"PALEONTOLOGY AND STRATIGRAPHY BRANCH"
10/7/59

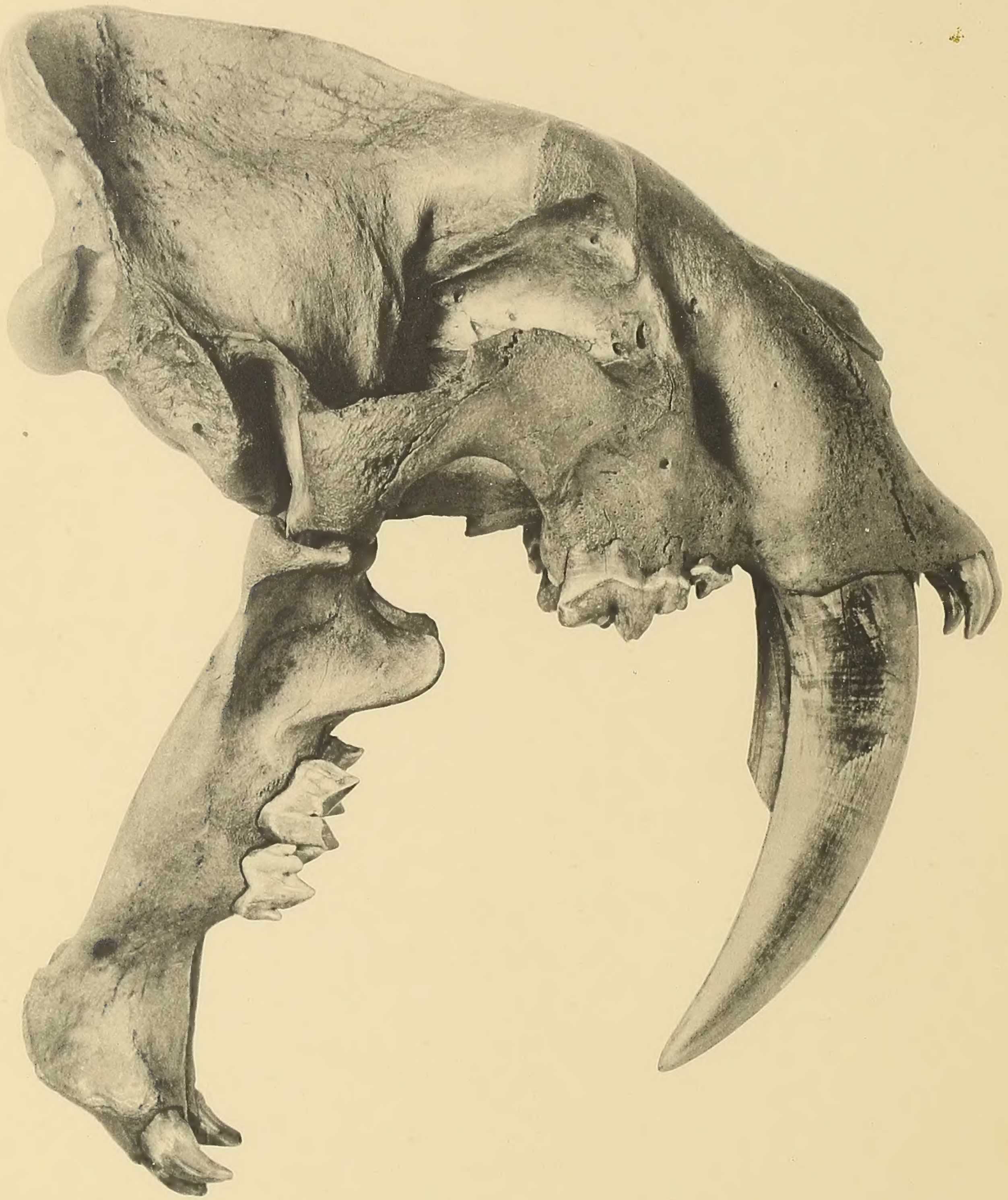

HELIOTYPE CO. BOSTON

SMILODON CALIFORNICUS

SKULL AND MANDIBLE, NO. 2001-2; X 1/2
LOS ANGELES MUSEUM COLLECTION. RANCHO LA BREA PLEISTOCENE

QE
882
C15M37
1932
VPAL

THE FELIDÆ OF RANCHO LA BREA

BY

JOHN C. MERRIAM

CHESTER STOCK

PUBLISHED BY
CARNEGIE INSTITUTION OF WASHINGTON
December, 1932

U. S. GEOLOGICAL SURVEY
BOOK 008147

CARNEGIE INSTITUTION OF WASHINGTON
PUBLICATION NO. 422

PRESS OF
W. F. ROBERTS COMPANY
LANMAN ENGRAVING COMPANY
HELIOTYPE COMPANY

U. S. G. S.
P&S BRANCH

CONTENTS

PAGE

INTRODUCTION ... 3
Acknowledgments ... 4
Review of Literature on Pleistocene and Late Tertiary Cats of Western North America ... 5
  Sabre-tooth Cats ... 5
  True Cats ... 6
Pleistocene sabre-tooth Cats of North America ... 8
Occurrence of Felidæ at Rancho La Brea ... 17
Habit and Habitat of Smilodon and of Felis atrox as Suggested by Occurrence at Rancho La Brea ... 21
Classification and Relationships of the Felidæ from the Asphalt ... 27
Smilodontinæ of Rancho La Brea ... 28
  Characters of the Genus Smilodon ... 28
Smilodon californicus Bovard ... 29
  Skull ... 29
    Palatine Region ... 35
    Foramina ... 36
  Endocranial Cast ... 38
  Mandible ... 41
  Hyoid Apparatus ... 45
  Dentition ... 45
    Superior Dentition ... 45
    Inferior Dentition ... 50
    Milk Dentition ... 53
    Notes on Skulls of Smilodon with Deciduous Canines Present or with Permanent Canines Partially Emerged ... 55
Comparative Study of Vertebral Column and Limbs of Smilodon and Felis atrox ... 60
  Vertebral Column ... 60
    Vertebral Formula ... 60
  Cervical Series ... 61
    Atlas ... 62
    Axis ... 64
    Third Cervical Vertebra ... 66
    Fourth Cervical Vertebra ... 67
    Fifth Cervical Vertebra ... 69
    Sixth Cervical Vertebra ... 70
    Seventh Cervical Vertebra ... 73
  Thoracic Series ... 77
    First Thoracic Vertebra ... 77
    Second Thoracic Vertebra ... 79
    Eleventh Thoracic Vertebra ... 85
    Twelfth Thoracic Vertebra ... 88
    Thirteenth Thoracic Vertebra ... 89
  Lumbar Series ... 91
    Sixth Lumbar Vertebra ... 94
    Seventh Lumbar Vertebra ... 96
  Sacrum ... 99
  Caudal Series ... 102
  Manubrium ... 103
  Mesosternum ... 105
  Xiphisternum ... 106
  Ribs ... 107
  Clavicle ... 108
  Scapula ... 108
  Comparison of Lengths of Limb Elements ... 110
  Humerus ... 111
  Ulna ... 115
  Radius ... 116
  Scapho-lunar ... 117
  Cuneiform ... 119
  Pisiform ... 119
  Trapezium ... 120
  Trapezoid ... 122
  Magnum ... 122
  Unciform ... 124
  Metacarpal Series ... 126
    Metacarpal I ... 126

PAGE
Metacarpal II 128
Metacarpal III 129
Metacarpal IV 131
Metacarpal V 134
Digit I, Proximal Phalanx 135
Innominate Bone 135
Femur 137
Patella 138
Sesamoids 138
Fabella 138
Phalangeal Sesamoids 139
Tibia 139
Fibula 140
Astragalus 142
Calcaneum 143
Entocuneiform 143
Mesocuneiform 146
Ectocuneiform 147
Cuboid 148
Navicular 150
Metatarsal Series 152
Rudimentary Metatarsal I 152
Metatarsal II 153
Metatarsal III 155
Metatarsal IV 157
Metatarsal V 160
Phalanges 160
Smilodon californicus brevipes, n. var. 161
Felis atrox Leidy 164
Status of Leidy's Species Felis imperialis 165
Comparison with Type Specimen of Felis atrox 167
Skull 168
Endocranial Cast 172
Mandible 175
Dentition 176
Superior Dentition 176
Inferior Dentition 178
Lower Milk Dentition 179
Relationship of Felis atrox to the Large Living Felines of the Old World 180
Comparison of the Large Extinct Cats of North America and Eurasia 190
Relationship of Felis atrox to the Jaguar 195
Smaller Cats of the Genera Felis and Lynx 199
Comparison of Skull and Dentition of Puma and Jaguar 205
Felis daggetti Merriam 207
Felis bituminosa, n. sp. 215
Lynx rufa fischeri Merriam 216
Occurrence and Description of Pleistocene Felidæ in Western North America 224
Pacific Coast Province 224
Great Basin Province 227
Literature 228

ILLUSTRATIONS

FRONTISPIECE

Smilodon californicus Bovard

Skull and mandible, No. 2001–2; lateral view; × 1/2. Los Angeles Museum Collection. Rancho La Brea Pleistocene.

PLATE 1

Smilodon californicus Bovard

FIG. 1, skull and mandible, No. 2001–1, lateral view; × 1/3.
FIGS. 2 and 3, skull No. 2001–1. FIG. 2, dorsal view; FIG. 3, ventral view; × 1/3.
Los Angeles Museum Collection. Rancho La Brea Pleistocene.

PLATE 2

Smilodon californicus Bovard

FIGS. 1 and 2, skull, No. 2001–1. FIG. 1, lateral view with portion of zygomatic arch removed to show infraorbital region; FIG. 2, posterior view; × 1/3.
FIG. 3, skull and mandible, No. 2001–1, anterior view; × 1/3.
FIGS. 4 and 5, mandible, No. 2002–1. FIG. 4, dorsal view; FIG. 5, lateral view; × 1/3.
FIG. 6, mandible, No. 2002–R–684, inner view; × 1/3.
Los Angeles Museum Collection. Rancho La Brea Pleistocene.

PLATE 3

Smilodon californicus Bovard

Smallest and one of the larger skulls of adult individuals, NOS. 2001–148, 2001–225. FIGS. 1 and 7, ventral views; FIGS. 2 and 5, anterior views; FIGS. 3 and 6, dorsal views; FIGS. 4 and 8, lateral views; × 2/9. Los Angeles Museum Collection. Rancho La Brea Pleistocene.

PLATE 4

Smilodon californicus Bovard

FIGS. 1–10, series of lower jaws including young and adult individuals showing variation in size, NOS. 2002–L–4, R–4, R–68, R–6, R–781, R–10, R–496, R–14, R–16 and R–15, incl. All specimens in lateral view; × 1/2. Specimens shown in FIGS. 1 to 7 possess milk teeth. Permanent dentition shown in FIGS. 8 to 10. Los Angeles Museum Collection. Rancho La Brea Pleistocene.

PLATE 5

Smilodon californicus Bovard

Skull, No. 2001–10. FIG. 1, lateral view; FIG. 2, anterior view; FIG. 3, dorsal view; FIG. 4, ventral view; × 2/5. The crowns of the permanent canine teeth are appearing along the inner sides of the deciduous canines. Los Angeles Museum Collection. Rancho La Brea Pleistocene.

PLATE 6

Smilodon californicus Bovard

FIGS. 1, 2, 3, and 4, skull, No. 2001–9. FIG. 1, lateral view; FIG. 2, anterior view; FIG. 3, dorsal view; FIG. 4, ventral view; × 2/5. Los Angeles Museum Collection. Rancho La Brea Pleistocene.

PLATE 7

Smilodon californicus Bovard

Skull, NO. 2001–7. FIG. 1, lateral view; FIG. 2, anterior view; FIG. 3, dorsal view; FIG. 4, ventral view; × 2/5. Note presence of deciduous and permanent canine teeth on left side. Los Angeles Museum Collection. Rancho La Brea Pleistocene.

PLATE 8

Smilodon californicus Bovard

Skull, NO. 2001–8. FIG. 1, lateral view; FIG. 2, anterior view; FIG. 3, dorsal view; FIG. 4, ventral view; × 2/5. Note partial emergence of permanent canine teeth. Los Angeles Museum Collection. Rancho La Brea Pleistocene.

PLATE 9

Smilodon californicus Bovard

Skull, NO. 2001–6. FIG. 1, lateral view; FIG. 2, anterior view; FIG. 3, dorsal view; FIG. 4, ventral view; × 2/5. Permanent canine teeth have not fully emerged in this specimen. Los Angeles Museum Collection. Rancho La Brea Pleistocene.

Plate 10

Smilodon californicus Bovard

Skull, No. 2001–19. Fig. 1, lateral view; Fig. 2, anterior view; Fig. 3, dorsal view; Fig. 4, ventral view; × 1/3. Note broken surfaces of canine teeth which were worn during life of individual. Los Angeles Museum Collection. Rancho La Brea Pleistocene.

Plate 11

Smilodon floridanus (Leidy)

Type specimen, skull, No. 4072, Wagner Free Institute of Science Collection. Fig. 1, ventral view; Fig. 2, lateral view; × 3/5. Pleistocene, Ocala, Marion Co., Florida.

Plate 12

Smilodon californicus Bovard

Figs. 1, 2 and 3, permanent and deciduous canines. Fig. 1, right canine, anterior, inner, outer and posterior views with cross-sections; Fig. 2, portion of crown of canine with anterior and posterior serrations somewhat magnified; Fig. 3, right deciduous canine, same views as in Fig. 1; × 1/2. Los Angeles Museum Collection. Rancho La Brea Pleistocene.

Plate 13

Smilodon californicus Bovard

Upper and lower teeth. Figs. 1-1a, $P\underline{4}$, outer and inner views; Figs. 2–2a, $P\underline{3}$, inner and outer views; Figs. 3–3a, Figs. 4–4a, $M\overline{1}$, $P\overline{4}$ respectively, outer and inner views; Figs. 5–5a, Figs. 6–6a, Figs. 7–7a, $I\underline{1}$, $\underline{2}$, $\underline{3}$ respectively, inner and posterior views; Figs. 8–8a, lower canine, inner and posterior views; Figs. 9–9a, Figs. 10–10a, Figs. 11–11a, $I\overline{1}$, $\overline{2}$, $\overline{3}$ respectively, outer and posterior views; × 1. Los Angeles Museum Collection. Rancho La Brea Pleistocene.

Plate 14

Felis atrox Leidy

Figs. 1, 2 and 3, endocranial cast of skull No. 2900–1. Fig. 1, dorsal view; Fig. 2, lateral view; Fig. 3, ventral view; × 2/3.

Smilodon californicus Bovard

Figs. 4, 5 and 6, endocranial cast of skull No. 2001–199. Fig. 4, dorsal view; Fig. 5, lateral view; Fig. 6, ventral view; × 2/3.

Los Angeles Museum Collection. Rancho La Brea Pleistocene.

Plate 15

Smilodon californicus Bovard

Fig. 1, left ear region of skull cut in transverse sections *a, b, c, d.* Sections *a′, b′, c′* viewed from posterior side; section d′ viewed from anterior side; pg.p., post-glenoid process; m.p., mastoid process; e.c., eustachian canal; f.r., foramen rotundum; f.o., foramen ovale; s.f., stylomastoid foramen; t-hy., tympanohyal pit; c.c., carotid canal; f.l.p., posterior lacerate foramen; c.f., condylar foramen; pa.p., paroccipital process; i.c., inner tympanic chamber; s., septum separating outer tympanic chamber from inner; e.a.m., external auditory meatus; bo., basioccipital; i.a.m., internal auditory meatus; fe.r., fenestra rotunda; pet., petrosal; × 3/4.

Fig. 2, three views of left incus; × 3.

Fig. 3, three views of left malleus; × 3.

Los Angeles Museum Collection. Rancho La Brea Pleistocene.

Plate 16

Smilodon californicus Bovard

Figs. 1 and 2, cervical vertebræ, lateral and dorsal views; × 1/3. These vertebræ are not all of the same individual.

Felis atrox Leidy

Figs. 3 and 4, cervical vertebræ, lateral and dorsal views; × 1/3. Cervicals III-VI are of one individual.

Los Angeles Museum Collection. Rancho La Brea Pleistocene.

Plate 17

Smilodon californicus Bovard

Figs. 1, 2 and 3, axis, No. 2039–1. Fig. 1, dorsal view; Fig. 2, posterior view; Fig. 3, lateral view; × 1/2.

Figs. 4, 5, 6 and 7, atlas, No. 2038–5. Fig. 4, dorsal view; Fig. 5, anterior view; Fig. 6, posterior view; Fig. 7, ventral view; × 1/2.

Los Angeles Museum Collection. Rancho La Brea Pleistocene.

Plate 18

Smilodon californicus Bovard

Figs. 1 and 2, thoracic vertebræ, lateral and dorsal views; × 1/3. a′, thirteenth vertebra, No. 2057–12; b′, twelfth vertebra, No. 2056–13; c′, eleventh vertebra, No. 2055–12; d′, seventh vertebra, No. 2051–2; e′, first vertebra, No. 2045–11; anterior views; × 4/9. Los Angeles Museum Collection. Rancho La Brea Pleistocene.

Plate 19

Smilodon californicus Bovard

Figs. 1 and 2, vertebral series from eighth thoracic to last sacral, incl., lateral and dorsal views; × 1/3. a′, seventh lumbar vertebra, No. 2064–12; b′, fourth lumbar vertebra, No. 2061–1; c′, first lumbar vertebra, No. 2058–1; d′, thirteenth thoracic vertebra, No. 2057–11; e′, twelfth thoracic vertebra, No. 2056–12; f′, eleventh thoracic vertebra, No. 2055–11; g′, eighth thoracic vertebra, No. 2052–2; anterior views; × 4/9. Los Angeles Museum Collection. Rancho La Brea Pleistocene.

Plate 20

Smilodon californicus Bovard and *Felis atrox* Leidy

Figs. 1–7, *Smilodon californicus* Bovard; Figs. 8–13, *Felis atrox* Leidy; right ribs. Figs. 1, 1a and Figs. 8, 8a, first rib; Figs. 2, 9, second rib; Figs. 3–7, Figs. 10–13, ribs posterior to the second; × 4/9. Los Angeles Museum Collection. Rancho La Brea Pleistocene.

Plate 21

Smilodon californicus Bovard

Figs. 1, 1a, right scapula, No. 2004–R–10, lateral view and view of articulating end; × 1/3.

Figs. 2, 3, 4 and 5, right humerus, No. 2005–R–6. Figs. 2, inner view; Fig. 3, outer view; Fig. 4, posterior view; Fig. 5, proximal, anterior and distal views; × 1/3.

Los Angeles Museum Collection. Rancho La Brea Pleistocene.

Plate 22

Smilodon californicus Bovard

Figs. 1, 2 and 3, right ulna, No. 2007–R–6. Fig. 1, radial view; Fig. 2, inner view; Fig. 3, anterior view; × 1/3.

Figs. 4 and 5, right radius, No. 2006–R–5. Fig. 4, ulnar view; Fig. 5, proximal, outer and distal views; × 1/3.

Fig. 6, right manus, dorsal view; × 1/3.

Los Angeles Museum Collection. Rancho La Brea Pleistocene.

Plate 23

Smilodon californicus Bovard

Figs. 1 and 2, right femur, No. 2009–R–11. Fig. 1, anterior view; Fig. 2, proximal, posterior and distal views; × 1/3.

Figs. 3, 4, 5 and 6, right tibia, No. 2010–R–5. Fig. 3, inner view; Fig. 4, outer view; Fig. 5, posterior view; Fig. 6, proximal, anterior and distal views; × 1/3.

Fig. 7, right patella, No. 2012–R–3, anterior and femoral views, and outline of lateral view; × 1/3.

Los Angeles Museum Collection. Rancho La Brea Pleistocene.

Plate 24

Smilodon californicus Bovard

Figs. 1 and 2, pelvis, No. 2008–7. Fig. 1, lateral view; Fig. 2, dorsal view; × 1/3.

Fig. 3, right pes, dorsal view; × 1/3.

Fig. 4, right fibula, No. 2011–R–1, outer, anterior and inner views; × 1/3.

Los Angeles Museum Collection. Rancho La Brea Pleistocene.

Plate 25

Smilodon californicus Bovard

Mounted skeleton, viewed from right side; approx. × 1/8. Los Angeles Museum Collection. Prepared by J. W. Lytle. Photograph by L. E. Wyman. Courtesy of Los Angeles Museum. Rancho la Brea Pleistocene.

Plate 26

Felis atrox Leidy

Fig. 1, skull and mandible, No. 20049, lateral view; × 1/3.

Figs. 2 and 3, skull, No. 20049. Fig. 2, dorsal view; Fig. 3, ventral view; × 1/3.

University of California Collection. Rancho La Brea Pleistocene.

Plate 27

Felis atrox Leidy

Figs. 1 and 2, skull, No. 20049. Fig. 1, lateral view with portion of zygomatic arch removed to show infraorbital region; Fig. 2, posterior view; × 1/3.
Fig. 3, skull and mandible, No. 20049, anterior view; × 1/3.
Figs. 4 and 5, mandible, No. 20049. Fig. 4, dorsal view; Fig. 5, lateral view; × 1/3.
Fig. 6, mandible, No. 2901–4, inner view; × 1/3.
No. 20049, University of California Collection. Rancho La Brea Pleistocene.

Plate 28

Felis atrox Leidy

Skull, No. 2900–6. Fig. 1, lateral view; Fig. 2, posterior view; Fig. 3, ventral view; Fig. 4, anterior view; Fig. 5, dorsal view; × 1/4. Skulls shown on this and on the three plates that follow represent individuals differing in age and sex. Los Angeles Museum Collection. Rancho La Brea Pleistocene.

Plate 29

Felis atrox Leidy

Skull, No. 2900–7. Fig. 1, lateral view; Fig. 2, posterior view; Fig. 3, ventral view; Fig. 4, anterior view; Fig. 5, dorsal view; × 1/4. Los Angeles Museum Collection. Rancho La Brea Pleistocene. (See note Plate 28.)

Plate 30

Felis atrox Leidy

Skull, No. 2900–9. Fig. 1, lateral view; Fig. 2, posterior view; Fig. 3, ventral view; Fig. 4, anterior view; Fig. 5, dorsal view; × 1/4. Los Angeles Museum Collection. Rancho La Brea Pleistocene. (See note Plate 28.)

Plate 31

Felis atrox Leidy

Skull, No. 2900–3. Fig. 1, lateral view; Fig. 2, posterior view; Fig. 3, ventral view; Fig. 4, anterior view; Fig. 5, dorsal view; × 1/4. Los Angeles Museum Collection. Rancho La Brea Pleistocene. (See note Plate 28.)

Plate 32

Felis atrox Leidy

Figs. 1–5, series of lower jaws including young and adult individuals showing variation in size and shape, Nos. 2901–6, –5, –21, –3, –22, incl.; all specimens × 1/3. Milk teeth present in No. 2901–22.
Figs. 6–6′, lower canine, inner and posterior views; × 2/3.
Figs. 7–7′, upper canine, inner and posterior views; × 2/3.
Los Angeles Museum Collection. Rancho La Brea Pleistocene.

Plate 33

Felis atrox Leidy

Upper and lower teeth. Figs. 1–1a, $P\underline{4}$, outer and inner views; Figs. 2–2a, $P\underline{3}$, outer and inner views; Figs. 3–3a, Figs. 4–4a, Figs. 5–5a, $I\overline{1}$, $\overline{2}$, $\overline{3}$ respectively, outer and posterior views; Figs. 6–6a, Figs. 7–7a, Figs. 8–8a, $M\overline{1}$, $P\overline{4}$, $P\overline{3}$ respectively, outer and inner views; Figs. 9–9a, Figs. 10–10a, Figs. 11–11a, $I\underline{1}$, $\underline{2}$, $\underline{3}$ respectively, inner and posterior views; × 1. Los Angeles Museum Collection. Rancho La Brea Pleistocene.

Plate 34

Felis atrox Leidy

Figs. 1, 2 and 3, axis, No. 2937–7. Fig. 1, dorsal view; Fig. 2, posterior view; Fig. 3, lateral view; × 1/2.
Figs. 4, 5, 6 and 7, atlas, No. 2936–1. Fig. 4, anterior view; Fig. 5, dorsal view; Fig. 6, ventral view; Fig. 7, posterior view; × 1/2.
Los Angeles Museum Collection. Rancho La Brea Pleistocene.

Plate 35

Felis atrox Leidy

Fig. 1, sacrum, No. 2963–2, lateral view; × 1/3.
Figs. 2 and 3, lumbar vertebræ, lateral and dorsal views; × 1/3. a′, seventh vertebra, No. 2962–11; b′, fourth vertebra, No. 2959–2; c′, first vertebra, No. 2956–2; anterior views; × 1/3.
Figs. 4 and 5, thirteenth thoracic vertebra, No. 2955–11, and twelfth thoracic vertebra, No. 2954–12, lateral and dorsal views; × 1/3.
Los Angeles Museum Collection. Rancho La Brea Pleistocene.

Plate 36

Felis atrox Leidy

Fig. 1, right scapula, No. 2902–R–1, lateral view and view of articulating end; × 1/3.
Figs. 2, 3, 4 and 5, right humerus, No. 2903–R–8. Fig. 2, inner view; Fig. 3, outer view; Fig. 4, posterior view; Fig. 5, proximal, anterior and distal views; × 1/3.
Los Angeles Museum Collection. Rancho La Brea Pleistocene.

Plate 37

Felis atrox Leidy

Figs. 1, 2 and 3, right ulna, No. 2905–R–8. Fig. 1, radial view; Fig. 2, inner view; Fig. 3, anterior view; × 1/3.
Figs. 4 and 5, right radius, No. 2904–R–7. Fig. 4, ulnar view; Fig. 5, proximal, outer and distal views; × 1/3.
Fig. 6, right manus, dorsal view × 1/3.
Los Angeles Museum Collection. Rancho La Brea Pleistocene.

Plate 38

Felis atrox Leidy

Figs. 1 and 2, right femur, No. 2907–R–11. Fig. 1, anterior view; Fig. 2, proximal, posterior and distal views; × 1/3.
Figs. 3, 4, 5 and 6, right tibia, No. 2908–R–10. Fig. 3, inner view; Fig. 4, outer view; Fig. 5, posterior view; Fig. 6, proximal, anterior and distal views; × 1/3.
Fig. 7, right patella, No. 2910–R–1, anterior and femoral views, and outline of lateral view; × 1/3.
Los Angeles Museum Collection. Rancho La Brea Pleistocene.

Plate 39

Felis atrox Leidy

Figs. 1 and 2, pelvis, No. 2906–1. Fig. 1, lateral view; Fig. 2, dorsal view; × 1/3.
Fig. 3, right pes, dorsal view; × 1/3.
Figs. 4a, 4b and 4c, right fibula, No. 2909–R–1. Fig. 4a, outer view; Fig. 4b, inner view; Fig. 4c, anterior view; × 1/3.
Los Angeles Museum Collection. Rancho La Brea Pleistocene.

Plate 40

Felis atrox Leidy

Mounted skeleton, viewed from right side; approx. × 1/9. Los Angeles Museum Collection. Prepared by J. W. Lytle. Photograph by L. E. Wyman. Courtesy of Los Angeles Museum. Rancho La Brea Pleistocene.

Plate 41

Felis bituminosa, n. sp.

Holotype, skull, No. X8628. Fig. 1, lateral view of skull and jaw; Fig. 2, dorsal view; Fig. 3, ventral view; × 1/2.
Los Angeles Museum Collection. Rancho La Brea Pleistocene.

Plate 42

Felis and *Lynx*

Figs. 1, 2 and 3, *Lynx rufa fischeri* Merriam, skull, No. X9489, dorsal, ventral and lateral views; × 1/2.
Fig. 4, *Lynx rufa fischeri* Merriam, type specimen, ramus of mandible, No. 11283, Univ. Calif. Coll., lateral view; × 1/2.
Fig. 5, *Felis* cf. *bituminosa*, n. sp., ramus of mandible, No. X9474, lateral view; × 1/2.
Fig. 6, *Felis daggetti* Merriam, type specimen, No. 21572, Univ. Calif. Coll., lateral view; × 1/2.
Fig. 7, *Lynx rufa fischeri* Merriam, ramus of mandible, No. X9490, lateral view; × 1/2.
Figs. 8 and 9, *Felis bituminosa*, n. sp., skull, No. X8629, dorsal and ventral views; × 1/2.
Los Angeles Museum and University of California Collections. Rancho La Brea Pleistocene.

FIG. 1. Topographic map of Rancho La Brea showing location of principal excavations of the Los Angeles Museum and University of California.

FIG. 2. Diagram showing relative number of individuals in the mammalian families (except rodents, lagomorphs, insectivores and bats) occurring in the Rancho La Brea Pleistocene fauna. Representation of the Felidæ is exceeded only by that of the Canidæ.

FIG. 3. Comparative study of head in (A) sabre-tooth cat (*Smilodon californicus* Bovard) and (B) great true cat (*Felis atrox* Leidy). Anterior views, greatly reduced and not to same scale. Restorations by Charles R. Knight under direction of J. C. Merriam.

FIG. 4. Comparative study of head in (A) sabre-tooth cat (*Smilodon californicus* Bovard) and (B) great true cat (*Felis atrox* Leidy). Lateral views, greatly reduced and not to same scale. Restorations by Charles R. Knight under direction of J. C. Merriam.

FIG. 5. Comparative study of (A) sabre-tooth cat (*Smilodon californicus* Bovard), approx. × 1/13, and (B) great true cat (*Felis atrox* Leidy), approx. × 1/12. Restorations by Charles R. Knight under direction of J. C. Merriam.

FIG. 6. *Smilodon californicus* Bovard. Skull, A, dorsal view; B, ventral view. Several sutures reproduced from considerably younger skulls than that shown. *pmx*, premaxillary; *n*, nasal; *mx*, maxillary; *la*, lachrymal; *ma*, malar; *fr*, frontal; *sq*, squamosal; *pa*, parietal; *so*, supraoccipital; *pl*, palatine; *pt*, pterygoid; *vo*, vomer; *ps*, presphenoid; *bs*, basisphenoid; *bo*, basioccipital; *as*, alisphenoid; *mt*, mastoid; *ty*, tympanic; *eo*, exoccipital. Rancho La Brea Pleistocene.

FIG. 7. *Smilodon californicus* Bovard. Lateral view of skull and view of infraorbital region with portion of zygomatic arch removed. *os*, orbitosphenoid; *pmx*, premaxillary; *n*, nasal; *mx*, maxillary; *la*, lachrymal; *ma*, malar; *fr*, frontal; *sq*, squamosal; *pa*, parietal; *so*, supraoccipital; *pl*, palatine; *as*, alisphenoid: *mt*, mastoid; *eo*, exoccipital. Rancho La Brea Pleistocene.

FIG. 8. View of occiput; × 1/3. A, *Smilodon californicus* Bovard, No. 2001-225; B, *Felis atrox* Leidy, No. 2900–9. *m.p*, mastoid process; *pa.p*, paroccipital process; *pg.p.*, postglenoid process; *t.b.*, tympanic bulla. The posterior processes and tympanic bulla are incomplete on the left side of the skull of *Felis atrox*. Rancho La Brea Pleistocene.

FIG. 9. Comparative views of skulls of sabre-tooth cat and true cat. A, C, superior view of muzzle B, D, anterior view; × 1/4. A, B, *Smilodon californicus* Bovard, No. 2001-225; C, D, *Felis atrox* Leidy, No. 2900–9. Rancho La Brea Pleistocene.

FIG. 10. *Smilodon californicus* Bovard. Vertical longitudinal section of skull, No. 2001-273; × 2/5. *n*, nasal; *fr*, frontal; *s*, frontal sinus; *pa*, parietal; *so*, supraoccipital; *ten.*, cut edge of tentorium; *bo*, basioccipital; *pet*, petrosal; *bs*, basisphenoid; *ps*, presphenoid; *ty*, tympanic; *pt.* pterygoid; *pl*, palatine; *pmx*, premaxillary; *mxt*, maxilloturbinal; *et*, ethmoturbinals; *ms*, mesethmoid; *st*, sella turcica; *cp*, clinoid plate; *mt*, mastoid; *pgp*, postglenoid process; *IX*, *X*, *XI*, foramen lacerum posterius, *XII*, condylar foramen. Rancho La Brea Pleistocene.

FIG. 11. *Smilodon californicus* Bovard. Endocranial cast from skull 2001-199. A, dorsal view; B, ventral view; C, lateral view; D, posterior view; × 2/3. *L.ol.*, lobus olfactorius; *L.p.*, lobulus pyriformis; *Hph.*, hypophysis; *Med.*, medulla oblongata; *II*, N. opticus; *f.l.a.*, N. trigeminus (ophthalmic); *f.r.*, N. trigeminus (maxillary); *f.o.*, N. trigeminus (mandibular); *VIII*, N. acusticus; *IX*, *X*, *XI*, N. glossopharyngeus, N. vagus, and N. accessorius; *XII*, N. hypoglossus; *V*, *cer.?*, cerebral veins?; *Sin. sag.*, sinus sagittalis; *S.so.*, supraorbital sulcus; *S.cr.*, cruciate sulcus; *S.cor.*, coronal sulcus; *S.an.*, sulcus ansatus; *S.lat.*, lateral sulcus; *S.ss.*, suprasylvian sulcus; *S.s.*, fissura Sylvii; *S.e.a.*, anterior ectosylvian sulcus; *S.e.p.*, posterior ectosylvian sulcus; *S.ps.*, postsylvian sulcus; *S.dg.*, diagonal sulcus; *S.rh.*, rhinal sulcus; *S.prh.*, postrhinal sulcus. Rancho La Brea Pleistocene.

FIG. 12. *Smilodon californicus* Bovard. Ramus and lower dentition showing presence of $P\overline{3}$; No. 2002–R–60; lateral view; × 1/2. Rancho La Brea Pleistocene.

FIG. 12*a*. Basihyal?, No. I-1, tentatively referred to *Smilodon californicus* Bovard; × 1. Rancho La Brea Pleistocene.

FIG. 13. *Smilodon californicus* Bovard. Specimens showing principally deciduous teeth. A, B, No. 2001–577, outer and inner views; C, No. 2001–578, inner view; D, E, No. 2001–579, inner and outer views; × 2/3. *DC*, deciduous canine; *Al*, alveolus for permanent canine; $Dm\underline{3}$, and $Dm\underline{4}$, third and fourth deciduous molars. Rancho La Brea Pleistocene.

FIG. 14. *Smilodon californicus* Bovard. Specimens showing deciduous and permanent teeth. A, B, No. 2001–580, outer and inner views; C, No. 2001–581, inner view; × 2/3. *DC*, deciduous canine; *C*, permanent canine; *Al*, alveolus for permanent canine; $Dm\underline{3}$, and $Dm\underline{4}$, third and fourth deciduous molars; $P\underline{4}$, fourth premolar. Rancho La Brea Pleistocene.

FIG. 15. *Smilodon californicus* Bovard. Specimens showing deciduous and permanent teeth. A, B, No. 2001–582, outer and inner views; C, No. 2001–583, inner view; × 2/3. *DC*, deciduous canine; *C*, permanent canine; $P\underline{3}$, and $P\underline{4}$, third and fourth premolars. Rancho La Brea Pleistocene.

FIG. 16. *Smilodon californicus* Bovard. $Dm\underline{3}$, No. 2001-584; lateral and occlusal views; × 1. Rancho La Brea Pleistocene.

FIG. 17. Atlas viewed from the antero-external side. A, *Smilodon californicus* Bovard, No. 2038–11; B, *Felis atrox* Leidy, No. 2936–1; × 1/2. Rancho La Brea Pleistocene.

FIG. 18. *Smilodon californicus* Bovard. 3d cervical vertebra, No. 2040–2. A, anterior view; B, dorsal view; C, lateral view; × 1/2. *az*, anterior zygapophysis, *pz*, posterior zygapophysis, *tp*, transverse process, *hy*, hyperapophysis. Rancho La Brea Pleistocene.

FIG. 19. *Felis atrox* Leidy. 3d cervical vertebra, No. 2938–1. A, B, C, same views as in fig. 18; × 1/2. Rancho La Brea Pleistocene.

FIG. 20. *Smilodon californicus* Bovard. 4th cervical vertebra, No. 2041–8. A, anterior view; B, dorsal view; C, lateral view; × 1/2. *az*, anterior zygapophysis, *pz*, posterior zygapophysis, *tp*, transverse process, *hy*, hyperapophysis, *il*, inferior lamella. Rancho La Brea Pleistocene.

FIG. 21. *Felis atrox* Leidy. 4th cervical vertebra, No. 2939–1. A, B, C, same views as in fig. 20; × 1/2. Rancho La Brea Pleistocene.

FIG. 22. *Smilodon californicus* Bovard. 5th cervical vertebra, No. 2042–5. A, anterior view; B, lateral view; × 1/2. *az*, anterior zygapophysis, *pz*, posterior zygapophysis, *tp*, transverse process, *il*, inferior lamella. Rancho La Brea Pleistocene.

FIG. 23. *Felis atrox* Leidy. 5th cervical vertebra, No. 2940–1. A, B, same views as in fig. 22; × 1/2. Rancho La Brea Pleistocene.

FIG. 24. *Smilodon californicus* Bovard. 6th cervical vertebra, No. 2043–4. A, anterior view; B, lateral view; × 1/2. *az*, anterior zygapophysis, *pz*, posterior zygapophysis, *tp*. transverse process, *il*, inferior lamella. Rancho La Brea Pleistocene.

FIG. 25. *Felis atrox* Leidy. 6th cervical vertebra, No. 2941–1. A, B, same views as in fig. 24; × 1/2. Rancho La Brea Pleistocene.

FIG. 26. *Smilodon californicus* Bovard. 7th cervical vertebra, No. 2044–6. A, anterior view; B, dorsal view; C. lateral view; × 1/2. *az*, anterior zygapophysis, *pz*, posterior zygapophysis, *tp*, transverse process. Rancho La Brea Pleistocene.

FIG. 27. *Felis atrox* Leidy. 7th cervical vertebra, No. 2942–1. A, B, C, same views as in fig. 26; × 1/2. Rancho La Brea Pleistocene.

FIG. 28. *Smilodon californicus* Bovard. 1st thoracic vertebra, No. 2045–4. A, anterior view; B, ventral view; C. lateral view; × 1/2. *az*, anterior zygapophysis, *pz*, posterior zygapophysis, *tp*, transverse process, *tr*, facet for tuberculum of rib, *cr*, facet for capitulum of rib, *df*, demifacet. Rancho La Brea Pleistocene.

FIG. 29. *Felis atrox* Leidy. 1st thoracic vertebra, No. 2943–1. A, B, C, same views as in fig. 28; × 1/2. Rancho La Brea Pleistocene.

FIG. 30. *Smilodon californicus* Bovard. 2d thoracic vertebra, No. 2046-3. A, anterior view; B, ventral view; C, lateral view; × 1/2. Processes and facets as in 1st thoracic vertebra. Rancho La Brea Pleistocene.

FIG. 31. *Felis atrox* Leidy. 2d thoracic vertebra, No. 2944–1. A, B, C, same views as in fig. 30; × 1/2. Rancho La Brea Pleistocene.

FIG. 32. *Smilodon californicus* Bovard. 3d thoracic vertebra, No. 2047–7. A, anterior view; B, ventral view; C, lateral view; × 1/2. Processes and facets as in 1st thoracic vertebra. Rancho La Brea Pleistocene.

FIG. 33. *Felis atrox* Leidy. 3d thoracic vertebra, No. 2945–1. A, B, C, same views as in fig. 32; × 1/2. Rancho La Brea Pleistocene.

FIG. 34. *Smilodon californicus* Bovard. 4th thoracic vertebra, No. 2048–1. A, anterior view; B, lateral view; × 1/2. Processes and facets as in 1st thoracic vertebra. Rancho La Brea Pleistocene.

FIG. 35. *Felis atrox* Leidy. 4th (?) thoracic vertebra, No. 2946–1. A, B, same views as in fig. 34; × 1/2. Rancho La Brea Pleistocene.

FIG. 36. *Smilodon californicus* Bovard. 5th thoracic vertebra, No. 2049–1. A, anterior view; B, lateral view; × 1/2. Processes and facets as in 1st thoracic vertebra. Rancho La Brea Pleistocene.

FIG. 37. *Smilodon californicus* Bovard. 6th thoracic vertebra, No. 2050–1. A, anterior view; B, lateral view; × 1/2. Processes and facets as in 1st thoracic vertebra. Rancho La Brea Pleistocene.

FIG. 38. *Smilodon californicus* Bovard. 7th thoracic vertebra, No. 2051–1. A, anterior view; B, lateral view; × 1/2. Processes and facets as in 1st thoracic vertebra. Rancho La Brea Pleistocene.

FIG. 39. *Smilodon californicus* Bovard. 8th thoracic vertebra, No. 2052–1. A, anterior view; B, lateral view; × 1/2. Processes and facets as in 1st thoracic vertebra. Rancho La Brea Pleistocene.

FIG. 40. *Smilodon californicus* Bovard. 9th thoracic vertebra, No. 2053–1. A, anterior view; B, lateral view; × 1/2. Processes and facets as in 1st thoracic vertebra. Rancho La Brea Pleistocene.

FIG. 41. *Smilodon californicus* Bovard. 10th thoracic vertebra, No. 2054–1. A, anterior view; B, lateral view; × 1/2. Processes and facets as in 1st thoracic vertebra. Rancho La Brea Pleistocene.

FIG. 42. *Felis atrox* Leidy. 10th thoracic vertebra, No. 2952–1. A, B, same views as in fig. 41; × 1/2. Rancho La Brea Pleistocene.

FIG. 43. *Smilodon californicus* Bovard. 11th thoracic vertebra, spineless type, No. 2055–3. A, anterior view; B, lateral view; × 1/2. *m*, metapophysis, *an*, anapophysis, *pz*, posterior zygapophysis, *tr*, facet for tuberculum of rib, *cr*, facet for capitulum of rib. Rancho La Brea Pleistocene.

FIG. 44. *Felis atrox* Leidy. 11th thoracic vertebra, No. 2953–8. A, B, same views as in fig. 43; × 1/2. Rancho La Brea Pleistocene.

Fig. 45. *Smilodon californicus* Bovard. 11th thoracic vertebra, No. 2055–2. A, anterior view; B, lateral view; × 1/2. Note well-developed neural spine. Rancho La Brea Pleistocene.

Fig. 46. *Smilodon californicus* Bovard. 12th thoracic vertebra, No. 2056–1. A, anterior view; B, lateral view; × 1/2. Processes and facets as in 11th thoracic vertebra. Rancho La Brea Pleistocene.

Fig. 47. *Felis atrox* Leidy. 12th thoracic vertebra, No. 2954-1. A, B, same views as in fig. 46; × 1/2. Rancho La Brea Pleistocene.

Fig. 48. *Smilodon californicus* Bovard. 13th thoracic vertebra, No. 2057–6. A, anterior view; B, lateral view; × 1/2. Processes and facets as in 11th thoracic vertebra. Rancho La Brea Pleistocene.

Fig. 49. *Felis atrox* Leidy. 13th thoracic vertebra, No. 2955–6. A, B, same views as in fig. 48; × 1/2. Rancho La Brea Pleistocene.

Fig. 50. *Smilodon californicus* Bovard. 1st lumbar vertebra, No. 2058–1. A, anterior view; B, lateral view; C, dorsal view; × 1/2. Rancho La Brea Pleistocene.

Fig. 51. *Felis atrox* Leidy. 1st lumbar vertebra, No. 2956–1. A, B, C, same views as in fig. 50; × 1/2. Rancho La Brea Pleistocene.

Fig. 52. *Smilodon californicus* Bovard. 4th lumbar vertebra, No. 2061–2. A, anterior view; B, dorsal view; C, lateral view; × 1/2. Rancho La Brea Pleistocene.

Fig. 53. *Felis atrox* Leidy. 4th lumbar vertebra, No. 2959–1. A, B, C, same views as in fig. 52; × 1/2. Rancho La Brea Pleistocene.

Fig. 54. *Smilodon californicus* Bovard. 6th lumbar vertebra, No. 2063–1. A, anterior view; B, dorsal view; C, lateral view; × 1/2. Rancho La Brea Pleistocene.

Fig. 55. *Felis atrox* Leidy. 6th lumbar vertebra, No. 2961–1. A, B, C, same views as in fig. 54; × 1/2. Rancho La Brea Pleistocene.

Fig. 56. *Smilodon californicus* Bovard. 7th lumbar vertebra, No. 2064–11. A, anterior view; B, dorsal view; C, lateral view; × 1/2. Rancho La Brea Pleistocene.

Fig. 57. *Felis atrox* Leidy. 7th lumbar vertebra, No. 2962–6. A, B, C, same views as in fig. 56; × 1/2. Rancho La Brea Pleistocene.

Fig. 58. *Smilodon californicus* Bovard. Sacrum, No. 2065–5. A, anterior view; B, dorsal view; C, ventral view; D, posterior view; × 1/2. Rancho La Brea Pleistocene.

Fig. 59. *Felis atrox* Leidy. Sacrum, No. 2963–2. A, B, C, D, same views as in fig. 58; × 1/2. Rancho La Brea Pleistocene.

Fig. 60. *Smilodon californicus* Bovard. 1st caudal vertebra, No. 2068–1. A, B, anterior and dorsal views. *Felis atrox* Leidy. 1st caudal vertebra, No. 2966–1. C, D, anterior and dorsal views; × 1/2. Rancho La Brea Pleistocene.

Fig. 61. *Smilodon californicus* Bovard. Representative caudal vertebræ, posterior to the first; dorsal and anterior views; × 1/2. Rancho La Brea Pleistocene.

Fig. 62. *Felis atrox* Leidy. Representative caudal vertebræ, posterior to the first; dorsal and anterior views; × 1/2. Rancho La Brea Pleistocene.

Fig. 63. *Smilodon californicus* Bovard. Manubrium, No. 2066–7. A, ventral view; B, lateral view; C, dorsal view; × 2/3. CcI, attachment of first costal cartilage. Rancho La Brea Pleistocene.

Fig. 64. *Felis atrox* Leidy. Manubrium, No. 2964–4. A, B, C, same views as in fig. 63; × 2/3. Rancho La Brea Pleistocene.

Fig. 65. *Smilodon californicus* Bovard. Manubria, Nos. 2066–11, 2066–12. A, ventral view; B, lateral view; × 2/3. Specimens show variation in size and shape. CcI, attachment of first costal cartilage. Rancho La Brea Pleistocene.

Fig. 66. Mesosternal elements. A, B, *Smilodon californicus* Bovard, No. J-8269; C, D, *Felis atrox* Leidy, No. X–7394; × 1. Rancho La Brea Pleistocene.

Fig. 67. *Smilodon californicus* Bovard. Xiphisternum, No. 2067–2. A, ventral view; B, lateral view; × 2/3. Rancho La Brea Pleistocene.

Fig. 68. *Felis atrox* Leidy. Xiphisternum, No. 2965–2. A, B, same views as in fig. 67; × 2/3. Rancho La Brea Pleistocene.

Fig. 69. Clavicles, presumably of *Smilodon californicus* Bovard. A to D, Nos. I–4, I–5, I–2, I–3; × 1. Rancho La Brea Pleistocene.

Fig. 69*a*. Diagram illustrating comparative lengths of appendicular elements of *Felis atrox* Leidy and *Smilodon californicus* Bovard from Rancho La Brea.

Fig. 70. Right humerus; anterior view; × 1/3. A, *Smilodon californicus* Bovard, No. 2005–R–6; B, *Felis atrox* Leidy, No. 2903–R–8. Note characteristic differences between sabre-tooth cat and true cat in proximo-internal profile of tuberosity and development of bicipital and deltoid crests. Rancho La Brea Pleistocene.

Fig. 71. Right humerus; lateral view; × 1/3. A, *Smilodon californicus* Bovard, No. 2005–R–6; B, *Felis atrox* Leidy, No. 2903–R–8. Note particularly difference in profile of tuberosity. Rancho La Brea Pleistocene.

Fig. 72. *Smilodon californicus* Bovard. Distal portions of right humeri; anterior views; × 1/2. A, specimen without entepicondylar foramen, No. 2005–R–11; B, normal specimen with foramen, No. 2005–R–4. Rancho La Brea Pleistocene.

Fig. 73. *Smilodon californicus* Bovard. Right scapho-lunar, No. 2023–R–3. A, distal view; B, proximal view; C, external view; D, dorsal view; × 2/3. Facets for trapezium (*Tm*), trapezoid (*Td*), magnum (*Mg*), unciform (*Un*), sesamoid (*Ses*), and radius (*R*). Rancho La Brea Pleistocene.

Fig. 74. *Felis atrox* Leidy. Right scapho-lunar, No. 2921–R–1. A, proximal view; B, distal view; C, dorsal view; D, external view; × 2/3. Facets as in fig. 73. Rancho La Brea Pleistocene.

Fig. 75. *Smilodon californicus* Bovard. Right cuneiform, No. 2024–R–2. A, outer view; B, inner view; C, dorsal view; × 2/3. Facets for pisiform (*Pi*), ulna (*U*), and unciform (*Un*). Rancho La Brea Pleistocene.

Fig. 76. *Felis atrox* Leidy. Right cuneiform, No. 2922–R–1. A, B, C, same views as in fig. 75; × 2/3. Rancho La Brea Pleistocene.

Fig. 77. *Smilodon californicus* Bovard. Right pisiform, No. 2025–R–2. A, distal view with view of head; B, radial view; C, ulnar view; × 2/3. Facets for cuneiform (*Cn*) and ulna (*U*). Rancho La Brea Pleistocene.

Fig. 78. *Felis atrox* Leidy. Right pisiform, No. 2923–R–1. A, B, C, same views as in fig. 77; × 2/3. Rancho La Brea Pleistocene.

Fig. 79. *Smilodon californicus* Bovard. Right trapezium, No. 2026–R–2. A, outer view; B, inner distal view; C, dorsal view; D, proximal view; × 2/3. Facets for trapezoid (*Td*), scapho-lunar (*S-L*), metacarpal I (*McI*), and metacarpal II (*McII*). Rancho La Brea Pleistocene.

Fig. 80. *Felis atrox* Leidy. Right trapezium, Nos. 2924–R–1, 2924–R–2. A, E, outer view; B, F, inner distal view; C, G, dorsal view; D, H, proximal view; × 2/3. Facets as in fig. 79. Rancho La Brea Pleistocene.

Fig. 81. *Smilodon californicus* Bovard. Right trapezoid, No. 2027–R–3. A, proximal view; B, distal view; C, dorsal view; D, inner view; × 2/3. Facets for scapho-lunar (*S-L*), metacarpal II (*McII*), magnum (*Mg*), and trapezium (*Tm*). Rancho La Brea Pleistocene.

Fig. 82. *Felis atrox* Leidy. Right trapezoid, No. 2925–R–1. A, B, C, D, same views as for fig. 81; × 2/3. Rancho La Brea Pleistocene.

Fig. 83. *Felis atrox* Leidy. Fused right trapezium and trapezoid, No. 2925–R–5. A, distal view; B, proximal view; C, dorsal view; × 2/3. Facets for scapho-lunar (*S-L*), metacarpal I (*McI*), and metacarpal II (*McII*). Rancho La Brea Pleistocene.

Fig. 84. *Smilodon californicus* Bovard. Right magnum, No. 2028–R–2. A, inner view; B, outer view; C, distal view; D, proximal view; × 2/3. Facets for scapho-lunar (*S-L*), trapezoid (*Td*), metacarpal II (*McII*), metacarpal III (*McIII*), metacarpal IV (*McIV*), and unciform (*Un*). Rancho La Brea Pleistocene.

Fig. 85. *Felis atrox* Leidy. Right magnum, No. 2926–R–1. A, B, C, D, same views as in fig. 84; × 2/3. Rancho La Brea Pleistocene.

Fig. 86. *Smilodon californicus* Bovard. Right unciform, No. 2029–R–2. A, outer view; B, inner view; C, distal view; D, proximal view; E, dorsal view; × 2/3. Facets for cuneiform (*Cn*), scapho-lunar (*S-L*), magnum (*Mg*), metacarpal IV (*McIV*), and metacarpal V (*McV*). Rancho La Brea Pleistocene.

Fig. 87. *Felis atrox* Leidy. Right unciform, No. 2927–R–1. A, B, C, D, E, same views as in fig. 86; × 2/3. Rancho La Brea Pleistocene.

Fig. 88. Diagram showing comparative maximum and minimum lengths of metacarpals and differences between maximum and minimum lengths of these elements in *Felis atrox* Leidy and *Smilodon californicus* Bovard from Rancho La Brea.

Fig. 89. *Smilodon californicus* Bovard. Right metacarpal I, No. 2013–R–1. A, dorsal view; B, distal view; C, proximal view; D, palmar view; E, inner view; × 2/3. Facets for trapezium (*Tm*) and first digit (*Di*); *tb*, tubercle. Rancho La Brea Pleistocene.

Fig. 90. *Felis atrox* Leidy. Right metacarpal I, No. 2911–R–3. A, B, C, D, E, same views as in fig. 89; × 2/3. Rancho La Brea Pleistocene.

Fig. 91. *Smilodon californicus* Bovard. Right metacarpal II, No. 2014–R–1. A, dorsal view with view of proximal end; B, outer view; C, inner view; × 2/3. Facets for trapezoid (*Td*), trapezium (*Tm*) and metacarpal III (*McIII*). Rancho La Brea Pleistocene.

Fig. 92. *Felis atrox* Leidy. Right metacarpal II, No. 2912–R–1. A, B, C, same views as in fig. 91; × 2/3. Facet for magnum (*Mg*); remaining facets as in fig. 91. Rancho La Brea Pleistocene.

Fig. 93. *Smilodon californicus* Bovard. Right metacarpal III, No. 2015–R–1. A, dorsal view with view of proximal end; B, outer view; C, inner view; × 2/3. Facets for unciform (*Un*), magnum (*Mg*), metacarpal II (*McII*), and metacarpal IV (*McIV*). Rancho La Brea Pleistocene.

Fig. 94. *Felis atrox* Leidy. Right metacarpal III, No. 2913–R–1. A, B, C, same views as in fig. 93; × 2/3. Rancho La Brea Pleistocene.

Fig. 95. *Smilodon californicus* Bovard. Right metacarpal IV, No. 2016–R–1. A, dorsal view with view of proximal end; B, outer view; C, inner view; × 2/3. Facets for unciform (*Un*), metacarpal III (*McIII*), and metacarpal V (*McV*). Rancho La Brea Pleistocene.

FIG. 96. *Felis atrox* Leidy. Right metacarpal IV, No. 2914–R–1. A, B, C, same views as in fig. 95; × 2/3. Rancho La Brea Pleistocene.

FIG. 97. *Smilodon californicus* Bovard. Right metacarpal V, No. 2017–R–1. A, dorsal view with view of proximal end; B, inner view; C, outer view; × 2/3. Facets for unciform (*Un*) and metacarpal IV (*McIV*). Rancho La Brea Pleistocene.

FIG. 98. *Felis atrox* Leidy. Right metacarpal V, No. 2915–R–1. A, B, C, same views as in fig. 97; × 2/3. Rancho La Brea Pleistocene.

FIG. 99. *Smilodon californicus* Bovard. Digit I, manus, proximal phalanx, No. 2073–1. A, dorsal view; B, distal view; C, proximal view; D, palmar view; E, inner view; × 2/3. Rancho La Brea Pleistocene.

FIG. 100. *Felis atrox* Leidy. Digit I, manus, proximal phalanx, No. 2968–1. A, B, C, D, E, same views as in fig. 99; × 2/3. Rancho La Brea Pleistocene.

FIG. 101. Sesamoids; × 1. A, B, *Smilodon californicus* Bovard, Nos. 2037–2 and 2037–1; C, D, *Felis atrox* Leidy or *S. californicus*, Nos. 2935–2 and 2935–1. Rancho La Brea Pleistocene.

FIG. 102. *Smilodon californicus* Bovard. Right astragalus, No. 2030–R–1. A, posterior view; B, calcaneal view; C, tibial view; D, distal view; × 2/3. Facets for tibia (*T*), fibula (*F*), navicular (*Na*), and calcaneum (Ca^1, Ca^2, Ca^3). Rancho La Brea Pleistocene.

FIG. 103. *Felis atrox* Leidy. Right astragalus, No. 2928–R–1. A, B, C, D, same views as in fig. 102; × 2/3. Rancho La Brea Pleistocene.

FIG. 104. *Smilodon californicus* Bovard. Right astragali; × 2/3. A and B, tibial views of long-necked and short-necked specimens, Nos. 2030–R–2, 2030–R–5; C, posterior view showing presence of large astragalar foramen, No. 2030–R–2. Rancho La Brea Pleistocene.

FIG. 105. *Smilodon californicus* Bovard. Right calcaneum, No. 2031–R–1. A, astragalar view; B, distal view; × 2/3. Facets for astragalus (As^1, As^2, As^3), navicular (*Na*), and cuboid (*Cu*). Rancho La Brea Pleistocene.

FIG. 106. *Felis atrox* Leidy. Right calcaneum, No. 2929–R–1. A, B, same views as in fig. 105; × 2/3. Rancho La Brea Pleistocene.

FIG. 107. *Smilodon californicus* Bovard. Right entocuneiform, No. 2032–R–2. A, proximal view; B, outer view; C, dorsal view; D, distal view; × 2/3. Facets for navicular (*Na*), mesocuneiform (*Me*), and metatarsal I (*MtI*). Rancho La Brea Pleistocene.

FIG. 108. *Felis atrox* Leidy. Right entocuneiform, No. 2930–R–1. A, dorso-internal and proximal views; B, plantar-external and distal views; × 2/3. Facets as in fig. 107. Rancho La Brea Pleistocene.

FIG. 109. *Smilodon californicus* Bovard. Fused right entocuneiform and metatarsal I, No. 2032–R–4. A, dorsal view; B, outer view; × 2/3. Facets for navicular (*Na*) and mesocuneiform (*Me*). Rancho La Brea Pleistocene.

FIG. 110. *Smilodon californicus* Bovard. Right mesocuneiform, No. 2033–R–2. A, posterior view; B, distal view; C, proximal view; D, inner view; E, outer view; × 2/3. Facets for entocuneiform (*En*), navicular (*Na*), and metatarsal II (*MtII*). Rancho La Brea Pleistocene.

FIG. 111. *Felis atrox* Leidy. Right mesocuneiform, No. 2931–R–1. A, B, C, D, E, same views as in fig. 110; × 2/3. Facets for entocuneiform (*En*), navicular (*Na*), ectocuneiform (*Ec*), and metatarsal II (*MtII*). Rancho La Brea Pleistocene.

FIG. 112. *Smilodon californicus* Bovard. Right ectocuneiform, Nos. 2034–R–2, 2034–R–5. A, distal view; B, proximal view; C, internal view; D, external view; E, dorsal view; F, proximal view; G, internal view; × 2/3. Facets for navicular (*Na*), cuboid (*Cu*), metatarsal II (*MtII*), and metatarsal III (*MtIII*). Rancho La Brea Pleistocene.

FIG. 113. *Felis atrox* Leidy. Right ectocuneiform, No. 2932–R–1. A, B, C, D, E, same views as in fig. 112, A-E; × 2/3. Facets for mesocuneiform (*Me*), navicular (*Na*), cuboid (*Cu*), metatarsal II (*MtII*), metatarsal III (*MtIII*), and metatarsal IV (*MtIV*). Rancho La Brea Pleistocene.

FIG. 114. *Smilodon californicus* Bovard. Right cuboid, No. 2035–R–3. A, proximal view; B, dorsal view; C, distal view; D, inner view; E, plantar view; × 2/3. Facets for calcaneum (*Ca*), navicular (*Na*), ectocuneiform (*Ec*), metatarsal IV (*MtIV*), and metatarsal V (*MtV*). Rancho La Brea Pleistocene.

FIG. 115. *Felis atrox* Leidy. Right cuboid, No. 2933–R–1. A, B, C, D, E, same views as in fig. 114; × 2/3. Rancho La Brea Pleistocene.

FIG. 116. *Smilodon californicus* Bovard. Right navicular, No. 2036–R–1. A, proximal view; B, distal view; C, external view; × 2/3. Facets for astragalus (*As*), ectocuneiform (*Ec*), mesocuneiform (*Me*), entocuneiform (*En*), calcaneum (*Ca*), and cuboid (*Cu*). Rancho La Brea Pleistocene.

FIG. 117. *Felis atrox* Leidy. Right navicular, No. 2934–R–1. A, B, C, same views as in fig. 116; × 2/3. Rancho La Brea Pleistocene.

FIG. 118. *Smilodon californicus* Bovard. Fused navicular and mesocuneiform, No. 2033–R–5. A, proximal view; B, distal view; C, external view; × 2/3. Facets for astragalus (*As*), entocuneiform (*En*), metatarsal II (*MtII*), ectocuneiform (*Ec*), and cuboid (*Cu*). Rancho La Brea Pleistocene.

Fig. 119. Diagram showing comparative maximum and minimum lengths of metatarsals and differences between maximum and minimum lengths of these elements in *Felis atrox* Leidy and *Smilodon californicus* Bovard from Rancho La Brea.

Fig. 120. *Smilodon californicus* Bovard. Right rudimentary metatarsal I, No. 2018–R–1. A, proximal view; B, dorsal view; C, inner view; × 2/3. Facet for entocuneiform (*En*). Rancho La Brea Pleistocene.

Fig. 121. *Felis atrox* Leidy. Right rudimentary metatarsal I, No. 2916–R–1. A, B, C, same views as in fig. 120; × 2/3. Rancho La Brea Pleistocene.

Fig. 122. *Smilodon californicus* Bovard. Right metatarsal II, No. 2019–R–1. A, dorsal view with view of proximal end; B, outer view; × 2/3. Rancho La Brea Pleistocene.

Fig. 123. *Felis atrox* Leidy. Right metatarsal II, No. 2917–R–1. A, B, same views as in fig. 122; × 2/3. Rancho La Brea Pleistocene.

Fig. 124. *Smilodon californicus* Bovard. Specimen showing fusion of right metatarsal II and rudiment of first metatarsal. A, dorsal and proximal views; B, inner view; No. 2019–R–4; × 2/3. Rancho La Brea Pleistocene.

Fig. 125. *Smilodon californicus* Bovard. Right metatarsal III, No. 2020–R–1. A, dorsal view with view of proximal end; B, outer view; × 2/3. Rancho La Brea Pleistocene.

Fig. 126. *Felis atrox* Leidy. Right metatarsal III, No. 2918–R–1. A, B, same views as in fig. 125; × 2/3. Rancho La Brea Pleistocene.

Fig. 127. *Smilodon californicus* Bovard. Right metatarsal IV, No. 2021–R–1. A, dorsal view with view of proximal end; B, outer view; C, inner view; × 2/3. Rancho La Brea Pleistocene.

Fig. 128. *Felis atrox* Leidy. Right metatarsal IV, No. 2919–R–1. A, B, C, same views as in fig. 127; × 2/3. Rancho La Brea Pleistocene.

Fig. 129. *Smilodon californicus* Bovard. Right metatarsal V, No. 2022–R–1. A, dorsal view with view of proximal end; B, inner view; × 2/3. Rancho La Brea Pleistocene.

Fig. 130. *Felis atrox* Leidy. Right metatarsal V, No. 2920–R–1. A, B, same views as in fig. 129; × 2/3. Rancho La Brea Pleistocene.

Fig. 131. *Smilodon californicus* Bovard. A, phalanx I, dorsal view; B, phalanx II, dorsal view; D, E, F, phalanx III, lateral, anterior and posterior views; × 2/3.

Felis atrox Leidy. C, phalanx II, dorsal view; × 2/3. Rancho La Brea Pleistocene.

Fig. 132. *Smilodon californicus brevipes*, n. var. Metapodials; × 1. A, B, type specimen, metatarsal III, No. 2070–L–1; A, dorsal and distal views; B, outer and proximal views. C, D, referred specimen, metatarsal II and fused rudimentary metatarsal I and entocuneiform, No. 2069–R–1; C, dorsal and proximal views; D, outer and distal views. E, F, referred specimen, metacarpal II, No. 2071–L–1; E, dorsal view; F, outer view. G, H, referred specimen, metacarpal V, No. 2072–R–1. G, dorsal view; H, inner view. Rancho La Brea Pleistocene.

Fig. 133. *Felis atrox* Leidy. Type specimen, No. 12546, Phila. Acad. Nat. Sci. Coll.; outline of lower cheek-teeth $P\overline{3}$–$M\overline{1}$; × 1. Pleistocene, Natchez, Mississippi.

Fig. 134. *Felis atrox* Leidy. Vertical longitudinal section of skull, No. 2900–16; × 2/5. Ethmoturbinals are not preserved in this specimen. *n*, nasal; *fr*, frontal; *s*, frontal sinus; *pa*, parietal; *so*, supraoccipital; *ten.*, cut edge of tentorium; *bo*, basioccipital; *pet*, petrosal; *bs*, basisphenoid; *ps*, presphenoid; *ty*, tympanic; *pt*, pterygoid; *pl*, palatine; *pmx*, premaxillary; *mxt*, maxilloturbinal; *ms*, mesethmoid; *st*, sella turcica; *cp*, clinoid plate; *pgp*, postglenoid process; *IX*, *X*, *XI*, foramen lacerum posterius; *XII*, condylar foramen. Rancho La Brea Pleistocene.

Fig. 135. *Felis atrox* Leidy. Endocranial cast from skull 2900–16. A, dorsal view; B, ventral view; C, lateral view; D, posterior view; × 2/3. For explanation of letters see fig. 11. Rancho La Brea Pleistocene.

Fig. 136. Comparison of skulls of Recent lion (1 and 3) and tiger (2 and 4). (After Boule.)

Fig. 137 Comparison of skulls and jaws of Recent lion (5 and 7) and tiger (6 and 8). (After Boule.)

Fig. 138 Comparison of humerus of Recent lion (9) and tiger (10). (After Boule.)

Fig. 139. *Felis atrox* Leidy. Lateral views of skulls; × 1/3. A, No. 2900–9; B, No. 2900–8; C, No. 2900–4. Compare dorsal profiles of these skulls with those of living tiger (see fig. 140, A, B). Rancho La Brea Pleistocene.

Fig. 140. Skulls of modern tiger and lioness; lateral views; × 1/3. A, skull of tiger (*Panthera tigris tigris)* from Central Provinces, showing typical shape in the Indian race; B, skull of Sumatran tiger *(Panthera tigris sumatrae)* from Sungei Kumbang, showing likeness to the lion's skull; C, skull of lioness from Mulema, Uganda, for comparison with A, B. After Pocock.

Fig. 141. Outline of nasals and portions of fronto-maxillary suture in skulls of Javan and Sumatran tigers. After Pocock. A, *Panthera tigris sondaica* Fitzinger, from Probolingo. B, *Panthera tigris sumatrae* Pocock, from Delhi; × 3/5.

Fig. 142. *Felis atrox* Leidy. A, B, skull, No. 2900–4, dorsal and anterior views of muzzle. C, D, mandibles, Nos. 2901–5 and 2901–15, lateral views to show variation in profile of ventral border; × 1/4. Rancho La Brea Pleistocene.

FIG. 143. Comparative outlines of skulls of Pleistocene felines. a, *Felis atrox* Leidy; Rancho La Brea, Calif. b, *Felis leo Edwardsi* (Bourguignat); Vence Cavern, Maritime Alps. (After Boule). c, *Felis leo spelaea* (Goldfuss); East side of Ural Mts., Province of Perm, Russia. (After Riabinin.) d, *Felis spelaea* Goldfuss; British Pleistocene. (After Dawkins and Sanford). × 1/3.

FIG. 144. Skull of modern jaguar *Felis onca*, No. 9703 U.S.N.M.; × 1/2. A, lateral view; B, dorsal view of facial region; C, anterior view; D, lateral view of mandible.

FIG. 145. Comparative views of basicranial region of skulls. A, *Felis onca*; B, *Felis leo*; C, *Felis atrox*; D, *Felis concolor*; × 2/3. *f.o.*, foramen ovale; *s.f.*, stylomastoid foramen; *f.l.p.*, foramen lacerum posterius; *c.f.*, condylar foramen; *v.n.c.*, canal for Vidian nerve; *n.*, median notch in posterior palatine border of palate; *en.p.*, entotympanic process; *ec.p.*, ectotympanic process; *pg.p.*, postglenoid process; *m.p.*, mastoid process; *p.p.*, paroccipital process; *t.hy.*, tympanohyal pit.

FIG. 146. Comparative views of humeri. A, A′, *Felis onca*, lateral and anterior views; B, B′, *Felis bituminosa*, n. sp., No. X8809 L.A. Mus Coll.; lateral and anterior views; × 1/2.

FIG. 147. Comparative views of femora. A, A′, *Felis*, possibly *daggetti* Merriam, No. X8848; B, B′, *Felis bituminosa*, n. sp., No. X8846; anterior and posterior views; × 1/2. Rancho La Brea Pleistocene.

FIG. 148. Study of the head of the puma (*Felis bituminosa*, n. sp.). Lateral view, greatly reduced. Restoration by Charles R. Knight under direction of J. C. Merriam.

FIG. 149. Comparative ventral views of skulls. A, *Lynx rufa;* B, *Lynx canadensis*; × 2/3. Note particularly differences in position of postpalatine foramina, size of postorbital processes of frontals, and shape of presphenoid.

FIG. 150. Study of the head of the wildcat (*Lynx rufa fischeri* Merriam). Lateral view, greatly reduced. Restoration by Charles R. Knight under direction of J. C. Merriam.

FIG. 151. Outline map showing Pleistocene occurrences of *Smilodon* and *Felis atrox* in western North America. 1, Rancho La Brea and vicinity, Los Angeles County; 2, McKittrick, Kern County; 3, Livermore Valley, Alameda County; 4, Hawver Cave, Eldorado County; 5, Carson City, Nevada, (occurrence questionable); 6, Astor Pass, Nevada; 7, Rome, Malheur County, Oregon; 8, Potter Creek Cave, Shasta County, Calif.; 9, Washtuckna Lake, Washington.

FIG. 152. *Felis* cf. *atrox* Leidy. Fragment of ramus, No. 647, lateral and dorsal views; × 1. Owyhee Pleistocene, Malheur Co., Oregon. California Institute of Technology Collections.

THE FELIDÆ OF RANCHO LA BREA

BY

JOHN C. MERRIAM and CHESTER STOCK

THE FELIDÆ OF RANCHO LA BREA

INTRODUCTION

Were one to select any single item to illustrate the most striking phase in the long list of exceptional features of our North American Pleistocene life as exhibited by the Rancho La Brea fauna, it would presumably be the representation of the Felidæ. Excepting only the dire wolves, no group in the fauna of Rancho La Brea is represented by such a multitude of specimens, ranging up to more than one thousand individuals of the sabre-tooth cat and an exceptionally large number of individuals of the great lion-like cat, with a limited number of smaller types.

It is certain that no other deposit thus far known in the history of paleontology has furnished such a marvelous abundance of perfectly preserved material. Moreover, there are to be found in this assemblage the highest and most efficient stages in evolution of two great divisions of the cat group; one being shown in the sabre-tooth, the acme of cat specialization on this line, the other represented in the magnificent *Felis atrox*, a veritable giant of the true cat tribe.

Among the smaller cats occurring at Rancho La Brea the puma and the wildcat are definitely recorded. While the frequency of occurrence of these various types undoubtedly reflects the environmental conditions prevailing in the vicinity of Rancho La Brea during the period of accumulation of the asphalt deposits, it likewise suggests the approach which the entire assemblage makes to the living fauna of the region. Thus, while the Rancho La Brea cats include in their number types like those of the present, such as puma and wildcat, the geologic antiquity of the fauna as a whole is emphasized by the preponderance of extinct representatives of the feline group.

In the number and variety of types represented, the Rancho La Brea group of cats exhibits a striking similarity to that described from the British caves. Increased appreciation of the unusual characteristics of the larger Pleistocene members of the cat tribe has come unquestionably with more intimate knowledge of the great living felines. A broad survey of the Quaternary history of the Felidæ emphasizes the wide distribution and importance of this family in the past, and illustrates that principle of change which has brought about restriction of range and extinction in so many groups of mammals.

ACKNOWLEDGMENTS

The following study was initiated at the University of California by John C. Merriam, then Professor of Paleontology and Historical Geology in the University. It was continued as a research project by Mr. Merriam as President of the Carnegie Institution of Washington with collaboration of Chester Stock, Professor of Paleontology at California Institute of Technology, Paleontologist at the Los Angeles Museum, and Research Associate of Carnegie Institution of Washington. Grateful acknowledgment is made to the institutions which have contributed toward furtherance of the research.

During the early stages in the study of the Felidæ from the asphalt, the important collections obtained by the Department of Paleontology, University of California, furnished the basis for first review of these types.

The splendid facilities offered by the Los Angeles Museum in the conduct of the research on the Rancho La Brea fauna and the cordial cooperation of those who have come to serve as guardians of this famous collection are responsible for progress made in forwarding these studies The unflagging interest shown in the pursuit of the investigation by the late director, Dr. Frank S. Daggett, and by the present director, Dr. Wm. Alanson Bryan, has been a source of helpfulness and encouragement. Our indebtedness to these gentlemen is gratefully acknowledged. Sincere thanks are due also to the Museum Board of Governors and to the Board of Supervisors of Los Angeles County for their generous support of research through opportunities afforded by this great collection.

The large number of specimens available from the asphalt deposits made necessary much patience and care on the part of those directly concerned with the preparation, cataloguing and mounting of the materials. The excellent mounted skeletons of the sabre-tooth cat and great true cat were prepared by James W. Lytle, Assistant Vertebrate Paleontologist. Mr. Lytle has likewise rendered much valuable aid in the assembling of specimens for study and display. H. A. Wylde of the Museum staff has also been of material assistance on numerous occasions. The wash drawings and text-figures were prepared with much care and patience by the artist, John L. Ridgway. In arranging the illustrative materials for text and plates the authors have profited likewise by Mr. Ridgway's long experience. Charles R. Knight has created the restorations of the Rancho La Brea cats shown in the text. The photographs, unless otherwise indicated, are the work of H. Wm. Menke. Where necessary, the latter illustrations have been retouched by Mr. Ridgway.

Skull and skeletal material representing the modern lion, tiger, and jaguar, of great value in making comparisons, were kindly loaned by the U. S. National Museum. Permission to study the series of skulls of Recent cats in the collections of the Museum of Vertebrate Zoology, University of California, was kindly granted by Dr. Joseph Grinnell, Director.

REVIEW OF LITERATURE ON PLEISTOCENE AND LATE TERTIARY CATS OF WESTERN NORTH AMERICA

SABRE-TOOTH CATS

The presence of remains of sabre-tooth cats in the asphalt deposits of Rancho La Brea was first mentioned in the literature by William Denton. In the account (1875, vol. 18, pp. 185-186) of a visit to the brea ranch of Major Henry Hancock in the vicinity of Los Angeles, Denton describes the asphalt beds which were then being excavated for their tar content. He relates furthermore how Major Hancock gave him a collection of fossil bones and teeth from the deposits. Among these specimens was a canine or sabre-tooth which Denton recognized and described as belonging to a machærodont cat.

Evidently on a later visit to the West, Denton either saw or heard of the remarkable series of tracks of Pleistocene mammals and birds which were being uncovered in the newly made excavations for the Nevada State Prison, one mile east of Carson City, Nevada. In an early account of these imprints by Gibbes [1] it is suggested that one type, a round track, five inches in diameter, was left by some feline animal, and in a footnote to this statement on page 2 the following remark is made: "In the spring of 1881, when Professor Denton was here he informed me that he found a tooth of the Machærodus (Sabre tooth Tiger), in the asphaltum beds of Los Angeles County. The animal that made these tracks may have been the Machærodus. C. D. G."

Apparently no further published record, with particular regard to the presence of fossil cats in the Rancho La Brea occurrence appeared until the preliminary notice twenty-four years later by J. C. Merriam (1906). This note was based on a small collection of vertebrate remains, including some fragmentary specimens of the sabre-tooth cat, secured at the locality in 1905 by Mr. W. W. Orcutt and Dr. Frank M. Anderson.

Additional materials of the sabre-tooth cat of Rancho La Brea formed the basis of a study by J. F. Bovard (1907, pp. 157-163, pl. 13, figs. 1-4) and the type was described as a new species under the name *Smilodon californicus*. An incomplete endocranial cast of this species was described by R. L. Moodie (1922). In addition, special investigations of the pathological lesions found in the cats of the asphalt have been conducted by Moodie (1926, 1927, 1929, 1930A, 1930B). In the cave deposits of northern California, sabre-tooth cat remains were recorded only from Hawver Cave in Eldorado County (Stock,

---

[1] Gibbes, C. D., *Prehistoric footprints in the sandstone quarry of the Nevada State Prison*, Proc. Calif. Acad. Sci., 8 pp., 4 photos., 3 diag., 1882.

1918, pp. 480-481, figs. 3*a*, 3*b*). Here the known material was extremely scanty.

The tentative record of sabre-tooth cats in the Pleistocene sandstones of the vicinity of Carson City, Nevada, has already been alluded to. Fragmentary materials from terrace accumulations exposed along the shore of San Pablo Bay may indicate the presence of *Smilodon* in the incomplete fauna known from this region.

Thus, for the region of western North America, the recognition of sabre-tooth cats, identified as *Smilodon californicus* or tentatively referred to this genus, is based principally on specimens secured in Pleistocene beds of California. Sabre-tooth cats possessing more primitive characters than those of *S. californicus* and occurring in formations of early Pleistocene or late Pliocene age have been described from California and Idaho. A fragmentary lower jaw provisionally referred to the genus *Machærodus* and designated *M.* (?) *ischyrus* was described by Merriam (1904, pp. 171-174, 1 fig.) from a locality at Asphalto, Kern County, not far from the present site of the village of McKittrick. In a later paper Merriam (1918A, p. 524, footnote) established the genus *Ischyrosmilus* on the basis of this specimen and a more extended discussion of the form appeared in the following year (Merriam, 1919, pp. 543-544). No definite determination was made of the age of the formation whence this specimen came, but the beds were regarded as either of the lower Pleistocene or of the late Pliocene. It has been generally assumed that *Ischyrosmilus ischyrus* Merriam and an associated form *Hyænognathus pachydon* Merriam came from the Tulare formation.

Among the mammals recorded from the Idaho formation of southwestern Idaho is a sabre-tooth cat described by Merriam (1918A, pp. 524-526, fig. 1) as *Ischyrosmilus*(?) *idahoensis.* Associated forms in the fauna include *Neotragocerus lindgreni* and *Equus idahoensis.* The character of the assemblage and the structural features of the sabre-tooth cat are suggestive of a faunal stage earlier than that recorded at Rancho La Brea. In 1918 Merriam (1918B, pp. 544-546, fig. 155), in the report on the Tertiary mammal faunas of the Mohave Desert, described the species *Ischyrosmilus osborni* from the Ricardo lower Pliocene.

TRUE CATS

Among the mammalian remains secured by Lorenzo G. Yates from Quaternary deposits in the Livermore Valley, California, was a skull fragment of a large cat which Leidy (1873B, pp. 228-229, pl. 31, fig. 3) used as type in the description of the species *Felis imperialis.* W. D. Matthew (1902, pp. 321-322) tentatively determined the presence of this species in the Washtuckna Lake Pleistocene fauna of eastern Washington. Mention of this species is made also by Bovard (1907, p. 164). In the same paper Bovard (1907, pp. 163-164, pl. 14, fig. 1) describes and figures an upper milk sectorial tooth from the Pleistocene of Potter Creek Cave, Shasta County, California, which resembles in size the comparable tooth in the African lion. A possible relationship to *Felis imperialis* was suggested. Jaws and teeth from this cavern, representing the puma and wildcat, were likewise identified by this writer (Bovard, 1907, pp. 165-166, pl. 14, figs. 2-5).

Two years later Merriam (1909) described from Rancho La Brea a very large skull of a cat and referred this specimen to a new variety of Leidy's species *Felis atrox*, designating the type as *F. atrox bebbi.* In 1910 W. Freudenberg (1910, pp. 223-230, pls. 27-28) recorded specimens from Pleistocene deposits in the region of Tequixquiac, valley of Mexico, which were referred to several species of cats including *Felis imperialis* and *Felis atrox.*

In the same year Merriam (1910, p. 395) described the type of *Lynx californicus fischeri* from the asphalt deposits. Two years later Merriam (1912, pp. 42-46, figs. 4-10) described a fragment of a mandible and several metapodials representing the puma group in the Rancho La Brea fauna. The specimens were referred to *Felis*, near *hippolestes* Merriam, C. H. It was suggested at that time that further materials might demonstrate the presence of a species distinct from the modern type. Later (Merriam, 1918B) a complete ramus of the mandible of a large puma from the asphalt was selected and described as the type of *Felis daggetti.*

A well-preserved skull of a puma from the Pleistocene deposits of Samwel Cave, Shasta County, California, is mentioned by Bovard (1907, p. 165). Two types of pumas [1] were recorded by Stock (1918, pp. 481-486, figs. 4a, 4b, 5 and 6) in the Hawver Cave fauna of Eldorado County. Among the materials secured during the early stages of the excavations in the asphalt deposits at McKittrick, Kern County, were skull remains of the large true cat, *Felis atrox*, and of a puma evidently distinct from the modern California form.[2] The lists which record the mammals known from the Upper San Pedro Pleistocene of Los Angeles County include the genus *Felis*, but the specific type remains too incompletely known to permit of much information regarding its relationships.

In the Great Basin Province of western North America large cats of the *Felis atrox* type have been described by Merriam (1915, p. 380, fig. 1) from Astor Pass, north of Pyramid Lake, Nevada. A recent review by Elftman [3] of the mammalian fauna of Fossil Lake, Oregon, reveals a fragmentary record of the cat group. One of the forms found here is intermediate in size between the puma and *Felis atrox.* Possibly its relationships are with individuals formerly included in the species *F. imperialis.* A cat smaller than the cougar is also recorded.

---

[1] The species *Felis hawveri* was established principally on the basis of peculiar shape of angle in the type specimen, a ramus of the mandible, No. 10636 Univ. Calif. Coll. Further acquaintance with the puma group has emphasized the fact that the particular structure of the angle seen in this specimen is an abnormal feature. Other than this character there are no notable differences between the type and the modern species *Felis concolor.* No. 10636 is referred therefore to the latter form.

[2] Merriam, J. C., and C. Stock, Science, n.s., vol. 54, pp. 566-567, 1921.

[3] Elftman, H. O., Amer. Mus. Novitates, No. 481, 21 pp., 10 figs. in text.

PLEISTOCENE SABRE-TOOTH CATS OF NORTH AMERICA

Several distinct genera of sabre-tooth cats have been described from the Pleistocene of North America. These include *Trucifelis* Leidy, *Dinobastis* Cope and *Smilodontopsis* Brown. Under the genus *Smilodon* Lund have come to be recorded four species, namely *S. fatalis* (Leidy), *S. floridanus* (Leidy), *S. californicus* Bovard and *S. nebrascensis* Matthew.

The species *Smilodon fatalis* (Leidy) was described from Hardin County, Texas. The type description (Leidy, 1868, pp. 175-176) follows:

FELIS (TRUCIFELIS) FATALIS, N. S.

An upper sectorial molar, contained in a small fragment of the jaw, which also includes the socket for a single fanged tubercular tooth. The specimen is thoroughly saturated with bitumen.

The sectorial tooth indicates a feline animal, approaching in size the lion or Bengal tiger. The form of the tooth is nearly like the corresponding one of the latter animals, but the crown is of less width and proportionately longer. The anterior lobe differs from that in the true cats not only in a greater proportionate development, but in its distinct separation in two sub-lobes, of which the anterior is rather more than half the depth of the succeeding one. The measurements of the tooth, in comparison with those in a similar one of a large skull of the Bengal tiger, are as follows:

	Fossil	Tiger
Breadth of crown	15¾ lines (33.4 mm.)	18 lines (38.2 mm.)
Depth of anterior lobe	7 " (14.8 ")	7¼ " (15.4 ")
Depth at principal cusp	9 " (19.1 ")	9 " (19.1 ")
Depth of posterior lobe	6½ " (13.8 ")	7 " (14.8 ")
Width at antero-internal abutment	7½ " (16 ")	8½ " (18 ")

Associated with this form are recorded the species *Equus complicatus, Mastodon americanus, Megalonyx validus, Canis* and *Emys petrolei.* Evidently the collection was secured at a locality in the vicinity of Sour Lake. The type of *Trucifelis fatalis* was later described again and figured by Leidy (1869, pp. 366-367, pl. 28, figs. 10, 11).

The tooth present in this specimen represents a right P$\underline{4}$. The corresponding tooth in the smallest skull of *Smilodon californicus* from Rancho La Brea is considerably more worn than the type of *Smilodon fatalis.* It is also more robust and the prostyle[1] is less well developed than in the latter. While there is close agreement between the two specimens in width across protocone, length of base of paracone, and length of base of parastyle, the tooth as a whole is distinctly smaller and more slender in *Smilodon fatalis* than in *Smilodon californicus.* It is a noteworthy fact that the fourth upper premolar, observed in skulls of *Smilodon californicus* from Rancho La Brea, is consistently larger than the comparable tooth of the Texan species. As a matter of fact it is questionable whether there are any upper fourth premolars of the sabretooth in the large collections from the California asphalt deposit which approach closely in size or at least in anteroposterior diameter the type of *Smilodon fatalis.* Largely on this basis does it appear reasonable to assume that the types from Texas and California are not specifically identical. Aside from this difference the characters displayed by $P\underline{4}$ in *Smilodon fatalis* offer nothing of value to exclude the species from the generic group to which the Californian species belongs.

---

[1] The style in front of the parastyle.

One may infer from a statement made by Cope (1880, vol. 14, p. 857) that a specimen collected in southwestern Texas and sent to him by G. W. Marnock was regarded as belonging to this species. Cope describes the material as follows: "It consists of that portion of a cranium, which is posterior to the orbits, and represents an animal of the size of the *S. necator*, or of a large tiger. The positions of the foramina and the conjunction of the posttympanic and postglenoid processes are as in the *S. necator.*"

More recently Lull (1921, pp. 160-163, fig. 1) has described the occipital portion of a sabre-tooth cat skull from the Dallas sand pits of Texas and has referred to this specimen as *Smilodon* cf. *fatalis* (Leidy). It is evident from his description that the mastoid process has not fused with the postglenoid process to close the auricular fossa below. In conclusion Lull states:

> "The Dallas specimen differs from *S. californicus* not only in its lesser size, but in its relatively narrower occiput, the proportions of which compare more nearly with those of the tiger. The brain-case, on the other hand, is relatively larger in the Texas specimen, and the sagittal crest thinner; another distinction lies in a sharp thin vertical keel on the basi-occipital in *S. californicus.* Some of these details, as in the more powerful occiput and greater size of the latter, may indeed have been sexual, but the assumption is that the species are distinct. I have, however, no assurance that the Dallas specimen is distinct from *S. fatalis,* with the proportions of which it approximately agrees. The discovery of a carnassial attached to the cranium in the Dallas sand pits alone can give assurance of identity or disagreement. Until then, this specimen must be referred provisionally to Leidy's species, and as it gives additional characters to those furnished by the original type, may be considered the plesiotype thereof."

Through courtesy of Mr. Carl Boyer, director of the Wagner Free Institute of Science, Philadelphia, it has been our privilege to study the type specimen of *Smilodon floridanus.* The fragmentary skull representing the type, No. 4072 Wag. Free Inst. Sci. Coll., came from Ocala, Marion County, Florida, and was described by Leidy (1889, pp. 13-16, pl. 3, fig. 1). The type, Plate 11, evidently resembles *Smilodon californicus* very closely in its structural characters. Obviously belonging to an adult individual, with permanent teeth present and with a number of the principal sutures closed in the skull, *S. floridanus* approaches in size individuals that are below rather than above those of average size from the asphalt deposits.

In discussing the relationships of the Pleistocene sabre-tooth cat of California, Bovard (1907, pp. 160-161) concluded that the skull of *Smilodon californicus* varied chiefly from that of *S. floridanus* in the presence of a shorter muzzle, more posterior position of the posterior nares, and possibly by the ridges on the palate. Aside from these characters Bovard recognized the close resemblance between the two species in structure of skull.

With the large series of skulls now available from Rancho La Brea, it becomes evident that the two species can not be distinguished on the basis of the characters selected by Bovard. Thus, for example, the length of the face (as measured from the anterior end of the premaxillary to a line tangent to the posterior surfaces of the maxillary parapets) relative to the length of the skull (as measured from the anterior end of the premaxillary to the posterior side of the occipital condyles) is not noticeably different in *S. californicus* from that in *S. floridanus.* In skull 2001-113 these measurements have the ratio 130:279, whereas in *S. floridanus* the ratio is 131: 285. Computed in terms of 100, the Rancho La Brea skull gives a value of 47, while the type of *S. floridanus* gives a value of 46. The comparable value in both the largest and smallest skull from the asphalt is 46. Moreover the position of the postnarial notch or the posterior nares in *S. californicus* is like that in the Florida species and the development of the ridges on the palate is similar in the two types.

The principal difference between the forms from Florida and California appears to be expressed in the region of the mastoid process. In *S. californicus* two rather well-defined areas can be discerned on the mastoid, namely an antero-distal and a postero-lateral. The latter forms a roughened surface, depressed somewhat longitudinally and generally clearly defined by an antero-dorsal and a postero-ventral border. The latter border separates this surface from a smoother surface which extends inward and backward to form the ventral side of the otic bulla. The oblique forward trend of the mastoid process in *S. californicus* is clearly seen in side view.

In *S. floridanus* the mastoid process, when viewed from the side, appears to turn more noticeably downward and to project less directly forward than in the species from Rancho La Brea. There are specimens available from the asphalt in which, however, the direction of the process approximates somewhat that in the Florida skull. In addition to the possible difference expressed in attitude of the process, the postero-lateral rugose area is much narrower in the skull of *S. floridanus,* while the major portion of the posterior surface is quite smooth. This difference is presumably not due to age for it is to be noted when comparisons are made with skulls of both adult and young individuals from Rancho La Brea.

The occiput has essentially the characters seen in skulls of *S. californicus.* The depression on each side of the median crest extends farther down toward the foramen magnum than is usually the case in the latter type. The jugal is relatively deep and in its diameter below the orbit is more nearly like that in considerably larger skulls of *S. californicus.*

A fourth species from the Pleistocene of North America to be assigned to the genus *Smilodon* is *S. nebrascensis.* This type was described by Matthew (1918, pp. 228-229) and consists of a lower jaw from the Hay Springs Quarry, Sheridan County, Nebraska. The type was not figured. Dr. Matthew describes the specimen as follows:

> "The postcanine diastema is decidedly shorter than *S. californicus* jaws with which I have compared it, the cheek-teeth about the same size, canine and incisors more robust. The specimen is not comparable with *S. floridanus* (type a skull with alveoli of upper teeth) although it accords in size. It is incommensurable save as to size with *S. fatalis* of Texas. *Dinobastis* and *Smilodontopsis* appear to be more specialized types of dentition, the cheek teeth more compressed and extended. *Machærodus ?, merceri* and *gracilis* and all other species of *Machærodus* are separated by the presence of $\overline{P3}$, deeper flange, etc."

He remarks furthermore:

> "I cite this as a new species but much doubt whether it is more than a geographic variant of the *californicus-floridanus-fatalis* group. Its interest is in its occurrence in the typical Hay Springs Pleistocene, correlated with the Aftonian of Iowa, and representing the Lower Pleistocene fauna of the Plains."

The genus *Dinobastis* was based by Cope (1893, pp. 896-897) on several teeth and skeletal elements found in western Oklahoma. With these specimens occurred the remains of an elephant *(Elephas columbi).* In the following year Cope (1894, pp. 454-456, pl. 21, figs. 1-13) described the cat material again and figured the specimens. While recognizing the similarity between *Dinobastis* and *Smilodon,* Cope noted that in the former the superior carnassial lacked the inner root. Among the specific characters by which *Dinobastis serus* differs from known sabre-tooth cats, those based on the dentition were stated by Cope to be as follows:

> "The canine teeth are large, with elongate compressed crowns, a little more convex on the external than the internal face. The cutting edges are finely serrate. The anterior edge differs from that of the *Smilodon neogæus* in that it turns inward toward the base of the crown, presenting inward. In the *S. neogæus* this edge is not incurved. The superior sectorial has a large anterior basal lobe and a rudiment of a second at its anterior base. It does not attain the importance of a lobe, as it does in the *S. fatalis.* The part of the crown anterior to the paracone forms about one-fourth of the longitudinal extent of the crown; in the *S. fatalis,* it forms about one-third. The paracone is prominent, and is strongly convex on the external face. The metacone has a nearly straight edge, and its external face displays a shallow vertical groove near the middle. The long diameter of its base is 1.5 as great as that of the paracone. The crowns of the

external incisors are oblique, and slightly incurved; they have robust cutting edges, which are finely serrate, and no basal lobes. The incisors 1 and 2 have small conic lobes at the base of the crown, which are well separated from each other at their bases. Those of I. 1 are subequal, while the external of I. 2 is smaller than the internal, and nearer the base of the crown. The crowns proper of 1 and 2 are acutely conic with semicircular section, the posterior face being flat. The edges of I. 2 are feebly crenate; those of I. 1 are smooth."

The principal character distinguishing this form is the absence of the inner root in $P\underline{4}$. Normally this root supports the protocone. In *Smilodon californicus* the inner cusp is considerably reduced or absent, but the fang is always present. Although no specific mention is made of $P\overline{3}$, a tooth figured by Cope (1894, pl. 21, figs. 6, 6a) may belong in this position. The specimen is single-rooted with principal cusp relatively high and without anterior and posterior basal cuspules.

While Cope speaks of the canine teeth of *D. serus* as being of large size, the illustrations clearly show that the upper canine tooth possessed a crown distinctly shorter than that in *Smilodon californicus.* While the individual represented is not fully adult, the canine is quite evidently not of the milk dentition. Judging from Cope's description and illustrations (Cope, E.D., 1894, pl. 21, figs. 4a, 4b) the anterior serrate border of this tooth swings inward more noticeably in its upward course than does the comparable border in the Californian form. In the first and second incisors the posterior basal cusps are situated farther apart than in the comparable teeth of *S. californicus.*

An upper canine tooth of small size, found in a cave near the village of Bulverde in the northern part of Bexar County, Texas, and figured by Hay (1920, pp. 107-108, pl. 28, fig. 4) was referred to this species. Skeletal remains from the Texas locality were later described by Hay (1921, pp. 142-143, pl. 5, figs. 1 and 2) and provisionally assigned to *Dinobastis serus.* The upper canine tooth figured by Hay is evidently not a milk tooth. The crown is apparently distinctly shorter than in *S. californicus* and the serrations, particularly those of the anterior border, are well defined.

The smilodont cats described by Brown (1908, pp. 188-191, pl. 19) from the Pleistocene deposit of Conard Fissure, Arkansas, as of the genus *Smilodontopsis* include the two species *S. troglodytes* and *S. conardi.* On the basis of the available material, this genus is regarded as differing from the South American *Smilodon* in the presence of an entepicondylar foramen in the humerus. In this particular character *Smilodontopsis* is like *Smilodon californicus.*

Passing for a moment the status of Brown's genus in the light of present studies, let us consider the characters of the two species of smilodonts recorded from the Conard cavern. Among the materials described under the species *S. troglodytes,* the upper carnassial is regarded particularly as furnishing characters distinguishing this type from other sabre-tooth cats of the North American Pleistocene· P$\underline{4}$ is stated by Brown to possess a well-developed metacone which is relatively greater than in *Trucifelis fatalis.* The external face of the paracone is flatter than in *Dinobastis serus,* and the inner face is nearly straight without sign of tubercle (protocone). The parastyle is large and high and the prostyle (preanterior cone) is a well-developed tubercle which is not so large as in *Trucifelis fatalis,* although the tooth is much longer anteroposteriorly. *Smilodontopsis troglodytes* differs from *S. conardi* in the presence of a shallower median depression developed on the external face of the metacone. The paracone is likewise relatively better developed in the former species than in the latter. Evidently the second species, *S. conardi,* differs principally from the first in greater depth of the median depression on the external surface of the metacone in P$\underline{4}$ and in the relatively small size of the prostyle in the tooth. Viewing the large series available from Rancho La Brea and the variability of the fourth premolar with regard to the two characters indicated above, it would appear entirely possible that individual rather than specific differences are in reality expressed by these two types. As has been stated by Brown, several skeletal elements referred to *S. conardi* may pertain equally well to *S. troglodytes.* We therefore propose to recognize but one type of sabre-tooth cat from the Conard Fissure, namely *Smilodontopsis troglodytes* Brown.

An interesting character noted in the description of the material from Conard Fissure is the presence of P$\overline{3}$. This tooth is usually absent in *Smilodon californicus,* occurring in approximately six per cent of the specimens found at Rancho La Brea. The occurrence of the tooth in so few individuals of *S. californicus* and the record of P$\overline{3}$ in jaws from the Conard Fissure locality suggest that the tooth was more frequently developed in the Arkansas form than in the type from California. Moreover, its presence may have been typical in *Smilodontopsis.* While single-rooted, the crown of P$\overline{3}$ shows as a rule less reduction than in the comparable tooth when present in *S. californicus.* According to Brown: "P$\overline{3}$ is single-rooted and oval in outline, with the internal face flattened; the middle cone is oblique and strongly inclined backwards and inwards; the apex of cone above the base of crown, inside measurement, is equal to the transverse measurement of the tooth at this point; there is a distinct anterior basal cone about half the size of the posterior basal cone. Two other separate teeth, P$\overline{3}$, show the same characters." In P$\overline{3}$ of *S. californicus* the crown is certainly not of this type, and the principal cusp as well as the accessory cuspules are considerably reduced. In these characters *Smilodontopsis* appears to be distinctly more primitive than the species from Rancho La Brea.

Several elements of the feet of *S. conardi* are available for comparison. These represent specimens 11786, 11787 and 11792 of the American Museum Collections. The scapho-lunar, Nos. 11786, 11787, is of relatively small size but resembles more closely in structure the comparable element in the sabre-tooth than that in the true cats. In anterior or dorsal aspect the surface between the articulating faces for the radius and trapezoid is narrow in proximodistal direction relatively perhaps more so than in *Smilodon californicus.* The palmar border of the surface for the magnum does not show the characteristic notching seen in specimens from the asphalt.

Metapodials representing front and hind feet are somewhat longer than the comparable elements of minimum size from the asphalt. These specimens range between metapodials of minimum and average size from Rancho La Brea, and are considerably larger than specimens referred to *Smilodon californicus brevipes.* Compare the measurements of *Smilodontopsis conardi* given below with those of the species from California.

Measurements (in millimeters) of metapodials of Smilodontopsis conardi Brown, No. 11792 Amer. Mus.

	Metac. II	Metac. V	Metat. II	Metat. IV	Metat. V
Greatest length	79.1	67	79.2	91	76.6
Greatest transverse diameter of proximal end	20.5	22.3	17.4	15.5	....
Greatest dorsoventral diameter of proximal end	27.2	23.3	....	26.1	20.2
Transverse diameter at middle of shaft	15.8	13.3	13.3	14	10
Dorsoventral diameter at middle of shaft	15.3	12.8	12.4	14.7	12.3
Greatest transverse diameter at distal end of shaft	23.6	20.1	20.8	20.2	17.6

Structurally these metapodials bear considerable resemblance to the comparable elements in *Smilodon californicus.*

All the characters, with one exception, which Brown (1908, p. 188) regarded as generically distinctive of *Smilodontopsis* are found to apply equally well to *Smilodon californicus.* The single exception, namely the presence and character of $\mathrm{P}\bar{3}$, has already been commented upon. As noted above, this tooth may have been more commonly represented in *Smilodontopsis* than in the Californian form. The close similarity between the types from the asphalt and Conard Fissure may warrant an assignment of the species from Rancho La Brea to the genus *Smilodontopsis.*

Unless characters can be ascertained which distinguish Brown's genus from the Pleistocene sabre-tooth of California, the validity of the former type and a further use of its generic name hinge upon definite allocation of the

Rancho La Brea species. If the latter can be assigned unequivocally to the genus *Smilodon* Lund, then there is evidently no reason for entertaining the view that the species should be included in *Smilodontopsis.* Should it be determined, however, that *Smilodon californicus* is generically distinct from the South American types, the name *Smilodontopsis* may be applicable to this form unless a sufficient number of characters is known to separate the two or some other name has priority. The characters exhibited by *Trucifelis fatalis* resemble closely those seen in *S. californicus,* and the two forms have come to be regarded as belonging to the same genus. Thus the name *Trucifelis* has precedence over *Smilodontopsis.*

On the other hand, *Smilodontopsis* may resemble the sabre-tooth cats described by Cope from the Pleistocene deposits of Port Kennedy cavern, Pennsylvania, in characters in which it differs from *Smilodon californicus.* Definite assignment of Cope's species *Machærodus (Smilodon) gracilis* and *M. (S.) mercerii* to *Smilodontopsis* has been made already by Brown. While serious question may be raised as to the validity of specific separation of the two types recorded from Port Kennedy Cave, the characters displayed by both forms certainly indicate the presence of a sabre-tooth cat distinct from that recorded at Rancho La Brea.

The species from the Pennsylvania locality were described and illustrated in the published, uncorrected manuscript of Cope (1899, pp. 239-247, pl. 20). Through courtesy of Mr. Childs Frick the authors have had available also for comparison an excellent cast of the type of *S. gracilis.* This form is characterized by teeth distinctly more slender than those of *Smilodon californicus.* The principal characters, however, on which a subgeneric or a generic separation can be made from the sabre-tooth cat of the California Pleistocene, are (1) presence of $P^{\overline{3}}$, and (2) greater inferior development of the forward flange of the mandible. To these may be added the noticeably smaller size of the lower canine. This tooth is only slightly more massive than the lateral incisor, whereas in *Smilodon californicus* the lower canine is distinctly larger. These characters are exhibited not only by *S. gracilis,* but also by *S. mercerii.*

Unfortunately the anterior portion of the lower jaw is not preserved in *Smilodontopsis conardi* and we are therefore unable to record the character of the mandibular flange. As indicated above, $P^{\overline{3}}$ is present in *Smilodontopsis.* Brown states that in *S. conardi* the lower canine is small and probably slightly larger than the incisors. He notes furthermore that the species from the Port Kennedy Cave are smaller than the types described from the Conard Fissure.

In character of dentition, presence of $P^{\overline{3}}$, and development of mandibular flange the types from Arkansas and Pennsylvania appear to be more primitive than *S. californicus.* Possibly these characters are indicative of difference in time of accumulation of the eastern cave deposits and the asphalt beds of California. It appears not improbable that one of the last and most specialized members of the sabre-tooth cat group in North America, represented by *Smilodon californicus*, may have evolved during the Pleistocene from a type possessing the characters of the species found at Port Kennedy Cave.

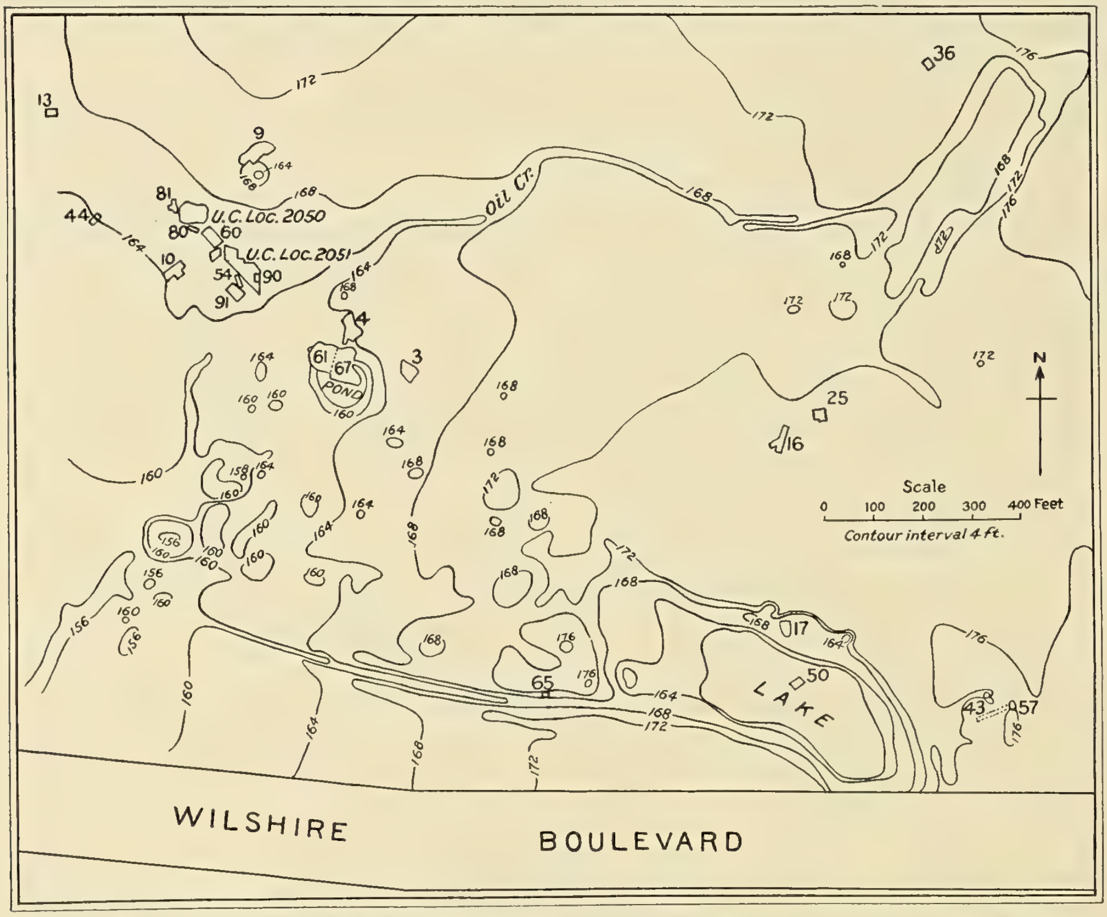

Fig. 1—Topographic map of Rancho La Brea showing location of principal excavations of the Los Angeles Museum and University of California.

In summary, the sabre-tooth cats of the North American Pleistocene may be grouped as follows:

Genus Smilodon Lund

This group is recognized in the broad sense in which it has been recently considered by Matthew (1929). It includes the South American type and allied forms as well as the North American species. Matthew recognizes the genus as occurring also in the Pleistocene of the Old World.

Subgenus Trucifelis Leidy

Under this division are included the sabre-tooth cats *Smilodon fatalis*, *S. floridanus*, *S. californicus* and *S. nebrascensis*. Collectively, these forms appear to be, in at least one character, less specialized than *Dinobastis,* and in several characters more advanced than *Smilodontopsis.*

Subgenus Dinobastis Cope

Type of *Dinobastis serus* from western Oklahoma; referred material from northern Texas.

Subgenus Smilodontopsis Brown

Represented by *Smilodontopsis troglodytes* from the Conard Fissure, Arkansas, and possibly by *S. gracilis* (Cope) from the Port Kennedy Cavern, Pennsylvania.[1]

The Californian type *Ischyrosmilus ischyrus,* from the late Pliocene or early Pleistocene, is certainly generically distinct from the sabre-tooth cats recorded by Cope from Port Kennedy Cave, and should not be included in the *Smilodontopsis* group as advocated by Brown.

OCCURRENCE OF FELIDÆ AT RANCHO LA BREA

The following felid forms are now recognized in the Pleistocene fauna of Rancho La Brea:

Smilodon californicus Bovard.
Smilodon californicus brevipes, n. var.
Felis (Panthera) atrox Leidy.
Felis daggetti Merriam.
Felis bituminosa, n. sp.
Felis concolor Linnæus.
Lynx rufa fischeri Merriam.

Among the larger mammals occurring at Rancho La Brea, the cats rank next to the canid tribe in number of individuals recorded in the asphalt deposits. A recent attempt to make a census of the mammals found at this locality (Stock, 1929) reveals an inordinately large group of these carnivores in the fauna. Doubtless the factors which in large measure influenced or controlled the representation of certain members of the Canidæ were equally responsible for the remarkable frequency of occurrence of such types as the sabre-tooth cats.

In number of individuals present, *Smilodon* bears a relationship to other types of cats similar to that which *Ænocyon* exhibits within the canid family. Unquestionably the dominant feline in the fauna, the sabre-tooth cat overshadows in numbers the great lion-like form and the cats of lesser size. Clearly apparent is also the fact that the puma and wildcat were not nearly so abundant as the species *Felis atrox.*

Of some interest is the distribution of the various types of cats in the individual pits excavated by the Los Angeles Museum.[2] Considering only those pits from which the Museum secured large collections of osseous remains, namely Pits 3, 4, 13, 60, 61, 67 and 77, a record of the number of individuals encountered in each excavation, although not based on complete counts, may still afford valuable means for determining the relative abundance of individual forms during the periods of accumulation. A number of skeletal elements were selected and counts were made with special reference to the occurrence of these bones in the individual excavations. While the average number of individuals (645) from the seven pits is probably distinctly less than the total number of sabre-tooth cats on record, the numerical results are perhaps sufficiently large to warrant the conclusions which may be drawn from them.[1]

---

[1] O. P. Hay (Proc. U. S. Nat. Mus., vol. 58, p. 107, pl. 4, figs. 21, 22, 1920) has described the species *Smilodontopsis mooreheadi* from the Pleistocene of Maryland.

[2] For additional information regarding the occurrence of mammals at Rancho La Brea, see C. Stock, *Cenozoic Gravigrade Edentates of Western North America,* etc., Carnegie Inst. Wash. Pub. No. 331, pp. 30-33, 1925.

The following table gives the results for *Smilodon*.

TABLE 1—*Distribution of Smilodon in Pits 3, 4, 13, 60, 61, 67 and 77*

Pit No.	Rt. Metac. II	Rt. Metac. IV	Rt. Metac. V	Lt. Metac. II	Lt. Metac. III	Lt. Metac. IV	Lt. Metac. V	Rt. Metat. IV	Rt. Metat. V	Lt. Metat. III	Lt. Metat. IV	Lt. Metat. V	Totals	Average No. Individuals	Percentage
3....	261	270	257	247	216	252	246	250	240	276	256	214	2985	248.7	38.6
4....	85	66	68	74	61	82	78	74	79	55	66	65	853	71	11
13....	36	41	36	31	42	35	30	40	30	40	37	33	431	35.9	5.5
60....	7	1	4	7	5	4	7	7	6	4	7	4	63	5.2	.81
61....	71	69	60	64	56	68	57	74	50	88	67	62	787	65.5	10.2
67....	92	79	93	102	105	94	87	92	110	92	127	80	1153	96	14.8
77....	125	125	131	140	142	117	134	104	103	124	120	105	1470	122.5	18.9
Totals	677	651	649	665	627	652	639	641	618	679	680	563	7741	645	99.81

Arranged in the order of decreasing abundance of individuals the information regarding the occurrence of *Smilodon* may be summarized as follows:

Pit No.	3	77	67	4	61	13	60
Percentage	38.6	18.9	14.8	11	10.2	5.5	.81

Considering the seven excavations which are listed, it is seen that the largest number of sabre-tooth cats are recorded from Pit 3, while the counts which were made of specimens excavated in Pits 77, 67, 4 and 61 reveal likewise a relatively large number of individuals. Distinctly fewer individuals are on record from Pit 13, and particularly from Pit 60. Apparently the size of the individual pit does not govern entirely the relative abundance of individuals occurring in the asphalt mass. As indicated previously (Stock, 1925, footnote *a*, p. 32), the excavations conducted in Pits 61 and 67, while initiated separately at the surface, soon developed into a single project, suggesting rather strongly that the pools responsible for these deposits were either connected or closely associated during their history. Yet from this combined source, with a mass probably in excess of that presented in Pit 3, has come a record of sabre-tooth cats somewhat less than that from the latter excavation.

---

[1] More complete counts will doubtless bring to light many interesting facts concerning the distribution of representatives of the Rancho La Brea fauna in the various excavations at this locality.

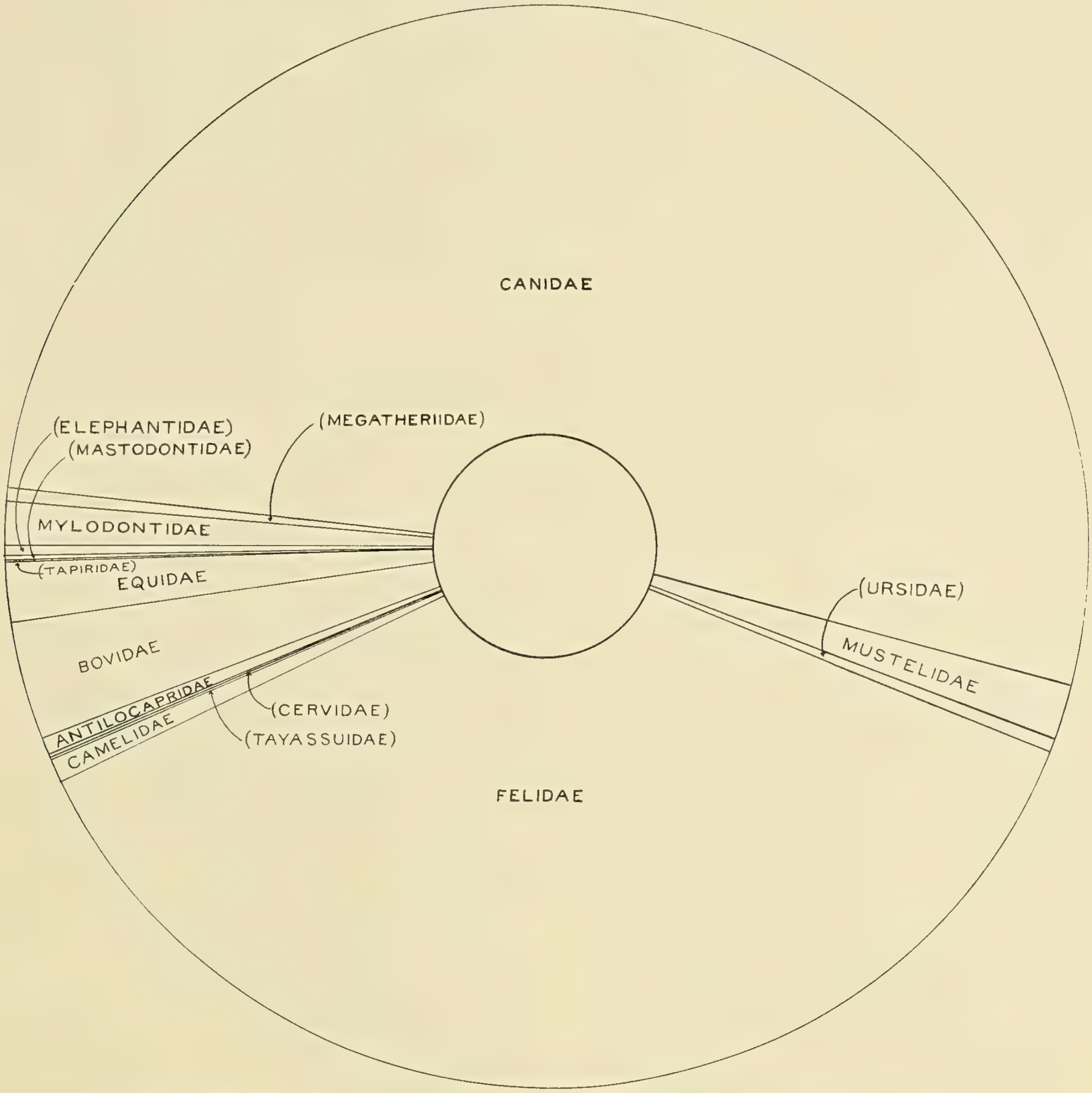

FIG. 2—Diagram showing relative number of individuals in the mammalian families (except rodents, lagomorphs, insectivores and bats) occurring in the Rancho La Brea Pleistocene fauna. Representation of the Felidæ is exceeded only by that of the Canidæ.

Strikingly apparent is the decidedly sparse representation of *Felis atrox* at Rancho La Brea in contrast to that of *Smilodon*. An attempt to determine the distribution of individuals of this species in the more productive pits must await the gathering of more complete data. While the results given in table 2 are based on limited evidence, they are offered as a tentative basis for comparison with those secured from a survey of the distribution of *Smilodon.*

TABLE 2—*Distribution of Felis atrox in Pits 3, 4, 13, 60, 61, 67 and 77*

Pit No.	Rt. Astragalus	Rt. Calcaneum	Lt. Metat. V	Lt. Metat. IV	Lt. Metat. III	Lt. Metat. II	Rt. Metac. V	Rt. Metac. IV	Rt. Metac. II	Rt. Metac. III	Totals	Average No. Individuals	Percentage
3.....	10	6	12	12	9	9	10	6	11	9	94	9.4	32.3
4.....	1	2	3	4	5	4	4	6	3	1	33	3.3	11.4
13.....	2	1	1	2	4	3	3	2	3	....	21	2.1	7.2
60.....	....	....	2	2	1	2	....	1	....	1	9	.9	3.1
61.....	3	4	6	4	5	5	7	7	4	6	51	5.1	17.5
67.....	8	4	5	6	6	7	6	6	7	7	62	6.2	21.3
77.....	....	1	4	2	1	1	4	2	2	4	21	2.1	7.2
Totals	24	18	33	32	31	31	34	30	30	28	291	29.1	100.0

In the order of decreasing importance the percentages of individuals in the seven pits arrange themselves as follows:

Pit No.	3	67	61	4	77	13	60
Percentage	32.3	21.3	17.5	11.4	7.2	7.2	3.1

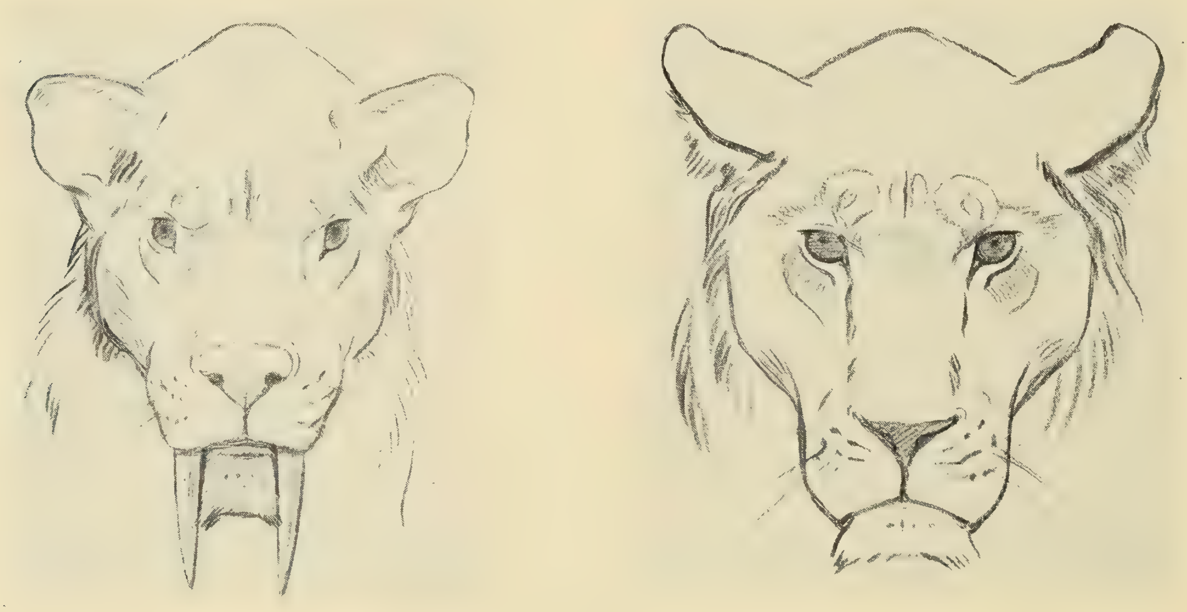
A B

FIG. 3—Comparative study of head in (A) sabre-tooth cat (*Smilodon californicus* Bovard) and (B) great true cat (*Felis atrox* Leidy). Anterior views, greatly reduced and not to same scale. Restorations by Charles R. Knight under direction of J. C. Merriam.

Perhaps all that may be claimed from this survey of the distribution of *Felis atrox* is the recognition of the latter type as a member of the typical Rancho La Brea mammalian fauna. It is interesting to note that when the percentages are combined for excavations 67 and 61 the total is greater than that recorded from 3. In this feature the result differs from that obtained from a representation of the sabre-tooth cats. Though definitely a contemporary of *Smilodon*, the sparse representation of the great cat can only be interpreted as indicating that this feline did not haunt the borders of the tar pools as persistently as the sabre-tooth.

The material record of the smaller cats, like the puma and wildcat, fails to show an abundance of individuals comparable to that of *Felis atrox*. Remains of the mountain lion appear to have been recorded in all of the more important excavations, while those of the wildcat may have been similarly distributed, though perhaps more commonly represented in the deposits of Pits 4 and 16.

HABIT AND HABITAT OF SMILODON AND OF FELIS ATROX AS SUGGESTED BY OCCURRENCE AT RANCHO LA BREA

The striking difference in representation of the two dominant feline types in the Rancho La Brea fauna can only be accounted for by assuming ecologic conditions at this particular locality more favorable to one group than to the other. A conservative estimate would seem to indicate that in the assemblage the sabre-tooth cats outnumber the true cats of the *Felis atrox* type approximately 30 to 1. Doubtless the numerical relationship does not express the actual representation of the sabre-tooth cat and true feline during this stage of Pleistocene time in the Californian area, but results largely from the conditions, physical and biotic, which prevailed at the specific locality of Rancho La Brea. It appears quite possible that in the region away from the pools, the lion-like form was more nearly a dominant type than the sabre-tooth cat. As a matter of fact, in Pleistocene faunas recorded from western North America, felines of the true cat tribe are of more common occurrence than those of the smilodont type.

Pleistocene occurrences of sabre-tooth cats are frequently identified with cave or fissure accumulations, although representatives of the group are not restricted to fossil assemblages found in such deposits. While remains of sabre-tooth cats have been found in cave deposits of California, Texas, Arkansas, Pennsylvania and Florida, such materials have been encountered at other localities in wholly different types of sediments. The susceptibility of this animal to the attractions offered by brea accumulations appears to be emphasized by the occurrences in California and Texas. On the other hand, *Felis atrox* may be regarded as a species occurring normally in faunas of the plains, although its range may have extended well beyond this environment, in some instances reaching into forested and more rugged upland areas.

The unusually large number of individuals of *Smilodon* found in the asphalt, and representing doubtless both sexes as well as animals ranging in

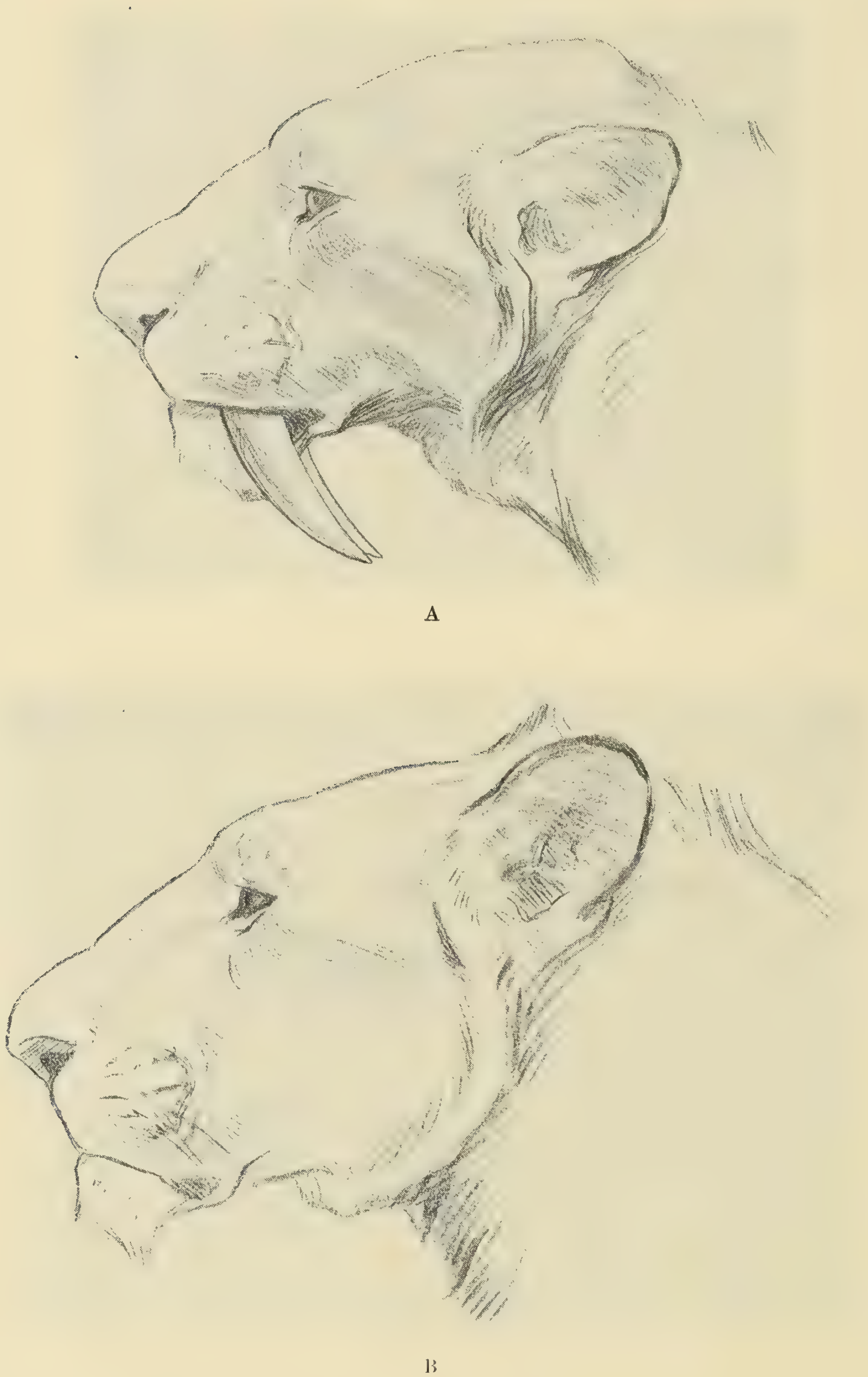

Fig. 4—Comparative study of head in (A) sabre-tooth cat (*Smilodon californicus* Bovard) and (B) great true cat (*Felis atrox* Leidy). Lateral views, greatly reduced and not to same scale. Restorations by Charles R. Knight under direction of J. C. Merriam.

age from youth to maturity and old age, indicates quite certainly a persistent representation of this predator about the borders of the pools during the active periods of the tar traps. Whether or not *Smilodon* possessed greater or less fecundity than the true felines can not of course be determined. It is conceivable and perhaps not unduly speculative to assume that with a relatively short period of maximum efficiency in the use of the biting mechanism, predicated by a long series of steps which brought about the remarkable specializations seen in this form, an increase in number of offspring would have been found useful as a compensatory feature offsetting in a measure these racial and individual disadvantages.

Aside from this it is true that both old and young fell victims to the tar traps, but with a majority of individuals taken apparently from within or close to the stage of maturity. Accustomed as they were in the Pleistocene to feeding on the thick-skinned, cumbersome, herbivorous mammals, developing an attack, perhaps from ambush, adapted particularly to a slow-moving target, the sabre-tooth cats doubtless found at and in the tar pools an added as well as an easier prey. So exceptional were the inherent characters of these traps, that the occasion of miring and holding animals in the tar frequently possessed a continuity in so far as space and time were concerned. In its simplest form, perhaps, one may visualize the miring of a large mammal, be it herbivore or carnivore, in the sticky mass, and the subsequent struggle which ensued. The lure presented by such a creature in distress would serve to bring to these pools numbers of carnivorous mammals and birds. With prey more or less fixed and relatively near at hand, no special cunning or care was required of the sabre-tooth in the dispatch of its victim. Least of all was *Smilodon* concerned apparently with the dangers which lurked in the physical characteristics of the trap itself. A fierce animal with small brain and powerful body, this cat was presumably intent on reaching and closing with its prey, while in its failure to appreciate the dangers it may have rivaled closely the dire wolf. Doubtless these were the reasons chiefly responsible for its own high mortality. Along the borders of the tar pools the struggles of *Smilodon* were frequently with members of its own tribe and with other carnivores. Its savage nature is also suggested by the many evidences of disease resulting from injury seen in elements of the vertebral column and appendicular skeleton and to a less extent in the skull. It is a fair assumption from evidence available that such troubles were of more common occurrence in the sabre-tooth than in the true cats, although they were not lacking in the latter.

An analysis of the structural characters of *Smilodon* and *Felis atrox* cleary emphasizes the dissimilarities in habits of the two creatures as well as the differences in their ecologic relationships. *Smilodon* approximated in size the

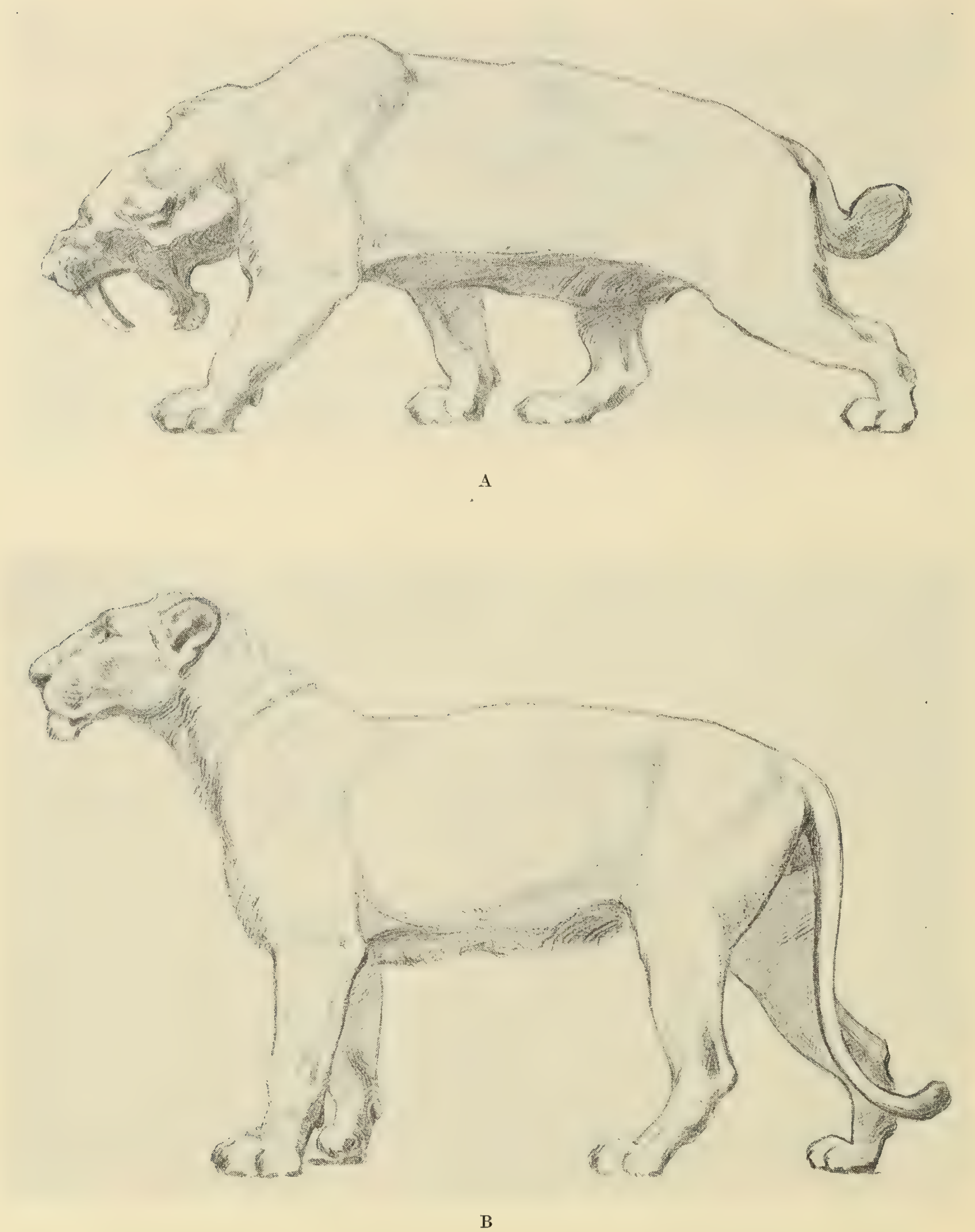

FIG. 5—Comparative study of (A) sabre-tooth cat (*Smilodon californicus* Bovard), approx. × 1/13, and (B) great true cat (*Felis atrox* Leidy), approx. × 1/12. Restorations by Charles R. Knight under direction of J. C. Merriam.

modern lion and tiger, with, however, a body not so high above the ground. With a build particularly sturdy in front, the strong front extremities and the powerful muscles which operated them denote great striking and grasping strength. In the face of this development, the hind quarters appear to be relatively slender, although the major hind limb elements are comparable in size to those in the large living felines, differing from them most strikingly in some of their proportions. In both front and hind limbs the epipodial and metapodial segments have been shortened, distinctly more so than in the true cats. It is evident that the sabre-tooth was not so fleet of foot as the lion or tiger. The shortened tail is also a noticeable difference. With added muscular development in front and with a more rigid series of lumbar vertebræ, a greater strain may have manifested itself in the lumbar region, due to repeated propulsion of the body as the animal leaped on or lunged against its prey. It is a curious fact that in this region vertebral lesions resembling the so-called *spondylitis deformans* are particularly prevalent among the sabre-tooth cats of the Rancho La Brea fauna.

In consummating an attack, the head would be drawn back by the powerful muscles lodged in the neck and attached to the occiput, while the lower jaw moving through a wide arc permitted the sabre-like canine teeth to function as stabbing weapons. The enlarged and strongly developed muscles, representing chiefly the sterno-cleido-mastoid group but assisted by the scalene muscles of the neck, furnished the equally important downward thrust, aided by a backward jerk, which accompanied the stab. With this action doubtless an open jagged wound was made. Unquestionably the serrated borders of the canines assisted in tearing or ripping the flesh and the scissor-like action of the compressed sectorial teeth enlarged the cut. With head buried deeply in the side of the victim, doubtless the backward position of the nasal opening permitted *Smilodon* to breathe during the concluding moments of the attack, while the heavily corrugated gum which presumably covered the hard palate may have been advantageous in blood sucking.

Sabre-teeth, as weapons of offense and defense, have been evolved on occasion in other mammals, but nowhere as in this culminating stage of the smilodont cats do we find their use enhanced by the presence of so many coordinated structures. This remarkable combination of characters obviously permitted a unique dental mechanism to function with superb effectiveness. In the action of the several parts of the dentition as here surmised, the lower jaw seemingly played a less important rôle. Yet the formidable row of lower incisor and canine teeth belies somewhat the relatively slender structure of the mandible in this form. While pronounced grasping strength of the jaws, manifesting itself by ability on the part of the animal to hold and drag heavy bodies, was evidently lacking in the sabre-tooth, the strongly developed incisor teeth and their penetrating power may have rendered service when *Smilodon* shook or worried its prey.

Cast in an entirely different light is the great true cat, *Felis atrox*. Evidently not a persistent participant in the struggles about the tar pools, this creature succumbed much less frequently in the asphalt than did the sabretooth. The material record of the presence of *F. atrox* hardly warrants, however, the assumption that these creatures were only sparsely represented in the region about Rancho La Brea. Doubtless from time to time the lure of the traps attracted these felines to the borders of the pools. Perhaps on occasion entire families were mired.

We are as yet wholly lacking in information concerning the pelage and coloration of *Felis atrox*. Whether or not these forms were spotted cats, only chance and unusual finds of the future may tell. The comparisons of the skull certainly indicate that the extinct cat and the jaguar while closely related are still distinct types, The tree-climbing habits of the jaguar are well known, but this cat is not restricted in its range to the tropical forests at the present time. On the other hand, the formidable size of *Felis atrox* and the elongation of its limbs lead one to regard the presumed habits to be more like those of the Quaternary lions of the Old World.

With average size of individual in the *Felis atrox* group larger than that in *Felis leo*, the extinct cat included types that were fully one-fourth larger than living forms. These creatures were comparable in size to the largest individuals of the extinct cave lion of the Pleistocene of the Old World. Among the carnivores of Rancho La Brea their only rivals in size were the tremarctotheres or short-faced bears. With powerful jaws and teeth, strong body and limb, with a litheness, agility and swift-footedness of the large living felines, *Felis atrox* doubtless preyed upon the larger ungulates of the Rancho La Brea fauna. In the more formidable male individuals of this species the massiveness of the head is a striking character and the biting strength of the jaws was probably tremendous. Such animals with a ferocity like that of the tiger might well have attacked herbivores of considerable size. In each instance, however, the method of attack was quite different from that of the sabretooth cat and doubtless resembled that of the true felines.

An open plain or a rolling country, probably grass-covered and supporting here and there a growth of trees and shrubs, presented in the vicinity of Rancho La Brea during Pleistocene time an environment in which one might reasonably expect to find such carnivores as the great cat. Recognizing the variety and richness of the vertebrate life which prevailed here during that period, it appears entirely reasonable to assume a habitat for this type closely similar to that in which the lion is found today on the African veldt. The similarities in structural characters between the fossil and living lions are perhaps sufficiently close to warrant this assumption.

CLASSIFICATION AND RELATIONSHIPS OF THE FELIDÆ FROM THE ASPHALT

Within the group of Felidæ found at Rancho La Brea two major divisions are represented, namely the sabre-tooth cats and the true cats. While *Smilodon* represents one of the most advanced and specialized stages in the history of the sabre-tooth cat group, the fundamental similarities which exist between this form and the true cats lead one to regard both divisions as belonging to a single family.

While *Smilodon* and the Tertiary genus *Hoplophoneus* represent the most completely known sabre-tooth cats, an adequate understanding of the development of the smilodont lineage in time is dependent upon the acquisition of additional information concerning the structural characters of types occurring in America and elsewhere in geologic horizons lying between the early Miocene and the later Pleistocene.

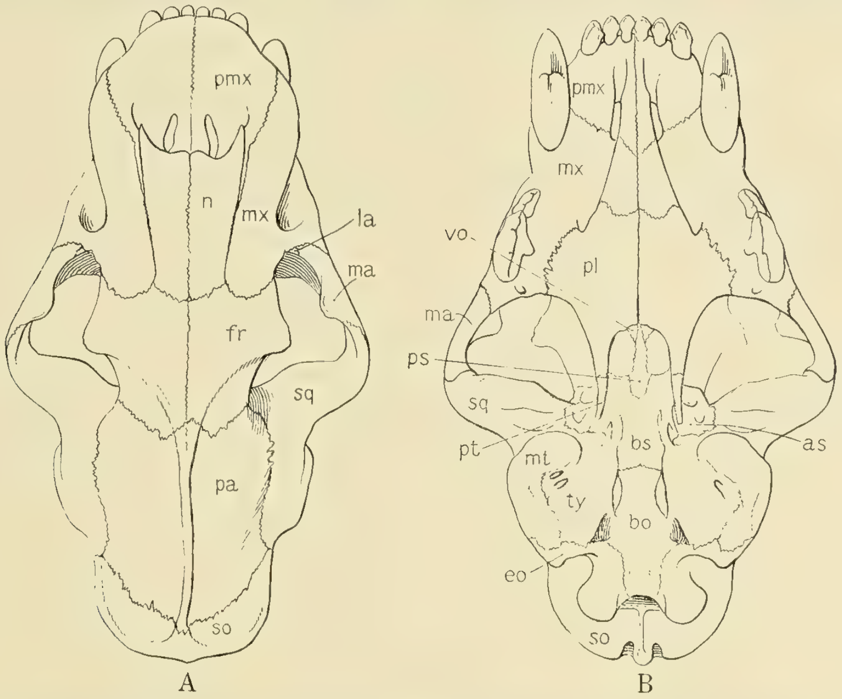

FIG. 6—*Smilodon californicus* Bovard. Skull, A, dorsal view; B, ventral view. Several sutures reproduced from considerably younger skulls than that shown. *pmx*, premaxillary; *n*, nasal; *mx*, maxillary; *la*, lachrymal; *ma*, malar; *fr*, frontal; *sq*, squamosal; *pa*, parietal; *so*, supraoccipital; *pl*, palatine; *pt*, pterygoid; *vo*, vomer; *ps*, presphenoid; *bs*, basisphenoid; *bo*, basioccipital; *as*, alisphenoid; *mt*, mastoid; *ty*, tympanic; *eo*, exoccipital. Rancho La Brea Pleistocene.

Ischyrosmilus of the Californian Pliocene is evidently more nearly related to the smilodont cats than is *Machærodus catocopis.* The important differences which distinguish the latter form from *Smilodon* have been clearly enumerated recently by Burt (1931). In view of the characters exhibited by the genus *Machærodus* and the noteworthy contrasting features that prevail between this type and the sabretooth genera including *Smilodon, Meganthereon, Hoplophoneus,* and *Ischyrosmilus,* it seems hardly fitting to place all these forms in a single subfamily. So distinctive are the differences that if *Machærodus* is retained in the group Machærodontinæ, at least one subfamily must be recognized to include the remaining genera. Kretzoi (1929) has proposed several subfamily names among which are the Hoplophoneinæ and Smilodontinæ. In the former are included the genera *Hoplophoneus*, *Eusmilus*, and *Pareusmilus* while under the latter are grouped *Smilodon* and its near allies as well as *Amphimachairodus* and *Protamphimachairodus*.

The grouping of smilodont forms in the present review would include under the Smilodontinæ at least the genera *Ischyrosmilus*, *Megantheréon*, the characteristic sabre-tooth cat of the asphalt and its near allies of the Pleistocene.

Among the Felinæ all of the forms with the exception of the wildcat have been retained within the generic group *Felis*. It should be emphasized, however, that the larger cats representing *Felis atrox* differ in important features from the pumas and resemble more the large living felines of the Old World, along with the Pleistocene *F. spelæa* and the jaguars of the New World. Pocock has shown that *F. leo*, *F. tigris*, the leopard and the jaguar, form a natural division of closely related forms for which he accepts the name *Panthera*. Following Owen, Pocock calls attention to the difference in structure of the hyoid apparatus between these larger cats and the genotype of *Felis catus* Linnæus.

The relationships of *Felis atrox* to these Quaternary cats of the Old World and to the American jaguar make it reasonable to conclude that if generic or subgeneric status is given to the name *Panthera* this designation should be applied also to the larger felids in the Rancho La Brea fauna. It has not been possible, however, to demonstrate definitely the characters of the hyoid arch in the forms from the asphalt. On the other hand, there seems no urgent need for applying the new generic name, *Neoleon*, to these cats as Kretzoi has done.

SMILODONTINÆ OF RANCHO LA BREA

CHARACTERS OF THE GENUS SMILODON

Skull with mastoid process greatly enlarged and extending forward close to postglenoid process. Posterior root of zygomatic arch greatly extended inferiorly. Antero-ventral flange on lower jaw present but not noticeably dependent. Coronoid process much reduced; condyle large; angle reduced. Dental formula $\frac{3}{3}, \frac{1}{1}, \frac{2}{2\text{-}1}, \frac{1}{1}.$ Incisors robust; upper canine a long, sabre-like tooth, flattened transversely and with serrated front and back edges of crown. P$\underline{3}$ with reduced size relative to upper carnassial; P$\underline{4}$ with prostyle usually present in front of parastyle, protocone reduced or absent. Lower canine incisiform; P$\overline{3}$ absent or vestigial when present; P$\overline{4}$ and M$\overline{1}$ with backward tilt to crowns. Shearing blade of M$\overline{1}$ with anterior and posterior basal cuspules present or absent.

Atlas with backwardly projecting transverse processes. Caudal vertebræ reduced in size and number generally less than 15. Epipodial and metapodial segments of appendicular skeleton shortened with reference to propodial segments. Propodial and epipodial elements of front limbs relatively massive. Astragalar foramen usually present.

SMILODON CALIFORNICUS BOVARD

SKULL

The numerous skull specimens [1] from the Rancho La Brea locality that have been examined illustrate collectively to a remarkable degree all the details of structure. As a rule skulls embedded in the asphalt have suffered no distortion from pressure or disturbance of the strata and are in practically as good condition for study as recently prepared skulls of modern felines. This unusual preservation doubtless indicates that no great rock mass has been present above the asphalt deposits to cause flattening or vertical compression of included specimens.

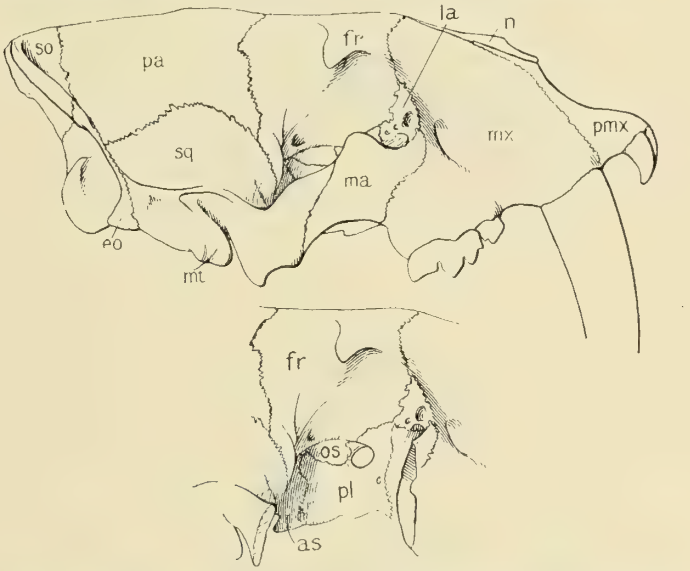

Fig. 7—*Smilodon californicus* Bovard. Lateral view of skull and view of infraorbital region with portion of zygomatic arch removed. *os,* orbitosphenoid; *pmx,* premaxillary; *n,* nasal; *mx,* maxillary; *la,* lachrymal; *ma,* malar; *fr,* frontal; *sq,* squamosal; *pa,* parietal; *so,* supraoccipital; *pl,* palatine; *as,* alisphenoid; *mt,* mastoid; *eo,* exoccipital. Rancho La Brea Pleistocene.

The extent of variation in the skulls is considerable, amounting probably to differences as great as have sometimes been considered specific. The gradation in skull form between variant types is, however, so close that there may be no valid reason to consider them as representing more than sexual or individual characters. Fortunately the collection includes skulls of young, adult and old individuals. The range in size is shown in table 3, in which are given the measurements of a representative series of 25 skulls, principally of adult animals in which the permanent dentition is present.

The skull considered as a whole is a most remarkable illustration of adaptation concentrated on an extreme phase of activity.

The facial region varies considerably in width among the individuals examined, the difference in width of muzzle being possibly due to specific variation or more probably to sexual difference. The form of the muzzle also shows noticeable variation according to the condition of the roots of the superior canines. In those skulls in which the canine teeth were in full function and normal position in the alveoli at the death of the animal, the roots of the superior canines extend practically to the extreme upper end of the nasal process of the maxillary, and the prominent external swollen tracts produced by these roots reach well above the middle of the orbits (see plate 1, figs. 1 and 2). In other specimens (plate 10, figs. 1 and 2) in which the canines have been broken off during life and the roots have been largely resorbed, or the canines have slipped downward in their sockets during life, the swollen tracts on the maxillary are much reduced and the form of the face is considerably modified. Where this has occurred on one side and not on the other a curious asymmetry of muzzle may result. In L. A. Mus. Skull 2001-19 (plate 10) and in Univ. Calif. specimen 10832 both canines were broken off before death and the portions remaining in the jaw are much worn on the broken surfaces. In No. 10832 the left canine shows more wear than the right and may have been broken at an earlier time. Corresponding to the evidence of wear, the upper portion of the original swollen tract on the left side is shrunken and reduced, showing that it was unoccupied for a long period antecedent to the death of the animal, while the alveolus of the right canine is nearly normal.

---

[1] Unless indicated otherwise all specimens bear the catalogue numbers of the Los Angeles Museum.

The nasal process of the maxillary ends with a transverse truncation (fig. 9A) which is almost normal to the long axis of the skull. This truncation is practically even with the line of truncation of the posterior ends of the nasals, and is also coincident with a line connecting the highest and most nearly approaching points on the orbits. No well-defined nasal process of the frontal is present, or there is at most a faint salient angle on the line of contact of maxillary and nasal.

The combined width of the anterior ends of the nasals closely approaches the greatest width of the anterior nasal opening. Posteriorly the nasal elements retain practically the same width as at the anterior extremity and end with an abrupt transverse truncation even with the nasal process of the maxillary and with a line connecting the highest points on the orbits. The anterior ends of the nasals are deeply notched, the portion external to the notch extending farther forward than the median side. The median angles are generally rather sharply bent downward.

The anterior nasal opening (fig. 9B) is less cordate in cross-section than in the true cats. The greatest diameter is reached at about the middle height of the opening, and the lower region is rather broadly rounded, instead of narrowed as in the lion and tiger. The upper margin of the opening is situated relatively far back, so that the plane of the opening faces upward more noticeably than in the lion or tiger.

In profile the superior outline of the skull is gently convex, the sagittal crest generally rising slightly above the frontal region and the nasals sloping gently downward and forward from their contact with the frontals. In face view the general outline of the frontal region is strongly convex across the postorbital processes. The frontal region immediately behind the postorbital processes may be flat or slightly concave. Situated over the anterior end of the frontals, but extending mainly over the nasals, there is usually a strongly marked depression 20 to 30 mm. wide and 40 to 50 mm. long. The postorbital processes of the frontal are very prominent and are usually characterized by the marked convexity of the posterior border.

The fronto-parietal sutures extend upward almost to the base of the sagittal crest on line nearly normal to the superior median line of the skull. At the base of the crest, the sutures suddenly turn backward and then forward so that a tooth of the frontal projects backward on each side of the base of the crest. At the summit of the crest the parietal barely reaches in front a line connecting the straight lateral fronto-parietal sutures.

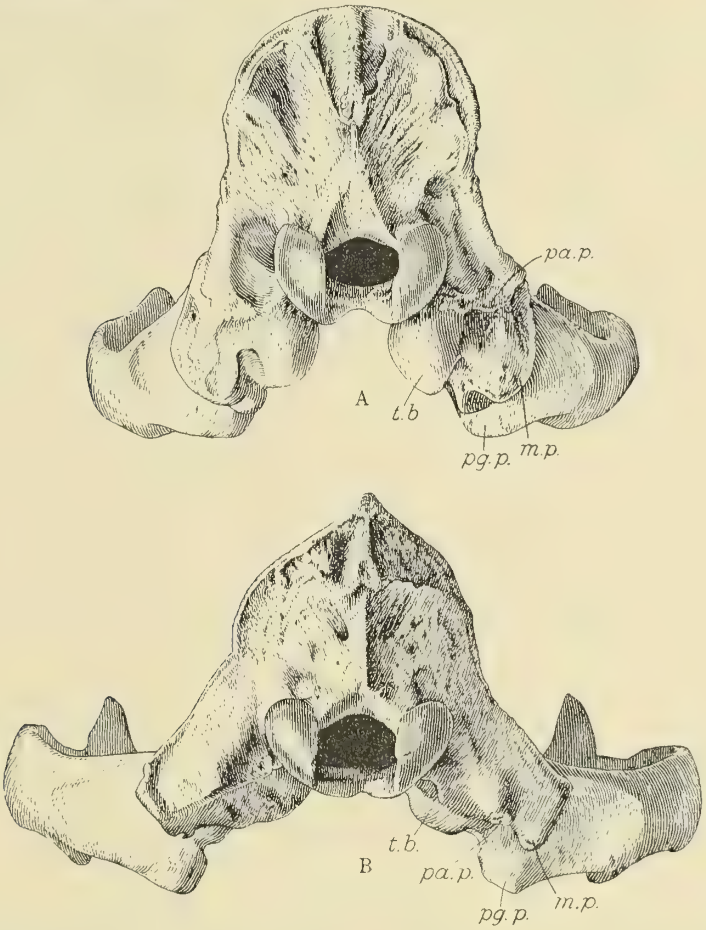

FIG. 8—View of occiput; × 1/3. A, *Smilodon californicus* Bovard, No. 2001-225; B, *Felis atrox* Leidy, No. 2900-9. ***m.p.***, mastoid process; ***pa.p***, paroccipital process; ***pg.p***, postglenoid process; ***t.b.***, tympanic bulla. The posterior processes and tympanic bulla are incomplete on the left side of the skull of *Felis atrox*. Rancho La Brea Pleistocene.

It is a noticeable feature of the frontal region that it is bounded anteriorly and posteriorly by almost straight transverse sutures running normal to the median superior line of the skull across practically the whole width of the frontal region (fig. 6A).

The parietal elements are rectangular in form, as the anterior and posterior sutures are both normal to the median line of the skull, while the squamosal suture follows a nearly even curve with that of the sagittal crest (see fig. 7). The sagittal crest is more strongly developed than in the lion or tiger, and the middle portion is usually elevated slightly above the frontal region.

The lambdoidal crest is very prominent and is continued downward to join the mastoid region with less reduction in height at the lower end than is shown in either the lion or the tiger. The upper or middle portion of the crest is greatly thickened, particularly in old specimens, and attains several times the strength of the corresponding region in the lion.

The occiput as seen in posterior view (fig. 8) is broadly rounded above instead of narrowly triangular as in *Felis atrox*, the broader superior region giving greater area for the attachment of muscles used in elevating the head. The occipital crest extends from the superior border of the foramen magnum to the inion as an extraordinarily high ridge bordered by cavernous lateral depressions. The crest usually maintains nearly the same transverse thickness for the greater part of the height and the summit is broadly rounded. Just below the inion there is a prominent narrow ridge corresponding to an upward continuation of the middle portion of the occipital crest. On either side of this ridge is a very deep, sharply incised pit in which the *rectus capitis posticus major* muscle was probably attached. The lower end of the occipital crest is usually nearly smooth and does not show two distinct lateral tubercles immediately above the foramen magnum for the attachment of the posterior occipito-atlantoid ligament as in Recent felines like the lion and tiger.

The region of the basioccipital varies considerably in different individuals. In a few specimens the portion situated between the otic bullæ is nearly flat anteriorly, and a low median ridge is developed in the region between the posterior ends of the bullæ. In most specimens a strongly developed median ridge extends from a point between the condylar foramina almost to the anterior end of the basioccipital. The rough surfaces, presumably for attachment of the *rectus capitis anticus major* muscle, are situated close to the median borders of the otic bullæ and their posterior ends usually extend a little behind the anterior ends of the posterior lacerate foramina. The posterior portion of the basisphenoid develops a trough-like form in accommodation to the uncommon narrowness of the posterior nasal openings.

The auditory bullæ vary greatly in size in different individuals. In some specimens (Univ. Calif. No. 10839) the bulla appears only as a slight swelling on the inner side of the heavy mastoid process; the swollen tract extends backward only as far as the anterior border of the posterior lacerate foramen and scarcely protrudes below the level of the opening of the stylomastoid foramen. In Univ. Calif. specimen 11256, the bulla is larger than the mastoid process, it extends backward as far as the posterior border of the condylar foramen, and the strongly domed surface protrudes downward almost as far as the lower end of the mastoid process.

In most of the skulls the auditory bullæ are apparently intermediate in form between those of the two skulls mentioned above, but the average of the specimens appears to be much nearer to the smaller form than to the larger. It is doubtful whether in any specimen in the collection the size of the bulla exceeds a stage halfway between the smaller and the larger form. In nearly all specimens it is also noticeable that, as in No. 10839 with the small bulla, the pit for reception of the tympano-hyal is separated by quite a distance from the median side of the stylomastoid foramen; while in the skull with large bulla, No. 11256, the pit is separated from the stylomastoid foramen by a very thin partition.

At the forward end of the ventral surface of the bulla and slightly posterior to and below the foramen lacerum medius and Eustachian canal a round pit is present. This small depression varies considerably in depth, and in some specimens may be replaced by a shallow concavity.

The paroccipital process is commonly present, but is developed only as a very weak prominence and may almost entirely disappear in some specimens.

The greatly enlarged mastoid process is lengthened until in some cases it may extend downward almost as far as the postglenoid process, although in many specimens its inferior extension falls considerably short of that of the postglenoid process. The mastoid process also swings forward so that the inferior end almost comes in contact with the postglenoid process. Only in rare cases are the two processes found to come into actual contact, and in no instance have they been found to fuse distally. In skull 2001–77 the anterior end of the mastoid process presses forward and to the inner side of the postglenoid process, reaching a point in advance of the level of the posterior border of the glenoid fossa. There is still a gap, however, between the antero-external border of the mastoid and the posterior surface of the squamosal process.

The attachments of muscles working from the mastoid process seem to be separated on two fairly distinct surfaces, a postero-lateral and an antero-distal. The large distal face is always deeply roughened and is usually marked by a transverse or oblique groove. This surface was probably occupied in large part by the *sterno-cleido-mastoid* muscle which also extended upward over the rough anterior edge of the lateral face.

The remarkable co-ordination of structures in the Pleistocene sabre-tooth cats as exemplified particularly by the enlarged mastoid processes and the great stabbing weapons represented by the upper canines has been thoroughly appreciated by Winge (1895, p. 55, see P.N. van Kampen, 1905, p. 502) and by Matthew (1910, p. 296).

The internal structure of the ear is clearly shown in dissected specimens (plate 15, figure 1). The external auditory meatus is generally rather small and takes on a tubular form in contrast to the ring-like form of the true felines. The upper side of the opening is roofed over very broadly by the ridge connecting the base of the zygomatic arch with the mastoid process, while the lower side of the opening is enclosed either by the ectotympanic portion of the bulla or possibly by a partial coalescing of the basal portion of the mastoid process extending over the ectotympanic region and reaching the postglenoid process.

As in the true felines the tympanic cavity is divided into two distinct chambers by an oblique bony septum, which is so situated that the fenestra ovalis occurs at the level of communication between them. The external or vestibular chamber is very small. It generally communicates with the inner chamber only by a small opening immediately over the fenestra ovalis, and the septum between the two chambers is otherwise complete.

The inner tympanic chamber is very large and is divided into two distinctly separated parts which are marked off by a prominent wall or septum which crosses the outer side of the cavity at the level of the fenestra rotunda. Apparently this septum shifts in relative position with inflation of the bulla. The external division of this chamber is sometimes considerably larger than the internal and extends well into the mastoid process, sometimes hollowing out a large part of this process.

In a young animal it appears that the mastoid grows over the outer chamber of the entotympanic cavity. The septum on the ventral surface seemingly marks the inner limit of the mastoid.

The internal of the two divisions of the entotympanic chamber is opposite the outer or vestibular cavity and extends forward beyond this ectotympanic chamber.

The malleus and incus have been recovered from skulls of *Smilodon californicus*, but the stapes has not been found. These ear bones are illustrated in plate 15, figures 2 and 3. The malleus resembles in shape and in major structural details the comparable element in *Felis*. The manubrium is relatively narrow and slender and as in the latter form is not strongly curved. The extremity of the process is slightly spatulate and distinctly recurved. The *processus muscularis* appears to be slightly blunter than in the living felines. While the lamina is thin, its development in breadth is not so great as in *Felis*. The *processus longus (processus gracilis)* is situated closer to the head in *Smilodon* than in the latter genus. The head is rather

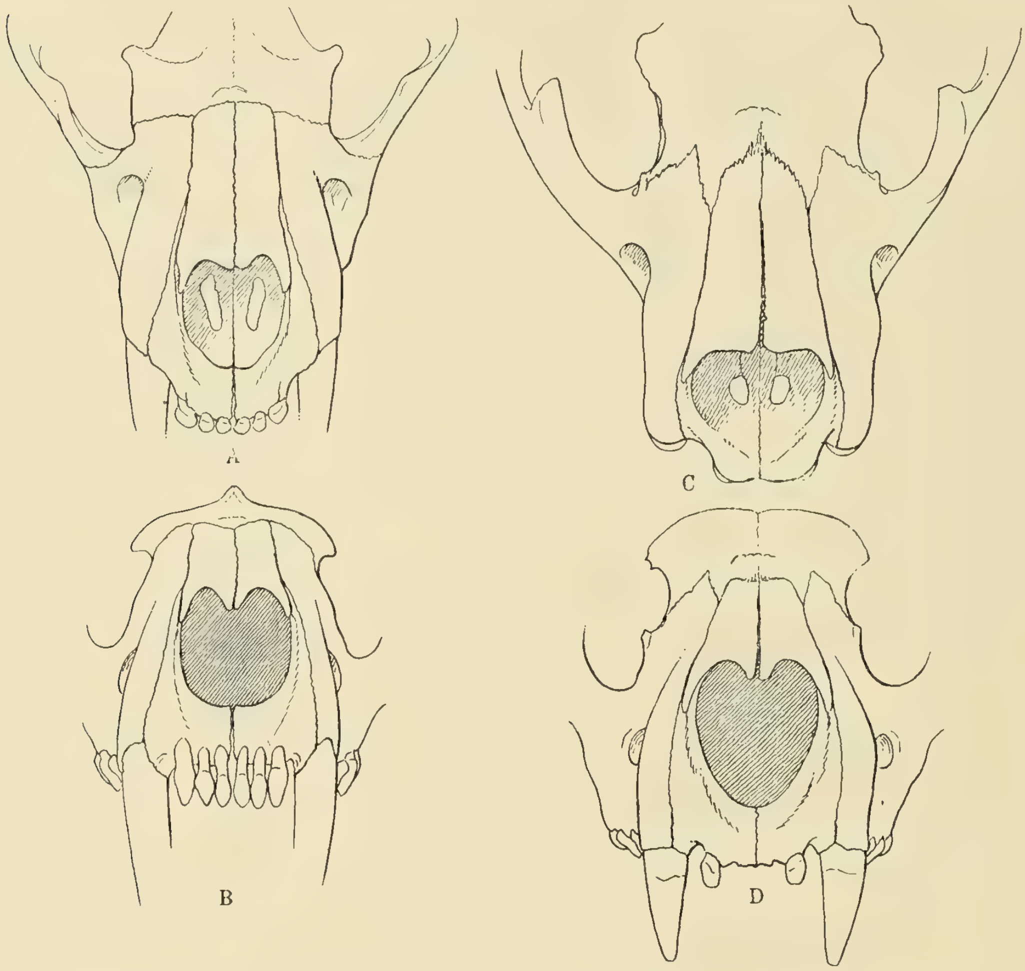

Fig. 9—Comparative views of skulls of sabre-tooth cat and true cat. A, C, superior view of muzzle; B, D, anterior view; × 1/4. A, B, *Smilodon californicus* Bovard, No. 2001-225; C, D, *Felis atrox* Leidy, No. 2900-9. Rancho La Brea Pleistocene.

sharply demarcated by a rim which encircles its base. Its outer border is broadly convex. Upper and lower facets are of subequal size and are separated by a groove having the characteristics of that in *Felis.*

In the incus, the articulating surface for the malleus is sharply defined. Its body is rather massive and this character is displayed also by the processes. The *processus brevis* tapers rapidly and the border of the incus connecting the extremity of this process with the articulating end is noticeably convex. The Sylvian apophysis, though small, is perhaps more prominently developed than in *Felis.* The stapes was probably quite small.

The structure of the zygomatic arch, particularly of the squamosal portion, is quite different from that of the true felines. The zygoma is short, relative to the length as measured from the postglenoid process to the anterior end of the skull. The arch possesses a strong upwardly convex curvature and the transverse diameter of the skull across this region is usually somewhat less than in the larger members of the true feline group (see measurements).

The elements composing the arch are relatively high compared with those of the African lion, but are thinner in transverse measurement. The postorbital process of the jugal is very low and blunt, compared with that of the lion and tiger, and is less acute than in the South American *Smilodon neogæus.* The posterior root of the arch is greatly extended inferiorly, and the lowest portion of the glenoid fossa has dropped to or below the level of the palate and is 30 or 40 mm. below the inferior surface of the basisphenoid. The posterior root of the arch and the glenoid fossa are also placed relatively farther forward than in *Felis* and the earlier and more primitive members of the sabre-tooth cat group.

PALATINE REGION

The roof of the mouth in *Smilodon californicus* is relatively much farther below the plane of the inferior side of the presphenoid than in *Felis.* The posterior narial opening is absolutely narrower than in lion and tiger skulls of somewhat smaller size, and is relatively much higher and narrower than in skulls of true felines with which comparisons have been made. The anterior border of the posterior nares, as in the true cats, is situated a considerable distance behind the posterior border of the superior molars. In adult animals the anterior border of the opening is usually flared downward and a prominent posterior nasal spine or ridge is commonly developed on the median portion and projects backward over the narial opening. The slender pterygoid processes extend nearly straight on a line about even with the lateral margins of the narial opening. So deep is the posterior root of the zygomatic arch that the pterygoid processes are only slightly lower than the glenoid fossæ.

On the superior side of the palatine plate a prominent median crest rises to meet the vomer. This crest is extended backward to the posterior nasal spine and its union with the vomer is carried extraordinarily far back so that the complete vertical septum is developed only a short distance in front of the posterior nasal opening.

In all of the specimens of *S. californicus* which have been examined, the palate is characterized by extraordinary development of the three longitudinal median ridges, which are indicated but are much less prominent in the true felines. In some cases the triangular median portion of the palatine plate included between the outer pair of the three ridges is much depressed below the roof of the lateral grooves which extend back from the anterior palatine foramina, and the median ridges are relatively weak. In other cases the median triangular area does not stand in relief and the ridges are relatively prominent. The lateral ridges are sharp where they occur on the premaxillaries and maxillaries. In their backward continuation on the palatines they lose their crested character and become noticeably heavier. Between the lateral ridges when in bold relief the region of greatest excavation occurs as a narrow trough along the median line slightly in front of and for a greater distance in back of the maxillo-palatine suture. Frequently occupying this position is a narrow bony element clearly defined in palatal view by suture from the maxilliary and from the palatine. In other specimens this element is absent and a normal intersection occurs between the transversely directed maxillo-palatine suture and the longitudinally directed median palatal suture. When the excavation occurs and when the median line of the palate is crested there is a very definite interruption of the ridge over the former area and this may become quite marked in some specimens. The lateral grooves, extending from the anterior side of the anterior palatine foramina backward to the posterior side of the palate, are very deep and are characterized by a marked roughening of the surface of the bone in this region. The extreme development of these grooves and the median ridges bounding them, taken with the other characters of the skull, seem to indicate that they have functioned as passage-ways for blood which the animal sucked from the gaping wounds produced by its sabres.

FORAMINA

The large infraorbital foramina are oval to triangular in form, and are so situated that the outer border is almost immediately over the anterior edge of the superior carnassial.

The small lachrymal foramen is situated farther in from the margin of the orbit than in the Recent lion or tiger, and a prominent lip or ridge is developed on the border of the orbit immediately in front of this foramen. Immediately behind the lachrymal foramen there are several small foramina.

The sphenopalatine opening may be situated in the border line between the palatine and the frontal with the posterior opening of the post-palatine foramen very close to the anterior border. In most cases it is, however, situated somewhat farther back in the palatine bone. While of large size this foramen is smaller than the sphenopalatine opening of *Felis atrox.*

The optic foramen, sphenoidal fissure and foramen rotundum are situated close together at the bottom of a deep groove bordered posteriorly and externally by a very strong, forwardly produced ridge of the alisphenoid. The foramen rotundum is deep down in this groove, close to the sphenoidal fissure, and is separated by quite a distance from the foramen ovale. A similar position is to be noted also in *Dinictis* and in *Nimravus.*

The foramen ovale is located at the lower end of the vertical face of the alisphenoid in which the foramen rotundum is situated. It usually opens mainly downward, but is so close to the edge of the vertical face that in many specimens it faces almost entirely forward. In *Nimravus, Pogonodon, Dinictis* and in *Hoplophoneus* the foramen ovale is on the inferior horizontal face of the alisphenoid, as in the true felines. In *Smilodon,* as in the true felines, there is no separate opening for the alisphenoid canal.

The postglenoid foramen varies considerably in size and may be minute in some specimens. Because of the close approximation of the postglenoid and mastoid processes this foramen is entirely hidden from view, situated high in the recess between these processes.

The stylomastoid foramen and the pit for the tympanohyal vary somewhat in position with relation to each other, being in some specimens very close together and in others separated by a distance of at least 10 mm. In those forms with the largest auditory bullæ the two openings are close together.

The openings of the posterior lacerate foramen and the condylar foramen may be as near each other as in the lion and tiger or in other true felines, and may be referred to as having a common opening (Univ. Calif. specimen 10839). In most cases, however, they tend to be separated somewhat, but are connected by a common groove. In some skulls, as in Univ. Calif. specimen 11074, the two foramina are about as far apart as in the dog, and the groove connecting them is relatively shallow.

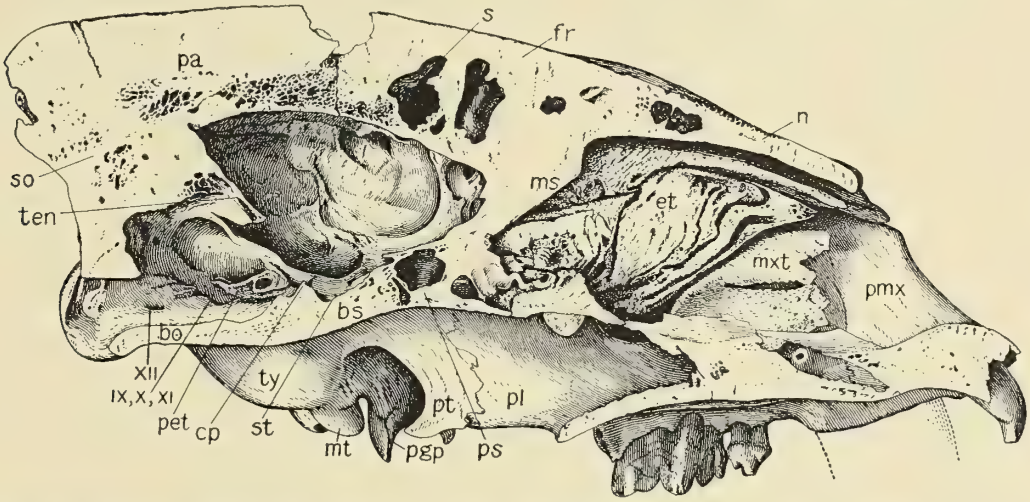

FIG. 10—*Smilodon californicus* Bovard. Vertical longitudinal section of skull, No. 2001-273; × 2/5. *n*, nasal; *fr*, frontal; *s*, frontal sinus; *pa*, parietal; *so*, supraoccipital; *ten*, cut edge of tentorium; *bo*, basioccipital; *pet*, petrosal; *bs*, basisphenoid; *ps*, presphenoid; *ty*, tympanic; *pt*, pterygoid; *pl*, palatine; *pmx*, premaxillary; *mxt*, maxilloturbinal; *et*, ethmoturbinals; *ms*, mesethmoid; *st*, sella turcica; *cp*, clinoid plate; *mt*, mastoid; *pgp*, postglenoid process; *IX*, *X*, *XI*, foramen lacerum posterius; *XII*, condylar foramen. Rancho La Brea Pleistocene.

When the skull is bisected vertically and either half is viewed from the sagittal plane (fig. 10), a number of interesting structural characters are brought to light. The most striking features, in contrast to those of *Felis*, are the relatively small size of the brain chamber and the extremely broad expanse of bone in back of and above this cavity. The latter development reflects in large measure the backward extension of the occiput and the high sagittal crest. Below and in front of the brain case is clearly shown the great depth of the posterior nares and post-narial passage. The enlarged opening causes the median line of the palate to dip noticeably downward toward its posterior end. Moreover, the recession of the nasal element with reference to the anterior end of the premaxillary is readily noted in this view. In contrast to *Felis atrox* (compare fig. 10 with fig. 134) the major trend of the basicranial axis is parallel to that of the principal fore and aft axis of the palate.

When the basicranial and basifacial axes are drawn on the respective sections of the skulls of these types, following the directions of these axes employed by Mivart (1881, pp. 83-85, fig. 48), the two are separated by an angle of 149° in *Smilodon* while in *F. atrox* they are separated by an angle of 126°. In other words, the facial region of the skull in the sabre-tooth is bent downward less, with reference to the basicranial axis, than in the extinct true cat.

The olfactory fossa is small. While the anterior fossa is relatively large and the middle fossa relatively small, in contrast to *Felis*, the cerebral chamber as a whole tapers forward more rapidly than in the latter type. The dorsal profile of this cavity meets the long axis of the tentorial process in a sharp angle. A marked characteristic is the very prominent development of the ridges on the inner cranial wall. The posterior or cerebellar fossa shows distinctly less extent in dorsoventral direction than in the true felines.

The tentorium is as well defined as in *Felis*, and in its lower anterior part exhibits on its superior surface a strong development of crests similar to that seen elsewhere on the cerebral wall. The petrosal is relatively small compared with that of the modern true felines and the pit for the appendicular lobe of the cerebellum is also relatively small. The floor of the cerebral cavity is thickened, relatively more so than in the true felines. The posterior clinoid plate ends dorsally in a thin edge which projects anteriorly. The base of the plate is broader anteroposteriorly than in *Felis*, while on the dorsal surface a small concavity situated immediately behind the process separates it from a lower posterior protuberance. The sella turcica appears to have been smaller than in *Felis*.

The presphenoidal sinus is of moderate size. Above the anterior fossa of the cerebrum and the olfactory fossa is situated the large posterior portion of the frontal sinus. In front of this is the anterior portion which, with the sinus of the nasal, contains the upper scrolls of the ethmoturbinal. The cavity in the nasal extends halfway down the length of this element.

Only portions of the mesethmoid plate are shown in figure 10. While the two upper scrolls are partly masked, the lower scrolls are clearly evident. The total number of major scrolls, as seen in this view, seems to correspond with that in *Felis*, although the individual scroll may vary somewhat in shape from the comparable structure in the latter type. The maxillo-turbinal is relatively large and is the principal turbinal element on each side of the mesethmoid to be seen when the nasal opening is viewed from in front. The coils of this scroll differ from those in true felines in lying entirely below and in front of the partition from which they spring.

Endocranial Cast

Plate 14, figs. 4, 5 and 6

The endocranial cast of *Smilodon californicus* displays a number of striking surface features. In shape and in proportions it likewise presents some noteworthy points of difference from that in *Felis*. The olfactory tract extends for a relatively short distance in front of the cerebrum, but is deep dorsoventrally. The cerebrum overlaps the cerebellum to a greater extent in this form than in *Felis atrox* and distinctly more so than in the Oligocene *Hoplophoneus*. In contrast to the latter type, the anterior half of the cerebrum has a fuller development. Viewed from the side, the cerebral portion, as a whole, is relatively deep, more so than in *Felis atrox*.

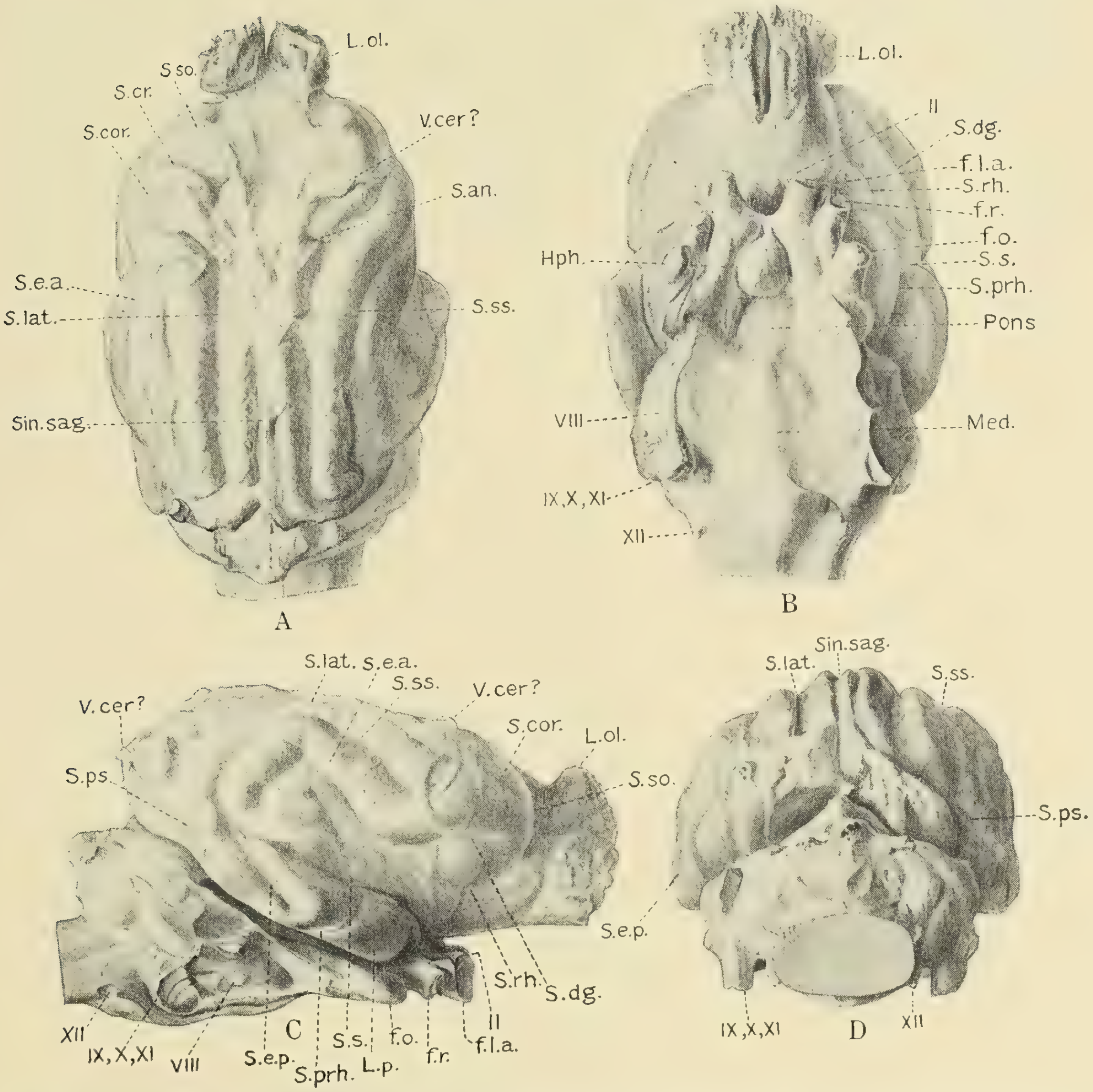

FIG. 11—*Smilodon californicus* Bovard. Endocranial cast from skull 2001-199. A, dorsal view; B, ventral view; C, lateral view; D, posterior view; × 2/3. *L.ol.*, lobus olfactorius; *L.p.*, lobulus pyriformis; *Hph.*, hypophysis; *Med.*, medulla oblongata; *II*, N. opticus; *f.l.a.*, N. trigeminus (ophthalmic); *f.r.*, N. trigeminus (maxillary); *f.o.*, N. trigeminus (mandibular); *VIII*, N. acusticus; *IX, X, XI*, N. glossopharyngeus, N. vagus, and N. accessorius; *XII*, N. hypoglossus; *V. cer.?*, cerebral veins?; *Sin. sag.*, sinus sagittalis; *S.so.*, supraorbital sulcus; *S.cr.*, cruciate sulcus; *S.cor.*, coronal sulcus; *S.an.*, sulcus ansatus; *S.lat.*, lateral sulcus; *S.ss.*, suprasylvian sulcus; *S.s.*, fissura Sylvii; *S.e.a.*, anterior ectosylvian sulcus; *S.e.p.*, posterior ectosylvian sulcus; *S.ps.*, postsylvian sulcus; *S.dg.*, diagonal sulcus; *S.rh.*, rhinal sulcus; *S.prh.*, postrhinal sulcus. Rancho La Brea Pleistocene.

Moodie (1922, pp. 357-359, fig. 16) in a description of an incomplete endocranial cast of the Rancho La Brea sabre-tooth, has directed attention to the large and prominent development of the gyri and the depth of the sulci. The pattern of the convolutions is remarkably well defined (fig. 11) and the gyri and sulci can be traced with greater ease in this form than in *Felis atrox*. At the anterior end of the sulcus lateralis is a short ansate sulcus. The cruciate sulcus is clearly defined.

TABLE 3—*Measurements (in millimeters) of skull of Smilodon*

	2001–24	2001–230	2001–225	2001–151	2001–77	2001–175	2001–111	2001–132	2001–288	2001–16	2001–181	2001–19	2001–65	2001–2	2001–5	2001–307	2001–311	2001–302	2001–90	2001–131	2001–4	2001–256	2001-113	2001-76	2001-148
Length from anterior end of premaxillary to posterior end of condyles	344.1	343.9	340.1	338.9	332.1	330.1	329.5	325.1	322.8	314.6	309.2	307.8	306.4	329.4	281.4	302.6	297.1	299	290.1	286	280.5	280.6	278.5	271.4	273.2
Basal length from anterior end of premaxillary to inferior notch between condyles	324.9	329.4	325.3	321.6	314.5	314	312	311.9	304	295.2	293.2	292.5	292.2	315.8	268.4	288.8	287.1	284.5	276.1	273.6	262.5	276.5	266.7	260	256.4
Length from anterior end of premaxillary to posterior end of inion	377.9	364	376.3	361	356.1	366.1	355.1	341.5	353.8	351.1	334.1	336	341.4	358	313.4	329.3	312.2	322.5	314.2	308.1	307.8	309	312.8	304.8	292.7
Length from anterior end of premaxillary to anterior end of posterior nasal opening	174.9	172	*a*170	174.9	164.5	164	162.3	164.8	168	168.1	159.1	166.5	164.5	173	145.2	158.3	160.6	157.8	149.5	144.4	138.6	143.3	142	137.6	142.4
Length of palate from anterior end of premaxillary to line tangent to posterior surfaces of maxillary parapets	158.3	151.6	152.4	157.6	156	.....	148.1	148.3	142	149.8	142.7	142.1	143.5	152	130.8	138.8	136.8	132.4	131.4	131	129	124.6	129.8	126.1	125.3
Length from posterior end of glenoid cavity to posterior end of condyles	109	117.8	113.7	112.2	113.8	.....	115.7	112	110	95	96.9	101	98.6	110.3	93.5	93.5	96.5	101.8	92.5	87.3	98.8	87.7	86.7	83.4	85.7
Anteroposterior diameter of nasals	85.9	95.1	86.1	88.9	80.1	99.5	79.9	83	85.9	84.9	*a*88.6	80.8	.....	94.4	89.3	80.9	80.2	78.5	73	71.6	81.4	78.9	66.8	69.7	73.2
Width of anterior nares	*a*63.4	59	62	59.8	55.6	.....	59.6	55.4	56.3	53.7	56.5	53.5	52.4	55.6	50.1	61.3	52.6	51.8	54.2	53.7	54.4	47.7	50.7	46.9	52.3
Greatest width across muzzle at canines	114.5	111.1	113	107.9	110	.....	*a*118.1	*a*113	108.9	108.6	106.2	100.8	101.1	114	101.3	111.6	112	101.3	97.1	100.1	106	93.1	93.6	93.6	93.9
Least width between superior borders of orbits	101	100.9	99.1	92.1	99.3	100.9	103.9	96.7	107	94.5	89.6	88.9	94.4	95.8	93.6	96.4	93.6	91.1	92	90.7	91.8	87.9	83.1	81.3	91.2
Width across postorbital processes	124.8	*a*127	117.8	111.9	118	.....	122.6	126	127.8	128.3	114	113.8	114.4	124.6	.....	130.2	129.6	104.1	118.3	116.7	120.5	110	104.9	109.1	111.4
Least width of postorbital constriction	63.9	65.5	60.5	63	58.6	64.5	65.9	59.4	66	55.2	57.4	60.1	54.9	62.5	62.6	62.8	61.5	54.3	58.5	56.6	64	59.1	52.9	60	60.6
Greatest width across zygomatic arches	232.4	.....	240.1	215	220.3	224	*a*216	214.9	224.1	211.2	205.4	195.3	202.6	214.5	209.7	220.3	219.4	200.4	204.1	192.2	203	185.2	191.9	186.3	182.9
Anterior palatal width between superior canines	63	62.3	61.1	56	60	.....	62.6	57.4	60.8	59.5	55.6	57.2	55.8	62	54.7	58.7	56.4	54.9	53.3	54.3	58.2	50	52.6	48.9	50.7
Posterior palatal width between inner roots of superior carnassials	106.5	108.6	105.2	106.4	110.5	.....	111.9	105.4	111	105.4	105.4	94	101.5	110.4	98.8	108	102.2	102	101.6	98.9	102.1	86.8	91.9	95.8	90.6
Width across palate between posterior alveoli of superior carnassials	129	135.4	132.4	128.2	130.2	.....	141	129.2	138.4	128.3	124.7	119	124.4	130.6	125.6	130.7	129.7	132.3	130.4	127.6	130.9	112	114.7	115.8	118.7
Greatest transverse diameter across auditory bulla, measured from foramen lacerum posterius to external auditory meatus	56.9	63.3	62.3	63.9	57.7	.....	58.4	59.3	59.3	57.6	51.1	55.6	50.9	56.3	47.5	53.8	55.8	50.5	48.8	48.4	51.4	49.5	47.4	47.9	46.7
Greatest width across mastoid processes	154.3	151.7	150.7	138	137.4	.....	143.4	138	144.7	144.6	131.3	129.1	126.1	140	128.9	139	139.1	122.4	119.7	130.7	127.3	125.7	120.8	122.8	122
Greatest diameter across condyles	70.4	69	66.5	72.3	70.5	64.1	67.5	70	67.1	63.2	66.9	67.8	63.4	64.6	*a*62.4	63.5	67	63.6	65.4	59.4	60.8	61.6	59.9	61	57.6
Height of anterior zygomatic pedicle	70.2	*a*60.7	61	64.4	54.5	.....	57.8	63.9	54.7	63.7	51.6	57.7	54.5	68	53.7	60.8	54	42.6	56.1	57.7	56.7	50	53.6	51.4	54.1
Length of anterior zygomatic pedicle	57.1	55.7	50.5	56.9	55	.....	55.5	57	53.7	51.2	51.2	50.4	50.3	56.5	51.6	52.5	52.9	51.8	49.9	51.2	50.9	47.2	45.9	45	45.8

a, Approximate.

Where this meets the mid-line of the cast, the dorsal surface is deeply depressed, evidently more so than in the true cats. The rhinal and post-rhinal sulci have positions as in *Felis.* The lobulus pyriformis projects to a noticeable extent in front of and below the temporal lobe. The latter is relatively narrow at its lateral extremity. This region presents a somewhat different appearance from that in *F. atrox.*

On the dorsal surface between the anterior end of the lateral sulcus and the cruciate sulcus is the course of a blood-vessel, presumably a cerebral vein. Elsewhere on the dorsal surface are indicated additional courses for vessels evidently leading to the sagittal sinus. The largest and longest of these is that situated in the posterior crest of the cerebral lobe.

A peculiar feature noted in ventral view is the position of the optic chiasma and optic nerves with reference to the ophthalmic nerves. In *Felis* the optic chiasma lies well out in front, whereas in *Smilodon* this structure tends to be more obscured by the inner base of the ophthalmic nerve (*f.l.a.*) of each side. The impression of the pituitary fossa is clearly marked.

Measurements (in millimeters) of the cerebrum are as follows: greatest length, 83.5; greatest width anteriorly, 61.4; greatest width across temporal lobes, 72. The endocranial cast displaces 223 c.c. of water.

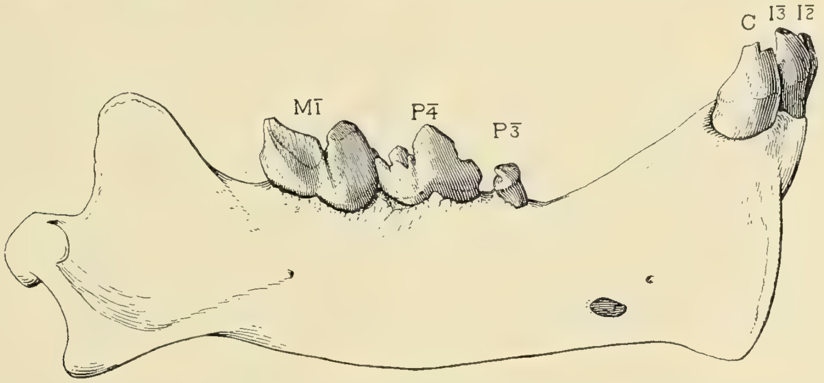

FIG. 12—*Smilodon californicus* Bovard. Ramus and lower dentition showing presence of $P_{\overline{3}}$; No. 2002-R-60; lateral view; × 1/2. Rancho La Brea Pleistocene.

MANDIBLE

The numerous lower jaws in the collection vary considerably in size and in form, but the gradation between them in size and in the apparent age of the individuals (plate 4) shows that there is no good reason for supposing that the variation is due to anything more than normal age, sex, or individual variation within a single species.

The mandible is on the whole a little weaker than that of an African lion of the same length. Compared with the Recent lion with particular relation to strength, the coronoid process is very small and the region of the diastema is relatively low and thin.

The symphyseal contact of the two rami is strongly constructed, but the rami do not come into contact gradually, thus forming an acute angle inferiorly between their anterior ends as in the true felines. At the posterior side of the symphysis, the inner borders of the rami turn toward each other sharply, so that the anterior end of the space between them is abruptly truncated instead of sharply angular.

TABLE 4—*Skull and dental indices of Smilodon**

	2001-24	2001-230	2001-225	2001-77	2001-175	2001-111	2001-288	2001-16	2001-181	2001-19	2001-65	2001-132	2001-151	2001-2	2001-5	2001-307	2001-311	2001-302	2001-90	2001-131	2001-4	2001-256	2001-113	2001 76	2001-148
Anterior narial index	19.5	18	19	18	. . . . .	19	18.5	18	19	18	18	18	18.5	18	19	21	18	18	20	20	21	17	19	18	20
Index of interorbital breadth	31	31	30	31.5	32	33	35	32	30.5	30	32	31	29	30	35	33	33	32	33	33	35	32	31	31	35.5
Breadth index of postorbital processes	38	39	36	37.5	. . . . .	39	42	43.5	39	39	39	40	35	39	. . . . .	45	45	36.5	43	43	46	40	39	42	43
Index of postorbital constriction	20	20	19	19	20.5	21	22	19	19.5	20.5	19	19	20	20	23	22	21	19	21	21	24	21	21	23	24
Bizygomatic index	71.5	. . . . .	74	70	71	69	74	72	70	67	69	69	67	68	78	76	76	70	74	70	77	67	72	72	71
Index of palatal length	49	46	47	50	. . . . .	47	47	51	49	49	49	48	49	48	49	48	48	47	48	48	49	45	49	48.5	49
Index of anterior palatal breadth	40	41	40	38	. . . . .	42	43	40	39	40	39	39	35.5	41	42	42	41	41	40.5	41	45	40	40.5	39	40
Index of posterior palatal breadth	67	72	69	71	. . . . .	76	78	71	74	66	71	71	68	73	75.5	78	75	77	77	75	79	70	71	76	72
Height index of anterior zygomatic pedicle	123	109	121	99	. . . . .	104	102	124	101	114	108	112	113	120	104	116	102	82	112	113	111	106	117	114	118
Mandible No. 2002—	72	335	324	333	350	53	443	233	32	70	213	234	103	299	338	41	52	157	292	34	365	138	69	313	104
Diametral index of $M\bar{1}\ \frac{WM\bar{1} \times 100}{L\ M\bar{1}}$	50	52	49	55	48	50	51.5	49	48	54	49	48	46	50	46	48	52	47	50	50	49	48	51	49	51
Length index of $P\bar{4}$—$M\bar{1}\ \frac{L\ P\bar{4} \times 100}{L\ M\bar{1}}$	81	90	83	87	82	83	88	86	85	79	78	87	86	89	85	97	86	87	81	94	85	89	83	92	85

* The skull indices adopted in this memoir are those defined by G. F. Eaton (1922, p. 443).

The lower margin of the symphyseal contact of the angle extends downward somewhat below the inner angle of the inferior side of the mandible immediately behind it. The amount of projection in this region is sometimes considerable, and the lower side of the symphysis may terminate in a sharp tubercle reaching below the inferior edge of the lateral flanges. In most instances, however, the inferior side of the symphysis projects only a few millimeters below the inner side of the inferior margin of the ramus immediately behind it or immediately external to it.

The anterior face of the symphyseal region is generally concave both transversely and vertically, without the development of a median ridge at the point of contact of the rami. The anterior face of each ramus is usually pitted by the openings of two to four large foramina. The posterior face of the symphysis slopes backward gently to the upper end of the lower half, where it suddenly dips downward and forward forming a prominent ridge above the geniohyal depression. The depression in the lower portion of this posterior face is much more pronounced than in the Recent lion or tiger, and the face of the symphyseal contact of the two rami is in consequence about twice as wide immediately above the geniohyal depression as it is just below the upper end of this depression.

The form and size of the characteristic lateral smilodont flanges vary considerably with age and possibly with sex. In all young individuals the flanges are relatively short and the margins obtuse. In many young specimens the inferior margin of the flange scarcely drops below the inferior line of that portion of the jaw below the cheek-teeth (see plate 4, figs. 1 to 6). In some older individuals the flanges may be a little more prominent, particularly anteriorly, and the edges may be somewhat thinner. The flanges seem on the whole to show about the same degree of development as in species of the South American *Smilodon*.

The coronoid process is always very poorly developed and does not reach much more than half the height in proportion to the length of the jaw that is developed in the Recent lion. The anteroposterior diameter of the base of this process is also small and the lower carnassial tooth has a position much nearer the condyle than in living *Felis*.

The masseteric fossa is strongly marked in comparison with the size of the coronoid process, and the inferior border of the jaw immediately below it shows a broadly horizontal expansion. The anterior end of the fossa is, however, in most cases much shallower than in the Recent lion or tiger, and the horizontal expansion of the inferior border does not extend so far forward as in the lion.

The angle is situated much nearer the condyle than in the true felines. It is also situated nearer the external or lateral end of the condyle, the posterior end of the inferior border being twisted outward rather sharply so that the angle is almost immediately below the outer end of the condyle.

The condyle is so situated that only a very small portion of the inner or median end extends beyond the plane of the inner or median face of the coronoid process. In the lion and in the true felines generally, the inner end of the condyle extends much farther inward beyond this plane. The articulating surface is very narrow at the outer end of the condyle and increases rapidly in the anteroposterior extent of the surface toward the inner end, where it is widest. The difference between the inner and outer ends is usually greater than in the lion and other true felines. The relative thickness of the condyle or the diameter of the circle into which the articular surface falls is also greater than in the lion, and the arc covered by the articular surface is larger.

TABLE 5—*Measurements (in millimeters) of mandible of Smilodon*

	2002-72	2002-335	2002-324	2002-350	2002-333	2002-53	2002-443	2002-233	2002-32	2002-70	2002-213	2002-234	2002-103	2002-299	2002-338	2002-41	2002-52	2002-157	2002-292	2002-34	2002-365	2002-138	2002-69	2002-313	2002-104
Length from anterior end of symphysis to posterior end of condyle	230	227	225.3	224	224.5	223.5	223.1	221.7	221.6	216.8	216	214	212.2	210.4	210	207.8	203.6	201.8	201.1	199.2	194.3	189.7	181.6	179.6	178.3
Length from anterior end of outer flange to posterior end of condyle	218.8	213.8	213.3	209.4	210	211.4	214.1	206.4	205.3	202.8	204.3	198.3	199	197.8	196.3	197.4	191.7	190.8	188	186.3	182.5	179.2	168.8	171.4	166.1
Length of symphysis measured along anterior border	72.7	71.4	73.8	64.3	75.5	70.5	70.7	67.7	67.7	74.3	72.5	71.5	76.8	62.6	65	62.5	60.8	66.6	55.5	63	59.4	52.2	61.9	53.8	48.7
Least depth of ramus below diastema	38.7	39.4	36.6	35.4	40.4	34.6	36.6	35.2	34.2	36.3	35.6	33.6	37.7	30.8	36.2	35.4	31	31.1	27.3	28.5	29.2	33.6	29.5	30.5	29.6
Depth of ramus below posterior end of M̅1̅	45.6	42.3	39.8	42.6	44.6	43	41.2	44	39.8	42	41.9	40.1	42.3	39.7	42.6	39.8	36.2	38.4	36.7	37.9	37.3	40.1	38.4	36	36
Thickness of ramus below M̅1̅	22.5	23	21.6	23.9	25	23.5	23.4	22.6	20.2	22.2	23.3	21.5	24	20.1	24.8	20.2	19	19.6	18.7	18.7	19.3	20.1	19	19.7	19.2
Height from inferior border of angle to summit of condyle	37.4	43.3	40	39.3	36.7	43	35.2	38.8	36.9	40.3	42.5	38	44	36	43.5	38.8	33.3	37.3	36.1	38.6	35.2	33.3	30.7	34.8	32.3
Height from inferior border of angle to summit of coronoid process	75.2	71.7	66.4	73.8	73.7	76.3	67.8	75.8	70.2	74.4	66.3	71.4	72.5	63.5	74.2	72.1	64	67	66.7	69.3	65.8	63.9	61.4	60.3	58
Transverse width of condyle	51.4	51.4	55.9	51.8	51.4	51.1	47.5	50.2	52.7	49.8	48.7	46.4	49.7	48	51.7	47	46.5	47.5	45.1	43.4	45.1	41.5	42.7	40.6	38.7
Greatest depth of condyle	18.9	20.7	17.1	18.3	19.8	20	18.2	18.8	19.4	18.3	18.5	17.2	19.2	17.2	19.8	19.1	17.5	16.5	16.5	18.4	17.6	18.4	16.6	16.8	15.8
Greatest width of mandible measured across symphysis and between outer walls of alveoli for lower canines	56.5	*a*63	60.5	57.9	64.6	58.7	60.5	57.5	59.8	61.6	60.1	56.5	63.5	53.6	60	*a*57.5	56.6	56.2	53.2	56.4	53.2	47.8	*a*55	50	48.1
Greatest width of mandible measured across outer flanges	58.6	53.4	53.8	54.7	57	55.5	56.7	59.1	56.8	56.4	51.6	48.5	62.3	50.6	63	*a*47	49.5	57	48.7	*a*49.4	52.3	40.2	45	52	47.5
Greatest width of mandible measured between outer ends of condyles	188.7	187.9	*a*208.7	198.7	192.3	184.1	184.7	176	196.2	182.3	183.3	187	188.3	165.6	181.7	164	173.4	178.9	171	168.5	169	158.2	152.4	147.4	147.9

a, Approximate.

HYOID APPARATUS

What appears to be the only representation at present available of the hyoid apparatus in the extinct cats of Rancho La Brea is specimen No. I 1, figure 12a. This element is regarded as a basihyal and is referred, at least tentatively, to *Smilodon.* No. I 1 is heavy and of relatively large size. The ends are broadened in anteroposterior direction. Each end is obliquely truncated by two surfaces for cartilaginous attachment.

Measurements (in millimeters) of No. I 1

Greatest length	80
Dorsoventral diameter at middle line	10.4
Anteroposterior diameter at middle line	9.5

DENTITION

Dental formula: $\frac{3}{3}, \frac{1}{1}, \frac{2}{2\text{-}1}, \frac{1}{1}$

SUPERIOR DENTITION

The crowns of the upper incisor teeth are characterized by a very prominent development of the principal cusp. The latter is cone-shaped and slightly recurved in its downward extent. On each tooth a ridge on the medial and lateral faces of the crown extends from the base to the tip. Even in $I\underline{3}$ the principal cusp is larger in its downward extent and more pointed than the comparable tooth in *Felis atrox,* but the most striking differences are seen when $I\underline{1}$ and $I\underline{2}$ of *Smilodon* are compared with the corresponding teeth in the great true cat. In the latter the principal cusp is low, rounded in transverse extent and flattened somewhat anteroposteriorly. The posterior tubercles are two in number and situated close together on the lingual side of the tooth. In the sabre-tooth, the tubercles while flattened and ridge-like are prominent and farther apart at the lower edge. Between them a V-shaped notch extends to the base of the crown. In $I\underline{1}$ the internal or medial cusp extends a little lower on the side of the tooth than the lateral cusp. In $I\underline{2}$, however, the external or lateral ridge is less prominent and extends a trifle lower than the internal cusp or ridge. Both teeth exhibit a slight development of cingulum at the base of the inner and outer sides of the front face. A very slight expression of this may be seen also on the antero-internal base of $I\underline{3}$. The strong development of these teeth and their extraordinary piercing and grasping power is emphasized also by the presence of strong roots. In this respect there is again a notable difference between *Smilodon* and *F. atrox.* In the former the fangs are decidedly longer and broader anteroposteriorly than in the latter (see plate 13, figs. 7 and 7a), and the differences are quite independent of the relative sizes of these animals.

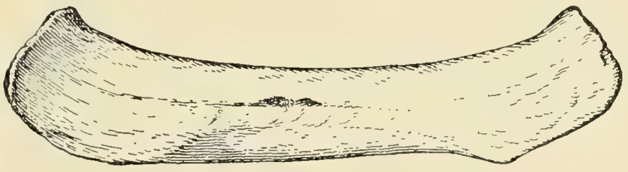

FIG. 12*a* Basihyal?, No. I-1, tentatively referred to *Smilodon californicus* Bovard; × 1. Rancho La Brea Pleistocene.

In the lateral incisor of *Smilodon*, the lateral crest of the crown may show, under magnification, a slightly serrate structure, but the serrations are never as coarse as those seen in *Dinobastis* or in the comparable tooth figured by Dawkins and Sanford (1872, p. 188, figs. 1–3) under *Machærodus latidens.*

As in the British specimen, the crown of I3 in *S. californicus* possesses a minute tubercle on the postero-lateral and postero-medial sides and near the base. The tubercle on the postero-medial side is situated at a point below that reached by the tubercle on the opposite side. The crown is somewhat more curved in its longitudinal extent than in *Machærodus latidens.* The root is flattened or slightly concave anteroposteriorly on its inner side and bulges slightly on the external side. The upward curvature of the fang is uniform.

In *Felis atrox*, on the other hand, the crown is shorter, slightly narrower at the base, than in *Smilodon.* Moreover, it differs decidedly in the development of a heavy ledge or cingulum, which extends backward from the base of the medial crest of the crown, diminishing considerably in prominence as it swings across the posterior base of the tooth. The root is distinctly shorter than in *Smilodon*, and when viewed from the rear is seen to possess a sinuous curve.

Evidently in the sabre-tooth cat, where the upper canines function chiefly as stabbing weapons, the grasping and holding of prey was accomplished largely with the aid of the strong penetrating incisor teeth. In the true feline, on the other hand, the strong grasp on the victim resulted in the main from an interlocking of the powerful upper and lower canines.

The superior canines are of approximately the same form as those of the South American smilodons, though differing in some minor details. In their normal position in the jaw, the sabres of *Smilodon californicus* have not projected as far beyond the alveolar margin as they are commonly shown to project in existing figures of the South American species. In a number of cases the sabres seem to have slipped down in the alveolus for varying distances and appear to be actually longer than in the other specimens. Apparently in some of these cases the abnormal protrusion of the sabre had occurred during the life of the animal.

The root of the tooth includes about two-fifths of its total length (plate 12, fig. 1). The upper end of the tooth is rather sharply tapered. Instead of being relatively heavy, as seems to be the case in some of the South American forms, the root is only slightly thicker than the extra alveolar portion and its width is practically the same as that of the lower part. However, the shape of the root varies and specimens are available from the asphalt in which this portion bulges more in anteroposterior direction than is shown in the tooth figured. Moreover while the root may end bluntly, in some specimens the end may be drawn out considerably.

The tooth as a whole is strongly curved anteroposteriorly, the total curvature of the anterior border amounting to 117° of arc. As the curvature is fairly regular for the whole length of the tooth, the curve of the exposed or functional portion is considerable, and it is probable that the downward stroke of the tooth must have been accompanied by a backward jerk in order to make it fully effective.

The whole tooth is much compressed laterally. The amount of flattening is a little less than half in a portion of the root and somewhat more than half in the greater part of the cutting blade. On perfectly preserved specimens the inner or median side of the tooth is slightly flatter than the lateral face.

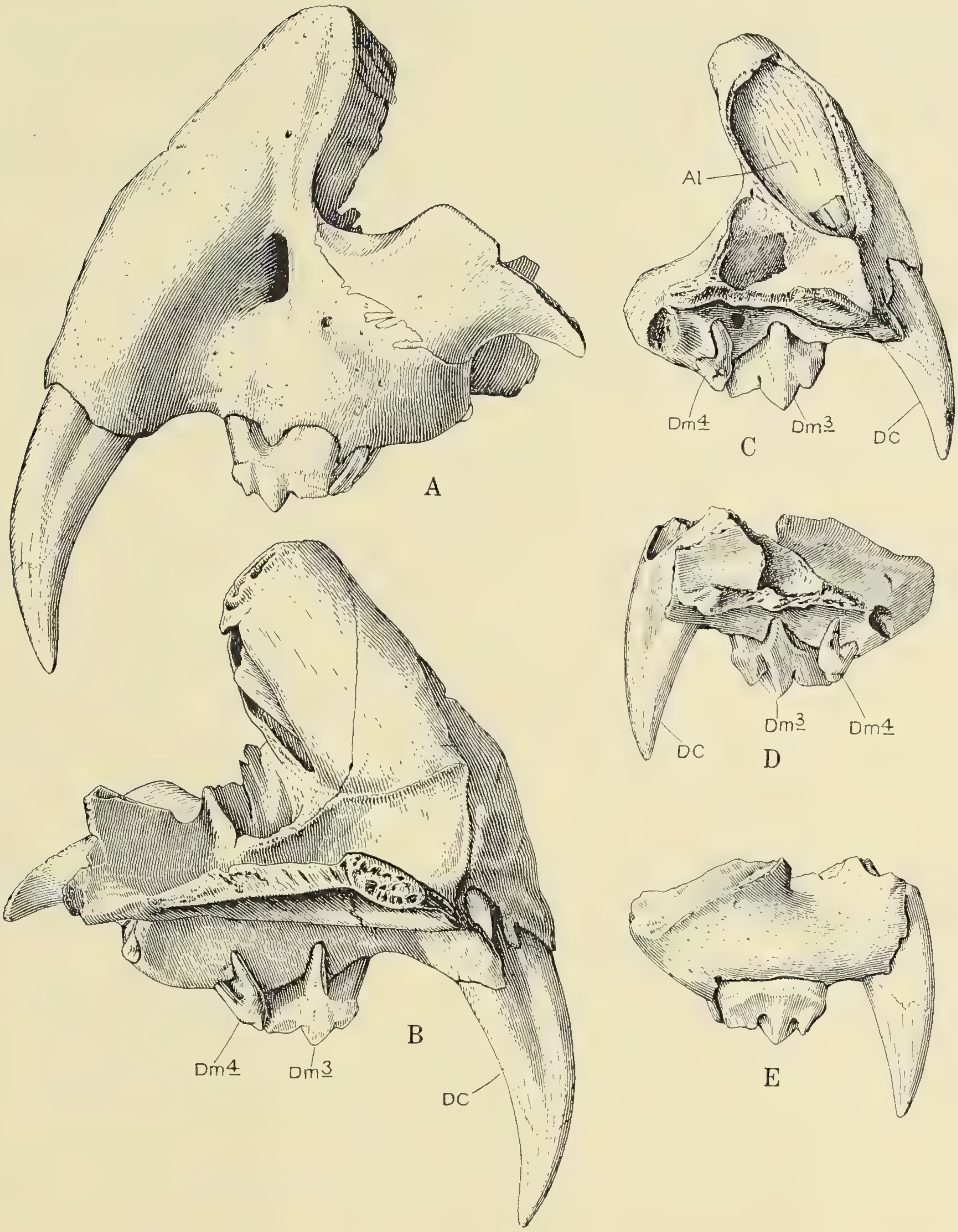

FIG. 13—*Smilodon californicus* Bovard. Specimens showing principally deciduous teeth. A, B, No. 2001-577, outer and inner views; C, No. 2001-578, inner view; D, E, No. 2001-579, inner and outer views; × 2/3. *DC*, deciduous canine; *Al*, alveolus for permanent canine; *Dm*$\underline{3}$ and *Dm*$\underline{4}$, third and fourth deciduous molars. Rancho La Brea Pleistocene.

The enamel extends much farther up from the point of the tooth on both the anterior and posterior edges than it does on the lateral faces. On the posterior edge it extends upward as a long narrow band, tapering to a sharp point exactly on the posterior margin somewhat more than halfway up from the point. On the outer side of the anterior edge the enamel reaches upward a little farther than it does over the middle of the external face of the tooth. On the inner side of the anterior edge it extends farther up than on the outer side and reaches to about the middle of the long diameter of the tooth.

The anterior and posterior edges of the tooth show beautifully marked serrations of the enamel (plate 12, fig. 2). The posterior cutting edge holds a median position on the tooth. At the upper end, the anterior cutting edge is noticeably nearer the inner or median side of the tooth.

Two specimens of the canine, selected from a large series of adults to represent a very long (No. 2000-L-26) and a very short tooth (No. 2000-L-2), furnish the following measurements in millimeters: Greatest length measured in a straight line from end of root to tip of crown 262-200; anteroposterior diameter of crown taken at upper end of enamel on forward edge 39-33.7; greatest anteroposterior diameter of root 41.8 (approx.)—36.8; greatest transverse diameter of root 21.2—17.3.

P$\underline{3}$—The third upper premolar varies considerably in size, ranging in anteroposterior diameter from 12 mm. to 19.7 mm. It is usually so placed in the jaw that its long diameter is parallel with the alveolar margin of the jaw, but in a considerable number of cases it is set obliquely or almost transverse to the alveolar margin. In L. A. Mus. skull 2001–162 where the position of P$\underline{3}$ is noticeably oblique, the diastema between P$\underline{3}$ and the canine is short. The crown generally bears an anterior and a posterior basal tubercle, but in rare cases the anterior tubercle may be absent. There is present in most specimens a small posterior basal tubercle. Occasionally this tubercle is not represented. In every specimen examined there is a small tubercle or ridge developed on the postero-external angle of the tooth. In some instances it is very weak, but in no case is it absent. In at least one specimen, a tubercle of this nature is present on the postero-internal portion of the cingulum. The posterior half of the tooth is much broader than the anterior, owing to the prominence of the postero-internal portion of the cingulum.

The two roots supporting the crown in P$\underline{3}$ may be separate or in some instances fused. Even in teeth in which the upper ends of the fangs are separate, fusion may take place immediately above the base of the crown for a variable distance. When the roots are distinct, it is clearly seen that the hinder fang is slightly longer but distinctly heavier than the forward fang.

P$\underline{4}$—The superior carnassial is a beautifully developed cutting tooth, resembling in general the *Smilodon* type. The antero-internal root is always present, but there is ordinarily no trace of a protocone upon it. In some specimens (Univ. Calif. No. 11291) a very small but distinct protocone is evident on the unworn teeth. In a number of other specimens absolutely unworn superior carnassials exhibit in the normal position of the protocone one or more very narrow ridges or wrinkles of the enamel.

The parastyle is always well developed, but varies in size in proportion to the size of the tubercle or cusp anterior to it. The latter tubercle, which may be conveniently designated the prostyle, is nearly always present but varies greatly in size. In several cases (L. A. Mus. No. 2001–225; Univ. Calif. No. 11249) it is entirely absent and the parastyle proportionately large. In one instance (Univ. Calif. No. 10829) it is absent on the left carnassial but is distinctly developed on the right side.

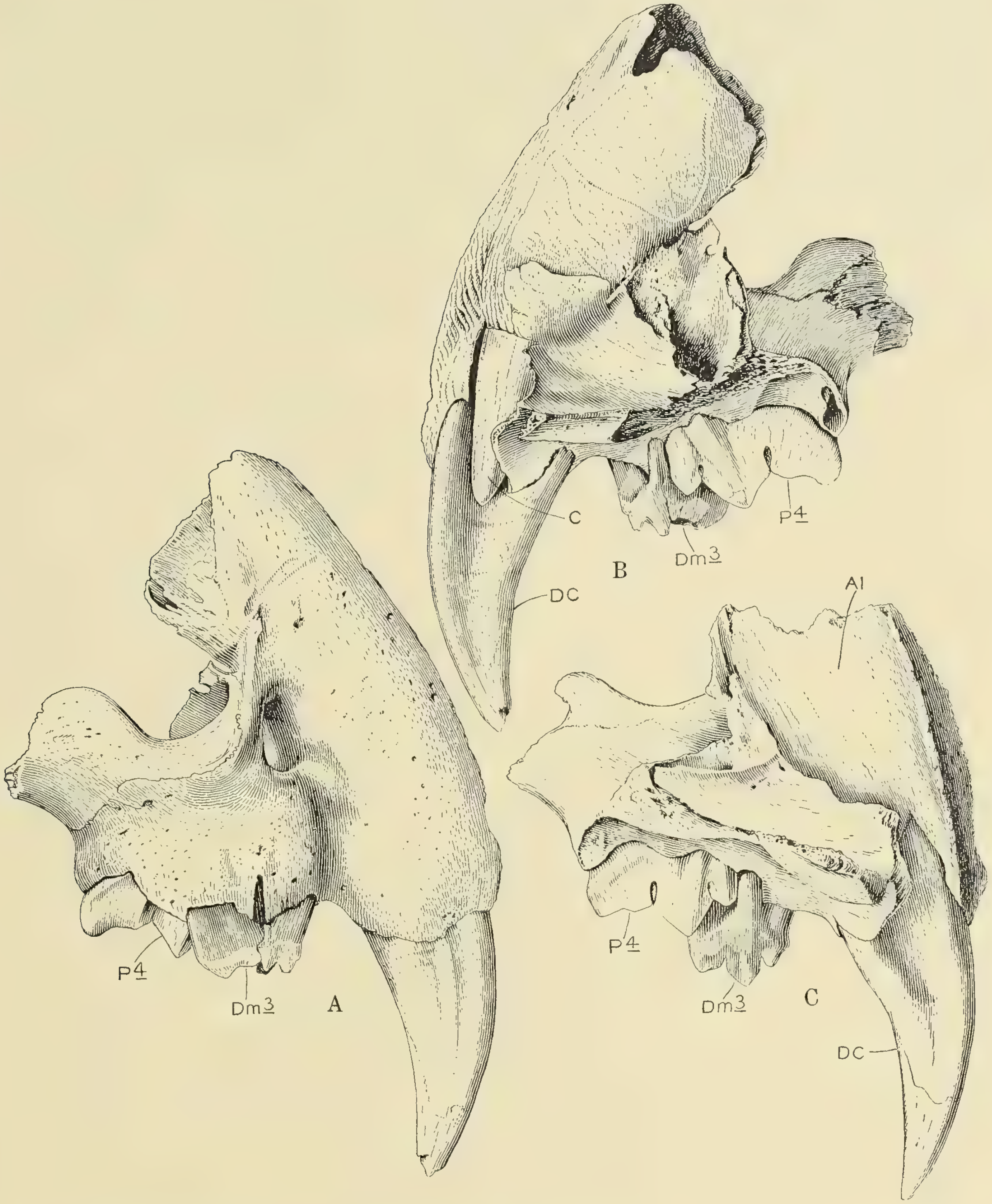

Fig. 14—*Smilodon californicus* Bovard. Specimens showing deciduous and permanent teeth. A, B, No. 2001-580, outer and inner views; C, No. 2001-581, inner view; × 2/3. *DC*, deciduous canine; *C*, permanent canine; *Al*, alveolus for permanent canine; $Dm\underline{3}$, and $Dm\underline{4}$, third and fourth deciduous molars; $P\underline{4}$, fourth premolar. Rancho La Brea Pleistocene.

The metacone is always somewhat longer anteroposteriorly than the paracone and is uniformly marked by a depression on the external face of the blade. The depth of this depression varies considerably in different individuals.

Normally P$\underline{4}$ possesses three roots, of which the largest is the posterior root. The latter fang rises above that portion of the crown which includes the metacone blade and approximately the posterior half of the paracone. The anterior root, next largest in size though considerably smaller than the posterior fang, rises above the rest of the crown anterior to the middle of the paracone. As indicated, an antero-internal root is always present. This rises from the inner anterior base of the protocone and projects inward. Both anterior and posterior roots curve inward in their upward course.

When comparison is made with P$\underline{4}$ of *Felis atrox,* having a size of crown approximately as large as that in *Smilodon* (compare plate 13, figs. 1, 1a with Plate 33, figs. 1, 1a), the roots in the latter form are seen to be slightly longer. The outer roots curve inward in their upward course and the posterior root shows this curvature more distinctly than does the comparable root of *F. atrox.* Moreover, this root possesses a broader base and is more compressed laterally than in *F. atrox.* The antero-internal fang is surprisingly well developed, but is subject to considerable variation in size. In some specimens it is quite slender.

A curious variation occurs in some individuals from the asphalt, namely an addition of a fourth fang to the root system of P$\underline{4}$. This, when present, is located at the antero-external corner of the posterior root and in its upward course may project outward and forward. The base of the fang thus lies above the middle of the external wall of the paracone. It occupies an alveolus distinct from those for the anterior and posterior roots. A fourth root of this type is present on each P$\underline{4}$ in skull 2001–120. Its diameter is less than that of the antero-internal root, but it reaches a length of 23 mm.

In some specimens, as for example in skull 2001-243, it is reduced to a very slender element, which, in occupying a tiny alveolus, persists in its separation from the anterior and posterior root. In its greatly reduced size, tucked away in the outer wall of the maxillary, this root may prevail more often than we are led at first glance to believe from an examination of skulls of *Smilodon californicus.* Considerable similarity exists between the permanent and milk carnassials in this particular character (see below, description of upper milk carnassial tooth).

M$\underline{1}$—The small molar tooth has approximately the same form and position and about the same relative size as in the African lion. The transversely elongated crown is nearly elliptical in cross-section, the long axis being nearly perpendicular to that of the superior sectorial. The elongated crown may be supported by two roots for the most part fused as in L. A. Mus. skull 2001-300, or the crown may be considerably reduced transversely, ovoid in shape, and with single fang as in L. A. Mus. skull 2001–159. The superior molar is present in only a few of the specimens. More often it has dropped from the alveolus.

Inferior Dentition

The inferior incisors are closely set in a transverse line which is slightly convex forward. I$\overline{1}$ is very much smaller than I$\overline{2}$ which is in turn much smaller than I$\overline{3}$. The crowns of these teeth are relatively narrow transversely, more so than in the lion. The principal cusp on each crown is distinctly higher than that in the comparable tooth of *Felis atrox*, and is moreover noticeably recurved. These cones would have a nearly round cross-section were it not for the presence of lateral ridges on the external and median sides. In I$\overline{1}$ the external lateral ridge terminates inferiorly at the anterior end of a prominent basal cusp which extends around the base of the tooth toward the middle of the posterior side. The median side of the base of I$\overline{1}$ bears no basal cusp though a faint ridge is present.

In I$\overline{2}$ the external lateral ridge terminates next a basal cusp similar to that on I$\overline{1}$, and a median lateral ridge swings backward over the posterior side of the base of the crown as a sharp ridge. The two posterior basal ridges are separated by a considerable space on the posterior side of the tooth, in contrast to the close proximity of the prominent basal cusps of the second superior incisor.

The form of I$\overline{3}$ is much as in I$\overline{2}$, except that the external basal tubercle is relatively smaller and may be continuous with the lower end of the external lateral ridge.

The roots of the inferior incisors, one to three inclusive, increase progressively in size. In an individual tooth the root is distinctly longer than that of the corresponding tooth in *Felis atrox*. In I$\overline{1}$ the root is not only decidedly longer than that of the extinct true cat, but it is likewise noticeably broader in anteroposterior direction. It differs furthermore in being relatively and absolutely narrower transversely than in the latter type.

The roots of I$\overline{2}$ and I$\overline{3}$, when compared with those of *Felis atrox*, exhibit the same pronounced differences seen in I$\overline{1}$. In these teeth the greatest anteroposterior diameter of the fang occurs in its lower half.

The inferior canine, in contrast to that of the lion, is very small and weak. The crown is more recurved than that of *F. atrox*. This tooth exceeds I$\overline{3}$ in size by about as much as I$\overline{3}$ is larger than I$\overline{2}$. A median lateral ridge is developed which is turned backward at the inferior end as in I$\overline{3}$. In some cases the basal end of this ridge may appear as a prominent basal cusp. In the place of the external or postero-external ridge of I$\overline{3}$, there is a sharp ridge on the middle of the posterior side which may show faint crenulation. The inferior canine is often quite similar to I$\underline{3}$ in form. In the inferior tooth, however, the posterior ridge has a median position, while in I$\underline{3}$ the ridge is situated on the postero-external region of the crown. The two teeth approach each other in size.

The root of the inferior canine is longer and heavier than that of the third lower incisor and tapers more noticeably to the lower end. In its downward course it shows no tendency to curve outward as in the comparable tooth of *Felis atrox*.

In a series of 678 mandibles of the sabre-tooth cat in the collection of the Los Angeles Museum, 41, or approximately 6 per cent, showed the presence of P$\overline{3}$. This tooth may be present on both sides of the lower jaw or may be present on one ramus and absent on the other. The tooth, when present on both rami, may not have the same anteroposterior diameter. In L. A. Mus. specimen 2001-213, for example, that of the left side measures 10.2 mm. in length while the comparable tooth of the right side has a length of 6.5 mm. P$\overline{3}$ is single-rooted with the crown reduced. On the latter a median cusp may be present from which a rudimentary crest extends anteriorly and posteriorly. The orientation of the crests may be oblique to the fore and aft axis of the tooth-row as in No. 2002-R-60 (figure 12).

In development of median cusp and in the more or less distinct retention of anterior and posterior basal cuspules P$\overline{3}$ of *Smilodontopsis* from the Conard Fissure

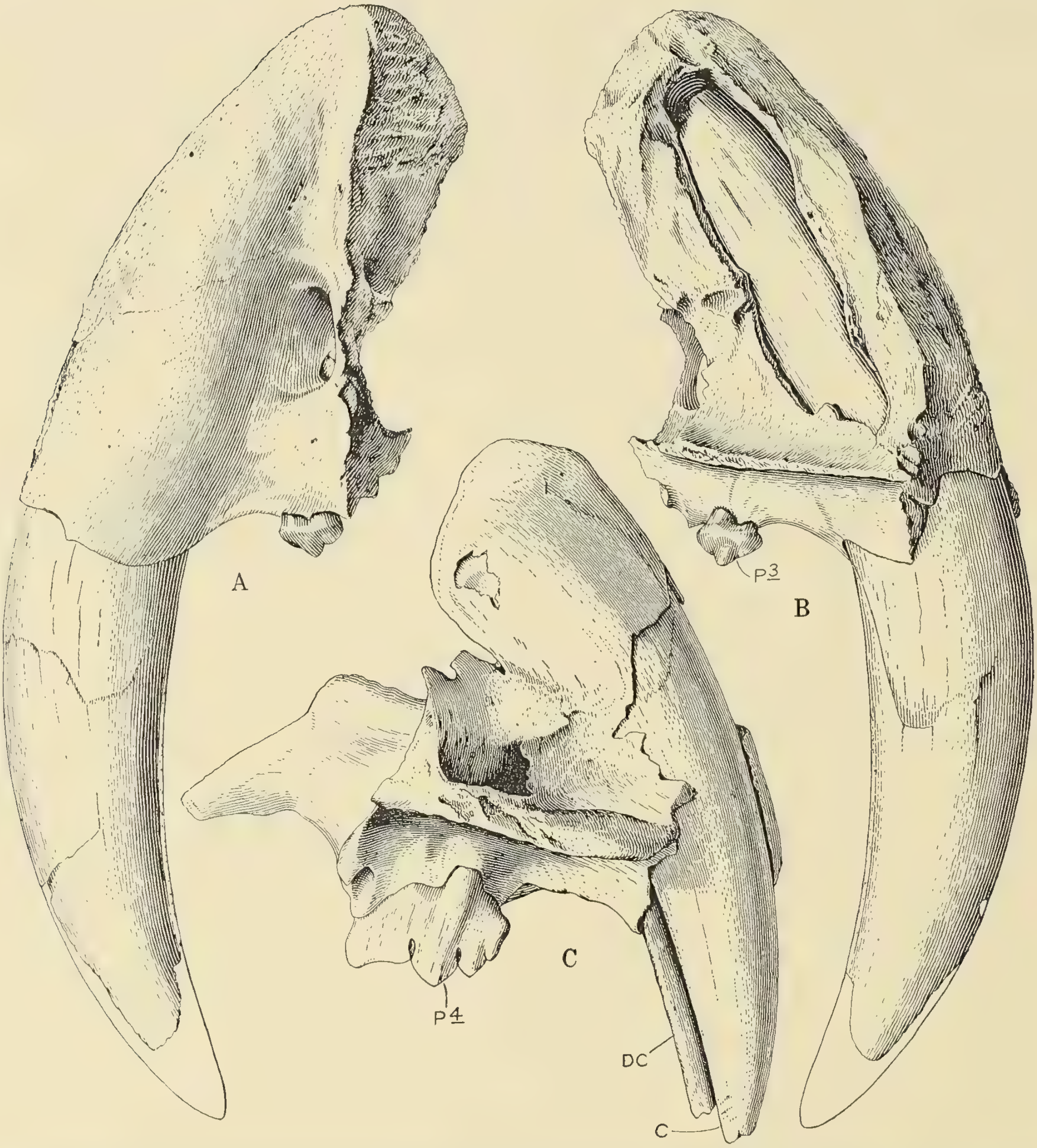

FIG. 15—*Smilodon californicus* Bovard. Specimens showing deciduous and permanent teeth. A, B, No. 2001-582, outer and inner views; C, No. 2001-583, inner view; × 2/3. *DC,* deciduous canine; *C,* permanent canine; $P\underline{3}$ and $P\underline{4}$, third and fourth premolars. Rancho La Brea Pleistocene.

Pleistocene appears less advanced than the comparable tooth in *Smilodon californicus.* Moreover this tooth may have been represented more persistently in the sabre-tooth from Arkansas than in the Californian form.

$P\overline{4}$ is a powerful tooth, only a little shorter than the inferior carnassial in anteroposterior diameter. It possesses well-developed anterior and posterior cusps and also a large posterior basal cusp. In many cases there is also a large tubercle on the postero-internal region of the cingulum, medial of the posterior basal tubercle. The roots may be relatively as long as those in *F. atrox.* The forward fang (plate 13, figs. 4, 4a) is longer and more slender than the hinder fang.

The crowns of P$\overline{4}$ and M$\overline{1}$ have a characteristic backward tilt .

On the inferior carnassial, as in later Tertiary sabretooth cats, the protoconid blade is considerably longer anteroposteriorly than the paraconid blade. The posterior border of the cingulum of this tooth nearly always bears a small heel. The anterior border of the paraconid in nearly all cases bears a small but distinctly separated cusp, as has been pointed out by Bovard (1907). This anterior cusp is sometimes entirely absent, but is commonly present and well developed. The base of the forward root in M$\overline{1}$ does not extend so far beneath the protoconid in *Smilodon* as in *F. atrox.* The roots are more slender than in the latter species and the posterior fang is shorter.

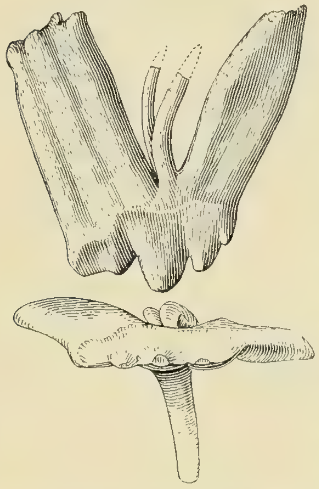

FIG. 16—*Smilodon californicus* Bovard, Dm$\underline{3}$, No. 2001-584; lateral and occlusal views; × 1. Rancho La Brea Pleistocene.

MILK DENTITION

A very large number of skeletons obtained at Rancho La Brea represent young individuals, and the milk dentition is well shown in many specimens.

In the upper milk dentition the form of the carnassial, Dm$\underline{3}$, corresponds in general to that of the permanent dentition. The paracone and metacone have about the same relative dimensions in anteroposterior diameter, the paracone is, however, a little more acute than in the permanent carnassial. The parastyle is well developed. The prostyle is usually distinctly developed, but as in the permanent carnassial it may also entirely disappear. As in the milk carnassial of some other carnivores there is a small but distinct tubercle developed on the antero-internal side of the tooth and some distance in front of the inner root.

The root system is essentially like that of P$\underline{4}$, except that the fangs are more widely divergent. The inner root, which is smaller in diameter than either the anterior or posterior root and is round or oval in cross-section, takes its origin opposite the base of the paracone and does not bear a basal tubercle (figure 16). It is much less removed from the inner side of the tooth than in Dm$\underline{3}$ of *Felis spelæa* (Dawkins and Sanford, 1868, pl. 13, fig. 1″). The anterior and posterior fangs are noticeably flattened transversely. All three curve inward in their upward course. As in P$\underline{4}$ a fourth root may be present, arising from the antero-external end of the posterior fang. This is usually slender, but it may bifurcate in its upward course.

The upper milk molar, Dm$\underline{4}$, is a triangular, three-rooted tooth nearly as large as the permanent molar. The inner root reaches somewhat nearer the median line of the palate than does the widely divergent inner root of the milk carnassial.

The enamel-covered portion of the upper milk canine (plate 12, figure 3) is relatively short, amounting only to about one-third of the total length of the tooth, while in the permanent canine the enamel extends somewhat more than half the length of the tooth. The disposition of the enamel on the crown is in its main

TABLE 6—*Measurements (in millimeters) of superior dentition of Smilodon*

	2001–24	2001–230	2001–225	2001–151	2001–77	2001–175	2001–111	2001–132	2001–288	2001–16	2001–181	2001–19	2001–65	2001–2	2001–5	2001–307	2001–311	2001–302	2001–90	2001–131	2001–4	2001–256	2001–113	2001–76	2001–148
Length from anterior end of canine alveolus to posterior end of P$\underline{4}$	126.3	118.9	*a*121	*a*120	120.3	.....	117.3	121.6	117.5	117.6	113.3	115.6	112.7	117.7	105.4	109.2	*a*107.7	*a*105	108.5	106.8	104.8	99.8	103.7	*a*102	97
Length from anterior end of P$\underline{3}$ to posterior end of P$\underline{4}$	63.7	60.6	*a*57.1	*a*58.5	58.1[1]	.....	58	55	54.3	58.3	52.5	60.7	53.8	57.5	.....	53	*a*53.8[1]	53.6[1]	56.7	55.9	53.3	54.5	51.2[1]	*a*48.8[1]	50.7[1]
Length of diastema from posterior end of alveolus for C to anterior end of alveolus for P$\underline{3}$	18	18.5	21.2	21.8	23.6	.....	19.3	21.2	18.8	19.8	17.7	13.8	13.8	17.5	11.5	17.8	15	12	12	7.8	12.8	10.2	15.1	15	12.4
I$\underline{1}$, greatest transverse diameter	7.6	6.6	6.9	7.5	.....	.....	6.9	7	6.4	7.1	6.4	7.4	6.4	7.3	6.7	6.3	6.3	5	.....	6.5	7	6	.....	6.3	.....
I$\underline{2}$, greatest transverse diameter	9.5	8.8	8.5	9.1	.....	.....	8.9	8.4	7.9	8.8	8.4	8.8	.....	9	8.5	8.2	8.5	7.7	7.6	9	9.7	.....	.....	7.9	7.6
I$\underline{3}$, greatest transverse diameter	13	12.9	12.4	12.5	.....	.....	11.2	11.6	12.5	11.5	11	12.6	.....	12	12.8	11.5	11.9	11.3	11.6	11.4	11.3	11.1	11.7	12	.....
$\underline{C}$, anteroposterior diameter of alveolus	46.1	44	43.7	41.7	41.4	.....	41.9	44.1	45.6	41.5	43	42.1	46.1	45	43.5	38.1	40	42.8	41	43	42.2	36	38.6	39	38.8
$\underline{C}$, transverse diameter of alveolus	22.9	21.7	24.1	22.2	18.8	.....	22.3	22.6	21.4	21.4	21.2	20.5	20.4	23	21	21.7	20.1	19.8	19.3	19.7	19.7	18.8	16.6	18	18
P$\underline{3}$, anteroposterior diameter	18.5	17.4	19	18	.....	.....	17.4	16.1	15.7	15.9	15.5	19.7	16.8	17.4	.....	15	.....	.....	17.9	18.5	16.1	16.1	.....	.....	.....
P$\underline{3}$, greatest transverse diameter	10.6	9.2	9.7	10.1	.....	.....	9.5	8.9	9.4	9	9.3	10.2	9.8	9.2	.....	8.4	.....	.....	8.7	9.1	8.8	8.4	.....	.....	.....
P$\underline{4}$, anteroposterior diameter	46	41.5	*a*39.5	41.6	39.5	.....	41.6	39	40	41.4	*a*37.3	42.7	38.8	41.4	41.6	40	.....	.....	42	41.7	41	37.9	37.8	*a*33.4	37.5
P$\underline{4}$, greatest transverse diameter across protocone	19.3	16	17.3	17.6	15.5	.....	15.3	16	16.3	16.7	15.7	19	15.8	16	19.9	15	.....	.....	15	18.3	17.4	15.9	14.5	14.2	16.8
P$\underline{4}$, anteroposterior diameter of base of paracone	13.7	12.8	11.2	.....	.....	.....	12	12.4	12	12.9	12	12.5	11.6	12.8	12.4	12.6	.....	.....	12	13	14.2	12	11.4	.....	11.1
P$\underline{4}$, length from base of paracone to anterior end of tooth	10.1	10.6	8	.....	.....	.....	11.5	10.9	9.7	10	.....	*a*9.4	9.6	10.2	10.2	9.9	.....	.....	*a*9	10	9.9	8.8	9.6	.....	9.2
P$\underline{4}$, length of metacone blade	15.2	16.5	.....	*a*15	.....	.....	15.2	14.6	13.4	*a*13.5	13.5	14.1	14.7	16.9	16.1	13.4	.....	.....	13.3	14.1	16.3	12.5	13.8	.....	11.5
Width of incisor series measured between outer sides of third upper incisors	63.5	61.4	58.5	58.3	.....	.....	59.3	58.3	.....	57.2	53.9	57.8	.....	57.6	55.9	54.9	.....	.....	51.9	.....	56.6	46.3	*a*49.2	50.5	.....

a, Approximate.

[1] Length from anterior end of aveolus for P$\underline{3}$ to posterior end of P$\underline{4}$.

features like that on the permanent tooth. The root is relatively long and is generally extremely wide anteroposteriorly. Its transverse diameter is relatively small, owing to the hollowing of the inner side to give place for the comparatively very large permanent canine. During a considerable part of the life of the milk canine a little less than half of the length of the tooth seems to have been exposed, and a large portion of the functioning region was not covered by enamel.

The nature of the milk canine and the generally primitive character in young animals of that portion of the mechanism of the skull which in adults is so highly specialized for stabbing indicate that the functions of the canines in young individuals were generally similar to the functions of the canines in true felines.

Owing to their great size, the development of the permanent canines has necessarily required an extraordinarily long growth period. These teeth are found to be represented by crowns 65 mm. in length in a kitten in which there is no evidence of formation of enamel for the crown of the permanent carnassial. The permanent canine was not erupted and in full function until the other teeth had begun to show some evidence of wear. It is therefore fair to assume that the peculiarly characteristic functions of the dentition of the sabre-tooth cat did not come into play until the animal had attained full maturity. With knowledge of the number of old animals showing loss of one or both canines through breakage, the period during which the peculiar mechanism of the animal was in active operation may perhaps be regarded as one of relatively short duration in a large percentage of cases; and the question may well be asked whether the degree of specialization exhibited here was not dangerously near the border line of over-specialization, or at any rate near the point where a slight change in environment might work a severe hardship.

The inferior cheek-tooth dentition includes two teeth, the anterior of which is followed by a permanent $P\overline{3}$ only in relatively few forms. In the milk carnassial the protoconid blade seems to be normally somewhat higher than the paraconid. Large metaconid and talonid cusps are present and show a noticeable tendency to project backward in most cases. The tooth anterior to the milk carnassial seems always to be tipped back against the milk carnassial, the root sloping backward strongly. The anterior margin of the principal cusp (protoconid) of this tooth may bear a minute basal tubercle or may be devoid of one. On the posterior border of the protoconid there is a broad posterior cusp and a basal cusp.

The milk incisors seem to have much the same structure as those of the permanent dentition. The inferior milk canine is considerably compressed transversely. The crown of this tooth is relatively small. A small but distinct tubercle is situated on the medial side of the principal cusp.

Notes on Skulls of Smilodon with Deciduous Canines Present or with Permanent Canines Partially Emerged

Skull No. 2001-10, plate 5—In this specimen the two deciduous canines are present.

Tip of the deciduous tooth is 62.8 mm. below outer alveolar border (measured in a straight line). This tooth measures 31.4 in anteroposterior diameter at base. Milk canines show very slight amount of wear at their tips, otherwise they have an unworn appearance. A considerable portion of the root region is exposed. Their inner sides are deeply concave.

Permanent canines are beginning to emerge in this specimen, that of right side having greater length of crown exposed than that of left. Approximately

TABLE 7—*Measurements (in millimeters) of inferior dentition of Smilodon*

	2002–72	2002–335	2002–324	2002–333	2002–350	2002–53	2002–443	2002–233	2002–32	2002–70	2002–213	2002–234	2002–103	2002–299	2002–338	2002–41	2002–52	2002–157	2002–292	2002–34	2002–365	2002–138	2002–69	2002–313	2002–104
Length from anterior end of C to posterior end of M$\overline{1}$	141.8	143.5	146.9	147.8	144.8	141.9	*a*143.6	138.4	*a*142	*a*140	141.7	135.6	134	134.9	136	135.8	129.4	129.7	127.3	128	126.5	119.9	113.5	114	115.7
Length from anterior end of P$\overline{4}$ to posterior end of M$\overline{1}$	57.8	56.4	57.9	60.9	54.7	54.4	55.6	55.4	*a*58	*a*51.5	55.5	52.8	54	51.4	56.5	55.6	55.9	52.6	53.2	48.4	52.7	51.7	48.3	49.3	52.8
Length of diastema measured between alveoli for C and P$\overline{4}$	65.5	68.5	71.8	69.3	69.7	69	72.6	65.3	65.3	70.4	53.8[1]	64	62.8	66.4	63.8	51.9[1]	55.9	60.3	60.7	59.3	60.6	51.2	*a*48	49.4	46.3
I$\overline{1}$, greatest transverse diameter	5	.....	.....	5.6	5	4.8	.....	5.2	5	5.5	.....	4.4	4.6	4.6	5.2	4.7	5.2	5	4.4	4.4	4.6	.....	.....	.....	.....
I$\overline{2}$, greatest transverse diameter	7.1	.....	.....	7.5	6.5	7.1	7.7	6.5	7.4	7.1	6.3	6.4	6.5	7	6.9	7.5	6.9	6.5	6.3	6.1	6.6	.....	.....	.....	.....
I$\overline{3}$, greatest transverse diameter	8.6	.....	.....	9	8.5	8.8	9	8.9	*a*9.2	9	8.4	7.5	8.3	8	8.9	8.8	.....	8.3	7.5	8	7.9	.....	.....	8.3	8
$\overline{C}$, greatest transverse diameter	10.5	.....	11.8	12.2	10.5	10.7	.....	11.2	9.8	10.2	11	9.7	10.3	10	11	10.7	.....	10.2	10.4	11.1	10.3	10.8	10.2	10.1	10.4
$\overline{C}$, greatest anteroposterior diameter at base of enamel	16	.....	15.3	14.7	14.6	15.7	.....	15.7	13	14.6	15.4	15.5	15.2	14.6	14.7	16.6	.....	16.1	13.4	14.2	13	14.1	13	13	14.7
P$\overline{3}$, anteroposterior diameter	.....	.....	.....	.....	.....	.....	.....	.....	.....	.....	L10.2 R 6.5	.....	.....	.....	.....	R 9.6	.....	.....	.....	.....	.....	.....	.....	.....	.....
P$\overline{3}$, greatest transverse diameter	.....	.....	.....	.....	.....	.....	.....	.....	.....	.....	L 7.1 R 5.7	.....	.....	.....	.....	R 7	.....	.....	.....	.....	.....	.....	.....	.....	.....
P$\overline{4}$, anteroposterior diameter	26	26.5	25	27.7	24.7	24.2	*a*26	24.9	25.6	22.5	23	24.2	*a*24.2	24	25.6	26.8	25.9	24.8	23.7	23.5	23.6	23.7	22.5	23.7	23.2
P$\overline{4}$, greatest transverse diameter	12.7	12.9	12	14.6	11.9	12	.....	12.3	12.1	.....	11.5	11.6	11.4	11.7	12.6	12.1	12.8	11.7	12	10.5	11.1	11.5	11.6	10.9	11.3
P$\overline{4}$, basal length of principal cusp	11.6	11	11	12.1	10.2	10	.....	11	10	10.7	10.1	9	10.9	9.4	9.8	10	9.6	10.4	9.6	9.2	10.5	9.7	9	9.4	10.5
M$\overline{1}$, anteroposterior diameter	32.1	29.4	30	*a*31.8	30	29.2	29.5	28.9	*a*30	28.5	29.6	27.9	28	27	30.1	27.7	30	28.4	29.3	25	27.8	26.7	27	25.9	27.4
M$\overline{1}$, greatest transverse diameter	16.1	15.4	14.7	17.6	14.4	14.5	15.2	14.1	14.3	15.4	14.5	13.5	12.8	13.5	13.9	13.4	15.7	13.3	14.6	12.4	13.7	12.9	13.8	12.8	14
M$\overline{1}$, length of protoconid blade	18	*a*15.5	16.8	15.4	16.1	15	17	15.1	.....	.....	15.5	15.1	14	14.3	15.8	14.3	15.8	16	15	12.8	14.8	14.8	13.9	13.8	16

a, Approximate.

[1] Length of diastema measured between alveoli for $\overline{C}$ and P$\overline{3}$.

25 mm. in length of crown is exposed on right side, whereas only 10 mm. of crown is exposed on left permanent canine. Serrations are sharp and clear-cut.

Permanent incisors are present. $P\underline{4}$ is almost completely emerged, that of right side slightly more than that of left. Very slight wear visible on inner side of metacone-blade in $P\underline{4}$, with even slighter indication on inner side of paracone-blade. $P\underline{3}$ is not completely emerged, although crown of this tooth extends for most part below alveolar border. $M\underline{1}$ was present.

Sutures of skull open and clearly defined.

Skull No. 2001–9—Deciduous canines are absent, but probably dropped from sockets during period of preservation. Permanent canines have emerged somewhat more than in No. 2001–10, with right one again, but only slightly, in advance of left. Right tooth measures approximately 47 mm. from tip of crown to inner alveolar border. Wide space present between outer wall of canine and outer wall of alveolus. Emergence of $P\underline{4}$ slightly more than in previous skull. Slightly more marked wear of inner surfaces of paracone and metacone blades in $P\underline{4}$ than in No. 2001–10. Sutures of skull open and clearly defined. Suture between basioccipital and basisphenoid open.

Skull No. 2001–7, plate 7—Milk canine present on left side with tip of permanent canine projecting down nearly as far as tip of milk tooth. Distance from tip of milk canine to outer alveolar border is 65.4 mm. in a straight line; greatest anteroposterior diameter at base is 31.2 mm.

Length in straight line from tip of permanent canine to inner alveolar wall is 67 mm.; anteroposterior diameter along alveolar border is 37.5 mm.

Cheek-teeth fully emerged; $P\underline{3}$ distinctly more so than in specimen No. 2001-10. Less wear on inner edges of paracone and metacone blades of $P\underline{4}$ than in No. 2001-9, but more than in No. 2001-10. Sutures open and well defined.

Skull No. 2001–8, plate 8—Deciduous canines absent. Permanent canines slightly farther emerged than in skull 2001–7, with right tooth slightly farther advanced than left. Length from tip of crown to inner border of alveolus of right tooth is 80 mm.; anteroposterior diameter of tooth measured at alveolar border is 29.7 mm. Permanent incisors and cheek-teeth present. Inner surfaces of paracone and metacone blades of $P\underline{4}$ exhibit a state of wear comparable to that in No. 2001–9.

Sutures open and clearly defined, including suture between basioccipital and basisphenoid.

Skull No. 2001–6, plate 9—Deciduous canines absent. Permanent canines more emerged than in 2001–8. Tip of right canine in straight line is 93 mm. removed from inner alveolar border; anteroposterior diameter of this tooth at alveolar border is 33 mm. Tip of right canine slightly worn (that of left canine is broken). In $P\underline{4}$ enamel surfaces along inner sides of paracone and metacone blades are deeply worn. Tip of principal cusp in $P\underline{3}$ slightly worn. Sutures open and clearly defined.

Skull No. 2001–3—Crown of permanent canine not quite fully emerged. Tip of canine not worn. Distance from tip of crown to inner alveolar border, measured in straight line, is 119.4 mm. Base of crown does not completely fill alveolus. Anteroposterior diameter at base of crown is 33.8 mm. Anterior and posterior upward extensions of enamel covered surface reach within alveolar wall. Between anterior and posterior tongues of enamel a small portion of external and internal surfaces, without enamel covering, extends for a short distance below alveolar rim.

Permanent incisors slightly worn. Paracone in $P\underline{4}$ well worn; prostyle and posterior end of metacone blade also worn.

Major sutures, including that in basicranial region between basioccipital and basisphenoid, still clearly defined.

Table 8—*Measurements (in millimeters) of skull of Smilodon (Skulls with deciduous canines or with permanent canines partially emerged)*

	2001–10	2001–7	2001–8	2001–9	2001–6	2001–3
Length from anterior end of premaxillary to posterior end of condyles	266.8	271	263.3	267.6	284.5	295.8
Basal length from anterior end of premaxillary to inferior notch between condyles	246.8	253.5	249.4	252.1	266.7	274.2
Length from anterior end of premaxillary to posterior end of inion	283	301.4	288.2	283.1	305.6	330
Length from anterior end of premaxillary to anterior end of posterior nasal opening	136.7	138.4	136.3	132.9	142.6	......
Length of palate from anterior end of premaxillary to line tangent to posterior surfaces of maxillary parapets	127.5	136	125.4	125.2	135	133.9
Length from posterior end of glenoid cavity to posterior end of condyles	80.4	74.7	75.6	79.8	81.2	90
Anteroposterior diameter of nasals	*a*78.5	77.5	76	70.6	......	84
Width of anterior nares	47.2	53	56.1	48.3	54.2	53.8
Greatest width across muzzle at canines	96.2	105.9	100.6	94	103.5	100.4
Least width between superior borders of orbits	*a*83.6	82.6	85.5	78.2	87.7	85.7
Width across postorbital processes	......	104.4	100.8	102	98.7	101.3
Least width of postorbital constriction	53	58.6	63.2	59.5	54.8	54.5
Greatest width across zygomatic arches	170.6	187	*a*185	180.3	182.7	192
Anterior palatal width between superior canines	53.3	49.5	48	43	48	52.7
Posterior palatal width between inner roots of superior carnassials	88.1	96.6	93.5	82.6	91.6	95.2
Width across palate between posterior ends of alveoli for superior carnassials	113.7	119.2	120	106	117	127
Greatest transverse diameter across auditory bulla, measured from foramen lacerum posterius to external auditory meatus	46.3	43.2	50.5	43.7	45.6	50.8
Greatest width across mastoid processes	120	123.7	124	116.7	122.9	121.5
Greatest diameter across condyles	64.7	61.6	60	62.4	59.3	64.6
Height of anterior zygomatic pedicle	48.6	58	52.9	55.2	50.3	53.1
Length of anterior zygomatic pedicle	47.5	51.7	50.4	50	50.7	49.8

a, Approximate.

Table 9—*Measurements (in millimeters) of superior dentition of Smilodon (Skulls with deciduous canines or with permanent canines partially emerged)*

	2001–10	2001–7	2001–8	2001–9	2001–6	2001–3
Length from anterior end of canine alveolus to posterior end of P$\underline{4}$	99	104.8	99	96.9	105.4	106.1
Length from anterior end of P$\underline{3}$ to posterior end of P$\underline{4}$	56	57.1	54.9	......	54.3	57.8
Length of diastema from posterior end of alveolus for C to anterior end of alveolus for P$\underline{3}$	13	13.6	13.6	13	15.3	13.2
I$\underline{1}$, greatest transverse diameter	6.6	7.6	......	......	6.8	6.9
I$\underline{2}$, greatest transverse diameter	8.4	9.6	8.5	......	8.1	8.4
I$\underline{3}$, greatest transverse diameter	12.2	12.7	11.8	11.6	10.4	12.1
$\underline{C}$, anteroposterior diameter of alveolus	33.2	35.5	34.4	35.3	37.8	37
$\underline{C}$, transverse diameter of alveolus	16.1	23.7	21.1	20.6	25.7	18.3
P$\underline{3}$, anteroposterior diameter	17.2	17.8	17.7	......	16.7	18.9
P$\underline{3}$, greatest transverse diameter	9.8	9.3	9	......	8.9	10
P$\underline{4}$, anteroposterior diameter	41	41.4	39.6	39.3	38.6	41
P$\underline{4}$, greatest transverse diameter across protocone	15.7	16.2	14.9	18.7	16.3	16.4
P$\underline{4}$, anteroposterior diameter of base of paracone	13	13.4	12.1	13.4	13.4	12.6
P$\underline{4}$, length from base of paracone to anterior end of tooth	10.3	10.3	10.5	10.1	8.7	11.4
P$\underline{4}$, length of metacone blade	16.7	16.9	15.9	15.5	15.6	16.1
Width of incisor series measured between outer sides of third upper incisors	56.8	60.3	54.5	52.3	56	56.3

TABLE 10—*Measurements (in millimeters) of ramus of mandible of Smilodon, based on specimens figured on plate 4*

	2002–L-4	2002–R-4	2002–R-68	2002–R-6	2002–R-781	2002–R-10	2002–R-496	2002–R-14	2002–R-16	2002–R-15
Length from anterior end of symphysis to posterior end of condyle	*a*95.4	97.4	116.7	129.5	142.3	161.4	169.2	193	204.4	217.8
Length from anterior end of outer flange to posterior end of condyle	.....	.....	.....	.....	134.4	150.1	159	181.5	192.9	205.6
Length of symphysis measured along anterior border	*a*27.4	28.5	33.3	*a*35.6	46.6	49.5	54.6	58.3	65.7	65.7
Least depth of ramus below diastema	17.8	16.7	21.4	20.6	26.2	29.7	25.6	29.7	38	32
Depth of ramus below posterior end of DM$\overline{4}$	22.8	20.5	28.1	28.2	32	33.6	32.3	.....	.....	.....
Depth of ramus below posterior end of M$\overline{1}$	.....	.....	.....	.....	.....	33.4	34.5	37.5	40.8	41.4
Thickness of ramus below DM$\overline{4}$	12.3	12.8	14.3	15.5	17.4	19.6	16.9	.....	.....	.....
Thickness of ramus below M$\overline{1}$	.....	.....	.....	.....	.....	19.2	19.1	20	21.3	19.8
Height from inferior border of angle to summit of condyle	.....	.....	20	26.4	24.8	28	31.6	31.8	31.7	38.7
Height from inferior border of angle to summit of coronoid process	*a*30.1	.....	35.8	46.8	48.7	51.5	57.8	60.6	67.9	73
Transverse width of condyle	.....	16.8	25.3	*a*26.6	28.2	32.2	32	38.4	42.8	52.2
Greatest depth of condyle	.....	8.7	10	12.6	12.9	15.6	15.6	17.5	19.4	16.7

a, Approximate.

TABLE 11—*Measurements (in millimeters) of inferior dentition of Smilodon, based on specimens figured on plate 4*

	2002–L-4	2002–R-4	2002–R-68	2002–R-6	2002–R-781	2002–R-10	2002–R-496	2002–R-14	2002–R-16	2002–R-15
Length from anterior end of DC to posterior end of DM$\overline{4}$	51.8	54.8	62.1	.....	.....	.....	.....	.....	.....	.....
Length from anterior end of DM$\overline{3}$ to posterior end of DM$\overline{4}$	28	28.9	30.9	27.8	30.2	32.7	30.1	.....	.....	.....
Length of diastema measured between alveoli for D$\overline{C}$ and DM$\overline{3}$	15.8	15.4	*a*18.7	24.6	28.7	27.1	36.2	.....	.....	.....
DC, anteroposterior diameter at base of enamel	7.7	8.3	9.3	.....	.....	.....	.....	.....	.....	.....
D$\overline{C}$, transverse diameter at base of enamel	5	5	5.5	.....	.....	.....	.....	.....	.....	.....
DM$\overline{3}$, anteroposterior diameter	11.5	12.2	13.4	12	13.1	14.9	12.4	.....	.....	.....
DM$\overline{3}$, greatest transverse diameter	5.1	5	5.4	5	5.3	6.5	5	.....	.....	.....
DM$\overline{4}$, anteroposterior diameter	17.8	18.3	19.4	16.3	17.7	18.7	17.8	.....	.....	.....
DM$\overline{4}$, greatest transverse diameter	7.1	7.3	7.3	6.5	6.5	8.9	6.8	.....	.....	.....
DM$\overline{4}$, length of base of protoconid	8.3	7.8	7.9	7.2	7.6	8.8	7.6	.....	.....	.....
Length from anterior end of DM$\overline{3}$ to posterior end of M$\overline{1}$	.....	.....	.....	.....	.....	.....	56	.....	.....	.....
M$\overline{1}$, anteroposterior diameter	.....	.....	.....	.....	.....	.....	25.7	26.1	30.5	*a*28.3
M$\overline{1}$, greatest transverse diameter	.....	.....	.....	.....	.....	.....	12.6	12.8	14.4	13.8
M$\overline{1}$, length of protoconid blade	.....	.....	.....	.....	.....	.....	13.4	12.4	15.6	15.8
P$\overline{4}$, anteroposterior diameter	.....	.....	.....	.....	.....	.....	.....	25.7	27.4	27
P$\overline{4}$, greatest transverse diameter	.....	.....	.....	.....	.....	.....	.....	11	12.5	12.2
P$\overline{4}$, basal length of principal cusp	.....	.....	.....	.....	.....	.....	.....	9.9	11.6	10.8
$\overline{C}$, greatest transverse diameter	.....	.....	.....	.....	.....	.....	.....	11	10.6	10.5
$\overline{C}$, greatest anteroposterior diameter at base of enamel	.....	.....	.....	.....	.....	.....	.....	16.7	14.8	14.3
I$\overline{1}$, greatest transverse diameter	.....	.....	.....	.....	.....	.....	.....	.....	.....	4.6
I$\overline{2}$, greatest transverse diameter	.....	.....	.....	.....	.....	.....	.....	.....	6.3	6.3
I$\overline{3}$, greatest transverse diameter	.....	.....	.....	.....	.....	.....	.....	.....	8.3	8
Length of diastema measured between alveoli for $\overline{C}$ and P$\overline{4}$	.....	.....	.....	.....	.....	.....	.....	50.3	60	66.5
Length from anterior end of P$\overline{4}$ to posterior end of M$\overline{1}$	.....	.....	.....	.....	.....	.....	.....	50.7	56	54
Length from anterior end of $\overline{C}$ to posterior end of M$\overline{1}$	.....	.....	.....	.....	.....	.....	.....	121.6	131.5	140.3

a, Approximate.

COMPARATIVE STUDY OF VERTEBRAL COLUMN AND LIMBS OF SMILODON AND FELIS ATROX

VERTEBRAL COLUMN

Vertebral Formula

The vertebral formula for *Smilodon* is usually C7, T13, L7, S3, Ca 13±. In other words, there is agreement between the sabre-tooth cat and the true felines in number of cervical, dorsal, and sacral vertebræ, and noticeable difference from such types as *Felis atrox* or the living lion and tiger in number of caudal vertebræ.

In several complete and incomplete vertebral series from Rancho La Brea, which have been assembled with considerable patience by J. W. Lytle, certain variations from the usual number of thoracic and lumbar vertebræ have been noted in *Smilodon.* Thus a type of column has been found by Mr. Lytle in which there are apparently 14 thoracic vertebræ and 7 lumbar vertebræ.[1]

The series possessing this peculiarity includes the vertebræ from the tenth thoracic to the sacrum inclusive. In other words, an additional thoracic vertebra is present. This variation in number of dorsal vertebræ is occasionally found in modern cats. A comparison of the series with one having the usual number of twenty dorsal vertebræ brings out the following relations:

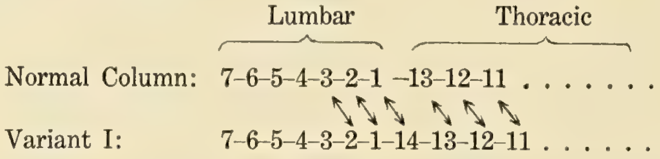
Lumbar
Thoracic
Normal Column: 7–6–5–4–3–2–1 –13–12–11 . . . .
Variant I: 7–6–5–4–3–2–1–14–13–12–11 . . . . . .

The arrows indicate resemblances between vertebræ in shape of neural spine, shape, size and direction of anapophysis. The fourteenth thoracic in the variant column differs from the first lumbar in the normal column in the presence of the capitular facet for a rib. The seventh lumbar vertebra in Variant I, while possessing several features characteristic of this segment in the normal column, differs from the latter in the peculiar form and size of the transverse processes and in the lowness of the neural spine.

Not only may the dorsal series be increased by one vertebra, but it may apparently be decreased also by one. In at least one individual from Rancho La Brea there are present behind the characteristic eleventh thoracic two additional thoracic vertebræ (twelfth and thirteenth) followed by six lumbar vertebræ. In this series the following relationships prevail:

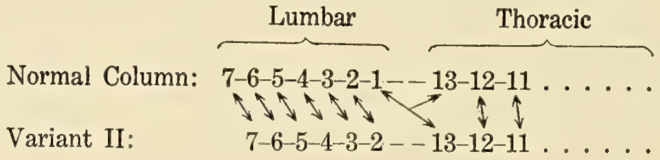
Lumbar
Thoracic
Normal Column: 7–6–5–4–3–2–1– – 13–12–11 . . . . . .
Variant II: 7–6–5–4–3–2 – – 13–12–11 . . . . . .

---

[1] It should be indicated that only in a few instances has it been found possible as yet to reassemble and articulate the vertebræ belonging to a single individual, furnishing thereby conclusive proof as to the number of vertebræ present in the column from the atlas to the sacrum inclusive. In the examples cited in which variations from the usual type of column occur, the number of thoracic and lumbar vertebræ is based on the recognition of certain "key vertebræ." Thus the eleventh or anticlinal vertebra in the dorsal series exhibits in its transformation of attitude of zygapophyses a character which readily distinguishes this segment from all other thoracic vertebræ. The twelfth also has several structural features clearly distinguishing this element in the thoracic series.

The arrows indicate similarity between individual vertebræ. The six lumbar vertebræ present in Variant II resemble the last six vertebræ in the normal column in progressive reduction of the anapophyses, in general shape of the neural spines and in type of transverse processes. The last thoracic vertebra in Variant II, presumably the thirteenth of the series because it is the second segment behind the vertebra having the characteristic structural features of the eleventh, appears to combine in a measure the characters of the first lumbar and thirteenth thoracic vertebræ of the normal column. A resemblance to the first lumbar is suggested by the shape of the anapophysis and perhaps by the shape of the neural spine. Moreover, when the first lumbar (second) and last thoracic (thirteenth) of Variant II are compared in front view, the metapophysis in the latter is seen to be heavier than that in the former. This relationship holds also for the metapophyses of the second lumbar (second) and first lumbar (first) in the normal column. The last thoracic in Variant II resembles the thirteenth thoracic of the normal column, particularly in the presence of the capitular facet for the rib.

Thus with regard to the variation in number and in type of dorsal vertebræ observed in *Smilodon*, the following vertebral formulæ presumably should be recorded:

7 — 13 — 7 — 3 — 13±
7 — 14 — 7 — 3 — 13±
7 — 13 — 6 — 3 — 13±

In *Felis atrox* the number of vertebræ in the cervical, thoracic, lumbar and sacral regions agrees with that of the modern lion and tiger, and may be recorded as follows:

7 — 13 — 7 — 3 — 21±

No complete series of caudal vertebræ has been obtained for a single individual of either the sabre-tooth or *Felis atrox* and the actual number of segments comprising these series can not be stated therefore with certainty. It is, however, clearly apparent that the number in *Smilodon* was distinctly less than that in *Felis atrox*. Presumably the number in the latter species approached that in *F. leo* or in *F. tigris*.

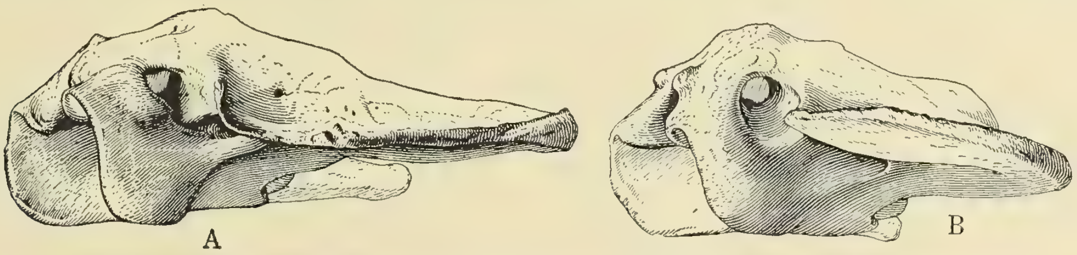

Fig. 17—Atlas viewed from the antero-external side. A, *Smilodon californicus* Bovard, No. 2038-11; B, *Felis atrox* Leidy, No. 2936-1; × 1/2. Rancho La Brea Pleistocene.

CERVICAL SERIES

Plate 16, figs. 1 to 4

Considerable dissimilarity exists between the sabre-tooth and the modern lion in the cervical series. In view of the essential similarity of the series between *Felis atrox* and *F. leo* there is likewise a noteworthy difference in this region of the column between the two dominant feline types from Rancho La Brea. Contrasting features are discussed more fully under the description of the individual vertebræ. The striking differences relate to the form of the transverse processes and the inferior lamellæ, suggesting quite clearly, as appreciated by Matthew (1910, pp. 296-297), a scalene musculature for the sabre-tooth which functioned somewhat differently from that in the lion. Viewed from above the transverse processes in the vertebræ posterior to the axis project farther out from the bodies of these segments in *Smilodon* than in *Felis*. The neural arch in the last three vertebræ particularly appears to be narrower in anteroposterior extent in the sabre-tooth than in *Felis atrox*. The neural spines increase progressively in length from the third to seventh vertebra inclusive as in the modern lion. The posterior spines do not show the peculiar bifurcation of the tip seen in *F. atrox*. In at least some individuals of the latter species the spines are relatively short.

ATLAS

Plates 17 and 34, figs. 4 to 7

The most striking difference between *Smilodon* and *Felis atrox* in the atlas is seen in the shape of the transverse processes. In the sabre-tooth the processes reach well behind the posterior articulating surfaces for the axis. In their backward extent they taper rapidly and at the posterior end where the inner and outer borders meet an acute angle is formed. The posterior end is, however, rounded. Occasionally specimens have the posterior end broadened laterally. The inner surface of the individual process is wide dorsoventrally and extends directly backward and outward from the outer end of the articulation for the axis. The anterior border of the process is deflected sharply upward. In *Felis atrox* the transverse process resembles in shape that of the large living cats and is broader transversely than in *Smilodon*. The process reaches but little behind the posterior border of the facet for the axis. The postero-internal border of the process is indented adjacent to the articulating surface.

The shape of the transverse process in *Smilodon* is subject to considerable variation, as seen in specimens available from the asphalt. In typical specimens the shape is like that in the figured atlas, No. 2038–5. In other specimens the process may be quite broad, both anteriorly and posteriorly, as in No. 2038–2. The dorsal surface may be flat or broadly concave, particularly when the border turns upward. The foramen transmitting a blood-vessel from the vertebrarterial canal to the neural canal may lie within the anterior portion of the vertebrarterial canal and be obscured from lateral view or it may lie in advance of this canal.

The contact surface for the axis may be narrower, in the direction taken normal to the vertical axis of the facet, in *Smilodon* than in *Felis atrox*. The surface within the neural canal, articulating with the odontoid process, is deflected sharply from the posterior articulation. The anterior articulation for the condyles of the skull is not so wide as in *F. atrox*, but is deeper than in the latter form. The median tuberosity on the dorsal surface of the neural arch is less prominent in *Smilodon* than in the true felines. The neural arch is longer in anteroposterior diameter in *Smilodon* and at the forward margin is less deeply indented than in the extinct true cat. In its forward extent it is deflected downward more than in the latter. On the ventral surface of the floor of the neural canal the median posterior tubercle for the *longus colli* muscle is heavy but may not project so prominently as in *F. atrox*. A broad excavation is present on each side of the ventral surface.

TABLE 12—*Measurements (in millimeters) of atlas of Smilodon*

	2038–1	2038–2	2038–3	2038–4	2038–5	2038–6	2038–7	2038–8	2038–9	2038–10
Greatest width across transverse processes	189.6	193	158.7	168.1	156.7	148.6	152.4	140.5	135.5	138.2
Greatest width of anterior end across articulation for condyles of skull	79.7	87.9	87.3	85.3	88.5	83	73.7	77.6	73.9	72.7
Greatest width across outer borders of articulation for axis	84.6	88.4	80.6	80.3	82.2	78	79.1	71.8	70.7	70.1
Length from anterior end of articulation for condyles to posterior end of articulation for axis	86	82.1	85.8	80.1	85.9	75	80	77.9	69.8	72.9
Length of neural arch along median line	45.4	39.2	42	39.2	46.7	39.4	42	38.5	36.9	36.4
Length of inferior arch along median line	33.4	28.1	30.4	26.9	31.3	24.9	31.6	29.7	24.3	26.1
Greatest length of transverse process, taken oblique to fore and aft axis of vertebra	111.8	100.2	107.8	106.8	98.6	102.4	89.9	92.7	80.1	74.8
Greatest height from ventral surface of inferior arch to dorsal surface of neural arch	56.7	56.6	54.8	51.7	53.3	50.1	54.9	50	46.0	50.7

TABLE 13—*Measurements (in millimeters) of atlas of Felis atrox*

	2936–1	2936–2	2936–3	2936–4	2936–5	2936–6	2936–7	2936–8	2936–9	2936–10
Greatest width across transverse processes	181.8	168.7	186.7	173.2	170.5	169.6	166.4	162	156.1	144.8
Greatest width of anterior end across articulation for condyles of skull	88.6	83.6	95	85.1	86.4	86.9	82	83	75.6	71
Greatest width across outer borders of articulation for axis	83.5	81.4	86.4	86.9	81.8	81.8	79.5	81.9	78.8	67.2
Length from anterior end of articulation for condyles to posterior end of articulation for axis	81.3	81.1	92.8	86.4	79.8	82.6	73.3	78.4	76.6	73.5
Length of neural arch along median line	39.7	34.3	42.2	33.6	36	36.7	34.4	34.4	32	31.2
Length of inferior arch along median line	30	22.6	35	25.6	26.9	29.3	27.2	24	22.4	24.6
Greatest length of transverse process, taken oblique to fore and aft axis of vertebra	73.2	70	74.8	67.7	67.7	66.8	67	66.4	58.8	58
Greatest height from ventral surface of inferior arch to dorsal surface of neural arch	57	54.5	52.7	58.5	53.8	57.3	55.3	54.9	50.9	47.4

The groove between the postero-internal border of the transverse process and the ventral border of the facet for the axis, which in *Felis* is broad and clearly defined, is only faintly discernible in *Smilodon*, where it notches the postero-internal border.

The neural canal, when viewed from the posterior side (plate 17, fig. 6), is more sharply defined ventrally and is less capacious than in *F. atrox*. The posterior opening of the vertebrarterial canal is situated immediately adjacent to the outer edge of the facet for the axis. In *Felis* it is situated in the recess adjacent to the facet. The opening may be smaller in *Smilodon* than in *F. atrox*. The depression in front of the anterior opening of the canal is noticeably deeper in the sabre-tooth, but is not so broad in that form as in the latter. In the latter a broad ridge separates the ventral depression from the dorsal opening into the neural canal. In the sabre-tooth a deep groove may extend from the lower depression to the upper foramen (fig. 17).

AXIS

Plates 17 and 34, figs. 1 to 3

In the second cervical vertebra of the sabre-tooth, the neural spine projects decidedly backward with reference to the position of the posterior zygapophyses. The crest line of the spine is straight. The anterior projection of the spine is shorter in *Smilodon* than in the extinct true cat type and does not overhang the anterior opening of the neural canal to the extent seen in the latter form. Between the posterior end of the spine and the posterior zygapophysis the posterior border is broadly indented. In *Felis atrox* this border is sinuous. The pedicle of the neural arch is broader anteroposteriorly in the sabre-tooth than in the true felines. The odontoid process is relatively short and heavy. The anterior articulating surface for the atlas faces more directly forward and less outward than in *F. atrox.* There is a greater expanse of bone between the anterior opening of the vertebrarterial canal and the posterior border of the transverse process, the opening being situated closer to the articulation for the atlas. The transverse process in *Smilodon* extends relatively not so far back but somewhat more ventrally, with reference to the lower rim of the posterior face of the centrum. The process may have a sharper termination in *Smilodon* than in *F. atrox.*

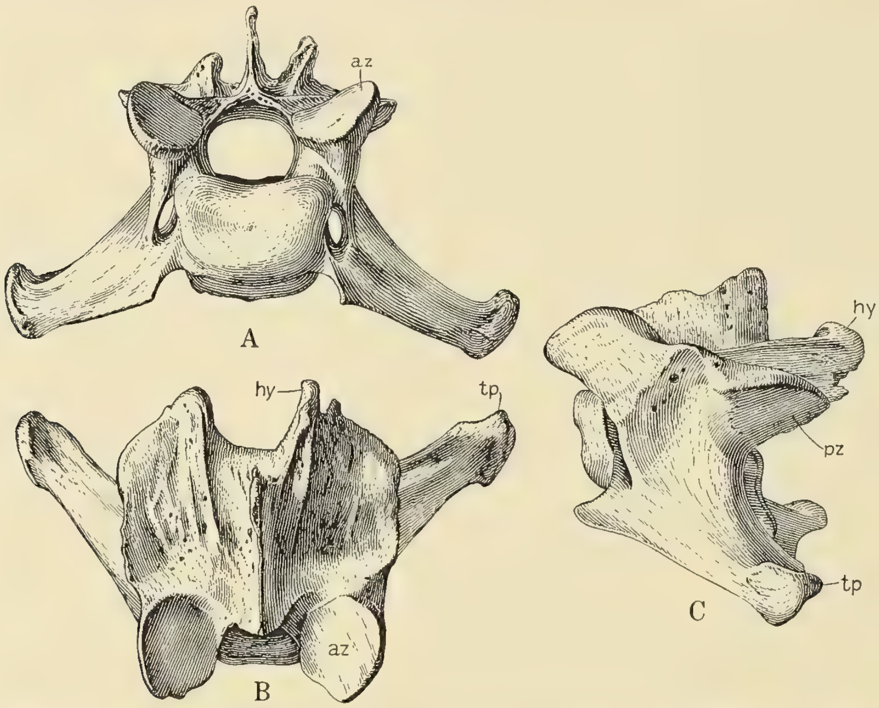

FIG. 18—*Smilodon californicus* Bovard. 3d cervical vertebra, No. 2040-2. A, anterior view; B, dorsal view; C, lateral view; × 1/2. *az,* anterior zygapophysis, *pz,* posterior zygapophysis, *tp,* transverse process, *hy,* hyperapophysis. Rancho La Brea Pleistocene.

The neural canal, as viewed from the posterior end, is triangular in cross-section and with rounded corners. The canal is narrower dorsally than in the extinct true feline. The great overhang of the neural spine is a noticeable feature in posterior view and presents a structure totally unlike that in the true felines. In *Felis atrox* the laminæ are carried backward and the rugose posterior surface

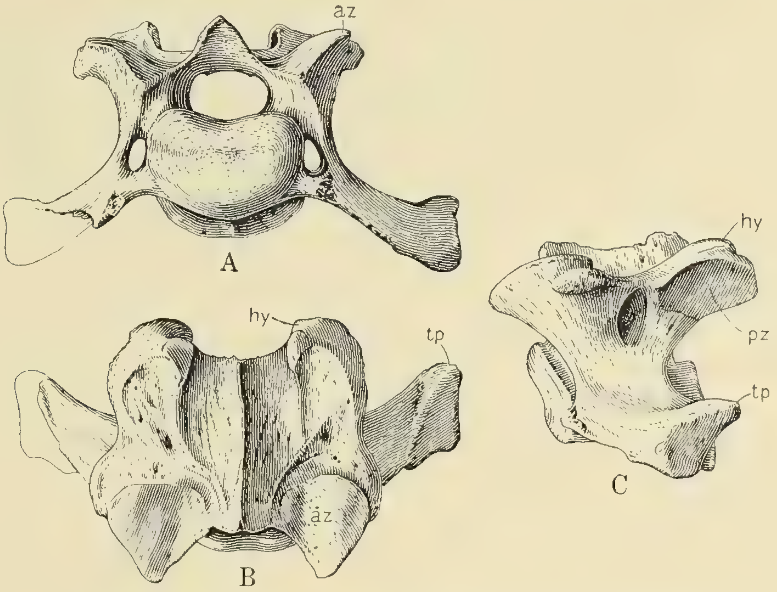

FIG. 19—*Felis atrox* Leidy. 3d cervical vertebra, No. 2938-1. A, B, C, same views as in figure 18; × 1/2. Rancho La Brea Pleistocene.

TABLE 14—*Measurements (in millimeters) of axis of Smilodon*

	2039–1	2039–2	2039–3	2039–4	2039–5	2039–6	2039–7	2039–8	2039–9	2039–10
Greatest length of neural spine	120.5	120.2	117.9	115.6	116.9	115.9	116.4	98.8	101.9	89.1
Greatest width of posterior end of neural spine	38.3	......	45.1	42	33.7	38	28.6	30.7	26.5	22.5
Length of centrum along median line measured parallel to lower surface from posterior end to tip of odontoid process	102.9	107.2	108.5	105.1	107	98.7	97.7	91.8	82.8	86.9
Depth of centrum measured normal to floor of neural canal and across posterior epiphysis	26	32.1	30	30	31.9	26.6	27	26.7	21.1	21.8
Greatest transverse width across posterior epiphysis of centrum	41.8	44.3	47	45.8	44.8	42.4	41	40.6	39.1	36.9
Width across articulating surfaces for atlas	77	81.7	84.2	80.6	80.7	76	75.7	70.2	67.6	63.6
Width across outer ends of transverse processes	92.4	116	102.7	107.7	105	93.8	92.9	93.5	89.4	94
Width across posterior zygapophyses	65	71.5	70.8	67.7	63	63.1	53.4	58.7	55.6	45.1
Distance measured in median line from lower border of posterior epiphysis of centrum to top of posterior end of neural spine	90	101.1	103.3	100.8	102.5	92.5	89.4	94.6	77.5	81.4

forms a deep cavity, encroaching well upon the smooth surface of the roof of the neural canal. In *Smilodon* the upper end of the overhanging portion of the spine is broad transversely. The great width of the end of the neural spine is very well shown in dorsal view (plate 17, figure 1).

The flattening of the dorsal surface of the posterior portion of the neural spine may extend forward for a considerable distance in some specimens. In No. 2039–12 the flattened surface is noticeably broad and tapers forward, extending well toward the anterior end of the neural crest. In a single specimen, No. 2039–11, the enlarged posterior portion of the spine is divided by a deep cleft into two parts.

Table 14a—*Measurements (in millimeters) of axis of Felis atrox*

	2937–1	2937–2	2937–3	2937–4	2937–5	2937–6	2937–7	2937–8
Greatest length of neural spine	111	*a*100.2	102.4	100.8	.....	88.1	108.2	99.9
Greatest width of posterior end of neural spine	54	47.3	53.4	47	48.3	41.5	43	50.6
Length of centrum along median line measured parallel to lower surface from posterior end to tip of odontoid process	99.8	95.9	101.1	96.1	87.9	85.5	103	103.7
Depth of centrum measured normal to floor of neural canal and across posterior epiphysis	29	30.6	28.7	27.8	24.8	24.4	29.3	30.7
Greatest transverse width across posterior epiphysis of centrum	47	47.8	45.3	44.3	39.8	39	46.8	46
Width across articulating surfaces for atlas	81.1	85.6	81.5	74.4	67.5	67.3	80.5	77.7
Width across outer ends of transverse processes	*a*93	*a*98	*a*89	.....	79.4	77	95.5	*a*94
Width across posterior zygapophyses	68.8	61.7	67.1	62	60.3	58	69.6	65.4
Distance measured in median line from lower border of posterior epiphysis of centrum to top of posterior end of neural spine	97.3	100.5	91	95.4	79.4	73.8	97.6	97.8

a, Approximate.

Third Cervical Vertebra

The centrum of the third cervical vertebra is deeper in comparison to its width in *Smilodon* than in *Felis atrox* (figs. 18, 19). The posterior epiphysis does not possess the ellipsoidal shape seen in the latter form. The neural canal may be relatively wide transversely. The neural spine may be considerably reduced in size and the remnant of the spine may be as low as or lower than the spine in *Felis atrox*. Two tubercles (hyperapophyses) are frequently present on the dorsal surface between the posterior zygapophyses and may project well beyond the posterior border. These tubercles appear to be much better developed in the sabre-tooth than in *F. atrox*.

The pedicle of the neural arch is distinctly narrower transversely than in the great true feline. At approximately the middle of the outer surface of the lateral wall of the canal there is frequently to be seen in the third cervical vertebra of *Felis atrox* a deep depression of varying size, at the forward end of which is a foramen through which a blood-vessel penetrates the bone. A similar depression is lacking in *Smilodon*, although small nutrient foramina are to be seen in this region. The transverse process is decidedly longer and more slender than in the true felines. The outer extremity of the process is small and shows slight bifurcation.

Table 15—*Measurements (in millimeters) of third cervical vertebra of Smilodon*

	2040–1	2040–2	2040–3	2040–4	2040–5	2040–6	2040–7	2040–8	2040–9	2040–10
Length from end of anterior zygapophysis to end of posterior zygapophysis	75.9	74.4	72.4	73.3	72	74.4	65.9	63.8	66.1	63.2
Greatest length from ends of anterior zygapophyses to ends of hyperapophyses	90.9	83.2	88.8	83.9	72	79.3	68.1	69.9	78.7	68.6
Length of centrum measured normal to posterior face and along median line	52	49.4	52	51.2	50.2	49.6	48.6	46.5	44.8	42.8
Width across anterior zygapophyses	69.6	64.6	67	61.4	64	63.1	57.8	56.9	56.2	53.8
Width across posterior zygapophyses	78.5	74.9	73.8	73	75.9	69.1	62.4	61.7	62.3	58.2
Greatest width of neural canal at anterior end	27.6	23.4	25.2	23.1	23.5	25	22.7	21.5	23.9	21.4
Greatest transverse width of posterior epiphysis of centrum	48.9	47	42.6	44.3	43.8	44.6	45	40.6	40.5	38.4
Greatest width across outer ends of transverse processes	148.6	141	129.1	128.1	126.8	134.9	137.3	118.6	113.8	108.3
Greatest length of transverse process from outer end to end of antero-internal projection of inferior lamella	77.7	80	83.2	76.6	75	74.2	66.2	64.9	70.1	66.3
Height from median posterior border of centrum to top of neural crest	*a*76	81.2	65.4	66.4	69.3	68.9	65.8	56.4	51.6	55.6
Depth of centrum measured normal to floor of neural canal and across posterior epiphysis	28.5	31	27.6	27.3	28.8	27.9	28.5	25.5	26.3	25.6

a, Approximate.

FOURTH CERVICAL VERTEBRA

The centrum of this vertebra is again relatively deeper in *Smilodon* than in *Felis atrox*, and the neural canal may be fully as large as in the latter form. The length of the dorsal surface, as measured from the end of the anterior zygapophysis to the end of the posterior zygapophysis, is relatively greater in the sabre-tooth than in *F. atrox.* The neural spine is situated at the front end of the neural arch and rises higher than in the great lion-like cat. The two tubercles or processes (hyperapophyses) lying posteriorly and between the posterior zygapophyses are well developed but less pronounced than in the third cervical vertebra. These processes are better developed than in the true felines. The anterior zygapophyses appear to be directed slightly more toward the inner side and less upward than in *F. atrox.* Likewise, the posterior zygapophyses are directed slightly more outward and backward and less downward than in the latter type. Rudimentary hypapophyses may be present in *Smilodon.*

When viewed from the front, the pedicle supporting the neural arch is relatively narrower transversely in the sabre-tooth. A deep and well-defined depression on the outer wall of the arch is present in *F. atrox* (fig. 21C). In *Smilodon* the depression is not so striking or is absent. The vertebrarterial canal is large. The transverse process is longer and on the whole more slender in *Smilodon* than in the true felines. The bifurcation of the outer end of the process is perhaps more clearly marked in the sabre-tooth, but the lower flange or lamella is not so deep as in *Felis atrox.*

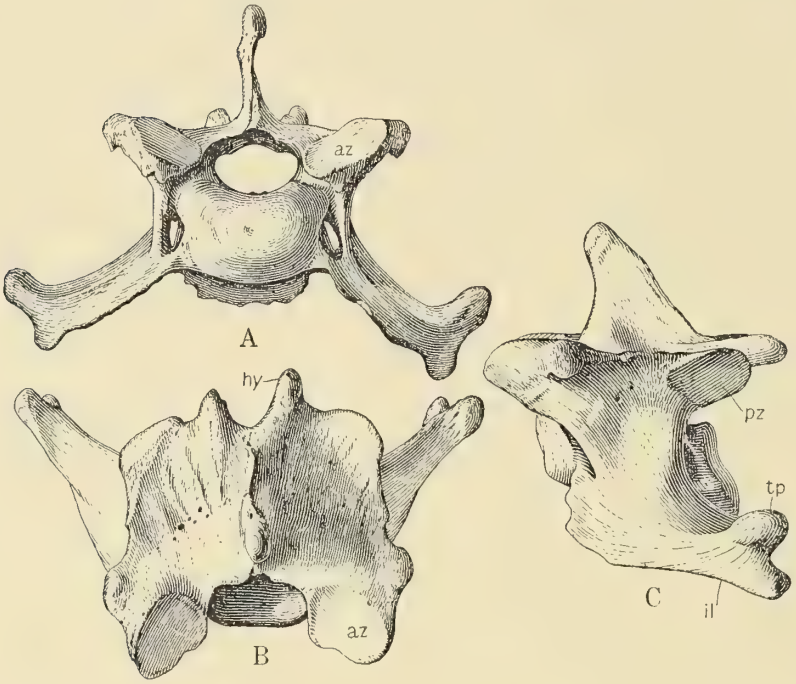

FIG. 20—*Smilodon californicus* Bovard. 4th cervical vertebra, No. 2041-8. A, anterior view; B, dorsal view; C, lateral view; × 1/2. *az*, anterior zygapophysis, *pz*, posterior zygapophysis, *tp*, transverse process, *hy*, hyperapophysis, *il*, inferior lamella. Rancho La Brea Pleistocene.

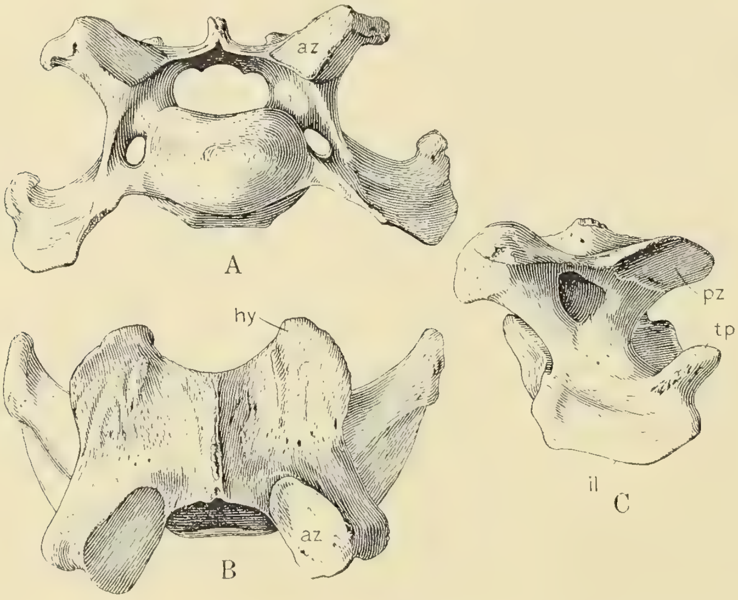

FIG. 21—*Felis atrox* Leidy. 4th cervical vertebra, No. 2939-1. A, B, C, same views as in figure 20; × 1/2. Rancho La Brea Pleistocene.

Table 16—*Measurements (in millimeters) of fourth cervical vertebra of Smilodon*

	2041–1	2041–2	2041–3	2041–4	2041–5	2041–6	2041 7	2041–8	2041–9	2041–10
Length from end of anterior zygapophysis to end of posterior zygapophysis	74.8	78.1	78.4	80.3	73.6	64.7	70.4	69.3	60.1	60.3
Greatest length from ends of anterior zygapophyses to ends of hyperapophyses	83.6	85	85	89.8	81.1	79	72.8	78.7	72.8	63.1
Length of centrum measured normal to posterior face and along median line	49.3	50	48.4	52.9	46.7	46.5	46.3	45.3	41.5	39.5
Greatest width across anterior zygapophyses	94.1	84.4	85.2	84.3	83	81.1	80.5	80.1	74.2	70
Width across posterior zygapophyses	84.8	83.4	84.8	79.5	73.3	70.2	78.7	78.4	74.9	65.3
Greatest width of neural canal at anterior end	35	28.2	26.2	27.5	28.4	27.5	24.5	25.9	25.6	25
Greatest transverse width of posterior epiphysis of centrum	45.7	43.5	47	44.1	47.9	43.6	41.5	42	37	36.7
Greatest width across outer ends of transverse processes	137.1	143.7	141.3	137.3	141.4	130.4	133.3	127.3	116.3	105.7
Greatest length of transverse process from outer end to end of antero-internal projection of inferior lamella	77.9	72.5	65.4	74.6	66.7	64.4	66.1	69.6	58.5	55.9
Height from middle of ventral border of posterior epiphysis of centrum to top of neural spine	99	105.3	102.1	93.2	96.6	95.4	90	88.9	83.1	80.1
Depth of centrum measured normal to floor of neural canal and across posterior epiphysis	29.7	29.5	28.9	26.9	28.9	26.3	27	29.8	23.8	22.6

Fifth Cervical Vertebra

The centrum is deeper than in *Felis atrox*. On the ventral surface a median keel is defined and the hypapophyses are more prominent than in the latter. The neural canal is relatively wide transversely and narrow dorsoventrally. The principal axis of the vertebrarterial opening, as viewed from the front (fig. 22A), is inclined less from the vertical than in *F. atrox*. The pedicles supporting the neural arch are slightly narrower than in *Felis* and are also shorter. The ends of the anterior zygapophyses are carried downward farther in front than in the extinct true feline and reach a level with the anterior upper border of the centrum. The dorsal surface of the vertebra is again longer in the sabre-tooth and the spine reaches to a greater height than in *F. atrox*. In the latter form the end of the spine is expanded transversely and the tip may be bifurcate.

While a well-marked depression may occur on the outer wall of the neural canal, it does not attain the size and depth seen in the great lion-like cat. The lateral processes exhibit considerable difference from those of the latter form. In *Felis atrox*, as in the modern cats, the transverse process is short, but the inferior lamella is deep, particularly at the forward end. In *Smilodon* the transverse process is long and projects considerably outward and backward. The inferior lamella has an entirely different shape from that in the true felines (see fig. 22B and fig. 23B). Its greatest depth is reached posteriorly where it extends well below the ventral surface of the centrum. The anterior border is nearly straight and extends obliquely downward to meet the ventral border.

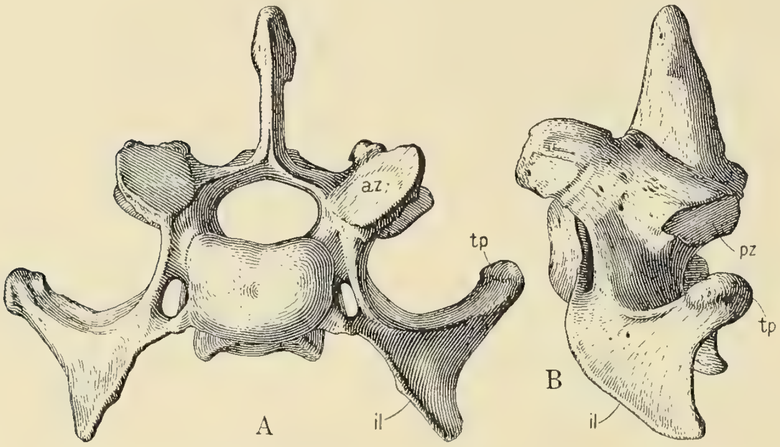

FIG. 22—*Smilodon californicus* Bovard. 5th cervical vertebra, No. 2042-5. A, anterior view; B, lateral view; × 1/2. *az,* anterior zygapophysis, *pz,* posterior zygapophysis, *tp,* transverse process, *il,* inferior lamella. Rancho La Brea Pleistocene.

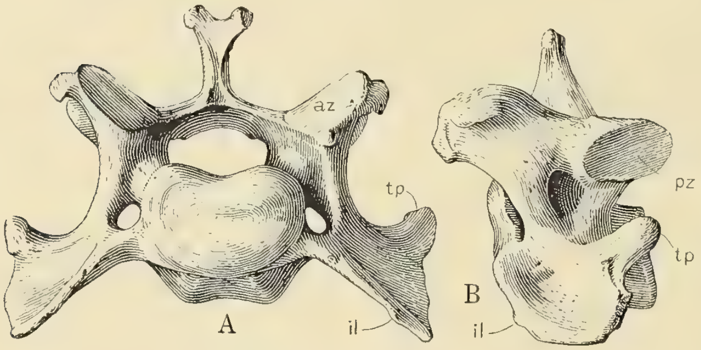

FIG. 23—*Felis atrox* Leidy. 5th cervical vertebra, No. 2940-1. A, B, same views as in figure 22; × 1/2. Rancho La Brea Pleistocene.

SIXTH CERVICAL VERTEBRA

The centrum is relatively deep and the vertebrarterial canal is large. The neural canal is relatively wide, but narrow dorsoventrally. The dorsal surface of the vertebra is comparable in length to that of *F. atrox.* The neural spine rises to greater height in *Smilodon* than in the true cat. In the latter, the end of the spine is broadened laterally and may show signs of a bifurcation. Immediately behind the anterior zygapophysis and situated on the dorsal surface is a tubercle from which a low ridge extends posteriorly. The anterior zygapophyses are narrow transversely and between them the anterior end of the dorsal surface is deeply excavated. The outer wall of the neural canal exhibits externally a broad depression in which are lodged several nutrient foramina, but a prominent fossa as in the Rancho La Brea great cat is not formed.

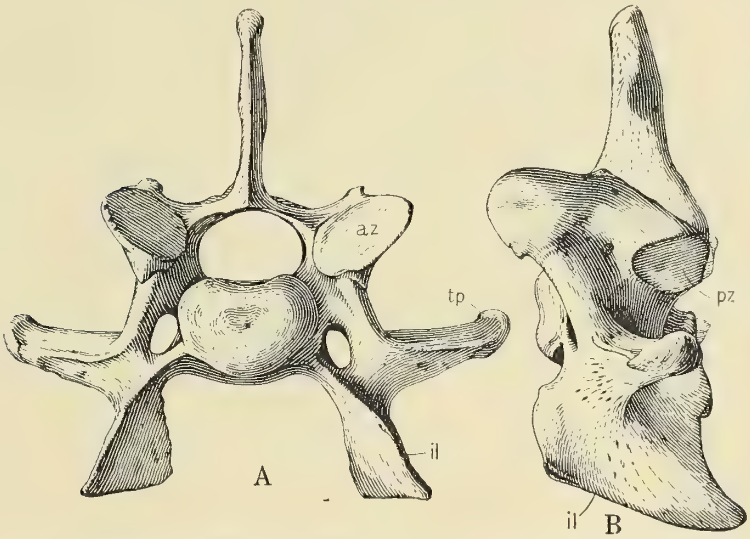

Fig. 24—*Smilodon californicus* Bovard. 6th cervical vertebra, No. 2043-4. A, anterior view; B, lateral view; × 1/2. *az*, anterior zygapophysis, *pz*, posterior zygapophysis, *tp*, transverse process, *il*, inferior lamella. Rancho La Brea Pleistocene.

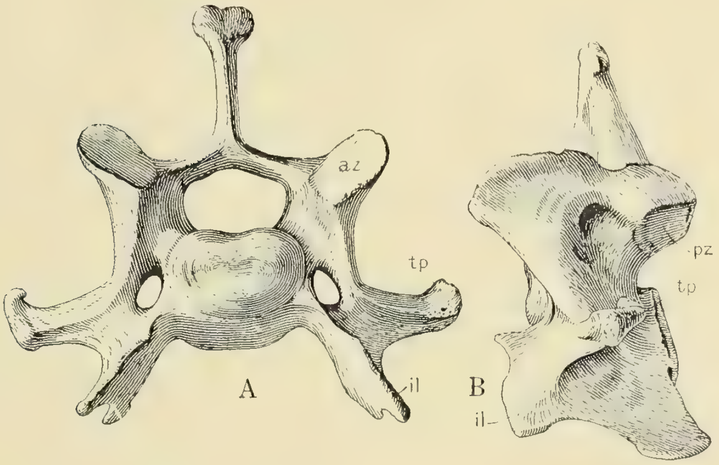

Fig. 25—*Felis atrox* Leidy. 6th cervical vertebra, No. 2941-1. A, B, same views as in figure 24; × 1/2. Rancho La Brea Pleistocene.

The transverse process extends farther outward and slightly backward in the sixth cervical vertebra of *Smilodon* than in that of the true felines. Its outer end is, however, not so tuberous as in the latter. The inferior lamella or plate forms a parallelogram and extends farther below the ventral surface of the centrum in *Smilodon* than in the great lion-like cat. Furthermore, the lamella extends more directly downward and less outward than in the latter form. The lower anterior edge flares slightly outward. Viewed from the side (fig. 24B), the lower border of the lamella is seen to be straight. In the true felines a notch is frequently present on the lower border and separates the lamella into two parts. In several specimens of *Felis atrox* a distinct notch is absent and the lower border may be straight or slightly concave.

TABLE 17—*Measurements (in millimeters) of fifth cervical vertebra of Smilodon*

	2042–1	2042–2	2042–3	2042–4	2042–5	2042–6	2042–7	2042–8	2042–9	2042–10
Length from end of anterior zygapophysis to end of posterior zygapophysis	64.8	66.2	69	64.8	62.5	69.5	65.5	54.9	56.6	54.9
Length of centrum measured normal to posterior face and along median line	45.7	43.5	42.7	43.6	41.9	41	44	38.2	36.8	38.3
Greatest width across anterior zygapophyses	86.4	82.1	86.3	87.7	79.6	81.7	81.9	74.9	70.5	71.5
Width across posterior zygapophyses	83	81.4	88	89.4	82.3	84.1	88	69.8	80.2	69.2
Greatest width of neural canal at anterior end	31.5	30.1	32.9	31	29.5	31.3	31.1	29.4	24.5	30.7
Greatest transverse width of posterior epiphysis of centrum	44.5	45.3	43.4	40.8	43.6	37.9	41.7	39.6	39.4	39.4
Depth of centrum measured normal to floor of neural canal and along median line of posterior epiphysis	30.2	26.9	28	26.4	29.5	26.3	28.9	23.8	25.9	25
Greatest width across outer ends of transverse processes	150.6	157.3	143	143.4	136.6	133.4	135.3	122.7	116	125.4
Greatest distance from end of transverse process to lower posterior end of lamella	51.4	43.6	44.1	52	49.2	32.5	47.9	37.4	40.4	41
Height from middle of ventral border of posterior epiphysis of centrum to top of neural spine	106.5	107.7	109.4	101.8	100.6	96.2	95.1	96.6	83.6	80.2

TABLE 18—*Measurements (in millimeters) of sixth cervical vertebra of Smilodon*

	2043–1	2043–2	2043–3	2043–4	2043–5	2043–6	2043–7	2043–8	2043–9	2043–10
Length from end of anterior zygapophysis to end of posterior zygapophysis	62.5	63.7	62.3	61.3	62.8	53.5	59.5	53.4	55.1	49.1
Length of centrum measured normal to posterior face and along median line	39.9	42.4	37.1	41.9	42	36.9	38.9	35	35.7	34
Greatest width across anterior zygapophyses	89.5	84	85.7	81.7	79.3	80.2	76.8	70.6	73.8	*a*73.8
Width across posterior zygapophyses	86	85.1	83.6	81.1	79.4	75.1	76.1	71.2	75.5	68.9
Greatest width of neural canal at anterior end	33.9	32.7	32.8	31	33	37.2	32.3	32.4	33.3	33
Greatest transverse width of posterior epiphysis of centrum	40	41.8	38.6	39.9	39.4	37.3	41.4	36.5	37.1	35.2
Depth of centrum measured normal to floor of neural canal and along median line of posterior epiphysis	27.5	26.6	23.9	26.2	28.1	26.3	27.3	26.7	24.2	23.5
Greatest width across outer ends of transverse processes	141.7	144.9	138.2	132.6	131.7	125.4	126.3	117	119	111.3
Greatest width across inferior lamellæ	*a*98	107	97.9	91.4	*a*105	80.1	90.4	85.5	76.4	75
Greatest length of inferior lamella measured along lower border	77.7	58.9	50.5	63	64.5	46.7	65.2	53	48.9	50.6
Height from middle of ventral border of posterior epiphysis of centrum to top of neural spine	116	*a*110	117.2	110	108.8	108.2	93.4	91.8	102	89.4

a, Approximate.

SEVENTH CERVICAL VERTEBRA

The ventral surface of the centrum is somewhat depressed or concave on each side of a low median ridge. The concave surfaces and the intervening ridge extend back to the posterior epiphysis. The surfaces are frequently marked by low sharp ridges which extend anteroposteriorly. In the extinct true feline, on the other hand, no distinct median ridge is formed and the posterior half of the ventral surface is broadly convex transversely. Slight as these characters may appear to be, they have been found useful in distinguishing the seventh cervical vertebræ of *Smilodon* and *Felis atrox* in the Rancho La Brea collections. Another distinguishing feature of value in separating these vertebræ at first glance is presented by the dorsal surface. In *Smilodon*, a low ridge or a series of small tubercles extends straight backward from the postero-inner end of each anterior zygapophysis. In *F. atrox*, this ridge is absent and a low but prominent tubercle situated on the dorsal surface of the posterior zygapophysis is separated from the posterior border of the anterior zygapophysis by an open groove or channel.

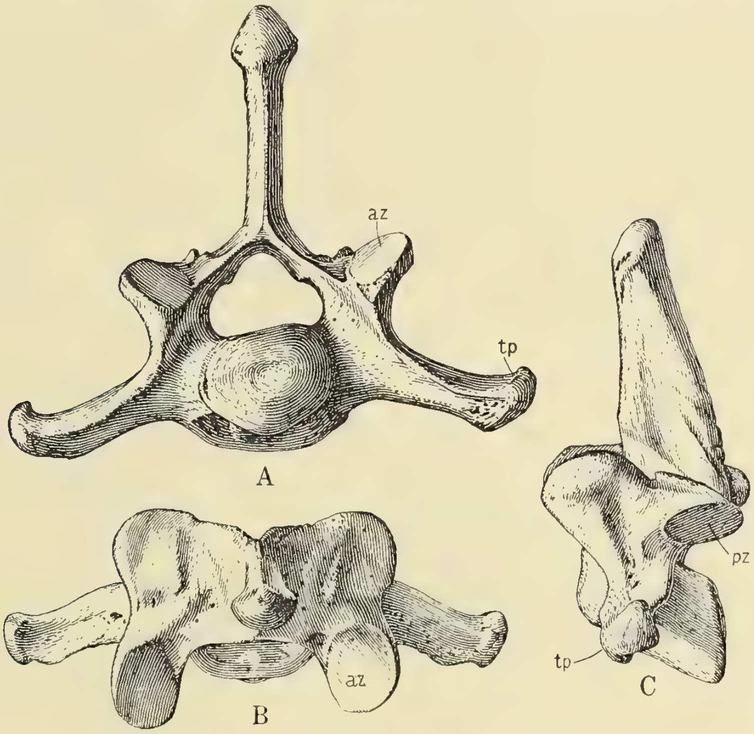

FIG. 26—*Smilodon californicus* Bovard. 7th cervical vertebra, No. 2044-6. A, anterior view; B, dorsal view; C, lateral view; × 1/2. *az*, anterior zygapophysis, *pz*, posterior zygapophysis, *tp*, transverse process. Rancho La Brea Pleistocene.

The neural spine is relatively heavy in *Smilodon.* The spine in typical specimens widens transversely below the dorsal end. The anterior zygapophyses appear in general to be narrower transversely than in *F. atrox* and extend farther forward with reference to the anterior face of the centrum. These differences, however, are not clearly evident in the figured specimens. The neural canal may be subtriangular in outline. The pedicle supporting the neural arch, as seen from the front (fig. 26A), appears to be slightly narrower in the sabre-tooth than in *F. atrox.* The transverse processes are distinctly longer and more slender than those of the Rancho La Brea true cat and their outer ends are not so heavy as in the latter form.

In a series of approximately 570 specimens representing the seventh cervical vertebra of *Smilodon,* at least 18 show evidences of a vertebrarterial canal. In five of these specimens a closed vertebrarterial canal is present on each side. The diameter of the canal may vary in size from 2.5 mm. to 16.3 mm. Seven specimens have the canal only on the right side, four only on the left. Two specimens exhibit a partial closing of the canal by development of a process extending inward and downward (No. 2044–11) or by the development of an inferior lamella extending down from the outer ventral surface of the centrum (No. 2044–12).

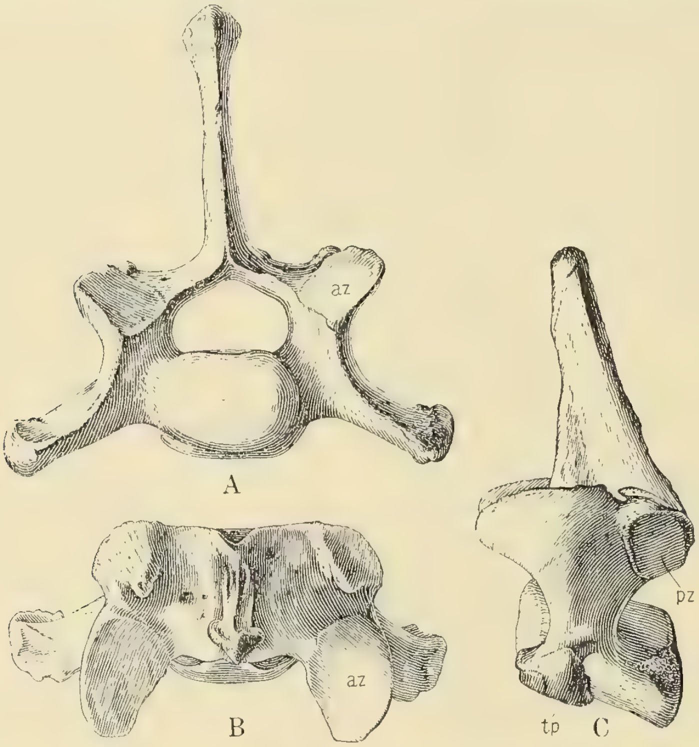

Fig. 27—*Felis atrox* Leidy. 7th cervical vertebra, No. 2942-1. A, B, C, same views as in figure 26; × 1/2. Rancho La Brea Pleistocene.

The position of the vertebrarterial canal when enclosed is always lower with reference to the centrum in the seventh vertebra than in the preceding vertebræ. The canal in nine vertebræ is closed by a bar of bone which extends outward from the ventro-external margin of the centrum to the transverse process. In one specimen, No. 2044–13, a well-defined suture is present where the contact is established with the transverse process. Several variations occur in the development of processes below the vertebrarterial canal. An inferior lamella may be present, as in specimen No. 2044–14, which extends well below the lower bar enclosing the canal. In specimen No. 2044–15 the inferior lamella, in contrast to the thin plate-like structure in preceding vertebræ, is quite thick and heavy. In this specimen, also, a small process extends forward and slightly inward and downward from the anterior border of the lower bar.

The twenty or more specimens of the seventh cervical vertebra of *Felis atrox* available from Rancho La Brea show none of the variations relating to the closing of the vertebrarterial canal and to the structures adjacent to this canal as seen in *Smilodon*.

TABLE 19—*Measurements (in millimeters) of seventh cervical vertebra of Smilodon*

	2044–1	2044–2	2044–3	2044–4	2044–5	2044–6	2044–7	2044–8	2044–9	2044–10
Greatest height measured from ventral border of posterior epiphysis of centrum to tip of neural spine......	137.1	132	130	123.6	128.2	123.1	118.1	107.5	105.1	101.4
Length of centrum measured normal to surface of posterior epiphysis and along median line...............	40.8	39.2	40.4	39.3	35.5	36.3	36.6	36	37.7	33.8
Depth of centrum measured normal to floor of neural canal and across posterior epiphysis.................	29.3	24.7	29.8	27.8	28.4	27.4	25	25.5	26.7	27.8
Greatest transverse width of posterior epiphysis of centrum....................	43.2	41.5	42.8	41.7	42.8	44.6	39.2	40.6	41.4	42
Width across transverse processes.....................	139.1	137.5	138.9	134.6	135.2	138.4	126.3	131.4	129.6	117.3
Width across anterior zygapophyses.................	88.6	83.4	81.1	84.6	78.4	76	79.2	71.9	82.9	71.5
Width across posterior zygapophyses.................	87.7	78.4	77.6	83.1	75.7	73.3	73.4	70.2	75.5	70.4
Length from ends of anterior zygapophyses to ends of posterior zygapophyses....	65	62.7	59	64.2	55.7	57.7	59	53.4	57.4	53
Greatest dorsoventral diameter of neural canal at anterior end..............	26	24.5	26	24.5	22.6	22.5	20.5	21	24.7	18.5

TABLE 20—*Measurements (in millimeters) of seventh cervical vertebra of Felis atrox*

	2942–1	2942–2	2942–3	2942–4	2942–5	2942–6	2942–7	2942–8	2942–9	2942–10
Greatest height measured from ventral border of posterior epiphysis of centrum to tip of neural spine......	132.7	*a*111.4	119.8	103.7	113.4	115.3	114.7	......	......	......
Length of centrum measured normal to surface of posterior epiphysis and along median line...............	38.6	38.5	41.9	34.5	36.9	34.6	35	37.6	36.2	36.6
Depth of centrum measured normal to floor of neural canal and across posterior epiphysis.................	29	29.9	31	24.4	25	25	27	31.9	31.2	31
Greatest transverse width of posterior epiphysis of centrum....................	45.4	42.6	47.9	37.5	39.6	37.5	43	45.8	45	42.6
Width across transverse zygapophyses.................	118	119.4	123.8	111.2	104.3	104	112.4	120.1	123.5	*a*117
Width across anterior zygapophyses.................	81	79.4	88	74.7	79.3	71.9	77.7	82.3	83.7	85.1
Width across posterior zygapophyses.................	75.3	76.4	84.1	69.5	73.9	69.5	69.9	75	75.4	77.4
Length from ends of anterior zygapophyses to ends of posterior zygapophyses....	57.4	57	59.2	53.3	53	50.8	55.5	59.8	63	57.3
Greatest dorsoventral diameter of neural canal at anterior end..............	21	19.5	23.7	21.2	21	21.3	20.7	21.4	20.8	18.6

a, Approximate.

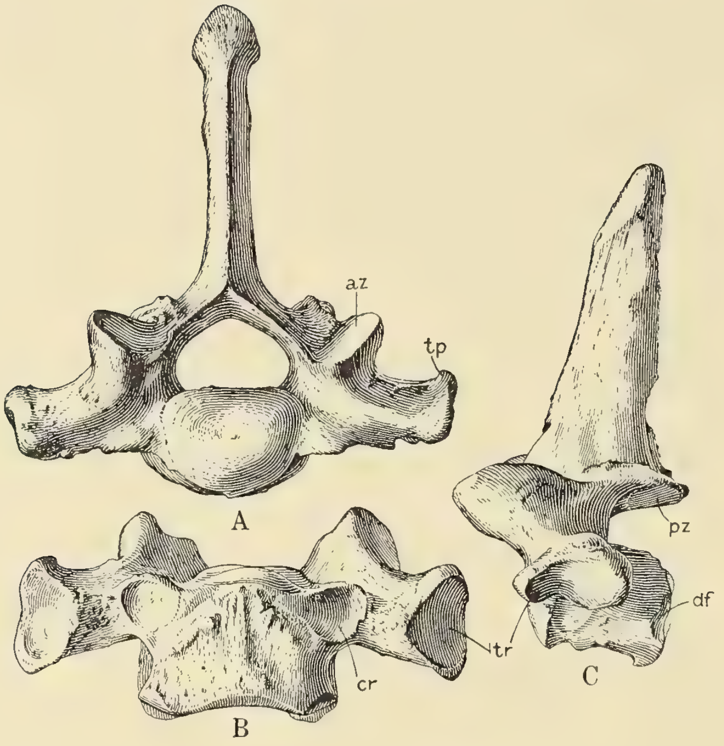

Fig. 28—*Smilodon californicus* Bovard. 1st thoracic vertebra, No. 2045-4. A, anterior view; B, ventral view; C, lateral view; × 1/2. *az,* anterior zygapophysis, *pz,* posterior zygapophysis, *tp,* transverse process, *tr,* facet for tuberculum of rib, *cr,* facet for capitulum of rib, *df,* demifacet. Rancho La Brea Pleistocene.

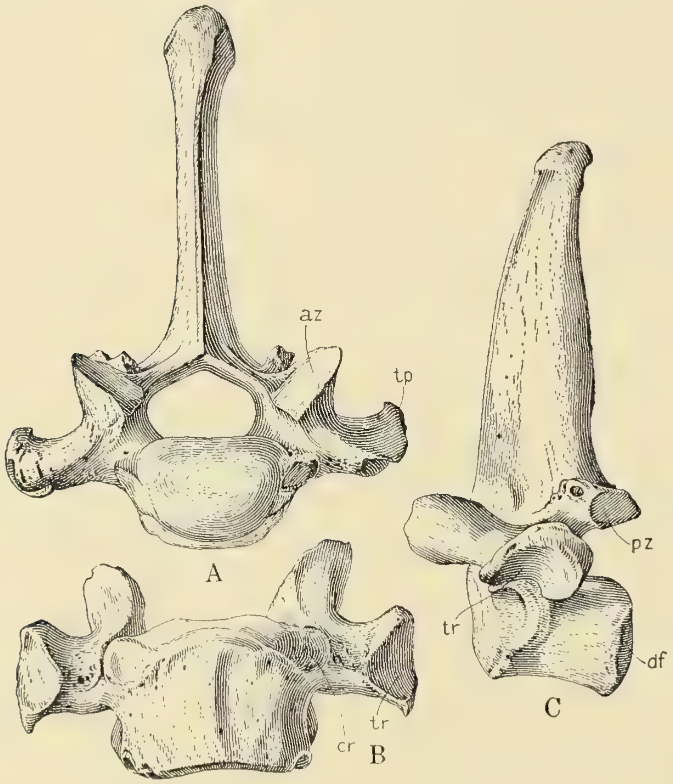

Fig. 29—*Felis atrox* Leidy. 1st thoracic vertebra, No. 2943-1. A, B, C, same views as in figure 28; × 1/2. Rancho La Brea Pleistocene.

THORACIC SERIES

Plates 18 and 19, figs. 1 and 2

In comparing the thoracic series of *Smilodon* with a series of the modern lion, having approximately the same total length, less difference is to be noted than exists in either the cervical or lumbar series of these types. The differences which exist in this region of the column involve to less extent structural details and are concerned primarily with the proportions of individual parts. In the sabre-tooth the segments are heavier, as revealed particularly by the greater breadth as measured across the centrum and transverse processes. The neural spines are likewise somewhat sturdier than in *F. leo*, but their length may not be appreciably different from, or may be actually less than that in the latter species. The centra in the sabre-tooth are relatively shorter anteroposteriorly than in the lion. This is particularly evident in the last two thoracics, the shortening here foreshadowing, as it were, the persistent shortness of the elements comprising the lumbar series. The facets for articulation of the ribs are also larger in the sabre-tooth than in the lion.

Table 21—*Measurements (in millimeters) of thoracic vertebræ of Smilodon*

Vertebræ	1	2	3	4	5	6	7	8	9	10	11	12	13
Length from end of anterior zygapophyses to end of posterior zygapophyses	60.3	57	57.2	56.4	60.7	58.7	58.2	57.4	60.8	57.6	61	65.5	73.5
Length of centrum measured normal to posterior face and along median line	36.7	34.7	34.8	35.5	35.1	35	34.5	34.9	34.8	34.5	38.7	40	41.3
Greatest width across anterior zygapophyses	74.5	55	45.1	40.8	38.8	38.4	37.5	35.9	33	32.7	33.6	37.7	27.8
Greatest width across posterior zygapophyses	50	46	41.6	39.3	39.9	40.6	38.2	34.8	34.6	36	36.4	26.4	34.4
Height of neural canal at anterior end	20.6	18.7	16.4	15	15.9	15	17.2	17.6	18.2	18.1	16.1	16.8	14.4
Greatest transverse width of posterior face of centrum across capitular facets	48	52.7	54	50.6	50.3	50.5	53.3	51.3	48.6	50.5	....	.....	...
Depth of centrum measured normal to floor of neural canal and along median line of posterior epiphysis	28	28.8	28.8	28.5	28.2	28.5	27.8	27.7	28.7	28.9	29.9	29.7	30.5
Greatest width across outer ends of transverse processes	110.6	93.3	*a*89	82.3	85.2	85.5	84.5	80.6	*a*77	78.7	73	59.1	60.5
Greatest anteroposterior diameter of outer end of transverse process	26.6	24.5	26.3	20	20.2	21.4	21.3	23	24.1	23.1	29.3	.....	.....
Height from middle of ventral border of posterior epiphysis of centrum to top of neural spine	*a*116.2	127.3	124.4	123.5	119.8	117.6	115.8	110.4	101.6	95.8	93.2	67.7	94
Length of spine from middle of notch between anterior zygapophyses to top measured parallel to anterior end	*a*74.4	86.1	93.3	98.9	95.7	95.2	96.5	99.8	92.5	85	76.9	.....	48 9
Greatest width across metapophyses	......	.....	.....	.....	.....	.....	.....	.....	.....	....	....	*a*66	67.9
Greatest width across outer ends of anapophyses	......	.....	.....	.....	.....	.....	.....	.....	.....	....	....	53.5	65
Greatest width of posterior epiphysis of centrum	......	.....	.....	.....	.....	.....	.....	.....	.....	....	41.9	41.8	42.8
Greatest length from end of metapophyses to end of anapophyses	......	.....	.....	.....	.....	.....	.....	.....	.....	....	....	48.2	67.7

a, Approximate

First Thoracic Vertebra

The centrum of the first thoracic vertebra, when measured posteriorly, generally exhibits a slightly greater depth in *Smilodon* than in *Felis atrox*. A distinct median keel on the ventral surface is present, and immediately adjacent to this

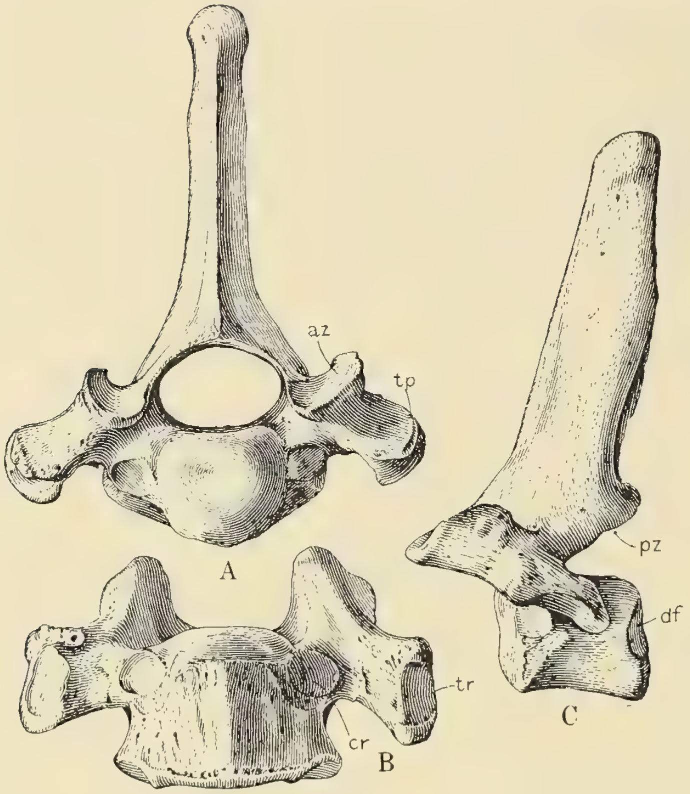

Fig. 30—*Smilodon californicus* Bovard. 2d thoracic vertebra, No. 2046-3. A, anterior view; B, ventral view; C, lateral view; × 1/2. Processes and facets as in 1st thoracic vertebra. Rancho La Brea Pleistocene.

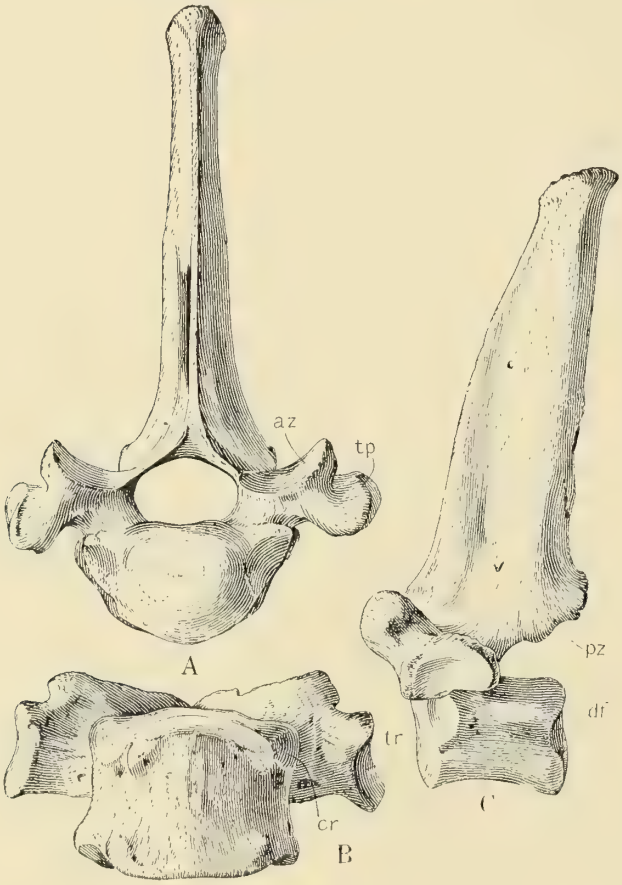

Fig. 31—*Felis atrox* Leidy. 2d thoracic vertebra, No. 2944-1. A, B, C, same views as in figure 30; × 1/2. Rancho La Brea Pleistocene.

ridge the surface is concave transversely. In the latter, the median ridge of the centrum is not so distinct and the surface adjacent to it on either side is not depressed to the extent seen in the sabre-tooth. The transverse processes are noticeably longer in *Smilodon* (fig. 28B) and differ also from those of *F. atrox* in their slight backward trend. The capitular facet (*cr*) is usually broader in the sabre-tooth and faces more toward the ventral side and less toward the outer side than in *F. atrox*. The neural spine is strongly developed and may be slightly expanded transversely at the tip. In most specimens the spine is relatively not so wide anteroposteriorly as in *F. atrox*. When viewed from the side the anterior border of the spine is seen to be slightly convex, straight or slightly concave in its upward extent. The anterior profile of the spine in *F. atrox* is broadly convex in its upward sweep from the neural arch to the tip and readily distinguishes this element from that of the sabre-tooth. Large nutrient foramina, which are frequently to be seen perforating the dorsal surface of the neural arch between the zygapophyses in *F. atrox*, are as a rule not so conspicuous in *Smilodon*. The height of the neural canal is greater in the sabre-tooth than in *F. atrox*. The anterior zygapophyses may be well developed in *Smilodon* and may be directed less steeply toward the median line than in the former type.

TABLE 22—*Measurements (in millimeters) of first thoracic vertebra of Smilodon*

	2045–1	2045–2	2045–3	2045–4	2045–5	2045–6	2045–7	2045–8	2045–9	2045–10
Length from end of anterior zygapophysis to end of posterior zygapophysis	67.8	64.6	61.3	60	57.5	61.6	58.2	56.1	55.2	57.4
Length of centrum measured normal to posterior face and along median line	40.4	39.7	37.3	37.4	38.5	37.3	36.8	35.3	33	34
Greatest width across anterior zygapophyses	81.4	85.6	80.3	76.4	71.9	80.4	74.7	78.1	77.4	71.7
Width across posterior zygapophyses	63.1	59.4	68.2	55.6	51.4	59.9	60.1	51.5	54.3	51.3
Height of neural canal at anterior end	23.7	22.7	24.5	20.8	20.5	21.2	19.6	21.8	18.5	19.5
Greatest transverse width of posterior face of centrum across capitular facets	57.4	59.1	54.6	51.7	54.4	55.3	53.3	51.5	51	48.6
Depth of centrum measured normal to floor of neural canal and along median line of posterior epiphysis	30.2	31.1	29.5	27.6	28.9	29.8	32	29.9	31.3	27.6
Greatest width across outer ends of transverse processes	134.5	135.5	131.1	118.6	115.6	122.9	119.4	112.3	112.4	110.7
Greatest anteroposterior diameter of outer end of transverse process	32	32	32.2	29.8	30	29.3	31.9	28.4	27.6	27
Height from middle of ventral border of posterior epiphysis of centrum to top of neural spine	152.5	139.7	142.7	129.8	127.6	128.3	138.4	130.3	117.9	115.6

SECOND THORACIC VERTEBRA

The centrum is not so wide as, but is deeper than, that of the second thoracic vertebra of *Felis atrox*. The ventral surface again exhibits the characteristic difference between the sabre-tooth and *F. atrox*, a median ridge being present in

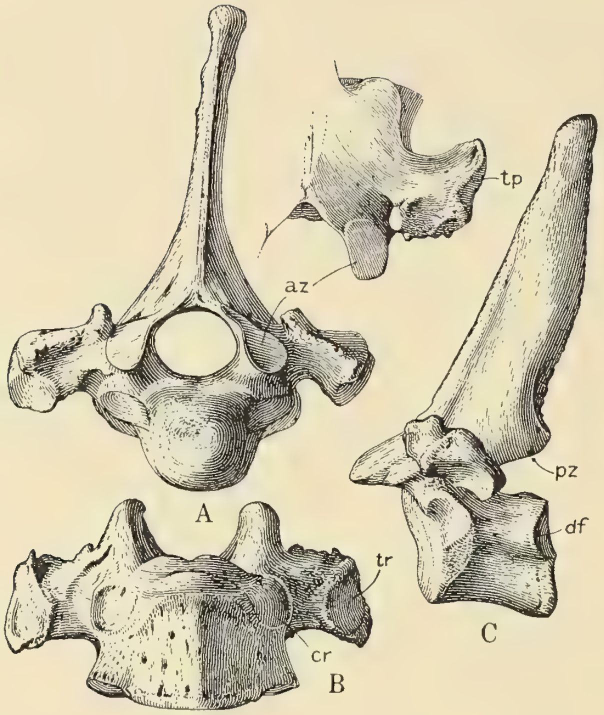

Fig. 32—*Smilodon californicus* Bovard. 3d thoracic vertebra, No. 2047-7. A, anterior view; B, ventral view; C, lateral view; × 1/2. Processes and facets as in 1st thoracic vertebra. Rancho La Brea Pleistocene.

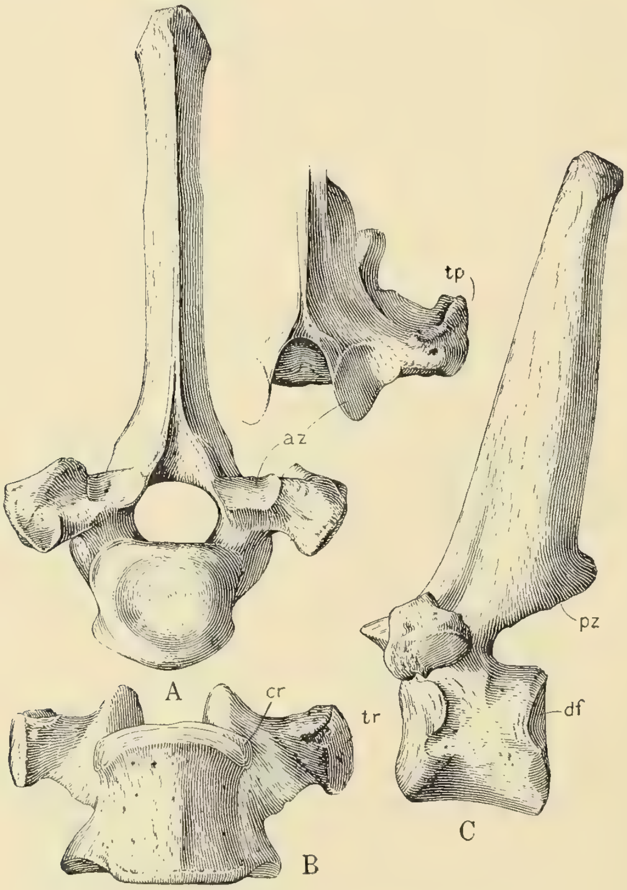

Fig. 33—*Felis atrox* Leidy. 3d thoracic vertebra. No. 2945-1. A, B, C, same views as in figure 32; × 1/2. Rancho La Brea Pleistocene.

Smilodon while in the latter no distinct ridge is formed. The transverse processes are longer in the sabre-tooth and the anterior zygapophyses project farther forward than in the true felines. The posterior zygapophyses may be farther apart than in the latter. As in the true felines, the anterior zygapophyses are directed for the most part inward and upward, in which respect they are like those of the first thoracic vertebra, while the posterior zygapophyses are slightly concave in their long axes and are directed downward. Occasionally the anterior zygapophyses are distinctly U-shaped or V-shaped, as viewed from the anterior side, the inner portion of the articulating surface extending upward along the face of the neural arch. The intervertebral notch is larger in the sabre-tooth than in *Felis atrox*.

The neural spine is thin in front but widens to the posterior side. Terminally the spine widens transversely. In *F. atrox* the thinness of the front portion of the lower half of the spine is, as a rule, somewhat more accentuated than in *Smilodon* by the presence of lateral depressions. However, in some specimens of the sabre-tooth from Rancho La Brea similar depressions have been noted. The spine is apparently not expanded at its dorsal end to the extent seen in *Smilodon*. The front profile of the spine in *F. atrox* may exhibit some of the character noted in the first thoracic vertebra of this form, differing in this respect from that of *Smilodon*.

TABLE 23—*Measurements (in millimeters) of second thoracic vertebra of Smilodon*

	2046–1	2046–2	2046–3	2046–4	2046–5	2046–6	2046–7	2046–8	2046–9	2046–10
Greatest length from end of anterior zygapophyses to end of posterior zygapophyses	48.5	56.9	64.7	56.6	52.4	57.1	62.4	52	55.4	52.4
Length of centrum measured normal to posterior face along median line	34.8	36.1	38.4	35	37.3	35.4	36.6	34	32	30.9
Greatest width across anterior zygapophyses	63.7	70.4	74.4	66.9	65.4	62	55.3	68.2	57.4	66.3
Greatest width across posterior zygapophyses	41.8	44.7	49.9	48	47	44.9	46.7	41	40	36.6
Height of neural canal at anterior end	22.1	20.9	22.8	23.5	19.1	22.3	18.3	20	16	15.7
Greatest transverse width of posterior face of centrum across capitular facets	51.4	57.2	59.1	54.5	59.8	58.5	57.8	55.4	53.4	48.3
Depth of centrum measured normal to floor of neural canal and along median line of posterior epiphysis	27.8	30.4	33.4	28.3	31	27.5	29.4	30.4	33	28.6
Greatest width across outer ends of transverse processes	97.3	109.1	109.8	109.3	105	101.8	96	101.9	91.8	89.1
Greatest anteroposterior diameter of outer end of transverse process	23.6	26.7	27.8	25.4	23.7	25.2	23.1	24	23.7	22.5
Height from middle of ventral border of posterior epiphysis of centrum to top of neural spine	152.6	152.5	149	141.3	142.4	138.4	129.2	131.2	123	114.4

TABLE 24—*Measurements (in millimeters) of third thoracic vertebra of Smilodon*

	2047–1	2047–2	2047–3	2047–4	2047–5	2047–6	2047–7	2047–8	2047–9	2047–10
Greatest length from end of anterior zygapophyses to end of posterior zygapophyses	56.5	60.7	61.6	56.2	53.1	59	54.6	54 8	52.5	53.2
Length of centrum measured normal to posterior face along median line	38.5	36.8	35.4	38.1	35.4	37.8	35.1	34.5	32.6	34.6
Greatest width across anterior zygapophyses	54.1	49.5	56.3	49.4	51.6	50.9	47	43.8	42.8	43.9
Greatest width across posterior zygapophyses	49.5	41.8	46.7	39.3	48	43.7	44.6	39.5	35.7	36.7
Height of neural canal at anterior end	22.1	17.7	21.4	18.4	20.6	17.1	19.3	16	17.8	17.5
Greatest transverse width of posterior face of centrum across capitular facets	58.9	56.9	62.5	63.1	58.4	62.5	54.7	54.9	50.1	51.4
Depth of centrum measured normal to floor of neural canal and along median line of posterior epiphysis	29.7	29	29.6	29.7	28.6	30.6	31.2	28.7	26.3	26
Greatest width across outer ends of transverse processes	105.8	94.9	97.9	98.8	95.9	101.7	95	92	86.4	85.6
Height from middle of ventral border of posterior epiphysis of centrum to top of neural spine	143.3	146.2	139.8	137.5	140.5	138.1	131	124.8	124.3	117.8

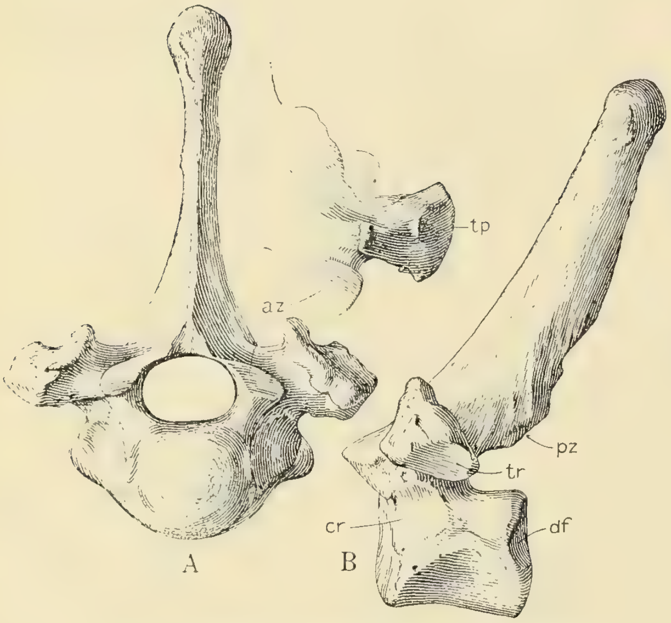

FIG. 34—*Smilodon californicus* Bovard. 4th thoracic vertebra, No. 2048-1. A, anterior view; B, lateral view; × 1/2. Processes and facets as in 1st thoracic vertebra. Rancho La Brea Pleistocene.

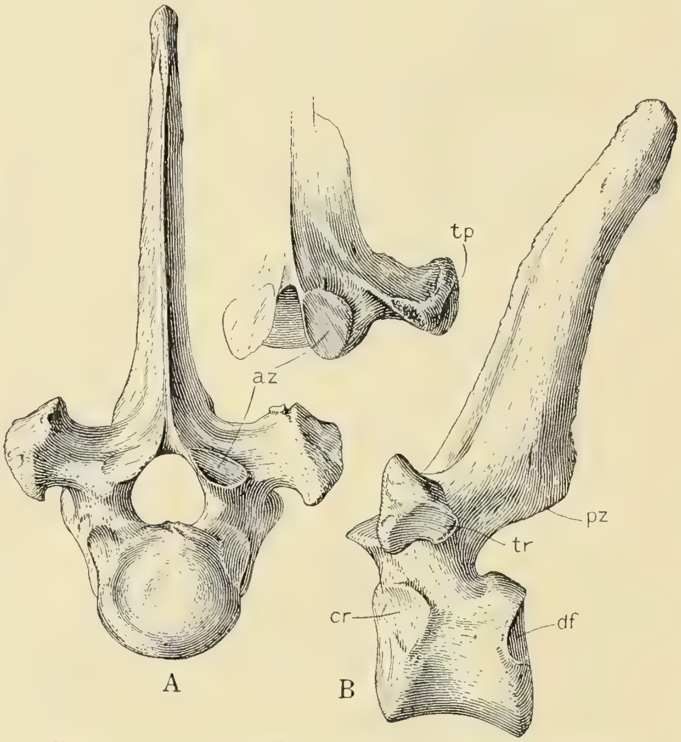

FIG. 35—*Felis atrox* Leidy. 4th (?) thoracic vertebra. No. 2946-1. A, B, same views as in figure 34; × 1/2. Rancho La Brea Pleistocene.

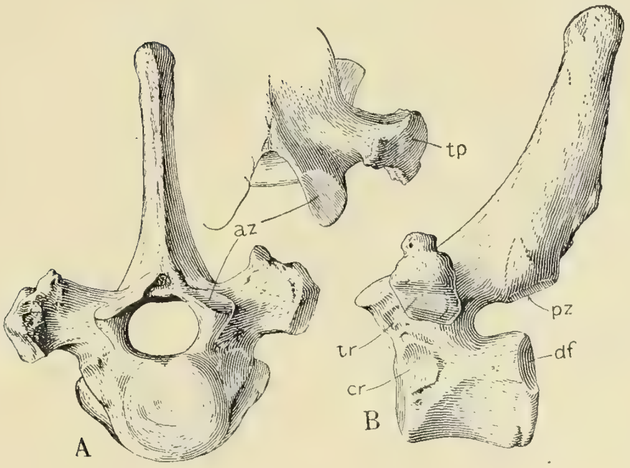

Fig. 36—*Smilodon californicus* Bovard. 5th thoracic vertebra, No. 2049-1. A, anterior view; B, lateral view; × 1/2. Processes and facets as in 1st thoracic vertebra. Rancho La Brea Pleistocene.

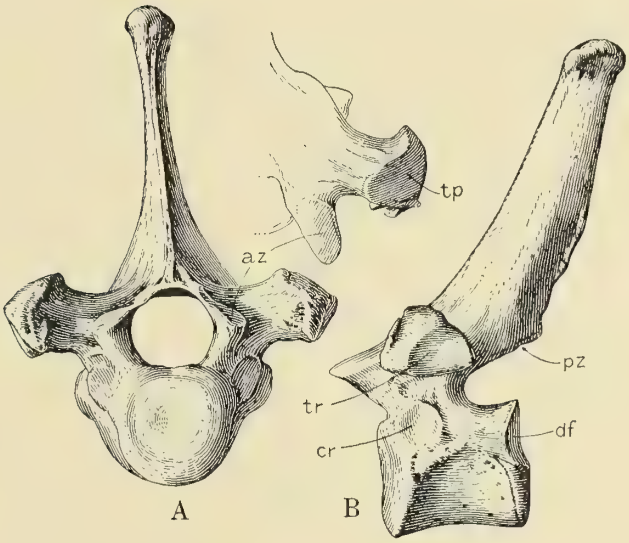

Fig. 37—*Smilodon californicus* Bovard. 6th thoracic vertebra, No. 2050-1. A, anterior view; B, lateral view; × 1/2. Processes and facets as in 1st thoracic vertebra. Rancho La Brea Pleistocene.

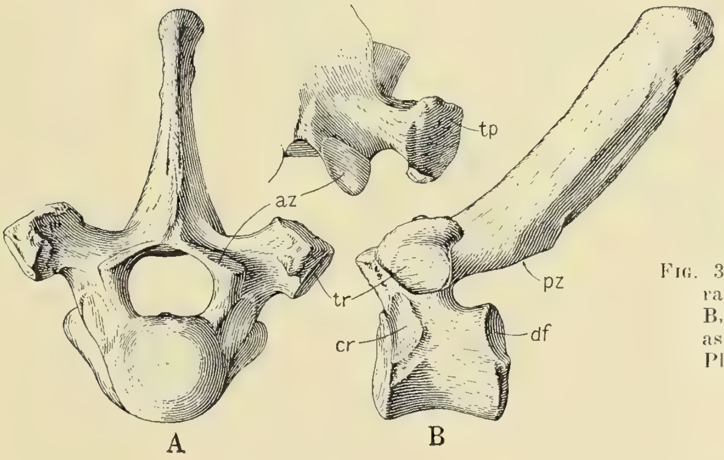

Fig. 38—*Smilodon californicus* Bovard. 7th thoracic vertebra, No. 2051-1. A, anterior view; B, lateral view; × 1/2. Processes and facets as in 1st thoracic vertebra. Rancho La Brea Pleistocene.

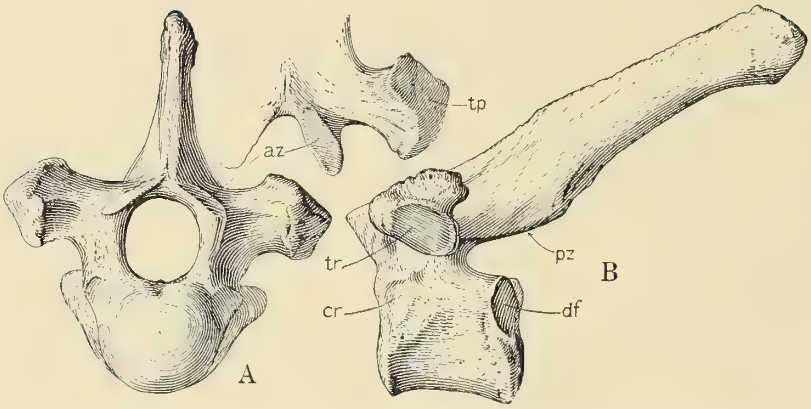

FIG. 39—*Smilodon californicus* Bovard. 8th thoracic vertebra, No. 2052-1. A, anterior view; B, lateral view; × 1/2. Processes and facets as in 1st thoracic vertebra. Rancho La Brea Pleistocene.

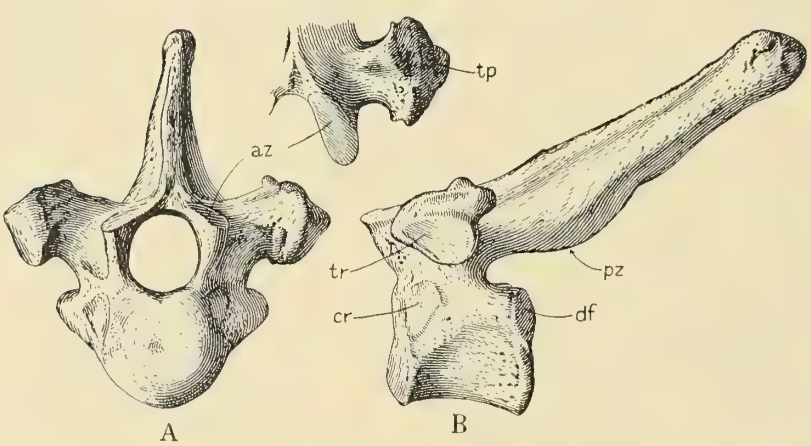

FIG. 40—*Smilodon californicus* Bovard. 9th thoracic vertebra, No. 2053-1. A, anterior view; B, lateral view; × 1/2. Processes and facets as in 1st thoracic vertebra. Rancho La Brea Pleistocene.

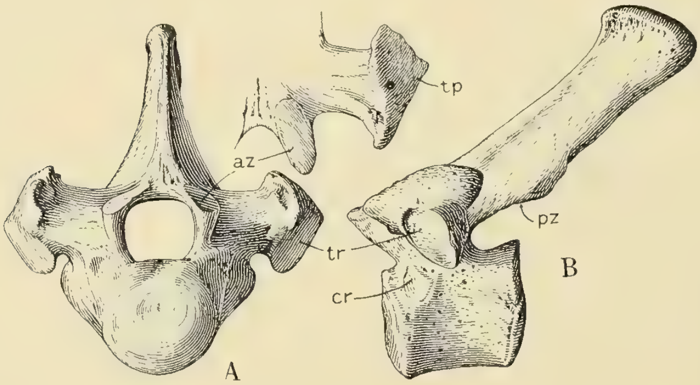

FIG. 41—*Smilodon californicus* Bovard. 10th thoracic vertebra, No. 2054-1. A, anterior view; B, lateral view; × 1/2. Processes and facets as in 1st thoracic vertebra. Rancho La Brea Pleistocene.

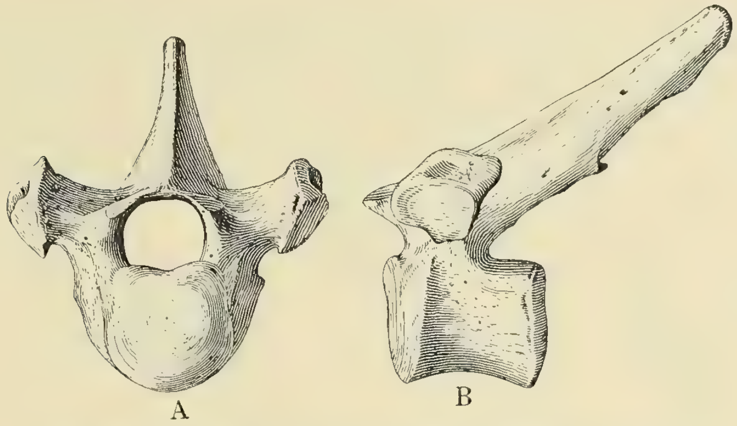

Fig. 42—*Felis atrox* Leidy. 10th thoracic vertebra, No. 2952-1. A, B, same views as in figure 41; × 1/2. Rancho La Brea Pleistocene.

Eleventh Thoracic Vertebra

The most striking feature of this vertebra in *Smilodon* and in the true felines, distinguishing it from preceding and following thoracic vertebræ in the column, is the difference between the anterior and posterior zygapophyses. In this segment the anterior zygapophyses have a shape and position like those of the thoracic vertebræ immediately in front of it. That is to say, the articulating surfaces are flattened or slightly convex and are directed for the most part upward. The posterior zygapophyses, however, are not directed downward for the most part as in preceding vertebræ, but face outward and resemble those in the vertebræ, which follow.

In a series of 487 specimens representing the eleventh thoracic vertebra, at least 29, or approximately 6 per cent of the total number, show the peculiarity of a division of the neural arch along the median line. This lack of fusion of the two halves of the arch is quite independent of age, since it occurs in both old and young specimens. When a distinct neural spine is present in vertebræ having this character, the major portion of the spine may lie to the left or to the right of the line of division.

The degree to which the neural spine develops in *Smilodon* is apparently subject to considerable variation. In a series of 448 specimens of this vertebra, a somewhat arbitrary grouping yields 117 specimens in which a spine is absent, 192 specimens have well-developed spines, and 139 specimens are regarded as intermediate in that the spines are small, rudimentary, or relatively slender. No sharp separation can be made, however, between the individual groups. When a well-developed spine is present, it resembles considerably the spine in the vertebræ which immediately precede the eleventh (tenth and ninth for example). It may be wider in anteroposterior direction than in the latter vertebræ. This type of spine is directed well posteriorly and overhangs the twelfth vertebra. The spine in some specimens, particularly when slender, may be directed more upward and less backward than in individuals in which a stout spine is present. In this respect the spine resembles that usually seen in the great lion-like cat. In specimens of the eleventh vertebra in which a spine is lacking, the posterior end of the crest of the neural arch may be bifurcate. Seemingly the backward trend of a well-developed spine is a more common occurrence in *Smilodon* than in *Felis atrox,* although no series of comparable size of the latter form is available for comparison. In a series of 25 specimens of the eleventh vertebra of *F. atrox,* only one shows a spine of distinctly larger size than that in the remaining 24. In this specimen, No. 2953–1, the spine, while broken at the top, appears to extend more directly upward and less backward than in the sabre-tooth.

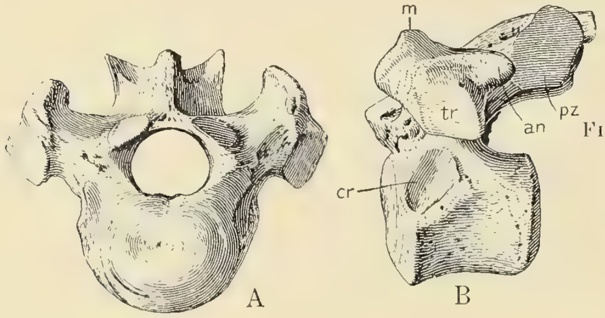

FIG. 43—*Smilodon californicus* Bovard. 11th thoracic vertebra, spineless type, No. 2055-3. A, anterior view; B, lateral view; × 1/2. *m,* metapophysis, *an,* anapophysis, *pz,* posterior zygapophysis, *tr,* facet for tuberculum of rib, *cr,* facet for capitulum of rib. Rancho La Brea Pleistocene.

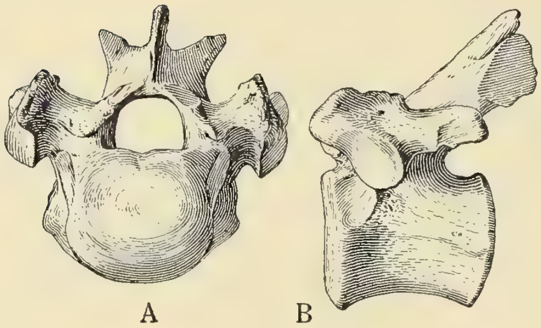

FIG. 44—*Felis atrox* Leidy. 11th thoracic vertebra, No. 2953-8. A, B, same views as in figure 43; × 1/2. Rancho La Brea Pleistocene.

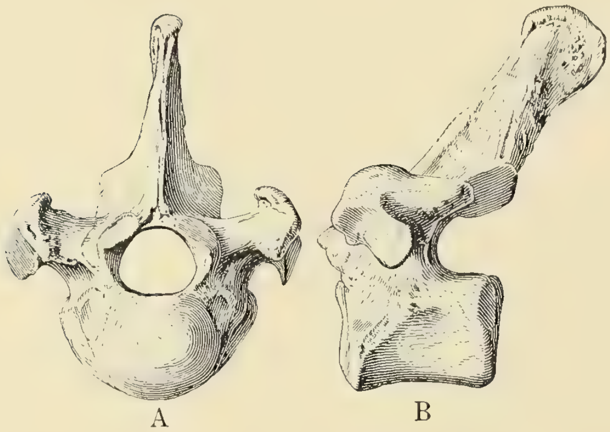

FIG. 45—*Smilodon californicus* Bovard. 11th thoracic vertebra, No. 2055-2. A, anterior view; B, lateral view; × 1/2. Note well-developed neural spine. Rancho La Brea Pleistocene.

Demifacets on the posterior epiphysis of the eleventh thoracic vertebra, articulating with the head of the twelfth rib, are occasionally present in *Smilodon.* In a series of 458 specimens of this segment 22 possess a demifacet on each side of the epiphysis, 12 have a demifacet only on the left side, and 12 only on the right. It is a curious fact that the facets occur in vertebræ having a neural spine and are absent in the series of 117 vertebræ in which no definite spine is present.

The centrum is relatively deep but not so wide in *Smilodon* as in *Felis atrox*. On the ventral surface a more or less well-defined median ridge is present in the sabre-tooth, while in *F. atrox* the ventral surface is broadly convex transversely and concave anteroposteriorly. At approximately the middle of the posterior end of the outer surface of the centrum in *F. atrox* a rudimentary process, which may be considered as a lower transverse process, can be seen. In posterior view this is expressed by a slight lateral projection from approximately the middle of the outer border of the epiphysis. In one specimen of *F. atrox* of Rancho La Brea, a styloid process is developed in this region. No kindred structures have been found in *Smilodon*.

TABLE 25—*Measurements (in millimeters) of eleventh thoracic vertebra of Smilodon*

	2055–1	2055–2	2055–3	2055–4	2055–5	2055–6	2055–7	2055–8	2055–9	2055–10
Greatest length from end of anterior zygapophysis to end of posterior zygapophysis	67.4	55	61.5	62.2	66	67	57.9	50.5	52.4	49
Length of centrum measured normal to posterior face along median line	41.3	41	38.7	39.4	41.4	40	37.5	33.5	34.6	31.8
Greatest width across anterior zygapophyses	40.2	32.1	35.5	40	35	41.8	33.5	35.4	30.8	32.9
Greatest width across posterior zygapophyses	36.4	32.3	30.9	35.4	27.7	44.8	28	29	27.1	20.8
Greatest transverse width of posterior face of centrum	45.4	50.8	42.8	44.5	43.1	45.5	36.8	36.6	37.9	34.5
Depth of centrum measured normal to floor of neural canal and along median line of posterior epiphysis	28.8	28	30.3	30.9	31.8	32.2	26	26.6	26.4	25.6
Greatest width measured from outer ends of facets for tubercle of rib	77	77.9	83.3	85.6	76	83.1	64.5	65.7	58.4	59.4
Height from middle of ventral border of posterior epiphysis of centrum to top of neural spine	111.4	104.4	70.7	97.7	103.3	102.5	59.6	88.7	82.9	64.2
Length of spine from middle of notch between anterior zygapophyses to top measured parallel to anterior end	87.7	78.9	......	78	84.3	80.3	......	68.5	60.5	41
Greatest anteroposterior diameter of plate above facet for tubercle of rib	42.2	38.7	35	33.8	34.3	34.6	35.6	27	32	27.1

In the sabre-tooth the neural canal is relatively large, as is also the intervertebral notch. In *Smilodon* the anterior zygapophyses project distinctly beyond the anterior face of the centrum. In the true cat of the asphalt, on the other hand, the zygapophyses usually do not reach beyond this face. The posterior zygapophyses may face squarely outward or slightly downward and backward as well. In *F. atrox* the ridge extending downward and forward from the lower end of the posterior zygapophysis to the posterior face of the pedicle of the neural arch is sharp. In *Smilodon* the ridge is usually broader.

The plate-like structure above the tubercular facet for the rib, from which are formed the metapophysis and anapophysis in the following vertebræ, occasionally permits an identification of these processes in the eleventh. The structure is never as long in anteroposterior direction as in *F. atrox*, due to a much less projection of the anapophyseal portion.

Twelfth Thoracic Vertebra

In this segment a median ridge is again defined or suggested on the lower surface of the centrum, in which respect *Smilodon* differs from *Felis atrox*. In the latter type the lateral projections, rudimentary transverse processes, are situated lower along the sides of the centrum than in the sabre-tooth. While the metapophysis and anapophysis are distinct in this vertebra, they are not so clearly differentiated in *Smilodon* as in *F. atrox*. In the latter the structures are slender. The anapophysis has usually a broader base in the sabre-tooth and the metapophysis often projects well outward from the margin of the anterior zygapophysis. A distinguishing feature of the twelfth vertebra in *Smilodon* is the presence of a relatively broad plate-like structure lying in front of a ridge extending downward and slightly backward from the anterior border of the metapophysis. This structure forms the outer wall of the front portion of the anterior zygapophysis and the side of the pedicle. Its separation from the lateral wall of the metapophysis and anapophysis is clearly defined by the ridge described above. There are, however, some specimens in the collection in which the separation is not so distinctly shown. In *Felis atrox* no surface or structure of comparable breadth, as measured in anteroposterior direction, is formed.

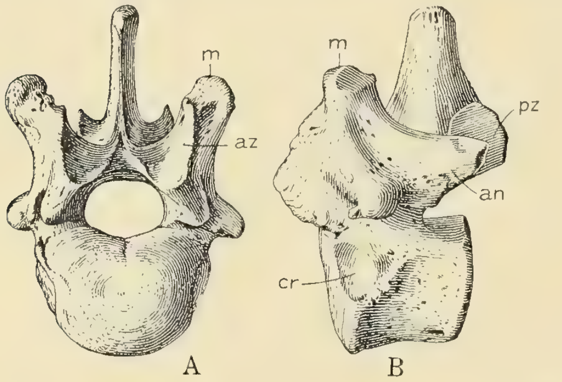

Fig. 46—*Smilodon californicus* Bovard. 12th thoracic vertebra, No. 2056-1. A, anterior view; B, lateral view; × 1/2. Processes and facets as in 11th thoracic vertebra. Rancho La Brea Pleistocene.

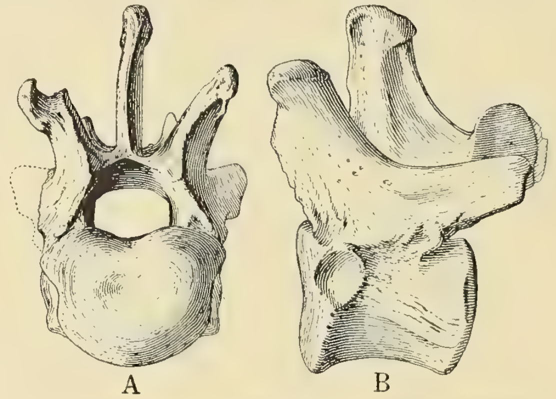

Fig. 47—*Felis atrox* Leidy. 12th thoracic vertebra, No. 2954-1. A, B, same views as in figure 46; × 1/2. Rancho La Brea Pleistocene.

Immediately behind the lower end of the ridge separating the two surfaces is situated the area which joins with the tubercle of the rib. In a series of 426 specimens representing the twelfth thoracic vertebra of *Smilodon*, a well-developed tubercular facet is present on each side in 73 vertebræ. In 124 specimens of this series, the facet may be present on one side and absent on the other or the two facets may be rudimentary. In 229 specimens the facet is entirely reduced and its place is frequently taken by a rounded tubercle. The facet, when present, is frequently supported on a short projection from the pedicle of the neural arch. A comparable facet for the tubercle of the rib is generally absent in the large cat of the asphalt. The anterior zygapophyses are noticeably larger in the sabre-tooth than in *F. atrox* and suggest a strong union of this segment with the preceding vertebra. In the latter species the size and shape of the anterior zygapophyses may be indicative of greater flexibility in this region of the vertebral column. The intervertebral notch is distinctly larger in the sabre-tooth.

In a series of 440 specimens, a neural spine is fully formed in 185; in 255 specimens of this series, the spine is either somewhat reduced or is absent. When a spine is lacking, a low crest is present on the neural arch. In a series of 16 specimens representing the twelfth thoracic vertebra of *Felis atrox*, all possess neural spines. In a series of more than 400 specimens of this vertebra in *Smilodon*, only 6 exhibit a median division of the neural arch. In other words, this peculiarity is slightly less frequent in its occurrence in the twelfth than in the eleventh vertebra of *Smilodon*.

Table 26—*Measurements (in millimeters) of the twelfth thoracic vertebra of Smilodon*

	2056–2	2056–3	2056–4	2056–5	2056–6	2056–7	2056–8	2056–9	2056–10	2056–11
Length from end of anterior zygapophyses to end of posterior zygapophyses...	66.8	69.9	*a*62	68.2	66.9	62.5	60.3	57	56.3	53.7
Length of centrum measured normal to posterior face along median line........	42.6	41.8	39.3	42.4	40.2	40	39.9	37.1	37	33.3
Greatest width across posterior zygapophyses......	34.9	31.6	30.9	34.4	27.8	28.5	30	24.1	27.5	26
Greatest width across metapophyses................	71	70.2	74.3	64.8	61.6	60.4	63.7	59.6	52.1	49.8
Greatest width across facets for tuberculum of rib.....	69.8	71.8	65.2	71.5	71.9	62	52.8	53.3	52.9	48.5
Greatest width of posterior epiphysis of centrum.....	44.6	44.4	42.6	44.5	44.3	43.7	42	38.4	37.3	35.6
Depth of centrum measured normal to floor of neural canal and along median line of posterior epiphysis.	28.5	30.3	28.7	28.7	29.5	30	26.7	26	24	22.7
Greatest length from end of metapophyses to end of anapophyses.............	59.4	53.2	40	58.7	53.2	48.2	47.1	51.3	55.7	37.1
Height of spine from inferior border of posterior epiphysis of centrum to top of neural spine...........	75.3	70.5	70	99.3	99	89.6	86.6	85.9	68.5	59.1

a, Approximate.

Thirteenth Thoracic Vertebra

In *Smilodon* the centrum of this vertebra is relatively smaller than in *Felis atrox* and differs also from that of the latter in the presence of a ventral ridge. In the latter the lateral tuberosities of the centrum are more prominently developed and in posterior view these projections are more conspicuous than in the sabre-tooth and form the outer inferior corners of the posterior epiphysis. The neural canal in *Smilodon* is comparatively large. The neural spine is practically always present in this vertebra of the sabre-tooth; in a series of more than 700 specimens, at least 8 were noted in which a spine was lacking. The spine is not so wide anteroposteriorly as in the great true feline and it has an erect position. The spine leans slightly forward in the latter. In *Smilodon* the posterior edge of the spine may extend downward and backward to a point on the posterior border of the arch between the posterior zygapophyses. In *Felis atrox* this edge ends on the dorsal surface between the zygapophyses, but does not extend back to the posterior border.

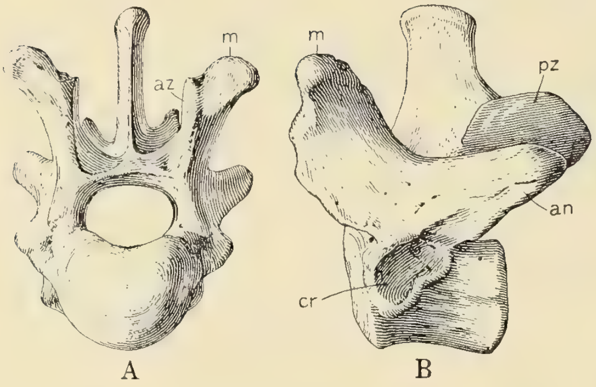

Fig. 48—*Smilodon californicus* Bovard. 13th thoracic vertebra, No. 2057-6. A, anterior view; B, lateral view; × 1/2. Processes and facets as in 11th thoracic vertebra. Rancho La Brea Pleistocene.

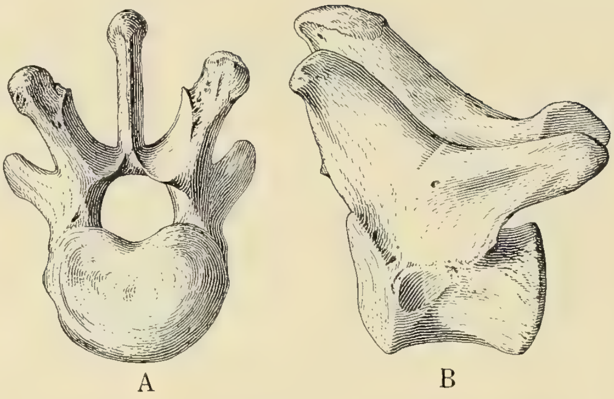

Fig. 49—*Felis atrox* Leidy. 13th thoracic vertebra, No. 2955-6. A, B, same views as in figure 48; × 1/2. Rancho La Brea Pleistocene.

The rugosity indicating the contact with the tuberculum of the rib, while small in *Smilodon*, is still more prominent in this form than in *F. atrox*. The lateral surface below the metapophysis and which extends forward to the anterior border is wider in anteroposterior direction than in *F. atrox*. The lower border of the anapophysis forms a more irregular edge in the former than in the latter. The anterior and posterior zygapophyses furnish apparently stronger bonds between this vertebra and adjacent vertebræ in *Smilodon* than in the *F. atrox*.

Table 27—*Measurements (in millimeters) of thirteenth thoracic vertebra of Smilodon*

	2057–1	2057–2	2057–3	2057–4	2057–5	2057–6	2057–7	2057–8	2057–9	2057–10
Length from end of anterior zygapophysis to end of posterior zygapophysis	83.7	80.9	76.6	86.8	78.4	79.3	71	75.7	65.2	63.5
Length of centrum measured normal to posterior face and along median line	47.2	45.1	45.3	45.9	47.5	40.6	40	41	38.3	38.8
Greatest width across posterior zygapophyses	39.7	33.4	40.6	41.4	39.3	28.5	38.1	25	23.6	29.5
Greatest width across metapophyses	65.5	76.6	77.5	74.9	78	67.1	62.7	59.7	52.6	56.9
Greatest width across outer ends of anapophyses	71	72.2	72.8	66.4	66.1	61.5	59.1	61	47.1	55.5
Greatest width of posterior epiphysis of centrum taken immediately above lateral projection of centrum	45.8	47.3	46.1	46.8	46.7	38.7	39.8	41.9	37.3	38.5
Depth of centrum measured normal to floor of neural canal and along median line of posterior epiphysis	32.6	29.4	34	31.9	34.1	27.1	27.4	30.3	26.4	25.9
Greatest length from end of metapophysis to end of anapophysis	84.3	81	82	81.7	79.7	74.4	59.8	70.4	57.8	62.8
Distance from median inferior border of anterior epiphysis to top of neural spine	102.6	104.6	99.1	97.1	100.9	92.1	80.6	93.3	81.1	77.8
Height of spine above roof of neural arch	58	59	50.9	51.9	50.8	50	37.6	48.7	45	39.1
Anteroposterior diameter of top of neural spine	21.2	19.4	22.5	20	17.4	20.4	18	21.3	19.7	16.3

Although a large number of specimens of this vertebra of the sabre-tooth are available in the collection, there are no examples which show the division of the neural arch along the median line.

LUMBAR SERIES

Plates 19 and 35

Normally the lumbar series in *Smilodon* is represented by seven vertebræ, in which respect the sabre-tooth is like the true felines. In reviewing the large number of lumbar series available from Rancho La Brea, it becomes evident that occasionally the lumbar vertebræ may be reduced to six in *Smilodon*. The length of the entire series, relative to the length of the thoracic series, is shorter than in the modern lion.

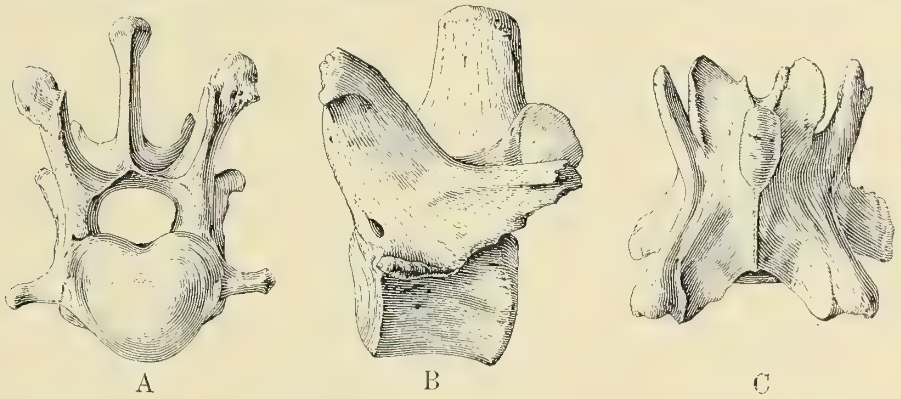

FIG. 50—*Smilodon californicus* Bovard. 1st lumbar vertebra, No. 2058-1. A, anterior view; B, lateral view; C, dorsal view; × 1/2. Rancho La Brea Pleistocene.

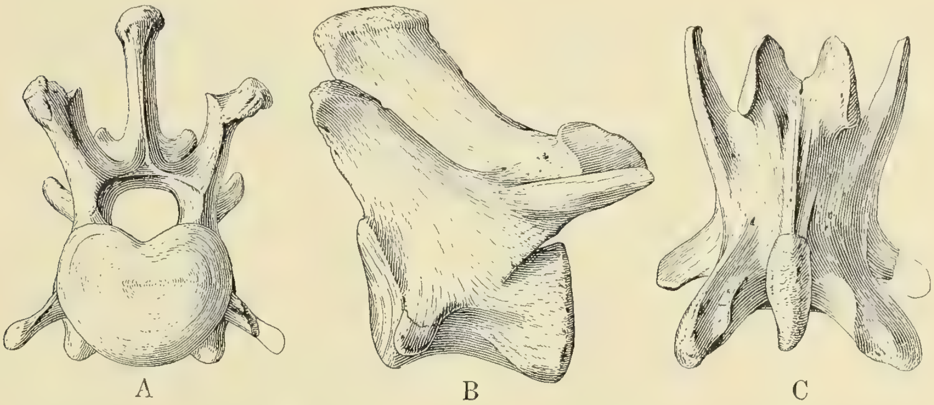

FIG. 51—*Felis atrox* Leidy. 1st lumbar vertebra, No. 2956-1. A, B, C, same views as in figure 50; × 1/2. Rancho La Brea Pleistocene.

This region of the vertebral column in the sabre-tooth exhibits a flexibility which is noticeably less than that in *F. atrox*, due in large measure to a firmer bond established between the zygapophyses of the individual vertebræ. The difference is apparently to be correlated with the habits of the animal and suggests that the sabre-tooth was not a lithe, swift-footed carnivore in the sense that the Pleistocene true cat or modern lion exhibits these characteristics.

The neural spines are relatively stout and the termini of these processes may be heavier than in *F. atrox.* Generally the spines of the first four lumbar vertebræ are broader anteroposteriorly than those of the last three vertebræ. They differ also from the latter in their more erect position, although this is not always the case in individuals from Rancho La Brea. At any rate, the forward border of the spine in the posterior three vertebræ may not descend so abruptly in these segments as in the anterior vertebræ. The attitude of the spines in *Smilodon* is somewhat different from that in *F. atrox.* In the latter form there is a distinct tendency on the part of the spines to lean forward. This is particularly true of the anterior lumbar vertebræ, the first, second and third, and the character becomes less evident in the fourth.

Reference has been made already to the zygapophyses. The anterior zygapophysis frequently exhibits a tendency to recurve inward dorsally and thus slightly enfolds the posterior zygapophysis with which it articulates, more so than in *F. atrox.* The metapophyses are relatively strong processes. The anapophyses in the anterior lumbar vertebræ, where they have not suffered posterior reduction, appear to project slightly less away from the sides of the vertebræ than in *F. atrox.* In their backward projection they frequently lie so close to the outer wall of the metapophyses of the succeeding vertebræ as to actually incise this surface. While this character may be seen occasionally in some lumbar vertebræ of the true felines, the impression is given that the relationship of the anapophysis to the metapophysis in the sabre-tooth furnishes an additional character promoting rigidity in this section of the column. The progressive reduction of the anapophysis in the lumbar series is approximately comparable to that in *Felis atrox.* In other words, the last distinct process is seen in the fifth; the sixth lumbar vertebra exhibits merely the rudimentary base of the anapophysis and even this is lacking in the seventh.

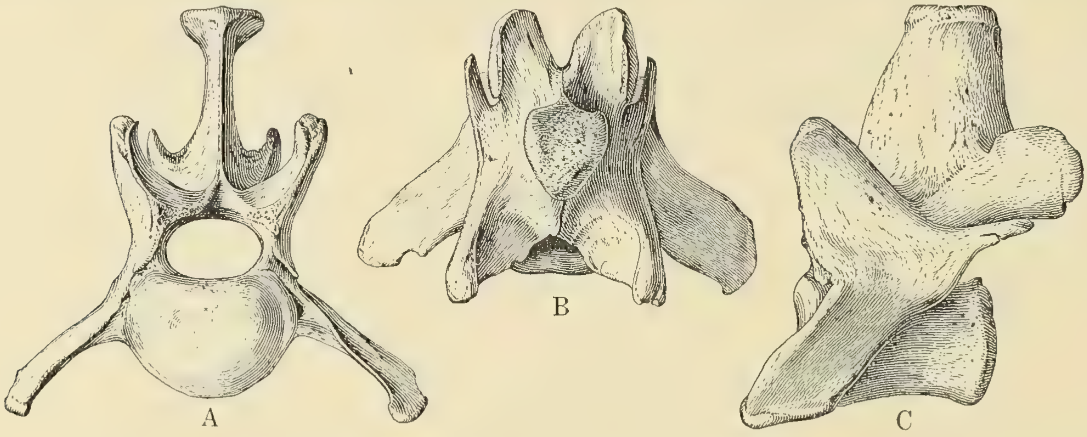

Fig. 52—*Smilodon californicus* Bovard. 4th lumbar vertebra, No. 2061-2. A, anterior view; B, dorsal view; C, lateral view; × 1/2. Rancho La Brea Pleistocene.

As in the true felines, the transverse processes of *Smilodon* increase in size from the first to the sixth lumbar vertebra. In the first four vertebræ the processes not only increase gradually in length but also in width. In the second, third and fourth vertebræ, the process does not curve forward to the extent seen in *F. atrox.* In the last three vertebræ (fifth, sixth and seventh lumbars) the processes are not so long

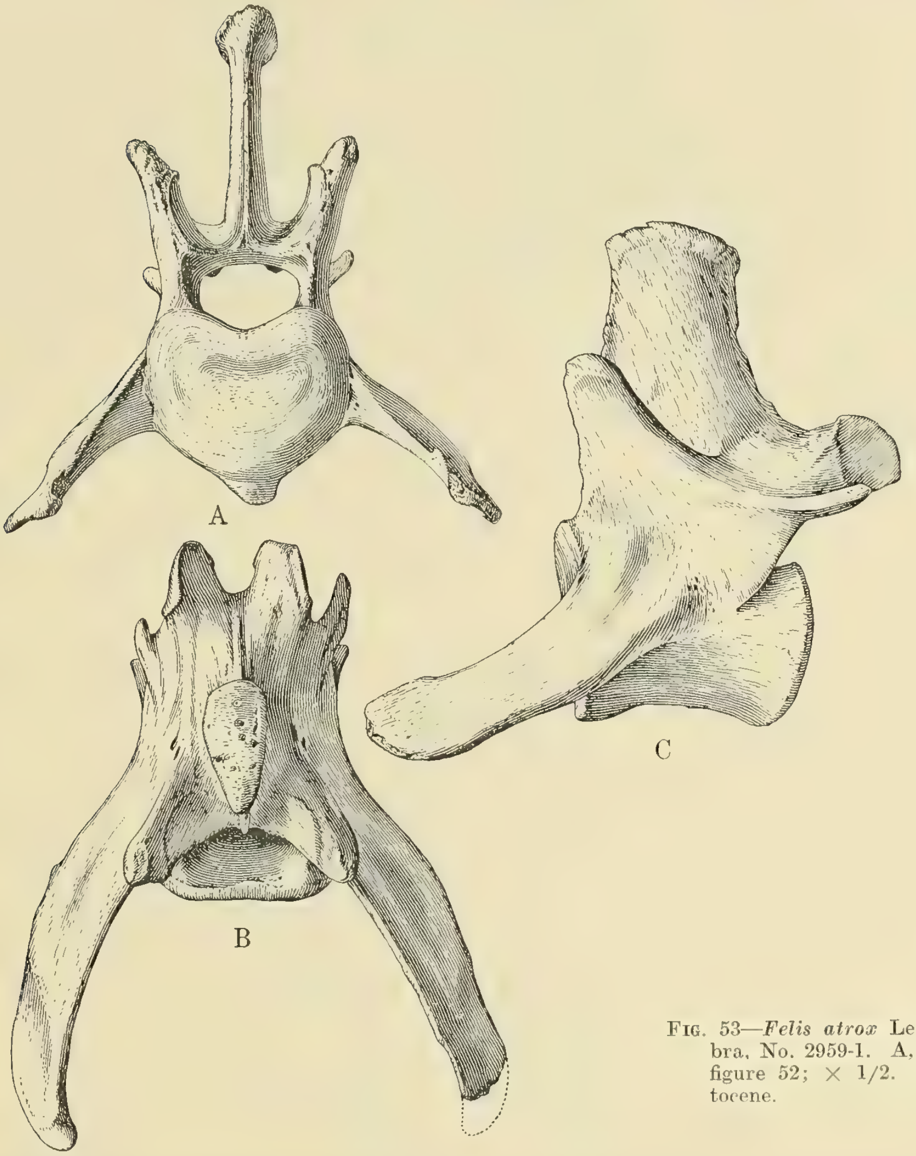

FIG. 53—*Felis atrox* Leidy. 4th lumbar vertebra, No. 2959-1. A, B, C, same views as in figure 52; × 1/2. Rancho La Brea Pleistocene.

nor do they extend so far forward as in the large true felines. In the seventh lumbar vertebra, the base of the transverse process is narrowed in anteroposterior direction, but the dorsoventral diameter is increased. The centra of the lumbar vertebræ are relatively not so long in *Smilodon* as in *Felis atrox.* The tendency to develop a median ridge on the ventral surface of the centrum is generally characteristic of the lumbar vertebræ of *Smilodon.* The character may become more accentuated in the fifth and sixth of the series, but the centrum of the seventh may also possess a distinct ridge. In *F. atrox* of the asphalt, the centra of the forward lumbar vertebræ have more or less smooth ventral surfaces, but a well-defined ridge may be definitely recognized on the centra of the third, fourth, fifth and sixth. It becomes much less defined or is totally absent in the seventh.

With exception of size the lumbar series in *Felis atrox* (plate 35, figs. 2 and 3) closely resembles that in the existing large felines.

Table 28—*Measurements (in millimeters) of lumbar vertebræ of Smilodon*

Vertebræ	1	2	3	4	5	6	7
Length of centrum measured normal to face of posterior epiphysis and along median line	42.9	45	46	48.5	49.1	49.2	46.5
Greatest length from anterior end of metapophyses to end of posterior zygapophyses	72.4	77.8	81.9	77	80	77	70.6
Greatest width across metapophyses	64.3	58.3	53.7	64.1	53.4	53.4	56
Greatest width across posterior zygapophyses	35.5	37	44	37.2	36.5	38	53.5
Greatest width across transverse processes	69.8	89.7	104.1	119.3	120.5	134.3	129.4
Width of posterior epiphysis of centrum	45.5	45.1	46	45.6	46	47	43.1
Depth of centrum measured normal to floor of neural canal and across posterior epiphysis	30.5	32	33.1	34.2	35	31.3	30.4
Height from middle ventral border of anterior epiphysis of centrum to top of neural spine	93.1	94.8	99.6	104	113.3	109	95.9

Table 29—*Measurements (in millimeters) of lumbar vertebræ of Felis atrox*

Vertebræ	1	2	3	4	5	6	7
Length of centrum measured normal to face of posterior epiphysis and along median line	54.2	57.2	60	62.7	65.2	65	55.5
Greatest length from anterior end of metapophyses to end of posterior zygapophyses	90.8	95.7	89.2	92.1	95	93.4	84.4
Greatest width across metapophyses	65.1	*a*60.5	*a*60	55.9	58.1	60.1	70
Greatest width across posterior zygapophyses	32.5	37.8	33.7	37	34.8	46.3	72.4
Greatest width across transverse processes	*a*77	*a*90	*a*96	*a*108	118	141.5	*a*120
Width of posterior epiphysis of centrum	49.7	50.3	50.8	50.6	52.4	52.5	53.2
Depth of centrum measured normal to floor of neural canal and across posterior epiphysis	34.5	36	36	35.6	37.3	38.6	35.6
Height from middle ventral border of anterior epiphysis of centrum to top of neural spine	95	.....	.....	115.6	112.4	105.4	98.7

a, Approximate.

Sixth Lumbar Vertebra

In view of a greater shortening of the sixth lumbar vertebra in *Smilodon*, the distance between the metapophysis and posterior zygapophysis is much less in the former type than in *Felis atrox*. The posterior portion of the neural arch projects well beyond the vertical plane of the posterior face of the centrum, frequently relatively more so than in *F. atrox*. The extent to which the anapophysis has been reduced in this vertebra of *Smilodon* is comparable to that in *F. atrox*. The intervertebral notch may be fully as large as in the latter form.

When the vertebra is viewed from the front the anterior zygapophyses may be seen to form a cup-shaped depression, the upper margin of each zygapophysis frequently extending inward. The pedicle of the neural arch is heavier in *Smilodon* than in *F. atrox*, and the neural canal is smaller. Within the canal, the median ridge traversing the length of the dorsal surface of the centrum is broader in the sabretooth than in *F. atrox*. Nutrient foramina pierce the surface on each side of the ridge. A deep groove is developed on the anterior face of the pedicle, extending outward from the neural canal and downward to the base of the transverse process. A similar groove is lacking in the large true cat.

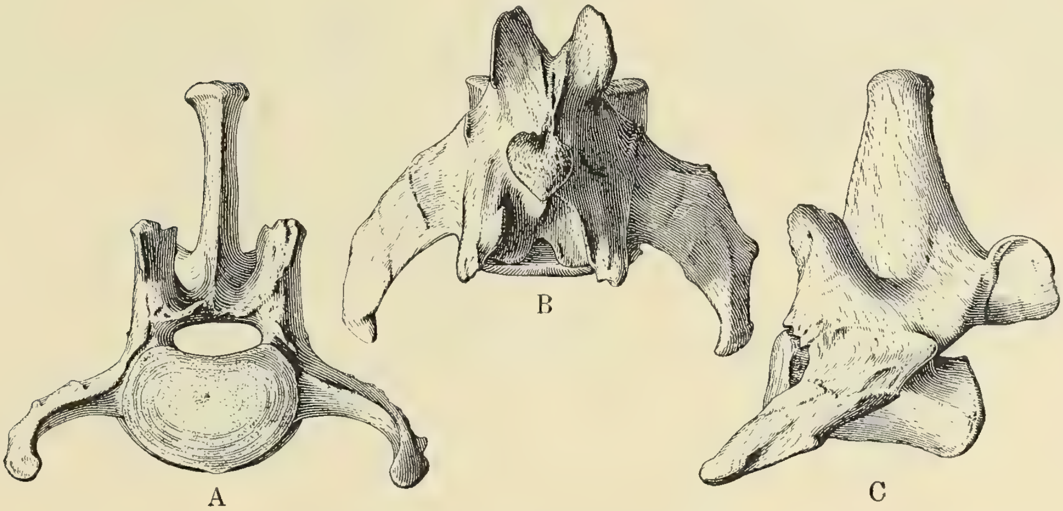

FIG. 54—*Smilodon californicus* Bovard. 6th lumbar vertebra, No. 2063-1. A, anterior view; B, dorsal view; C, lateral view; × 1/2. Rancho La Brea Pleistocene.

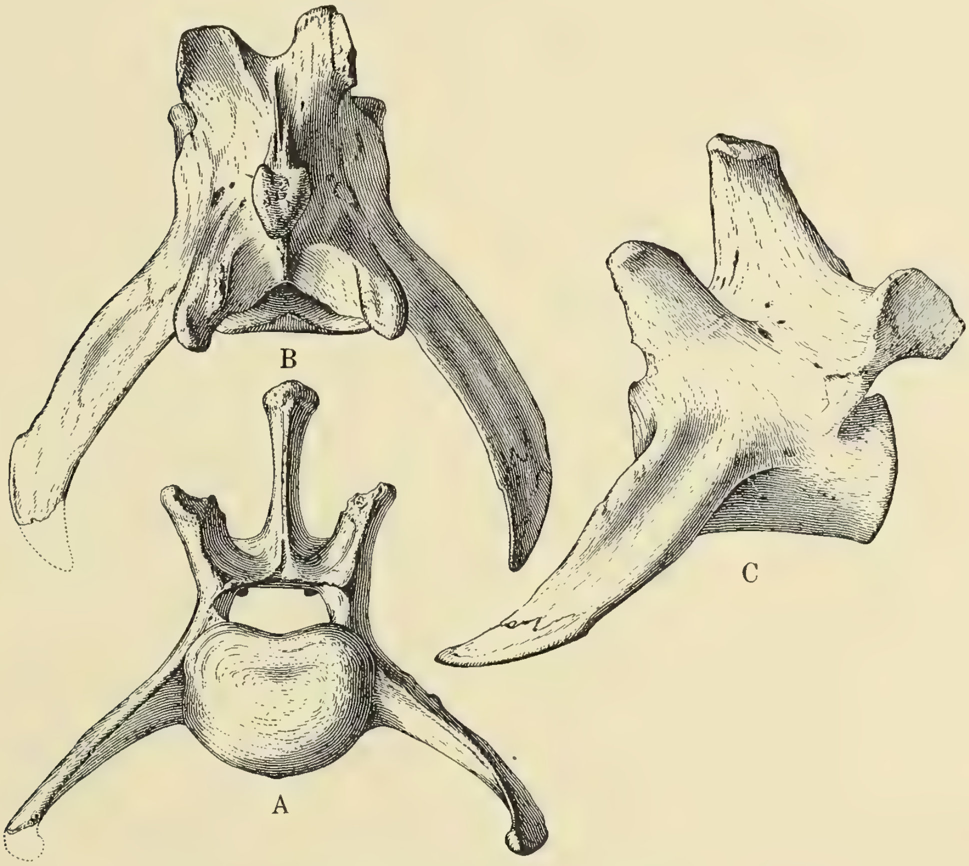

FIG. 55—*Felis atrox* Leidy. 6th lumbar vertebra, No. 2961-1. A, B, C, same views as in figure 54; × 1/2. Rancho La Brea Pleistocene.

Before swinging forward, the transverse processes extend directly outward farther in *Smilodon* than in *Felis atrox.* In the latter species they extend more directly downward and forward. The base of the process is thicker in the sabre-tooth. Its front face is notched by a groove which extends downward from the neural canal.

TABLE 30—*Measurements (in millimeters) of sixth lumbar vertebra of Felis atrox*

	2961–1	2961–2	2961–3	2961–4	2961–5	2961–6	2961–7	2961–8	2961–9	2961–10
Length of centrum measured normal to face of posterior epiphysis and along median line	72.7	63.7	67.6	69.8	68.9	64.5	63.1	64.8	60.7	61.5
Greatest length from anterior end of metapophyses to end of posterior zygapophyses	99.5	94.8	97.1	92	89.4	86.3	85.3	93.3	87.7	84.9
Greatest width across metapophyses	67.3	60.6	60.6	50.9	48.9	......	63.2	60	48	56
Greatest width across posterior zygapophyses	47.3	48.3	41.6	33.9	44.4	44.3	41	45.8	38.8	39.4
Greatest width across transverse processes	......	*a*160	......	......	......	*a*133	......	141.3	......	......
Width of posterior epiphysis of centrum	61.2	59.5	58.3	54.4	59.4	52	50.9	52.5	48.6	49.4
Depth of centrum measured normal to floor of neural canal and across posterior epiphysis	43.8	39.9	43	39.3	42	40	39.2	38.7	35.4	35.4
Height from middle ventral border of anterior epiphysis of centrum to top of neural spine	......	110.5	116.7	108.5	107.1	......	102.4	105.7	95.3	93.9

a, Approximate.

SEVENTH LUMBAR VERTEBRA

Viewed from the front (fig. 56A), the metapophyses are seen to project as a rule straight upward in *Smilodon,* while in *F. atrox* they lean slightly more outward. From the side, the metapophysis is seen also to be slightly more erect than in the great lion-like cat. Between the metapophysis and the posterior zygapophysis a deep valley is formed, which extends downward and slightly backward. The anterior zygapophyses may be large, relatively more so than in *F. atrox.* However, the size of the articulating surfaces varies considerably in the sabre-tooth, and so also does the distance between the anterior zygapophyses. The posterior zygapophyses project farther beyond the vertical plane of the posterior epiphysis of the centrum in *Smilodon* than in *Felis atrox.* The posterior portion of the neural arch is also carried farther backward. Viewed from the top, the posterior border of the neural arch is seen to be incised by a V-shaped notch. Frequently, however, a broader indentation occurs. In *Felis atrox* the posterior border forms a thin edge between the zygapophyses, while in the sabre-tooth the border is formed by a rugose surface.

The base of the transverse process is thicker in dorsoventral diameter than in preceding vertebræ. The ventral surface of the process is smooth, while the dorsal surface, particularly of that portion of the process which extends forward, is rugose. The neural spine varies in size; it may have a height fully as great as that in *F. atrox.*

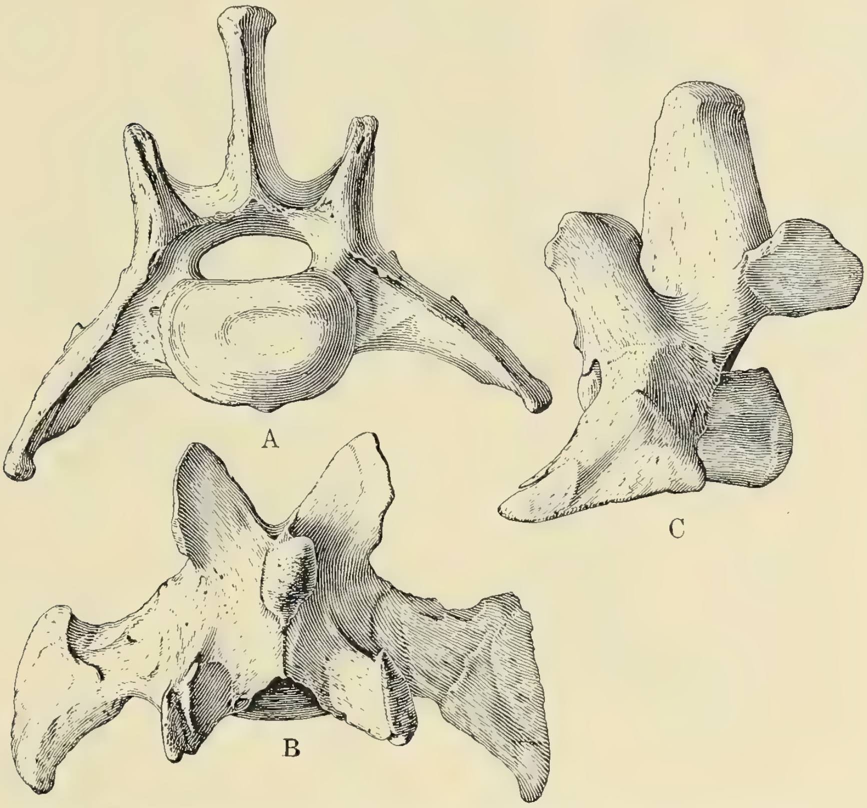

Fig. 56—*Smilodon californicus* Bovard. 7th lumbar vertebra, No. 2064-11. A, anterior view; B, dorsal view; C, lateral view; × 1/2. Rancho La Brea Pleistocene.

Table 31—*Measurements (in millimeters) of seventh lumbar vertebra of Smilodon*

	2064–1	2064–2	2064–3	2064–4	2064–5	2064–6	2064–7	2064–8	2064–9	2064–10
Length of centrum measured normal to face of posterior epiphysis and along median line	54.3	56.4	53.9	51.9	47.1	48.8	54.1	44	40.8	36.7
Greatest length from anterior end of metapophyses to end of posterior zygapophyses	79.6	83	85.8	74	69.8	73	85.2	68.4	53.2	52.8
Greatest width across metapophyses	64.6	65.7	69.9	50.5	56.6	59.7	55.3	48.5	56.6	48.6
Greatest width across posterior metapophyses	54.9	57.1	57.8	43.8	53.8	54.4	49.8	59.8	51	52.3
Greatest width across transverse processes	143	145.5	140.6	134.7	130.7	128.2	123	104.4	*a*115	......
Width of posterior epiphysis of centrum	52.9	51.5	52.3	51.2	46.4	46	51.7	41.8	36.3	37.4
Depth of centrum measured normal to floor of neural canal across posterior epiphysis	35.1	31.5	31.8	31.1	31.3	31.8	33.7	26.1	25.8	24.2
Height from middle of ventral border of anterior epiphysis of centrum to top of neural spine	105.3	111.4	106.4	114.9	105.3	106.5	106.6	90.6	80.7	74.5

a, Approximate.

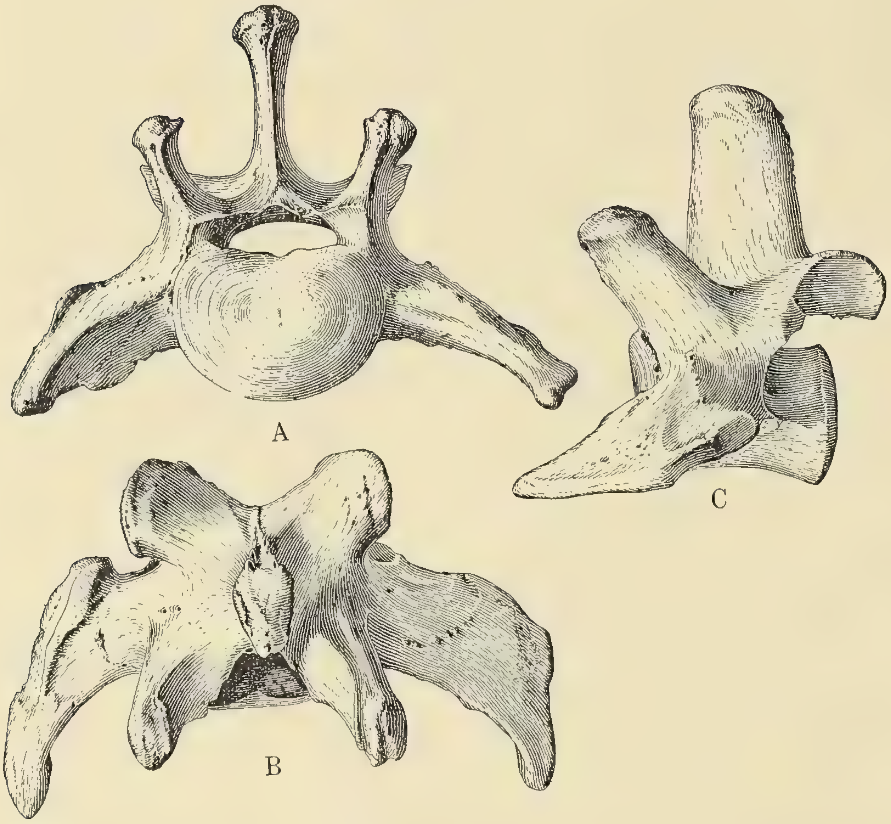

Fig. 57—*Felis atrox* Leidy. 7th lumbar vertebra, No. 2962-6. A, B, C, same views as in figure 56; × 1/2. Rancho La Brea Pleistocene.

Table 32—*Measurements (in millimeters) of seventh lumbar vertebra of Felis atrox*

	2962–1	2962–2	2962–3	2962–4	2962–5	2962–6	2962–7	2962–8	2962–9	2962–10
Length of centrum measured normal to face of posterior epiphysis and along median line	62.6	58.4	63.8	56.7	60.4	53	57.3	55.6	55.3	52
Greatest length from anterior end of metapophyses to end of posterior zygapophyses	90.9	84	94.5	90.3	83.3	82.4	75.4	82.3	84.4	81.4
Greatest width across metapophyses	74	75.4	*a*75	66.4	69	73	68.5	68.5	70	58.9
Greatest width across posterior zygapophyses	77	71.2	77.3	71.2	64.4	70.8	68.6	71.7	72.4	65.5
Greatest width across transverse processes	*a*165	......	......	......	147	148.7	......	......	......	*a*118.5
Width of posterior epiphysis of centrum	61.2	63	61	58.2	59.6	52.3	55.1	51.6	53.2	49.4
Depth of centrum measured normal to floor of neural canal across posterior epiphysis	41.3	41.4	41.9	39.3	39.5	35.2	37.9	37	35.7	34.1
Height from middle of ventral border of anterior epiphysis of centrum to top of neural spine	114	113.6	115.5	108.4	98	103.4	107.5	103.2	99	95.7

a, Approximate.

SACRUM

The sacrum of *Smilodon* exhibits considerable sturdiness and possesses a particularly strong surface for attachment with the pelvis.[1] The centra of the vertebræ show a more noticeable decrease in size from the first to the third than in *Felis atrox;* the last centrum being distinctly smaller in the sabre-tooth and clearly indicating the presence of a shorter tail in the latter form. A narrowing of the sacrum posteriorly is seen in dorsal view (fig. 58B), for with the reduction of the transverse processes of the third vertebra, the difference between the transverse widths of the anterior and posterior end is more striking in the sabre-tooth than in the true cat.

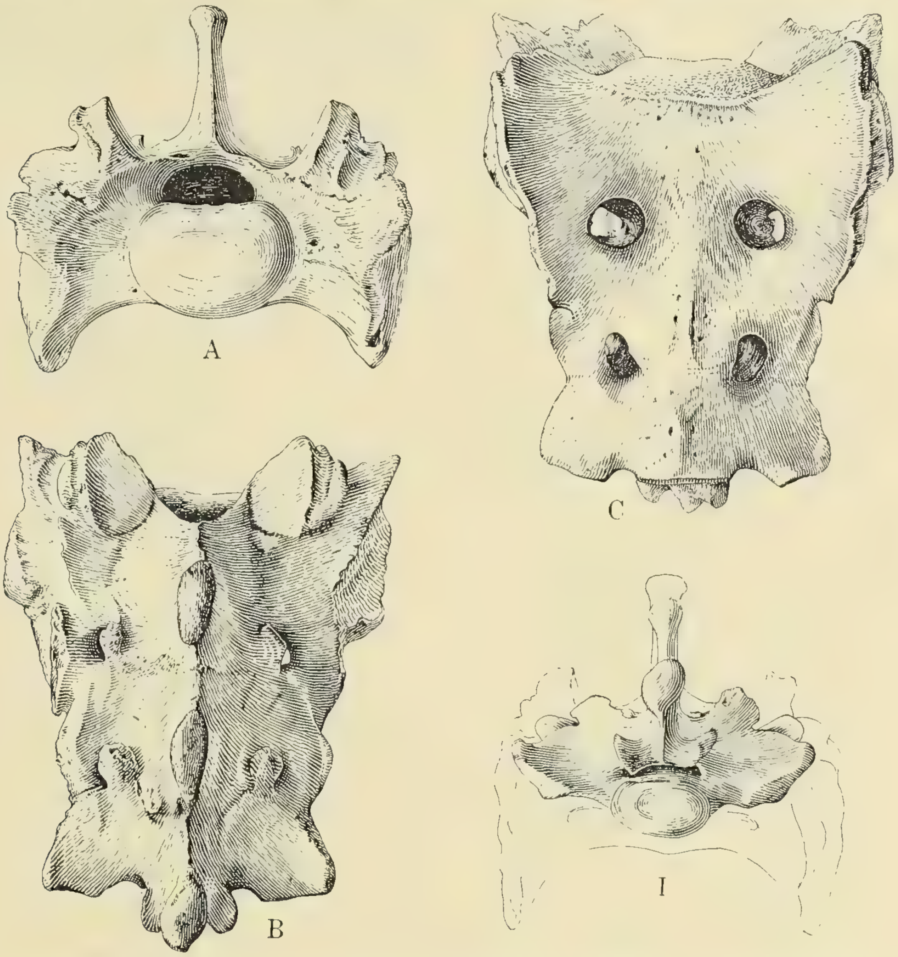

FIG. 58—*Smilodon californicus* Bovard. Sacrum, No. 2065-5. A, anterior view; B, dorsal view; C, ventral view; D, posterior view; × 1/2. Rancho La Brea Pleistocene.

The neural spines of the three vertebræ are broad anteroposteriorly and are strongly developed. The spine of the first vertebra is vertical, that of the second leans slightly backward, and that of the third vertebra leans more decidedly backward. In the extinct lion-like form, as in the living true felines, the spines of the vertebræ are relatively more slender. In *Felis atrox* there is a distinct tendency on the part of the spines to lean forward rather than backward. In the sabre-tooth the posterior border of the spine of the third vertebra rises directly upward and backward from a point on the margin of the neural canal between the posterior zygapophyses. In *F. atrox*, on the other hand, the posterior base of the spine is situated well in advance of the rim of the canal and farther forward with reference to the posterior zygapophyses. Distinct spines may be occasionally lacking in sacra of *Smilodon* from Rancho La Brea.

---

[1] The sacrum described and figured by Merriam and Stock (Carnegie Inst. Wash. Pub. No. 347, p. 21, pl. 6, figs. 9, 9*a*, 1925) as of *Arctotherium* probably represents a large sabre-tooth cat.

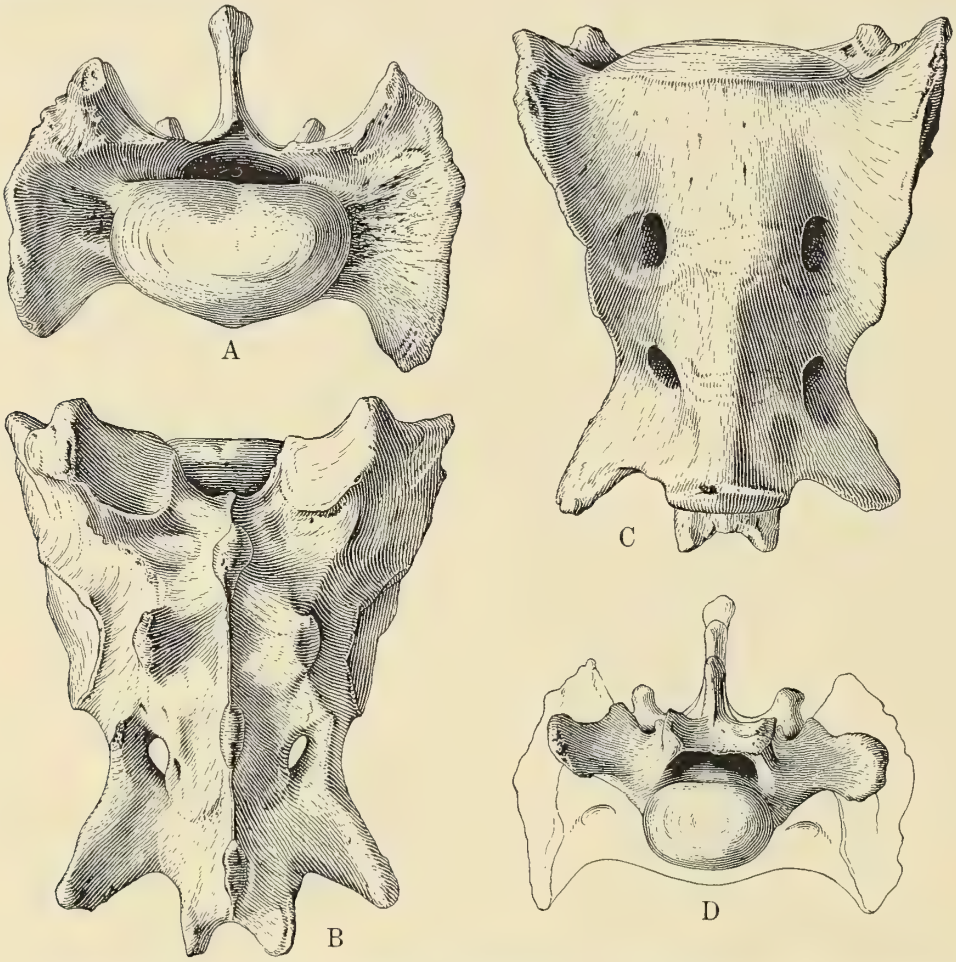

FIG. 59—*Felis atrox* Leidy. Sacrum, No. 2963-2. A, B, C, D, same views as in figure 58; × 1/2. Rancho La Brea Pleistocene.

The anterior zygapophyses are oval in shape and are not so large as in the *Felis atrox*. The united articular processes between the first and second vertebræ show greater reduction than in *F. atrox*. The dorsal sacral foramina are relatively large. When the sacrum is viewed from the front (fig. 58A), the alæ are seen to project farther downward in the sabre-tooth than in *F. atrox*. The wings do not extend so far forward with reference to the plane of the front face of the centrum in the former as in the latter. As viewed from the anterior end, the neural canal may have dimensions similar to those of *F. atrox*. Posteriorly, however, the opening of the neural canal may be somewhat smaller in the sabre-tooth.

Situated laterad to the metapophyses supporting the anterior zygapophyses of the first vertebra is a well-defined groove which extends from the dorsal surface be-

TABLE 33—*Measurements (in millimeters) of sacrum of Smilodon*

	2065–1	2065–2	2065–3	2065–4	2065–5	2065–6	2065–7	2065–8	2065–9	2065–10
Greatest length measured parallel to median line	137.3	145.9	141.8	137.7	132.1	118.6	120.8	122.2	117.6	110.9
Greatest width at anterior end and from outer sides of surfaces for ilia	111.5	105.7	107.8	106.8	105.4	98.4	101.6	85.4	88.5	77
Greatest width of third sacral vertebra across transverse processes	74.9	87.7	*a*70	67.4	78.7	70	59.8	57.8	60.8	54.3
Greatest width between dorsal borders of anterior zygapophyses	64.6	59.6	51.4	69.9	58	56.7	52.4	50	52.5	47.5
Width across posterior zygapophyses of third sacral vertebra	18.7	26.3	27.4	......	25.8	15.4	15.9	19.7	16.3	13.4
Width across posterior zygapophysis of third sacral vertebra	21	23.8	23.3	22.6	25	20.6	20.6	18.3	20.3	19
Depth of centrum of first sacral vertebra measured normal to floor of neural canal and across anterior epiphysis	30.8	29.3	33.9	28.8	30	29.7	25.5	26.4	25.5	23
Greatest distance from dorsal margin of anterior zygapophysis to ventral border of surface joining with ilium	82.2	86.1	90.6	80.7	81.3	78	74.4	*a*68	76.2	....
Height from median ventral surface of first sacral vertebra to top of first neural spine	79.2	65.6	82.8	49.1	72.7	78.3	63.2	63.5	63	....
Depth of centrum of third sacral vertebra measured across posterior epiphysis	14.5	15.4	14.7	13.7	14.4	14.4	12.7	12.2	12.9	11.6

a, Approximate.

TABLE 34—*Measurements (in millimeters) of sacrum of Felis atrox*

	2963–1	2963–2	2963–3	2963–4	2963–5	2963–6	2963–7	2963–8	2963–9	2963–10
Greatest length measured parallel to median line	150.5	148.6	144.2	141	139.3	131.7	131.8	*a*118	118	117
Greatest width at anterior end and from outer sides of surfaces for ilia	*a*118	119.3	*a*105	106	102.8	101.8	99.5	100.8	100.1	98.5
Greatest width of third sacral vertebra across transverse processes	95.5	90	96.8	*a*90	82.5	85.8	*a*75.5	......	76.9	.....
Greatest width between dorsal borders of anterior zygapophyses	77.6	75.4	73.5	70.5	69	64.3	64.4	70.2	*a*64.5	60.1
Width across posterior zygapophyses of third sacral vertebra	30.7	28.7	23	30.8	28.7	22.6	24.7	......	25.2	23.5
Width across posterior epiphysis of third sacral vertebra	34.7	33.4	30.7	30.9	31.6	29.6	29.6	29.7	27.5	27.5
Depth of centrum of first sacral vertebra measured normal to floor of neural canal and across anterior epiphysis	37.6	36.6	30.7	33.8	33.6	28.2	31.4	31.3	30.8	29.7
Greatest distance from dorsal margin of anterior zygapophysis to ventral border of surface joining with ilium	80.8	77.8	71.6	76.7	71.7	67.7	67.5	66.3	65.6	63
Height from median ventral surface of first sacral vertebra to top of first neural spine	.....	79.6	75.6	77.2	69.3	67.8	.....	68.2	69.7	.....
Depth of centrum of third sacral vertebra measured across posterior epiphysis	25	22.4	21	21.2	21.9	20.1	22	20.4	18.6	19.7

a, Approximate.

hind the process to the forward side. Occasionally the metapophysis stands forth as a very distinct process. The contact surface with the ilium is less clearly ear-shaped in the sabre-tooth and is not deeply excavated posteriorly as in *Felis atrox*. The area for attachment of the sacro-iliac interosseous ligaments is decidedly rugose.

On the ventral surface of the sacrum (fig. 58C), a noticeable difference between the sabre-tooth and *F. atrox* is seen in the size of the ventral sacral foramina. These are of large size in *Smilodon*, the anterior opening particularly being larger than in *F. atrox*. The ventral surface is flattened with a suggestion of a median keel on the second and third vertebræ. In the great lion-like cat the median surface of the sacrum, particularly of the second and third vertebræ, is convex. As indicated above, the transverse process of the third vertebra is reduced in *Smilodon* and does not project outward and backward to the extent seen in the true felines.

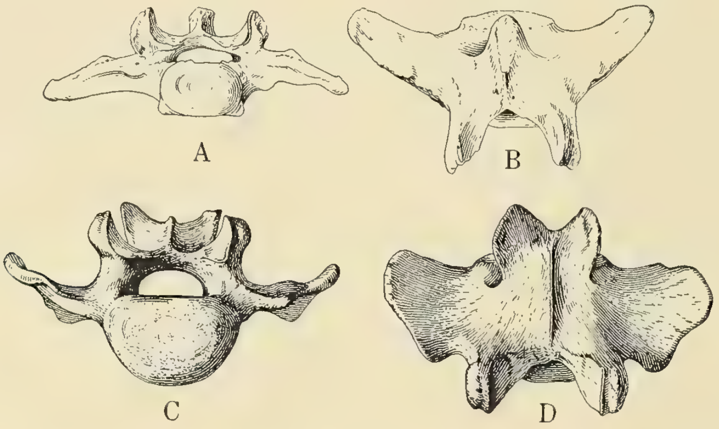

FIG. 60—*Smilodon californicus* Bovard. 1st caudal vertebra. No. 2068-1. A, B, anterior and dorsal views. *Felis atrox* Leidy. 1st caudal vertebra, No. 2966-1. C, D, anterior and dorsal views; × 1/2. Rancho La Brea Pleistocene.

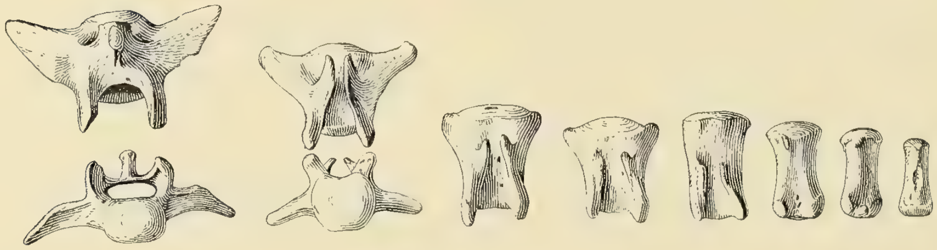

FIG. 61—*Smilodon californicus* Bovard. Representative caudal vertebræ, posterior to the first; dorsal and anterior views; × 1/2. Rancho La Brea Pleistocene.

CAUDAL SERIES

With the shortening of the tail in *Smilodon* a striking difference prevails between this type and the true felines, like the modern lion or tiger. Not only are there fewer vertebræ in the sabre-tooth, but there is likewise a greater shortening of the individual segments and greater specialization in the reduction of particular structures than in the large true felines. Thus the first caudal is considerably smaller than the comparable element in *Felis atrox* (see fig. 60A, B and C, D). In contrast to this type and the modern lion, *Smilodon* exhibits considerable reduction of the neural arch. Moreover, the posterior zygapophysis may disappear entirely, but the neural spine may be more prominently developed. The transverse process is comparatively narrow anteroposteriorly and projects backward in its outward curve. In *F. atrox* on the other hand it is broader and more wing-like. The centrum is compressed dorsoventrally with a short ridge giving prominence to each ventrolateral border at the forward end. The neural canal is likewise compressed in dorsoventral direction and is less capacious than in *F. atrox.*

In the vertebræ immediately posterior to the first, the neural arch becomes incomplete and this failure to roof over the canal is initiated farther forward in the series than in *Felis atrox.* In the extinct form the reduction of the neural arch is like that in the caudal series of *F. leo* and *F. tigris.* Likewise, the anterior zygapophyses in *Smilodon* become reduced more rapidly than in *F. atrox.* Some of the vertebræ posterior to the first in *Smilodon* are shown in figure 61.

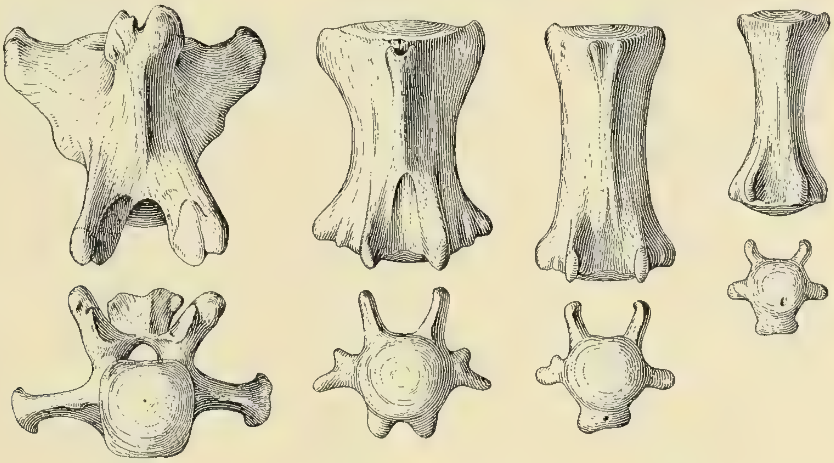

FIG. 62—*Felis atrox* Leidy. Representative caudal vertebræ, posterior to the first; dorsal and anterior views; × 1/2. Rancho La Brea Pleistocene.

In the caudal appendage of *Felis atrox* the individual vertebræ are strongly developed and evidently possessed characters closely similar to those seen in the comparable elements of the large living felines. Representative vertebræ of the extinct type of Rancho La Brea, but not all of the same individual, are shown in figure 60C and D and in figure 62.

MANUBRIUM

While the manubrium of *Smilodon* may be similar in width to that of *Felis atrox*, it exceeds that of the latter form distinctly in depth. The dorsal surface of the body of this element may be flattened, but frequently the dorsal and ventral surfaces develop a median ridge. On the dorsal surface of the projecting forward portion of the manubrium, the median ridge extends anteriorly to the tip. In *F. atrox*, the dorsal surface may be flat or slightly concave transversely, particularly between the first costal cartilages. In both dorsal and lateral views, the projecting portion of the first sternal element is seen to taper toward the anterior

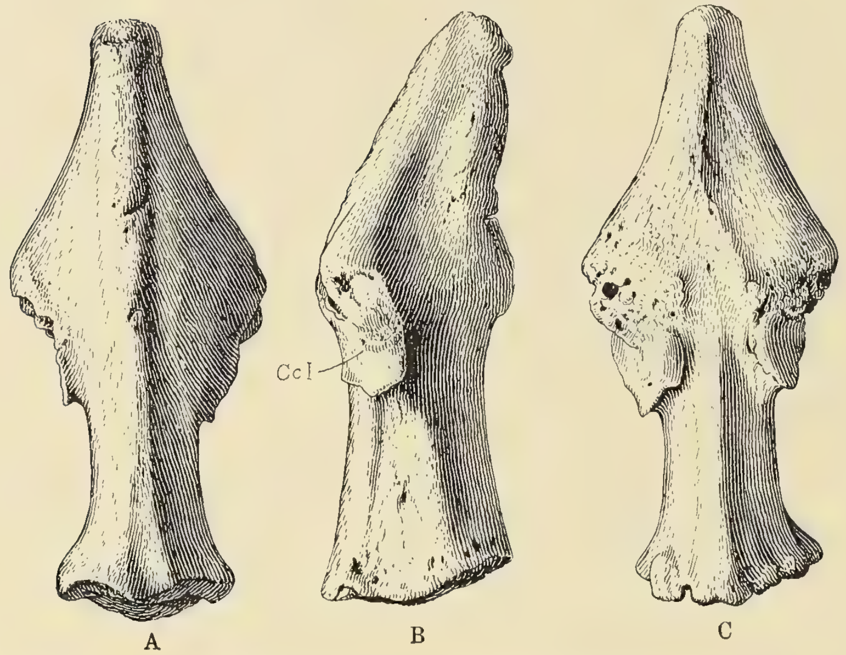

Fig. 63—*Smilodon californicus* Bovard. Manubrium, No. 2066-7. A, ventral view; B, lateral view; C, dorsal view; × 2/3. *CcI*, attachment of first costal cartilage. Rancho La Brea Pleistocene.

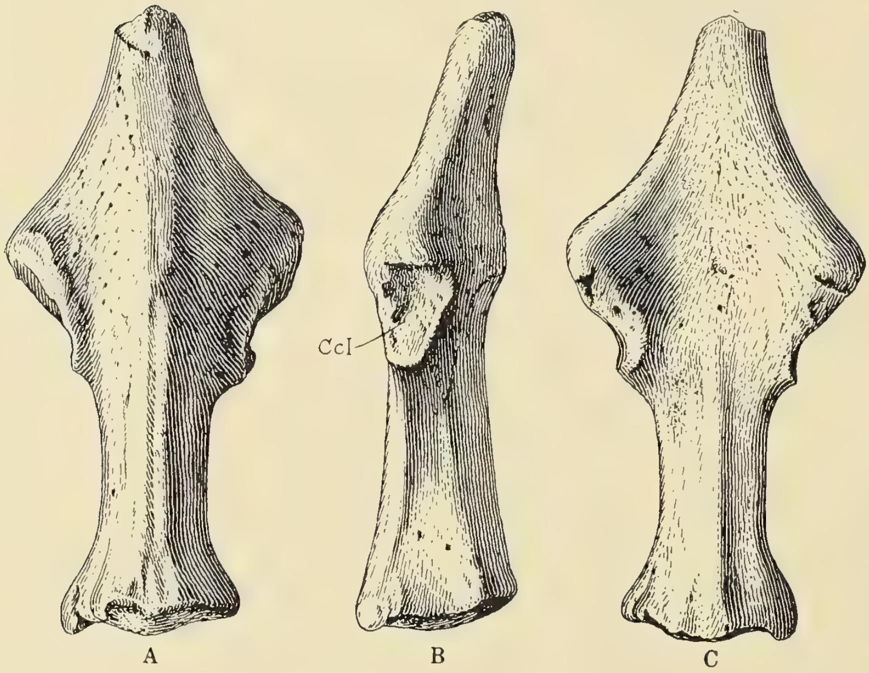

Fig. 64—*Felis atrox* Leidy. Manubrium, No. 2964-4. A, B, C, same views as in figure 63; × 2/3. Rancho La Brea Pleistocene.

end. The principal fore and aft axis of this part may be in line with that of the body, but frequently it is deflected downward from that of the latter. The anterior end may be rugose, terminating apparently in cartilage, or the end may be rounded and knob-like. The median ventral keel or ridge of the anterior projecting portion is often incompletely formed and was apparently also covered with cartilage. The surfaces for attachment of the first costal cartilages are relatively large in *Smilodon*, and are not separated by so great a distance as in *F. atrox*.

TABLE 35—*Measurements (in millimeters) of manubrium of Smilodon*

	2066–1	2066–2	2066–3	2066–4	2066–5	2066–6	2066–7	2066–8	2066–9	2066–10
Greatest length measured parallel to long axis through middle of body of manubrium	141.1	135.6	141	137.4	123.8	127	117.9	122.2	100.5	101.6
Greatest width at forward end of surfaces joining with first costal cartilages	56.5	51.9	44.8	41.7	50.7	52.9	51.3	58.7	47.6	36.7
Greatest depth measured from point between rugose surfaces for costal cartilages	46.7	42.1	39.9	44.9	41	44.3	36.8	41.5	27	32.5
Depth of distal end	39.6	42.4	36.5	40.8	45.4	39	38.3	41.7	38.3	34.6
Width of distal end	34.8	31.7	29	28.6	32.9	32	34.8	37.7	30.7	23.4
Least depth behind surfaces for costal cartilages	32.6	30.2	29.7	26.9	33	30.4	26.5	32.7	21.3	23.2

TABLE 36—*Measurements (in millimeters) of manubrium of Felis atrox*

	2964–1	2964–2	2964–3	2964–4	2964–5	2964–6	2964–7	2964–8	2964–9
Greatest length measured parallel to long axis through middle of body of manubrium	130	116.8	120	123.6	*a*102.8	*a*99.4	108	104.7	103.6
Greatest width at forward end of surfaces joining with first costal cartilages	58	63.4	50.8	57.3	49	51.7	50	58.8	54.2
Greatest depth measured from point between rugose surfaces for costal cartilages	30.6	25.1	23.5	23.7	25	21	21.4	29	19.4
Depth of distal end	37.7	33.5	34.7	33.8	29.9	36.6	31.6	35.5	39.7
Width of distal end	34	34.8	35	34	25	30.9	25	34	33.8
Least depth behind surfaces for costal cartilages	27.9	22	20.6	19.8	20.3	20.7	20.6	24.4	21.2

a, Approximate.

MESOSTERNUM

Elements in this region of the sternum of *Smilodon* offer, as perhaps their most striking characteristic, a noticeable depth in comparison to the length. In this respect the sabre-tooth appears to differ from *Felis atrox*. Individual segments are heavy, but vary in width and in length. Specimens representing the sabre-tooth and lion-like form of Rancho La Brea are shown in figure 66.

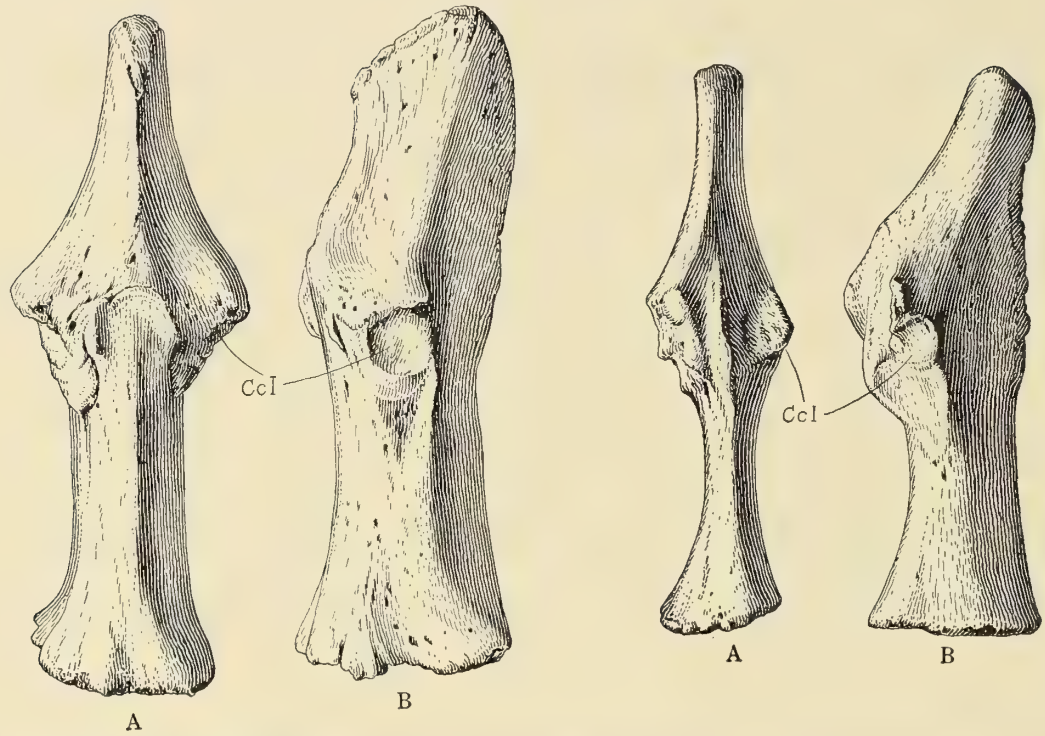

Fig. 65—*Smilodon californicus* Bovard. Manubria, Nos. 2066-11, 2066-12. A, ventral view; B, lateral view; × 2/3. Specimens show variation in size and shape. *CcI* attachment of first costal cartilage. Rancho La Brea Pleistocene.

XIPHISTERNUM

The last sternal segment is less expanded transversely and is thicker dorsoventrally in the sabre-tooth than in the extinct true feline. This element, except for the slight expansion of the proximal end, is rod-shaped. The distal end, as a rule, does not flare greatly. The greatest dorsoventral diameter is situated not far behind the proximal end. The ventral surface develops a median ridge. The dorsal surface is not flattened to the extent seen in *Felis atrox*. The xiphisternum reflects in its structure the sturdiness of the sternum.

Table 37—*Measurements (in millimeters) of xiphisternum*

	Smilodon californicus										Felis atrox		
	2067–1	2067–2	2067–3	2067–4	2067–5	2067–6	2067–7	2067–8	2067–9	2067–10	2965–1	2965–2	2965–3
Greatest length through middle	74.2	72.6	62.1	62.4	61.3	55.3	52.6	50.9	47.2	43.2	81	80	66.7
Greatest width of proximal end	25.6	22.5	25.8	21	26	21.7	18	21.5	17.1	19.9	30.1	27.1	20.8
Greatest width of distal end	19	15.6	17.7	15.3	22.3	15.8	15.7	15.5	17.7	20.6	25.6	25.3	33.3
Greatest dorsoventral diameter	22	19.4	22.8	22.3	16.6	17.3	17.2	18	14	15.3	17	13.5	14

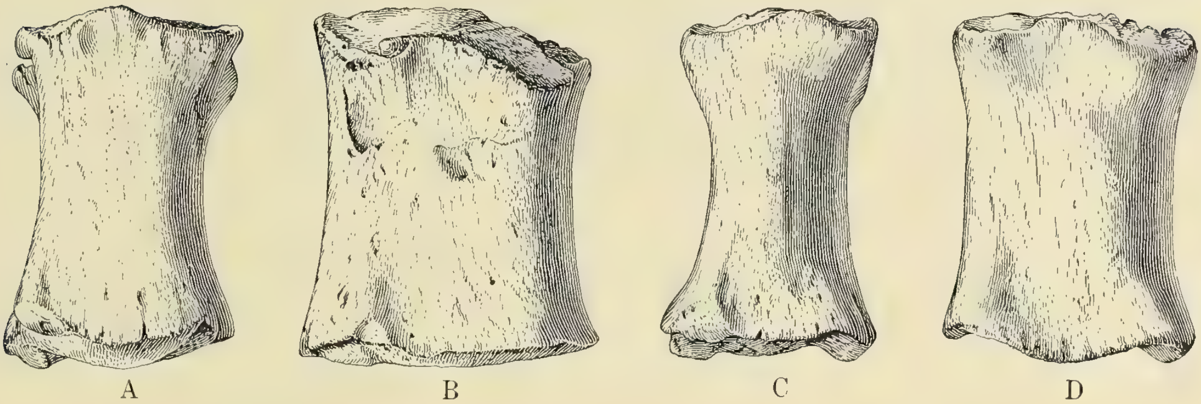

Fig. 66—Mesosternal elements. A, B, *Smilodon californicus* Bovard, No. J-8269; C, D, *Felis atrox* Leidy, No. X-7394; × 1. Rancho La Brea Pleistocene.

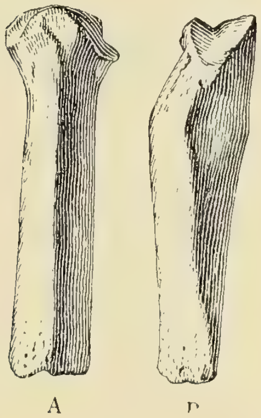

Fig. 67—*Smilodon californicus* Bovard. Xiphisternum, No. 2067-2. A, ventral view; B, lateral view; × 2/3. Rancho La Brea Pleistocene.

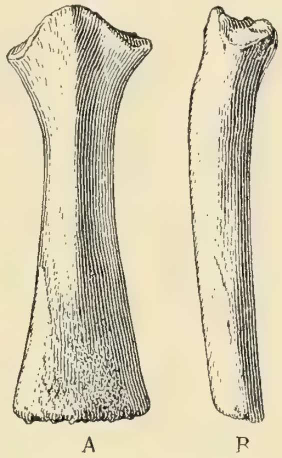

Fig. 68—*Felis atrox* Leidy. Xiphisternum, No. 2965-2. A, B, same views as in figure 67; × 2/3. Rancho La Brea Pleistocene.

RIBS

Plate 20, figs. 1 to 13

The ribs of *Smilodon* are generally shorter but stouter than those of *Felis atrox*. The first costal rib with its expanded vertebral and sternal end is a particularly strong element in the sabre-tooth. The tuberculum and capitulum in this element are separated by a broad notch which is, however, not so deep relatively as in *F. atrox*. The outer and inner borders of the posterior surface of the shaft are sharply defined. In mid-costal region the shafts are broad. In all the ribs of *Smilodon* the surface texture of the bone appears to be coarser than in *F. atrox*. Moreover, the ridges and roughened areas for muscle attachment may be more pronounced in the former than in the latter type.

CLAVICLE

Four specimens, fig. 69, represent felid clavicles and are presumably to be referred to *Smilodon*. These elements show some variation in size as well as in shape. It is possible that one or more of these specimens should be assigned to *Felis atrox*, but the numerical representation of the sabre-tooth in the collections from Rancho La Brea makes it more probable that they belong to the latter form.

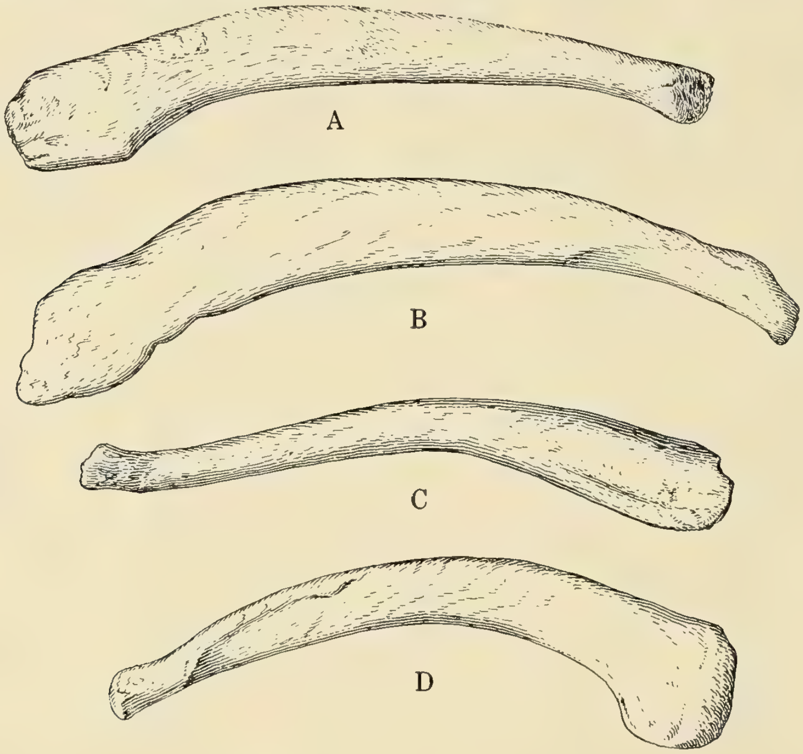

FIG. 69—Clavicles, presumably of *Smilodon californicus* Bovard. A to D, Nos. I-4, I-5, I-2, I-3; × 1. Rancho La Brea Pleistocene.

In essential characters the clavicle resembles that in *Felis* and the reduction is similar to that in the latter. In the largest of the four specimens, No. I-5, the shaft is relatively heavy. At each end a small roughened surface suggests cartilaginous or ligamentous attachment. In No. I-3 the outer end is wider than that in the remaining specimens.

Measurements (in millimeters) of Clavicle

	I-2	I-3	I-4	I-5
Greatest length in straight line from outer to inner end	84	80.1	91.8	101.1

SCAPULA

Plates 21 and 36, figs. 1 and 1a

The shoulder blade of *Smilodon* differs in several respects from that of the true felines. It is relatively narrow in fore and aft direction and high dorsoventrally. The vertebral border is sharply angulate as a result of the projection of the ossified suprascapular cartilage above and in front of the upper end of the spine. The ossified cartilage in this region is distinctly wider dorsoventrally than in the scapula of *F. atrox*. No distinct superior angle is formed where the vertebral border meets the anterior superior border as in *Felis*, although an angle is at least suggested in scapulæ of *Smilodon* from Rancho La Brea. The anterior superior border is broadly rounded and curves directly into the border of the suprascapular notch without an intervening angulation. The inferior angle formed at the point of meeting of the vertebral border and the axillary border is greater in *Smilodon* than in the true felines. In the Pleistocene *Felis atrox* this angle is slightly greater than 90°. The axillary border is not quite so straight in *Smilodon* as in the former species.

TABLE 38—*Measurements (in millimeters) of scapula of Smilodon*

	2004–R-8	2004–R-6	2004–R-1	2004–R-3	2004–R-2	2004–R-10	2004–R-9	2004–R-5	2004–R-4	2004–R-7
Greatest length from coracoid process to suprascapular border, measured along axis of spine	358	343	342	*a*327	324	322	316	310	298	266
Greatest width of articulating end measured across glenoid cavity	87.1	79.8	79.5	78.7	72.7	78.6	75.0	75.9	74.2	67.0
Greatest transverse diameter across glenoid cavity	57.9	49.5	54.6	53.0	50.6	50.5	46.3	44.0	40.8	41.5
Distance from inner border of glenoid cavity to top of spine	......	89.0	96.6	*a*85.3	86.0	80.0	78.7	76.5	79.3	70.1
Width of scapular blade, measured obliquely across spine	191	186	193	197	175	170	162	167	167	148
Least width of neck across articulating end	73.2	76.4	72.9	73.9	61.3	66.2	61.4	59.5	64.3	55.1

a, Approximate.

TABLE 39—*Measurements (in millimeters) of scapula of Felis atrox*

	2902–R-1	2902–R-2	2902–R-3
Greatest length from coracoid process to suprascapular border, measured along axis of spine	354	*a*309	290
Greatest width of articulating end measured across glenoid cavity	85	78	65.1
Greatest transverse diameter across glenoid cavity	56.8	50	44
Distance from inner border of glenoid cavity to top of spine	98	89.7	81.5
Width of scapular blade, measured obliquely across spine	*a*215	181	169
Least width of neck above articulating end	77.8	64.2	58.7

a, Approximate.

A noticeable difference between the sabre-tooth and the true felines is seen in the scapular spine. The free margin of the spine is not carried backward over the infraspinous fossa as in *F. atrox*. A slight backward curving of the outer portion is sometimes to be seen at approximately the middle of the spine in *Smilodon*, but it is never so general in its extent as in the true cats. A distinct metacromial process, like that of *F. atrox*, is absent in the sabre-tooth. The acromion is relatively heavy. The glenoid cavity may be longer anteroposteriorly and narrower transversely in *Smilodon* than in *Felis*. The outer border of the cavity below the base of the spine may be incised by a deeper and broader notch in the sabre-tooth than in *F. atrox*. The coracoid process has a length comparable to that in the great lion-like cat and is fairly stout.

The supraspinous fossa is slightly larger than the infraspinous fossa. The surface of each fossa slopes medially and forms a deep depression on each side of the base of the spine. These surfaces lack the undulations seen in the shoulder blade of *Felis*. The inner surface is broadly convex in anteroposterior direction.

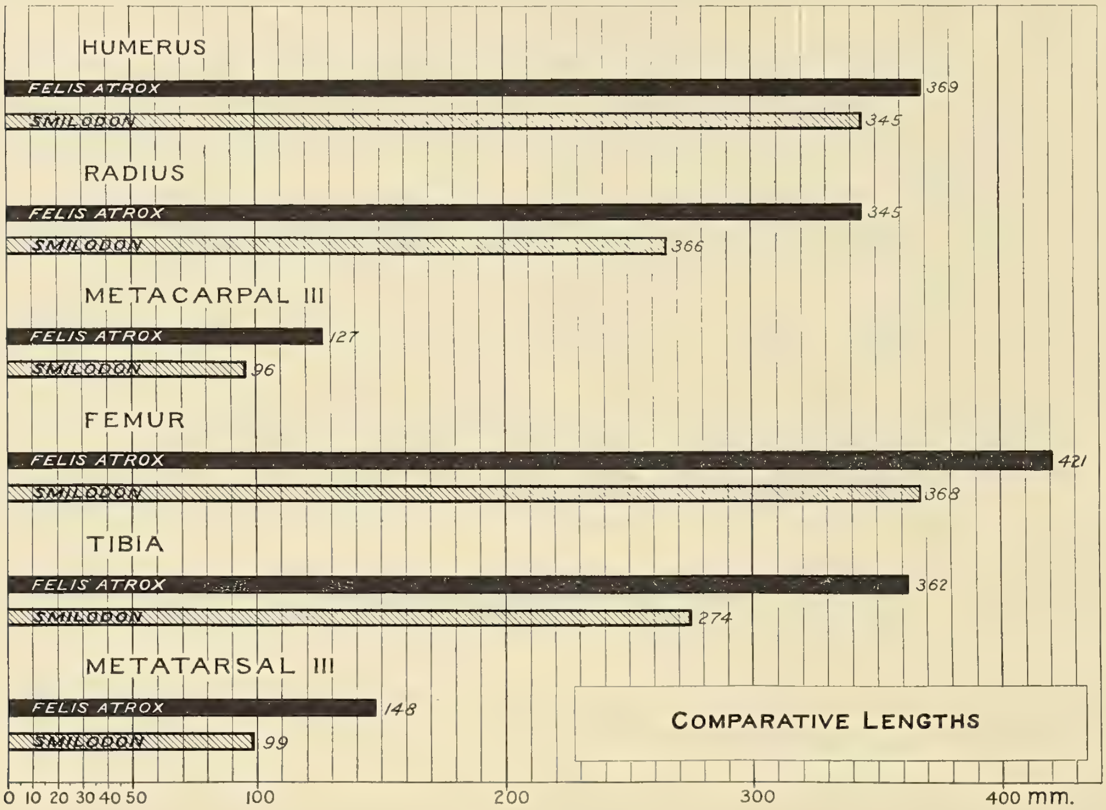

FIG. 69a—Diagram illustrating the comparative lengths of appendicular elements of *Felis atrox* Leidy and *Smilodon californicus* Bovard from Rancho La Brea.

COMPARISON OF LENGTHS OF LIMB ELEMENTS

Figure 69a displays graphically the differences between *Smilodon californicus* and *Felis atrox* in the length of individual elements of the front and hind limbs. Each bar represents an average of the series of measurements of total length given in the tables of measurements. While the specimens selected for measurement include both the longest and shortest adult elements, the series for *Smilodon* is based upon a decidedly larger group of individuals than is that for *F. atrox*.

In the front limb of *Smilodon* the shortening of the epipodial region furnishes a distinct point of contrast between this cat and *F. atrox*. A shortening of the metapodial region in the former type is also apparent.

A similar shortening of the epipodial region is noticeable in the hind limb of *Smilodon* and the shortening of the metapodial segment in this form is more apparent than in the front limb.

In *Felis atrox* the length of femur in relation to the length of humerus is greater than in the sabre-tooth.

The following ratios may be recorded:

TABLE 40—*Comparison of Ratios of Limb Segments*

	F. atrox	*F. leo*	*F. leo*	*F. tigris*	Jaguar	Jaguar	Jaguar	*Smilodon californicus*
$\frac{\text{Radius}}{\text{Humerus}}$	0.93	0.89	0.93	0.86	0.79	0.82	0.87	0.77
$\frac{\text{Metac. III}}{\text{Humerus}}$	.34	.35	.36	.37	.30	.31	. . .	.28
$\frac{\text{Tibia}}{\text{Femur}}$	.86	.86	.88	.84	.85	.85	.87	.74
$\frac{\text{Metat. III}}{\text{Femur}}$	.35	. . .	.37	.36	.32	.33	. . .	.27
$\frac{\text{Humerus}}{\text{Femur}}$	.88	.92	.89	.88	.91	.87	.91	.94

Comparisons of ratios between the extinct *Felis atrox* and the modern lion, tiger, and jaguar are handicapped unfortunately by lack of large series of specimens representing the latter types. From the materials available it would appear that the limb proportions of the jaguar are less like those of *F. atrox* than are those of *F. leo*. On the other hand, judged in the light of the three individuals available of the jaguar, at least some variation in the values obtained can be demonstrated. All that can be stated at present is that in the jaguar the epipodial and metapodial segments in both front and hind limbs show a greater shortening, but not a much greater shortening, with reference to the propodial segments than in the extinct form. The differences are certainly not so great as those which distinguish the sabre-tooth cat from *F. atrox*.

HUMERUS

Plates 21 and 36, figs. 2 to 5

The humerus in *Smilodon* may be as long as or longer than that of the living species, *Felis leo* and *F. tigris*. This element may be as long as the humerus in some individuals of the Pleistocene *F. atrox*, but is generally heavier.

At the proximal end the articulating head of the humerus is narrower transversely and the surface is perhaps flatter than in the true cats. The greater tuberosity extends farther backward along the side of the articulating surface in the sabre-tooth than in the Pleistocene *F. atrox*. The proximal surface of this tuberosity, to which are attached the supraspinatus and the anterior part of the deep pectoral muscles, is bent somewhat as it extends inward and forward from the outer side. In *F. atrox* as in the modern cats, this surface extends obliquely inward and forward. The lesser tuberosity is not so well developed in *Smilodon* as in *Felis*, although the inner surface for attachment of the subscapularis muscle is broader and flatter in the former than in the latter. The reduction of a distinct tuberosity makes the bicipital groove, as viewed from above, a more open channel in the sabre-tooth than in the true cats.

A noticeable difference between *Smilodon* and the true felines is seen in the contour of the front end of the greater tuberosity. In the Pleistocene *F. atrox* the proximal border of the tuberosity descends gradually from a point above and in front of the depression for the supraspinatus to the pectoral ridge. In this respect the latter appears to be somewhat intermediate between the living lion and tiger. In *Smilodon*, on the other hand, the proximal border extends for some distance inward and forward from a point above and in front of the depression for the infraspinatus at approximately the same level or with a slight ascent before turning downward to the pectoral crest (compare fig. 70, A and B).

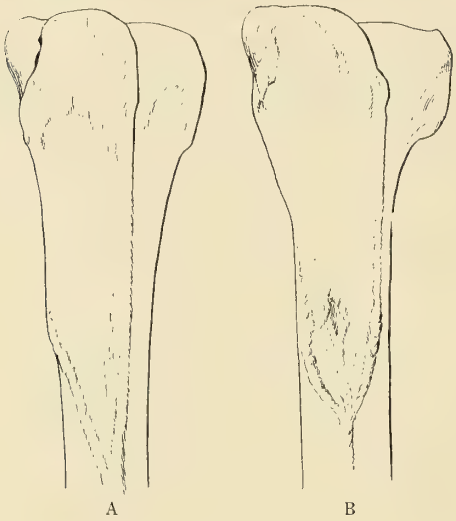

Fig. 70—Right humerus; anterior view; × 1/3. A, *Smilodon californicus* Bovard, No. 2005-R-6; B, *Felis atrox* Leidy, No. 2903-R-8. Note characteristic differences between sabre-tooth cat and true cat in proximo-internal profile of tuberosity and development of bicipital and deltoid crests. Rancho La Brea Pleistocene.

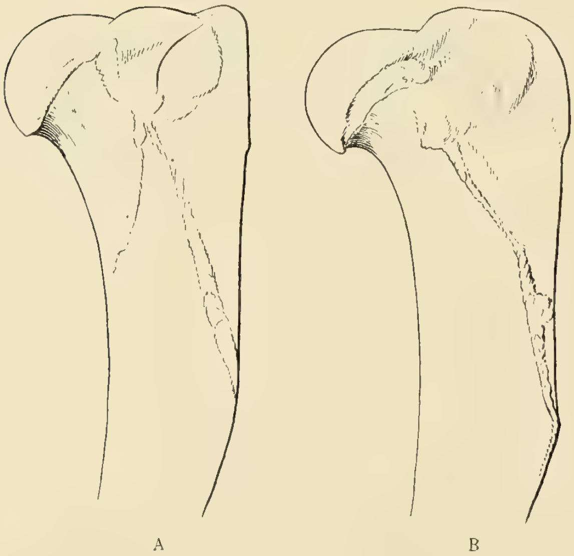

Fig. 71—Right humerus; lateral view; × 1/3. A, *Smilodon californicus* Bovard, No. 2005-R-6; B, *Felis atrox* Leidy, No. 2903-R-8. Note particularly difference in profile of tuberosity. Rancho La Brea Pleistocene.

The small tubercle situated between the bicipital groove and pectoral ridge, to which is attached the anterior part of the deep pectoral muscle, may not be so well defined in some specimens of *Smilodon* as in the true cats. The depressed area on the outer side of the greater tuberosity for the insertion of the infraspinatus is larger in the sabre-tooth than in *F. atrox*. Below this the area for the attachment of the teres minor muscle is seemingly not so well defined in *Smilodon* as in *F. atrox*. The rugose area on the inner surface of the shaft for the attachment of the inner humeral head of the triceps muscle appears to be larger in *Smilodon* than in the extinct true feline. The pectoral ridge is straight, and near its union with the deltoid crest it is not curved inward as is frequently the case in the Recent lion and tiger and in the Pleistocene *F. atrox*. The union of the two ridges is apparently situated lower on the shaft in *Smilodon* than in the great lion-like cat. The entepicondylar foramen may be distinctly larger in *Smilodon* than in the extinct *F. atrox*, but the bridge of bone enclosing the foramen may be narrower. In *Smilodon* the supracondylar ridge of the outer side, when viewed from the front, does not have the sinuous curve seen in the true cats. This ridge extends farther along the shaft in *Smilodon*.

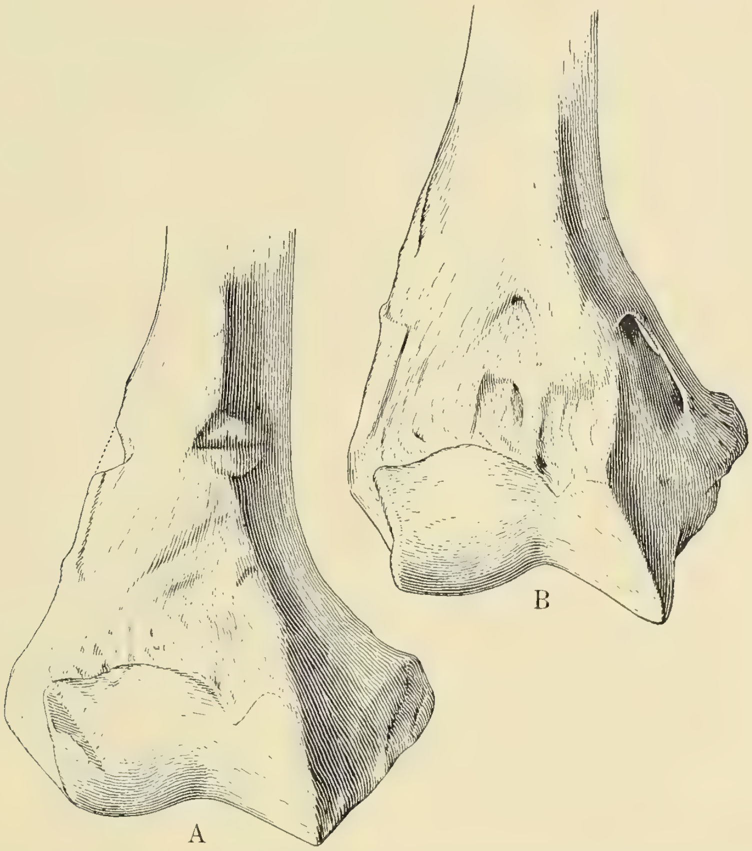

FIG. 72—*Smilodon californicus* Bovard. Distal portions of right humeri; anterior views; × 1/2. A, specimen without entepicondylar foramen, No. 2005-R-11; B, normal specimen with foramen, No. 2005-R-4. Rancho La Brea Pleistocene.

In posterior view the distal end of the shaft widens rapidly below, and the distal extremity is wider in the sabre-tooth than in *F. atrox*. The olecranon fossa may be relatively larger in the former than in the latter. The inner condyle, while more prominent in the sabre-tooth than in *F. atrox*, is not situated so far back with reference to the distal articulating surface in the former as in the latter type. The outer condyle is deeper in proximo-distal direction, but relatively not so long anteroposteriorly in *Smilodon* as in *F. atrox*.

An interesting variation in the humerus of *Smilodon* from Rancho La Brea is seen in specimen No. 2005–R–11. This element lacks the entepicondylar foramen, a character in which it differs from humeri of a series of 238 individuals from the asphalt. Evidently the absence of the entepicondylar foramen is an extremely rare occurrence in the Californian species. The absence of this foramen has been noted in sabre-tooth cats of the South American Pleistocene and may occur more frequently in these types than in *S. californicus*. The character was regarded by some authors as of value in distinguishing *Smilodon* from *Machærodus*. On the other hand, Burmeister (1881, p. v) considered the absence as due to individual variation. Cope (1880, p. 857, fig. 15) figured a humerus of *Smilodon necator* in which the structural characters, including the absence of the entepicondylar foramen, resemble those in the upper arm bone from the asphalt.

TABLE 41—*Measurements (in millimeters) of humerus of Smilodon*

	2005–R-1	2005–R-2	2005–R-3	2005–R-4	2005–R-5	2005–R-6	2005–R-7	2005–R-8	2005–R-9	2005–R-10
Greatest length measured parallel to longitudinal axis	385	370	363	360	348	342	328	321	323	309
Greatest transverse diameter of proximal extremity	92.4	90.9	98	83.3	82.6	77.3	79.2	79.4	77.7	75.4
Greatest anteroposterior diameter of proximal extremity	117.6	113	118.2	105	100.7	95.8	97.8	95.9	95.7	92
Transverse diameter at middle of shaft	41.7	41.4	43.4	33.4	33.2	33.1	34.2	36.7	34.3	32.2
Anteroposterior diameter at middle of shaft	57.7	61	56.2	51.3	50	48.7	51.9	46.3	42.5	47.5
Greatest width of distal extremity	125	116.8	128.3	106.6	106.3	98.7	108	106.6	99.3	98.8
Least anteroposterior diameter of articulating surface for ulna	35.4	31.5	36	30.3	31.1	31.3	30.5	30.1	28.4	27.5

TABLE 42—*Measurements (in millimeters) of humerus of Felis atrox*

	2903–R-1	2903–R-2	2903–R-3	2903–R-4	2903–R-5	2903–R-6	2903–R-7	2903–R-8	2903–R-9
Greatest length measured parallel to longitudinal axis	409	396	389	380	363	368	347	337	328
Greatest transverse diameter of proximal extremity	100.2	97.8	92.5	88.4	90.5	92.3	82.3	81.7	78.7
Greatest anteroposterior diameter of proximal extremity	123.4	121.6	122.7	112.8	111.2	112	102.8	101.7	99.1
Transverse diameter at middle of shaft	38.2	41.4	39.2	35	38.6	37.8	33.4	34.4	33
Anteroposterior diameter at middle of shaft	59.4	69.5	70	60.8	64.4	58.2	53.4	53.6	53.8
Greatest width of distal extremity	107.6	111.3	108.8	98.4	101	101.2	96.8	89.9	85.7
Least anteroposterior diameter of articulating surface for ulna	35	36	35.2	30.8	34	34	30.6	29.5	30

The specimen, No. 2005–R–11, from Rancho La Brea is considerably abraded. The scarring of the surface may be due to "pit wear," namely the result of an attrition of this bone and other skeletal elements caused by movement of the material in the mass of tar or asphalt after entombment. It is entirely possible that the external surfaces show also the work of other carnivorous mammals. The distal portion of the specimen is shown in figure 72A. The characters displayed by this element are clearly those of the sabre-tooth and not those of *F. atrox.* Greatest width of distal extremity 112.3 mm.; least anteroposterior diameter of articulating surface for ulna 31 mm.

ULNA

Plates 22 and 37, figs. 1 to 3

The ulna of *Smilodon,* in contrast to that of the extinct true cat of Rancho La Brea and of the modern cats, *Felis leo* and *F. tigris,* is distinctly shorter and decidedly heavier.

TABLE 43—*Measurements (in millimeters) of ulna of Smilodon*

	2007-R-1	2007-R-2	2007-R-3	2007 R-4	2007-R-5	2007-R-6	2007-R-7	2007-R-8	2007-R-9	2007-R-10
Greatest length measured parallel to longitudinal axis of ulna	372	372	361	358	348	338	318	306	301	287
Greatest width of posterior surface of olecranon process	48.8	48.8	48	45.3	48	42.3	43.5	41.3	39	33.6
Greatest transverse width of greater sigmoid cavity	60.2	52.2	60.1	56	56.7	53.5	48	47.1	42.2	41.5
Anteroposterior diameter measured from posterior border to top of coronoid process	78.8	70.8	77.6	69.3	77.8	68.7	61.8	62.6	60.2	57.3
Anteroposterior diameter of shaft at proximal end of tendon scar	47.6	41.4	43.1	39.1	47.1	40.6	36.7	37.6	30	34.8
Transverse diameter of shaft at proximal end of tendon scar	29.9	25.8	28	23.4	28.7	26.6	24.2	21.2	19.8	20.9
Greatest anteroposterior diameter of distal extremity	46.6	45.4	44.6	38.9	45.2	42.3	39.4	36.7	31.3	33.3
Greatest width of distal extremity	33.8	28.2	27.5	23.2	30.6	24.4	22.3	21.7	19.1	20.4

Viewed from above, the proximal surface of the olecranon process is seen to be much wider in *Smilodon* than in *F. atrox.* The surface for attachment of the scapular head of the triceps muscle is broader and more rugose. The broadening of the proximal surface furnishes also in transverse direction a longer area for attachment of the posterior humeral head of the triceps. The fossa in front of this area is not so well defined as that of the true cats. The outer anterior tubercle to which is attached the anconeus muscle is heavier, but is not so prominently developed as in *Felis atrox, F. leo* and *F. tigris.*

In *Smilodon,* in contrast to *Felis atrox,* the heaviness of the ulna is expressed in anterior view in greater width of olecranon process, in width of upper portion of articulating surface of the greater sigmoid cavity, and in width of shaft and distal end. The shaft as seen in this view is straighter in its longitudinal extent than that in the ulna of *Felis atrox.* The articulating surface for the radius is larger than that of the latter species.

In outer view, the ulna is again seen to be straighter in its longitudinal extent than that of *Felis.* The shaft is noticeably wider. The area for attachment of the outer humeral head of the triceps is distinctly larger in *Smilodon.* The articulating surface for the head of the radius is relatively large and the coronoid process is decidedly more prominent in the sabre-tooth than in *Felis.* The rugose area for attachment of the interosseous ligament is broad and in its downward extent, toward the distal extremity, is presumably better defined than in *Felis.* Apparently a strong bond between ulna and radius existed in the sabre-tooth, and the areas for muscle attachment suggest considerable power in the use of the forearm and front paw in this form.

A nutrient foramen perforates the shaft at a point approximately comparable in its position below the coronoid process to that in *Felis.* The foramen is situated close to the anterior border. The articulating surface for the pisiform is not so broad in the sabre-tooth as in *F. atrox.*

Table 44—*Measurements (in millimeters) of ulna of Felis atrox*

	2905–R-1	2905–R-2	2905–R-3	2905–R-4	2905–R-5	2905–R-6	2905–R-7
Greatest length measured parallel to longitudinal axis of ulna	438	437	420	435	402	396	384
Greatest width of posterior surface of olecranon process	47.7	45.1	40.9	42.4	40.8	35.4	35.9
Greatest transverse width of greater sigmoid cavity	65	69.7	65.1	67.3	59.2	55.6	48
Anteroposterior diameter measured from posterior border to top of coronoid process	87.5	87.8	79.6	84.5	74.8	68.9	68.5
Anteroposterior diameter of shaft at proximal end of tendon scar	56.7	57.7	50	54.3	51.3	43.7	42.5
Transverse diameter of shaft at proximal end of tendon scar	24	22.8	24.7	25	21.8	21	20.7
Greatest anteroposterior diameter of distal extremity	44.6	47.5	44.1	45.2	41.2	37	36.2
Greatest width of distal extremity	27.5	27.7	28.5	28.4	27.7	24	23

RADIUS

Plates 22 and 37, figs. 4 and 5

The radius is distinctly shorter and relatively heavier than the comparable element in *Felis atrox* and in the modern large felines. The stoutness of the radius is particularly noticeable in the proximal and distal extremities and in the lower half of the shaft as viewed from the side. While the long diameter of the head is not so great as that in the extinct true cat, the diameter normal to the long axis is greater in the sabre-tooth. The proportions of the proximal extremity furnish a broader articulating surface for the humerus. The articulating surface for the lesser sigmoid cavity is relatively large.

The tubercle situated on the anterior surface and below the head is not so large as in the lion and tiger and is directed less anteriorly and more toward the ulnar border in the sabre-tooth than in the Pleistocene *F. atrox* and in the living cats. The nutrient foramen is situated not so far below the tubercle in *Smilodon* as in the true cats. The shaft is more bowed in its longitudinal extent in *Smilodon* than in *Felis atrox.*

At the distal extremity, the facet for the ulna is smaller and the styloid process is heavier than in *F. atrox.* The groove for the tendon of the extensor ossis metacarpi pollicis muscle is well defined and deep. The groove for the extensores carpi radialis longior and brevior muscles is broad and deep. That for the extensor communis digitorum muscle is also broad but shallower than in the Pleistocene true feline. The articulation for the scapho-lunar is not so long in *Smilodon* as in *F. atrox*, but the surface is broader in the former than in the latter.

Table 45—*Measurements (in millimeters) of radius of Smilodon*

	2006–R-1	2006–R-2	2006–R-3	2006–R-4	2006–R-5	2006–R-6	2006–R-7	2006–R-8	2006–R-9	2006–R-10
Length measured along internal border	289	295	294	269	264	257	260	258	236	235
Long diameter of proximal end	49.8	55.5	47	50.3	46	45.6	45.4	47.1	41.3	41.8
Greatest diameter taken at right angles to long diameter of proximal end	42	44	38	40.2	37	33.9	35.9	37.6	33.5	32.2
Width of shaft at middle	38.8	33.8	34.6	34.3	29.8	31	30.5	27.5	33	26
Thickness of shaft at middle	22	24.6	19.7	24.1	20.6	18.9	21.1	19.5	19.6	16.5
Greatest width at distal end taken normal to internal face	62.8	67.3	60.3	61.8	59.2	56.4	55.3	57	49.4	50.8
Greatest thickness of distal end	46.7	48.2	45.1	47	44.4	41.4	42.2	41.6	36.4	35.6

Table 46—*Measurements (in millimeters) of radius of Felis atrox*

	2904–R-1	2904–R-2	2904–R-3	2904–R-4	2904–R-5	2904–R-6	2904–R-7	2904–R-8	2904–R-9	2904–R-10
Length measured along internal border	411	364	366	347	343	330	330	318	319	317
Long diameter of proximal end	58.1	56	55.7	51	53	48.6	50.1	47	49.7	*a*44
Greatest diameter taken at right angles to long diameter of proximal end	47.2	40.7	38.8	38.3	38.9	37.3	37.1	33.7	37.5	*a*33
Width of shaft at middle	36.3	45.6	39.6	39.8	38.4	38.2	33.4	35.8	38.7	38.1
Thickness of shaft at middle	23.4	26.4	27.5	23.1	25.3	23.6	20.7	21.4	21.9	20.8
Greatest width of distal end	72.7	75.2	77.6	70.7	69.9	67.4	63.5	63.6	62	61.5
Greatest thickness of distal end	47.4	47	48.7	44.8	45.7	43.8	39.7	38.6	39.9	38.3

a, Approximate.

SCAPHO-LUNAR

The scapho-lunar of *Smilodon* resembles in its general characteristics the comparable element in *Felis atrox* (figs. 73, 74), although differing from the latter in several details. When the proximal surface is viewed, the ulnar side of the articulation for the radius (*R*) is seen to be wider in dorsopalmar direction in the sabre-tooth than in *F. atrox*. Furthermore, the process situated at the radio-palmar corner projects more to the inner or radial side and less to the palmar side than in *F. atrox*. The concavity for the reception of the styloid process of the radius is relatively broad in *Smilodon*.

In dorsal view the principal difference between *Smilodon* and *F. atrox* is seen in depth of the dorsal surface toward the ulnar side of the element and above the articulation for the magnum. This depth is greater in the sabre-tooth than in the latter. In distal view the articulating surfaces for the distal row of carpal elements are in area not so extensive as in *Felis atrox*. The surface for the trapezium does not extend toward the palmar border quite so far in the sabre-tooth as in *F. atrox*. The palmar border of the surface for the magnum may be deeply notched. The

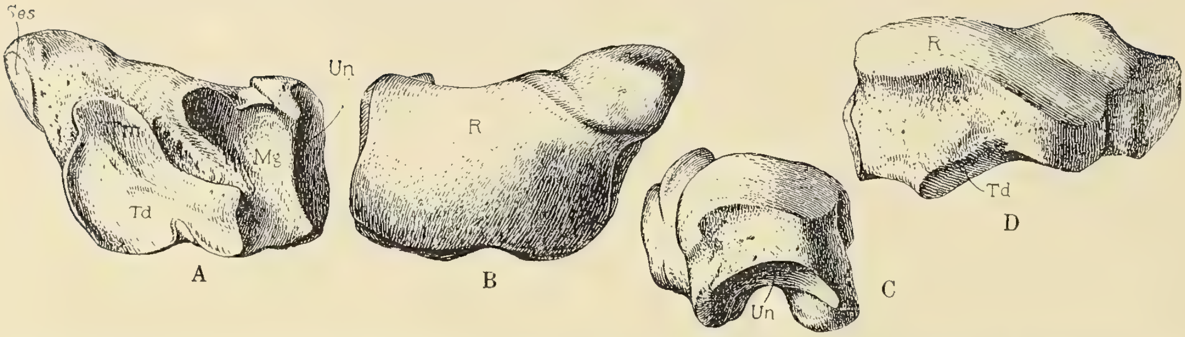

FIG. 73—*Smilodon californicus* Bovard. Right scapho-lunar, No. 2023-R-3. A, distal view; B, proximal view; C, external view; D, dorsal view; × 2/3. Facets for trapezium (*Tm*), trapezoid (*Td*), magnum (*Mg*), unciform (*Un*), sesamoid (*Ses*), and radius (*R*). Rancho La Brea Pleistocene.

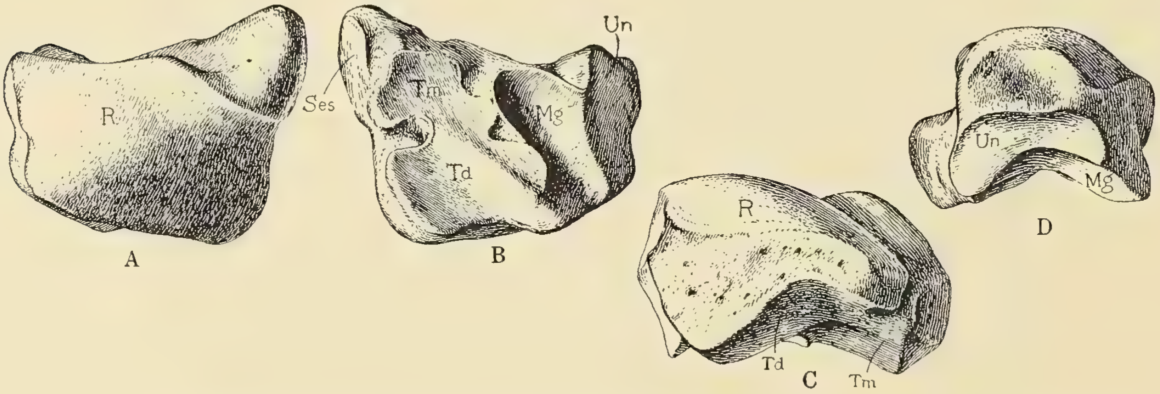

FIG. 74—*Felis atrox* Leidy. Right scapho-lunar, No. 2921-R-1. A, proximal view; B, distal view; C, dorsal view; D, external view; × 2/3. Facets as in figure 73. Rancho La Brea Pleistocene.

TABLE 47—*Measurements (in millimeters) of scapho-lunar*

	Smilodon californicus*				Felis atrox		
	2023–R-1	2023–R-2	2023–R-3	2023–R-4	2921–R-1	2921–R-2	2921–R-3
Greatest transverse diameter measured normal to external border of proximal surface	63.1	57.2	57.7	45.5	58	61.7	50.7
Greatest dorsopalmar length	37.8	42.5	40.4	31.6	43.8	49.3	37.2
Greatest proximal distal diameter	35.4	32	32.5	25.3	32.1	35.6	29.3

* Selected from a series of 662 individuals.

unciform surface in *Smilodon*, while fully as long in dorsopalmar direction as in *F. atrox*, is noticeably narrower in the former type. The external surface of the scapho-lunar above the rim of the unciform facet may not be so deeply indented in the sabre-tooth as in *Felis atrox*.

CUNEIFORM

The cuneiform of *Smilodon,* while somewhat smaller than that of *Felis atrox* (compare figures 75 and 76), differs also from the latter in shape and in size and configuration of the articulating surfaces. On the proximal surface the facet for the pisiform widens noticeably toward the radial side. The ulnar surface is relatively not so broad as in *F. atrox.* On the distal surface the facet for the unciform is not infrequently rather small and does not extend very far in a radio-ulnar direction. Numerous exceptions to this type of facet are to be noted for the surface varies considerably in shape. A greater emargination on the ulnopalmar side of this facet is present in *Smilodon* than in *Felis.* Viewed in dorsal aspect the ulnar facet slopes more abruptly downward to the ulnar side than in *F. atrox.*

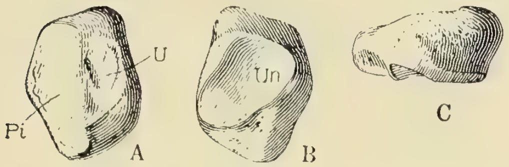

FIG. 75—*Smilodon californicus* Bovard. Right cuneiform, No. 2024-R-2. A, outer view; B, inner view; C, dorsal view; × 2/3. Facets for pisiform (*Pi*), ulna (*U*), and unciform (*Un*). Rancho La Brea Pleistocene.

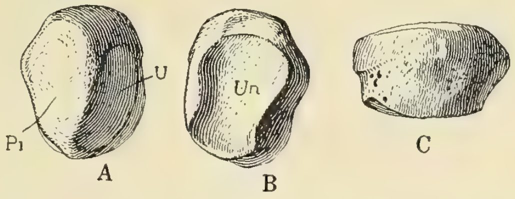

FIG. 76—*Felis atrox* Leidy. Right cuneiform, No. 2922-R-1. A, B, C, same views as in figure 75; × 2/3. Rancho La Brea Pleistocene.

TABLE 48—*Measurements (in millimeters) of cuneiform*

	Smilodon californicus*				Felis atrox			
	2024–R-1	2024–R-2	2024–R-3	2024–R-4	2922–R-1	2922–R-2	2922–R-3	2922 R-4
Greatest length measured parallel to ridge separating pisiform and ulnar facets	32.1	30	29.8	23.9	30.1	35.3	26.4	27.9
Diameter normal to line of greatest length	23.9	22.4	21.3	17.3	25.1	25.5	21.7	22
Greatest thickness	15.8	14.4	13.4	12.8	17.9	18	15	14.7

* Selected from a series of 116 individuals.

PISIFORM

The pisiform is a relatively heavy element in *Smilodon,* in which the head is more compressed in its proximo-distal diameter and is more extended in ulnar-radial direction than in *Felis atrox* (figs. 77, 78). The shaft is also broader when viewed distally. This character is seen in figure 77A. It continues to the articulating end, for the maximum width between the borders of the facets for ulna and unciform may be actually greater in the sabre-tooth than in *F. atrox.* The articulating surface for the ulna does not encroach so far upon the shaft as in *F. atrox.*

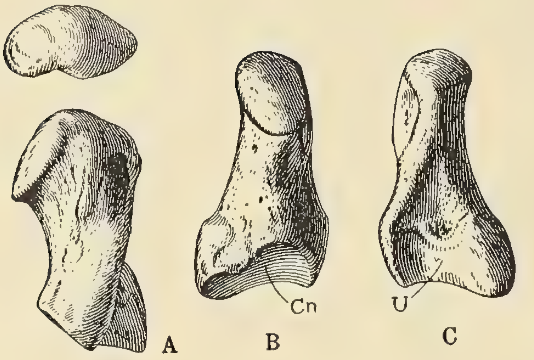

Fig. 77—*Smilodon californicus* Bovard. Right pisiform, No. 2025-R-2. A, distal view with view of head; B, radial view; C, ulnar view; × 2/3. Facets for cuneiform (*Cn*) and ulna (*U*). Rancho La Brea Pleistocene.

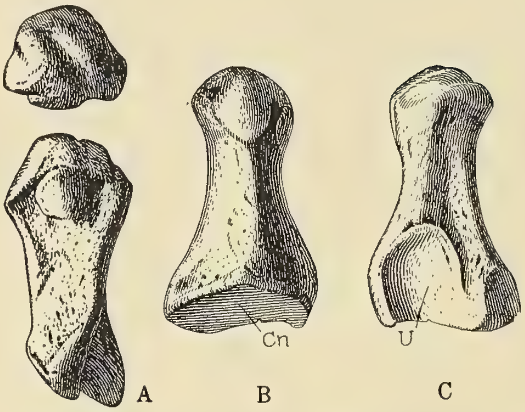

Fig. 78—*Felis atrox* Leidy. Right pisiform, No. 2923-R-1. A, B, C, same views as in figure 77; × 2/3. Rancho La Brea Pleistocene.

Table 49—*Measurements (in millimeters) of pisiform*

	Smilodon californicus*				Felis atrox					
	2025-R-1	2025-R-2	2025-R-3	2025-R-4	2923-R-1	2923-R-2	2923-R-3	2923-R-4	2923-R-5	2923-R-6
Greatest length measured from and normal to the contact edge of ulnar and unciform facets to the head	49.4	46.5	41.8	36	52.4	47.9	50.2	50.6	42.4	40.7
Long diameter of articulating end	26.8	26.7	25.4	21.9	30	29.7	31.4	29.3	27.9	25.1
Long diameter of head	29.6	26.5	23.5	17.4	24.3	25.3	26.1	24.2	24.2	21
Greatest proximodistal diameter of head normal to long diameter	16.1	14	14.9	12	19.6	18	20.2	17.6	18.2	17.5

* Selected from a series of 484 individuals.

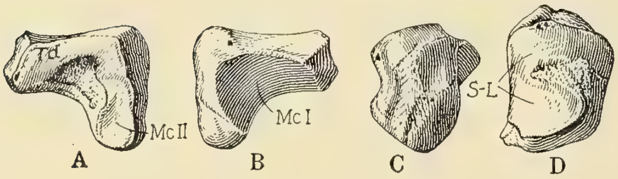

Fig. 79—*Smilodon californicus* Bovard. Right trapezium, No. 2026-R-2. A, outer view; B, inner distal view; C, dorsal view; D, proximal view; × 2/3. Facets for trapezoid (*Td*), scapho-lunar (*S-L*), metacarpal I (*McI*), and metacarpal II (*McII*). Rancho La Brea Pleistocene.

TRAPEZIUM

This element, as seen in dorsal or anterior view and in proximal view (fig. 79), is relatively broader than the trapezium of *Felis atrox*. The dorsal surface does not extend downward so far as in *F. atrox*, although the character is subject to some variation in the latter form. When viewed from the side, the dorsal surface is seen to be at right angles to the surface articulating with the scapho-lunar. In *F. atrox* the dorsal surface in its extent downward projects forward, making an obtuse angle with the surface for the scapho-lunar.

On the outer side of the trapezium of *Smilodon* the facet for the second metacarpal (*McII*) extends well up along the border of the dorsal surface, and in the specimen figured it is confluent with, but demarcated by, a ridge from the facet for the trapezoid. In *F. atrox* the two facets are distinctly separated. The concave articulating surface for metacarpal I is relatively broad.

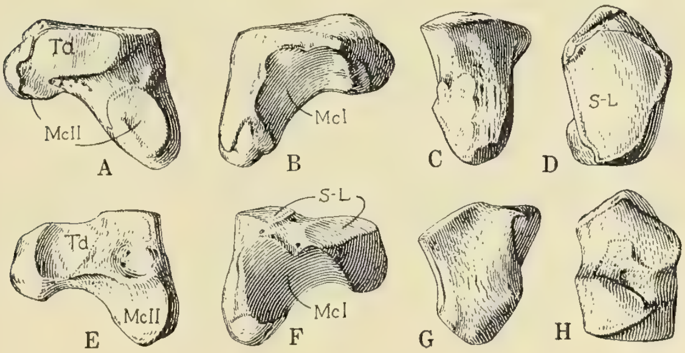

Fig. 80—*Felis atrox* Leidy. Right trapezium, Nos. 2924-R-1, 2924-R-2. A, E, outer view; B, F, inner distal view; C, G, dorsal view; D, H, proximal view; × 2/3. Facets as in figure 79. Rancho La Brea Pleistocene.

Table 50—*Measurements (in millimeters) of trapezium*

	Smilodon californicus*			Felis atrox		
	2026-R-1	2026-R-2	2026-R-3	2924-R-1	2924-R-2	2924-R-3
Greatest dorsopalmar length	28.6	27.7	21.7	31	29.1	25.6
Greatest proximodistal diameter	23.8	24.3	19.3	28.2	27.4	25
Greatest width of proximal surface	20.7	20.5	17	19.8	20.8	16

* Selected from a series of 119 individuals.

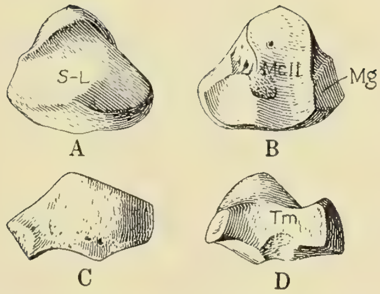

Fig. 81—*Smilodon californicus* Bovard. Right trapezoid, No. 2007-R-3. A, proximal view; B, distal view; C, dorsal view; D, inner view; × 2/3. Facets for scapho-lunar (*S-L*), metacarpal II (*McII*), magnum (*Mg*), and trapezium (*Tm*). Rancho La Brea Pleistocene.

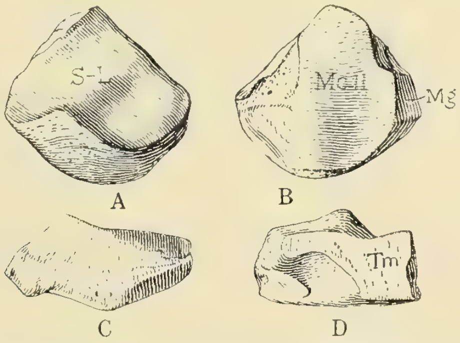

Fig. 82—*Felis atrox* Leidy. Right trapezoid, No. 2925-R-1. A, B, C, D, same views as for figure 81; × 2/3. Rancho La Brea Pleistocene.

TRAPEZOID

The trapezoid of *Smilodon* approximates in size that of the Recent *Felis leo* and *F. tigris.* On the proximal surface the concave portion of the articulation for the scapho-lunar is relatively wider in *Smilodon* than in *Felis atrox* (compare figures 81 and 82) and the flattened portion of the articulation is correspondingly smaller in the former than in the latter. The two divisions are not separated by so sharp a ridge as in *F. atrox*. Because of increased size of the concave portion of the proximal surface, the dorsal border of the surface may be fully as long as that in *F. atrox.*

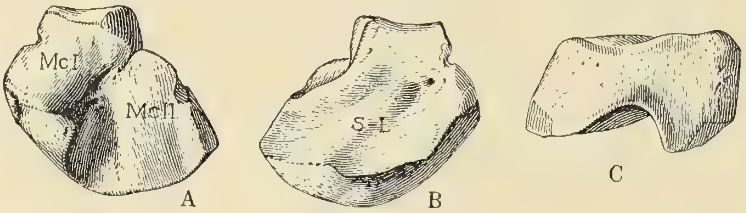

Fig. 83—*Felis atrox* Leidy. Fused right trapezium and trapezoid, No. 2925-R-5. A, distal view; B, proximal view; C, dorsal view; × 2/3. Facets for scapho-lunar (*S-L*), metacarpal I (*McI*), and metacarpal II (*McII*). Rancho La Brea Pleistocene.

The distal articulation for the second metacarpal (*McII*) is distinctly bilobate and the surface adjacent to the magnum facet (*Mg*) is noticeably smaller than in the extinct true cat and in the Recent large Eurasiatic cats. The surface for the magnum (*Mg*) may be relatively large. Likewise, the articulation for the trapezium (*Tm*) is relatively large, the dorsal portion of this surface extending distally and touching the articulating facet for metacarpal II.

Table 51—*Measurements (in millimeters) of trapezoid*

	Smilodon californicus*				Felis atrox			
	2027–R-1	2027–R-2	2027–R-3	2027–R-4	2925–R-1	2925–R-2	2925–R-3	2925–R-4
Greatest dorsoplantar length	27.9	26	23.8	21.6	33.4	29.6	31.3	25
Greatest transverse diameter	29.3	31.5	28.7	22.4	36.5	33.7	33.4	30
Greatest proximodistal diameter	17.8	16.3	16.3	12.8	19.7	22.9	20.8	17.3

* Selected from a series of 101 individuals.

MAGNUM

The dorsal surface of the magnum of *Smilodon* may be fully as wide in proximodistal direction as the comparable surface in *Felis atrox*, although toward the outer side the articulation for the scapho-lunar may encroach more on this surface in the former than in the latter. On the inner side (fig. 84A) the facet for metacarpal II situated near the palmar border has a shape similar to that in *F. atrox* and may be comparable in size to or larger than the facet in the latter form. The facets situated near the dorsal border and lying between the proximal articulation for the scapholunar and the distal articulation for metacarpal III consist of two rectangular surfaces. The proximal facet articulates with the trapezoid, the distal one with metacarpal III. In other words, there is no contact established between the magnum and metacarpal II in this region, in which respect the Rancho La Brea sabre-tooth differs from *F. atrox.* The facet for the trapezoid (*Td*) is relatively large and more distinctly outlined and demarcated from the articulating surface for the scapholunar than in *F. atrox.* The facet for the third metapodial (*McIII*) is not so long in dorsopalmar direction in *Smilodon* as in *F. atrox.*

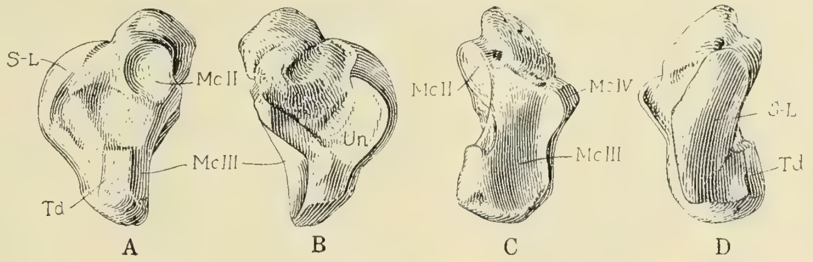

Fig. 84—*Smilodon californicus* Bovard. Right magnum, No. 2028-R-2. A, inner view; B, outer view; C, distal view; D, proximal view; × 2/3. Facets for scapho-lunar (*S-L*), trapezoid (*Td*), metacarpal II (*McII*), metacarpal III (*McIII*), metacarpal IV (*McIV*), and unciform (*Un*). Rancho La Brea Pleistocene.

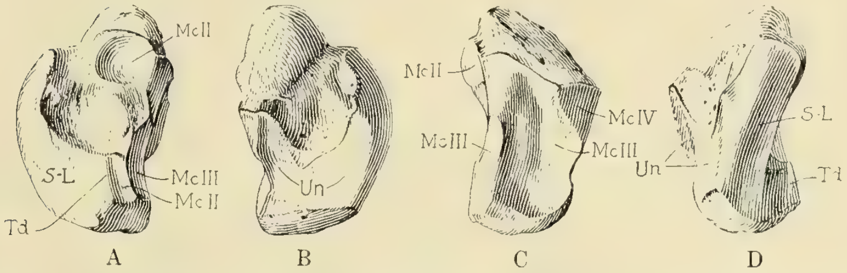

Fig. 85—*Felis atrox* Leidy. Right magnum, No. 2926-R-1. A, B, C, D, same views as in figure 84; × 2/3. Rancho La Brea Pleistocene.

The unciform surfaces (*Un*) are not so broad as in *F. atrox.* The facet for this element flanking the distal border is distinctly concave in dorsopalmar direction. In distal view a noticeable difference between *Smilodon* and *F. atrox* is seen in the relatively small size of the facet for the fourth metacarpal (*McIV*). Frequently, however, this facet is larger than in the specimen figured. The surface for the scapho-lunar is flattened. The palmar end of the lower unciform facet is carried outward farther in the sabre-tooth than in the true felid type.

Table 52—*Measurements (in millimeters) of magnum*

	Smilodon californicus*			Felis atrox		
	2028-R-1	2028-R-2	2028-R-3	2926-R-1	2926-R-2	2926-R-3
Greatest dorsoplantar length	41.9	41	31.6	44.2	40.8	35
Greatest proximodistal diameter	27.3	27.8	22.4	29	29.4	25.3

* Selected from a series of 299 individuals.

UNCIFORM

In dorsal view (fig. 86E), the articulating facet for the scapho-lunar is seen to truncate obliquely the proximal end of the dorsal surface and it extends generally farther down in a distal and inner direction than in *Felis atrox.* The proximal contour of the articulation for the scapho-lunar is distinctly sinuous, the surface being decidedly convex dorsally and concave toward the palmar end. As viewed from either the outer or inner side, the palmar end of this surface is situated higher above the distal surface than in the large extinct *Felis.* In other words, the proximo-distal diameter of the palmar end of the unciform is relatively greater in the sabre-tooth than in *F. atrox.* The palmar end is also relatively and absolutely thicker transversely in *Smilodon.* This is particularly noticeable toward the proximal surface. On the outer side of the unciform, the facet for the cuneiform is not so broad as in *Felis.* Below this articulation or toward the palmar side, a deeper and broader depression is present in the sabre-tooth than in *F. atrox.* On the inner side and situated along the dorsal portion of the distal border is a surface, not clearly defined, which articulates with metacarpal III. This surface lies below the area of articulation for the magnum and between it and the distal surface for metacarpal IV.

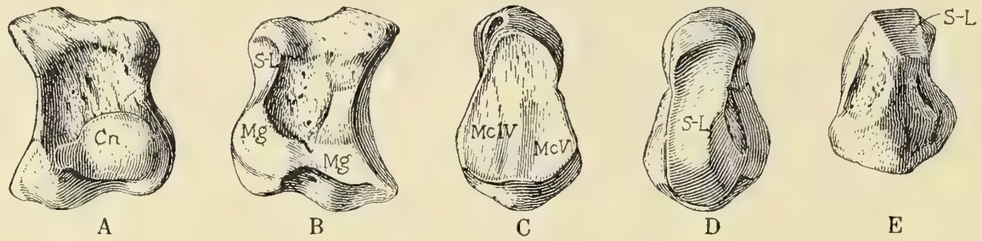

FIG. 86—*Smilodon californicus* Bovard. Right unciform, No. 2029-R-2. A, outer view; B, inner view; C, distal view; D, proximal view; E, dorsal view; × 2/3. Facets for cuneiform (*Cn*), scapho-lunar (*S-L*), magnum (*Mg*), metacarpal IV (*McIV*), and metacarpal V (*McV*). Rancho La Brea Pleistocene.

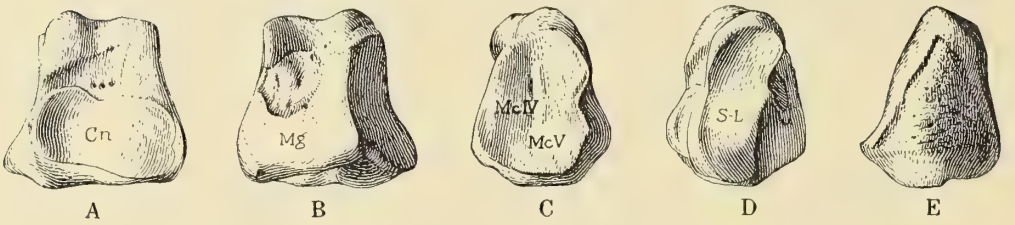

FIG. 87—*Felis atrox* Leidy. Right unciform, No. 2927-R-1. A, B, C, D, E, same views as in figure 86; × 2/3. Rancho La Brea Pleistocene.

At the distal end the concave articulating surface for the metacarpals is not so broad as in *F. atrox.* A faint ridge indicates the separation of the articulating areas for the fourth and fifth metapodials. The surface for metacarpal V is distinctly narrower transversely than that for metacarpal IV.

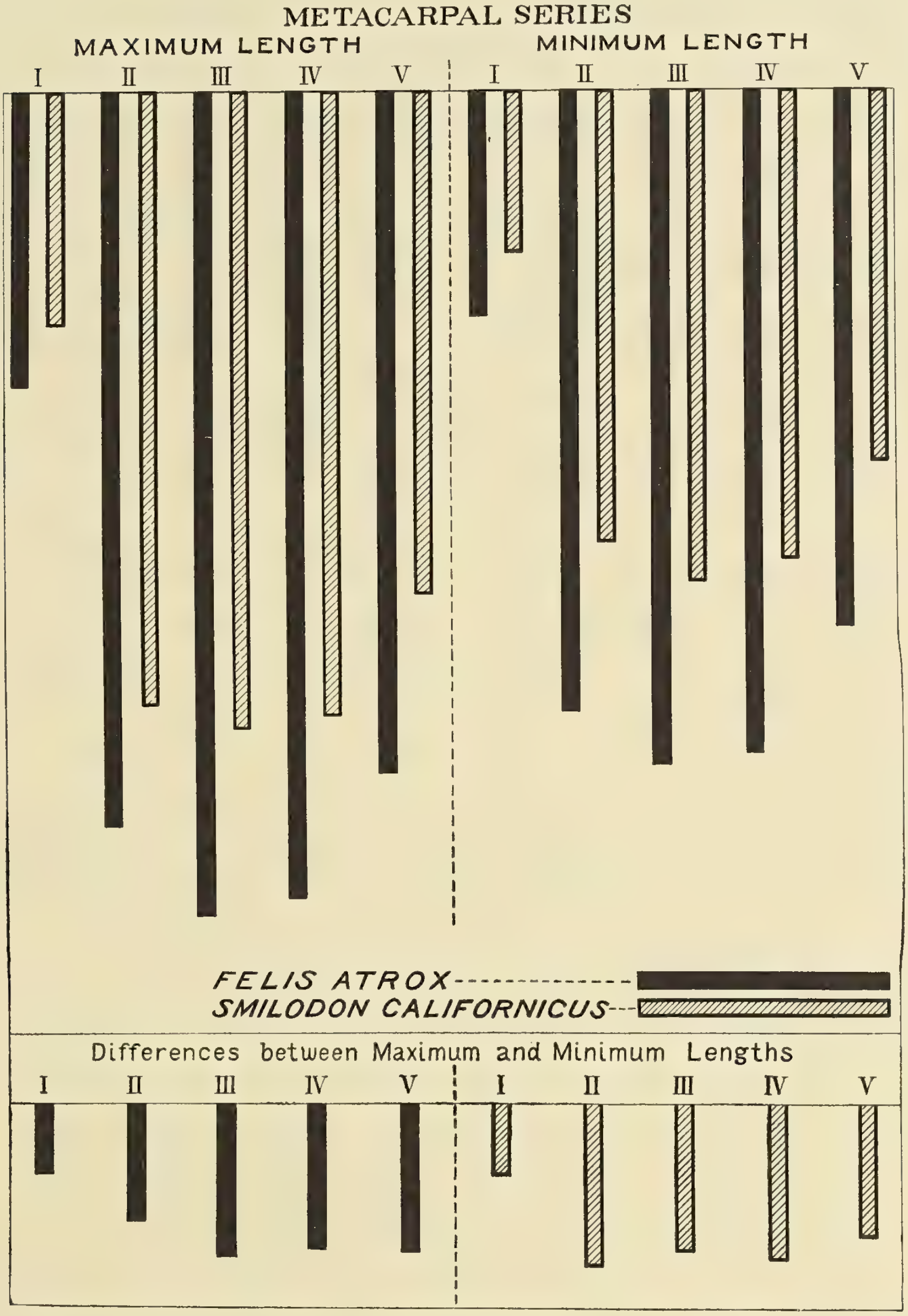

FIG. 88—Diagram showing comparative maximum and minimum lengths of metacarpals and differences between maximum and minimum lengths of these elements in *Felis atrox* Leidy and *Smilodon californicus* Bovard from Rancho La Brea.

METACARPAL SERIES

The diagram shown in figure 88 gives the comparative lengths of the metacarpals in *Smilodon californicus* and in *Felis atrox* for specimens of maximum and minimum size in series of adult individuals from the asphalt beds. The diagram illustrates also the differences in length between the longest and shortest specimens of comparable metacarpals in each type of cat, thus expressing the extent of variation in this particular character in the sabre-tooth and in *F. atrox.* With regard to the variation displayed in this measurement it should be borne in mind that the differences between maximum and minimum lengths of metacarpals are based on a much larger series of specimens in *S. californicus* than in *Felis atrox.*

In both types of cats the differences in lengths of metacarpals are approximately of the same order of magnitude for the maximum and minimum series. When the length of the third metacarpal is used as a basis for reference, the first metacarpal is seen to be slightly shorter, the second metacarpal slightly longer in the sabre-tooth than in *F. atrox.* Distinctly greater variation in length is apparently displayed by the second metacarpal of *Smilodon* than by the comparable element in *F. atrox.*

Table 53—*Measurements (in millimeters) of unciform*

	Smilodon californicus*				Felis atrox					
	2029-R-1	2029-R-2	2029-R-3	2029-R-4	2927-R-1	2927-R-2	2927-R-3	2927-R-4	2927-R-5	2927-R-6
Proximodistal diameter measured normal to plane level with dorsal and palmar borders of distal articulation	34.2	32.2	30.5	23.8	33.3	33	33	32.4	30.2	26.2
Greatest dorsopalmar diameter	40.8	38.7	35.7	28.7	35	36.1	38.3	36.8	33.7	29.4
Greatest width across dorsal surface	27.1	25.2	23.4	20.1	26.2	28.4	25.8	28.8	26.3	22.8

* Selected from a series of 313 individuals.

When the metacarpals are in articulation, this portion of the front foot is relatively broad but apparently no more spreading than in *F. atrox.* The total width of the metapodial region, due to the heaviness of the individual elements, combined with a noticeable abbreviation in length, furnish in this region the chief points of contrast between the sabre-tooth and *Felis atrox.*

METACARPAL I

The first metacarpal is distinctly shorter and relatively heavier than that of *Felis atrox* (compare figures 89 and 90). The dorsal surface develops a ridge which extends obliquely from the inner border of the facet for the trapezium (*Tm*) to a point above the outer portion of the distal articulating surface. This ridge is absent in metacarpal I of the large true felid and of the Recent large cats. The outer border of the facet for the trapezium is not so long in proximo-distal direction in the sabre-tooth as in *F. atrox,* and the outer surface of the element in this region forms a tuberosity in the former which is lacking in the latter. The tuberosity to the inner palmar side of the facet is larger in *Smilodon* than in *F. atrox.*

The distal end of the metacarpal, as viewed particularly from the palmar side, is noticeably different from that in *F. atrox*. The articulating surface for the first digit (*Di I*) is deeply notched in front and distinctly concave transversely. The outer portion of the surface is carried forward for some distance, noticeably more so in the sabre-tooth than in *F. atrox*. The median keel of the articulating surface is sharp and relatively more prominent in *Smilodon* than in *F. atrox*.

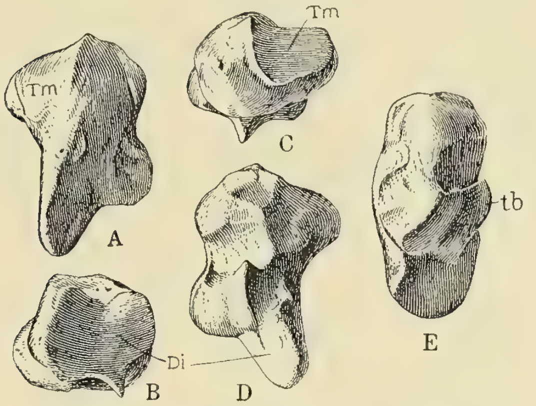

FIG. 89—*Smilodon californicus* Bovard. Right metacarpal I, No. 2013-R-1. A, dorsal view; B, distal view; C, proximal view; D, palmar view; E, inner view; × 2/3. Facets for trapezium (*Tm*) and first digit (*Di*); *tb*, tubercle. Rancho La Brea Pleistocene.

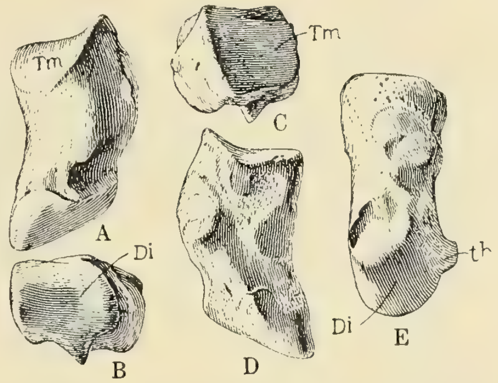

FIG. 90—*Felis atrox* Leidy. Right metacarpal I, No. 2911-R-3. A, B, C, D, E, same views as in figure 89; × 2/3. Rancho La Brea Pleistocene.

In addition to the shortness and heaviness of the shaft, the characters of the distal end serve to distinguish readily this element from the comparable metacarpal of *Felis atrox*.

One specimen in the Los Angeles Museum collections, No. 2013–R–5, selected from a series of more than 300 elements of the right side, differs from the normal type of the first metacarpal in possessing a relatively long shaft. This character gives the specimen a greater resemblance to that of *F. atrox*. The facet for the trapezium in No. 2013–R–5 is flatter than is generally the case in *Smilodon*, and it differs also in the manner in which it extends over the dorsal surface. The remaining characters clearly indicate that the specimen belongs to a sabre-tooth cat.

TABLE 54—*Measurements (in millimeters) of metacarpal I*

	Smilodon californicus*				Felis atrox			
	2013–R-3	2013–R-2	2013–R-1	2013–R-4	2911–R-1	2911–R-2	2911–R-3	2911–R-4
Greatest length measured normal to proximal end	39.6	39.2	38.9	27.5	50	43.1	42.9	38.3
Greatest width of proximal end	29.6	27.3	27.3	22.8	27.2	26.5	21	22.4
Transverse width of distal articulating surface	23.1	20.9	23	18	23.4	21.4	21	18.6

* Selected from a series of 344 individuals.

METACARPAL II

The proximal surface of the second metacarpal of *Smilodon*, articulating with the trapezoid, lacks the triangular shape seen in the extinct true cat and in Recent felines. The palmar base of this surface is broad, due to the relatively much larger hook-like process for attachment of the first palmar interosseous muscle. In the sabre-tooth the dorso-internal corner of the surface for the trapezoid is elevated distinctly above the remaining facet, and this elevation interrupts the general concavity of the proximal end but accentuates the depression immediately adjacent to it. In this character, *Smilodon* differs noticeably from *Felis atrox* (compare figures 91A and 92A).

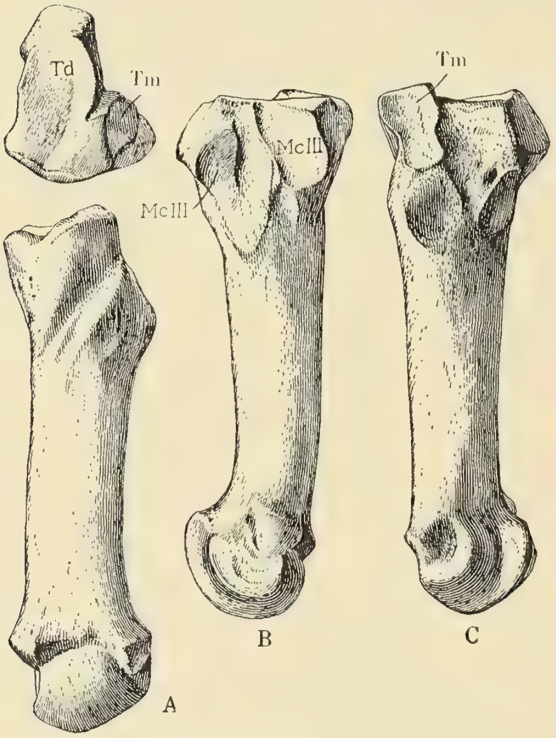

FIG. 91—*Smilodon californicus* Bovard. Right metacarpal II, No. 2014-R-1. A, dorsal view with view of proximal end; B, outer view; C, inner view; × 2/3. Facets for trapezoid (*Td*) trapezium (*Tm*), and metacarpal III (*McIII*). Rancho La Brea Pleistocene.

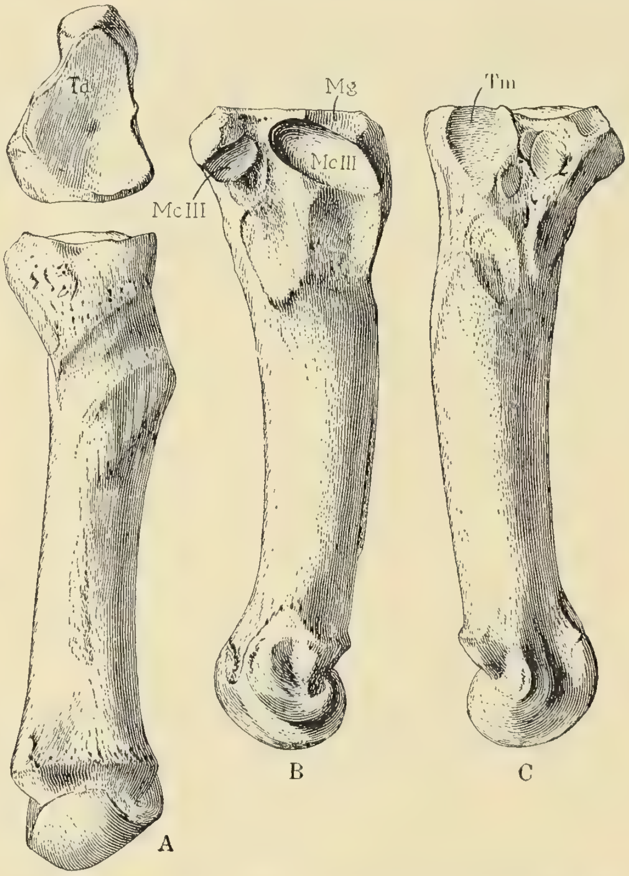

FIG. 92—*Felis atrox* Leidy. Right metacarpal II, No. 2912-R-1. A, B, C, same views as in figure 91; × 2/3. Facet for magnum (*Mg*); remaining facets as in figure 91. Rancho La Brea Pleistocene.

On the dorsal face of the metapodial and below the proximal end, the oblique groove for the radial artery is deeply marked. The dorsal surface does not widen in its extent from the groove to the proximal border, as in the true felines. The swelling on the dorso-internal border below the groove is more pronounced in *Smilodon* than in *Felis atrox* and in Recent cats. On the inner surface of the proximal end the facet for the trapezium (*Tm*) is elongate proximo-distally and relatively larger than in *F. atrox.* In side view the facet is seen to project above the proximal border.

On the external side of the proximal end the dorsal facet for metacarpal III (*McIII*) is not elongated obliquely from the proximo-palmar end to the dorsal end, as in the extinct true felid and Recent cats. In *Smilodon* the major axis of the facet is more nearly longitudinal. A facet articulating with the magnum and present in *Felis atrox* is lacking in the sabre-tooth.

Table 55—*Measurements (in millimeters) of metacarpal II of Smilodon californicus*

	Right*			Left†		
	2014–R-1	2014–R-2	2014–R-3	2014–L-1	2014–L-2	2014–L-3
	Max.		*Min.*	*Max.*		*Min.*
Greatest length	103.8	90.2	76.4	105.5	90.8	76.4
Greatest transverse diameter of proximal end	22.1	22.1	20.6	22.1	21.4	21.6
Greatest dorsoventral diameter of proximal end	34	29.8	28	34	32.8	27.2
Transverse diameter at middle of shaft	18.7	18	15	17.9	18	15.7
Dorsoventral diameter at middle of shaft	16.5	17.8	13.9	17.8	16.3	14.8
Greatest transverse diameter at distal end of shaft	27.6	25.6	22	26.4	25.2	22.6

* Based on a series of 676 specimens. † Based on a series of 753 specimens.

Table 56—*Measurements (in millimeters) of metacarpal II of Felis atrox*

	Right*			Left†		
	2912–R-1	2912–R-2	2912–R-3	2912–L-1	2912 L-2	2912 L-3
	Max.		*Min.*	*Max.*		*Min.*
Greatest length	124.4	116	104.6	122.8	115.7	100.4
Greatest transverse diameter of proximal end	29	28.4	23.8	29	25.8	22.9
Greatest dorsoventral diameter of proximal end	38.5	35.8	32.3	36.4	34.1	32
Transverse diameter at middle of shaft	19.3	18.1	16.4	19.8	18.8	16.7
Dorsoventral diameter at middle of shaft	20.8	18.8	17.1	20.8	18.6	17.4
Greatest transverse diameter at distal end of shaft	29	26.6	24.3	27.7	26.2	23

* Based on a series of 32 specimens. † Based on a series of 31 specimens.

The shaft is relatively broad. At the distal end the tuberosity situated on each side of the proximal surface and at the point of union of shaft with distal epiphysis is perhaps more prominent than in *F. atrox.* The depression lying between these tuberosities and above the distal articulating surface is broader and extends farther along the dorsal surface in *Smilodon* than in *F. atrox.*

METACARPAL III

The shaft of the third metacarpal of *Smilodon* is not only broader than that of the great lion-like cat, but it also widens more distally than that of the latter form. At the proximal end the articulating surface for the magnum is wide and for the most part broadly concave. Toward the palmar border this surface is distinctly wider than in the true felines. Along the lateral border the surface for the magnum is sharply separated from a lateral facet for the unciform. Along the inner border where the dorsal facet for the second metacarpal meets the surface for the magnum, a sharp ridge is formed which is more conspicuous than in *Felis atrox.* As viewed from the proximal end, a broad and deep notch penetrates the magnum surface between the dorsal and palmar facets for metacarpal II. In *F. atrox* this notch is acute and is not so deep as in the sabre-tooth.

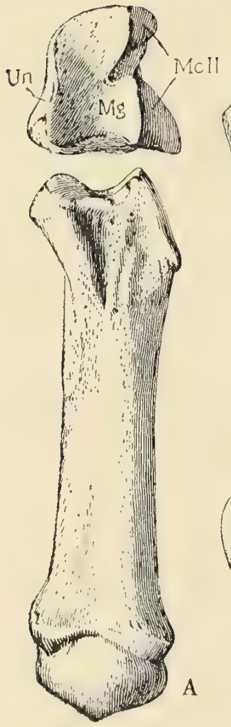

Fig. 93—*Smilodon californicus* Bovard. Right metacarpal III, No. 2015-R-1. A, dorsal view with view of proximal end; B, outer view; C, inner view; × 2/3. Facets for unciform (*Un*), magnum (*Mg*), metacarpal II (*McII*), and metacarpal IV (*McIV*). Rancho La Brea Pleistocene.

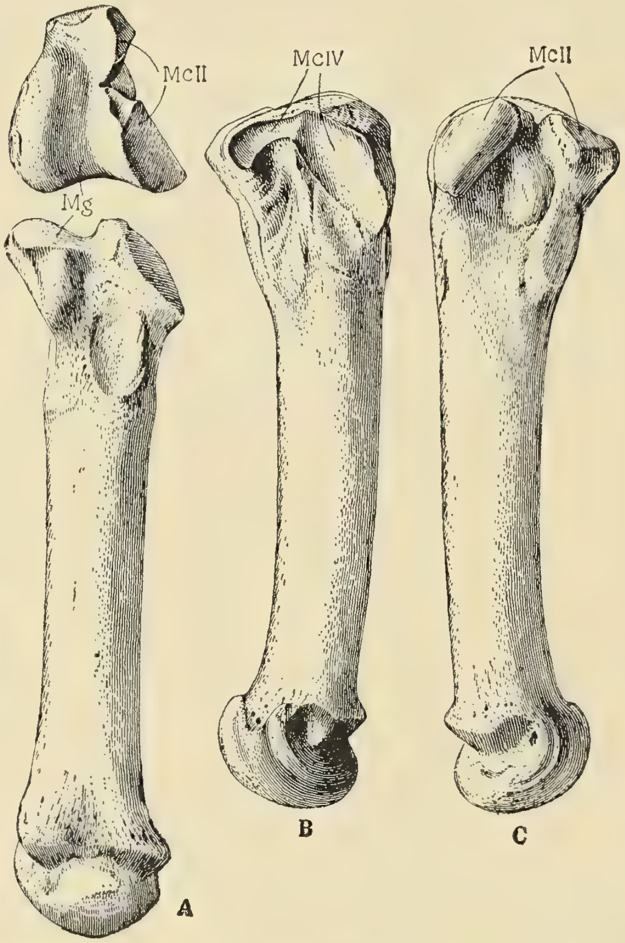

Fig. 94—*Felis atrox* Leidy. Right metacarpal III, No. 2913-R-1. A, B, C, same views as in figure 93; × 2/3. Rancho La Brea Pleistocene.

Viewed from the inner side (compare figures 93C and 94C), the dorsal facet for metacarpal II is seen to be of large size. This facet is flatter than the corresponding surface in the extinct true felid. Its long axis tends to be longitudinal, whereas in *F. atrox* the long axis is oblique to the longitudinal axis of the metapodial. On the outer side of the proximal end, the facet for metacarpal IV is broad with the palmar portion of the surface broader in proximo-distal direction than in *F. atrox.* Above this surface and lying between it and the outer margin of the dorsal surface for the magnum is a relatively large articulating facet for the unciform

(*Un*), indicative of a broad contact with the latter element. This facet is absent in *Felis atrox.*

When the third metacarpal is viewed from the side, the distal portion of the shaft is seen to be thinner in dorso-palmar direction than in *F. atrox.* The palmar keel of the distal articulation is well developed.

TABLE 57—*Measurements (in millimeters) of metacarpal III of Smilodon californicus*

	Right*			Left*		
	2015–R-1	2015–R-2	2015–R-3	2015–L-1	2015–L-2	2015–L-3
	Max.		*Min.*	*Max.*		*Min.*
Greatest length	107.8	95.8	83	109.6	96.4	83.2
Greatest transverse diameter of proximal end	30.7	27	24.6	29.6	27.6	24.2
Greatest dorsoventral diameter of proximal end	28.8	25.4	23	29.2	26	22.8
Transverse diameter at middle of shaft	19.5	17.6	14.6	20	17	14.8
Dorsoventral diameter at middle of shaft	15.7	13	13.2	15.1	13.6	12.3
Greatest transverse diameter at distal end of shaft	29.4	25.6	23.7	29.3	27.7	22.4

* Based on a series of 737 specimens. † Based on a series of 709 specimens.

TABLE 58—*Measurements (in millimeters) of metacarpal III of Felis atrox*

	Right*			Left†		
	2913–R-1	2913–R-2	2913–R-3	2913–L-1	2913–L-2	2913–L-3
	Max.		*Min.*	*Max.*		*Min.*
Greatest length	139.4	130.6	113.9	138.8	126.6	116
Greatest transverse diameter of proximal end	34.2	30.6	27	34	31	27.8
Greatest dorsoventral diameter of proximal end	35.2	31.9	28.3	33.2	31.1	25.8
Transverse diameter at middle of shaft	19.4	19.7	16	21.3	19.6	14.4
Dorsoventral diameter at middle of shaft	17.7	17.9	14.8	18	16.2	13
Greatest transverse diameter at distal end of shaft	29	26.4	24	29.2	26.5	23

* Based on a series of 30 specimens. † Based on a series of 31 specimens.

METACARPAL IV

The proximal end of the fourth metacarpal of the sabre-tooth differs somewhat in shape and in outline from that of *Felis atrox* (compare figures 95A and 96A). Toward the palmar side, the proximal end is relatively not so broad in *Smilodon* as in *F. atrox.* The outer border of the surface articulating with the unciform (*Un*) curves into the palmar border. In the latter, as in the living cats, the outer border is straight. In the great lion-like cat the inner border of the proximal end is deeply notched near the middle, while in *Smilodon* the indentation is not so distinct. Likewise, an indentation of the dorsal border occurs between the surfaces for unciform and metacarpal III in *Felis atrox.* This indentation is absent in the sabre-tooth. Viewed from the dorsal side, the plane of the unciform surface in *Smilodon* is seen to form a distinct angle with the plane of the surface for the third metacarpal. In *F. atrox,* however, the impression is strongly given in comparable view that the plane of one surface is not strongly deflected from the plane of the other.

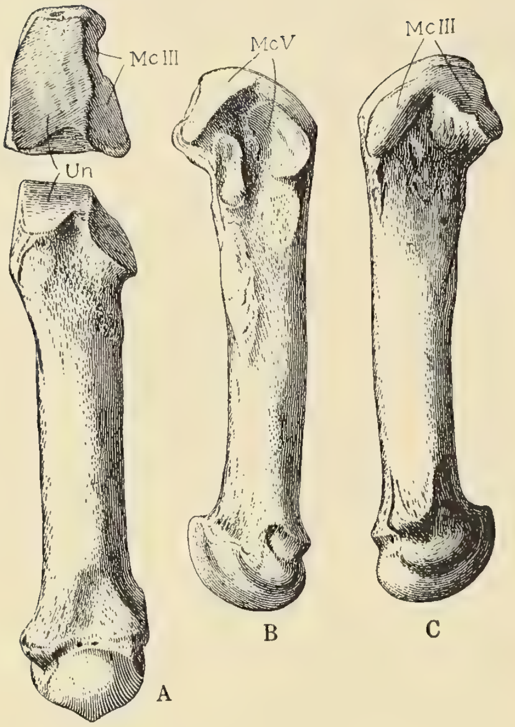

FIG. 95—*Smilodon californicus* Bovard. Right metacarpal IV, No. 2016-R-1. A, dorsal view with view of proximal end; B, outer view; C, inner view; × 2/3. Facets for unciform (*Un*), metacarpal III (*McIII*), and metacarpal V (*McV*). Rancho La Brea Pleistocene.

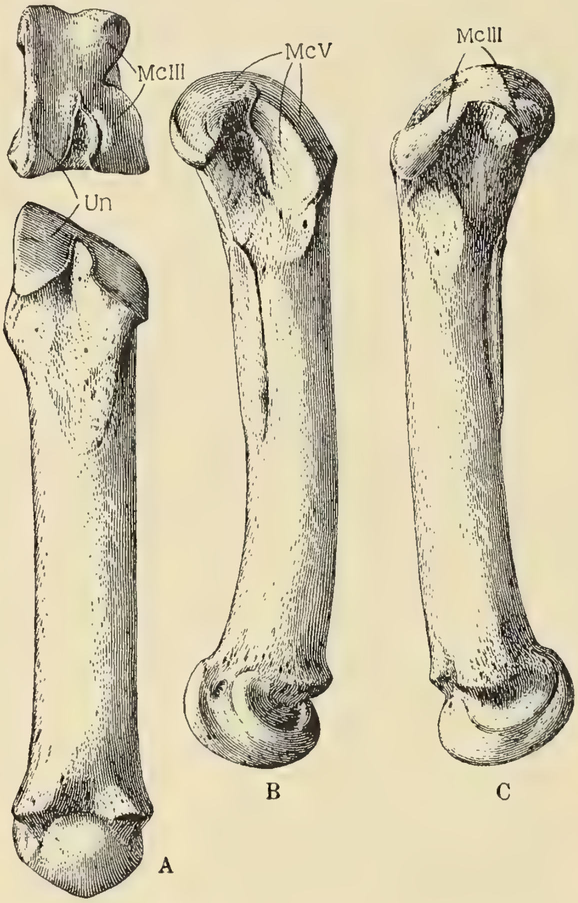

FIG. 96—*Felis atrox* Leidy. Right metacarpal IV, No. 2914-R-1. A, B, C, same views as in figure 95; × 2/3. Rancho La Brea Pleistocene.

TABLE 59—*Measurements (in millimeters) of metacarpal IV of Smilodon californicus*

	Right*			Left†		
	2016-R-1	2016-R-2	2016-R-3	2016-L-1	2016-L-2	2016-L-3
	Max.		*Min.*	*Max.*		*Min.*
Greatest length	105.6	92.2	79.4	107.4	92.3	79.4
Greatest transverse diameter of proximal end	24.2	21.4	20.4	26.6	21.8	18.9
Greatest dorsoventral diameter of proximal end	27.4	24.7	22.8	25.8	26	20.6
Transverse diameter at middle of shaft	16	15.3	12.4	15.9	15.8	12.3
Dorsoventral diameter at middle of shaft	14.9	14.4	12.8	14.4	14.5	12.2
Greatest transverse diameter at distal end of shaft	24.6	23	19.6	22.7	21.9	20.2

* Based on a series of 733 specimens. † Based on a series of 742 specimens.

The facet for metacarpal III, situated toward the palmar side of the proximal end, is more extensive in *Smilodon* than in *F. atrox*. On the outer side of the proximal end two articulating surfaces for metacarpal V are clearly outlined. The facet situated dorsally may, however, extend to the proximal border as in *F. atrox.*

As in the third metacarpal of *Smilodon,* the lower portion of the shaft is compressed somewhat in dorso-palmar direction, more so than in *F. atrox.* Likewise, the palmar keel of the distal end is more prominent than in *F. atrox.*

TABLE 60—*Measurements (in millimeters) of metacarpal IV of Felis atrox*

	Right*			Left†		
	2914-R-1	2914-R-2	2914-R-3	2914-L-1	2914-L-2	2914 L-3
	Max.		*Min.*	*Max.*		*Min.*
Greatest length	136.4	129	112	142.7	127.1	112.1
Greatest transverse diameter of proximal end	27.6	26.7	22.2	25.7	26.3	22.9
Greatest dorsoventral diameter of proximal end	31.7	30.1	26.9	29.3	30	27
Transverse diameter at middle of shaft	18.9	17.3	15.1	17.4	17.4	15
Dorsoventral diameter at middle of shaft	17.2	15.7	14.8	16.9	17.6	14.6
Greatest transverse diameter at distal end of shaft	27.4	24.2	21.6	26.3	24.3	21.7

* Based on a series of 32 specimens. † Based on a series of 37 specimens.

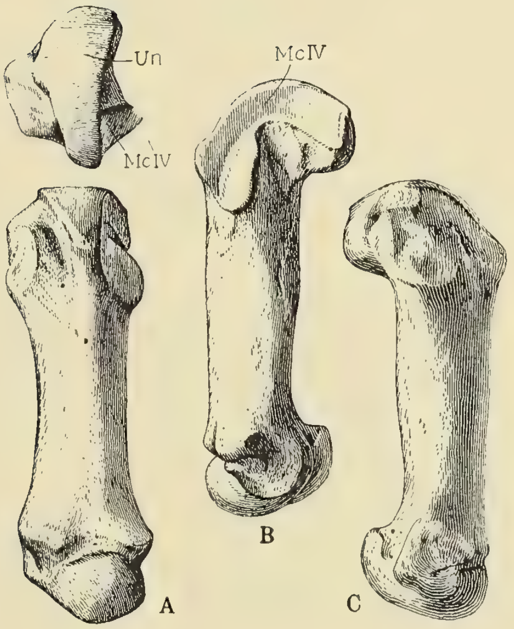

FIG. 97—*Smilodon californicus* Bovard. Right metacarpal V, No. 2017-R-1. A, dorsal view with view of proximal end; B, inner view; C, outer view; × 2/3. Facets for unciform (*Un*) and metacarpal IV (*McIV*). Rancho La Brea Pleistocene.

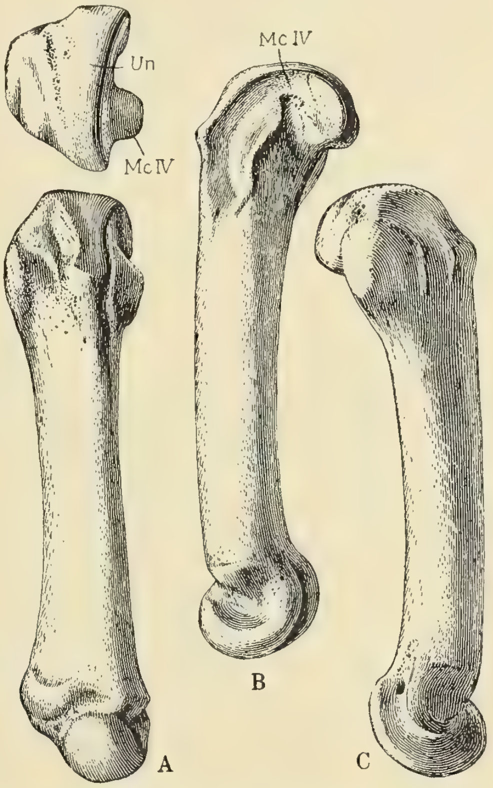

FIG. 98—*Felis atrox* Leidy. Right metacarpal V, No. 2915-R-1. A, B, C, same views as in figure 97; × 2/3. Rancho La Brea Pleistocene.

METACARPAL V

The proximal surface articulating with the unciform is relatively broad, more so than in *Felis atrox*. Viewed from the inner side (compare figures 97B and 98B), the plane of this surface is seen to dip not so steeply into the plane of the dorsal surface in *Smilodon* as in the large true cat type. The inner ear-shaped projection of the proximal end, supporting a portion of the articulating surface for the fourth metacarpal, is not so large in the sabre-tooth as in *F. atrox*. To the palmar side of this projection, the notch which indents the margin of the facet for metacarpal IV is broad. In *F. atrox* the notch is narrower and the articulating surface for the adjacent metapodial swings farther along the palmar border of the proximal end than in *Smilodon*.

TABLE 61—*Measurements (in millimeters) of metacarpal V of Smilodon californicus*

	Right*			Left		
	2017–R-1	2017–R-2	2017–R-3	2017–L-1	2017–L-2	2017–L-3
	Max.		*Min.*	*Max.*		*Min.*
Greatest length	85	75.3	62.8	86.6	74.9	61.6
Greatest transverse diameter of proximal end	28.8	22.8	20.3	27.9	24.4	20.1
Greatest dorsoventral diameter of proximal end	31	25.8	25.2	32.2	28.8	23.3
Transverse diameter at middle of shaft	17.2	14.4	13.3	17.9	15.4	12.9
Dorsoventral diameter at middle of shaft	14.2	12.7	11.7	16.1	13	10.8
Greatest transverse diameter at distal end of shaft	25.7	22.2	20.4	26.6	24.4	19.6

* Based on a series of 745 specimens. † Based on a series of 733 specimens.

TABLE 62—*Measurements (in millimeters) of metacarpal V of Felis atrox*

	Right			Left		
	2915–R-1	2915–R-2	2915–R-3	2915–L-1	2915–L-2	2915–L-3
	Max.		*Min.*	*Max.*		*Min.*
Greatest length	115.3	105	90.6	113	106.6	91.7
Greatest transverse diameter of proximal end	27.7	28.7	25.1	30	27.8	24.9
Greatest dorsoventral diameter of proximal end	30.8	31.3	27	33.2	29.8	27.3
Transverse diameter at middle of shaft	15.8	17	14.2	17.6	16.3	14.2
Dorsoventral diameter at middle of shaft	15.2	15	13.2	15.8	14.1	12.2
Greatest transverse diameter at distal end of shaft	25.2	24.9	21.2	26.7	24.8	22.2

On the outer side of the proximal end the surface of the tuberosity is frequently depressed or may be flattened in the sabre-tooth, while in the extinct true felid it is often convex. The shaft of metacarpal V is relatively stout. The inner and palmar surfaces are flat and sharply separated along the inner palmar border. In *F. atrox* the cross-section of the shaft at the middle is oval and no sharply defined borders are present. The palmar keel of the distal articulation is prominent.

DIGIT I, PROXIMAL PHALANX

Compare this element of *Smilodon* with that of *Felis atrox* (see figs. 99 and 100). The proximal phalanx in the sabre-tooth is relatively wider than that of *F. atrox*, but not so deep dorsoventrally. The latter difference is seen best in side view, but the distal articulation for the ungual phalanx likewise shows a greater depth in *F. atrox*. The dorsal surface of the distal end appears to be more deeply incised by a longitudinal groove in the latter than in the sabre-tooth. The notch which indents the palmar border of the proximal end is deep and acute in *Smilodon*, while in *F. atrox* it is wide and more open. Behind the distal articulation the palmar surface of the phalanx is broadly excavated, apparently more so in the former than in the latter.

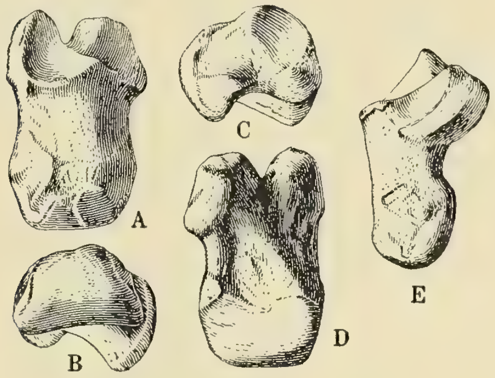

FIG. 99—*Smilodon californicus* Bovard. Digit I, manus, proximal phalanx, No. 2073-1. A, dorsal view; B, distal view; C, proximal view; D, palmar view; E, inner view; × 2/3. Rancho La Brea Pleistocene.

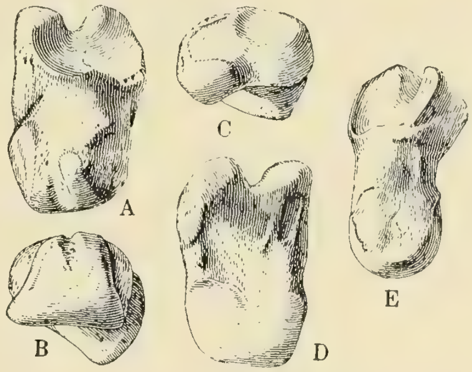

FIG. 100—*Felis atrox* Leidy. Digit I, manus, proximal phalanx, No. 2968-1. A, B, C, D, E, same views as in figure 99; × 2/3. Rancho La Brea Pleistocene.

INNOMINATE BONE

Plates 24 and 39, figs. 1 and 2

The os innominatum of *Smilodon* differs from that of *Felis atrox* in several noteworthy structural details. The anterior inferior spine and the posterior inferior spine are quite prominent in *Smilodon*, more so than in *F. atrox*. The anterior inferior spine has moved farther forward with reference to the crest of the ilium in the sabre-tooth, and the anterior border behind or below the spine is formed by a sharper ridge than in *F. atrox*. The crest of the ilium is not quite so pointed or is at least not so acutely rounded in *Smilodon* as in the true felines. The external surface of the ilium is not so deeply excavated as in the great lion-like cat. In the specimen under observation, the line bordering the area of attachment of the gluteus medius muscle lies closer to the anterior border than to the posterior border. In *F. atrox* the reverse is the case. On the inner side of the ilium the area to which the sacrum is attached suggests a strong union with this element. The ilium may be thicker or heavier through the region which joins the sacrum than that of *F. atrox*. Two prominent rugose surfaces lie above or in front of the rim of the acetabulum and presumably indicate strong attachments for the rectus femoris and gluteus quartus muscles. The ilio-pectineal eminence is very distinct.

The innominate bone of *Smilodon* is actually broader as measured from the border of the lesser sacro-sciatic notch to the symphyseal border than that of *F. atrox*. The tuberosity of the ischium is not so heavy as in the latter, but the body of the ischium is quite wide. The body of the pubis as well as the horizontal ramus of this element are narrow, distinctly more so than in *F. atrox*. The inner surface of the cotyloid bone may be decidedly convex in *Smilodon*. The symphyseal union in the pubic region does not appear to have been as strong in the sabre-tooth as in *F. atrox*. While the long diameter of the obturator foramen is shorter than that of the extinct true felid, the greatest diameter of this opening taken normal to it exceeds that in *F. atrox*. The even curve of the border of the obturator foramen is broken by the presence of a distinct spine on the pubis. The articulating surface within the acetabulum for the head of the femur is broader in *Smilodon* than in *F. atrox*.

TABLE 63—*Measurements (in millimeters) of innominate bone of Smilodon*

	2008–R-1	2008–R-2	2008–R-3	2008–R-4	2008–R-5	2008–R-6	2008–R-7	2008–R-8	2008–R-9	2008–R-10
Length from anterior end of ilium to posterior border of ischium	368	363	363	347	341	332	323	307	309	*a*283
Greatest depth of ilium	94	90.7	91.8	85.8	91.9	81.5	81.1	76.9	76.2	73.8
Length of symphysis	125	......	119	......	117.8	114	101.3	102	......	......
Width of ischium measured from ischial tuberosity to posterior end of ischial symphysis	117.7	117.3	112.6	114.5	103.3	111.4	109.4	107	108.6	88.6
Diameter of acetabulum measured at right angles to long axis of internal notch	54.7	54.2	54.8	52.9	48.9	50.6	50.8	44.3	44.8	46.4
Long diameter of obturator foramen	74.2	78.4	82.4	70	75	80.6	69.9	72.2	73.1	69.9
Greatest diameter of obturator foramen taken normal to long diameter	52.8	56.8	57.4	46.3	51.9	53.9	48.3	47.7	......	45

a, Approximate

TABLE 64—*Measurements (in millimeters) of innominate bone of Felis atrox*

	2906–R-1	2906–R-2	2906–R-3	2906–R-4	2906–R-5
Length from anterior end of ilium to posterior border of ischium	370	365	345	*a*338	347
Greatest depth of ilium	90.6	83.4	74.8	78.2	83
Length of symphysis	146.2	136.8	134.5	138	128
Width of ischium measured from ischial tuberosity to posterior end of ischial symphysis	111.1	111.2	101	106.4	101.3
Diameter of acetabulum measured at right angles to long axis of internal notch	54.8	54.7	51	49.4	47.3
Long diameter of obturator foramen	85	82.4	87.9	84.4	79.4
Greatest diameter of obturator foramen taken normal to long diameter	46.9	46.5	47.4	50.3	46.9

a, Approximate.

FEMUR

Plates 23 and 38, figs. 1 and 2

The thigh bone of the sabre-tooth is a shorter and relatively heavier element than that of *F. atrox*. The shaft is noticeably broader throughout its length than in the latter and widens gradually from a point near the middle of the femur toward the proximal and distal extremities. The shaft appears to be slightly bowed in its longitudinal extent. The distal portion of the shaft is flatter, less cylindrical than in *F. atrox*. A nutrient foramen on the inner side of the posterior surface of the shaft is situated midway between the lesser trochanter and the distal articulation.

Several structural characters seen at the proximal end serve to distinguish the femur of *Smilodon* from that of *Felis atrox* and from the large living cats. The greater trochanter rises distinctly above the level of the head and is obliquely truncated on its lateral side. The outer surface of the trochanter extends farther down the proximal extremity of the femur. Viewed from the posterior side, the lesser trochanter is seen to be situated at a point distinctly below the head. This distance is greater in the sabre-tooth than in *F. atrox*. The digital fossa is a larger depression than in the latter. Between the fossa and the head the posterior surface of the neck develops a rounded and prominent tuberosity. The head is essentially like that in *F. atrox*, but may be relatively larger than in the latter type.

Table 65—*Measurements (in millimeters) of femur of Smilodon*

	2009-R-1	2009-R-2	2009-R-3	2009-R-4	2009-R-5	2009-R-6	2009-R-7	2009-R-8	2009-R-9	2009-R-10
Greatest length from top of greater trochanter to distal condyles, measured parallel to long axis of femur	408	399	390	388	381	370	353	342	329	317
Transverse diameter of proximal end, outer face of greater trochanter to inner side of head, taken normal to median longitudinal plane	108.8	98.1	106.3	98.7	102.9	96	92	86.4	82.7	83
Greatest antero-posterior diameter of head	50.7	44.4	47.4	45.7	48	45.6	43.2	39.7	39.1	39.4
Transverse diameter of shaft at middle	40.4	35.2	35.6	38.4	39	37.3	38.1	30.8	33.5	30.1
Antero-posterior diameter of shaft at middle	35.4	31.4	33.8	31.9	33.2	33.6	31.5	29.2	28.3	26.8
Greatest width of distal extremity	90.2	76.8	84.7	82.9	84.9	82.3	76.2	73.4	68.3	65.2
Greatest antero-posterior diameter of the distal extremity, at right angles to longitudinal axis of femur	80.3	74.3	76.6	74.5	77	77.2	72.7	69.4	64	63.9
Greatest width of rotular surface	60	47.8	53.3	53.6	52.3	54.8	52	44.9	42	43.4
Greatest width of intercondylar notch	21.7	21.1	22.5	16.9	23.3	22.7	15.4	18.6	19.8	14.5
Greatest width of articular surface of inner condyle	35.7	29.9	33.9	33.8	32.7	31	33.2	28.4	24.9	26.5

The patellar surface is slightly more excavated than in *F. atrox* and the lateral borders appear to be more prominent dorsally in the sabre-tooth. The inner and outer tibial articulations are of nearly equal size. In contrast to the great lion-like cat these surfaces are separated by a decidedly narrower intercondyloid notch in *Smilodon*. The rugose areas at the lower end of the shaft and above the outer and inner articulating surfaces of the distal end, to which are attached the gastrocnemius muscle, are much less pronounced in *Smilodon* than in *Felis atrox.*

Table 66—*Measurements (in millimeters) of femur of Felis atrox*

	2907–R-1	2907–R-2	2907–R-3	2907–R-4	2907–R-5	2907–R-6	2907–R-7	2907–R-8	2907–R-9	2907–R-10
Greatest length from top of greater trochanter to distal condyles, measured parallel to long axis of femur	402	455	460	437	435	423	415	402	*a*393	391
Transverse diameter of proximal end, outer face of greater trochanter to inner side of head, taken normal to median longitudinal plane	100.6	120.3	112.8	105.7	101.5	107	99	100.6	*a*97	97.9
Greatest anteroposterior diameter of head	47	54.3	53.8	47.9	50.3	49.7	46.6	47	48	44.2
Transverse diameter of shaft at middle	37	45.3	41	41.3	41.7	40.3	35	36.5	35.6	36.2
Anteroposterior diameter of shaft at middle	32.5	42.5	37.6	36.3	37.8	35.6	32.2	32.3	32.8	33.1
Greatest width of distal extremity	87.1	105.4	95.5	90	92.8	92.5	85.8	90	89.3	79.9
Greatest anteroposterior diameter of the distal extremity, at right angles to longitudinal axis of femur	85.4	98.6	96.4	87.9	91.8	93.7	85	85.4	86.7	82.6
Greatest width of rotular surface	53	60	56	52	52.4	46.5	42	47	44.3	40.7
Greatest width of intercondylar notch	24.7	32.6	29.5	22	24	23.6	22.7	26	24.3	18.6
Greatest width of articular surface of inner condyle	32.1	39	35.2	35	36.7	34.4	32.5	32	30.8	31.3

a, Approximate.

PATELLA

Plates 23 and 38, fig. 7

The patella of *Smilodon* approximates in size the kneecap of the modern cats, *Felis leo* and *F. tigris.* The element differs from the patella of *Felis atrox* and of the living cats in its relative heaviness, particularly as indicated by the anteroposterior diameter. The transverse convexity of the femoral articulation is more pronounced in the sabre-tooth than in *F. atrox.* The end of the distal tongue is broadly rounded, not pointed as in the extinct true cat type.

Table 67—*Measurements (in millimeters) of patella*

	Smilodon californicus*				Felis atrox			
	2012–R-1	2012–R-2	2012–R-3	2012–R-4	2910–R-1	2910–L-1	2910–L-2	2910–L-3
Greatest proximodistal diameter	64.2	57.7	57.7	44.7	75.7	73.8	66.8	63.8
Greatest transverse width	47	45.3	40	33.6	46.6	54.9	43.8	42.7
Anteroposterior diameter through middle of articulating surface	29.6	29.4	25	19.7	27.6	31.4	25.6	26.4

* Selected from a series of 679 individuals.

SESAMOIDS

Fabella

Several nodular elements appear to represent these femoral sesamoids. These specimens are heavier than the comparable bones in the lion or tiger. Measurements (in millimeters) of No. 2037–2 are as follows: Greatest length 17, greatest width 13.3, greatest thickness through articulating facet 9.9.

Phalangeal Sesamoids

A number of phalangeal sesamoids are available in the collection. These vary in size and in shape. Those of larger size (fig. 101C, D) may represent *Felis atrox*, while the smaller elements (fig. 101B), of which there are a greater number, presumably belong to *Smilodon*. The characters displayed by the specimens from the asphalt are essentially like those in the large living felines. In some of the elements referred to *Smilodon*, the ridge behind the articulating surface appears to be relatively heavy.

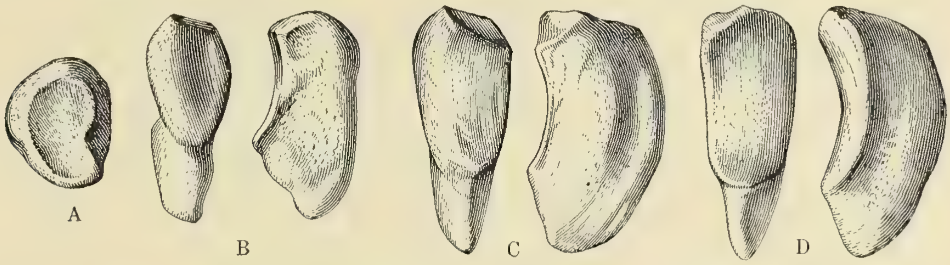

Fig. 101—Sesamoids; × 1. A, B, *Smilodon californicus* Bovard, Nos. 2037-2 and 2037-1; C, D, *Felis atrox* Leidy, or *S. californicus*, Nos. 2935-2 and 2935-1

Table 68—*Measurements (in millimeters) of phalangeal sesamoids*

	2037–1	2935–1	2935–2
Greatest length. .	27.3	31.9	32
Greatest width. . .	11.1	12.4	12.4

TIBIA

Plates 23 and 38, figs. 3 to 6

The elements of the lower segment of the hind limb, like those of the forearm, are short, but the tibia is relatively not so heavy in *Smilodon* as in *Felis atrox*. At the proximal end the articulating surfaces for the femur are not so large nor is the spine so prominent as in the latter type. The tubercle for attachment of the ligamentum patellæ is relatively broad and the cnemial crest is heavier in the sabretooth than in *F. atrox*. In side view, the crest is seen to project farther forward in *Smilodon* than in *Felis leo* or in *F. tigris*. In this view also the border extending forward from a point in front of the femoral articulation to the tubercle makes a more rapid descent in *Smilodon* than in the Pleistocene *F. atrox*.

The proximal and distal articulations for the fibula are larger in the sabre-tooth than in *F. atrox*. Viewing the tibia from the outer side, the posterior face of the upper half of the shaft is seen to round gradually into the outer surface. Thus the nutrient foramen on the posterior surface becomes clearly in evidence in lateral view. In *Felis atrox* and in the modern cats, on the other hand, the lateral and posterior surfaces of this region of the shaft are sharply demarcated and the nutrient foramen is not seen in lateral view. The posterior surface below the head is not so deeply nor so broadly excavated in *Smilodon* as in *F. atrox*. The posterior surface of the distal third of the shaft is flat, not distinctly convex as in the Rancho La Brea lion-like type.

At the distal extremity the grooves for the tendons of the flexor longus digitorum and tibialis posticus muscles are well defined. A distinct tubercle on the posterior side of the distal extremity separates the course of the tendon of the flexor longus digitorum muscle from that of the flexor longus hallucis muscle. The notch incising the anterior border of the distal surface is noticeably smaller than in *F. atrox*.

Table 69—*Measurements (in millimeters) of tibia of Smilodon*

	2010–R-1	2010–R-2	2010–R-3	2010–R-4	2010–R-5	2010–R-6	2010–R-7	2010–R-8	2010–R-9	2010–R-10
Greatest length measured parallel to long axis	305	301	284	288	291	282	264	241	239	241
Greatest transverse diameter of proximal end	84.4	89	90.4	87.4	86	84.9	83.1	76.4	72.5	74.8
Transverse diameter of shaft at middle	26.8	32.3	33	29.5	29.5	28.2	25.7	27.9	25.1	25.7
Greatest transverse diameter of distal end	63.3	61.3	60	58.6	56.5	57.8	55.4	51.9	45	50.2
Greatest anteroposterior diameter of distal end	40.8	38.2	40.2	41.1	40.8	36.6	40.4	34.4	34.8	33.3

Table 70—*Measurements (in millimeters) of tibia of Felis atrox*

	2908–R-1	2908–R-2	2908–R-3	2908–R-4	2908–R-5	2908–R-6	2908–R-7	2908–R-8	2908–R-9	2908–R-10
Greatest length measured parallel to long axis	400	382	381	369	362	355	353	339	338	338
Greatest transverse diameter of proximal end	107	102.7	106.7	97.9	98	95.4	95.1	95.4	93.6	86.7
Transverse diameter of shaft at middle	40	36.6	43.4	37.5	37.5	33.8	37	33.3	32	33
Greatest transverse diameter of distal end	74.8	71.4	77.4	65.5	68.3	65	65.8	66	62	59.1
Greatest anteroposterior diameter of distal end	52.3	50.3	51	46	49.4	45.3	45.3	44.2	41.7	42.4

FIBULA

Plates 24 and 39, fig. 4

The fibula in *Smilodon* is not only stouter and relatively heavier than the comparable element in *Felis*, but exhibits also a number of structural peculiarities unique to this form. The proximal end, as viewed from the inner side, is fan-shaped. The anterior and posterior borders of this end descend rapidly to form the comparable borders of the shaft. The anterior and posterior ends of the proximal extremity are tuberous. Immediately below the proximal end the outer surface of the shaft is broadly and deeply excavated.

The shaft when viewed from the inner side does not increase in anteroposterior diameter from the upper to the lower end. The inner surface is not bent in the manner seen in the fibula of *Felis atrox*. The shaft is relatively wider transversely in *Smilodon* than in *Felis*. The ridge for attachment of the interosseous membrane is not so sharply emarginate in the sabre-tooth as in the latter. The distal end is not so long in anteroposterior diameter as that of *F. atrox,* but the transverse diameter is greater in *Smilodon.* The articulating surface for the astragalus is convex. The external malleolus is large and prominent.

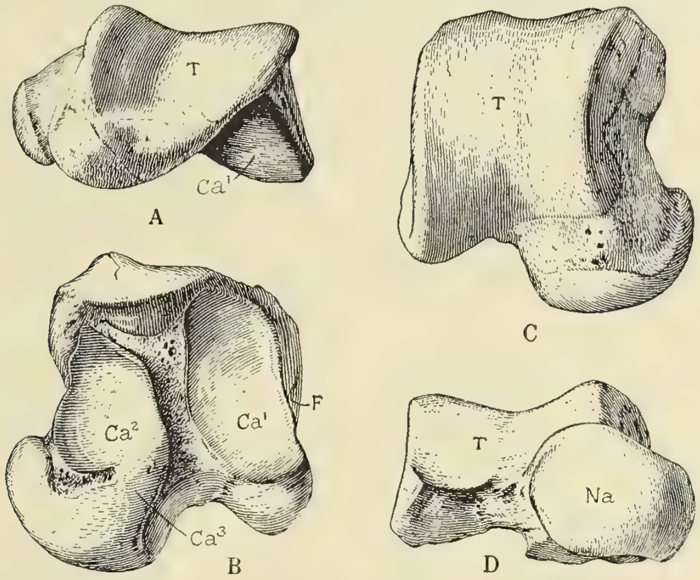

Fig. 102—***Smilodon californicus*** Bovard. Right astragalus, No. 2030-R-1. A, posterior view; B, calcaneal view; C, tibial view; D, distal view; × 2/3. Facets for tibia (*T*), fibula (*F*), navicular (*Na*), and calcaneum (*Ca*¹, *Ca*², *Ca*³). Rancho La Brea Pleistocene.

Table 71—*Measurements (in millimeters) of fibula of Smilodon*

	2011–R-1	2011–R-2	2011–R-3	2011–R-4	2011–R-5	2011–R-6	2011–R-7	2011–R-8	2011–R-9	2011–R-10
Greatest length	265	284.7	271	258.8	250.3	247	237	232	223.4	212.7
Greatest anteroposterior diameter of proximal end	39.2	45.9	43.4	40.1	40.3	41	35.6	37.9	36.8	32.5
Greatest anteroposterior diameter of distal end	22.8	*a*26.4	24.8	24	26.7	25.6	24.3	23.5	24.8	17.2
Greatest transverse diameter of distal end	29.9	.....	33.4	28.6	34	32.2	29.3	27.4	30.5	24.4
Anteroposterior diameter of shaft at middle	10.7	11.9	10.4	9.4	11.1	11.4	9.2	9.2	10.8	9.2
Transverse diameter of shaft at middle	11.3	13.5	16	15.3	12.2	11.9	12	13.7	11.2	9.4

a, Approximate.

Measurements, in millimeters, of fibula of *Felis atrox,* No. 2909-R-1, are as follows: greatest length, 369; long diameter of proximal end, 35.4; diameter of proximal end taken normal to long diameter, 22.1; greatest width of shaft at middle, 16.1; greatest thickness of shaft at middle, 10.9; long diameter of distal end, 39.4; diameter of distal end taken normal to long diameter, 21.

ASTRAGALUS

The trochlear surface of the astragalus is relatively broad and less deeply grooved in *Smilodon* than in the large extinct *Felis*. The articulating surface for the fibula may be deeply excavated. The neck is not so long as in *F. atrox*, although short-necked and relatively long-necked astragali of the sabre-tooth occur in the collections from Rancho La Brea (see fig. 104A, B).

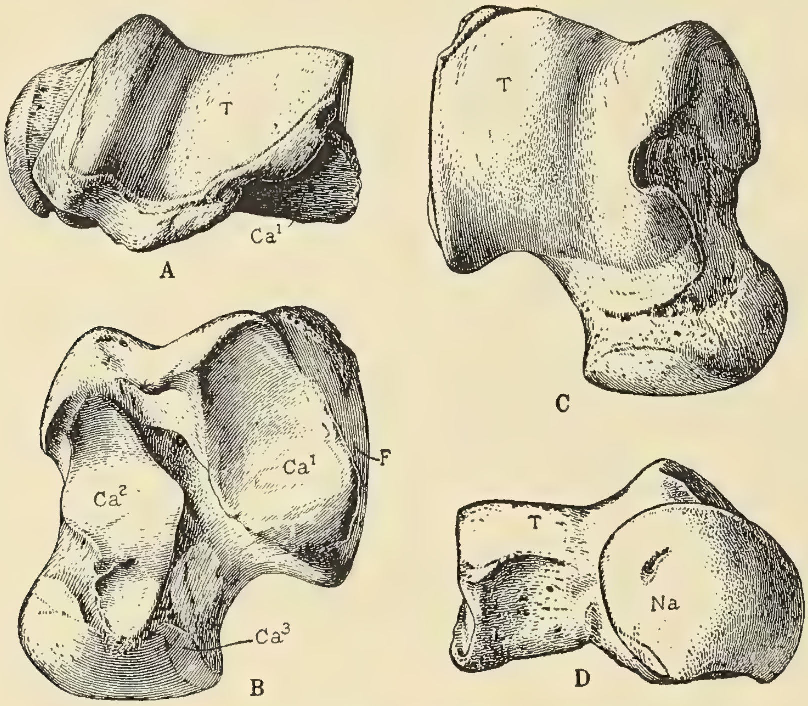

Fig. 103—*Felis atrox* Leidy. Right astragalus, No. 2928-R-1. A, B, C, D, same views as in figure 102; × 2/3. Rancho La Brea Pleistocene.

An astragalar foramen is frequently present in *Smilodon* (fig. 104C). This opening is absent in the astragalus of *Felis atrox*. The foramen varies considerably in size. In a series of 368 specimens, the following variations were noted:

11 specimens with foramen varying in diameter from approximately 6 mm. to 7.8 mm.
52 specimens with foramen varying in diameter from 4.2 mm. to 5.8 mm.
123 specimens with foramen varying in diameter from 1 mm. to 3.7 mm.
138 specimens show a single opening in the dorsal or tibial face and several small foramina on the calcaneal or plantar face.
44 specimens with no dorsal foramen but with several small foramina visible on the plantar side.

The head articulating with the navicular (fig. 102D, *Na*) is flattened and less hemispherical in shape than that of *F. atrox*. The inner calcaneal facet, *Ca*^{2}, is concave and broadly connected distally with the third surface (*Ca*^{3}) of articulation with the calcaneum. Facets *Ca*^{2} and *Ca*^{3} are as a rule separate and distinct articulating surfaces in *F. atrox* and in the Recent cats, *F. leo* and *F. tigris*. The groove for the interosseous ligament is long.

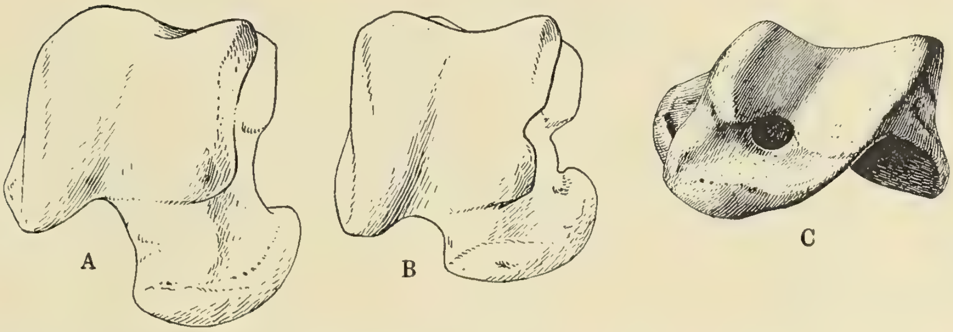

Fig. 104—*Smilodon californicus* Bovard. Right astragali; × 2/3. A and B, tibial views of long-necked and short-necked specimens, Nos. 2030-R-2, 2030-R-5; C, posterior view showing presence of large astragalar foramen, No. 2030-R-2. Rancho La Brea Pleistocene.

Table 72—*Measurements (in millimeters) of astragalus*

	Smilodon californicus*				Felis atrox									
	2030–R-1	2030–R-2	2030–R-3	2030–R-4	2928–R-1	2928–R-2	2928–R-3	2928–R-4	2928–R-5	2928–R-6	2928–R-7	2928–R-8	2928–R-9	2928–R-10
Greatest length	61.2	59.4	52.8	44.6	74.1	71.7	70	69.6	68	69.6	64	66.7	58.7	61.8
Greatest width	61.2	59.4	52.4	46	66	63.2	63.5	62	61.3	60	57	58	53.8	51.8
Least distance across neck	29.5	27.7	27.1	23.3	35.4	31.9	33.7	33.8	32	31.9	30.6	29.3	26.3	27.8
Greatest diameter of head	35.1	36.2	32.8	29	43	40.7	41.7	41.5	40.1	40.4	38.6	38.6	35.1	36.4

* Selected from a series of 838 individuals.

CALCANEUM

The tuber calcis is long and heavy and the astragalar facets are situated relatively close to the cuboid border (fig. 105A). The two astragalar facets of the inner side (As^2 and As^3) are broadly connected, not separate as in *Felis atrox*. The inner process supporting the second or sustentacular facet (As^2) is relatively smaller than in the great lion-like cat. The large outer facet (As^1) for the astragalus does not apparently encroach upon the surface of the tuber calcis so far as in *F. atrox*. This facet is broad. Distad to facet As^1 the outer portion of the calcaneum of *Smilodon* is more tuberous than that in the large true felines of the Pleistocene and Recent.

The articulating facet for the cuboid (*Cu*) differs in shape from that of *F. atrox* and may be distinctly concave. It is flanked on the inner side by a small concave surface (*Na*) for the navicular. This facet is absent in the true cats.

ENTOCUNEIFORM

The entocuneiform of *Smilodon* is a small and thickened element noticeably different in shape from the corresponding bone in *Felis atrox* (compare figures 107 and 108). The entocuneiform is triangular in cross-section, with the base of the triangle facing the mesocuneiform. At the proximal end a rounded tuberosity pro-

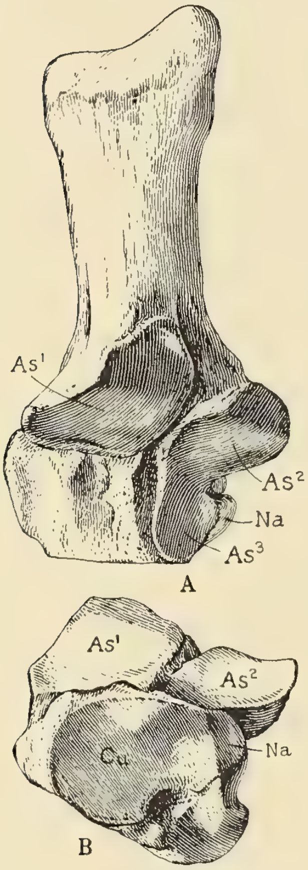

FIG. 105—*Smilodon californicus* Bovard. Right calcaneum, No. 2031-R-1. A, astragalar view; B, distal view; × 2/3. Facets for astragalus (*As*¹, *As*², *As*³), navicular (*Na*), and cuboid (*Cu*). Rancho La Brea Pleistocene.

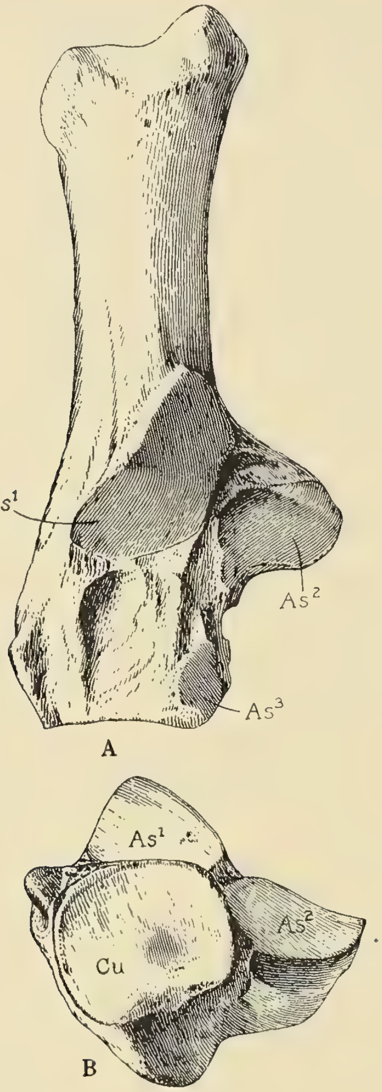

FIG. 106—*Felis atrox* Leidy. Right calcaneum, No. 2929-R-1. A, B, same views as in figure 105; × 2/3. Rancho La Brea Pleistocene.

jects upward and inward. The facet for the navicular (*Na*) may be broad and shallow, and it differs in shape from that in *F. atrox*. It varies considerably in size and in shape. The facet for the mesocuneiform (*Mc*) is relatively large and in a number of specimens from Rancho La Brea is convex in its dorsoplantar extent. This surface, however, may be flattened or even concave. The distal surface for the metatarsal is flattened or slightly concave and is rudely triangular in outline.

TABLE 73—*Measurements (in millimeters) of calcaneum*

	Smilodon californicus*			Felis atrox									
	2031–R-1	2031–R-2	2031–R-3	2929–R-1	2929–R-2	2929–R-3	2929–R-4	2929–R-5	2929–R-6	2929–R-7	2929–R-8	2929–R-9	2929–R-10
Greatest length	106.8	96.7	79.4	142	140.3	140.5	137.7	131.5	131.5	125	118	117.8	109
Greatest width measured across astragalar facets As^1 and As^2	50.8	45.5	40.4	56	55.2	53.2	54	50.9	52.4	45.9	47	47.9	41.5
Greatest width across cuboid surface measured from astragalar facet As^3 to outer side†	44.2	39.8	32.7	37.8	34.3	35.2	34.4	33.3	34.1	30.2	30	29.3	26
Greatest width of outer face measured normal to plantar border and to edge of outer astragalar facet	48.9	40.3	36.3	59	60.3	58.5	56.4	56.4	54.3	51.5	49.2	47.4	46.5

* Selected from a series of 841 individuals.

† This measurement in *Smilodon* is taken from the inner border of the navicular facet (Na) to the outer side

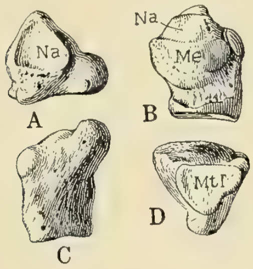

FIG. 107—*Smilodon californicus* Bovard. Right entocuneiform, No. 2032-R-2. A, proximal view; B, outer view; C, dorsal view; D, distal view; × 2/3. Facets for navicular (*Na*), mesocuneiform (*Me*), and metatarsal I *MtI*). Rancho La Brea Pleistocene.

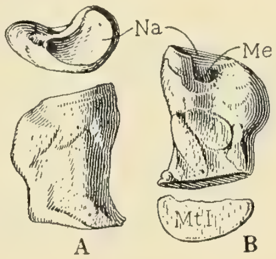

FIG. 108—*Felis atrox* Leidy. Right entocuneiform, No. 2930-R-1. A, dorso-internal and proximal views; B, plantar-external and distal views; × 2/3. Facets as in figure 107. Rancho La Brea Pleistocene.

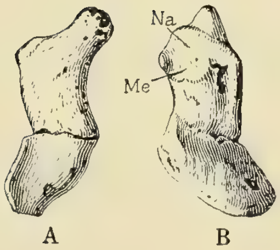

FIG. 109—*Smilodon californicus* Bovard. Fused right entocuneiform and metatarsal I, No. 2032-R-4. A, dorsal view; B, outer view; × 2/3. Facets for navicular (*Na*) and mesocuneiform (*Me*). Rancho La Brea Pleistocene.

In a series of 43 specimens of the right entocuneiform of *Smilodon californicus*, 13 showed fusion with the rudimentary metatarsal I and one showed fusion with the mesocuneiform.

MESOCUNEIFORM

The mesocuneiform of the sabre-tooth is quite dissimilar in shape from that of *Felis atrox* (compare figures 110 and 111). This element is slightly sinuous in its dorsoplantar extent. The proximal articulating surface for the navicular (*Na*) is more deeply concave than in *Felis.* The outer side is decidedly narrower in proximo-distal direction than in the latter type. At the proximo-plantar side of the inner surface of the mesocuneiform is a concave facet for the entocuneiform (*En*). This facet is generally distinctly larger than in the true cat. The position of the articulation is also somewhat different from that in *F. atrox*, in which form the facet is situated on the plantar surface.

Table 74—*Measurements (in millimeters) of entocuneiform*

	Smilodon californicus*			Felis atrox		
	2032–R-1	2032–R-2	2032–R-3	2930–R-1	2930–R-2	2930–R-3
Greatest proximo-distal diameter	23.9	22.4	21	26.6	23.6	24.2
Greatest width	14.5	17.9	13.4	21.9	20.1	19.7
Greatest thickness of proximal end	.....	.....	.....	12.3	11	12.4

* Selected from a series of 57 individuals.

On the latter surface in *Smilodon* is a small facet, which at first sight appears to be comparable to the facet having this position on the mesocuneiform of *Felis atrox* (*En*). But in the latter the facet clearly articulates with the entocuneiform which swings around to the plantar side of the mesocuneiform. This quite clearly is not the case in *Smilodon.* Possibly the facet articulates with a nodular rudiment. It is rarely present in the sabre-tooth, for in a series of 34 specimens representing the right mesocuneiform the element figured is the single example showing the facet.

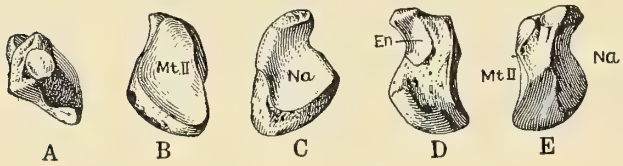

Fig. 110—*Smilodon californicus* Bovard. Right mesocuneiform, No. 2033-R-2. A, posterior view; B, distal view; C, proximal view; D, inner view; E, outer view; × 2/3. Facets for entocuneiform (*En*), navicular (*Na*), and metatarsal II (*MtII*). Rancho La Brea Pleistocene.

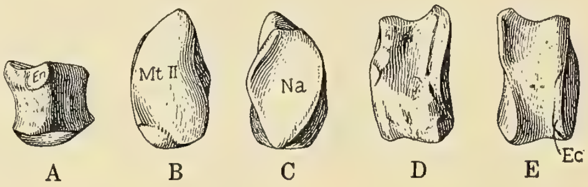

Fig. 111—*Felis atrox* Leidy. Right mesocuneiform, No. 2931-R-1. A, B, C, D, E, same views as in figure 110; × 2/3. Facets for entocuneiform (*En*), navicular (*Na*), ectocuneiform (*Ec*), and metatarsal II (*MtII*). Rancho La Brea Pleistocene.

In No. 2033-R-5 (fig. 118) the mesocuneiform has fused in part with the navicular. One specimen is also available in which the mesocuneiform has fused with the entocuneiform.

ECTOCUNEIFORM

The ectocuneiform is distinctly more compressed in proximo-distal direction than that of the Pleistocene and Recent true cats. The plantar projection with groove for the tendon of the peroneus longus muscle is more hook-like and less tuberous than in *F. atrox* of the asphalt. This envelops a deeper and broader groove for the tendon than is found in the ectocuneiform of either the extinct true cat or the living large cats. Occasionally the hook is absent in the sabre-tooth, the process being truncated as seen in specimen No. 2034-R-5 (fig. 112, F and G). When this occurs the truncated end bears a small facet which articulated apparently with a nodule of bone. Specimens also have been noted in which the truncated process has a surface like that of the process when normally developed.

Table 75—*Measurements (in millimeters) of mesocuneiform*

	Smilodon californicus*				Felis atrox			
	2033–R-1	2033–R-2	2033–R-3	2033–R-4	2931–R-1	2931–L-1	2931–L-2	2931–L-3
Greatest long diameter as measured along outer surface	28.6	25.1	25.6	21.2	25.8	29.3	28.2	25.3
Greatest proximodistal diameter	12.9	13.2	11.9	10.9	15.7	17.5	15.3	17.9
Width of articulating surface for metatarsal	14.2	11.7	13.7	9.6	15	14.3	13.7	14

* Selected from a series of 35 individuals.

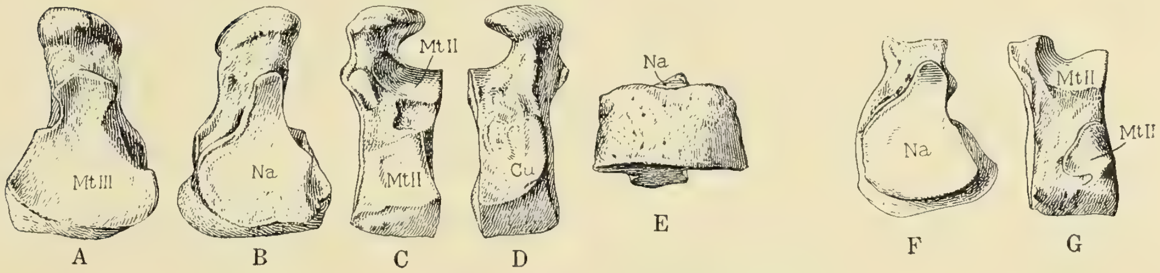

FIG. 112—*Smilodon californicus* Bovard. Right ectocuneiform, Nos. 2034-R-2, 2034-R-5. A, distal view; B, proximal view; C, internal view; D, external view; E, dorsal view; F, proximal view; G, internal view; × 2/3. Facets for navicular (*Na*), cuboid (*Cu*), metatarsal II (*MtII*), metatarsal III (*MtIII*). Rancho La Brea Pleistocene.

In a series of 120 specimens of the ectocuneiform, 85 possess a well-developed posterior process while 35 show this structure completely reduced.

The facet articulating with the navicular (*Na*) tapers to the plantar side and extends relatively farther in this direction than in the Pleistocene *Felis*. The opposite facet for the third metatarsal resembles in outline that of the true cats. The plantar projection of this surface is, however, relatively small. Viewed from the inner side, the plantar facet for the second metatarsal extends farther proximally from the distal border in the sabre-tooth than in *F. leo*, *F. tigris* and *F. atrox*, and encroaches upon the lower surface of the plantar process. On the outer surface the facet for the cuboid may extend along the proximal border or may reach distally along the dorsal border.

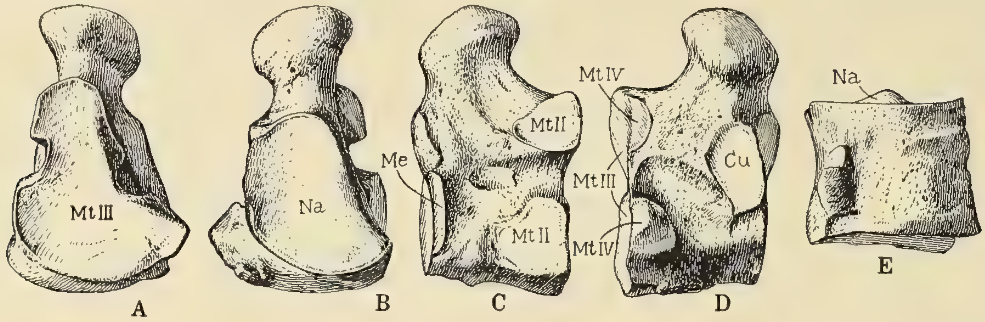

Fig. 113—*Felis atrox* Leidy. Right ectocuneiform, No. 2932-R-1. A, B, C, D, E, same views as in figure 112, A-E; × 2/3. Facets for mesocuneiform (*Me*), navicular (*Na*), cuboid (*Cu*), metatarsal II (*MtII*), metatarsal III (*MtIII*), and metatarsal IV (*MtIV*). Rancho La Brea Pleistocene.

Table 76—*Measurements (in millimeters) of ectocuneiform*

	Smilodon californicus*				Felis atrox			
	2034-R-1	2034-R-2	2034-R-3	2034-R-4	2932-R-1	2932-R-2	2932-R-3	2932-R-4
Greatest dorsoplantar length	48.9	43.9	40.8	33.1	55.2	51.8	48	43.8
Greatest proximodistal diameter	15.7	15.8	19.1	12.8	28.2	26.4	23	23.1
Greatest width across metatarsal articulation	26.6	29.7	26.7	22	33.8	31.2	29.2	25

* Selected from a series of 298 individuals.

CUBOID

In the cuboid of *Smilodon*, the facet for the navicular (*Na*) is situated at the dorsoplantar corner of the inner surface. The narrow, elongate facet for the ectocuneiform (*Ec*) is situated relatively farther toward the distal border of the inner surface in *Smilodon* than in *F. atrox*. On the distal face of the cuboid the facet for metatarsal IV is smaller and that for metatarsal V is larger than in the Pleistocene *F. atrox* or Recent *F. leo* and *F. tigris*. The tuberosity on the plantar surface is situated relatively farther distally in the cuboid of the sabre-tooth than in that

Table 77—*Measurements (in millimeters) of cuboid*

	Smilodon californicus*				Felis atrox			
	2035-R-1	2035-R-2	2035-R-3	2035-R-4	2933-R-1	2933-R-2	2933-R-3	2933-R-4
Greatest proximodistal diameter	31.4	29.5	27.4	25	38.5	37.3	34.5	32.9
Greatest transverse diameter	31.4	33.6	32.5	24.7	39.3	39.3	33.3	33.7
Greatest dorsoplantar length	42.3	37.7	35.6	27.5	42.7	39.2	35.5	33.9

* Selected from a series of 475 individuals.

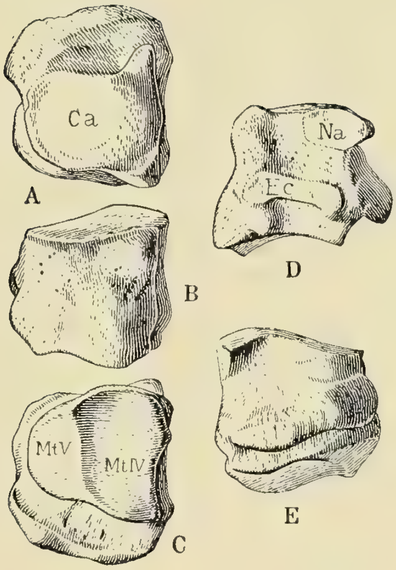

FIG. 114—*Smilodon californicus* Bovard. Right cuboid, No. 2035-R-3. A, proximal view; B, dorsal view; C, distal view; D, inner view; E, plantar view; × 2/3. Facets for calcaneum (*Ca*), navicular (*Na*), ectocuneiform (*Ec*), metatarsal IV (*MtIV*), and metatarsal V (*MtV*). Rancho La Brea Pleistocene.

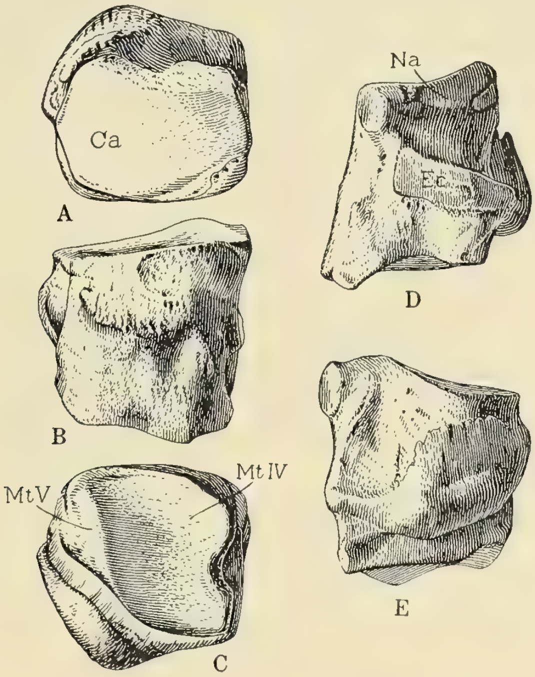

FIG. 115—*Felis atrox* Leidy. Right cuboid, No. 2933-R-1. A, B, C, D, E, same views as in figure 114; × 2/3. Rancho La Brea Pleistocene.

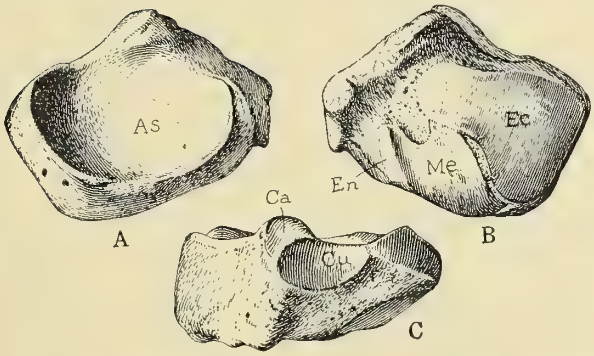

FIG. 116—*Smilodon californicus* Bovard. Right navicular, No. 2036-R-1. A, proximal view; B, distal view; C, external view; × 2/3. Facets for astragalus (*As*), ectocuneiform (*Ec*), mesocuneiform (*Me*), entocuneiform (*En*), calcaneum (*Ca*), and cuboid (*Cu*). Rancho La Brea Pleistocene.

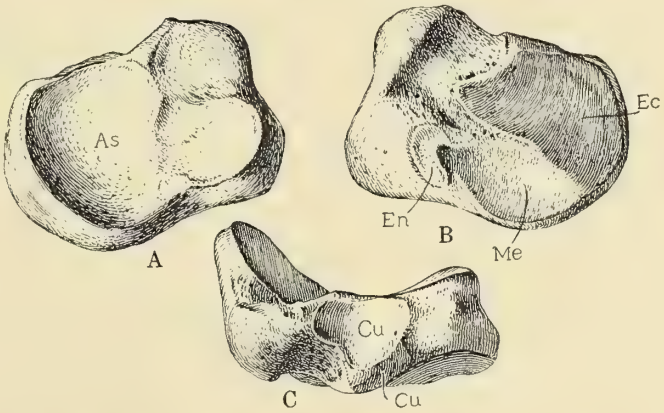

FIG. 117—*Felis atrox* Leidy. Right navicular, No. 2934-R-1. A, B, C, same views as in figure 116; × 2/3. Rancho La Brea Pleistocene.

of the Pleistocene *Felis,* and it projects farther in the former than in the latter. The tuberosity is more fully developed toward the inner side in *Smilodon* than in *F. atrox.* The groove for the peroneus longus muscle, while well defined and broad, is apparently not so deep as in the latter type.

NAVICULAR

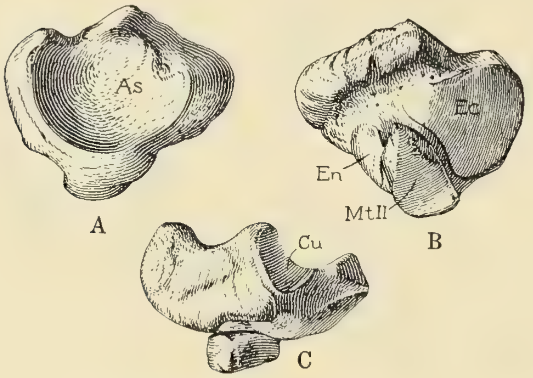

FIG. 118—*Smilodon californicus* Bovard. Fused navicular and mesocuneiform, No. 2033-R-5. A, proximal view; B, distal view; C, external view; × 2/3. Facets for astragalus (*As*), entocuneiform (*En*), metatarsal II (*MtII*), ectocuneiform (*Ec*), and cuboid (*Cu*), Rancho La Brea Pleistocene.

The navicular of *Smilodon* lacks a well-developed plantar-proximal tuberosity, thus differing distinctly from that of *Felis atrox* and of the modern cats (compare figures 116 and 117). While the astragalar surface is perhaps more deeply excavated in the sabre-tooth, the plantar portion of the surface is not carried so far proximally in this form as in the Pleistocene true cat because of the absence of the tuberosity. On the outer side of the navicular there is frequently to be seen a facet for the calcaneum (*Ca*). Occasionally specimens of the sabre-tooth are found in which the facet is absent. It is always absent in *F. atrox* of the asphalt and in the living cats, *F. leo* and *F. tigris.*

The outlines of the facets for the cuneiform bones in *Smilodon* differ from those seen in *F. atrox.* To the plantar side of these articulating surfaces the rugose area for the interosseous ligament is not so extensive in the sabre-tooth as in the true cats. The plantar surface is, however, more extensive in proximo-distal direction in the former than in the latter.

TABLE 78—*Measurements (in millimeters) of navicular*

	Smilodon californicus*			Felis atrox									
	2036-R-1	2036-R-2	2036-R-3	2934-R-1	2934-R-2	2934-R-3	2934-R-4	2934-R-5	2934-R-6	2934-R-7	2934-R-8	2934-R-9	2934-R-10
Dorsoplantar length........	48	43.5	37	52.5	52.7	50.8	47.6	50.8	46.8	49.6	44.9	43.7	43
Transverse diameter.......	37.4	34.1	28.5	38.2	39.6	39.7	39.5	38.8	33.9	37.3	34.6	32.6	33.7

* Selected from a series of 496 individuals.

Specimen No. 2033-R-5 represents a coossification of the navicular and mesocuneiform.

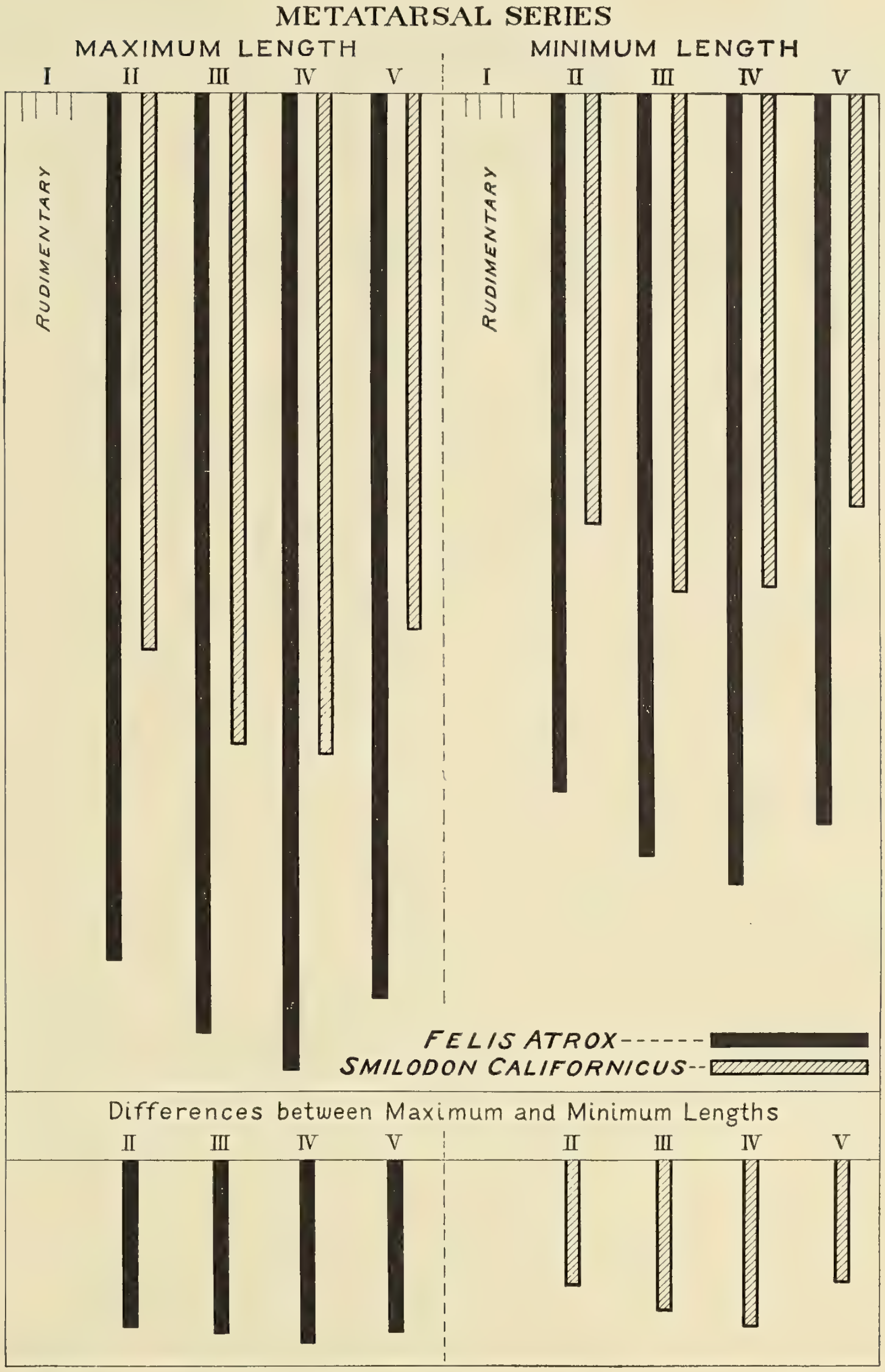

FIG. 119—Diagram showing comparative maximum and minimum lengths of metatarsals and differences between maximum and minimum lengths of these elements in *Felis atrox* Leidy and *Smilodon californicus* Bovard from Rancho La Brea.

METATARSAL SERIES

The diagram (fig. 119) illustrates graphically the comparative lengths of the four metatarsals in *Smilodon californicus* and in *Felis atrox* for specimens of maximum and minimum size in series of adult individuals from Rancho La Brea. The differences in length between longest and shortest specimens of comparable metatarsals in each type of cat are also expressed, furnishing information as to the extent of variation in this particular character in the sabre-tooth and in *F. atrox*. As in the metacarpal series, it should be recalled that the differences are not based on series of comparable size, since the sabre-tooth cat is much better represented in the Rancho La Brea fauna than is *F. atrox*.

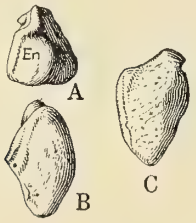

Fig. 120—*Smilodon californicus* Bovard. Right rudimentary metatarsal I, No. 2018-R-1. A, proximal view; B, dorsal view; C, inner view; × 2/3. Facet for entocuneiform (*En*). Rancho La Brea Pleistocene.

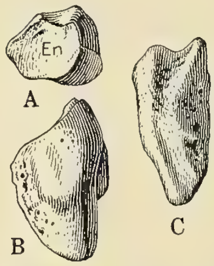

Fig. 121—*Felis atrox* Leidy. Right rudimentary metatarsal I, No. 2916-R-1. A, B, C, same views as in figure 120; × 2/3. Rancho La Brea Pleistocene.

Metatarsals III and IV appear to approach each other more closely in length in the sabre-tooth than in *F. atrox*.

The metatarsals of *Smilodon* are decidedly shorter than those of *F. atrox*, this difference being much greater than the comparable difference between the metacarpals of the two types (compare fig. 88, p. 125).

The metatarsals in articulation give a width to this region of the paw which does not differ noticeably from that in *F. atrox*. The difference here is less than that seen in the metacarpal series. On the other hand, the entire series of hind metapodials emphasizes again the extreme shortening which characterizes this region in *Smilodon*.

Rudimentary Metatarsal I

It is interesting to note that the inner or first metatarsal of *Smilodon* exhibits the same amount of reduction seen in the extinct *Felis atrox* and in the living large cats. The rudiment which remains is approximately half the size of the comparable element in the extinct true cat (compare figures 120 and 121). Viewed from the plantar side, this element is seen to be thicker than that of *F. atrox*. When articulated or fused with the entocuneiform, the rudimentary metatarsal is directed away from and forms a distinct angle with the principal axis of the tarsal bone (see fig. 124).

Metatarsal I is frequently fused with the entocuneiform, less often with metatarsal II.

TABLE 79—*Measurements (in millimeters) of rudimentary metatarsal I*

	Smilodon californicus			Felis atrox		
	2018–R-1	2018–R-2	2018–R-3	2916–R-1	2916–R-2	2916–R-3
Greatest length	22.8	22.5	21.3	31.5	31.4	27.5
Greatest dorso-plantar diameter	13.4	13.7	12.5	18.1	17	17.5
Greatest width of proximal end	14.4	14.8	14.3	15.7	15.1	12.7

METATARSAL II

In the second metapodial of the pes, the proximal facet for the mesocuneiform extends relatively not so far back as in *Felis atrox.* It is also a narrower facet in *Smilodon.* The external facets articulating with the ectocuneiform frequently extend to the proximal end of the element in the sabre-tooth, while in *F. atrox* this is often not the case.

TABLE 80—*Measurements (in millimeters) of metatarsal II of Smilodon californicus*

	Right*			Left†		
	2019–R-1	2019–R-2	2019–R-3	2019–L-1	2019–L-2	2019–L-3
	Max.		*Min.*	*Max.*		*Min.*
Greatest length	95.4	83.7	73.7	96.5	84.6	74.1
Greatest dorsoventral diameter of proximal end	29.4	31	26.2	31.7	28.9	26.6
Greatest transverse diameter of proximal end	16.7	16.4	14.6	17	15.6	14.8
Transverse diameter at middle of shaft	13.8	14.8	13.2	16	13.1	13.4
Dorsoventral diameter at middle of shaft	15.8	15	15	15	14.6	15
Greatest transverse diameter at distal end of shaft	22	22	20.3	23.7	19.9	20.5

* Based on a series of 716 specimens. † Based on a series of 699 specimens.

A second metatarsal of *Smilodontopsis conardi* from the Pleistocene of Conard Fissure, Nebraska, agrees in size and in structure with the corresponding metapodial situated near the mean of the series from Rancho La Brea.

A cast of metatarsal II of *Smilodon neogæus*, No. 11101 Amer. Mus. Nat. Hist. Coll., represents an element slightly shorter but stouter than the largest second metatarsal of *S. californicus* in the series from the asphalt deposits.

In a series of approximately 600 specimens of the second metatarsal of the left side, seven showed fusion with the rudimentary metatarsal I.

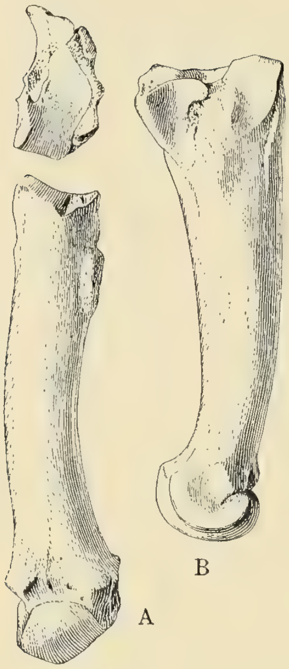

FIG. 122—*Smilodon californicus* Bovard. Right metatarsal II, No. 2019-R-1. A, dorsal view with view of proximal end; B, outer view; × 2/3. Rancho La Brea Pleistocene.

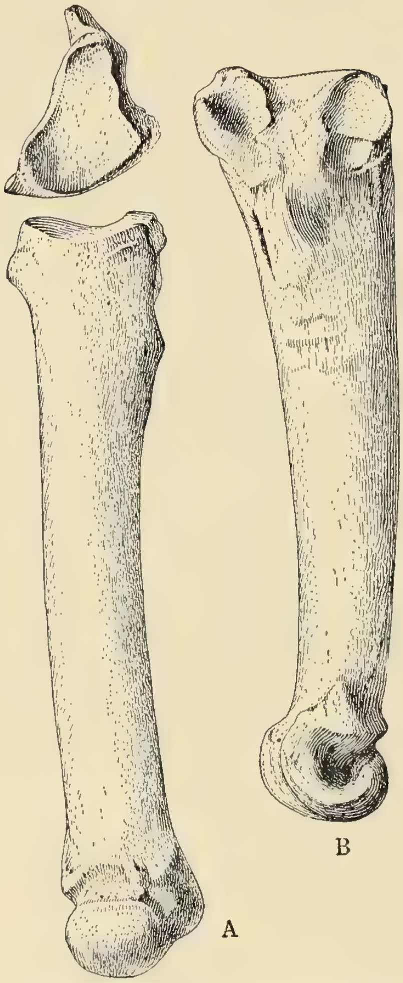

FIG. 123—*Felis atrox* Leidy. Right metatarsal II, No. 2917-R-1. A, B, same views as in figure 122; × 2/3. Rancho La Brea Pleistocene.

TABLE 81—*Measurements (in millimeters) of metatarsal II of Felis atrox*

	Right*			Left†		
	2917–R-1	2917–R-2	2917–R-3	2917–L-1	2917–L-2	2917–L-3
	Max.		*Min.*	*Max.*		*Min.*
Greatest length	148.5	134.9	119.7	147.6	135.3	120.3
Greatest dorsoventral diameter of proximal end, measured across outer face	38	35.8	30.8	37.7	34.3	32.5
Greatest transverse diameter of proximal end	22	20	18.4	21.8	19	18.8
Transverse diameter at middle of shaft	19.4	15.6	16.2	18.8	16.3	15.7
Dorsoventral diameter at middle of shaft	21	18.8	15.9	19.3	20.1	17.4
Transverse diameter at distal end of shaft	27.9	25	23.7	27.8	25.1	23.6

* Based on a series of 36 specimens. † Based on a series of 33 specimens.

METATARSAL III

As indicated by the measurements, the largest specimen of this element of *Smilodon* recorded from Rancho La Brea (a series representing more than 600 individuals) is shorter than that of the smallest adult of *Felis atrox* (more than 30 individuals). It is, however, relatively stouter, although the distal portion of the shaft is thinner dorsoventrally than in the corresponding element of *F. atrox*. The shaft proximal to the middle differs from that of *F. atrox* in being less cylindrical and rudely triangular in cross-section. This character of shaft usually permits the medullary foramen to be seen in ventral view, whereas in *F. atrox* the foramen is usually hidden in this aspect and can be seen best when the metapodial is viewed from the inner side. The rugose tendinal area on the ventral side below the proximal end appears to be more conspicuous in the sabre-tooth and often extends farther down the shaft than in *Felis*. When viewed from the side, the shaft is seen to be slightly more curved in *Smilodon* than in *F. atrox*. The ventral arm of the hammer-shaped facet for the ectocuneiform is shorter. In the sabre-tooth the proximal end of metatarsal III exhibits a greater extent of bone lying ventral to this facet than in *F. atrox*. Frequently the dorsal facet for articulation with metatarsal IV reaches back to the proximal end of the element, and the ventral facet, also for the fourth metatarsal, does not reach the proximal end. In *F. atrox* the situation is reversed for these two surfaces. The border of the median ventral keel of the distal articulation, when viewed from the side, is quite straight. In *F. atrox* the keel usually curves dorsally and the border is convex.

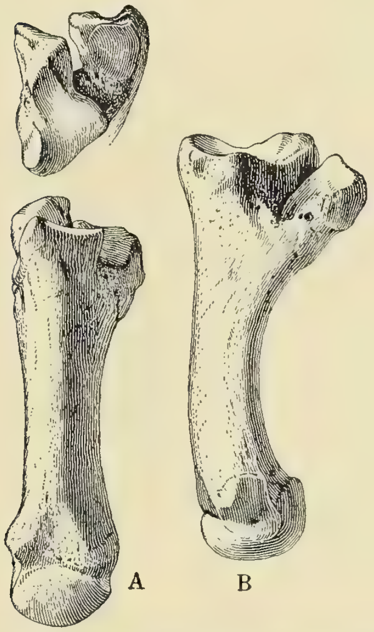

FIG. 124—*Smilodon californicus* Bovard. Specimen showing fusion of right metatarsal II and rudiment of first metatarsal. A, dorsal and proximal views; B, inner view; No. 2019-R-4; × 2/3. Rancho La Brea Pleistocene.

The third metatarsal of *Smilodon neogæus*, No. 11101 Amer. Mus. Nat. Hist. Coll., as represented by a cast, is decidedly larger than the corresponding element of the Californian species selected from near the mean of the series recorded from Rancho La Brea. No. 11101 is not so long as the third metatarsal of maximum size from the asphalt, but is stouter.

In summary, metatarsal III of *Smilodon* differs from that of *Felis atrox*, as follows:

1. Shaft shorter and slightly more curved.
2. Distal portion of shaft thinner dorsoventrally.
3. Ventral arm of hammer-shaped facet for ectocuneiform shorter.
4. Dorsal facet articulating with metatarsal IV reaches back to proximal end; ventral facet articulating with metatarsal IV does not reach proximal end.

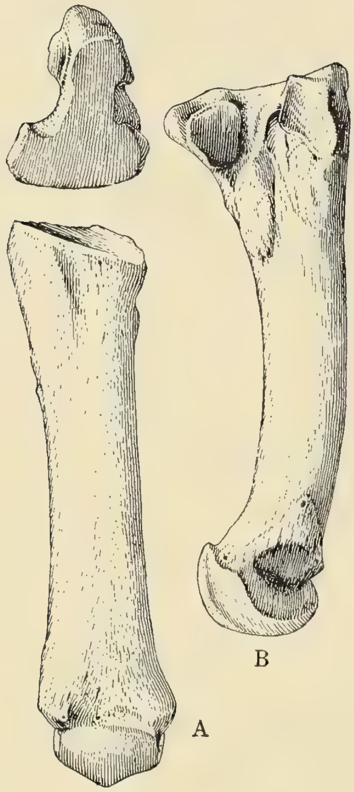

Fig. 125—*Smilodon californicus* Bovard. Right metatarsal III, No. 2020-R-1. A, dorsal view with view of proximal end; B, outer view; × 2/3. Rancho La Brea Pleistocene.

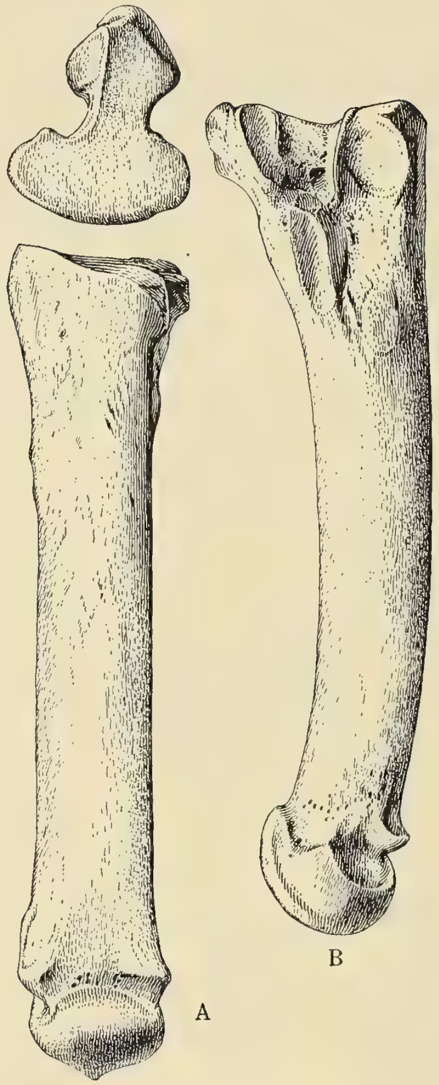

Fig. 126—*Felis atrox* Leidy. Right metatarsal III, No. 2918-R-1. A, B, same views as in figure 125; × 2/3. Rancho La Brea Pleistocene.

Table 82—*Measurements (in millimeters) of metatarsal III of Smilodon californicus*

	Right*			Left†		
	2020–R-1	2020–R-2	2020–R-3	2020–L-1	2020–L-2	2020–L-3
	Max.		*Min.*	*Max.*		*Min.*
Greatest length	111.5	98.9	85.5	112.6	98.8	85.6
Greatest transverse diameter of proximal end	27.1	24.9	25.8	27	27.4	25.6
Greatest dorsoventral diameter of proximal end	36.2	29.8	28.8	36.4	32.2	29.7
Transverse diameter at middle of shaft	17.9	17.3	17.7	18.2	18	15.8
Dorsoventral diameter at middle of shaft	16.3	15.7	15.1	16.4	15.7	12.8
Greatest transverse diameter at distal end of shaft	26.4	23.5	23.8	26.7	25	22.7

* Based on a series of 766 specimens. † Based on a series of 798 specimens.

TABLE 83—*Measurements (in millimeters) of metatarsal III of Felis atrox*

	Right*			Left†		
	2918–R-1	2918–R-2	2918–R-3	2918–L-1	2918–L-2	2918–L-3
	Max.		*Min.*	*Max.*		*Min.*
Greatest length	161	141.3	131.2	163.4	147.3	132.3
Greatest transverse diameter of proximal end	33.2	30.1	26.9	34.2	30.1	28.2
Greatest dorsoventral diameter of proximal end	43	38.6	35.1	42.7	39.2	36.4
Transverse diameter at middle of shaft	23.3	20.4	19.3	23.4	20.5	20.3
Dorsoventral diameter at middle of shaft	20.5	17.4	16.8	20	18.5	18.4
Greatest transverse diameter at distal end of shaft	29.7	25.5	24.3	30	26.8	24.9

* Based on a series of 33 specimens. † Based on a series of 37 specimens.

METATARSAL IV

The shaft is slightly more curved in the lower portion than that in metatarsal IV of *Felis atrox*. When the dorsal face of the proximal third of the metapodial is held in horizontal position the lower third of the element is directed noticeably less inward than in the Pleistocene true cat (compare figures 127 and 128). The more forwardly directed surface for the first phalanx reflects perhaps a greater spread of the toes with an increase in clawing power than in *F. atrox*. The medullary foramen is frequently on the ventral side of the proximal third of the shaft, while in *F. atrox* this foramen is often seen when the metatarsal is viewed from the inner side. The proximal articulating surface for the cuboid is relatively and absolutely less extensive than in the latter. This facet is narrower posteriorly and is more strongly convex in *Smilodon* than in *F. atrox*. In the sabre-tooth the ventral tuberosity extends a considerable distance behind the ventral margin of the cuboid facet. The dorsal facet articulating with metatarsal V may be a simple oval or elliptical surface, while the ventral facet is frequently set off from the base of the ventral tuberosity and rests on a distinct pedicel. On the inner side of the proximal end the ventral facet for metatarsal III is situated relatively farther distally with reference to the dorsal facet than that of the large extinct *Felis*.

TABLE 84—*Measurements (in millimeters) of metatarsal IV of Smilodon californicus*

	Right*			Left†		
	2021–R-1	2021–R-2	2021–R-3	2021–L-1	2021–L-2	2021–L-3
	Max.		*Min.*	*Max.*		*Min.*
Greatest length	113.3	98.9	84.6	113.8	99.1	83.6
Greatest transverse diameter of proximal end	18.6	17.5	16.3	19.9	16.5	16.1
Greatest dorsoventral diameter of proximal end	30.9	26.3	25.8	30	26.4	25.8
Transverse diameter at middle of shaft	16	15.1	13	17	16.3	13.4
Dorsoventral diameter at middle of shaft	17	14.6	13.8	14.9	13.4	13
Greatest transverse diameter at distal end of shaft	25.2	21.9	19	22.3	22	18.5

* Based on a series of 748 specimens. † Based on a series of 462 specimens.

TABLE 85—*Measurements (in millimeters) of metatarsal IV of Felis atrox*

	Right*			Left†		
	2919–R-1	2919–R-2	2919–R-3	2919–L-1	2919–L-2	2919–L-3
	Max.		*Min.*	*Max.*		*Min.*
Greatest length	167.3	154.3	135.8	166.9	152.1	135.1
Greatest transverse diameter of proximal end	23	22.9	18.7	25.8	22.9	20.6
Greatest dorsoventral diameter of proximal end	35	34	28.7	33.4	32.4	28.8
Transverse diameter at middle of shaft	19.7	17.8	17	20.4	19.2	17.4
Dorsoventral diameter at middle of shaft	21.6	20.3	17.2	21.3	19.5	18.8
Greatest transverse diameter at distal end of shaft	26.6	25.1	22.8	27.7	25.1	21.7

* Based on a series of 30 specimens. † Based on a series of 35 specimens.

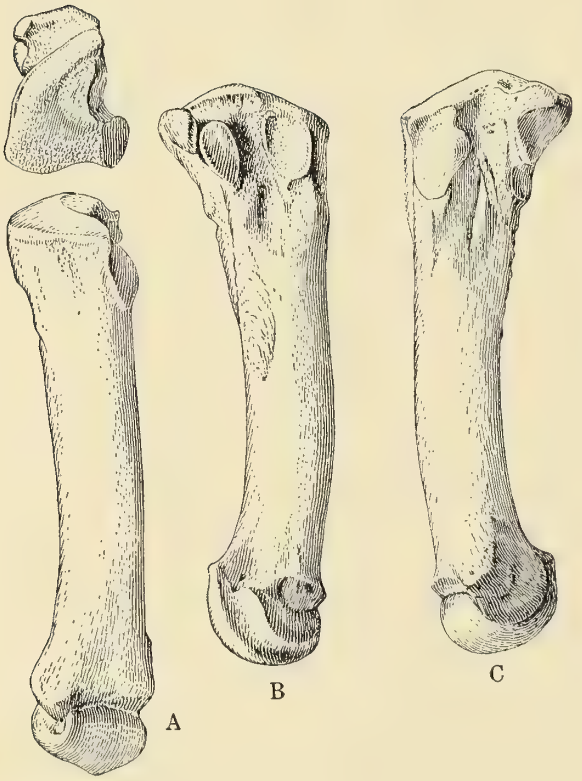

FIG. 127—*Smilodon californicus* Bovard. Right metatarsal IV, No. 2021-R-1. A, dorsal view with view of proximal end; B, outer view; C, inner view; × 2/3. Rancho La Brea Pleistocene.

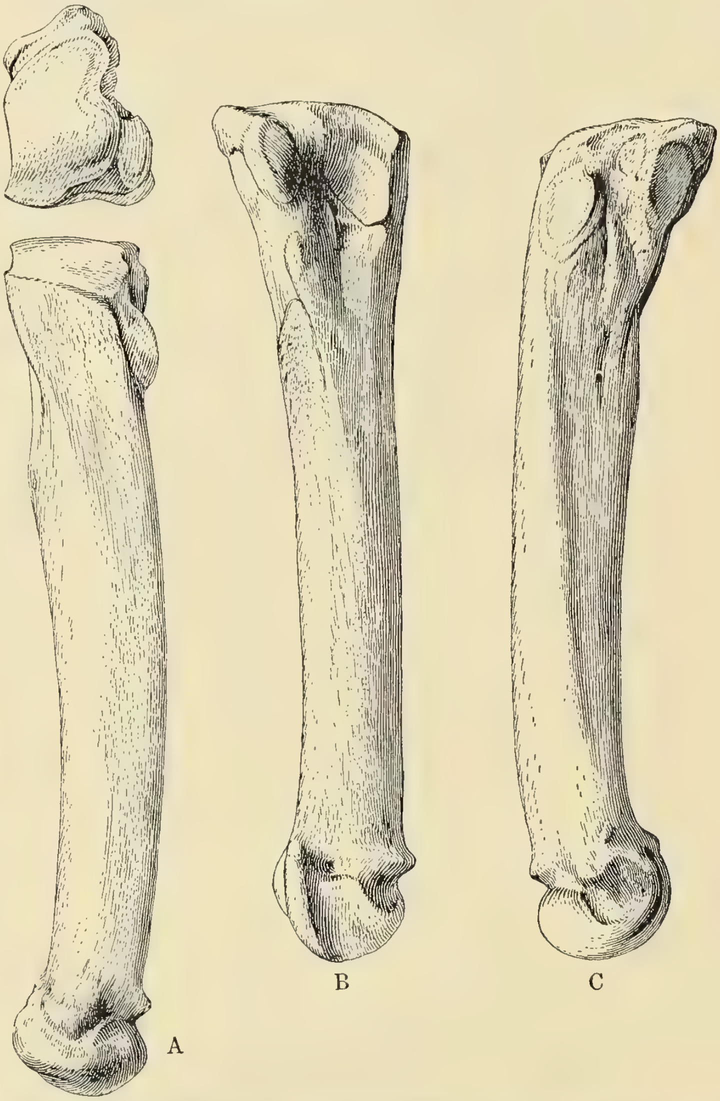

FIG. 128—*Felis atrox* Leidy. Right metatarsal IV, No. 2919-R-1. A, B, C, same views as in figure 127; × 2/3. Rancho La Brea Pleistocene.

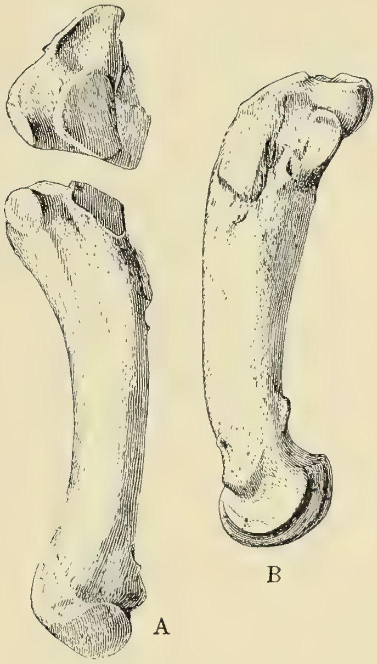

FIG. 129—*Smilodon californicus* Bovard. Right metatarsal V, No. 2022-R-1. A, dorsal view with view of proximal end; B, inner view; × 2/3. Rancho La Brea Pleistocene

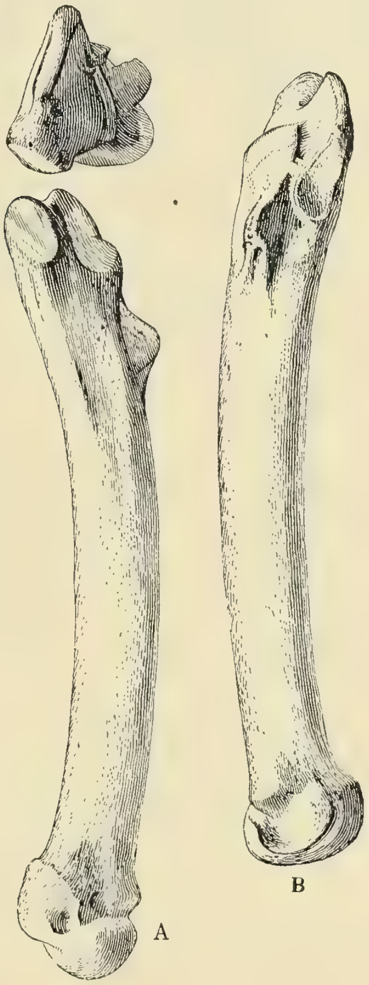

FIG. 130—*Felis atrox* Leidy. Right metatarsal V, No. 2920-R-1. A, B, same views as in figure 129; × 2/3. Rancho La Brea Pleistocene.

METATARSAL V

The fifth metatarsal of *Smilodon* differs from that of *Felis atrox* in the following characters:

1. Stoutness of shaft and proximal extremity.
2. More angulate cross-section of shaft below proximal extremity.
3. Presence of well-defined tendinal scar below ventral facet for metatarsal IV. This is situated on border separating ventral and inner sides.

4. Absence of wing-like proximal process, which in *F. atrox* extends noticeably beyond the articulating surface for cuboid.
5. Outer posterior surface of proximal extremity frequently notched in middle.
6. Frequent larger size of facet for cuboid.
7. Dorsal facet articulating with metatarsal IV relatively smaller and notch between this facet and that for cuboid not sharp.
8. Relatively wider separation of the two facets articulating with metatarsal IV.

TABLE 86—*Measurements (in millimeters) of metatarsal V of Smilodon californicus*

	Right*			Left†		
	2022–R-1	2022–R-2	2022–R-3	2022–L-1	2022–L-2	2022–L-3
	Max.		*Min.*	*Max.*		*Min.*
Greatest length	91.9	80.6	70.8	94.8	84	72.7
Greatest dorsoventral diameter of proximal end	28.6	27.2	24.4	28.2	26.6	24.9
Transverse diameter at middle of shaft	13.6	12	10.5	13.5	11.1	13.8
Dorsoventral diameter at middle of shaft	16	16.3	12.1	14.9	14.7	13.9
Greatest transverse diameter at distal end of shaft	21.2	19.3	17.1	21.6	18.5	19

* Based on a series of 722 specimens. † Based on a series of 677 specimens.

TABLE 87—*Measurements (in millimeters) of metatarsal V of Felis atrox*

	Right*			Left†		
	2920–R-1	2920–R-2	2920–R-3	2920–L-1	2920–L-2	2920–L-3
	Max.		*Min.*	*Max.*		*Min.*
Greatest length	155	136.6	125.4	153.3	137.1	123.6
Greatest dorsoventral diameter of proximal end	27.7	22.6	23.7	31.6	24.7	23.3
Transverse diameter at middle of shaft	14.9	13.3	12.1	16.6	13.7	13
Dorsoventral diameter at middle of shaft	15	13.3	12.7	15.8	13.7	13
Greatest transverse diameter at distal end of shaft	23.7	21.6	20	25.7	22.4	20.2

* Based on a series of 23 specimens. † Based on a series of 36 specimens.

PHALANGES

An extremely large number of phalangeal elements occur in the collection, but because of the scattered distribution of this material in the asphaltic mass it has been found impossible at present to bring together in their proper position all of the segments of the digits belonging to the manus and pes. Moreover, it is not always possible, because of range of variation, to distinguish with certainty between the sabre-tooth and *Felis atrox* on the basis of the structural characters of particular segments.

In general, there is considerable resemblance between the phalanges of *Smilodon* and those of the large true felines. The first and second segments may be shorter in the former than in *F. atrox*, but there is evidently considerable range in size. In the first segment the proximal and distal ends are relatively heavy and the tendonal scar on each ventrolateral border of the shaft is well marked. The proximal articulation may be quite broad in dorsoventral direction, perhaps more so than in *F. atrox*. The distal end may be somewhat more compressed in this direction than in the latter.

In the second phalanx the shaft is short and stout. The transverse axis of the proximal extremity is oblique to the fore and aft axis of the segment in *Smilodon*, whereas in *Felis atrox* these two axes tend to form a right angle (see fig. 131 B and C). Because of this difference the lateral projection of the distal extremity appears to be more pronounced in the latter species than in the sabre-tooth. The position of the distal end with reference to the principal axis of the shaft appears to imply a foot with more spreading toes than in the true felines.

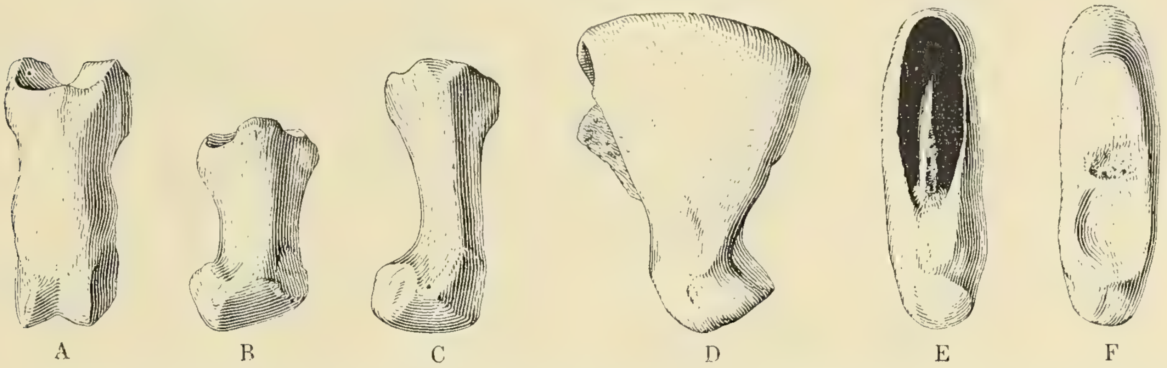

Fig. 131—*Smilodon californicus* Bovard: A, phalanx I, dorsal view; B, phalanx II, dorsal view; D, E, F, phalanx III, lateral, anterior and posterior views; × 2/3. *Felis atrox* Leidy: C, phalanx II, dorsal view; × 2/3. Rancho La Brea Pleistocene.

The ungual phalanges are sturdily built with the bony core of the claw encompassed by a strongly developed hood. Viewed from the side these elements have a triangular shape with upper border slightly convex. The posterior face of the hood is broad and flattened with a slight indentation of the surface above the articulation for the second phalanx. Subungual foramina are present.

SMILODON CALIFORNICUS BREVIPES, N. VAR

The presence at Rancho La Brea of a sabre-tooth cat with shortened feet is indicated by the occurrence in the Los Angeles Museum collection of several metapodials whose length falls distinctly below the minimum length of the comparable elements of *Smilodon californicus*. Presumably further remains of this type will be identified in the collection when segregation of the materials is completed. The presence of more than one individual possessing the shortened metapodials is suggested by the fact that at least four specimens having this character are known, the specimens coming from different excavations at Rancho La Brea. Thus the characters assigned to *S. californicus brevipes* are apparently not restricted to a single type, but are shared by several individuals, although the total number of sabre-tooth

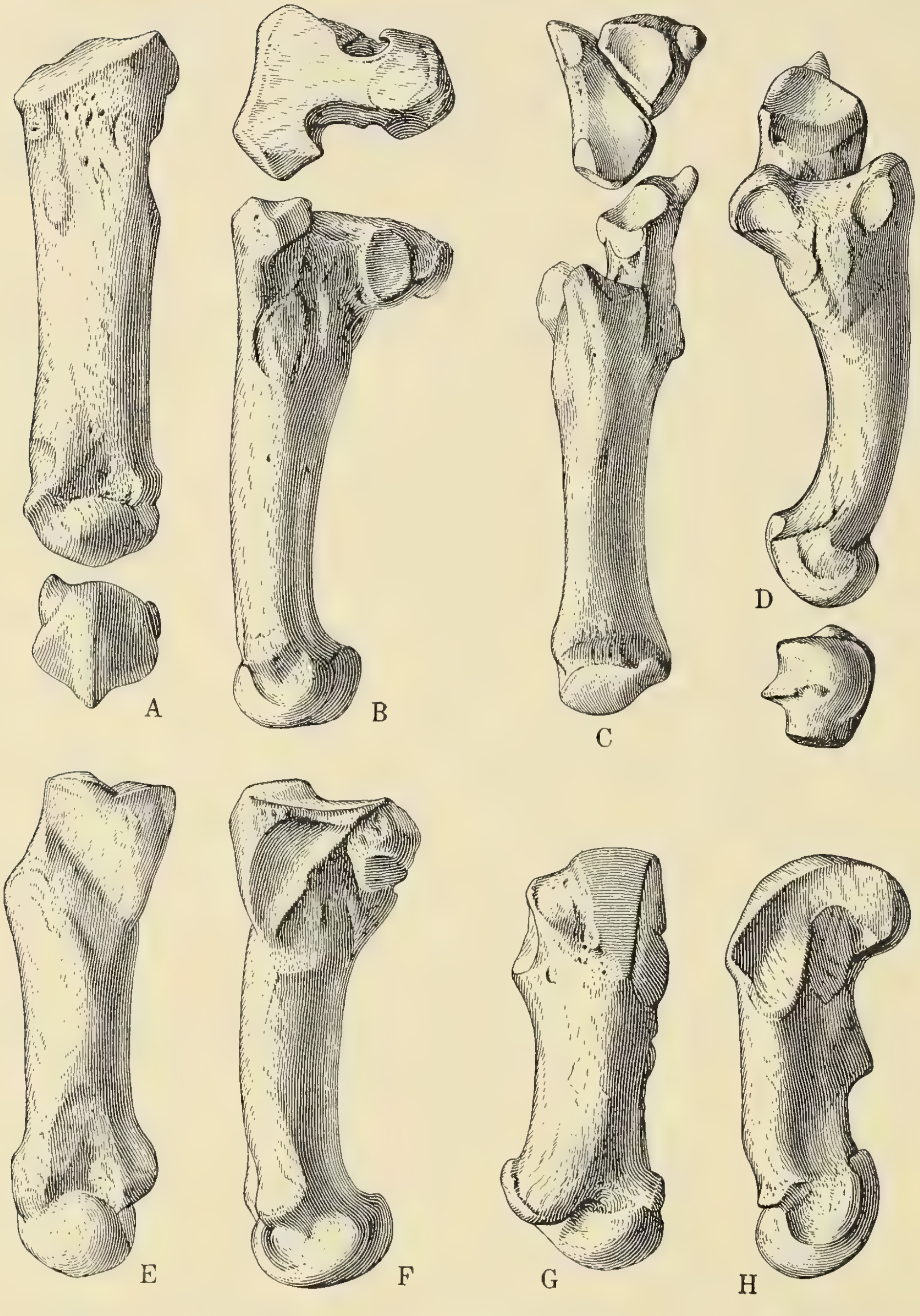

Fig. 132—*Smilodon californicus brevipes,* n. var. Metapodials; × 1. A, B, type specimen, metatarsal III, No. 2070-L-1; A, dorsal and distal views; B, outer and proximal views. C, D, referred specimen, metatarsal II and fused rudimentary metatarsal I and entocuneiform, No. 2069-R-1; C, dorsal and proximal views; D, outer and distal views. E, F, referred specimen, metacarpal II, No. 2071-L-1; E, dorsal view; F, outer view. G, H, referred specimen, metacarpal V, No. 2072-R-1. G, dorsal view; H, inner view. Rancho La Brea Pleistocene.

cats having the peculiarity of a shortened metapodial region is extremely small in contrast to those forms falling within the normal range of variation of *Smilodon californicus.* The specimens belong to adult forms.

Type specimen—A third metatarsal, No. 2070-L-1, Los Angeles Museum Collection. Rancho La Brea Pleistocene (figs. 132 A and B).

Referred specimens—A second and a fifth metacarpal, No. 2071-L-1 and No. 2072-R-1 respectively, and a second metatarsal, No. 2069-R-1, Los Angeles Museum Collection. Rancho La Brea Pleistocene (figs. 132, C to H).

Given the maximum and minimum lengths of the comparable metapodials in *Smilodon californicus* each as 100, the following values are obtained for the specimens referred to *S. californicus brevipes:*

	Max.	Min.
Metacarpal II	63.9	87.9
Metacarpal V	64.9	87.8
Metatarsal II	61.8	81
Metatarsal III (type specimen)	61.8	81.3

In other words, the type and referred metapodials of this subspecies show approximately the same degree of shortening when comparisons are made with the corresponding elements, representing the maximum and minimum sizes among adult individuals of the typical form, *S. californicus.*

TABLE 88—*Measurements (in millimeters) of metapodials*

	Metac. II	Metac. V	Metat. II	Metat. III
	2071–L-1	2072–R-1	2069–R-1	2070–L-1
Greatest length	67.2	55.2	60.3	69.6
Greatest transverse diameter of proximal end	17.3	20.4	[a]12.2	22.5
Greatest dorsoventral diameter of proximal end	25.2	24.3	23.6	28.3
Transverse diameter at middle of shaft	14	14.1	10.6	14.7
Dorsoventral diameter at middle of shaft	12.6	11.9	10.7	11.9
Greatest transverse diameter at distal end of shaft	19.8	21.7	16.3	18.8

a, Approximate.

Metatarsal III (figs. 132 A and B) exhibits for the most part the structural features seen in *Smilodon.* It differs from *Felis* and resembles the sabre-tooth in shape of the proximal end and in outline of articulating surface for the ectocuneiform. On the outer side of the proximal extremity the dorsal facet for metatarsal IV is separated from the proximal surface by a distinct facet (for cuboid) which is apparently much better developed in this form than in typical specimens of *Smilodon* from Rancho La Brea. In dorsal view, the shaft does not show the slight widening toward the distal end seen in *S. californicus.* The shape and size of the plantar keel of the distal end is more like that in *Smilodon* than like that in *Felis.* Aside from the shorter length and the structural differences which have been noted the proportions of this element compare favorably with those of the specimen of minimum size belonging to *S. californicus* (compare measurements).

The second metatarsal (figs. 132 C and D) is fused with the rudiment of the first metatarsal to which is also joined the entocuneiform.

Metacarpal II and metacarpal V, referred to *S. californicus brevipes*, are shown in figures 132 E to H.

The characters distinguishing the second metacarpal of *Smilodon* from that of *Felis* are all clearly shown in specimen 2070-L-1. No noticeable differences, aside from the shorter length, exist between this specimen and the shortest second metacarpal of the series belonging to *Smilodon californicus*.

The fifth metacarpal is relatively heavy but resembles *S. californicus* in those characters which distinguish this form from *Felis*. A distinct tuberosity is present on the inner palmar border of the shaft and midway between the proximal and distal ends.

FELIS ATROX LEIDY

Felis atrox Leidy. Trans. Amer. Philos. Soc., n.s., vol. 10, p. 319, 1853.
Felis imperialis Leidy. Proc. Acad. Nat. Sci. Phila., p. 259, 1873.
Felis imperialis, Matthew, W. D. Bull. Amer. Mus. Nat. Hist., vol. 16, p. 321, 1902.
Felis sp. indet., Bovard, J. F. Univ. Calif. Pub. Bull. Dept. Geol., vol. 5, p. 163, 1907.
Felis atrox bebbi Merriam. Univ. Calif. Pub. Bull. Dept. Geol., vol. 5, p. 301, 1909.
Felis atrox, Freudenberg, W. Geol. u. Palæ. Abh., n.f., Bd. 9, p. 31, 1910.
Felis imperialis, Freudenberg, W. Ibid, p. 33, 1910.
Felis atrox, Merriam, J. C. Univ. Calif. Pub. Bull. Dept. Geol., vol. 10, pp. 517, 520, 1918.
Felis atrox, Merriam, J. C., and Stock, C. Science, n. s., vol. 54, p. 567, 1921.
Neoleon atrox, Kretzoi, N. Mag. Kir. Földt. Int. Haziny. Budapest, V. 24, 1929[1]

The fauna of Rancho La Brea contains a group of gigantic felines which seem distinct from the other large cats of the world and are apparently more closely related to *Felis atrox*, the great lion described by Leidy from Natchez, Mississippi, than they are to any other forms. They include the enormous form described by Merriam (1909) as *Felis atrox bebbi* and a number of specimens representing a much smaller type which is indistinguishable from *Felis imperialis* Leidy. There are considerable differences among the individuals included in this group, especially in point of size, but there is also a noteworthy similarity in nearly all of the characters in which they differ from other forms. The community of characters shown seems to indicate pretty distinctly that these individuals form a natural group, and if the subdivisions were to be recognized as species the including division would be of generic or subgeneric rank. Inasmuch as size appears to be the most important distinguishing feature, it has seemed to the writers advisable to consider all the forms as of one species.

Taking the characters of all the forms available, the following diagnosis may serve for the group included in *Felis atrox*.

Muzzle very wide compared with the length of the skull. Nasals short, never extending distinctly behind the frontal processes of the maxillaries posteriorly. Fronto-nasal region relatively flat. Superior diamond-shaped area of the frontal longer anteroposteriorly than in the lion. Brain-case small, fronto-parietal suture nearly straight, as in the African lion. Anterior spine of ectotympanic region of auditory bulla extending much farther forward than entotympanic portion.

Coronoid process of mandible high, wide, situated near medial end of and generally projecting backward beyond the condyle. Masseteric fossa very deep and showing a marked excavation as far forward as the middle of the inferior carnassial. Anterior outline of symphyseal region generally more nearly normal to the inferior line of the mandible than in the lion or tiger. Angle produced inferiorly somewhat farther than in the lion.

---

[1] This paper unfortunately has not been available to the writers.

Infra-orbital foramen oval. Condylar foramen tending to be separated from the foramen lacerum posterius.

Canines large, and the incisors small or set in a relatively narrow space. $\mathrm{I}\overline{3}$ with a very small lateral tubercle. Principal cusp of $\mathrm{P}\overline{3}$ and $\mathrm{P}\overline{4}$ nearly triangular in horizontal cross-section. $\mathrm{P}\underline{3}$ occasionally with third or inner root. Superior carnassial with prominent antero-internal root but without a distinctly separated protocone. $\mathrm{M}\underline{1}$ two-rooted or with a divided root. Anterior border of paraconid blade of $\mathrm{M}\overline{1}$ sloping backward more than in lion or tiger.

This group interpreted in the broad sense in which it is used here includes the following forms:

F. atrox Leidy. Type specimen, Natchez, Mississippi.
F. imperialis Leidy. Type specimen, Livermore Valley, California.
F. imperialis, Matthew, W. D. Washtuckna Lake, Washington.
F. sp. indet., Bovard, J. F. Potter Creek Cave, California.
F. atrox bebbi Merriam. Type specimen, Rancho La Brea, California.
F. atrox, Freudenberg, W. Mexican Plateau.
F. imperialis, Freudenberg, W. Mexican Plateau.
F. atrox, Merriam, J. C. Astor Pass, Nevada.
F. atrox, Merriam, J. C., and Stock, C. McKittrick, California.

All the forms included in the above list have been considered as Pleistocene, both from the nature of their occurrence and from the character of the fauna associated with them.

STATUS OF LEIDY'S SPECIES FELIS IMPERIALIS

The type of Leidy's species *Felis imperialis* (Leidy, 1873A, p. 259) was obtained by Dr. Lorenzo G. Yates in a gravel deposit at Livermore Valley, California. Bovard (1907, p. 164) records the locality as occurring 25 miles east of San Leandro, California. In the same beds there were also obtained remains of *Bison latifrons*, *Auchenia hesterna (Camelops hesternus)*, *Elephas*, *Equus* and *Canis indianensis (Ænocyon dirus)*. Several of these mammals are now known also from Rancho La Brea. This collection taken as a whole indicates the Quaternary age of the deposit. There is, however, no definite statement as to how closely the specimens represented in the collection were associated.

The type specimen consisted of an upper jaw fragment containing $\mathrm{P}\underline{3}$ and showing the alveoli of $\mathrm{P}\underline{2}$ and the canine. Leidy suggested that *F. imperialis* might be found to represent a young individual of the *F. atrox* type. While this material represents a cat of distinctly smaller size than that on which the type of *Felis atrox bebbi* was based by Merriam (1909), additional specimens now available from Rancho La Brea include individuals that resemble closely in size as well as in structure the type of *F. imperialis*. As will be seen from the description and measurements given below, there are apparently no noteworthy structural characters distinguishing the small forms from the larger cats in the series of skulls now known from the asphalt beds. In nearly all the points in which skulls of the small forms differ from other cats they resemble the *F. atrox bebbi* type, so that there are a considerable number of common characteristics. In character of size it becomes evident that within the series a number of specimens bridge the gap between the smallest and largest skulls. In this connection it may be noted that, particularly in the asphalt collections, great variation in size is to be expected, as the asphalt victims are presumed to include in their number the inexperienced young with the infirm aged, so that extremes of size might well occur.

The small skulls, in contrast to those of larger size may show larger auditory bullæ, wider occiput, and less prominent anterior angle to the symphyseal region. Size of auditory bullæ and form of the occiput are characters which change greatly with age and sex, while the antero-inferior angle of the symphysis is also subject to considerable variation. Several of the small skulls are obviously of young individuals with entirely unworn teeth and open cranial sutures.

Several specimens of very large cats described by Freudenberg (1910) from Pleistocene deposits of the Mexican Plateau are closely similar to the forms from Rancho La Brea and show the same variation in size. A portion of a skull (Freudenberg, No. 163), including the premaxillary and a part of the maxillary and showing the form of the alveoli for the insertion of the canine and premolars two and three, represents a very large animal evidently to be included in *F. atrox.* In the cross-section of the alveolus for the superior canine, this specimen is slightly larger than Univ. Calif. specimen 18598 of the smaller or *imperialis* group from Rancho La Brea, and in the anteroposterior diameter of $P\underline{3}$ it is at least as large as that specimen. It therefore partly bridges the gap between the *F. atrox bebbi* form and the *F. imperialis* form.

A much smaller specimen (Freudenberg No. 23) consisting of premaxillary, maxillary, jugal and the greater part of the upper dentition, is near the size of the type of *F. imperialis*, and is almost identical in dimensions with smaller specimens obtained at Rancho La Brea. Freudenberg refers this specimen to *F. imperialis*, and it would evidently be included with *imperialis*, whatever rank that form may have.

A somewhat similar example may be cited from the McKittrick deposits along the western border of the San Joaquin plain in California. Early in the study of the McKittrick collection the presence of *F. atrox* was recognized on the basis of fragmentary skull remains. Additional collections at this locality include two fairly complete skulls of large cats. The larger skull, Calif. Inst. Tech. No. 648, compares favorably in size with the larger skulls of *F. atrox* from Rancho La Brea. The second specimen, Calif. Inst. Tech. No. 649, is smaller but still possesses a size greater than that of the smaller skulls of the *imperialis* group from Rancho La Brea.

The fact that in the large cats of the *F. atrox* type, variation in size without marked deviation in structure is noted at such widely separated localities as Rancho La Brea, the Mexican Plateau, and possibly McKittrick would seem to indicate that the variation was sexual and individual rather than specific. The same individual and sexual variation might presumably be expressed wherever a given species is found, however wide its geographic distribution may be; while the occurrence of two very closely related species in the same place is uncommon, as geographic separation is certainly one of the most important factors in the development of new species of mammals, even if it be not concerned in their origin. The association of two closely related species over as wide an area as that extending from California to the Mexican Plateau seems highly improbable. If existing within the same period, two closely related forms will generally be found in different places, or if occurring in the same place they will belong to different periods.

Taking all of the circumstances into consideration there appear substantial reasons for regarding specimens which have been referred to *F. imperialis* as representing young individuals, or possibly young females of the *F. atrox* type.

COMPARISON WITH TYPE SPECIMEN OF FELIS ATROX

Through the courtesy of Witmer Stone of the Academy of Natural Sciences of Philadelphia, it has been our privilege to examine the type specimen of *Felis atrox* and to compare it with specimens of the large felines of Rancho La Brea.

The type specimen of *F. atrox*, No. 12546 Phila. Acad. Nat. Sci., as figured by Leidy and as preserved at the present time in the Museum of the Philadelphia Academy consists of the anterior half of a mandible enclosed in a very hard concretionary layer which is nearly 8 mm. thick over the masseteric fossa. It is thicker than 8 mm. at some points and thinner than this measurement at other points. The bone is exposed only at the posterior end of the specimen and around the alveolus for the canine. The outlines of the specimen as represented in Leidy's illustration which accompanied the original description are entirely the outlines of the enclosing concretion. The bony material of the jaw is very imperfectly preserved and badly rotted.

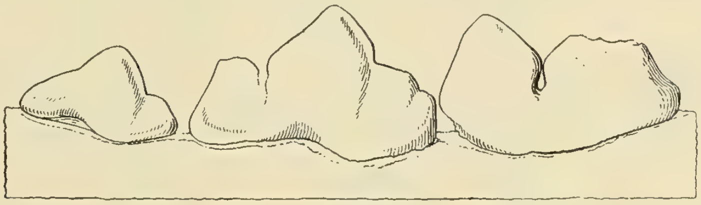

Fig. 133—*Felis atrox* Leidy. Type specimen, No. 12546, Phila. Acad. Nat. Sci. Coll.; outline of lower cheek-teeth $P\overline{3}$-$M\overline{1}$; × 1. Pleistocene, Natchez, Mississippi.

The portion of the jaw present does not show the form of the mandible with certainty, but there seems reason to believe that it gives approximately the outline of the anterior region. The antero-inferior margin appears to be slightly less angulate than in specimens from the asphalt. The convexity of the inferior border representing the ramal process is largely matrix but there may have been a small inferior prominence. In the masseteric region there is evidence of a moderately deep fossa. The ridge of bone to be seen immediately above the lower side of the masseteric fossa may represent the bony plate on the outer side of the inferior dental foramen.

The dentition is represented by the canine and the cheek-teeth. A considerable part of the canine is broken away and the lower carnassial has lost the tip of the protoconid. The cheek-teeth fortunately project through the concretion and are most satisfactorily exposed for study. In comparing the type specimen with material from Rancho La Brea it is possible to obtain a very clear idea as to the form of the teeth, although the transverse diameters of the cheek-teeth can not be obtained. The following comparisons (fig. 133) may be noted:

$P\overline{3}$ possesses approximately the form and dimensions shown in specimens from Rancho La Brea as nearly as can be determined by examination of the type. An anterior basal tubercle is absent. Instead a sharp ridge runs from the anterior side of the principal cusp to the anterior margin of the tooth. While an anterior basal tubercle is present on P$\overline{3}$ in most of the jaws of *Felis atrox* available from the asphalt, this cuspule may be absent in some specimens.

P$\overline{4}$ of the type specimen shows anterior and posterior basal tubercles of nearly equal size, but the posterior tubercle is divided in the posterior half by a shallow but distinct notch separating the posterior basal cusp from a posterior basal tubercle. The anterior tubercle seems to have its blade a little longer anteroposteriorly and relatively narrower than in Rancho La Brea forms. The shape of this tooth does not differ greatly from that in Univ. Calif. specimen 20049 from Rancho La Brea in the proportions of the anterior and posterior cusps, but in the type specimen the tooth is less worn and the subsidiary anterior and posterior cusps are somewhat higher. Compared with specimen 20049 the type seems to show the posterior cusps to have a wider base and this coupled with their height gives a slightly different form to the tooth.

M$\overline{1}$ is unfortunately not fully exposed so that the width of the tooth in the type can not be satisfactorily determined. The general outlines of the tooth are similar to those in No. 20049 with the exception that the posterior end of this tooth exhibits practically no prominence of the cingulum.

The portion of the mandible present in the type specimen No. 12546 extends from the anterior end of the jaw to the middle of the masseteric fossa. The portion present is insufficient to indicate more than that the masseteric fossa is deep and that the inferior border of the mandible below this fossa is possibly not so widely extended as in the larger specimens of *Felis atrox* from Rancho La Brea.

SKULL

The collection of crania of *Felis atrox* in the Los Angeles Museum represents a series of 16 good skulls and an additional number of incomplete specimens. The crania fall into two groups, which may be characterized as the large and the small forms. There are clearly 9 skulls which may be referred to the class of large individuals and 6 or 7 representing the small individuals. The differences in size are indicated in the table of measurements (table 89). It is interesting to note that the measurements reveal a more or less uniform increase in size from the smallest to the largest type. The type of *F. atrox bebbi* (Univ. Calif. No. 14001) exceeds in length the largest specimen (No. 2900–3) in the Los Angeles Museum collection, but its larger size is not maintained throughout the series of measurements.

The large skulls may be divided into two types, one represented by L. A. Mus. No. 2900–9, an individual of middle age with the sutures well closed and dentition very moderately worn. In this skull the zygomatic arches are very broad, the sagittal crest is nearly straight and is relatively high. The same characters are seen in the very large skull, No. 2900–3. In a number of other specimens, which represent uniformly rather young individuals, as for example L. A. Mus. No. 2900–10, the sutures are open, dentition very little worn, the sagittal crest less prominent and the zygomatic arches are somewhat narrower. In a large specimen, L. A. Mus. No. 2900–11, with moderately worn dentition and closed sutures the zygomatic arches are apparently a little less extended than in No. 2900–9 and are wider than in the somewhat younger specimens, as No. 2900–10.

In the smaller skulls some individuals, as L. A. Mus. No. 2900–4, show closed sutures, moderately worn dentition and rather wide arches. In other individuals the width seems to be relatively somewhat less.

The question arises as to the relation of these two groups to each other. It is possible that they represent two species corresponding to *Felis atrox* and *F. imperialis*, but there seem good reasons to believe that the difference between the most extreme types of the large skulls is not in any sense comparable to the difference between male and female skulls in large cats of the lion type. If the large forms do represent a distinct species, the individuals with wide zygomatic arches would presumably be males and those with narrow arches females. In the group of smaller skulls there is perhaps somewhat greater difference between the individuals. This may be due in part to the fact that the group of small skulls includes young individuals of the males, as well as adult females. The difference between the groups of larger and smaller skulls is not materially different from that between males and females of the living African lion.

In all of the skulls of *Felis atrox*, both large and small, from Rancho La Brea, the superior outlines of the cranium are approximately intermediate between those of *Felis leo* and *Felis tigris.* The fronto-nasal region is generally flatter anteroposteriorly than in the tiger. It may be as flat as in the lion, as is true especially of skull, L. A. Mus. 2900–9. This is true also of a very small skull, L. A. Mus. No. 2900–4. The postero-superior contours of the cranium form a sharper angle with the fronto-nasal contour than in *F. leo*, and in this respect approach more nearly the form in the tiger. The superior anteroposterior contour of the cranium may approach quite closely to the form seen in the tiger. There seems to be no great difference in this respect between the large and small skulls, although there is perhaps a tendency for the large skulls to be flatter above and for the small skulls to be more convex above.

The superior face of the frontal region is usually nearly flat, but it may show a distinct median depression. The transverse contour of this region in some respects approaches that of the tiger, at least as closely as it approaches the lion, as the postorbital processes drop laterally rather more than in the lion.

The width of the skull across the zygomatic arches seems to vary considerably, even among the large skulls. In No. 2900–9, a large skull with basal length of 359.4 mm., the arches are very wide (296.5 mm.). In L. A. Mus. No. 2900–12, a large skull with basal length of 346.3 mm., the width across the zygomatic arches is 247.6 mm. In the large skull, No. 2900–9, the upper carnassial is smaller than that in No. 2900–12. In No. 2900–9 the anteroposterior diameter of $P\underline{4}$ is 39.5 mm. and in No. 2900–12 the anteroposterior diameter of $P\underline{4}$ is 42.2 mm. In No. 2900–9 the sagittal crest is high and full, in No. 2900–12 it is low and concave. In No. 2900–9 the frontal region is quite flat superiorly and shows a slight median depression. In No. 2900–12 the frontal region is convex and without median depression. No. 2900–9 represents a much older animal than No. 2900–12, the sutures being generally closed and the teeth well worn, while in No. 2900–12 the sutures are open and the teeth show a little less wear.

In all specimens, both large and small, the posterior ends of the nasal bones are relatively much wider than in the Recent lion, and in this respect approach the type of nasals seen in the tiger. On the other hand, the posterior ends of the nasal elements resemble the lion in that they do not extend posteriorly as far as the upper end of the frontal processes of the maxillary. The latter processes are truncated anteroposteriorly at the upper end, somewhat as in the modern lion, and the nasal processes of the frontal bone are wide, somewhat as in this type. In the modern tiger the frontal processes of the maxillaries are not truncated and the anterior processes of the frontal are therefore relatively narrow.

In side view of the skull (plate 26, fig. 1), the anterior projection of the nasals seems to be almost intermediate between that of the modern lion and the modern tiger. In the lion the nasal opening is directed more distinctly upward than in the tiger and the anterior ends of the nasals are situated farther away from the anterior end of the premaxillary.

In front view (plate 27, fig. 3; see also fig. 142, B), the nasal opening is in some respects more like that of the tiger, as the opening is more distinctly pointed inferiorly, instead of relatively wide inferiorly as in the lion.

The turbinal elements are beautifully preserved in specimen No. 2900–9. They are very largely developed, and the superior fold of the maxillo-turbinal seems larger than that in specimens of either the modern lion or tiger available for comparison.

In the Rancho La Brea specimens of *F. atrox* at the Los Angeles Museum, the orbits tend to be nearer oval in outline than in the modern lion, the lower end of the orbit being distinctly narrower. In these respects the fossil forms more closely resemble the tiger. In the specimens from the asphalt, the orbits possibly look upward a little more than in the tiger, but possibly not so much as in the modern lion.

The postorbital constriction in the Rancho La Brea specimens is not so pronounced as in some skulls of the modern lion and tiger. In the skulls from the asphalt the cranial region is generally fuller behind the postorbital processes than in the lion and tiger. The less-marked postorbital constriction is in part due to the relatively smaller size of the brain and the more pronounced fullness behind the postorbital processes.

As viewed from above the brain-case in all the specimens of *F. atrox* is relatively smaller than in either the modern lion or modern tiger.

In *F. atrox* the posterior end of the frontal process of the maxillary is truncated on the median side, on a line nearly parallel with the median plane of the skull. In the lion the truncation of the frontal process is more distinctly oblique, and the lines of truncation extended forward would meet at a point situated about the middle of the nasal bones. The posterior ends of the frontal processes are truncated on a line making an angle of approximately 80° with the anteroposterior line of truncation. The extreme posterior end of the frontal process of the maxillary is commonly sharply pointed in the Rancho La Brea specimens, while in the lion and tiger it is blunt, or perhaps truncated transversely.

The occipital region in *F. atrox* exhibits a prominent median ridge which is generally high and more distinctly angular than in either the modern lion or tiger. There is considerable variation in this respect, the large skulls showing the ridge more strongly developed. Even in the small skulls the difference is very marked. In one large skull, L. A. Mus. No. 2900–11, there is an unusual modification of the occipital region in that two very deep pits are developed on either side of the occiput immediately above the condyles. These pits may be present in other skulls, but are very much less marked.

The narrowing of the occipital region immediately above the mastoid as described in the type of *Felis atrox bebbi* is not evident in the Los Angeles Museum specimens. This character is not more marked than in the modern lion.

The auditory bullæ in the Los Angeles Museum specimens generally show approximately the same relative size seen in the modern lion and in nearly all cases are relatively larger than in the type of *F. atrox bebbi.* In the large skulls, L. A. Mus. Nos. 2900–9 and 2900–13, the bullæ are relatively small. In the gigantic skull, No. 2900–3, the bullæ are apparently more strongly inflated than in the type of *F. atrox bebbi.* As in the latter form, the anterior spine of the ectotympanic region extends farther forward than the anterior extension of the entotympanic region. The ectotympanic spine commonly extends forward to a point a short distance behind the middle of the glenoid fossa. The inferior border of the external auditory meatus does not normally extend unusually far out from the median plane of the skull, as was reported in the type of *F. atrox bebbi.*

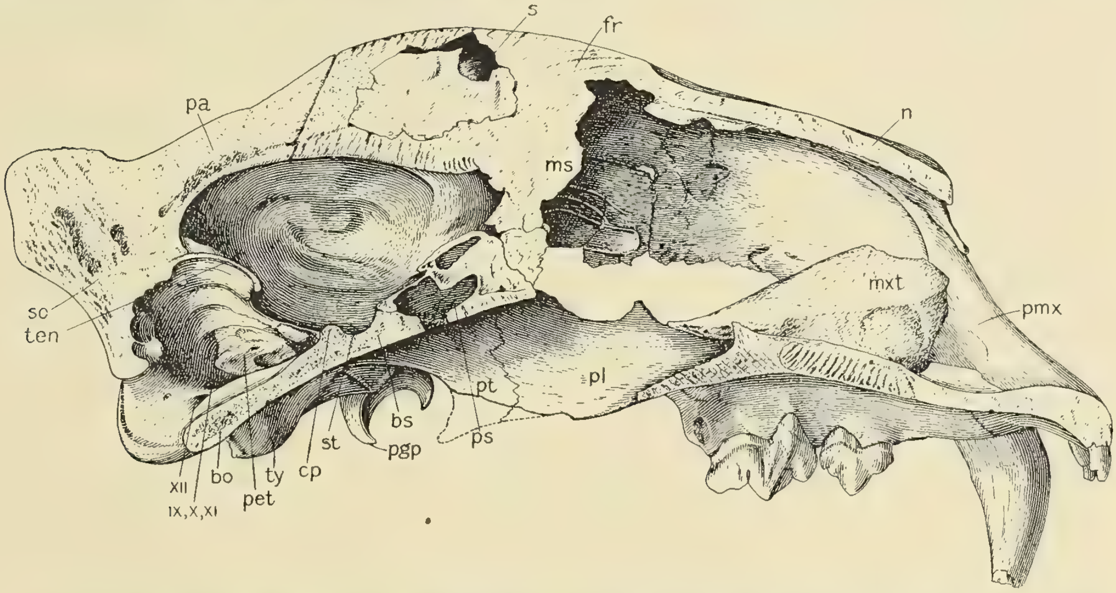

Fig. 134—*Felis atrox* Leidy. Vertical longitudinal section of skull, No. 2900-16; × 2/5. Ethmoturbinals are not preserved in this specimen. *n,* nasal; *fr,* frontal; *s,* frontal sinus; *pa,* parietal; *so,* supraoccipital; *ten,* cut edge of tentorium; *bo,* basioccipital; *pet,* petrosal; *bs,* basisphenoid; *ps,* presphenoid; *ty,* tympanic; *pt,* pterygoid; *pl,* palatine; *pmx,* premaxillary; *mxt,* maxilloturbinal; *ms,* mesethmoid; *st,* sella turcica; *cp,* clinoid plate; *pgp,* postglenoid process; *IX, X, XI,* foramen lacerum posterius; *XII,* condylar foramen. Rancho La Brea Pleistocene.

In the region of the basioccipital, the roughened area for attachment of the *rectus capitis anticus* muscle is generally situated far back, so that it is immediately adjacent to the opening of the posterior lacerate foramen.

Skull No. 2900–16 has been cut in two along the median longitudinal plane to reveal the internal structures (fig. 134). Unfortunately the ethmoturbinate elements are not preserved in this specimen. Attention has been directed already to the difference in orientation of the basicranial and basifacial axes between the extinct cat and the sabre-tooth. While the brain-chamber is larger than in the sabre-tooth, it is relatively smaller than in modern cats. It is noteworthy that a considerable expanse of bone representing the frontal, parietal and supraoccipital comes to view in this section. The dorsomedian contour of the cerebral and olfactory chambers possesses a somewhat different curvature from that in *Smilodon.* The ridges on the wall of the cerebral cavity, while clearly defined, are not so well developed as in the sabre-tooth. The cerebellar cavity is noticeably larger in *Felis* *atrox* than in *Smilodon.* The impressions of the lobules of the cerebellum are well defined in this specimen. The petrosal is distinctly larger than in the sabre-tooth, but the internal auditory meatus is smaller. In median line the cut edge of the tentorium presents a thinner surface in *F. atrox* than in the sabre-tooth, although the plate may be no thicker in one than in the other. This edge appears to project more downward, less forward, than in modern *Felis.* The tip of the clinoid plate is broken away. The base of the plate resembles that in modern *Felis.* The pituitary fossa (*st*) is more sharply defined in this section than in that of the sabre-tooth. It is more deeply excavated. The presphenoidal sinus is more capacious than in *Smilodon.* Likewise, the frontal sinus is of large size.

The infraorbital foramina are generally somewhat smaller and narrower transversely than in the modern lion. In these characters *F. atrox* may be more like the tiger.

The sphenopalatine opening is distinctly larger than that in *Smilodon.*

The postpalatine foramina are situated farther back than in the lion and tiger. They are usually behind the posterior end of $P\underline{4}$. Occasionally they may be situated as far forward as the extreme posterior end of $P\underline{4}$.

The foramen rotundum is normally much nearer the sphenoidal fissure than in *Felis leo.* This foramen is commonly separated from the sphenoidal fissure by a relatively thin blade of bone. In L. A. Mus. specimen 2900–14 the foramen rotundum seems not to have been separated externally from the sphenoidal fissure, or if a separation was represented it consisted at most of a very thin thread of bone. The space separating the foramen rotundum from the foramen ovale appears comparatively wide.

The condylar foramina are commonly well outside the openings of the posterior lacerate foramina. In four or five cases out of more than twenty crania the situation is approximately as in *F. leo.*

The inferior nasal openings in the Rancho La Brea specimens always have the anterior palatine border cleft and never with a median spine, as in the tiger.

ENDOCRANIAL CAST

Plate 14, figs. 1 to 3

Two endocranial casts are available of *Felis atrox,* one taken from skull 2900–1 (plate 14), the other from skull 2900–16 (fig. 135). These cats show considerable resemblance in size, shape and surface features, although the skulls varied somewhat in size, No. 2900-1 being larger than No. 2900–16.

As commented upon in the description of the endocranial cast of *Smilodon,* there is considerable difference between the sabre-tooth and the extinct true cat of Rancho La Brea in this structure. *Felis atrox* had, quite evidently, a larger brain than *S. californicus.* The proportions of the casts in the two forms are different. The form of the cast resembles the form of the brain in modern cats, although the anterior portion of the cerebrum does not appear to be so deep in *F. atrox* as in the latter types. The olfactory lobe is placed well in front of the cerebrum and the olfactory tract is long, giving this region of the cast a quite different appearance from that of *Smilodon.*

The gyri and sulci are more faintly defined in *Felis atrox* than in *S. californicus,* and this is true of both casts taken from skulls of the former species.

Table 89—*Measurements (in millimeters) of skull of Felis atrox*

	2900–3	2900–9	2900–11	2900–12	2900–10	2900–20	2900–15	2900–8	2900–7	2900–5	2900–18	2900–16	2900–17	2900–4	2900–19	2900–6	Univ. Calif. 20049	Univ. Calif. 14001
Length from anterior end of premaxillary to posterior end of condyles	410	380.8	374.9	368.9	368.6	366	361	348.7	336.6	332	.....	328	311.3	302	*a*293.3	290	406	424.3
Basal length from anterior end of premaxillary to inferior notch between condyles	388	359.4	348.9	346.3	344.2	344	340.4	321.9	313.7	314.6	338.9	306.8	290	287.9	*a*275.3	269	375.2	404.7
Length from anterior end of premaxillary to posterior end of inion	458	429.5	*a*432.8	*a*417.3	419.2	406.8	400	391.9	373.5	367	.....	368.9	.....	325.8	*a*322.9	310.3	447.5	467.5
Length from anterior end of premaxillary to anterior end of posterior nasal opening	212	194.4	192.8	179.7	179.6	*a*193	*a*184	175.8	169.3	167.4	180.9	156.9	155.3	156.7	*a*142.9	148.4	209.2	.....
Length of palate from anterior end of premaxillary to line tangent to posterior surfaces of maxillary parapets	134.4	148	.....	152.6	156	156	144	136.5	140.8	140.8	.....	138.2	134.8	126.1	122.8	121.7	158.5	159
Length from posterior end of glenoid cavity to posterior end of condyles	112.5	108.5	*a*86.7	100.2	102	93.4	.....	99.5	93	97.8	.....	87.8	88.4	82.8	80	80.5	97.5	105
Anteroposterior diameter of nasals	.....	101.6	114	99	104.2	93.5	*a*99	96	90.9	.....	105.8	92.4	.....	82.7	.....	79.2	104.5	.....
Width of anterior nares	73	67	.....	*a*62	65.2	*a*72	67	63.9	63.2	62.4	.....	58.8	53.7	53.2	*a*47	51.4	69.9	66.6
Greatest width across muzzle at canines	141.4	122.8	128.3	122.6	110	127.3	*a*115	116.9	111.8	113.2	*a*116	104.3	98.8	98.3	98.7	98	127.3	135.9
Least width between superior borders of orbits	.....	98.3	106.6	91.3	87.5	91.9	.....	83.6	83.3	80.4	*a*88.3	74.6	77	75.3	73.7	68.8	93.5	.....
Width across postorbital processes	.....	*a*132	.....	119.8	121.4	121	*a*114	113.3	119.6	*a*110.5	.....	101.4	101	107.6	*a*109	99	129.4	.....
Least width of postorbital constriction	.....	85	78	89	80.8	81	79	75.5	78.8	74.3	86.6	71	71	72	77.3	70.7	84.8	84.9
Greatest width across zygomatic arches	294	296.5	*a*280	247.6	244	248	.....	245	235.3	238.3	.....	.....	212.2	*a*225.2	*a*203	*a*205.7	276.3	304.3
Anterior palatal width between superior canines	71.4	66.2	.....	59	59	64.4	62	59.8	58.2	58	.....	55.5	49.6	52.8	48	49.9	65.4	68
Posterior palatal width between inner roots of superior carnassials	107.8	97.6	.....	90	85.3	96	88	85	85	86.4	.....	81.4	76	86.7	76	78.2	103.5	108.4
Width across palate between posterior alveoli of superior carnassials	147.8	140.8	138.4	131.8	121.9	134.2	.....	125.4	125.7	120.5	132.8	*a*111.3	110	122.9	117.3	114.4	126.6	133.9
Greatest transverse diameter across auditory bulla, measured from foramen lacerum posterius to external auditory meatus	29.6	29.2	29.2	26.2	29.9	27.9	29	28	22.3	25.2	27	21.1	22.7	23	24.7	22	30.8	35.9
Greatest width across mastoid processes	173.6	.....	.....	*a*151	165.4	160.7	.....	144.8	140.8	138.2	.....	132.2	133.5	132.7	122.8	126.7	158.2	170.8
Greatest diameter across condyles	76.8	74.1	78.6	70.6	76.2	73	71.9	70.4	68.4	63.5	.....	62.4	69	58.4	64.2	60.4	72.1	73.7
Height of anterior zygomatic pedicle	78.8	84.4	.....	70.1	77.3	74.6	69	75.8	71.3	70.4	.....	65.2	61.1	66.9	65	57.6	83.5	89.7
Length of anterior zygomatic pedicle	52.5	44.7	.....	46.3	47.5	50.7	45.5	39.9	42.2	39.3	.....	43.2	42	39	42.3	38.9	48.8	53.7

a, Approximate.

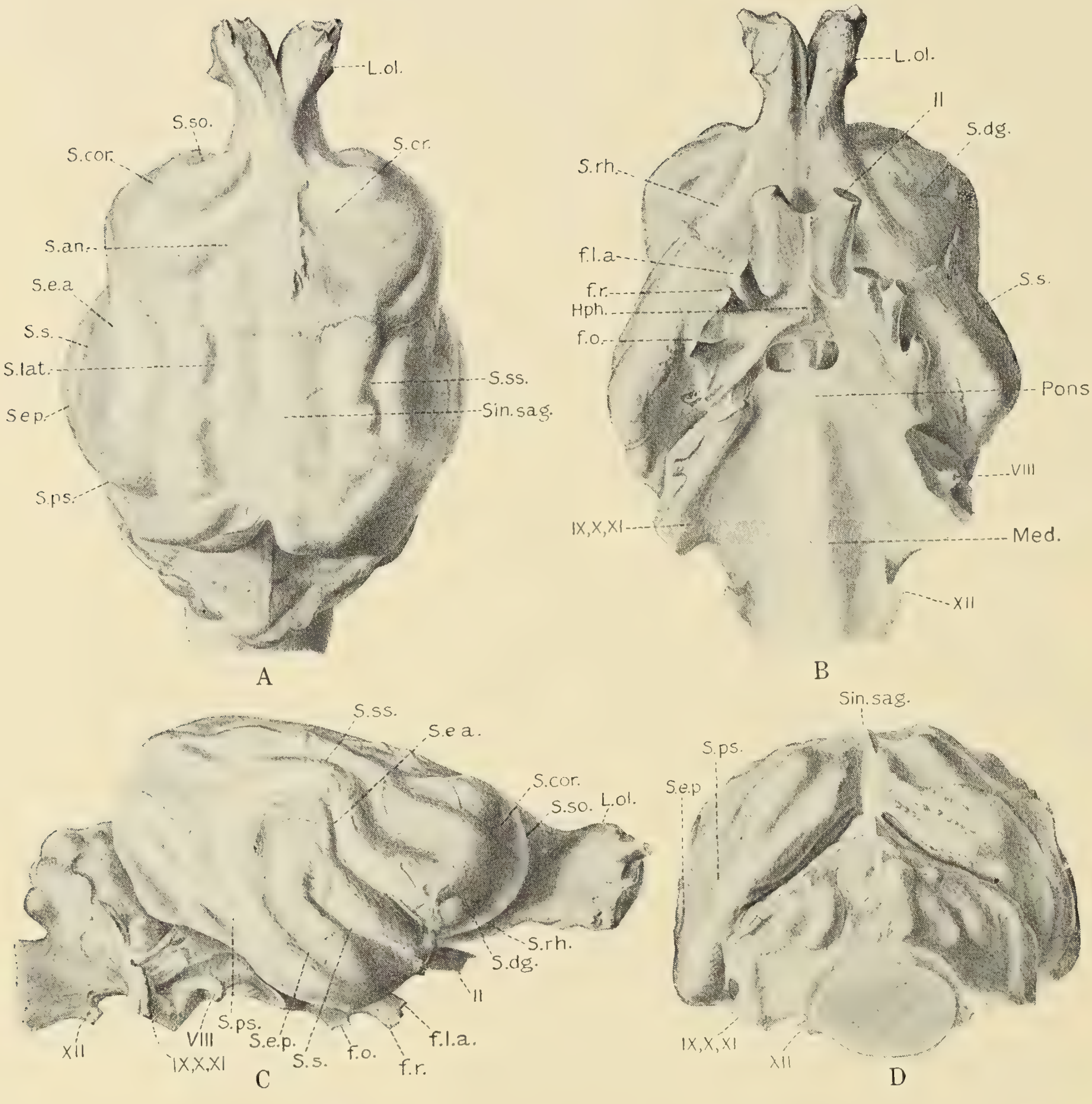

Fig. 135—*Felis atrox* Leidy. Endocranial cast from skull 2900-16. A, dorsal view; B, ventral view; C, lateral view; D, posterior view; × 2/3. For explanation of letters see figure 11. Rancho La Brea Pleistocene.

Table 90—*Skull and dental indices of Felis atrox*

	2900–3	2900–9	2900–11	2900–12	2900–10	2900–20	2900–15	2900–8	2900–7	2900–5	2900–18	2900–16	2900–17	2900–4	2900–19	2900–6	Univ. Calif. 20049	Univ. Calif. 14001
Anterior narial index	18	18	.....	18	19	20	19	19	20	19	.....	19	17	18	17	19	19	17
Index of interorbital breadth	.....	27	30	26	25	26	.....	26	26	25	25	.....	26	26	26	25	25	.....
Breadth index of postorbital processes	.....	36	.....	34	35	35	33	35	38	35	.....	32	34	37	39	36	34	.....
Index of postorbital constriction	.....	23	22	25	23	23	23	23	25	23	25	.....	24	25	28	26	23	21
Bizygomatic index	75	82	80	71	70	72	.....	76	74	76	.....	.....	71	78	70	76	74	75
Index of palatal length	47	41	.....	44	45	45	42	42	45	44	.....	44	45	43	42	45	42	39
Index of anterior palatal breadth	40	44	.....	38	38	41	43	43	41	41	.....	40	37	42	39	41	41	43
Index of posterior palatal breadth	61	66	.....	59	54	61	61	62	60	61	.....	58	56	69	61	64	65	68
Height index of anterior zygomatic pedicle	149	186	.....	152	159	212	150	190	169	179	.....	152	145	171	154	148	.....	.....
Diametral index of superior canine	70	69	.....	.....	74	80	82	71	.....	.....	.....	72	76	72	69	.....	.....	.....
Mandible No. 2901	3	15	20	24	5	7	16	25	23	26	4	27	6	....	...	....	....	.....
Diametral index of $\mathrm{M}\bar{1}$ $\frac{\mathrm{W\ M}\bar{1} \times 100}{\mathrm{L\ M}\bar{1}}$	53	53	53	50	52	54	46	53	46	48	52	46	48	.....	.....	.....	.....	.....
Length index of $\mathrm{P}\bar{4}$—$\mathrm{M}\bar{1}$ $\frac{\mathrm{L\ P}\bar{4} \times 100}{\mathrm{L\ M}\bar{1}}$	94	103	97	97	100	100	93	100	100	94	96	100	96	.....	.....	.....	.....	.....

MANDIBLE

Specimens of the mandible of *Felis atrox* from Rancho La Brea vary considerably in size (see measurements, table 92). These may fall into two groups, the difference between the two types being comparable in a general sense to the differences between the large and small crania. Here again, however, the measurements reveal a more or less uniform increase in size from the smallest to the largest mandible, with no tendency toward a sharp separation into two groups. The largest specimen in the Los Angeles Museum collection, No. 2901–3, is in some measurements, but not in all, slightly smaller than that of the type of *F. atrox bebbi.*

Table 91—*Measurements (in millimeters) of endocranial casts*

	No. 2900–1	No. 2900–16
Greatest length of cerebrum	91.7	91.6
Greatest width across anterior end of cerebrum	73.6	73.8
Greatest width across temporal lobes	88.6	92
Cast displaces c.c. of water	340	319

The symphyseal region may slope downward and backward a little more distinctly in the smaller jaws than in some of the larger specimens. As a rule, however, the anterior face of this region drops off quite steeply and the form is distinctly different from that in the modern *F. leo.* At the lower side of the symphyseal region there is not infrequently a dependent process or tubercle.

In rare cases the inferior border of the ramus may be almost straight below the cheek-teeth. Normally the ramal process is clearly developed below the anterior or middle region of $M\bar{1}$. In most specimens from Rancho La Brea the jaw when placed on a table can not be rocked, with the inferior surface of the ramal process serving as a pivot. In this respect a greater resemblance prevails between *F. atrox* and the tiger than between the extinct species and the lion. The stability of the mandible when placed on a flat surface depends upon the development of the inferior symphyseal process or tubercle and upon the lower prominence of the angle. Examples are present, however, as in L. A. Mus. specimen 2901–23, in which a closer approach is made toward the lion than the tiger (see also fig. 142, C and D).

TABLE 92—*Measurements (in millimeters) of mandible of Felis atrox*

	2901–3	2901–15	2901–20	2901–24	2901–5	2901–7	2901–16	2901–25	2901–23	2901–26	2901–4	2901–27	2901–6	2901–10	Univ. Calif. 20049	Univ. Calif. 14001
Length from anterior end of symphysis to posterior end of condyle immediately behind coronoid process	309.5	276.8	273.1	257.5	243.8	242	242	237.8	238.3	235	217	218	206	273.4	309.3	318
Length of symphysis measured along anterior border	94	79.5	82.7	71.2	82.2	71	72.2	76	75.3	74	69.5	67.6	67.2	85.2	87.9	99.3
Depth of ramus below anterior end of $P\bar{4}$	60.7	55.6	53	54	46.8	48.9	45	49.3	47.5	47	45.3	43	38.9	52.9	56.5	59.7
Depth of ramus below posterior end of $M\bar{1}$	63.4	57.4	57.6	56.1	49.7	51.8	47.3	50.4	53.4	49.9	49.4	46.1	46	57.5	62.3	67.1
Thickness of ramus below posterior end of $M\bar{1}$	29.2	27.3	27.8	25.3	23.6	23.4	20	23.8	23.8	21.4	23.3	21.4	20.2	23.9	26.6	36.9
Height from inferior border of angle to summit of condyle	66.4	52.2	52.3	57.6	51.7	46.8	45.8	44	46.5	45.5	45.2	45.8	42	56	64.8	62.3
Height from inferior border of angle to summit of coronoid process	150	132.6	129	131	124.6	117.3	111.5	111.8	121.5	112	107.6	107.4	96.3	129.3	142.8	.....
Transverse width of condyle	74.9	70.2	64.7	*a*59	58.9	59.4	55.5	58.3	53.1	*a*50.5	54.3	55.3	*a*44.5	63.6	71.4	67.8
Greatest depth of condyle	26.7	25.7	25.3	24	21.4	19.3	18.8	20.8	20.7	20.6	20.2	20.4	18.4	24.6	27.2	24.9

a, Approximate.

The masseteric fossa is very deep, and its extreme anterior border reaches forward to a point opposite the middle or posterior part of the inferior carnassial. The inferior border of the anterior portion of the masseteric fossa is marked by a sharp upward twist occurring just below the deepest portion of the fossa. The coronoid process is normally high and broad. Frequently the superior portion sweeps backward somewhat as in the tiger, so that the posterior extremity extends behind the condyle. The form of the angle is intermediate between that of the lion and the tiger, as it projects inferiorly more than in the lion, and less than in the tiger posteriorly.

The posterior mental foramen is frequently of large size in *F. atrox*.

DENTITION

$$\text{Dental formula: } \frac{3}{3}, \frac{1}{1}, \frac{3}{2}, \frac{1}{1}$$

SUPERIOR DENTITION

The anterior face of the row of upper incisors is generally convex forward or nearly straight across, and commonly possesses a slight indentation backward in the middle due to slightly smaller size of the median incisors $I\underline{1}$ and $I\underline{2}$. $I\underline{1}$ is somewhat

Table 93—*Measurements (in millimeters) of superior dentition of Felis atrox*

	2900–3	2900–9	2900–11	2900–12	2900–10	2900–20	2900–15	2900–8	2900–7	2900–5	2900–18	2900–16	2900–4	2900–19	2900–6	2900–17	Univ. Calif. 20049	Univ. Calif. 14001
Length from anterior end of canine alveolus to posterior end of P$\underline{4}$	139.4	120.4	.....	128.8	122.5	125.2	117.2	112	119.7	117.3	.....	111.7	104.2	103.8	101.2	109.3	129.4	*a*136
Length from anterior end of alveolus for P$\underline{2}$ to posterior end of alveolus for P$\underline{4}$	91.6	77.7	.....	88.7	82.9	84.8	78.4	76.7	79	77.7	.....	77.5	73.8	71.3	71.4	76.9	86.8	89.4
I$\underline{1}$, greatest transverse diameter	6.3	5.9	.....	.....	6.5	5.8	.....	.....	.....	.....	.....	5.7	.....	.....	.....	5.8	5.9	.....
I$\underline{2}$, greatest transverse diameter	.....	.....	.....	.....	7.2	7	7.4	6.8	.....	.....	.....	.....	.....	.....	.....	6.5	6 9	.....
I$\underline{3}$, greatest transverse diameter	12.8	11	.....	12.3	11.7	11.4	12	10.2	11.4	.....	.....	9.4	9.8	9.7	10	12	11.2	.....
$\underline{C}$, anteroposterior diameter at base of enamel	36.8	29.3	.....	.....	30.7	30	*a*28	30.5	.....	.....	.....	25.2	25.6	25.6	.....	25.3	*a*30.6	.....
$\underline{C}$, transverse diameter	*a*25.7	20.4	.....	.....	22.6	23.7	22.8	22	.....	.....	.....	18	18.3	18.4	.....	18.6	22.7	.....
P$\underline{2}$, anteroposterior diameter of alveolus	11.4	10.2	.....	9.6	10.1	10	7.3	9	9.8	9	.....	7.6	10	8	8.2	8.7	10.5	9
P$\underline{3}$, anteroposterior diameter	30.4	26.2	.....	30.6	28	28.3	25.3	27.8	26.7	25.6	.....	25.9	25	25.7	23.9	.....	30.4	.....
P$\underline{3}$, greatest transverse diameter	16.2	14.4	.....	15.5	15.9	14.5	14.9	13.7	13.4	12	.....	12.3	12	12	12.7	.....	14.9	13.7
P$\underline{4}$, anteroposterior diameter	45	39.5	.....	42.2	40.5	40	40.8	40.3	40	39	.....	38.3	*a*35	36.5	36.6	37	40.8	.....
P$\underline{4}$, greatest transverse diameter across protocone	*a*19	20.9	.....	21.2	20.4	20.8	21.4	21	20	19.6	.....	19.3	18.4	18.7	18.3	19.2	22.9	*a*21
P$\underline{4}$, anteroposterior diameter of base of paracone	17	14.7	.....	17	15.6	16	15.8	15.5	13.9	14.5	.....	14	12.4	14	14.1	14.5	15.7	.....
P$\underline{4}$, anteroposterior diameter of parastyle	8.1	7.7	.....	7	7.9	7.3	6.6	7	8.9	6.7	.....	7.4	6.4	6.6	7.6	7.6	9.4	.....
P$\underline{4}$, length of metacone blade	16.4	15.2	.....	16.5	15.2	15.5	14.7	15.8	15.5	15.1	.....	15.1	.....	13.9	14	14.4	14.5	.....
M$\underline{1}$, anteroposterior diameter	.....	.....	.....	.....	6	.....	.....	.....	.....	.....	.....	.....	.....	.....	.....	.....	.....	.....
M$\underline{1}$, transverse diameter	.....	.....	.....	.....	11.6	.....	.....	.....	.....	.....	.....	.....	.....	.....	.....	.....	.....	.....

a, Approximate.

Table 94—*Measurements (in millimeters) of inferior dentition of Felis atrox*

	2901–3	2901–15	2901–20	2901–24	2901–5	2901–7	2901–16	2901–25	2901–23	2901–26	2901–4	2901–27	2901–6	2901–10	Univ. Calif. 20049	Univ. Calit. 14001
Length from anterior end of C to posterior end of M$\overline{1}$	156.7	142.7	144.5	134.9	131.6	132.8	127.4	*a*135	129.5	.....	119.3	.....	116.4	143.5	150	*a*156
Length from anterior end of P$\overline{3}$ to posterior end of M$\overline{1}$	89	80.7	80.1	79.8	77.3	74.8	71.7	81.7	*a*75.5	79.1	70.7	72.8	68.3	78.8	84.2	86
I$\overline{1}$, greatest transverse diameter	.....	4.3	.....	.....	.....	.....	4	.....	.....	.....	4	.....	.....	4.4	.....	.....
I$\overline{2}$, greatest transverse diameter	.....	5.9	.....	.....	.....	.....	5.4	.....	.....	.....	5	.....	.....	6.1	.....	.....
I$\overline{3}$, greatest transverse diameter	.....	8	7.7	.....	.....	.....	6.7	.....	7.3	.....	6.8	.....	.....	.....	7.3	8.3
$\overline{C}$, anteroposterior diameter at base of enamel	30.4	27.3	29.3	*a*27.5	25.2	.....	25.8	.....	24.4	.....	23.6	.....	21.8	28.9	30.2	.....
$\overline{C}$, transverse diameter	21.6	19.3	20	*a*22	19	.....	16.4	.....	15.5	.....	15.1	.....	15.1	19.8	20.8	.....
P$\overline{3}$, anteroposterior diameter	21	20.2	20	*a*19.6	18.1	18.9	18.2	20.6	.....	21	17	19.6	17	19.5	21.6	20.5
P$\overline{3}$, greatest transverse diameter	13.2	12.5	11.7	*a*11.3	10.3	10.2	9.4	11.5	.....	11.4	8.9	10.5	9.8	11.3	12	11.7
P$\overline{4}$, anteroposterior diameter	32.3	30.5	28.5	*a*29	28.7	27.7	26.4	32.3	28.1	29	26.3	27.5	25.8	29.5	31.3	32.1
P$\overline{4}$, greatest transverse diameter	16.8	14.4	15	*a*15.4	14	13.5	12.6	15.7	13.7	14	12	13.4	12.6	14	14.7	16.9
P$\overline{4}$, basal length of principal cusp	14.5	13.6	14.6	13.2	13	12.6	12.4	15	12.5	14	11.9	12	12.2	12.9	14.3	14
M$\overline{1}$, anteroposterior diameter	33.7	30	29.9	29.6	28.5	27.5	28.3	32	28.3	30.5	26.9	27.7	27.1	29.8	30.7	33.9
M$\overline{1}$, greatest transverse diameter	17.5	15.5	15.6	14.8	14.9	14.6	13	16.8	13.4	14.5	13.5	13.4	13.4	14.9	16	17.2
M$\overline{1}$, length of protoconid blade	16	16	15	15	13.2	14.7	14.8	14.8	14.7	15	12.4	12.7	14.7	.....	15.1	14.2

a, Approximate.

smaller than I$\underline{2}$, and both of these teeth have a strong posterior cusp which is separated from the spatulate anterior cusp by a deep transverse groove. The form of these two teeth is nearly the same. The tip of the crown of I$\underline{2}$ may be a little more pointed or narrowed than that of I$\underline{1}$. I$\underline{3}$ is large and the lateral angle is turned far back in accommodation to the bend of the outer margin of the premaxillary. The low posterior median cusp or tubercle is almost on the median side.

The upper canine is possibly a little more flattened in the smaller forms than in the larger types from Rancho La Brea. The posterior angle of the crown is well developed, the antero-internal angle is faintly marked, and the internal face is much flatter than the outer face.

The alveolus for P$\underline{2}$ is present, but the tooth has not been observed in any of the skulls of *F. atrox* from Rancho La Brea (see p. 225).

P$\underline{3}$ may not differ greatly from that in *F. leo*. The crown of this tooth is generally somewhat lower than in the lion, and in this respect it resembles the tiger.

A curious variation in fang development occurs occasionally in this tooth. A third or inner root situated above the inner base of the principal cusp may be present, in which case it is distinct from the posterior fang. No similar root has been observed in *Felis leo spelæa*. This character occurs in specimens 2900–9 and 2900–8 of *F. atrox* from Rancho La Brea. In No. 2900–9 the extra root is present in P$\underline{3}$ of the left side but absent in the comparable tooth of the right side. In No. 2900–8 the extra root is present in P$\underline{3}$ of both sides. At least 19 specimens show a right P$\underline{3}$ with two roots and 15 specimens show a left tooth with two roots. In specimen No. 2900–17, in which the teeth are missing from the skull, the posterior alveolus of each side shows an inner bulge. The anterior root while distinctly smaller than the posterior is only a trifle shorter.

The cusps of P$\underline{4}$ seem not quite so low as in the tiger. The cusps appear lower generally than in *F. leo*, although this is not always the case. The parastyle is not so strongly developed as in the tiger. The condition in this respect is much as in the lion. The proportions of the cusps on P$\underline{4}$ do not seem to be materially different from those in the modern lion. The protocone is much as in skulls of *F. leo*. The root system (plate 33, figs. 1, 1a) is similar to that in P$\underline{4}$ of *F. l. spelæa* with the posterior root perhaps not so broad anteroposteriorly as in the latter type. The outer fangs curve inward in their upward course. This is particularly noticeable in the antero-external fang. The antero-internal root is well developed, more so than in *Smilodon*, but is shorter than the antero-external root.

M$\underline{1}$ is a small tooth with oval crown. It has commonly two roots which may be quite widely separated as in L. A. Mus. specimen No. 2900–18, or it may have only one root as in L. A. Mus. specimen 2900–19.

Inferior Dentition

The transverse line of the incisor teeth may be bowed slightly forward or slightly backward or may be approximately straight across. The space occupied by the incisors is relatively small. I$\overline{1}$ is much smaller than I$\overline{2}$. The medial incisor has the merest trace of an external lobe as shown in L. A. Mus. specimen 2901–16. I$\overline{2}$ has a very small external lobe which reaches back a little more than half the distance to the posterior border of the enamel. The inferior canines possess stout roots and have a greater anteroposterior diameter compared with that of the inferior carnassial than in the lion, but are smaller in comparison with the upper canines.

The longitudinal ridge on the inner face may not be situated so far forward as in the tiger.

The diastema between canine and P$\overline{3}$ is relatively a little shorter than in the Recent lion or tiger.

In P$\overline{3}$ the postero-internal portion of the cingulum is more strongly swollen laterally than in the lion or tiger. Usually a distinct anterior tubercle is present on this tooth. In a few cases, as in L. A. Mus. specimen 2901–28, P$\overline{3}$ lacks a separate anterior tubercle. The fangs, with reference to the vertical axis of the crown, are directed somewhat anteriorly. The posterior root is slightly larger than the anterior. On the basis of material available from the Mexican Pleistocene Freudenberg (1910, p. 226) concludes that *Felis atrox* is characterized by a single-rooted P$\overline{3}$, in which respect it differs from the double-rooted tooth in *F. spelæa*. In all of the specimens of *F. atrox* from Rancho La Brea P$\overline{3}$ is two-rooted.

P$\overline{4}$ resembles quite closely the form of this tooth in the African lion, excepting that the anterior and posterior cusps are perhaps a little more compressed laterally and are less acute. In L. A. Mus. No. 2901–21, the superior crest of the anterior tubercle curves inward rather noticeably. The principal cusp is approximately triangular in cross-section, the inner angle of the triangle extending down to the cingulum as a rather prominent ridge. Occasionally a minute tubercle may be discerned on the ledge extending inward from behind the posterior cusp at the postero-internal corner of the tooth. The fangs are of subequal size.

M$\overline{1}$ corresponds in relative size and proportions quite closely to the inferior carnassial of the African lion. It possesses, however, a rather distinct heel, and a minute cusp corresponding to the metaconid may or may not be present. The anterior margin of the paraconid blade slopes backward more strongly than the nearly vertical anterior border of this portion of the tooth as it may appear in the African lion. The crown is supported principally by the anterior fang, which is strongly developed. The posterior root is slender, small in cross-section, and shorter than the anterior fang.

Lower Milk Dentition

The inferior cheek-tooth dentition of *Felis atrox* includes two teeth, Dm$\overline{4}$ and Dm$\overline{3}$. In the lower milk carnassial the anterior root is relatively not so large as in the comparable tooth of *Smilodon*. The crown is likewise not so high in the former as in the latter, so that the notch between the paraconid and protoconid blades is closer to the base of the crown. The difference in length between the anterior border of the protoconid and the posterior border of the paraconid is not so great in the large true feline as in the sabre-tooth cat. A single cusp is present behind the protoconid, and its position with reference to the latter cusp is more posterior and less internal than in *Smilodon*. While a posterior cingulum is evident in this tooth, no distinct basal cusp (talonid) is present as in the sabre-tooth cat.

Dm$\overline{3}$ leans backward, but the slope is not so pronounced as in the comparable tooth of *Smilodon*. This tooth, in comparison to the milk carnassial, is relatively larger in the extinct true felid than in the sabre-tooth cat. In front of the principal cusp (protoconid) is a well-developed basal cusp. Behind the protoconid is a posterior cusp, the tip of which does not project away from that of the protoconid to the extent seen in *Smilodon*. A low posterior basal tubercle or ridge is present which, in side view, does not appear quite so prominently developed as in the sabre-tooth cat.

The milk canine is compressed and the crown is relatively higher than in *Smilodon*. On the inner base of the crown is a small ledge, but no minute cusp has been noted as in the latter form.

RELATIONSHIP OF FELIS ATROX TO THE LARGE LIVING FELINES OF THE OLD WORLD

In studies of the large true cats of the Quaternary, attempts have been made from time to time to determine the relationship of fossil forms to the living lion and tiger, based on the recognition of characters which distinguish the latter species. Particularly is this true of investigations which have been conducted on Pleistocene representatives of the group in the Old World, although the problem of distinguishing the lion from the tiger on characters seen in the skull, skeleton and dentition has been treated also by systematists concerned principally with the modern forms.

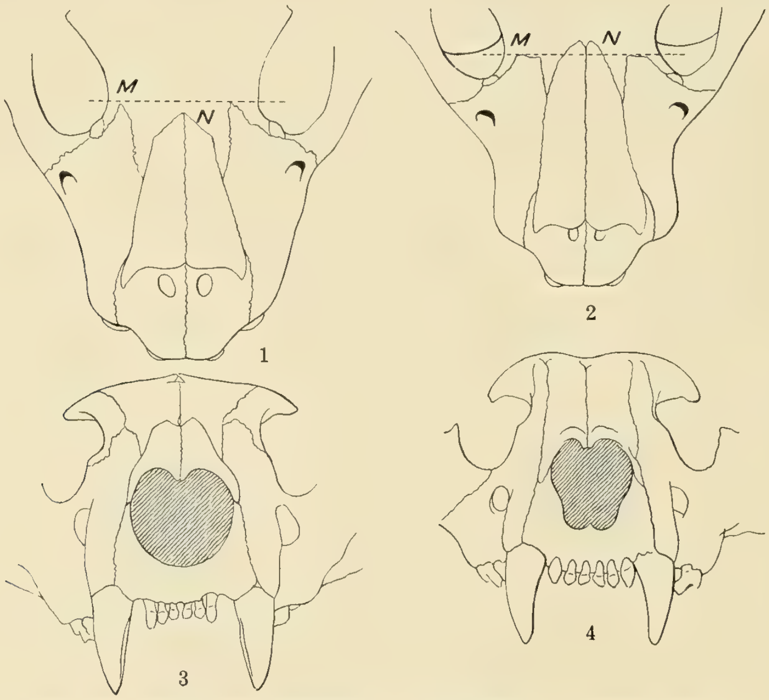

FIG. 136—Comparison of skulls of Recent lion (1 and 3) and tiger (2 and 4). (After Boule.)

Curiously enough while the two living species furnish striking external dissimilarities, a survey of structures revealed in the skull and skeleton and in the dentition has offered as yet no very reliable basis or no extensive series of differences on which a satisfactory separation can always be made. Doubtless the history of this group in the Old World has been such as to bring about in late geologic time noteworthy differences in the distribution of particular types and in the specific adjustments of these forms to their individual environments without incurring much change in their more fundamental structures.

Boule (1906, pp. 69–95), following the important contribution by Dawkins and Sanford (1868, pp. 62–64), has indicated certain structural differences between the modern lion and tiger, based principally on characters of the skull, and has emphasized their functional value as related to the habits of these animals. In view of the rather full yet concise treatment of this subject it will be of interest to render the following translation from Boule:

1. SKULL

LION	TIGER
1. The frontal process of the superior maxillary (fig. 1, *M*) reaches the level of the fronto-nasal suture, or extends back of this suture.	1. The frontal process of the superior maxillary, *M*, does not reach the fronto-nasal suture, *N* (fig. 2).
2. The summit of this process is more or less acute (fig. 1).	2. The summit of this process is truncated (fig. 2).
3. The nasal bones are flat or slightly convex, especially toward their frontal extremities.	3. The nasal bones are very convex throughout their length.
4. The external opening of the nasal fossæ is relatively wider; it widens regularly beginning at the lower part (fig. 3).	4. The external opening of the nasal fossæ is relatively narrower; it widens regularly, only up to a certain height, beginning at the lower part.
5. The interorbital space formed by the frontals is wider, flatter and even commonly excavated; the Lion has a forehead which is wide and flat, transversely as well as longitudinally.	5. The interorbital space is narrower and always convex: the Tiger has a forehead which is narrower and more arched.
6. The temporal part of the frontals is relatively less developed; the fronto-parietal sutures are placed further forward (*ss*, fig. 5).	6. The temporal part of the frontals is relatively more developed; the fronto-parietal sutures are placed further back (*ss*, fig. 6).
7. The posterior palatine foramen is closer to the orbital border.	7. The posterior palatine foramen is further removed from the orbital border.

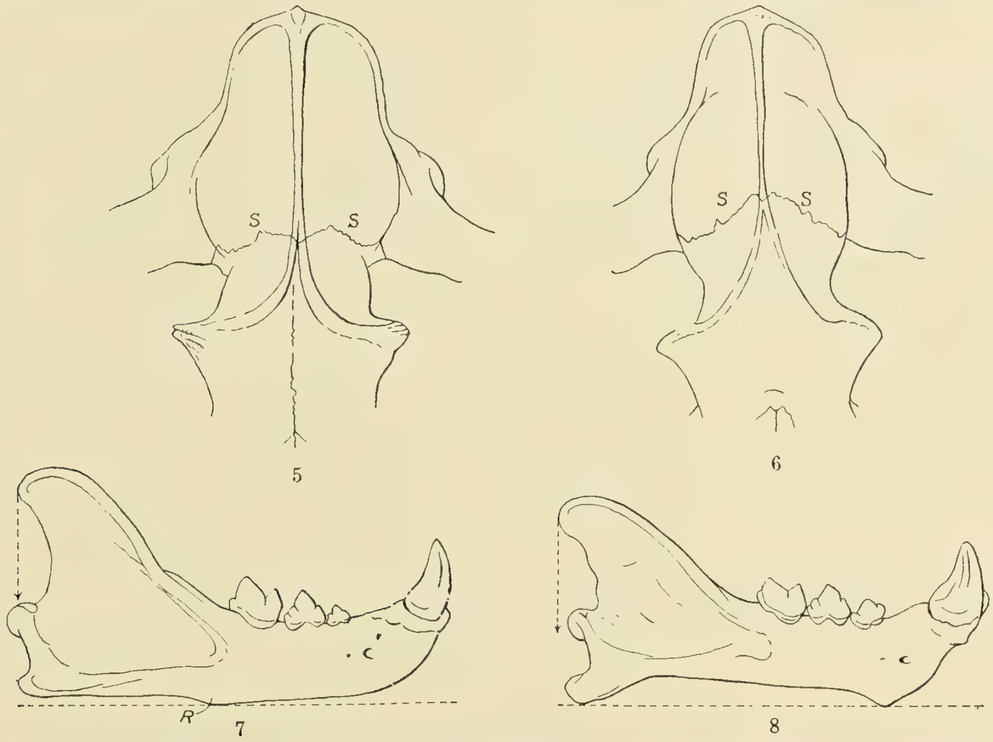

FIG. 137—Comparison of skulls and jaws of Recent lion (5 and 7) and tiger (6 and 8). (After Boule.)

8. The inferior border of the mandible has a rather convex form; below the carnassial, this border presents a sort of tuberosity which is more or less pronounced (*ramal process* of English authors [fig. 7, *R*]). This shape is such that a mandible of a Lion lying on a table on this inferior border can not touch the table at the symphysis and the angular process at the same time. It follows, likewise, that the mandible is lower in front of the molars than in the back.	8. The inferior border of the mandible has a rather straight and even concave form; there is no tuberosity below the carnassial (fig. 8). The mandible placed on a table rests on the symphysis and on the angular process at the same time. The height of the mandible, in front of the molars and back of the molars, is obviously equal.
9. The coronoid process does not project behind the condyle (fig. 7).	9. The coronoid process projects behind the condyle (fig. 8).

2. DENTITION

Lion	Tiger
10. The canines have a more rounded section; their internal face is more convex; the edges are less sharp. These characters are more clearly indicated on the superior canines than on the inferior ones.	10. The canines have a more flattened section; their internal face is less convex; the edges are more separated and sharper.
11. In general, the molars, while being slightly more elevated, have their cusps less compressed transversely, with edges more blunt; the premolars are thicker in their posterior part.	11. In general, the molars, while being less elevated, have their cusps more compressed transversely, with sharper edges; the premolars are less thick in the posterior part.

3. LIMB BONES

Lion	Tiger
The glenoid cavity of the scapula is more circular.	The glenoid cavity of the scapula is more oval.
The humerus is less curved in its superior part, the articular head projecting less in back.	The humerus is more curved in its superior part, the articular head projecting farther backward.
The anterior part (fig. 9) of the summit of the great tuberosity (or large trochanter), in front of the insertion of the sub-spinous muscle (*s. e.*), is more elevated; it nearly reaches the level of the posterior part.	The anterior part (fig. 10, *a*) of the summit of the great tuberosity is less elevated and less marked than the posterior part (fig. 10).

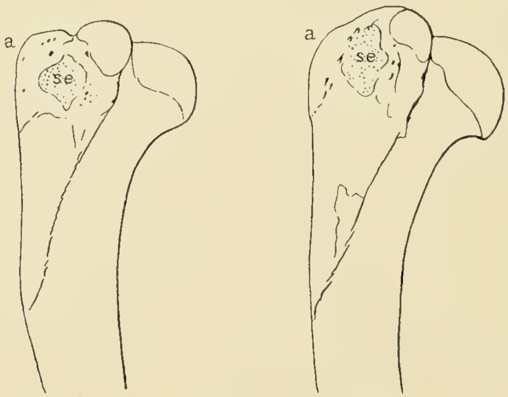

9 10

FIG. 138—Comparison of humerus of Recent lion (9) and tiger (10). (After Boule.)

The difference is very noticeable in a comparative study of the external face of the bones in profile (figs. 9 and 10). The summit of the great tuberosity (*a*) forms, with the anterior edge of the bone, a right angle in the Lion, and an obtuse angle in the Tiger. It denotes, in the Tiger, greater facility for movements of the arms.

The olecranon fossa is less deep and more open toward the top.	The olecranon fossa is deeper and its limit better defined toward the top.
The radius is proportionately longer and more slender, less curved. In the Lion, the forearm appears to be relatively longer than in the Tiger. The articular cup of the superior head has a more oval form.	The radius is proportionately shorter, thicker, and more curved. In the Tiger, the forearm appears relatively shorter than in the Lion. The articular cup of the superior head has a rounder form.
The femur has a neck more distant; the large trochanter is more elevated; the digital cavity is more spacious, and deeper.	The femur has a neck less distant; the large trochanter is less elevated (which denotes a more climbing animal); the digital cavity is less spacious, shallower.
The patellar trochlea is less developed anteroposteriorly; its area is less extensive.	The patellar trochlea is more developed anteroposteriorly; its area is greater.
The tibia is more curved, particularly on its anterior edge; in its inferior, or distal half, its section is more rounded, the edges being less distinct.	The tibia is less curved, the anterior edge is nearly straight; the transverse section, in the inferior half of the bone, is more triangular, for the edges are more distinct.
The superior portion of the external face is less concave, because the external and anterior tuberosities are less developed.	The superior portion of the external face seems more hollowed because the external and anterior tuberosities are more projecting.

The bones of the feet offer individual variations at least as considerable as those sometimes indicated as specific differences. In the Tiger, the head of the astragalus is more warped externally than in the Lion. One may note also that the distal articulations of the metacarpals and the metatarsals are more inflated, more spherical in the Tiger than in the Lion; the furrow which bounds them is deeper, the tubercles for the insertion of the lateral ligaments appear more distinct and more protruding; all this is in agreement with the more ferocious habits of the Tiger.

Blanford and more recently Pocock have given consideration to the differences noted in the skulls of the large living felines. Pocock concludes that many of the characters which have been regarded as diagnostic of the lion and tiger are inconstant in their occurrence. Variation in profile of skull and in backward extent and shape of nasals in the tiger is shown for example in figures 140 and 141, taken from Pocock. He states furthermore: "All indeed, that can be said with regard to the cranial differences between these two species is that tigers on the average have more vaulted skulls, with longer, narrower nasal bones, narrower anterior nares, the facial part shorter as compared with the cranial part and the lower edge of the mandible straighter than in lions."

Since the large true cat of the Rancho La Brea Pleistocene has come to be commonly designated the great lion, it is of some interest to determine whether or not the type from the asphalt can be regarded with equal right as belonging to a large species of tiger. Leidy, in the description of the type specimen of *Felis atrox* from the vicinity of Natchez, Mississippi, was the first to apply the name American lion to this species. With regard to the relationship of the Natchez specimen to the lion and tiger, it is of interest to note the following statement by Leidy (1853, p. 320): "The exact outline of the jaw in the specimen is difficult to ascertain, from its thick ferruginous coating, but from several exposed points of the body along its base,

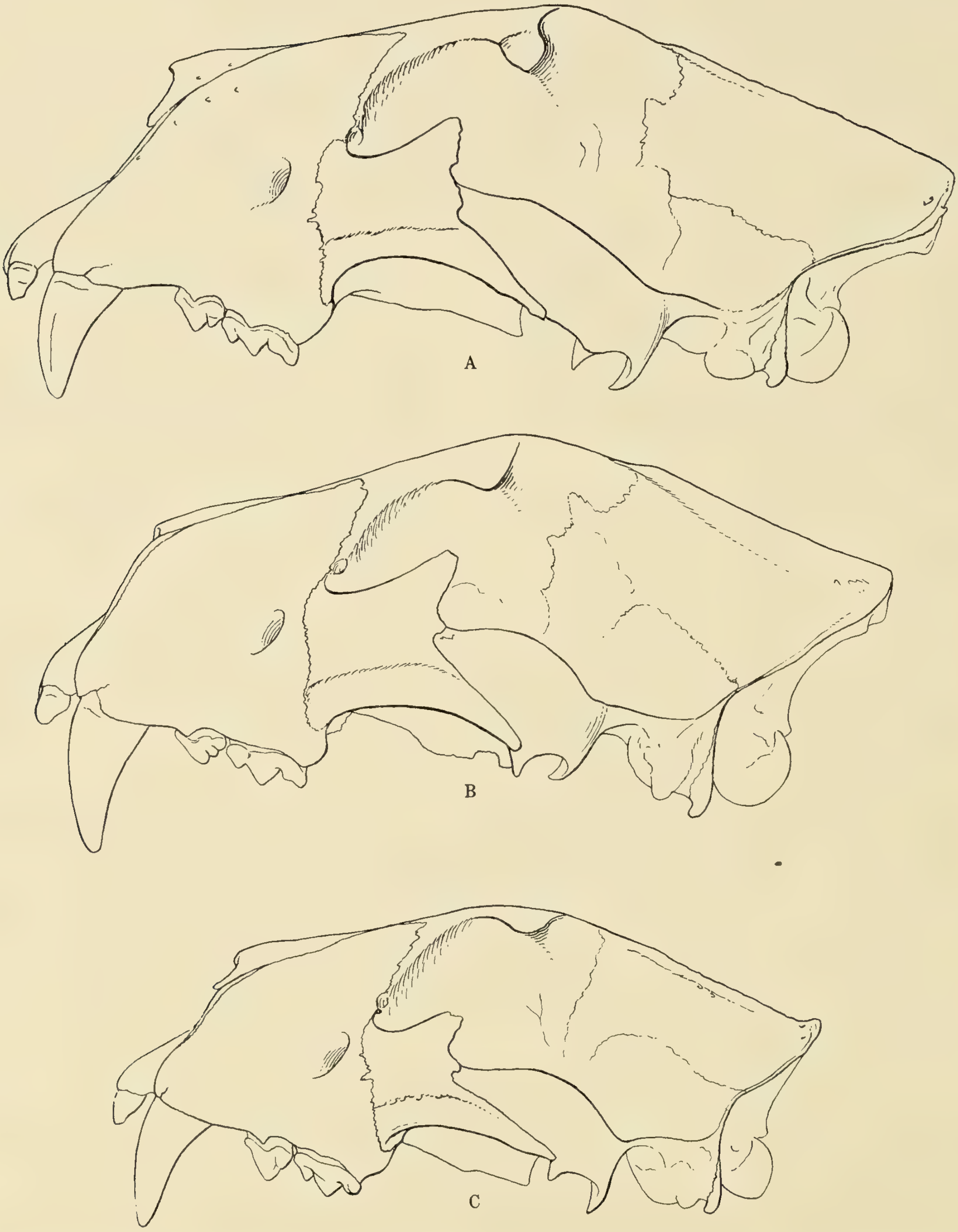

Fig. 139—*Felis atrox* Leidy. Lateral views of skulls; × 1/3. A, No. 2900-9; B, No. 2900-8; C, No. 2900-4. Compare dorsal profiles of these skulls with those of living tiger (see fig. 140, A, B,). Rancho La Brea Pleistocene.

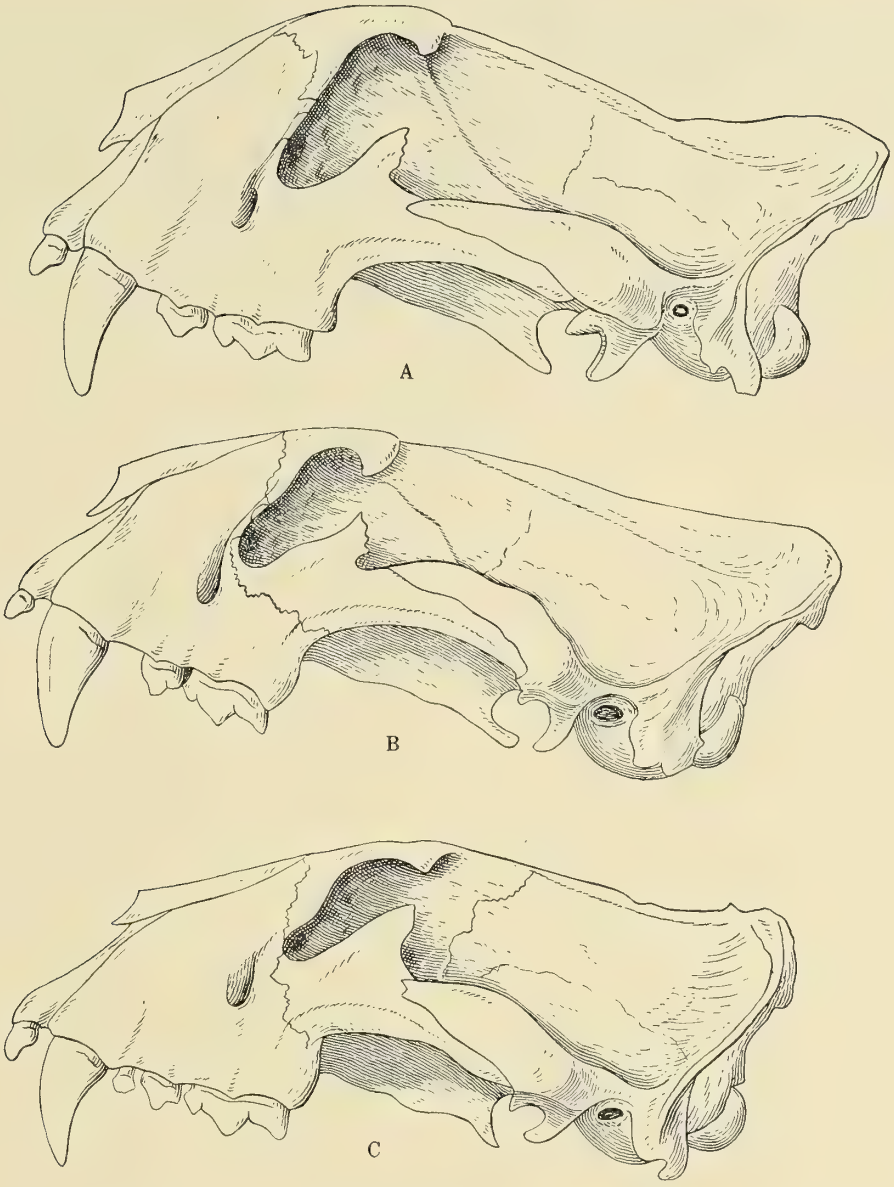

Fig. 140—Skulls of modern tiger and lioness; lateral views; × 1/3. A, skull of tiger (*Panthera tigris tigris*) from Central Provinces, showing typical shape in the Indian race; B, skull of Sumatran tiger (*Panthera tigris sumatræ*) from Sungei Kumbang, showing likeness to the lion's skull; C, skull of lioness from Mulema, Uganda, for comparison with A, B. After Pocock.

it appears to have been a little convex downwards, as is frequently the case in the lion. The symphysis rises in the gradual convex manner more usual in the latter than in the Tiger. The hiatus anterior to the molars is long, in correspondence with the size of the animal, but as in the Lion it rises relatively higher in its advance to the canine alveolus than is commonly the case in the Tiger."

Large cats, closely related to *F. atrox*, were widely distributed over the land masses of the northern hemisphere during Quaternary time. Types allied to *Felis leo spelæa* are known not only from localities in western Europe and northern Africa, but have been recorded from Quaternary deposits of Poland, Bessarabia, Russia, and more recently by Riabinin (1919) in the Urals and in the region of the Volga. In view of this range it should be remembered that the lion today is found in the Ethiopian region and in a restricted section of the northwestern portion of peninsular India, while the tiger has likewise a wide distribution in the asiatic area. Pocock (1929, p. 509) regards central and northern Asia as the original home of the latter species and states that it survives in Mongolia, Amurland, Manchuria and Korea. Pocock also calls attention to the former, more northerly distribution of these types as indicated by the occurrence of remains indistinguishable from those of modern types, in association with mammals of the Glacial Period, in deposits of northern Siberia well within the Arctic Circle (Tscherski, J., 1892, pp. 51-64, pl. 1).

During the Quaternary the known range of the large felines of the *Felis atrox* type in North America extended westward from the Mississippi Valley to the Pacific coast and southward to the Mexican Plateau. Of considerable interest is the recently recorded occurrence of *Felis atrox alaskensis* by Frick (1930, pp. 78-79) in the tundra region of Alaska. Thus in so far as their distributional areas are concerned, the range of the American form might imply a closer relationship between *F. atrox* and the tiger than between the former species and the lion. Our knowledge, however, of the faunal relationships of North America and western Europe during Quaternary time is still in a formative stage.

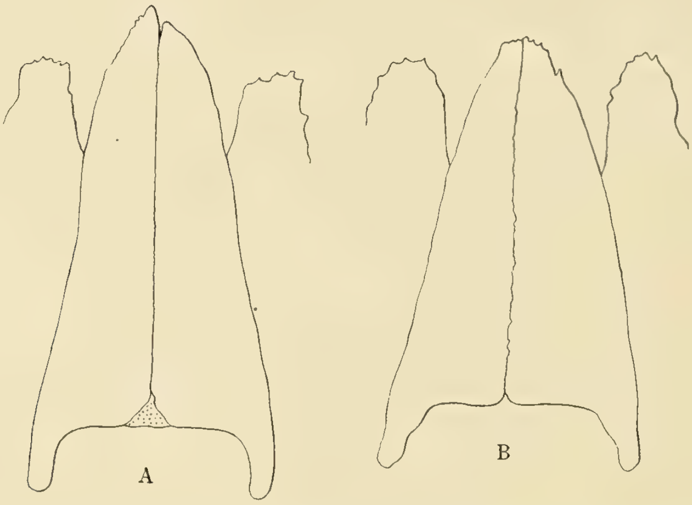

FIG. 141—Outline of nasals and portions of fronto-maxillary suture in skulls of Javan and Sumatran tigers. After Pocock. A, *Panthera tigris sondaica* Fitzinger, from Probolingo. B, *Panthera tigris sumatræ* Pocock, from Delhi; × 3/5.

Aside from the relationships which may exist between the great cats of the Quaternary of the New and Old Worlds, it is well to remember that representatives of the Felidæ may occur in Pliocene deposits of western North America. With acquisition of more complete materials from the later Tertiary it appears possible that a reasonable demonstration of the derivation of the Pleistocene types from antecedent forms in the North American area may be effected. Were this ultimately established, the structural characters displayed by *F. atrox* might receive added support as pointing toward an ancestral relationship to both the lion and tiger. Let us then consider the structural characters of *F. atrox* with a view to determining the possible resemblances of this form to the lion and tiger, employing in this survey of the Rancho La Brea materials the distinguishing features selected by Dawkins and Sanford, Boule and others principally in a study of the skulls of the modern species. See also the comparisons which have been made in the study of the skull of *Felis atrox* (pp. 168-172).

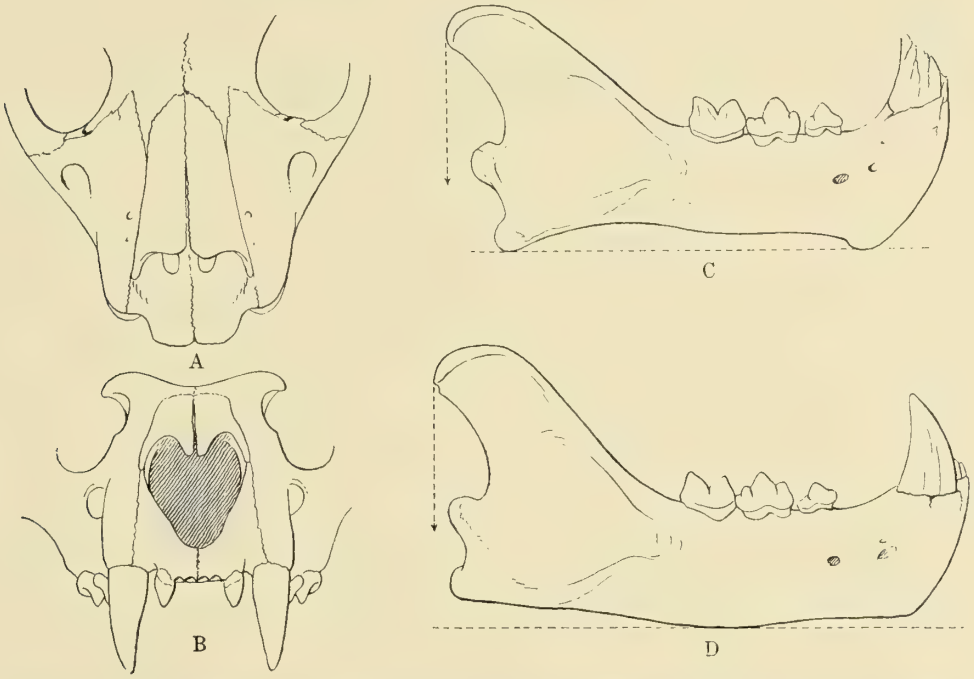

FIG. 142—*Felis atrox* Leidy. A, B, skull, No. 2900-4, dorsal and anterior views of muzzle. C, D, mandibles, Nos. 2901-5 and 2901-15, lateral views to show variation in profile of ventral border; × 1/4. Rancho La Brea Pleistocene.

I. 14 skulls examined.
  In three the frontal processes of the superior maxillaries reach a level distinctly posterior to the posterior ends of the nasals.
  In six the processes reach only slightly behind the level of the ends of the nasals.
  In five the processes reach a level with the posterior ends of the nasals.
  In no instance are the posterior ends of the nasals projected distinctly behind the level of the ends of the frontal processes of the superior maxillaries, as in the tiger.

II. 12 skulls examined.
  In one specimen the summit of the frontal process of the maxillary is distinctly acute.
  In nine the summit of this process is more or less acute.
  A slight tendency toward truncation of process is observed in two specimens.

III. 9 skulls examined.
  In six the nasal bones are flat or slightly concave from their middle back to the posterior ends.
  In two the surface is slightly convex.
  In one the surface is more distinctly convex.

IV. 12 skulls examined.

In eleven the widest diameter of the anterior nares occurs immediately below the lower outer ends of the nasal bones. From this level the opening narrows below and the lower margin is perceptibly incised as in the tiger.

In one specimen the opening appears slightly wider below, but this perhaps is due to the worn surface of the bone.

V. 12 skulls examined.

In all specimens the interorbital surface formed by the frontals is wide, slightly concave in front and more deeply so behind. A deep median concavity is usually present behind the fronto-nasal suture. The frontal surface appears to be generally flatter in skulls of comparatively young individuals.

VI. 9 skulls examined.

In attempting to state the relative position of the fronto-parietal (coronal) suture in these specimens the following cranial index was determined:

$$\frac{\text{Length from anterior end of premaxillaries to point of intersection of coronal and sagittal sutures} \times 100}{\text{Length from anterior end of premaxillaries to posterior end of inion}}$$

Three skulls give an index of......	74
Two skulls give an index of........	75
Three skulls give an index of......	77
One skull gives an index of........	78

Unfortunately no comparable index is available for modern skulls of the lion and tiger.

VII. 12 skulls examined.

In eleven skulls the position of the postpalatine foramen is relatively close to the orbital border.

In one skull the position of the foramen is slightly farther forward.

VIII. 19 mandibles examined.

In nine specimens the mandible rests on both the inferior end of the symphyseal region and the angular process, but the inferior border of the horizontal ramus is slightly to noticeably convex beneath the posterior cheek-teeth.

In one specimen it rests on the two ends of the inferior border and on the convex border of the middle portion of the horizontal ramus.

In nine specimens the convexity of the inferior border of the horizontal ramus is sufficiently prominent to cause the jaw not to rest on a plane with both the inferior end of the symphyseal region and the angular process in contact with this surface at the same time.

IX. 17 mandibles examined.

In sixteen specimens the coronoid process projects backward beyond the posterior end of the condyle.

In one specimen the coronoid process does not project backward beyond the posterior end of the condyle.

X. Canines with internal face flattened, but perhaps no more so than in the lion. Edges well defined; intermediate in their development between those of lion and those of tiger.

XI. Crowns of premolars ($P\underline{3}$, $P\overline{3}$, and $P\overline{4}$) increase in width posteriorly, slightly more so than in tiger. Cusps in some of the premolars may be lower than those in lion.

Skeletal elements—In the humerus of *Felis atrox* the articular head, when viewed from the outer side, appears to extend slightly farther back than in the lion. The upper border of the greater tuberosity descends slightly in its forward course and curves gently into the anterior border (see figs. 70, 71, B). This curvature does not give a right angle where the upper and anterior borders meet as in the modern lion, but it is not so pronounced as in the tiger. In other words, while *F. atrox* resembles the lion in this character some approach is also made to the tiger. The characters of the olecranon fossa, as distinguished by Boule, are more like those of the tiger than like those of the lion.

The radius is relatively heavier than in the lion, but the shaft is less curved than in the tiger.

In the femur of *Felis atrox* the great trochanter does not project distinctly above the level of the head. The proximal end may be level with the proximal surface of the head or may reach a point slightly below this level. The digital fossa is relatively small.

The shaft of the tibia is more curved in its longitudinal extent and in the inferior half its cross-section is more rounded than in the tiger. In some specimens from Rancho La Brea the shaft is straighter.

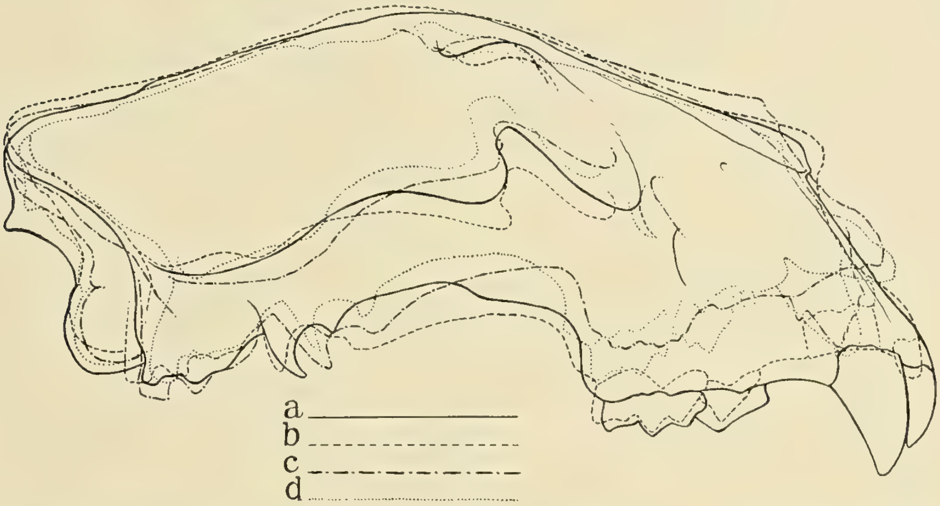

Fig. 143—Comparative outlines of skulls of Pleistocene felines. a, *Felis atrox* Leidy; Rancho La Brea, Calif. b, *Felis leo Edwardsi* (Bourguignat), Vence Cavern, Maritime Alps. After Boule. c, *Felis leo spelæa* (Goldfuss); East side of Ural Mountains, Province of Perm, Russia. After Riabinin. *d, Felis spelæa* Goldfuss; British Pleistocene. After Dawkins and Sanford. × 1/3.

Thus we note that in several characters, as seen especially in the skull, the Rancho La Brea species makes a closer approach to the lion than to the tiger. In at least two particulars, namely, shape of the external nasal orifice and extent of posterior projection of the coronoid process, does *Felis atrox* resemble the tiger. While in some specimens the inferior border of the horizontal ramus may approach in straightness that seen in the tiger, it more frequently resembles in its convexity that in the lion.

If we consider the characters which Pocock regards as distinctive on the average of the modern tiger, it follows that the large cats of the *Felis atrox* type from Rancho La Brea differ from the latter in possessing less vaulted skulls, shorter and broader nasal bones, facial portion of the skulls longer in comparison with the cranial portion, and in the more convex lower border of the horizontal ramus of the mandible. In most of these characters a closer approach is made to the lion. In form of anterior narial opening a close approach may be made to the tiger.

The North American form clearly presents structural characters in which it resembles in part the lion and in part the tiger. This combination of characters together with certain primitive features, as for example the relatively smaller size of brain, suggests a close approach of *F. atrox* to the ancestral stock from which the large felines of the Old World may have been derived.

COMPARISON OF THE LARGE EXTINCT CATS OF NORTH AMERICA AND EURASIA

The large lion, *Felis spelæa,* of the Pleistocene of the Old World, recognized and described by Goldfuss (1821) as specifically distinct from the existing lion, is now recorded from a number of localities in Eurasia and northern Africa. The well-preserved remains of this cat secured in cavern deposits of the British Isles were fully discussed and illustrated in the classic monograph by Dawkins and Sanford (1866-68). Important materials found at localities widely spread on the continent have been described by many students of Quaternary mammalian faunas, notably by Boule (1906), Pavlow (1908), Wurm (1912) and Riabinin (1919). While most authors have regarded the extinct lion as specifically different from the modern form, Boule and more recently Riabinin consider the former type as a racial variation of *Felis leo.*

If we compare the skulls of *F. leo spelæa* from the Pleistocene of the French caves and of the Ural Mountains with the series of specimens available from Rancho La Brea, it becomes evident that the former approach more nearly in size the mean rather than the extremes of the skulls from the asphalt. Below is given a table of comparative measurements of the Cajarc and Vence skulls of Boule, of the Ural specimen of Riabinin, and of three skulls of *Felis atrox* chosen from near the mean of the Rancho La Brea series. The skull from the Ural Mountains, of which excellent illustrations are given by Riabinin (1919, pls. 1 to 4) is slightly smaller than No. 2900–7 of *Felis atrox.*

Not only is there close correspondence in size, but there is likewise considerable resemblance in structural details between the American and Eurasiatic types. In figure 143 the outline of Riabinin's specimen, shown in lateral view reversed, is superimposed on the outline of skull No. 2900–7 from Rancho La Brea. The former skull as represented in this relationship exhibits less vertical depth of muzzle than in *F. atrox* with, however, a larger posterior cranial region than in the latter. The asphalt type resembles the Russian form in the expanse of nasal shown in lateral view and in the position of the orbit and postorbital processes. The orbit is, however, smaller in the latter species, while the paroccipital process is larger than in the American form. The shape of the external nares, as viewed from the front, resembles that usually seen in skulls of *F. atrox.*

In the mandible the ventral outline of the horizontal ramus, position of mental foramina, and character of ventral border of masseteric fossa are features in which Riabinin's specimen resembles *Felis atrox.* The diastema between the alveolus for $\overline{P3}$ and that for the canine is shorter in the former species than in the latter. In the American species, the angle projects downward slightly more and the coronoid process is less erect and sweeps backward farther than in the former type. Moreover, the anterior end of the masseteric fossa is narrower dorso-ventrally than in *F. leo spelæa.*

Unfortunately the dentition in the skull from the Ural Mountains is not sufficiently complete to permit of adequate comparisons. The lower teeth are better preserved in the mandible which Riabinin refers to *Felis leo* cf. *Edwardsi* (Riabinin, 1919, pl. 5). This specimen is nearly comparable in size to mandible No. 2901-5 of *F. atrox* from Rancho La Brea. While the length of the cheek-tooth series approximates closely that in the latter, the diastema between the alveolus for P$\overline{3}$ and the lower canine is shorter. There is correspondence between the two types in size of canine and in the principal features displayed by the cheek-teeth. In this specimen the front end of the masseteric fossa is again broader in dorso-ventral direction than in *F. atrox*, although the difference may not be great.

The skull from the cavern of Vence, which has been referred to the race *F. leo Edwardsi* and has been figured by Boule (1906, pl. 3) again exhibits structural features that are similar to or identical with the characters seen in *F. atrox*. The pro-

TABLE 95—*Comparative measurements (in millimeters) of skulls of Felis spelæa Goldfuss and Felis atrox Leidy*

List of measurements*	Sandford Hill Cave	Hutton Cave	Sundwig British Museum	Sandford Hill Cave No. 2	*Felis atrox* R. L. B. No. 2900–8	*Felis atrox* R. L. B. No. 2900–7	*Felis atrox* R. L. B. No. 2900–5	*Felis atrox* R. L. B. No. 2900–9
1 Basal length (median)	330.2	294.6	266.7	....	321.9	313.7	314.6	380.8
2 Zygomatic width	231.4	233.6	....	....	245	235.3	238.3	296.5
3 Height from palate to supra-orbital	124.4	106.6	121.9	....	120.4	108.9	115.8	138.2
4 Extreme length	....	335.2	304.8	....	391.9	373.5	367	429.5
5 Sagittal length of parietal	....	101.6	86.3	....	115	*a*107	*a*90	139.6
6 Median frontal length	116.8	114.3	104.1	....	134	*a*125.7	*a*121.5	131.2
7 Median nasal length	....	....	....	....	96.3	89.5	91.5	104.1
8 Maximum parietal width	91.4	88.9	83.8	....	95.4	96.2	95	97
9 Maximum frontal width	....	114.3	96.5	....	113.3	119.6	*a*110.5	*a*132
10 Width at parieto-frontal suture	68.5	76.2	63.5	....	74.4	79.4	77.2	87.4
11 Minimum width at orbits	81.2	68.5	63.5	....	83.6	83	80.3	98
12 Maximum width of nasals	....	63.5	58.4	73.6	64.7	72.5	70	*a*76.6
13 Malar width at maxillary suture	162.5	152.4	149.8	177.8	171.4	167.1	163.6	186.8
14 Infra-orbital width of maxillaries	101.6	99.0	91.4	104.1	....	....	....	....
15 Width of maxillaries above Pm$\underline{2}$	....	99	99	121.9	116.8	112	112.6	122.5
16 Maximum width of premaxillaries	....	71.1	71.1	93.9	78.2	81.1	76.5	86.6
17 Incisal width	....	45.7	45.7	55.8	51.6	51	49	51.5
18 Paroccipital width	....	109.2	....	....	109.7	*a*108.8	96	123.7
19 Occipital height	....	99	....	....	116.1	103.6	106.5	120
20 Mastoidal width	139.7	134.6	124.4	....	144.8	140.8	138.2	....
21 Maximum tympanic width	93.9	93.9	91.4	....	112	104	110.2	133.5
22 Minimum between tympanics	33.0	33.0	38.1	....	35	33.5	34.4	33.5
23 From paroccipital to anterior border of articular	....	81.2	....	....	89.3	89.6	88.7	102.4
24 Glenoid cavity to alveolar border	99.0	88.9	86.3	....	100.4	96.4	92.1	125.1
25 Maximum internal width of zygoma	73.6	78.7	....	....	82.4	79	82.1	105.1
26 Minimum width of posterior nares	....	....	33.0	....	37.5	35.5	40	37.8
27 Minimum palatal width	....	....	45.7	....	78	75.6	75.6	86.1
28 Maximum width, palatal bones	....	88.9	58.4	....	88.7	89.1	88.6	100.6
29 Width of maxillaries at Pm$\underline{4}$ (internal)	129.5	127	109.2	152.4	125.4	125.7	120.5	140.8
30 Width at premaxillary suture	....	58.4	50.8	71.1	59.4	59.3	59.5	65.8
31 Median length of entire palate	....	....	147.3	....	167.3	162.3	161.2	185
32 From alveolar border of M$\underline{1}$ to external edge of premaxillary	....	134.6	127	175.2	132.2	140.6	137	150.3
33 Lachrymal to infra-orbital process	55.8	50.8	....	....	63.5	63	66.3	69.8
34 Maximum from malar to supra-orbital process	73.6	66	63.5	....	86	85.2	81.2	86.7
35 Thickness of arch of infra-orbital foramen	15.2	15.2	15.2	22.8	17.1	19.2	15.8	20.5
36 Maximum width of anterior nares	....	55.8	45.7	68.5	63.9	63.2	62.4	67
37 From posterior palatal foramen to posterior edge of palate	15.2	15.2	15.2	17.7	17.7	20.8	17.9	13.7
38 Temporal length of frontals	55.8	55.8	55.8	....	....	....	....	....

* The list of measurements and the measurements in the first four columns of table are from W. Boyd Dawkins and W. Ayshford Sanford (1868) and are based on skulls from the British Pleistocene.

a, Approximate.

TABLE 96—*Comparative measurements (in millimeters) of mandibles of Felis spelæa Goldfuss and Felis atrox Leidy*

List of measurements	*Felis spelæa**										*Felis atrox*			
	Taunton Museum							Dr. Spurrel's Collection						
	Bleadon Cavern Bl. B. I.	The same, left ramus	Sandford Hill S.H.B.I.	The same, left ramus	Sandford Hill Cave. S. H. B. 2	Bleadon Cavern B. L. B. 2	Mendip. William's Collection Wms.	Crayford Brick-earth	Crayford Brick-earth	Ilford Brick-earth. Mr. Brady's Collection	R. L. B. No. 2901–3	R. L. B. No. 2901–15	R. L. B. No. 2901–5	R. L. B. No. 2901–6
1 Symphysis to condyle	251.5	251.5	228.6	228.6	....	....	....	....	....	....	308.6	273.7	251.9	209.6
2 Length of the inferior border from symphysis to angle	205.7	203.2	203.2	203.2	....	....	....	....	....	104.1	238	231.2	196.4	173.5
3 Length of exterior border of symphysis	91.4	91.4	76.2	76.2	....	....	....	....	....	....	97.4	83.7	84	66.6
4 Height of coronoid process from angle	127	....	....	....	....	....	....	121.9	....	....	151.6	133.7	125.5	97
5 Transverse measurement of condyle	....	....	....	....	....	....	....	55.4	....	....	74.2	70	56.8	....
6 Vertical measurement of condyle	....	....	20.3	30.5	....	....	....	35.6	....	....	27	26.1	23	18.3
7 Canine to $\overline{M1}$, inclusive	127	129.5	114.3	116.8	....	....	....	....	....	....	154.7	142.5	131.8	116.2
8 Canine to $\overline{Pm3}$, exclusive	22.9	22.9	35.6	33	....	....	....	....	....	....	67	61.9	55.4	49.7
9 Molar series, length of	81.3	96.5	66	66	78.7	83.8	73.7	....	78.7	....	89.1	82.1	77.2	68.2
10 Depth of jaw anterior to $\overline{Pm3}$	61	53.3	43.2	43.2	....	73.7	....	....	....	....	59.4	51.8	48.4	40
11 Depth of jaw posterior to $\overline{M1}$	63.5	58.4	50.8	48.3	50.8	71.1	....	....	....	....	61.3	57.4	49.6	46
12 Extreme length from symphysis to end of coronoid process	256.5	....	....	....	....	....	....	....	....	....	330.4	282.9	267	213.7

* Measurements from W. Boyd Dawkins and W. Ayshford Sanford (1866) and based on specimens from the British Pleistocene.

portions of this skull are like those of No. 2900–7 from Rancho La Brea. The masseteric fossa does not extend forward below the posterior portion of M$\overline{1}$ as in *F. atrox*. Likewise the diastema is a trifle shorter.

TABLE 97—*Comparative measurements (in millimeters) of skulls of extinct true felines*

Measurements	*F. leo spelæa* Cajarc skull (after Boule)	*F. leo Edwardsi* Vence skull (after Boule)	*F leo spelæa* Ural Mts. skull (after Riabinin)	*F. atrox* R. L. B. No. 2900–8	*F. atrox* R. L. B. No. 2900–7	*F. atrox* R. L. B. No. 2900–5
Length in straight line from incisive border to posterior surface of occipital condyles	350	320	330	348.7	336.6	332
Total length	393	393	355	391.9	373.5	367
Greatest width across zygomatic arch	265	241	244	245	235.3	238.3
Length of canine at alveolar margin	27	27	30	30.5	32	.....
P$\underline{2}$, length	9	9	10	9	9.8	9
P$\underline{3}$, length	26	26	25.5	27.8	26.7	25.6
P$\underline{4}$, length	37	39	37	40.3	40	39
M$\underline{1}$, length	5	...	7	.....	.....	.....
M$\underline{1}$, width	10	...	15	.....	.....	.....
Mandible	...	...	...	No. 2901–16 R. L. B.	No. 2901–7 R. L. B.	No. 2901–5 R. L. B.
Length from incisive border to condyle	254	235	238	242	242	243.8
Height in front of P$\overline{3}$	47	47	49	.....	47	.....
Height behind M$\overline{1}$	54	51	55	47.3	51.8	49.7
C, length at alveolar border	23	24	29	25.8	*a*29	25.2
P$\overline{3}$, length	20	18	19	18.2	18.9	18.1
P$\overline{4}$, length	26	28	27	26.4	27.7	28.7
P$\overline{4}$, width	13	13	13	12.6	13.5	14
M$\overline{1}$, length	28	29	28	28.3	27.5	28.5
M$\overline{1}$, width	15	14	14.5	13	14.6	14.9

a, Approximate.

In P$\underline{3}$ of *F. atrox* the cusp anterior to the principal cusp lies more noticeably to the inner side of the median fore and aft axis of the tooth than in the specimen described by Boule. This is clearly seen when comparison is made with the illustration of the upper cheek-teeth of the Vence skull (Boule, 1906, pl. 3, figs. 2, 2*a*). In the Californian specimens the greatest transverse swelling of the crown of P$\underline{3}$ is slightly farther back than in *F. leo Edwardsi.* Moreover, while P$\underline{4}$ in the latter compares favorably in length with the upper carnassial of No. 2900–7, its width particularly across the protocone is somewhat greater, although it does not exceed in this measurement P$\underline{4}$ of somewhat larger skulls from Rancho La Brea. The paracone in this tooth may not stand quite so high as in *F. atrox.* There are no marked differences in the lower teeth.

Measurements of the principal skeletal elements of the Cajarc and Vence skeletons, as given by Boule, are listed in table 98. In the third column of this table are given the comparable measurements of *Felis atrox.* Individual measurements of the latter type represent the average of the measured specimens from Rancho La Brea. While we may conclude from the comparisons that individuals of *Felis atrox* of average size were slightly larger than either the Cajarc or Vence animals, this difference is not very great.

Skulls and teeth of *Felis spelæa* from the British Pleistocene, described by Dawkins and Sanford, include both large and small forms. Judging from the measurements given by these authors this species was apparently subject to considerable variation in size, in which respect there is resemblance to the American type. In measurements of individual teeth and of some skeletal elements occasional specimens are found to be actually larger than the largest types of *F. atrox* recorded from Rancho La Brea. In tables 95, 96 are given the measurements of the skull and mandible in British specimens, after Dawkins and Sanford, followed by comparable measurements of some of the specimens from the asphalt.

TABLE 98—*Measurements (in millimeters) of skeletal elements of extinct true felines*

	Cajarc skeleton (after Boule)	Vence skeleton (after Boule)	*Felis atrox* Leidy avg. of meas. spec.
Scapula:			
Greatest diameter of the glenoid cavity	62	59	76
Humerus:			
Total length	380	336	368.5
Anteroposterior diameter at middle	55	58	60.3
Transverse diameter at middle	36	33	36.7
Maximum width of distal extremity	102	88	100
Width of trochlea	66	65	
Radius:			
Total length	327	308	344.5
Greatest diameter of articulating cup	45	41	51.3
Smallest diameter of articulating cup	31	31	38.3
Anteroposterior diameter at middle	23	39	23.4
Transverse diameter	37	40	38.4
Width of distal extremity	71	69	68.4
Width of carpal articulation	48	48	
Ulna:			
Total length	403	379	416
Metacarpal III:			
Total length	121	120	126.6
Transverse diameter at middle	17	17	17.7
Femur:			
Total length	410	382	421.3
Anteroposterior diameter at middle	33	33	35.3
Transverse diameter at middle	37	36	39
Width across condyles	88	84	90.8
Tibia:			
Total length	353	341	361.7
Transverse diameter of proximal extremity	93	91	97.9
Anteroposterior diameter at middle	38	41	
Transverse diameter at middle	36	33	36.4
Transverse diameter of distal extremity	64	63	67.5
Fibula:			
Maximum thickness at middle	16	...	16.1
Metatarsal III:			
Total length	144	137	146.1
Transverse diameter at middle	20	20	21.3

In the series of measurements recorded for nine specimens of both P$\underline{3}$ and P$\underline{4}$ of *F. spelæa*, the greatest anteroposterior diameters are seen to be slightly in excess of those in the largest skull (No. 2900–3) of the Museum collection from Rancho La Brea. Similar measurements for P$\overline{4}$ and M$\overline{1}$ reveal a closer resemblance between *F. spelæa* and *F. atrox*.

A comparison of the structural details of the crowns of individual teeth emphasizes again the essential similarity between *Felis atrox* and *F. spelæa*. In the latter the incisors, both upper and lower, have longer fangs than in the true cat of the asphalt. The roots of the lower incisors appear, however, to be slightly wider in *F. atrox*.

RELATIONSHIP OF FELIS ATROX TO THE JAGUAR

In nearly all of the characters in which the jaguar differs decidedly from the puma (see below under the discussion of the puma the list of comparative characters) this cat resembles the large true felids of the Quaternary of the northern hemisphere.

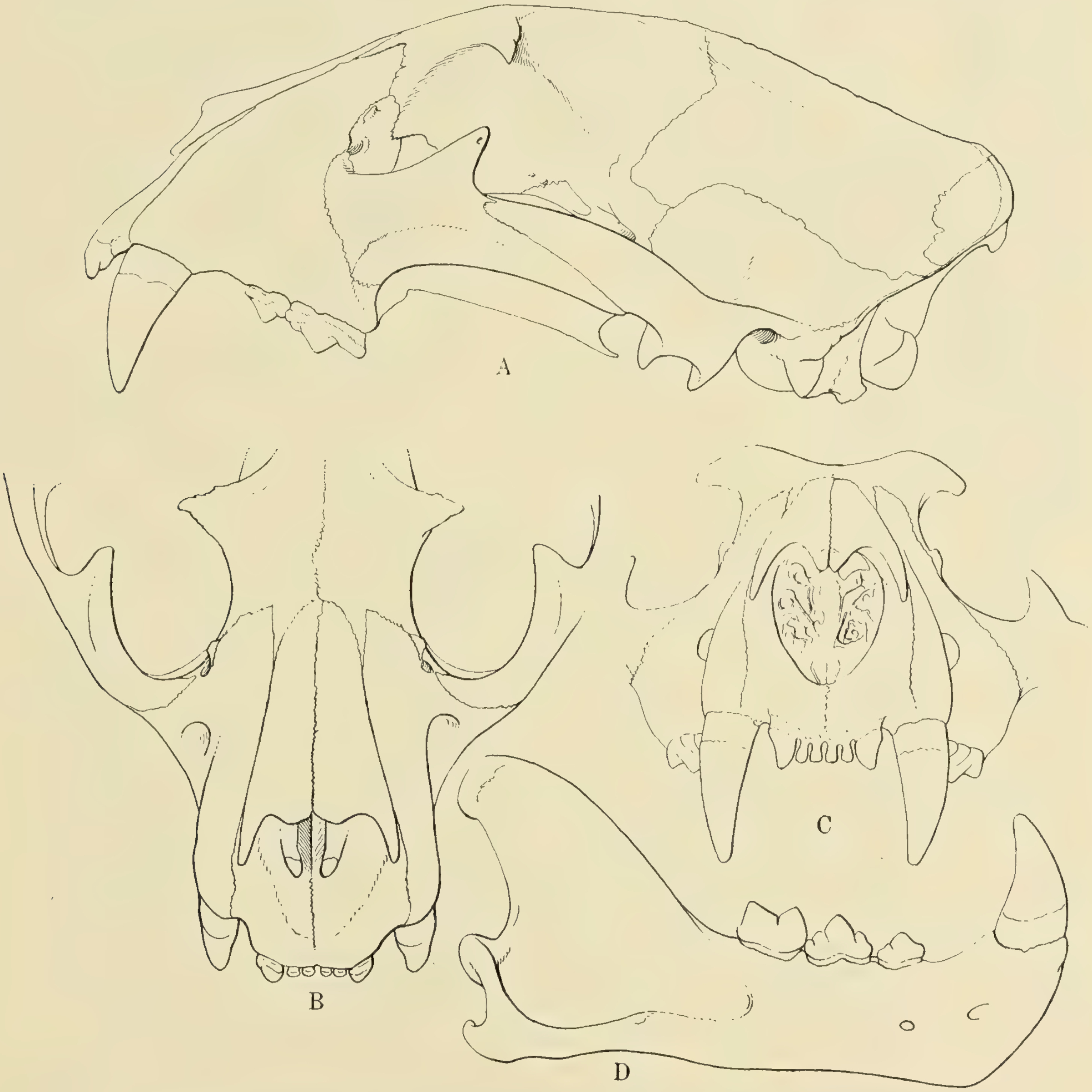

Fig. 144—Skull of modern jaguar *Felis onca*, No. 9703 U. S. N. M.; × 1/2. A, lateral view; B, dorsal view of facial region; C, anterior view; D, lateral view of mandible.

The jaguar resembles *Felis atrox* in the shape and proportions of the skull (compare cranial indices), in shape of occiput, and in the important features of the basicranial region. The latter characters are shown in figure 145, A to D. In the structure of the anterior end of the tympanic bulla and particularly the forward extension of the ectotympanic process (fig. 145, A, *ec. p.*) the jaguar is more like the lion and *Felis atrox* than like the puma. The entotympanic process (*en. p.*) is flattened as in *F. atrox*, not ridged as it usually is in the puma. In the mandible considerable similarity is to be noted between the jaguar and *F. atrox* in the development of the angle and in the form and depth of the anterior end of the masseteric fossa.

The principal differences in the skull between the jaguar and the large Pleistocene cat of North America are (1) smaller size, (2) narrower frontal development between orbits and an average greater bizygomatic width, (3) greater median indentation of the postnarial border of the palatine, (4) greater development of lachrymal eminence. Additional differences may be noted. These are however not always constant when comparisons are made with all the skulls in the Ranch La Brea collection. When the jaguar skull is viewed from in front the orbits appear to be round-oval with long diameter relatively not so great as in *F. atrox*. The external nares may be quite narrow in the jaguar, although the nasals are relatively broad. Moreover, the outer forward ends of the nasals may be relatively heavier than in *F. atrox*.

The maxillary region lying between the orbital rim and the nasal boundary is depressed somewhat more than in the Rancho La Brea species, although this character may occur in some specimens (No. 2900-4) from the asphalt as well as in the modern lion. The depression of the maxillary tends to accentuate the difference in slope between the side of the face and the dorsal surface of the nasals. In the jaguar this angulation of the lateral and dorsal surface of the face may be carried backward on the frontal so that the surface above the dorsal rim of the orbit is distinct from the upper surface of the frontal sloping inward to the median line.

When the face is viewed from the side the upper end of the maxillary, as measured between the nasal and orbital borders, is narrower in the jaguar than in the lion and in *F. atrox*. The transverse narrowing of the skull across the frontals behind the postorbital processes appears to be distinctly greater in the jaguar than in the Pleistocene species. However, a tendency toward this narrowing is seen in specimen No. 2900-8 and in No. 2900-9. The latter skull, it should be recalled, is featured by a distinctly large bizygomatic width. The brain-case in the jaguar exhibits relatively greater lateral expansion than in the Pleistocene species. The postpalatine foramina are usually somewhat farther removed from the orbital border than in *F. atrox*. The postnarial passage gives the appearance of being longer in proportion to its width. However, in narrowness of the postnarial passage *Felis atrox* is intermediate between the jaguar and the African lion. In *F. atrox* the median portion of the palatine, forming a floor to this passage, appears to extend slightly farther back than in the jaguar. Of perhaps greater importance is the anteroposterior extent of the pterygoid plate, which may be as great as or even greater than that in the skulls from the asphalt.

The mandible in the jaguar may rest on a flat surface with the symphyseal end and angle touching this surface. Specimens are available in which a third point of contact with the flat surface may be established by the convex inferior

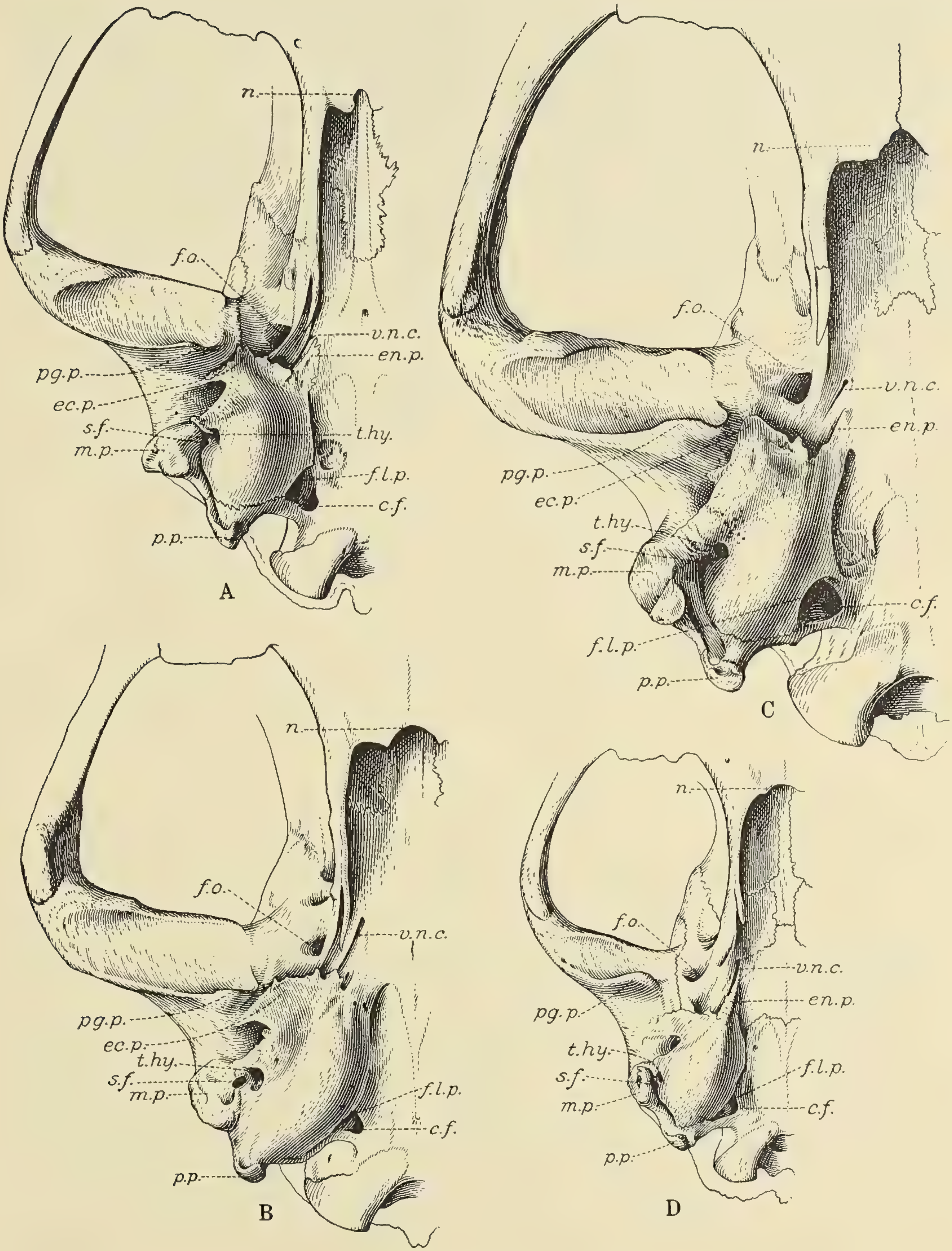

FIG. 145—Comparative views of basicranial region of skulls. A, *Felis onca*; B, *Felis leo*; C, *Felis atrox*; D, *Felis concolor*; × 2/3. *f.o.*, foramen ovale; *s.f.*, stylomastoid foramen; *f.l.p.*, foramen lacerum posterius; *c.f.*, condylar foramen; *v.n.c.*, canal for Vidian nerve; *n.*, median notch in posterior palatine border of palate; *en.p.*, entotympanic process; *ec.p.*, ectotympanic process; *pg.p.*, postglenoid process; *m.p.*, mastoid process; *p.p.*, paroccipital process; *t.hy.*, tympanohyal pit.

border of the horizontal ramus. In other specimens the convexity of the inferior border is such as to prevent the contact of the angle and the symphyseal end with a horizontal plane at the same time. In other words, the range in variation of this character appears to be as great in the living species as in *F. atrox.* The backward sweep of the coronoid process is not so great in the jaguar as in the Rancho La Brea form. The shape of this process is also somewhat different for the lower half is broader anteroposteriorly than in the extinct cat from the asphalt.

In the dentition there is again a much greater resemblance between the jaguar and the great Quaternary cats of the northern hemisphere, including *F. atrox*, than between the former type and the living or fossil pumas. In $P\underline{3}$ the anterior end may be relatively narrower transversely than in *Felis atrox.* The principal cusp in this tooth and in $P\overline{3}$ may be lower than in the living lion, in which respect a greater resemblance exists with at least some specimens from the asphalt.

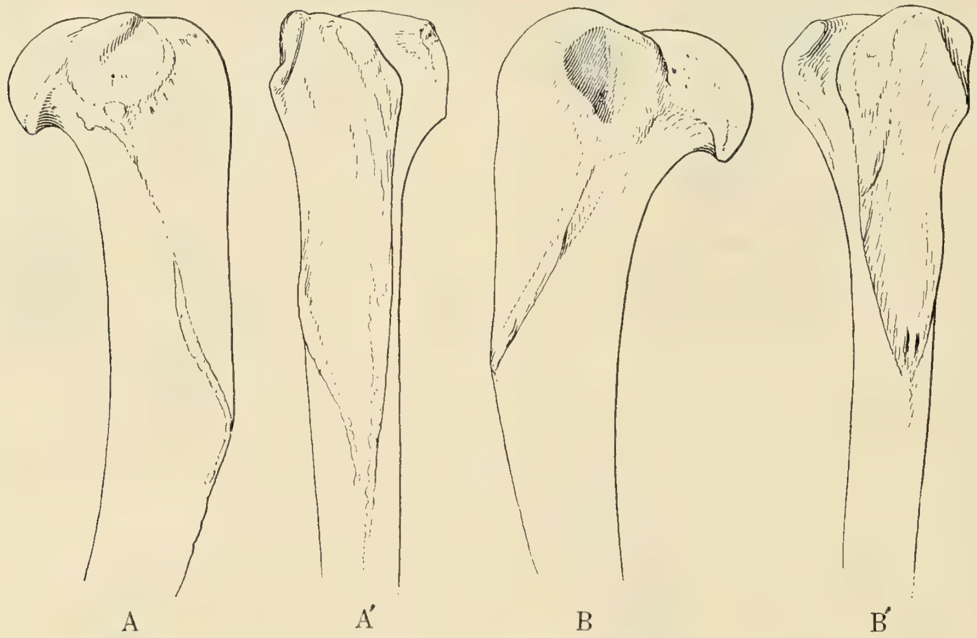

FIG. 146—Comparative views of humeri. A, A′, *Felis onca*, lateral and anterior views; B, B′, *Felis bituminosa* n. sp., No. X8809 L. A. Mus. Coll.; lateral and anterior views; × 1/2.

Comparison of appendicular elements.—Resemblance between *Felis atrox* and the jaguar is seen in the profile of the greater tuberosity of the humerus (compare fig. 71B and fig. 146A). Less difference in this character is presented by the modern lion (see p. 182, fig. 9) than by the puma (fig. 146, B, B′).

The ulna of the jaguar, in radial aspect, is straighter in its longitudinal extent than in either the lion or in *F. atrox.* In the latter forms the end opposite and above the greater sigmoid cavity sweeps backward more than in the jaguar, and gives a somewhat different appearance to this portion of the ulna. Moreover, the olecranon process projects relatively farther above the sigmoid notch in the jaguar than in the lion and in the form from the asphalt. *F. atrox* deviates less from the jaguar in this character than does the African lion. When viewed from in front the anterior surface of the process above the notch is broadly rounded transversely, whereas in *F. atrox* and in *F. leo* a sharp ridge is usually developed. The fossa on the proximal surface of the olecranon process is shallower in the jaguar and the eminence on each side of the forward end of the fossa is not so conspicuous as in the extinct cat and in *F. leo.*

The metapodials, particularly the third, when viewed from the side show more bowing in their longitudinal extent in the jaguar than in *F. atrox.* In this character the latter form likewise exhibits a greater resemblance to the lion.

Differences in the proportions of the principal limb segments have already been noted (see page 111).

That there are important resemblances between the Rancho La Brea *Felis atrox* and the living jaguar may well be expected. In this connection it is interesting to mention that Freudenberg (1910, pp. 230-231) speaks of *Felis imperialis* as a giant jaguar. Doubtless the jaguars find their ancestry in antecedent forms of the North American later Cenozoic and the large cats of the *Felis atrox* type may be regarded as the last representatives of a group whose lineage leads back to the stem from which these southern Nearctic and Neotropical species have also been derived.

The differences which prevail between the jaguar and *F. atrox* are certainly not of the fundamental order seen to exist between the jaguar and the puma. Rather are they to be regarded as the result of adjustments whose impress during the Quaternary has developed in *Felis atrox* a creature like the jaguar but with certain lion-like characteristics. Recognition of the wide distribution of the great cats of the Pleistocene over the northern hemisphere, and of the relationship existing between *F. atrox* and the jaguar, furnishes added reasons for regarding all these forms as of a distinct group to which the name *Panthera* might be applied.

The history of the great cats of the *Felis atrox* type and of the jaguars may parallel that of the great short-faced bears and of the spectacle bear in the New World. Presumably in each instance the living form is related rather closely to the extinct type. Moreover, insofar as an independent history is concerned, the puma would have a relationship to this branch of the Felinæ similar to that of the black bear—grizzly bear group to the Tremarctinæ.

SMALLER CATS OF THE GENERA FELIS AND LYNX

Remains of pumas from the asphalt are distinctly less numerous than those of the larger cats of the *Felis atrox* group. At least two and possibly three forms are to be distinguished on the basis of the material available. Of the two types of pumas recognized as specifically distinct from the modern *Felis concolor*, *F. daggetti* is regarded as differing to a greater degree and is more widely divergent from this species than is *F. bituminosa.* Some jaw specimens in the collection can not be distinguished readily from those of *F. concolor.* Possibly the latter form was also present in the Pleistocene fauna. On the other hand, the range of variation in size of jaw and teeth in *F. bituminosa* may have been greater in that species than in the existing *F. concolor* and of such extent as to include individuals which, in at least character of size, are indistinguishable from the latter species. The series of specimens from the asphalt is not however sufficiently large nor continuous to demonstrate this definitely. The species *Felis concolor* is therefore retained, at least for the present, in the list of cats from Rancho La Brea.

The skull and dentition in these cats present so many points of contrast with those of the jaguars that in many instances a ready identification of specimens can be made. Before referring more particularly to the characters of the pumas from

TABLE 99—*Measurements (in millimeters) of skull of jaguar*

	Felis onca No. 100122 Brazil U. S. Biol. Surv.	*Felis onca* No. 100123 Brazil U. S. Biol. Surv.	*Felis onca* No. 49393 Brazil U.S.N.M.	*Felis onca* No. 12176 ♂ Costa Rica U.S.N.M.	*Felis onca* No. 239343 Costa Rica U.S.N.M.	Jaguar No. 244507 ♂ Arizona U. S. Biol. Surv.	Jaguar No. 247337 ♂ Arizona U. S. Biol. Surv.	*Felis hernandesii* No. 9703 Tehuantepec U.S.N.M.	Jaguar No. 231961 ♀ Arizona U. S. Biol. Surv.	Jaguar No. 137039 Venezuela U. S. Biol. Surv.	Jaguar No. 179171 Mexico U. S. Biol. Surv.	*Felis hernandesii* No. 249824 ♀ Guatemala U.S. Biol. Surv.
Length from anterior end of premaxillary to posterior end of condyles	242.6	235.6	234	233	198 1	237.3	241.8	237.8	193.9	213.1	186.7	183.9
Basal length from anterior end of premaxillary to inferior notch between condyles	227.4	219.5	218.7	216.9	186	222.4	225.1	222.9	179.8	198.3	173.2	169.9
Length from anterior end of premaxillary to posterior end of inion	268.2	267.4	268.7	263.1	222.8	272.5	275.9	268	217.3	237.6	201.3	202.6
Length from anterior end of premaxillary to anterior end of posterior nasal opening	110.2	105.4	106.9	100.9	88.2	108.4	106.3	108.3	85.9	97.4	82.6	88
Length of palate from anterior end of premaxillary to line tangent to posterior surfaces of maxillary parapets	96	94.3	95.7	95.4	80	96.6	99.4	92.5	78.7	85	77.7	77.4
Length from posterior end of glenoid cavity to posterior end of condyles	66.6	66	63.3	60.7	54.5	62	65	66.5	53.3	59.6	54.1	52
Anteroposterior diameter of nasals	65.3	59.7	56.2	65.8	55.5	62.3	64.3	61.8	51.6	55.3	48.8	50
Width of anterior nares	37.6	38.2	37.9	39.7	33.4	40.7	38.4	41.2	34.1	37.3	30.7	30.9
Greatest width across muzzle at canines	75	71.6	72.8	70.1	60.4	76.3	77.9	70.7	64.2	66.7	55.5	59.5
Least width between superior borders of orbits	46.7	46.7	46.1	44	42.3	50.8	52.1	50.4	44.2	45.6	38.3	35.5
Width across postorbital processes	74.1	81.4	78	70	70.3	76.2	73.1	80	68.5	74.3	53.6	55.6
Least width of postorbital constriction	46.9	49.3	44.7	43.2	43.9	46.4	47.8	46.8	43.5	47.5	44.8	38.8
Greatest width across zygomatic arches	181.2	175.3	181.9	175.9	150	188.5	183.6	187.6	154.9	163.8	143.3	139.4
Anterior palatal width between superior canines	35.9	36.4	35.5	36.7	28.9	39.1	38.8	36.5	34.2	33.8	27	27.6
Posterior palatal width between inner roots of superior carnassials	61.1	58.6	60.6	55.3	50.5	59.6	59.3	55.8	54.2	54.8	46.5	49
Greatest transverse diameter across auditory bulla, measured from foramen lacerum posterius to external auditory meatus	27.8	26.5	26.8	24.7	21.8	26	26.9	27.2	23.5	25.9	21.8	22.1
Greatest width across mastoid processes	114	110.3	115.7	104.6	95.5	111.6	116.6	111.8	95.9	101	85.2	86.7
Greatest diameter across condyles	48.6	46	49.4	45.9	44.4	46.7	48.8	50.7	42.6	47	43.4	44.8

TABLE 100—*Skull and dental indices of jaguar*

	Felis onca No. 100122 Brazil U. S. Biol. Surv.	*Felis onca* No. 100123 Brazil U. S. Biol. Surv.	*Felis onca* No. 49393 Brazil U.S.N.M.	*Felis onca* No. 12176 ♂ Costa Rica U.S.N.M.	*Felis onca* No. 239343 Costa Rica U.S.N.M.	Jaguar No. 244507 ♂ Arizona U. S. Biol. Surv.	Jaguar No. 247337 ♂ Arizona U. S. Biol. Surv	*Felis hernandesii* No. 9703 Tehuantepec U.S.N.M.	Jaguar No. 231961 ♀ Arizona U. S. Biol. Surv.	Jaguar No. 137039 Venezuela U. S. Biol. Surv.	Jaguar No. 179171 Mexico U. S. Biol. Surv.	*Felis hernandesii* No. 249824 ♀ Guatemala U.S. Biol. Surv.
Anterior narial index	17	17	17	18	18	18	17	18	19	19	18	18
Index of interorbital breadth	21	21	21	20	23	23	23	22	24	23	22	21
Breadth index of postorbital processes	33	37	36	32	38	34	32	36	38	37	31	33
Index of postorbital constriction	21	22	21	20	24	21	21	21	24	24	26	23
Bizygomatic index	80	80	83	81	81	85	82	84	86	83	83	82
Index of palatal length	42	43	44	44	43	43	44	42	44	43	45	46
Index of anterior palatal breadth	37	39	37	38	36	40	39	39	39	40	35	36
Index of posterior palatal breadth	64	62	63	58	63	62	60	60	69	64	60	63
Diametral index of superior canine	83	75	..	78	80	..	79	78	81	77	83	83
Diametral index of $\mathrm{M}\overline{1}$ $\frac{\mathrm{W\ M}\overline{1} \times 100}{\mathrm{L\ M}\overline{1}}$	51	52	55	52	52	51	49	53	49	49	50	52
Length index of $\mathrm{P}\overline{4} - \mathrm{M}\overline{1}$ $\frac{\mathrm{L\ P}\overline{4} \times 100}{\mathrm{L\ M}\overline{1}}$	99	95	104	103	91	95	93	95	97	95	95	94

Table 101—*Measurements (in millimeters) of mandible of jaguar*

	Felis onca No. 100122 Brazil U. S. Biol. Surv.	*Felis onca* No. 100123 Brazil U. S. Biol. Surv.	*Felis onca* No. 49393 Brazil U.S.N.M.	*Felis onca* No. 12176 ♂ Costa Rica U.S.N.M.	*Felis onca* No. 239343 Costa Rica U.S.N.M.	Jaguar No. 244507 ♂ Arizona U. S. Biol. Surv.	Jaguar No. 247337 ♂ Arizona U. S. Biol. Surv.	*Felis hernandesii* No. 9703 Tehuantepec U.S.N.M.	Jaguar No. 231961 ♀ Arizona U. S. Biol. Surv.	Jaguar No. 137039 Venezuela U. S. Biol. Surv.	Jaguar No. 179171 Mexico U. S. Biol. Surv.	*Felis hernandesii* No. 249824 ♀ Guatemala U.S. Biol. Surv.
Length from anterior end of symphysis to posterior end of condyle immediately behind coronoid process	181.1	176.7	178.5	176.5	149.8	181.6	180.2	179.4	143.2	157.8	138	136.7
Length of symphysis measured along anterior border	58.4	55.8	62.5	58.2	47.6	58.6	62	57.6	49.6	53.4	44	46
Depth of ramus below anterior end of P$\overline{4}$	38.9	31.6	35.3	33	26.8	35.3	36.3	33.2	27.1	30.3	25.5	24.8
Depth of ramus below posterior end of M$\overline{1}$	42.4	36.6	36.5	35.7	31	39.4	39.5	36.3	33.2	34.3	29.6	28.9
Thickness of ramus below posterior end of M$\overline{1}$	16.5	17.3	17.6	15	12.2	16.6	15.4	15.4	13.8	14	12.2	12
Height from inferior border of angle to summit of condyle	38.3	36.1	38	33.7	30.8	38.4	40.3	37.5	30.5	33.6	27.8	28.1
Height from inferior border of angle to summit of coronoid process	93.2	88.5	90.2	82.4	71.1	92.8	92	89.2	71.3	77.4	64.8	64.3
Transverse width of condyle	45.2	47.2	43.6	40.8	36.1	43.2	43.3	45.6	34.7	35	30	31.2
Greatest depth of condyle	16.3	15	15	14	11.8	16.6	15.2	14.8	12	13.1	10	10.7

TABLE 102—*Measurements (in millimeters) of superior dentition of jaguar*

	Felis onca No. 100122 Brazil U. S. Biol. Surv.	*Felis onca* No. 100123 Brazil U. S. Biol. Surv.	*Felis onca* No. 49393 Brazil U.S.N.M.	*Felis onca* No. 12176 ♂ Costa Rica U.S.N.M.	*Felis onca* No. 239343 Costa Rica U.S.N.M.	Jaguar No. 244507 ♂ Arizona U. S. Biol. Surv.	Jaguar No. 247337 ♂ Arizona U. S. Biol. Surv.	*Felis hernandesii* No. 9703 Tehuantepec U.S.N.M.	Jaguar No. 231961 ♀ Arizona U. S. Biol. Surv.	Jaguar No. 137039 Venezuela U. S. Biol. Surv.	Jaguar No. 179171 Mexico U. S. Biol. Surv.	*Felis hernandesii* No. 249824 ♀ Guatemala U.S. Biol. Surv.
Length from anterior end of canine alveolus to posterior end of P$\underline{4}$	81.8	77.2	78.6	81.2	69.1	82.1	84.3	77.3	69.9	72.4	66	68.3
Length from anterior end of alveolus for P$\underline{2}$ to posterior end of alveolus for P$\underline{4}$	55.1	51.4	52.3	52.3	44.8	53.5	54.4	49.8	48.9	50.1	45.6	46.9
I$\underline{1}$, greatest transverse diameter	...	...	4.1	2.8	...	4.3	3.7	3.8	3.5	4.2	3.4	3.6
I$\underline{2}$, greatest transverse diameter	...	...	...	4	...	4.8	4.3	4.2	4	4.7	3.8	4.3
I$\underline{3}$, greatest transverse diameter	7.4	...	...	7	...	8	7.4	6.8	6.9	7.5	6.6	6.6
Transverse width of entire upper incisor series	31.8	...	...	33.1	...	33.8	32.3	31.8	30.8	33	27.4	28.3
$\underline{\text{C}}$, anteroposterior diameter at base of enamel	20	19.3	...	17.7	17.1	...	18.9	18	15.5	18	15.2	15.9
$\underline{\text{C}}$, transverse diameter	16.6	14.5	...	13.8	13.7	...	14.9	14	12.5	13.9	12.6	13.2
P$\underline{2}$, anteroposterior diameter	...	6.4	...	7.1	...	7.1	6.8	...	6.2	8.4	6.4	...
P$\underline{3}$, anteroposterior diameter	19.4	17.1	18.7	17.9	16	18	17.6	16.9	16	18.2	16	15.4
P$\underline{3}$, greatest transverse diameter	10	9.9	12.5	9.2	8.6	10.2	9.4	9.7	8	9.5	9.3	9.3
P$\underline{4}$, anteroposterior diameter	27.3	26.5	27	25.9	24.4	27.7	27	24.6	25	26.8	23.4	25.5
P$\underline{4}$, greatest transverse diameter across protocone	15.3	14.5	15.4	14	13	15	14.2	14.4	12.9	14.6	12.5	12.4
P$\underline{4}$, anteroposterior diameter of base of paracone	11	10	10.4	10.3	9.2	10.1	10.3	9.6	9.4	10.3	9.3	10.4
P$\underline{4}$, anteroposterior diameter of parastyle	4.7	4	4.7	4.9	4.4	4.8	5	4.1	4.4	5	4.1	4.2
P$\underline{4}$, length of metacone blade	10.4	10	10	10.1	9.2	10.5	10	9.7	9.5	9.8	9	9.5
M$\underline{1}$, anteroposterior diameter	4.8	4.7	...	4.1	...	4.3	4.4	4.8	3.6	3.7	3.4	...
M$\underline{1}$, transverse diameter	8.8	8.5	...	7.6	...	8.6	8.8	8.3	8.9	7.3	7.5	...

TABLE 103—*Measurements (in millimeters) of inferior dentition of jaguar*

	Felis onca No. 100122 Brazil U. S. Biol. Surv.	*Felis onca* No. 100123 Brazil U. S. Biol. Surv.	*Felis onca* No. 49393 Brazil U.S.N.M.	*Felis onca* No. 12176 ♂ Costa Rica U.S.N.M.	*Felis onca* No. 239343 Costa Rica U.S.N.M.	Jaguar No. 244507 ♂ Arizona U. S. Biol. Surv.	Jaguar No. 247337 ♂ Arizona U. S. Biol. Surv.	*Felis hernandesii* No. 9703 Tehuantepec U.S.N.M.	Jaguar No. 231961 ♀ Arizona U. S. Biol. Surv.	Jaguar No. 137039 Venezuela U. S. Biol. Surv.	Jaguar No. 179171 Mexico U. S. Biol. Surv.	*Felis hernandesii* No. 249824 ♀ Guatemala U.S. Biol. Surv.
Length from anterior end of $\overline{C}$ to posterior end of M$\overline{1}$	98.3	91.7	94.6	94.7	81.2	96.3	96.2	92	79	83.9	77.3	77.8
Length from anterior end of P$\overline{3}$ to posterior end of M$\overline{1}$	57.3	52.8	54.9	50.4	...	55.2	55	53.1	46.3	52.7	48	...
Length of lower diastema between canine and P$\overline{3}$	18.7	19.4	17	25.2	14.1	21.9	21.3	19.7	17	12.9	12	13
I$\overline{1}$, greatest transverse diameter	...	3	...	3.9	...	3	3	...	2.4	3	2.3	2.6
I$\overline{2}$, greatest transverse diameter	...	4.3	...	4.5	...	4.2	4	3.7	3.8	4.3	3.4	4
I$\overline{3}$, greatest transverse diameter	...	4.4	...	4.3	...	5.5	4.8	4.6	4.7	5.3	3.8	4.6
Transverse width of entire lower incisor series	...	...	...	24.4	...	24.4	24.3	23.4	23	24.7	22.4	22.3
$\overline{C}$, anteroposterior diameter at base of enamel	20.3	18.7	19.1	17	15.7	18.1	17.8	17.8	15	17.2	14.9	16.3
$\overline{C}$, transverse diameter	14.8	13.6	...	13.2	11.8	13.3	13.8	12.9	10.6	12.4	11.3	11.9
P$\overline{3}$, anteroposterior diameter	15.9	14.3	15.2	13.7	...	14.8	14.2	13.3	11.7	14.7	12.5	...
P$\overline{3}$, greatest transverse diameter	9.5	7.7	8.8	7.3	...	7.4	7.6	7	6.2	7.6	6.5	...
P$\overline{4}$, anteroposterior diameter	22.6	19.4	21.4	19.4	17.6	20.4	20.1	19.3	17.7	19.5	18.1	17.6
P$\overline{4}$, greatest transverse diameter	11.7	10.3	11	9.4	8.2	10.2	10.5	9.4	8.4	9.4	8.3	8.3
P$\overline{4}$, basal length of principal cusp	11.2	9.5	9.4	8.7	8.4	9.3	9.7	7.8	8.5	9.6	8.4	8.4
M$\overline{1}$, anteroposterior diameter	22.8	20.5	20.6	18.9	19.3	21.5	21.7	20.3	18.3	20.5	19	18.7
M$\overline{1}$, greatest transverse diameter	11.6	10.6	11.3	9.8	10	10.9	10.7	10.8	9	10.1	9.5	9.7
M$\overline{1}$. length of protoconid blade	10.4	9.6	9.6	8.7	8.3	10	10	9.6	9.3	9.5	9.2	9.7

Rancho La Brea, a list of the important differences in skull and dentition between the puma and jaguar will serve to indicate how remote their relationships are and how distinct their antecedent histories must have been (*vide supra*). The comparisons are based on large series of skulls of modern types in the collections of the U. S. National Museum.

COMPARISON OF SKULL AND DENTITION OF PUMA AND JAGUAR

	Felis concolor	*Felis onca* *Felis hernandesii*
Side view of skull:	Plane of anterior two-thirds of nasals descends more sharply downward than posterior third; the change in slope occurring where these two portions meet.	Plane of nasals descends evenly from posterior end to anterior end.
	Sagittal crest when well developed frequently reaches greatest elevation in mid-section of parietal and from this point descends to lambdoidal crests.	In male skulls sagittal crest reaches highest point where it meets lambdoidal crests, giving considerable prominence to this region.
Jugal:		Inner anterior portion overlaps maxillary to less extent above infraorbital canal than in puma. As seen from in front there is a greater expanse of maxillary above upper rim of foramen than in puma.
Lachrymal:	Conspicuous lachrymal eminence absent. Weakly developed in a few specimens.	Frequently has greater facial development than in puma and lachrymal foramen is situated closer to orbital rim. Conspicuous lachrymal eminence which in some specimens becomes very prominent.
Nasals:		Broad; less noticeably tapering posteriorly than in puma.
	Posterior end reaches behind line connecting posterior ends of fronto-maxillary sutures usually distinctly farther than in jaguar.	Posterior end reaches line connecting posterior ends of fronto-maxillary sutures or reaches point slightly behind this line.
Occiput:	Lambdoidal crests display a full lateral development. Inion with recessed dorsal border.	Narrows noticeably upward above foramen magnum and lambdoidal crests without full lateral development. Inion well developed.

	Felis concolor	*Felis onca* *Felis hernandesii*
Mastoid:		Mastoid process projects more directly outward, less forward than in puma. Mastoid and paroccipital processes display greater individuality than in puma. Mastoid process conspicuous because of lateral development and clearly defined separation of an antero-external and a postero-external or posterior surface.
Bulla:	Antero-internal process is frequently compressed transversely forming a wall which projects downward from its position adjacent to the canal for the Vidian nerve.	Antero-internal process of entotympanic flattened and conspicuous in ventral view as it reaches over basisphenoid.
		Forward fringe of ectotympanic lying beneath foramen lacerum medius is much more conspicuous than in the puma. Laterally this fringe is carried forward as an antero-external process much farther than in puma. In some skulls anterior end reaches point in front of level of inner surface of postglenoid process.
		Bulla exhibits less pronounced elongation in anterointernal-posteroexternal direction and appears less inflated than in puma.
Posterior nares:	Postnarial passages broad.	Postnarial passage walled by palatines and pterygoids is narrow.
	Notch shallow, widely open posteriorly.	Median portion of palatine border deeply notched.
Postpalatine foramina:		Situated closer to orbital rim of palate than in puma.

	Felis concolor	*Felis onca* *Felis hernandesii*
Premaxillaries:	Anterior border convex forward. In ventral view crowns of incisors are seen to lie back of border.	Anterior border tends to be concave forward. Viewed from ventral side crowns of upper incisors obscure anterior border.
Mandible:	Anterior end of masseteric fossa reaches a point below and behind posterior end of $M\overline{1}$.	Forward end of masseteric fossa narrows dorsoventrally. Anterior end of fossa reaches point below posterior portion of $M\overline{1}$.
	Angle projects conspicuously backward.	Angle does not project conspicuously backward but is well developed in dorsoventral direction.
$P\underline{3}$		Antero-internal cusp usually more prominently developed than in puma.
$P\overline{3}$		Height of principal cusp, relative to basal length of cusp, not so great as in puma.
$P\overline{4}$		Length, relative to length of $M\overline{1}$, greater than in puma.

FELIS DAGGETTI MERRIAM

This species of puma from Rancho La Brea was described by J. C. Merriam (1918B) and based on a left ramus of the mandible (plate 42, fig. 6) No. 21572 Univ. Calif. Coll. from locality 2050. Several more fragmentary specimens from the asphalt evidently show the same characters seen in *Felis daggetti* and may belong to the same species.

As indicated in the original description the type specimen has approximately the dimensions seen in the Recent puma of California, but is distinguished by unusual massiveness of the cheek-teeth and of the jaw, by unusual width of the angle of the mandible, and by the decided backward curve or sweep of the coronoid process compared with that in Recent pumas.

Felis daggetti represents an animal equaling or perhaps exceeding in size the largest pumas of the present day. In a series of modern skulls of *F. concolor* whose measurements are given in Table 106, the largest specimen is No. 108681 U. S. National Museum. This individual, a male, exceeds the type of *F. daggetti* in several measurements, but the massiveness of the ramus and dentition in the latter is clearly shown. The relatively large size and massiveness of the cheek-teeth, the extreme width of the posterior region of $P\overline{3}$ and $P\overline{4}$, and the stronger backward curvature of the long coronoid process are features in which No. 21572 differs most noticeably from pumas of the *F. concolor* group.

Table 104—*Comparative measurements (in millimeters) of skull*

	Felis bituminosa		Felis concolor											
	Type No. X8628 Rancho La Brea	No. X8629 Rancho La Brea	No. 108681 ♂ Colorado U. S Biol. Surv.	No. 242603 ♂ Montana U. S. Biol. Surv.	No. 213135 ♂ Idaho U. S. Biol. Surv.	No. 224575 ♂ Nevada U. S. Biol. Surv.	No. 234453 ♂ New Mexico U. S. Biol. Surv.	No. 248226 ♂ Oregon U. S. Biol. Surv.	No. 226427 ♂ New Mexico U. S. Biol. Surv.	No. 228617 ♀ Wyoming U. S. Biol. Surv.	No. 228615 ♀ Wyoming U. S. Biol. Surv.	No. 167967 Arizona U. S. Biol. Surv.	No. 139144 New Mexico U. S. Biol. Surv.	No. 227698 ♂ Idaho U. S. Biol. Surv.
Length from anterior end of premaxillary to posterior end of condyles	188	170.4	209.5	200	198.1	193.1	198.8	198.7	192.4	173	163.5	200	193.3	183.7
Basal length from anterior end of premaxillary to inferior notch between condyles	175.1	154.9	195.3	187.4	186	178.3	185.8	183.8	180	160.4	152.5	187.4	181.1	170.6
Length from anterior end of premaxillary to posterior end of inion	209.8	189.3	237.2	224	214.8	209	223.4	217	217.2	189.9	181.6	217	214.7	205.8
Length from anterior end of premaxillary to anterior end of posterior nasal opening	83.4	76.9	90.2	90.1	85.9	85.6	87.6	86.3	85.6	74.5	71	83.3	87.7	80.7
Length of palate from anterior end of premaxillary to line tangent to posterior surfaces of maxillary parapets	73.8	70.6	80.7	77.9	80	73.3	77	75.5	74.3	67.4	64.4	76.4	74.8	70
Length from posterior end of glenoid cavity to posterior end of condyles	59.8	53	62.8	57	56.5	58.7	60.1	59.5	57	53	49.3	64.2	59.2	55.3
Anteroposterior diameter of nasals	53	41.3	59	50.7	49.6	47.8	53.1	51	48	43.7	42.7	57.3	52.1	48.6
Width of anterior nares	[a]36.3	30.8	38	35.1	34.4	33.7	34.5	33	35.1	28	26.9	36.6	32.9	33.5
Greatest width across muzzle at canines	59	....	69.8	64	61	59.3	60	60.5	62.1	57	52	61	61.7	62.5
Least width between superior borders of orbits	43.2	38.6	46.3	47.3	41.5	41.7	42.6	47.2	42.5	39.7	36.2	43.3	43.3	42.3
Width across postorbital processes	[a]77	....	83.4	84.8	76.6	75	78	79.3	76.8	69.6	73.2	79.2	80.8	76.7
Least width of postorbital constriction	45	43.2	42.4	46.4	44.8	40.4	43.8	41.8	42.7	42.5	41.8	41.8	43.6	41.6
Greatest width across zygomatic arches	147.2	132.4	163	162.3	154	145	148.5	156.6	148.9	136.4	128.3	143.1	148.7	153
Anterior palatal width between superior canines	32.2	31.5	40.6	37.1	35.2	33.8	34.9	34.6	36.1	30.7	28.5	33.2	34.4	35
Posterior palatal width between inner roots of superior carnassials	56	50	59.7	59	53.9	54	53.8	54.7	53.5	52.4	49.5	53.1	55.6	57
Greatest transverse diameter across auditory bulla, measured from foramen lacerum posterius to external auditory meatus	22.5	19.3	20.4	20	21.5	21.7	22.4	22	19.8	18.1	18.3	19.4	22.1	18.3
Greatest width across mastoid processes	83.6	76.7	97	....	90.5	89.5	89.7	91.4	90.4	83.9	78.3	87.8	91	85.6
Greatest diameter across condyles	45.2	38.9	42.2	....	40.9	40.4	42.5	42.5	42.3	36.8	40.3	42.7	41.9	40.7

a, Approximate.

Table 105—*Comparison of cranial and dental indices*

	Felis bituminosa		Felis concolor											
	Type No. X8628 Rancho La Brea	No. X8629 Rancho La Brea	No. 108681 ♂ Colorado U. S. Biol. Surv.	No. 242603 ♂ Montana U. S. Biol. Surv.	No. 213135 ♂ Idaho U. S. Biol. Surv.	No. 224575 ♂ Nevada U. S. Biol. Surv.	No. 234453 ♂ New Mexico U. S. Biol. Surv.	No. 248226 ♂ Oregon U. S. Biol. Surv.	No. 226427 ♂ New Mexico U. S. Biol. Surv.	No. 228617 ♀ Wyoming U. S. Biol. Surv.	No. 228615 ♀ Wyoming U. S. Biol. Surv.	No. 167967 Arizona U. S. Biol. Surv.	No. 139144 New Mexico U. S. Biol. Surv.	No. 227698 ♂ Idaho U. S. Biol. Surv.
Anterior narial index	21	20	19	19	18	19	18	18	20	17	20	18	18	20
Index of interorbital breadth	25	25	24	25	23	24	23	26	24	25	24	23	24	25
Breadth index of postorbital processes	44	..	43	45	41	42	42	43	43	44	48	42	45	45
Index of postorbital constriction	26	28	22	25	24	23	24	23	24	27	27	22	24	25
Bizygomatic index	84	85	84	87	83	81	80	85	83	85	84	76	82	89
Index of palatal length	42	46	41	42	43	41	41	41	41	42	41	41	42	41
Index of anterior palatal breadth	44	45	50	48	44	46	45	46	49	46	44	46	43	50
Index of posterior palatal breadth	76	71	74	76	67	74	70	73	72	78	70	74	77	81
Diametral index of superior canine	..	..	77	79	..	85	82	79	87	82	84	82	79	79
Diametral index of $\mathrm{M}\overline{1}$ $\frac{\mathrm{W\ M}\overline{1} \times 100}{\mathrm{L\ M}\overline{1}}$	48	..	49	48	49	53	49	49	50	51	49	52	51	48
Length index of $\mathrm{P}\overline{4} - \mathrm{M}\overline{1}$ $\frac{\mathrm{L\ P}\overline{4} \times 100}{\mathrm{L\ M}\overline{1}}$	88	..	90	85	87	95	93	92	88	89	92	89	90	88

Table 106—*Comparative Measurements (in millimeters) of mandible*

	Felis bituminosa	Felis daggetti	Felis concolor											
	Type No. X8628 Rancho La Brea	Type No. 21572 U. C. Coll. Rancho La Brea	No. 108681 ♂ Colorado U. S. Biol. Surv.	No. 242603 ♂ Montana U. S. Biol. Surv.	No. 213135 ♂ Idaho U. S. Biol. Surv.	No. 224575 ♂ Nevada U. S. Biol. Surv.	No. 234453 ♂ New Mexico U. S. Biol. Surv.	No. 248226 ♂ Oregon U. S. Biol. Surv.	No. 226427 ♂ New Mexico U. S. Biol. Surv.	No. 228617 ♀ Wyo.-ming U. S. Biol. Surv.	No. 228615 ♀ Wyoming U. S. Biol. Surv.	No. 167967 Arizona U. S. Biol. Surv.	No. 139144 New Mexico U. S. Biol. Surv.	No. 227698 ♂ Idaho U. S. Biol. Surv.
Length from anterior end of symphysis to posterior end of condyle immediately behind coronoid process	137	145.7	158.9	147.8	144.8	142	146	148.3	144.7	127.4	120.6	143.7	144.4	137.4
Length of symphysis measured along anterior border	39.9	48	47.8	44.1	43.8	40.7	45.9	44.2	44.9	35.1	35	41.6	41.4	42
Depth of ramus below anterior end of $P\overline{4}$	23	27.6	29	25.8	25.1	26.1	25.7	26.1	24.1	21.6	20.5	24.1	25	24.8
Depth of ramus below posterior end of $M\overline{1}$	27.9	31.4	33.9	31.5	30.1	29.4	28	28.7	27.2	25.6	24.6	29.7	28.7	29.6
Thickness of ramus below posterior end of $M\overline{1}$	13.6	16.3	14.3	14.5	13.6	14.1	12.5	13.8	12.6	12	10.4	12.6	12.8	13.5
Height from inferior border of angle to summit of condyle	31	31	36.5	34.2	31.4	30.3	31.7	29.6	33.4	25.2	25.3	34.2	31.8	30.7
Height from inferior border of angle to summit of coronoid process	71.4	76.3	83.6	79.3	75.8	74.8	75	72.6	73.3	64	60.4	76	74.3	72.6
Transverse width of condyle	31.3	36.2	37.4	34.8	35	32.6	33.7	34.8	30.6	29	29.3	32.3	35.7	35.7
Greatest depth of condyle	9.4	9.7	11.4	11.4	11.1	12	10.5	11	10.5	9.3	9.1	10.3	11.1	10.3

TABLE 107—*Comparative measurements (in millimeters) of superior dentition*

	Felis daggetti	Felis bituminosa		Felis concolor											
	No. 29524 U. C. Coll. McKittrick	Type No. X8628 Rancho La Brea	No. X8629 Rancho La Brea	No. 108681 ♂ Colorado U. S. Biol. Surv.	No. 242603 ♂ Montana U. S. Biol. Surv.	No. 213135 ♂ Idaho U. S. Biol. Surv.	No. 224575 ♂ Nevada U. S. Biol. Surv.	No. 234453 ♂ New Mexico U. S. Biol. Surv.	No. 248226 ♂ Oregon U. S. Biol. Surv.	No. 226427 ♂ New Mexico U. S. Biol. Surv.	No. 228617 ♀ Wyoming U. S. Biol. Surv	No. 228615 ♀ Wyoming U. S. Biol. Surv.	No. 167967 Arizona U. S. Biol. Surv.	No. 139144 New Mexico U. S. Biol. Surv.	No. 227698 ♂ Idaho U. S. Biol. Surv.
Length from anterior end of canine alveolus to posterior end of P$\underline{4}$	68	63.5	61.5	67	66.6	67.4	61	64.7	63.9	62.8	57.7	56.5	63.3	62.5	61.4
Length from anterior end of alveolus for P$\underline{2}$ to posterior end of alveolus for P$\underline{4}$	49.2	45	45.6	44.2	46.6	46.3	40.4	....	44.6	42.9	41	40.1	43.8	42	41.8
I$\underline{1}$, greatest transverse diameter	3.5	....	3.3	....	2.9	3.3	3.1	....	3.4	3	3.1	2.8	2.9	2.9	....
I$\underline{2}$, greatest transverse diameter	4.2	....	3.5	....	3.5	3.7	3.3	....	3.8	3.6	3.5	3.1	3.3	3	....
I$\underline{3}$, greatest transverse diameter	6.3	....	5.9	....	5.1	5.6	4.4	....	5.4	5.4	4.6	4.8	5	5.1	5
Transverse width of entire upper incisor series	*a*29	....	....	....	24.2	24.8	22.3	....	25.4	24.7	23.2	21.4	22.9	25.7	23.6
C$\underline{}$, anteroposterior diameter at base of enamel	15	....	....	15.1	14.7	....	13.7	13.7	14.9	13.6	12.3	12.3	14.1	14	14.9
C$\underline{}$, transverse diameter	12.2	....	....	11.6	11.6	....	11.6	11.3	11.8	11.8	10.1	9.7	11.8	11.5	11.7
P$\underline{2}$, anteroposterior diameter	6.4	....	....	3.9	4.3	5.6	4	....	4.2	4.5	5.1	4.5	5	....	....
P$\underline{3}$, anteroposterior diameter	17.4	16.4	16.4	15.5	17	16.5	15.2	15.4	17	15.4	14.8	15.1	15.8	17.1	16.3
P$\underline{3}$, greatest transverse diameter	9.8	9.7	9.4	8.6	9.4	9	9.3	8	9.6	8.4	9.4	8.2	8.9	9.4	9
P$\underline{4}$, anteroposterior diameter	26.4	24.4	23.3	22.8	22.2	24.5	21.6	23	25.3	23	21.6	21	23	23.2	21.2
P$\underline{4}$, greatest transverse diameter across protocone	12.6	11.8	12.7	12.3	12.1	12.7	11.2	11.5	13.2	12.4	10.7	11	12	13	12.1
P$\underline{4}$, anteroposterior diameter at base of paracone	10.4	10.1	8.6	9.2	9.1	9.5	8.7	8.8	9.8	9.2	8.4	8.6	9.3	9	8.4
P$\underline{4}$, anteroposterior diameter of parastyle	4.6	4.2	4.3	3.5	3.8	3.7	3.4	3.4	3.9	3	3.3	3.2	3.1	3.6	3.7
P$\underline{4}$, length of metacone blade	10.6	9.4	9.7	8.4	8.7	9.4	8.5	9	10.3	9.5	8.6	8.4	9.5	8.9	9.5
M$\underline{1}$, anteroposterior diameter	....	....	....	2.8	2.8	3.5	3.6	2.4	3	3.5	2	3.6	....	3.7	2.8
M$\underline{1}$, transverse diameter	....	....	....	4.7	5.3	6.3	5.9	4.1	6.8	5.6	2.7	6.1	....	6.9	5.3

a, Approximate.

TABLE 108—*Comparative Measurements (in millimeters) of inferior dentition*

	Felis bituminosa	Felis daggetti	Felis concolor											
	Type No. X8628 Rancho La Brea	Type No. 21572 U. C. Coll. Rancho La Brea	No. 108681 ♂ Colorado U. S. Biol. Surv.	No. 242603 ♂ Montana U. S. Biol. Surv.	No. 213135 ♂ Idaho U. S. Biol. Surv.	No. 224575 ♂ Nevada U. S. Biol. Surv.	No. 234453 ♂ New Mexico U. S. Biol. Surv.	No. 248226 ♂ Oregon U. S. Biol. Surv.	No. 226427 ♂ New Mexico U. S. Biol. Surv.	No. 228617 ♀ Wyo.-ming U. S. Biol. Surv.	No. 228615 ♀ Wyo-ming U. S. Biol. Surv.	No. 167967 Arizona U. S. Biol. Surv.	No. 139144 New Mexico U. S. Biol. Surv.	No. 227698 ♂ Idaho U. S. Biol. Surv.
Length from anterior end of $\overline{\mathrm{C}}$ to posterior end of M$\overline{1}$	72.7	80.6	78	77.2	78	71.5	73.8	73.9	73.4	65.8	65	73.2	72.1	71
Length from anterior end of P$\overline{3}$ to posterior end of M$\overline{1}$	46.2	51.9	46.6	47	49.3	46.4	44.6	48.4	45.4	41.8	42.5	45	46.3	....
Length of lower diastema between canine and P$\overline{3}$	11.9	10.5	17.1	14.1	12.2	12.7	15.5	11.8	15	12	9.7	13	12.8	12.4
I$\overline{1}$, greatest transverse diameter	....	....	....	2	2.4	....	....	2.4	2	2.2	1.9	2	2.4	2.1
I$\overline{2}$, greatest transverse diameter	....	3.1	....	2.9	3.3	3	....	3.1	3	3.3	2.9	2.7	3	3.3
I$\overline{3}$, greatest transverse diameter	....	....	....	4.2	3.9	3.9	....	4	4.5	4.4	4.1	3.9	4.1	4.3
Transverse width of entire lower incisor series	....	....	17.3	19	18.6	18	17.8	19	18.8	18.8	17.1	17.4	19.8	....
$\overline{\mathrm{C}}$, anteroposterior diameter at base of enamel	14	16.4	13.4	15	15.1	13.6	13.8	13.8	13.4	11.9	12.4	13.7	13.4	14.2
$\overline{\mathrm{C}}$, transverse diameter	10.5	11.9	9.8	10.5	11.3	10	10	10	10.1	8.6	8.6	10	9.8	10.1
P$\overline{3}$, anteroposterior diameter	13.4	14.7	13	13.8	14.3	13	12.9	13.8	12.7	12.4	12.7	13.8	14	....
P$\overline{3}$, greatest transverse diameter	8.1	9.1	7.2	7.7	7.3	6.9	6.9	7.8	7.2	7	6.8	7.5	8.6	....
P$\overline{4}$, anteroposterior diameter	16.2	17.6	15.9	16.2	17	15.7	15.6	17.5	15.7	14.6	14.8	15.9	16.1	15.8
P$\overline{4}$, greatest transverse diameter	9	10.5	8.5	9	8.8	8.6	8.3	8.6	8.5	8.3	8.1	8.7	9	8.7
P$\overline{4}$, basal length of principal cusp	8.3	8.6	8.4	8.4	8.7	8.6	8.1	8	8.3	7.3	7.7	8.3	8.3	7.6
M$\overline{1}$, anteroposterior diameter	18.4	21	17.7	19	19.5	16.6	16.8	19	17.9	16.4	16.4	17.2	18	18
M$\overline{1}$, greatest transverse diameter	8.9	10.8	8.8	9.1	9.5	8.8	8.3	9.4	8.9	8.3	8.4	8.4	9.3	8.6
M$\overline{1}$, length of protoconid blade	8.2	9.5	8.4	9	8.6	9	7.5	8.1	8	8.5	7.7	8.6	8.4	8.3

No. 21572 is clearly allied with the pumas rather than with the jaguars and differs from the latter in the shape and direction of the angle, in the narrowness of the base of the coronoid process and to some extent in the greater degree of backward curvature of this process, in the height of the principal cusp in $P\overline{3}$, in the greater width of $P\overline{3}$ and $P\overline{4}$, in the more massive lower cheek-teeth, and in the relatively shorter anteroposterior diameter of $P\overline{4}$.

Among the skeletal remains in the Los Angeles Museum collection representing the pumas from the asphalt are several specimens which, although resembling somewhat in length the comparable elements that have been referred to *Felis bituminosa*, are distinctly heavier and differ in certain structural details.

No. X8805, a left humerus lacking the proximal epiphysis, resembles the comparable element in the puma and differs from that in the jaguar in several characters. Although the bicipital crest is not clearly defined in this specimen the point of union of this crest and the deltoid ridge is situated higher on the front face of the shaft than in the jaguar. Moreover, the supra-condylar ridge of the outer side resembles much more nearly in its development and in its straight course upward and inward that in the puma than that in the jaguar. In the characters which have been noted the jaguar resembles much more closely the large *Felis atrox*.

No. X8805 differs from No. X8809, a specimen referred to *F. bituminosa,* in greater length and more particularly in massiveness as exhibited by the shaft and distal extremity. The olecranon fossa is large. Possibly No. X8805 represents a large male individual of the species *F. bituminosa*. However, among the several specimens of the humerus referred to the latter species none reaches the size seen in No. X8805.

A comparable or even greater difference in size and massiveness is revealed in a comparison between an adult femur, No. X8848, referred tentatively to *Felis daggetti,* and femora referred to *F. bituminosa* (see fig. 147). This specimen is slightly longer than the comparable element in the puma, but is decidedly heavier. It is distinctly larger than femora of the jaguar available for comparison and shorter than the shortest femur referred to *Felis atrox*. In heaviness of shaft and in narrowness of intercondyloid notch this element resembles *Smilodon*. With increase in width of shaft there is a tendency to flatten this portion of the femur, in which respect again a greater resemblance to the sabre-tooth is indicated. The noticeable transverse widening of the femur from a point near the middle of the shaft toward the extremities seen in *Smilodon* is not so evident in No. X8848. The latter type differs furthermore from *Smilodon* in the characters of the proximal end, in which respect it is more like the true cats. The rugose area on the posterolateral surface of the shaft above the outer condyle is much more strongly marked than in the sabre-tooth and resembles that in the puma from Rancho La Brea. The patellar surface is broad, much more so than in femora of the puma which display a shorter length.

No. X8848 is presumably longer than the estimated length of femur in *Smilodon californicus brevipes*. No femur having the outstanding characteristics of *Smilodon* and which might be correlated with the shortened metapodials referred to this variety has been noted in the collection from Rancho La Brea. No. X8848 appears to represent a true cat. The difference in size between this specimen and femora regarded as representing either *Felis bituminosa* or *F. concolor* may be correlated perhaps with the differences in size of ramus and lower teeth in these forms.

A comparison with the jaguar is based on a limited number of specimens. The femur in one individual of *Felis onca*, No. 12296 U. S. N. M., exhibits a relatively wider shaft at the middle than in the puma. The shaft throughout its length is narrower in anteroposterior direction. In the latter character a possible resemblance is seen to the femur from the asphalt. The great trochanter projects well above the level of the head, in which respect No. 12296 differs from femora of *F. concolor*, *F. bituminosa*, and from No. X8848. The intercondyloid area is nar-

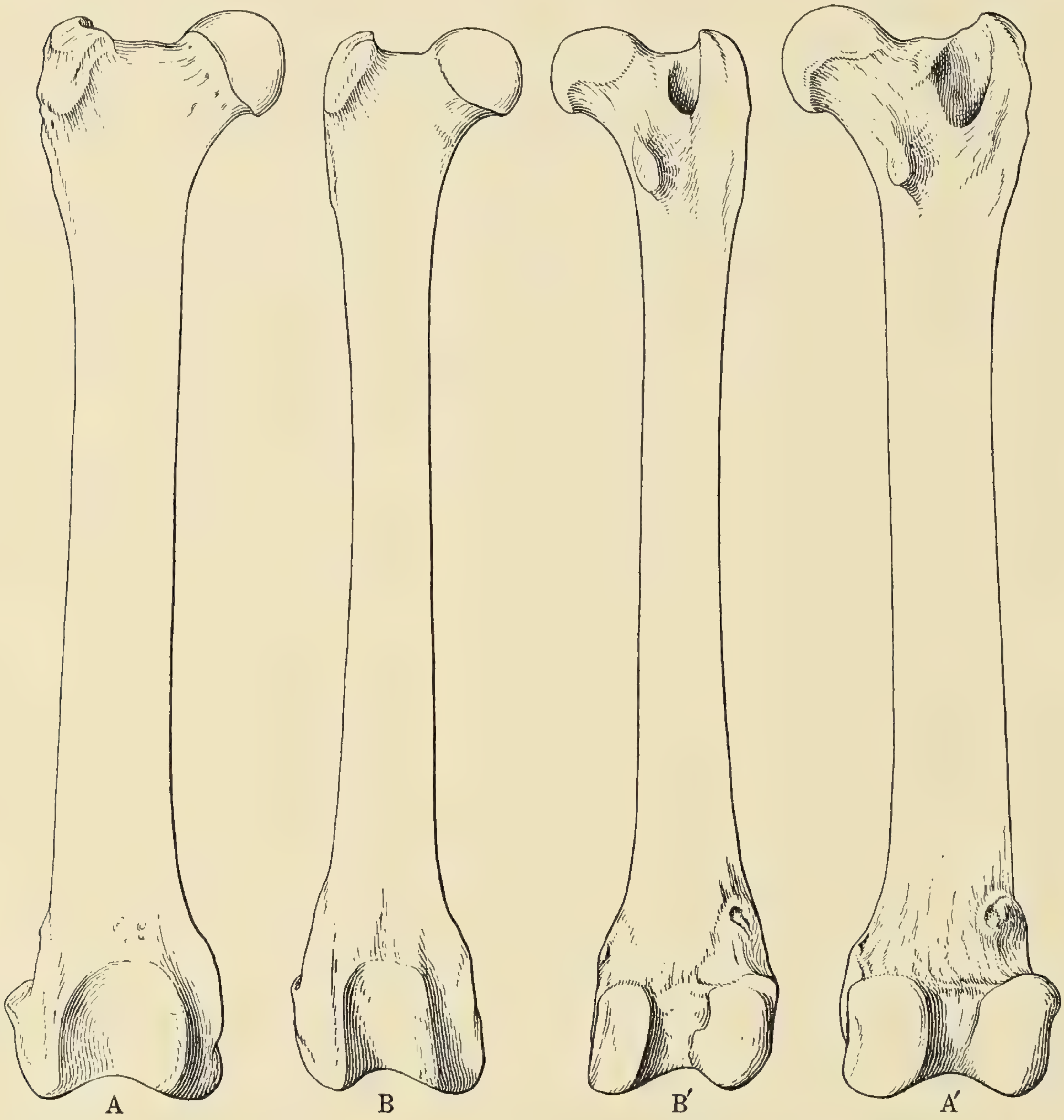

Fig. 147—Comparative views of femora. A, A′, *Felis*, possibly *daggetti* Merriam, No. X8848; B, B′, *Felis bituminosa*, n. sp., No. X8846; anterior and posterior views; × 1/2. Rancho La Brea Pleistocene.

row, more so than in the puma. In this character there is again resemblance to No. X8848. The rugose area above the outer condyle is conspicuous and while similarly developed in a femur of *F. concolor* or *F. bituminosa* and in No. X8848, is much less in evidence in a specimen (No. 4968 U. S. N. M.) of the modern puma.

No. X8848 (compare fig. 147, A, A′ and B, B′) is featured by unusual massiveness, as exhibited particularly by the shaft, by relatively small size of the lesser trochanter, large size of digital fossa with corresponding narrow wall laterally adjacent to fossa, more directly inwardly projecting surface of the head, by unusual narrowness of intercondylar space, and by unusual width of patellar surface.

TABLE 109—*Measurements (in millimeters) of femur*

	Felis possibly *daggetti* No. X8848	*Felis bituminosa* No. X8846
Greatest length from top of head to distal condyles, measured parallel to long axis of femur	294.	287.
Transverse diameter of proximal end, outer face of greater trochanter to inner side of head, taken normal to median longitudinal plane	67.8	54.2
Greatest antero-posterior diameter of head	31.1	27.4
Transverse diameter of shaft at middle	29.2	22.8
Antero-posterior diameter of shaft at middle	25	21.3
Greatest width of distal extremity	59	51.2
Greatest antero-posterior diameter of the distal extremity, at right angles to longitudinal axis of femur	53.5	51.5
Greatest width of rotular surface	35.3	27
Greatest width of intercondylar notch	12.2	14.4
Greatest width of articular surface of inner condyle	22.5	16.6

FELIS BITUMINOSA, N. SP.

Holotype, No. X8628 L. A. Mus. Coll., plate 41, figs. 1-3.

Referred specimen, No. X8629 L. A. Mus. Coll., plate 42, figs. 8-9.

Specific characters.—Differs from *Felis daggetti* and resembles modern pumas in size. Differs from *Felis concolor* in broader interpterygoid fossa, with sides more markedly divergent posteriorly. The auditory bullæ are more flattened anteriorly, the anterior margin forming a more nearly even transverse line. Dentition is relatively heavy.

We are indebted to Mr. E. A. Goldman, senior biologist of the U. S. Biological Survey, for his kindness in pointing out the differences between this type from Rancho La Brea and the modern species *Felis concolor* based on comparisons made with a very large series of modern skulls at his command. Mr. Goldman calls attention also to the shallowness of the fronto-nasal pit in the asphalt type. In No. X8628 the sagittal crest appears straighter and the frontal above the supra-orbital rim is flattened somewhat more than in existing puma skulls. The posterior end of the tympanic bulla is narrower than in specimens of the North American puma and in this character the material from the Rancho La Brea Pleis-

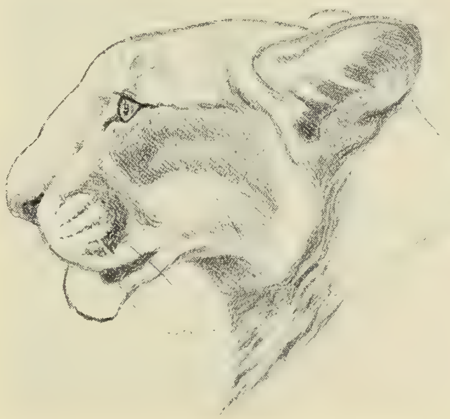

FIG. 148—Study of the head of the puma (*Felis bituminosa*, n. sp.). Lateral view, greatly reduced. Restoration by Charles R. Knight under direction of J. C. Merriam.

tocene resembles skulls of South American representatives of the puma group. The lower jaw does not have the pronounced curvature of the ventral border seen in *F. daggetti*, nor does the coronoid process show the backward sweep seen in the latter.

This species is clearly more closely related in structural characters and in size to *F. concolor* than is *F. daggetti.* To it are referred not only the second skull, No. X8629, but also the greater number of scattered skeletal elements of pumas from the asphalt deposits.

LYNX RUFA FISCHERI MERRIAM

Lynx californicus fischeri, n. var. Merriam, John C., Univ. Calif. Publ., Bull. Dept. Geol., vol. 5, p. 395, 1910.

Type specimen.—No. 11287, Univ. Calif. Col. Vert. Palæ. Rancho La Brea, California.

Type description.—Two small cats of the *Felis* type are represented in the asphalt fauna by lower jaws. One specimen closely resembles in all of its characters *Lynx californicus* found at the present time in southern California. In another form which is made the type of the new variety, *fischeri*, the jaw has about the same length as in the living species but is much more slender and the carnassial is somewhat larger. As yet incomplete skeleton material of this form has been obtained.

Measurements

	No. 11287
Length, posterior side of canine alveolus to posterior side of $\overline{M1}$	33.9 mm.
$\overline{M1}$, anteroposterior diameter	11.2
Height of mandible below protoconid of $\overline{M1}$	12.2
Thickness of mandible below protoconid of $\overline{M1}$	7.5

Additional materials of Pleistocene wildcats now available in the collections of the Los Angeles Museum include a nearly complete skull, several fragmentary rami of the lower jaw and a number of scattered skeletal elements. It is clear from the numerical representation that the wildcat, like the mountain lion, is not found so abundantly in the asphalt as the sabre-tooth or *Felis atrox.*

The lower jaw specimens show considerable range in size. At least two rami, No. X9490 and No. X9262 are characterized by relatively large cheek-teeth, in which respect these specimens differ noticeably from living representatives of the *Lynx rufa* group and approach the Canada lynx. While in these two rami the horizontal portion of the jaw is larger than in the type of *L. r. fischeri* the presence of cheek-teeth larger than those occurring typically in the Recent geographic races of *L. rufa* may for the present be sufficient reason for referring the specimens to Merriam's variety.

In characters of lower jaw, mentioned below, distinguishing *rufa* from *canadensis*, No. X9490 and No. X9262 differ from the latter and resemble the former.

Comparisons of the skull have been made with the splendid series of specimens in the collections of the California Museum of Vertebrate Zoology. Materials available here represent the several sub-species known from the Californian region, namely *Lynx rufa pallescens, L. r. fasciatus, L. r. baileyi,* and *L. r. californicus,* and the Canada lynx (*Lynx canadensis*) of more northerly distribution. In the study of the modern types, particularly from California, frequent reference was made to the revision of the genus *Lynx* occurring in this area by Grinnell and Dixon .[1]

[1] Grinnell, J. and J. Dixon, Univ. Calif. Pub. Zool., vol. 21, pp. 339-354, pl. 11, 1 fig. in text, 1924.

The Canada lynx, *Lynx canadensis*, is readily separated from the species *L. rufa* on the basis of characters observed in the skull. The following are some of the more evident differences:

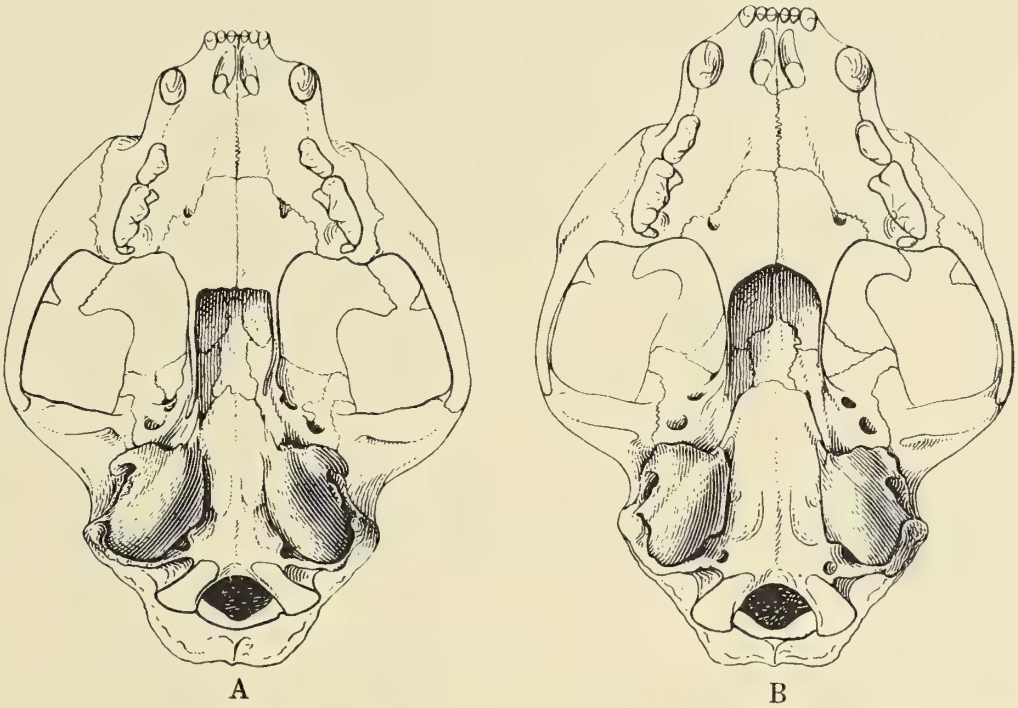

FIG. 149—Comparative ventral views of skulls. A, *Lynx rufa*; B, *Lynx canadensis*; × 2/3. Note particularly differences in position of postpalatine foramina, size of postorbital processes of frontals and shape of presphenoid.

1. Large size (*L. canadensis* compares favorably with *L. rufa pallescens* in this character.)
2. Relatively small auditory bullæ.
3. Postpalatine foramina situated nearer to orbital rim of palate. Associated with this is the greater forward extent of the palatine as outlined by the maxillo-palatine suture.
4. Shape of presphenoid. In *canadensis* this element, as seen in ventral view (compare figure 149, B and A) is contracted anteroposteriorly and widened transversely. In *rufa* the presphenoid is elongate and narrow.
5. Small postorbital process (see breadth index of postorbital processes).
6. Condyle of ramus with shortened transverse diameter.

Correlated with the larger skull size in *canadensis* is the heavier dentition as exhibited especially by the cheek-teeth in this form. Evidently in the lower jaw the most constant difference between the two species occurs in the width of the condyle. The angle appears to be less prominent in *canadensis* than in *rufa*, a difference seen chiefly in a comparison of adult specimens. The masseteric fossa is deeper in *canadensis.* In the latter form the distance from the posterior end of $M\overline{1}$ to the condyle is relatively shorter than in *rufa,* a difference which is presumably due to the presence of larger teeth in *canadensis.* The coronoid process appears to be relatively shorter in the latter than in *rufa.*

The characters displayed by the skull, No. X9489 (plate 42, figs. 1-3), from Rancho La Brea, clearly indicate that the Pleistocene type is widely removed from *Lynx canadensis* and much more closely related to the *Lynx rufa* group. The largest representatives of the latter species occurring today in the Californian region belong to *L. r. pallescens.* The Rancho La Brea specimen is smaller than typical skulls belonging to members of this geographic race. No. X9489 is larger than skulls of average individuals of *L. r. californicus* and compares more favorably in size with representatives of *L. r. baileyi.* Unfortunately, no typical representatives of the northwest race of wildcat, *L. r. fasciatus,* were available for comparison. No. X9489 is featured by the large size of the tympanic bullæ. These structures approach each other more closely in the region of the basioccipital in the asphalt specimen than in most skulls of the Recent species. In at least one skull of *Lynx rufa baileyi* in the collection of the Museum of Vertebrate Zoology, No. 7087, are the bullæ as large as in X9489. Moreover, in skulls 7150, 7085, 31998 of *L. r. baileyi* and in No. 18995 of *L. r. fasciatus* is the distance separating the bullæ no greater than in the Pleistocene skull. Lastly, the occiput in No. X9489 is distinctly narrow dorsally and no skull of the modern types has been observed in which the narrowing of this region is as great as in the former specimen. The teeth in No. X9489 do not appear to differ noticeably in size from those of *L. rufa.* It is possible that the superior dentition is slightly heavier than that in average individuals of the *rufa* group. In $P\underline{3}$ the posterior tubercle has undergone some reduction and this feature gives added prominence to the median cusp. Presumably the tubercle has been reduced by wear and this attrition occurs in $P\underline{3}$ of both right and left sides.

FIG. 150—Study of the head of the wildcat (*Lynx rufa fischeri* Merriam). Lateral view, greatly reduced. Restoration by Charles R. Knight under direction of J. C. Merriam.

Absence of a character which might reasonably be expected if the skull belongs to *Lynx rufa fischeri,* namely enlargement of the cheek-teeth, may indicate that No. X9489 is more closely related to existing forms than are the type of *L. r. fischeri* and the remaining specimens which have been referred to the latter form. Indeed, lower jaw fragments, including No. X9077, are available which resemble closely the existing races of the Californian region in character of dentition. On the other hand, the presence of at least one feature in the skull, namely the relatively great narrowing dorsally of the occiput, serves to distinguish No. X9489 from the living forms unless ultimately found in a skull of a Recent wildcat, and the specimen is therefore assigned for the present to *L. r. fischeri.*

TABLE 110—*Comparative measurements (in millimeters) of skull*

Key to Identification of Recent Species or Race in Each Rectangle[1]

Lynx canadensis	×	×	*L. rufa baileyi*
L. rufa pallescens	×	×	*L. rufa californicus*

	Lynx rufa fischeri Merriam R. L. B. No. X9489 L. A. M.	4797 ♂ 24739	♂ 47239 ♂ 4906	♀ 4340 ♀ 23837	♀ 16247 ♂ 29808	♀ 4362 24607	♀ 32442 ♂ 28794	4796 ♀ 11324	♂ 10605 ♂ 3243	♂ 4213 24620	♂ 32458 ♂ 2333	♂ 4214 ♂ 24592	♂ 25919 ♂ 2335	4209 ♂ 23795	♂ 16366 ♀ 21398	4192 37330	♂ 32460 ♂ 21415	4186 37325	♂ 7150 ♀ 23880	♂ 4153 37298	♂ 7087 ♂ 23881	♀ 4149 37301	♂ 16248 ♂ 12874	♂ 4155 ♀ 37302	♀ 7085 ♀ 19748	♀ 4162 ♀ 37299	♂ 43937 ♂ 29786
Length from anterior end of premaxillary to posterior end of condyles		115	111.7	109.6	98.9	119.6	100	117.9	106	114	115.6	118.8	113.5	123.4	115.3	124.1	113.3	121.2	112.7	119.2	113	113	115.5	120	104.7	115.5	115.2
	113.5	121	106.4	105.8	109.6	117	108	109	104.6	118	105.9	112.2	105.1	119	113	120.2	112.5	114.3	101.5	117.6	108.5	113.2	108	102.4	106	105.3	114.2
Basal length from anterior end of premaxillary to inferior notch between condyles		104	104	100.4	90.7	109	91.4	107.8	98	103.5	106.8	108.5	104	113	106.2	113	104.4	110.8	104	108.5	103.2	102.8	105.8	109.4	96.4	104.8	105.6
	105	110.8	97 5	97.3	101	107.5	99.8	100.4	95.8	108.9	97.2	102.6	96.2	109	104.7	109.6	102.8	104.4	92.8	107.3	100	104.3	99.1	93.6	96.6	97.5	105.5
Length from anterior end of premaxillary to posterior end of lambdoidal crests		125.2	122.5	119.4	107.7	129.4	108.4	132	117.2	126	128.3	130.4	125	133.3	128.4	135.5	125.6	133.6	127.7	130.6	125	122.6	127	130.2	115	125.8	128
	125.6	135.1	118	118.7	120.2	128	119.6	119 5	116	129.8	118	124	115	135.5	123.8	134	123	125.5	112.2	127.8	120.8	124.8	119	113.6	115.6	118.7	125.7
Length from anterior end of premaxillary to anterior end of posterior nasal opening		47.8	49	46.3	41.1	48.9	42.8	49.7	48.4	46.4	48.7	50.6	48.2	50.3	51.3	52	49.8	51.5	48.8	48.1	50.4	47.8	49.7	50.4	45.5	46.9	47.5
	49	52.9	47.8	45.1	47.4	48	45.2	46.4	44.1	48.6	45 3	50	43.4	54.4	50	53.2	47.8	47.8	44	49.3	47	47.4	47.7	44.4	44.7	44.9	47.4
Length of palate from anterior end of premaxillary to line tangent to posterior surfaces of maxillary parapets		45.2	44.2	43.3	37.5	45.3	38.5	46	41.7	43.9	44 6	47.7	45.5	48.4	46.4	49.3	44.6	47.1	44.3	46.4	46	44.6	46.3	46.7	40.8	45.2	44.3
	43.7	46.4	42.5	41	44	44.3	42	42.4	40.9	45.4	42.4	44.5	40	45.9	44.5	49.5	42.6	46.2	40.1	44.3	42.4	43.6	41.1	40.4	41.4	41.4	45.1
Anteroposterior diameter of nasals along median line		26.2	22.2	23	21.6	28	20.6	28.6	25.4	28.3	26.3	26.7	25.6	27	30.3	29.2	27.3	25.4	26.1	29	25	26.1	27	28.2	25.4	26.9	27.2
	*a*24.3	29.7	25.2	26	24.3	27.2	25.4	*a*22.5	23.7	26.5	23.9	26.8	22.4	28.4	25.4	27.2	26.6	27.4	23.4	23.5	24.8	23.5	23.1	24	24.1	26.2	26
Width of anterior nares		18.8	15.5	17	14.3	19	14.3	18	14.9	17.8	16.6	18.7	16.5	20.3	17	20.3	17	19.4	17.2	18.1	17.5	17.6	18.3	18.3	15.9	18	17.4
	16.4	18.2	15.7	16	15.6	17.6	15.8	16.4	15.4	17.4	15.5	16.8	15.4	17.7	16.2	18.5	14.7	17.7	14.3	16.7	14.8	16.1	15.5	14.3	15.1	15.7	16.4
Greatest width across muzzle at canines		33.8	32.6	34.4	28.4	34.8	30.3	36.3	31.4	34	35.4	35.8	34.1	36.2	33	37	33.7	36	33.2	35.5	35.6	33.7	35.2	35.3	32.5	35.8	34
	34.3	35	31.7	31.6	33.1	32.6	32.6	32.8	30.5	34.2	32.3	34.2	32.5	35.8	33.6	35.3	31.8	36	32	33.9	33	30.4	32.5	33	31.6	31	33.2
Least width between superior borders of orbits		28.3	25.8	27.1	23.2	28	21.4	28.9	25	27	26.1	29	26	29.1	26.4	31.6	23.1	28.1	25.3	29	25.1	27.6	28	29.2	25.2	26.8	26.3
	26.7	27	25.5	24.8	23.3	26	23.4	26.5	24.8	27.4	21.6	25.8	25.4	26.3	26.4	28.8	22.8	27.5	21.5	25	24	24.7	23.9	24.1	23.5	22.3	24.4
Width across postorbital processes		55.2	62.4	56.5	57	57.2	55.3	*a*59	62.6	56	60.5	58	58.7	59	65.7	61.6	61	57.7	60	58.5	60.3	58.2	62.1	59.4	55.5	56.7	61
	61.3	65.2	61.5	60.1	58.3	62.3	61	62.7	58.7	66.4	55.7	62.7	60	60.7	66.5	67.3	57.1	62.8	55.6	*a*61	60.4	59	61.1	55.8	55.1	57.4	57.5
Least width of postorbital constriction		40.8	39.2	41.9	40	38.7	40.1	39.4	41.5	37.9	39	37.7	40	38.8	42.5	42	36.4	38.6	36.1	39	38.8	40.8	40.2	39.3	38.4	39.3	40.8
	40.2	39.4	41.4	40.5	37.2	40.2	39.9	42.4	40.9	41.7	39.4	39.5	43.7	37.7	38.7	45.3	37	*a*40.3	42.3	39.7	43	38.3	38.7	41	37.6	37.3	40
Greatest width across zygomatic arches		88.9	88.6	86.9	79.5	92.1	77.2	94.5	85.7	88.4	91.2	89.6	89.4	93.5	88.7	96	91	92.4	90.1	91.7	87.3	87	89.1	92.8	81	90	88
	*a*90	94.3	85.2	85.3	87.6	89.4	87.5	90.7	82.4	93.2	82.4	87.5	83.3	94.1	90.5	95	84.4	89.4	80.1	91	87.2	86.5	86.7	80.5	81.3	84.3	87.9
Anterior palatal width between superior canines		20.3	18.7	18.8	16.6	20	16.1	21.2	18	20.6	19.2	20.8	17.9	21.1	18.8	21.6	19.3	21.5	18.8	21	19.6	19.8	20	21	18	20	17.8
	18.7	19	17.8	18	18.7	19.4	17.9	18.4	16.9	19.6	17.5	19.6	18	19.6	19.7	20	17.1	19.9	16.4	18.8	18	18.2	17.8	17.4	17.2	18.3	18.7
Posterior palatal width between inner roots of superior carnassials		32.7	30.7	31.9	27.6	34	27.1	34.5	31.8	33.8	32.7	33.7	30.8	35.8	31.2	36	32.7	35.6	32.5	35.7	31.8	32.7	30.8	35.2	29.8	33.3	31
	32.9	32.7	29.9	29.6	30.3	32.7	29.8	31.7	28	32.9	29.5	31.7	29.8	34.8	30.8	33.6	30.8	32.2	27.9	34.2	30.8	30.6	30.7	27.9	29.8	31.1	29.8
Greatest transverse diameter across auditory bulla, measured from foramen lacerum posterius to external auditory meatus		13.2	14.8	13.1	13.7	13.3	13.6	14.1	14.5	13.7	14.4	13.4	14.7	14.4	14.9	14.7	15.9	14.1	15.6	12.8	15.9	13.5	15.2	14.6	13.8	13.2	15.6
	15.7	15.3	13.8	14.5	14.9	15.1	14.7	14.7	14.4	15.8	14.8	14.4	13.7	16.4	13.8	15.9	13.8	14.3	13.7	15.9	14.1	15.8	13.8	13.5	13.8	14.7	14.9
Greatest width across mastoid processes		54.2	54.7	50.6	49.8	54.2	48	56	51.5	54	55.8	55.3	51.3	56.5	53.9	57.2	56	55.5	57	55.9	56	53.3	54.8	56.7	51.2	54.8	58
	53.2	58.2	53.5	55	51	55.7	53.5	53.8	53	55.5	52.1	54.9	52	59.9	52.8	57.4	53.7	54	50.8	56.5	53.8	56	51.5	50.5	51.7	54.2	55.3
Greatest diameter across condyles		31.5	29	29.4	27.4	31.8	25.9	31	26.8	30.2	29	32.8	29.8	33.7	29.4	33.9	30.5	31.7	31.4	32.1	29.3	30.6	28.4	32.3	27	31.8	31.4
	27.9	32.3	29.3	31.3	29	29.5	28.4	29	29.6	30.3	27.7	29.1	28.5	32.6	28	32.4	31.1	29.1	27.5	30.3	28.9	30.8	28.6	29.6	28.6	30	28.3

---

[1] Based on specimens in the collections of the Museum of Vertebrate Zoology, University of California.

a, Approximate.

TABLE 111—*Comparison of cranial and dental indices*

	Lynx rufa fischeri Merriam R. L. B.	Key to Identification of Recent Species or Race in Each Rectangle[1] *Lynx canadensis* × × *L. rufa baileyi* *L. rufa pallescens* × × *L. rufa californicus*																									
	No. X9489 L. A. M.	4797	♂ 47239	♀ 4340	♀ 16247	♀ 4362	32442	4796	♂ 10605	♂ 4213	♂ 32458	♂ 4214	♂ 25919	4209	♂ 16366	4192	♂ 32460	4186	♂ 7150	♂ 4153	♂ 7087	♀ 4149	♂ 16248	♂ 4155	♀ 7085	♀ 4162	♂ 43937
		♂ 24739	♂ 4906	♀ 23837	♂ 29808	24607	♂ 28794	♀ 11324	♂ 3243	24620	♂ 2333	♂ 24592	♂ 2335	♂ 23795	♀ 21398	37330	♂ 21415	37325	♀ 23880	37298	♂ 23881	37301	♂ 12874	♀ 37302	♀ 19748	♀ 37299	♂ 29786
Anterior narial index	15.5	18	15	17	16	17.5	15.5	17	15	17	15.5	17	16	18	16	18	16	17.5	16.5	16.5	17	17	17	17	16.5	17	16.5
		16.5	16	16.5	15.5	16	16	16	16	16	16	16	16	16	15.5	17	14	17	15.5	15.5	15	15.5	15.5	15	15.5	16	15.5
Index of interorbital breadth	25.5	27	25	27	25.5	25.5	23.5	27	25.5	26	24.5	27	25	26	25	28	22	25	24	27	24	27	26.5	26.5	26	25.5	25
		24	26	25.5	23	24	23.5	26	26	25	22	25	26.5	24	25	26	22	26	23	23	24	23.5	24	26	24	23	23
Breadth index of postorbital processes	58.5	53	60	56	63	52.5	60.5	*a*55	64	54	56.5	53.5	56.5	52	62	54.5	58.5	52	58	54	58.5	56.5	58.5	54	57.5	54	58
		59	63	62	57.5	58	61	62	61	61	57	61	62	55.5	63.5	61.5	55.5	60	60	*a*57	60.5	56.5	61.5	59.5	57	59	54.5
Index of postorbital constriction	38	39	38	42	44	35.5	44	36.5	42	36.5	38	35	38.5	34	40	37	35	35	35	36	37.5	40	38	36	40	37.5	38.5
		35.5	42.5	41.5	37	37	40	42	42.5	38	40.5	38.5	45.5	34.5	37	41	36	38.5	45.5	37	43	37	39	44	39	38	38
Bizygomatic index	*a*85.5	85.5	85	86.5	87.5	84.5	84.5	88	87.5	85.5	85.5	82.5	86	82.5	83.5	85	87	83.5	86.5	84.5	84.5	84.5	84	85	84	86	83
		85	87	87.5	87	83	87.5	90	86	85.5	85	85.5	86.5	86	86.5	86.5	82	85.5	86	85	87	83	87.5	86	84	86.5	83
Index of palatal length	41.5	43.5	42.5	43	41	41.5	42	42.5	42.5	42.5	42	44	44	43	43.5	43.5	43	42.5	42.5	43	44.5	43.5	44	42.5	42	43	42
		42	43.5	42	43.5	41	42	42	42.5	41.5	43.5	43.5	41.5	42	42.5	45	41.5	44	43	41	42.5	42	41.5	43	43	42.5	43
Index of anterior palatal breadth	43	45	42	43.5	44	43	42	46	43	47	43	43.5	39	43.5	40.5	44	43	45.5	42.5	45	42.5	44	43	45	44	44	40
		41	42	44	42.5	44	42.5	43.5	41	43	41	44	45	43	44	40.5	40	43	41	42.5	42.5	42	43	43	41.5	44	41.5
Index of posterior palatal breadth	75	72.5	69.5	74	73.5	75	70.5	75	76	77	73.5	70.5	67.5	74	67	73	73	75.5	73.5	77	69	73.5	66.5	75	73	74	70
		70.5	70	72	69	74	71	75	68.5	72.5	69.5	71	74.5	76	69	68	72.5	70	69.5	77	72.5	70	74.5	69	72	75	66
Diametral index of superior canine	*a*88	80	75.5	80	79	78.5	81	76.5	79	80	80	75	79	77	83	76	85	79	87	75.5	86.5	79	80.5	81.5	81.5	78.5	86
		84	85	86	80.5	82	79	82	84.5	78	83	82	78.5	84.5	82	88	83	85	80.5	84	83	81	83	76	83.5	82	78
Diametral index of $M\bar{1}$ $\frac{W\ M\bar{1} \times 100}{L\ M\bar{1}}$	...	43	44.5	42	43.5	41.5	43	48	46	43	42	42	47	44	44	43.5	46	41	*a*49	43	43	44	43	46	44.5	42	42.5
		46.5	46	47.5	45	45	44	48	45.5	49.5	40	50.5	45	48.5	45	47	41	43	46.5	47.5	47	48.5	43	42	42	47	44
Length index of $P\bar{4} - M\bar{1}$ $\frac{L\ P\bar{4} \times 100}{L\ M\bar{1}}$	...	90	83.5	79	82.5	82	82.5	85	87	88	78	87	81	84	78	84	89	84	*a*89	89	79	88	82	92	82	86	83.5
		83.5	87	87.5	81	87	88.5	85	88	96	83	86	79.5	84.5	90.5	83	78	85	80	84	81	87.5	81.5	85	79	83	80.5

---

[1] Based on specimens in the collections of the Museum of Vertebrate Zoology, University of California.

a, Approximate.

TABLE 112—*Comparative measurements (in millimeters) of mandible*

	Lynx rufa fischeri Merriam Rancho La Brea			Key to Identification of Recent Species or Race in Each Rectangle[1] *Lynx canadensis* × × *L. rufa baileyi* *L. rufa pallescens* × × *L. rufa californicus*												
	No. X9490 L.A.M.	No. X9262 L.A.M.	No. X9082 L.A.M.	4797 ♂ 47239 ♂ 24739 ♂ 4906	♀ 4340 ♀ 16247 ♀ 23837 ♂ 29808	♀ 4362 ♀ 32442 24607 ♂ 28794	4796 ♂ 10605 ♀ 11324 ♂ 3243	♂ 4213 ♂ 32458 24620 ♂ 2333	♂ 4214 ♂ 25919 ♂ 24592 ♂ 2335	4209 ♂ 16366 ♂ 23795 ♀ 21398	4192 ♂ 32460 37330 ♂ 21415	4186 ♂ 7150 37325 ♀ 23880	♂ 4153 ♂ 7087 37298 ♂ 23881	♀ 4149 ♂ 16248 37301 ♂ 12874	♂ 4155 ♀ 7085 ♀ 37302 ♀ 19748	♀ 4162 ♂ 43937 ♀ 37299 ♂ 29786
Length from anterior end of symphysis to posterior end of condyle immediately behind coronoid process	83.7	83.4	....	81.5 78.7 86 75.3	78 68.3 74 76.8	84.3 69.3 81.5 78	85 74.7 77.3 72.7	80.7 81 84.2 74	84.6 79 80.2 74.5	86.3 82 83.4 81	88.3 80 86.4 77.7	85.5 80 80 70	85 78.5 82.3 76.5	80 81 77.6 76.6	84.7 73.4 71.4 72.5	81.2 81 75.7 80
Length of symphysis measured along anterior border	21.5	22.1	20.6	20.7 21.2 22 19.1	18.8 19.1 20.5 20.3	20.6 17.9 22 20	22 19.3 20.2 18.9	21.2 20.6 22 19.5	21.5 20.7 21.8 17.2	22.4 21 21 21	22.8 22.2 23.7 22.3	22 21.8 22.5 19.6	22 20 21.8 22.2	22.2 19.1 19.8 19.6	22.6 18.5 19 19	21.6 21.8 19.9 22.7
Depth of ramus below anterior end of P̄3	14.9	15.4	14.1	14.7 14.6 15.6 13	13.8 12.8 14.1 13	14 12.7 14.2 14	15.6 12.7 13.7 12.7	15 14.4 14.1 13.9	16.2 14.5 14.7 12.2	15.7 14.3 15 14.5	16.1 15.6 15.2 14.9	15.2 13.7 14.5 12.8	15.6 14.3 13.9 13.3	15 13.8 12.5 13.3	15.1 13.2 13.6 13	14.8 14.2 13.7 14.8
Depth of ramus below posterior end of M̄1	15.5	15.8	14.7	16.9 15.4 16.3 15.8	16.9 13.8 14.9 14.5	17.3 13.6 15.1 15.8	18 13.8 16 13.8	16.9 15.8 17.1 14.5	18 16.5 16.3 13	18 16.9 16.1 16	17.9 16.3 17.2 14.7	17.7 15.1 16.6 13.8	16.9 14 16.2 15.7	16.7 15.2 15.1 15.2	18.4 14.8 14.8 13.5	17.8 16.2 14.3 15.8
Thickness of ramus below posterior end of M̄1	6.6	6.7	6 4	6.3 6.3 7.5 6.5	7 6 6.2 7.4	6.9 5.6 6.9 6.1	7 6.1 7.5 6	6.2 6.9 6.9 6.7	6.8 6.9 6.2 6.3	6.3 6.8 7.2 6.3	6.6 7.7 7.9 6.5	6.8 7.1 6.8 6.3	6.8 6.6 6.7 6.6	6.3 6.8 6.4 7.4	6.6 6.1 6.3 6.7	6.7 7.1 6 6.9
Height from inferior border of angle to summit of coronoid process	....	....	....	34.3 36.8 41.1 35.1	31.9 29.6 31.7 34.9	35 30.5 35.2 35.8	37.9 36.8 34.6 32	36.4 38.8 38.9 32.8	36.6 33.7 37.4 31.9	37.7 36.2 39.2 36.5	38.3 39 42.8 36.8	38.1 38.6 36.6 32	38.1 34.6 37.8 34.8	32.3 37.8 36.3 36.8	37.7 34.1 32 30.5	33.8 37.6 33.3 37.4
Transverse width of condyle	....	19.4	....	16.2 18.2 19.9 17	16.6 15 16.8 17.1	17.7 16 17.9 16.8	17.6 17 17.1 15.3	16.3 18.5 18.8 16.4	17.2 17.7 17.6 16	17 18.3 18.8 18	18 19.2 19.3 17.2	17.7 17.3 17.6 16.4	17.7 17.2 17.8 16.8	15.8 19.5 17.6 17.9	17.3 15 15.1 15.8	17.2 17.2 16.9 18.6

[1] Based on specimens in the collections of the Museum of Vertebrate Zoology, University of California.

TABLE 113—*Comparative measurements (in millimeters) of superior dentition*

Key to Identification of Recent Species or Race in Each Rectangle[1]

Lynx canadensis	×	×	*L rufa baileyi*
L. rufa pallescens	×	×	*L. rufa californicus*

	Lynx rufa fischeri Merriam R. L. B. No. X9489 L. A. M.	4797	♂ 47239	♀ 4340	♀ 16247	♀ 4362	♀ 32442	4796	♂ 10605	♂ 4213	♂ 32458	♂ 4214	♂ 25919	4209	♂ 16366	4192	♂ 32460	4186	♂ 7150	♂ 4153	♂ 7087	♀ 4149	♂ 16248	♂ 4155	♀ 7085	♀ 4162	♂ 43937
		♂ 24739	♂ 4906	♀ 23837	♂ 29808	24607	♂ 28794	♀ 11324	♂ 3243	24620	♂ 2333	♂ 24592	♂ 2335	♂ 23795	♀ 21398	37330	♂ 21415	37325	♀ 23880	37298	♂ 23881	37301	♂ 12874	♀ 37302	♀ 19748	♀ 37299	♂ 29786
Length from anterior end of canine alveolus to posterior end of P$\underline{4}$		39.4	36.7	38.6	32.2	39.7	32.5	39.9	34.6	38.6	38.8	41.6	38.2	42.2	38.3	43.2	37.6	40.9	36.5	39.8	37.2	38.2	37.6	40.8	33.6	39.1	37.3
	37.4	38.2	36	34	35.7	37.1	36.8	35.3	34.4	38.2	35.6	37.5	34	38.2	36.8	40	36.1	38.4	33.2	37.5	35.5	36.1	34	33.9	33.6	35.2	37.5
Length from anterior end of P$\underline{3}$ to posterior end of P$\underline{4}$		26.8	23.7	26.7	22.4	26.3	21.5	26.7	21.5	26.4	25.3	27.3	24.6	27.9	24.2	28.4	24.4	26.2	22	26.2	23.9	25.3	24.1	26.9	21.7	26.2	24.7
	24	24.4	23	23.7	24.3	24.2	24.8	23.6	22.5	23.8	23.6	24	21.4	23.8	24	24.8	23.3	24.5	22	23.6	22.5	22.9	22.5	23.6	22.6	22.4	24
Transverse width of entire upper incisor series		14.1	12.3	13.7	12.6	13.6	11.3	14.7	....	13.3	13.5	14.3	13.4	14.1	12.4	14.9	12.4	14.3	12.4	14.1	14.7	14.1	13	13.7	12.4	14.6	12.2
	13.3	12.2	13	12.7	12.6	....	12.4	....	11.8	12.1	12.8	12.9	12.2	12.7	13.2	13.8	12.5	12.9	12.1	13	13.8	12.2	12.8	12.5	12.6	12.8	....
$\underline{\mathrm{C}}$, anteroposterior diameter at base of enamel		7	6.5	7.4	5.2	7	5.7	7.6	6.1	7.1	7.5	8.1	7.2	7.8	6.6	8.3	6.7	7.7	6.2	7.7	6.6	7.1	6.7	7	5.9	7.5	7.2
	*a*6.6	7.5	6.8	5.7	6.6	6.8	7.1	6.1	5.8	7.3	6.6	6.7	6.1	7.1	7.2	6.7	6.4	6.7	6.1	6.8	6.5	6.3	6.6	6.6	6.1	6.1	7.4
$\underline{\mathrm{C}}$, transverse diameter		5.6	4.9	5.9	4.1	5.5	4.6	5.8	4.8	5.7	6	6.1	5.7	6	5.5	6.3	5.7	6.1	5.4	5.8	5.7	5.6	5.4	5.7	4.8	5.9	6.2
	*a*5.8	6.3	5.8	4.9	5.3	5.6	5.6	5	4.9	5.7	5.5	5.5	4.8	6	5.9	5.9	5.3	5.7	4.9	5.7	5.4	5.1	5.5	5	5.1	5	5.8
P$\underline{3}$, anteroposterior diameter		10.6	9.6	10.6	8.8	10.4	8.3	10.7	8.6	10.6	9.7	10.8	9.4	11.5	9.5	11.5	9.3	10.2	8.7	10.4	9	10	9.6	10.9	8.3	10.6	9.6
	9.3	9.5	9.1	9.9	10	9.3	10	9.3	8.6	9.9	9.3	9.2	8.4	9.6	9.9	10	9	10	8.8	9.2	8.7	9.4	9.1	9	8.8	8.7	9.6
P$\underline{3}$, greatest transverse diameter		4.8	4.5	5	4.3	5	4.2	5.3	4.1	4.9	5.1	5.1	4.9	5.2	4.7	5.4	4.7	4.9	4.8	5	4.7	4.9	4.9	5.1	4	5.1	4.8
	5	5	4.9	4.7	4.8	4.9	5.1	4.8	4.3	4.8	5	5	4.2	5	4.8	5.1	4.3	4.8	4.4	4.8	4.5	4.6	4.7	4.3	4.8	4.4	4.8
P$\underline{4}$, anteroposterior diameter		16.4	14.3	16.3	13.7	16	13.3	15.9	13.1	16	15.4	16.8	15.1	16.9	14.7	17.1	14.9	16.1	13.8	16	14.8	15.4	14.6	16	13.5	15.8	14 9
	14.6	15	14.1	13.8	14.8	14.8	14.7	14	8.6	14	14.5	14.3	12.9	14.3	14.4	14.7	14.3	14.8	13.4	14.4	13.9	13.6	13.5	14.8	14	13.8	14.6
P$\underline{4}$, greatest transverse diameter across protocone		7.4	6.6	7.8	6	7.5	5.8	7.9	5.6	7.2	7	7.8	7	7.9	6.1	8	6.6	7.6	6.5	7.3	6.6	7.3	6.7	7.7	6	7.7	6.9
	7.1	7.3	6.3	6.5	6.6	6.7	7.2	6.7	4.1	7.1	6.8	7.1	5.8	7.2	6.5	7	6.3	6.6	6.3	6.2	6.1	6.1	6.4	6.7	6.7	5.7	6.8
P$\underline{4}$, anteroposterior diameter at base of paracone		6	6.2	6.3	5.7	6.1	5.5	6.5	5.3	6	6.5	6.4	6.2	6.1	6.1	6.8	6.4	6.4	5.8	6.4	6.7	5.9	6.2	6.1	6	6.1	6.2
	6.8	6.2	5.8	5.8	6.2	6	6.2	5.8	6.2	5.9	6.1	6	5.7	5.8	6.1	5.8	6	6.1	5.9	5.8	5.4	5.8	5.7	5.8	5.7	5.7	5.9

[1] Based on specimens in the collections of the Museum of Vertebrate Zoology, University of California.

a, Approximate.

TABLE 114—*Comparative measurements (in millimeters) of inferior dentition*

	Lynx rufa fischeri Merriam Rancho La Brea			Key to Identification of Recent Species or Race in Each Rectangle[1] *Lynx canadensis* × × *L. rufa baileyi* *L. rufa pallescens* × × *L. rufa californicus*																									
	No. X9490 L.A.M.	No. X9262 L.A.M.	No. X9082 L.A.M.	4797 ♂ 24739	♂ 47239 ♂ 4906	♀ 4340 ♀ 23837	♀ 16247 ♂ 29808	♀ 4362 24607	♀ 32442 ♂ 28794	4796 ♀ 11324	♂ 10605 ♂ 3243	♂ 4213 24620	♂ 32458 ♂ 2333	♂ 4214 ♂ 24592	♂ 25919 ♂ 2335	4209 ♂ 23795	♂ 16366 ♀ 21398	4192 37330	♂ 32460 ♂ 21415	4186 37325	♂ 7150 ♀ 23880	♂ 4153 37298	♂ 7087 ♂ 23881	♀ 4149 37301	♂ 16248 ♂ 12874	♂ 4155 ♀ 37302	♀ 7085 ♀ 19748	♀ 4162 ♀ 37299	♂ 43937 ♂ 29786
Length from anterior end of $\overline{C}$ to posterior end of M$\overline{1}$	*a*45.7	*a*46	43.9	44.8 44.7	41.8 40.5	44.9 40.2	36.4 42	45.8 42.7	37.4 42.6	46.8 40	39.4 39.3	44.9 44	44.4 41.4	48.2 42.2	43.5 38.4	48.2 44.5	43.5 43.1	49.4 45.2	43.2 41.6	47.5 44.5	42.6 38	45.5 43.4	43.3 41	44.5 40.8	42.4 40.8	46.2 39	39 39	45.5 40.2	43.7 43.7
Length from anterior end of P$\overline{3}$ to posterior end of M$\overline{1}$	29	29.1	30.2	30.6 28.3	27.5 25	31.3 26.8	24.9 27.2	30.2 27.9	24.6 28.2	32.3 26.1	25.5 25.5	31 27.2	28.2 28.3	32.1 27.2	28.3 24.6	32.5 27.1	27.6 27.8	33.5 28.2	28 27.1	31 28.4	26.3 25.1	30.7 27	28.9 25.5	30.5 25.4	27.8 26.8	30.9 26.9	24.7 25.5	31.4 26.2	28.5 27.6
Length of lower diastema between canine and P$\overline{3}$	9.3	9.6	6.5	7.1 8.5	7.5 9.2	6.1 7.3	6.1 8.3	8.4 8.2	6.8 7.6	7.9 8	7.3 7.8	6.5 9.3	8.6 6.8	8.2 8.3	7.8 6.8	9 9.6	9.4 8.1	7.7 10	8.7 7.8	9.1 8	9.8 6.6	7.1 9.2	7.5 8.9	6.8 9.1	7.8 7.9	8.5 5.8	8.7 7.6	7 8.4	8 8.7
Transverse width of entire lower incisor series	....	....	....	11.7	10	11.3	10.6 9.5	11.2	8.7 9.7	12.8	... 9.3	11 9.3	.... 10.6	11.3	11 10.4	11.1	10.1 9.9	12.5	....	11.8 10.3	*a*8.8 9.9	11.9	*a*11.8 10.7	12.2	10.5 10.4	11.8	9.8 10.3	11.5 10.4	10.3 10.5
$\overline{C}$, anteroposterior diameter at base of enamel	....	....	7.5	6.5 7.4	6.4 6.3	6.8 5.8	5.1 6.2	6.4 6.1	5.6 6.4	6.9 5.8	5.9 5.9	7 6.7	7 6.1	7.4 6.1	6.6 6.1	7.2 6.6	6.4 6.9	7.7	6.2 6.1	7.2 6.8	6.2 5.9	7.2 6.6	6.4 6.3	6.5 5.8	6.1 6.3	6.7 6.3	5.5 6	7 5.8	7.1 6.8
$\overline{C}$, transverse diameter	....	....	5.7	5 5.8	5.6 5.1	5.4 4.2	4.3 5.2	5 4.9	4.3 5.2	4.9 4.8	4.7 4.4	5 5.3	5.4 5	5.3 4.9	5.5 4.9	5.2 5.4	5.1 5.5	5.8	5.2 4.9	5.4 5.3	5.1 4.7	5.3 5.3	5 5	4.7 4.8	4.9 5.1	5 4.7	4.7 4.5	5.1 4.8	5.4 5.5
P$\overline{3}$, anteroposterior diameter	7.5	7.7	8.2	8.3 7.8	7.6 6.8	8.1 7.2	6.5 7.1	7.6 7.7	6.6 7.5	8.6 7.1	7.1 6.7	8.1 7	7.1 7.5	8.8 7.1	7.5 6.1	8.8 7.3	7.2 7.3	9 7.2	7.5 6.8	8.3 7.4	6.7 6.7	8 7.3	6.9 6.1	7.8 6.6	7.3 7.1	7.8 7.1	6 6	8.1 7.2	7.7 7.1
P$\overline{3}$, greatest transverse diameter	4.1	4.2	4.6	4.3 4.2	4 3.7	4.4 3.7	3.5 3.7	4.3 3.8	3.3 4.2	4.7 4	3.6 3.5	4.3 4.2	4 3.8	4.4 4	4.1 3.4	4.3 4	3.8 3.9	4.7 4.1	3.9 3.5	4.5 4	3.8 3.4	4.4 4.2	3.7 3.5	4.2 3.7	3.8 3.7	4.1 3.6	3.1 3.5	4.4 3.8	3.9 3.9
P$\overline{4}$, anteroposterior diameter	10.2	10.4	10.1	10.8 9.7	9.2 8.7	10.6 9.2	8.5 9	10.1 9.5	8.1 10	10.8 9.2	8.5 8.7	10.8 9.9	9.2 9.8	11.1 9.4	9.3 8.5	11.1 9.2	9.3 9.7	11.2 9.3	9.6 8.9	10.6 10	8.9 8.1	10.5 9	9.2 8.6	10.4 8.5	9.2 8.9	10.6 9.7	8.3 8.8	11 8.8	9.6 9.5
P$\overline{4}$, greatest transverse diameter	4.9	5	5.2	4.6 5	4.5 4.4	5.1 4.3	4 4.5	4.6 4.5	4 4.6	5 4.5	4 4.2	4.8 4.7	4.7 4.6	5 4.7	4.8 4.2	4.9 4.8	4.4 4.5	5.2 4.8	4.5 4.3	4.8 4.8	4.2 3.9	4.7 4.7	4.5 4.1	4.5 4.4	4.5 4.4	4.8 4	3.9 4.4	4.9 4.2	4.4 4.6
P$\overline{4}$, basal length of principal cusp	5	5	4.9	5.3 4.9	5 4.2	5.3 4.6	4.2 4.8	4.8 4.9	4.5 4.8	5.2 4.8	4.8 4.4	5 4.9	4.8 5	5.3 4.6	4.7 4.8	5.2 4.5	5 4.8	5.7 4.6	4.8 4.9	5.3 5.1	4.8 4.1	5 4.8	4.7 3.7	5 4.6	4.5 4.1	5.1 4.8	4.4 4.3	5.1 4.8	4.9 4.4
M$\overline{1}$, anteroposterior diameter	12.3	12.7	13.3	12 11.6	11 10	13.4 10.5	10.3 11.1	12.3 10.9	9.8 11.3	12.7 10.8	9.8 9.9	12.3 10.3	11.8 11.8	12.8 10.9	11.5 10.7	13.2 10.9	11.9 10.7	13.3 11.2	10.8 11.4	12.6 11.8	*a*10 10.1	11.8 10.7	11.6 10.6	11.8 9.7	11.2 10.9	11.5 11.4	10.1 11.1	12.8 10.6	11.5 11.8
M$\overline{1}$, greatest transverse diameter	5.2	5.5	5.5	5.2 5.4	4.9 4.6	5.6 5	4.5 5	5.1 4.9	4.2 5	6.1 5.2	4.5 4.5	5.3 5.1	5 4.7	5.4 5.5	5.4 4.8	5.8 5.3	5.2 4.8	5.8 5.3	5 4.7	5.2 5.1	4.9 4.7	5.1 5.1	5 5	5.2 4.7	4.8 4.7	5.3 4.8	4.5 4.7	5.4 5	4.9 5.2
M$\overline{1}$, length of protoconid blade	....	5.7	5.1	5.9 6	5.1 4.8	6.5 5.6	5.4 5.3	6.2 5.7	5.2 5.4	6 4.8	4.6 5	5.8 5.3	5.7 5.6	6.2 5	4.9 4.8	6.1 5.8	5.5 4.8	6.4 4.8	5.4 5.1	6 5.1	4.8 5.3	5.9 5.5	5.6 5.2	6 4.9	5.2 5	6.2 5.4	4.9 4.8	6.2 5.1	5.4 4.6

[1] Based on specimens in the collections of the Museum of Vertebrate Zoology, University of California.

a, Approximate

OCCURRENCE AND DESCRIPTION OF PLEISTOCENE FELIDÆ IN WESTERN NORTH AMERICA

PACIFIC COAST PROVINCE

In the review of the literature relating to the Pleistocene and late Tertiary cats of western North America mention has been made of the known occurrences of these types. There remain to be considered here the later acquisitions of ma-

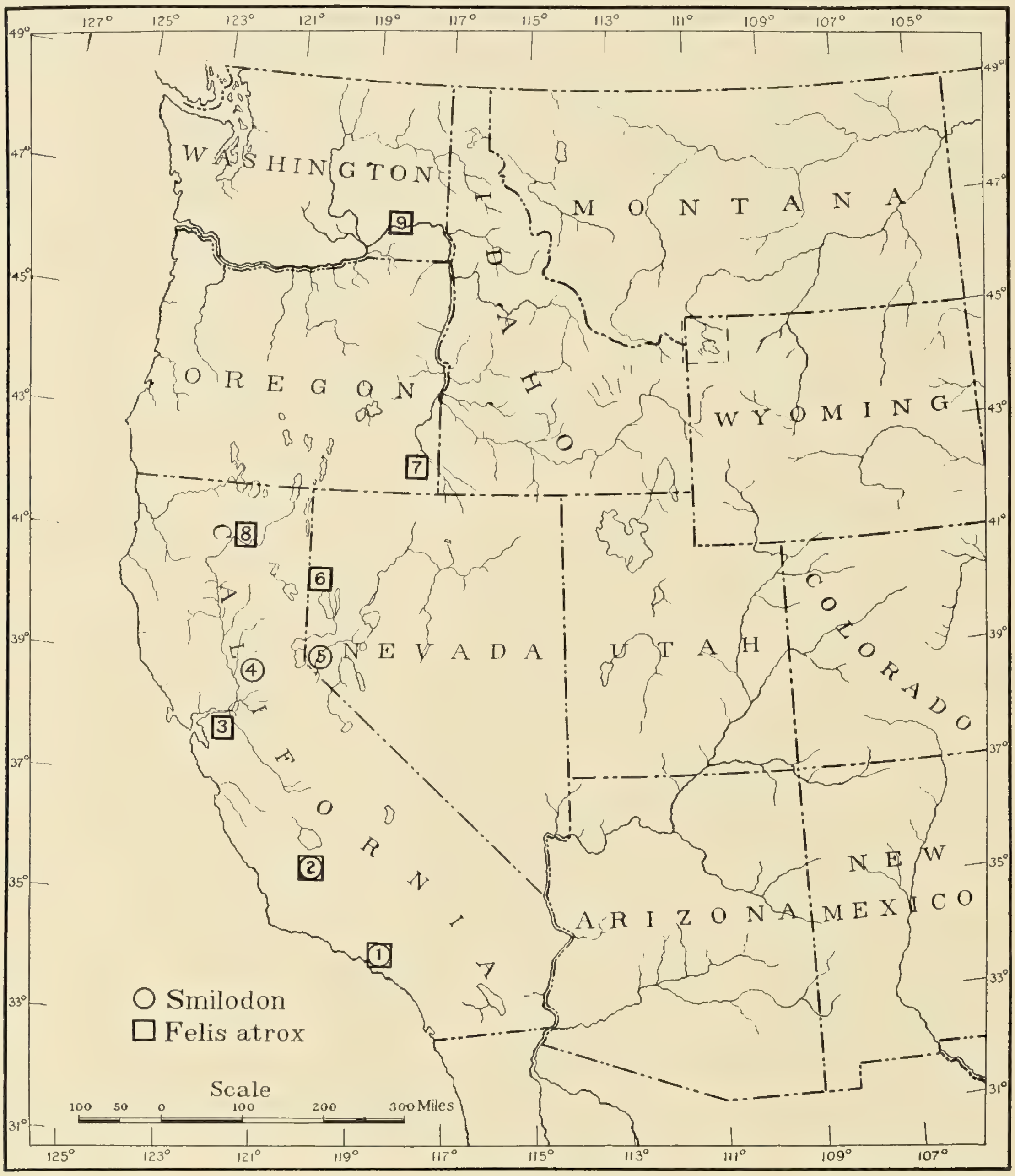

FIG. 151—Outline map showing Pleistocene occurrences of ***Smilodon*** and ***Felis atrox*** in western North America. 1, Rancho La Brea and vicinity, Los Angeles County; 2, McKittrick, Kern County; 3, Livermore Valley, Alameda County; 4, Hawver Cave, Eldorado County; 5, Carson City, Nevada (occurrence questionable); 6, Astor Pass, Nevada; 7, Rome, Malheur County, Oregon; 8, Potter Creek Cave, Shasta County, California; 9, Washtuckna Lake, Washington.

terial and the additional information obtained at new localities. The map, figure 151, shows the occurrences of the larger felids in this western region.

McKittrick, California.—Clearly of major importance is the occurrence of the Pleistocene fauna in the asphalt, tar and clay of McKittrick, Kern County, California. While collections obtained from these deposits are considerably smaller than those from Rancho La Brea, a large and diversified assemblage of mammals and birds is now known from the former locality. The Felidæ are by no means as numerous as at Rancho La Brea, but the larger types are represented by the sabre-tooth and by the species *Felis (Panthera) atrox,* while the smaller forms include the puma and the wildcat. Materials of the latter form are still incomplete.

In view of the small number of individuals recorded it is perhaps unsafe to draw conclusions as to the factors responsible for the numerical representation of individual forms. However, the larger cats apparently do not dominate in numbers the puma and wildcat to the extent seen in the Rancho La Brea fauna. Nor is the sabre-tooth cat particularly well represented at this locality. Indeed, there is some reason for believing that the great true felines are better represented than is the sabre-tooth.

Skull and skeletal material of the sabre-tooth clearly indicates the presence of a form specifically identical with *Smilodon californicus.* The only skull and lower jaw available from the McKittrick deposits is No. 650, Calif. Inst. Tech. Coll. Vert. Pale. This belongs to an old individual in which many of the sutures are obliterated and practically all the teeth, when not broken, are worn. No. 650 corresponds in size to the larger specimens whose masurements are given in Table 3. Indeed, in some measurements of the skull and dentition No. 650 exceeds the larger skulls from Rancho La Brea.

The species *Felis atrox* was recorded in the original list of the mammals found in the McKittrick beds. Skull and skeletal remains indicate the presence of several individuals and two nearly complete skulls are now available in the collections of the California Institute, Nos. 648 and 649. No. 648 corresponds in size to one of the larger skulls of *Felis atrox* from Rancho La Brea, having a total length and a width across the zygomatic arches close to that in No. 2900-9 from the latter locality. No. 649, also of an adult, is distinctly smaller than No. 648 and is smaller than skulls of average size from Rancho La Brea. In No. 649 the second upper premolar is present and measures 8.8 mm. in anteroposterior diameter and 7 mm. in transverse diameter. The crown of the tooth resembles that in *Felis spelæa.* It possesses a low ridge extending in the direction of the long diameter with a depressed area on the inner side and a very small depressed area on the postero-external side.

The puma is represented in the McKittrick assemblage by a skull of an adult individual, No. 29524 Univ. Calif. Coll. Unfortunately this specimen is somewhat distorted and not completely preserved so that a series of measurements can not be given. The teeth, however, are well preserved. No. 29524 is characterized particularly by a heavy dentition, the dimensions of the teeth being in excess of those for the type of *Felis bituminosa* (see measurements, Table 107). In size of teeth this specimen may resemble *Felis daggetti,* judged in the light of the lower teeth present in the type of the latter species from Rancho La Brea. When No. 29524 and No. 21572 (type of *F. daggetti*) are compared with the skull and jaw of *F. bituminosa* (No. X8628) respectively, the differences in size of upper dentitions corresponds closely to that which exists between the lower. No. 29524 may represent a large male individual of the *F. bituminosa* group or it may be more nearly related to *F. daggetti.* It is provisionally referred to the latter species.

In P3 the postero-external corner of the crown is prominently developed. For measurements of upper teeth see Table 107.

Los Angeles basin.—Two fused vertebræ of a sabre-tooth cat were found during the excavation of section X of the trench for the north outfall sewer of the City of Los Angeles in 1924. The locality occurs immediately to the north of the Baldwin Hills in the region of Ballona Plain and approximately three miles south and slightly west of Rancho La Brea. The specimens were said to have been found at the base of the upper boulder bed exposed in this section. According to Tieje[1] this boulder bed represents material carried in an ancient stream course through this region of the Los Angeles basin in post-upper San Pedro (Palos Verde) time. Not only is the boulder bed later than marine strata of the upper San Pedro, but overlying the latter and beneath the former are also fresh-water clays in which fresh-water shells and bones of the Pleistocene ground-sloth *Mylodon* occurred. The late Pleistocene series has a dip of approximately 15° to the northeast. The two vertebræ, No. 881 L. A. Mus. Coll. representing the eleventh and twelfth of the thoracic series, show the characteristic pathologic lesion with development of excess bone tissue seen frequently in vertebræ of the sabre-tooth from Rancho

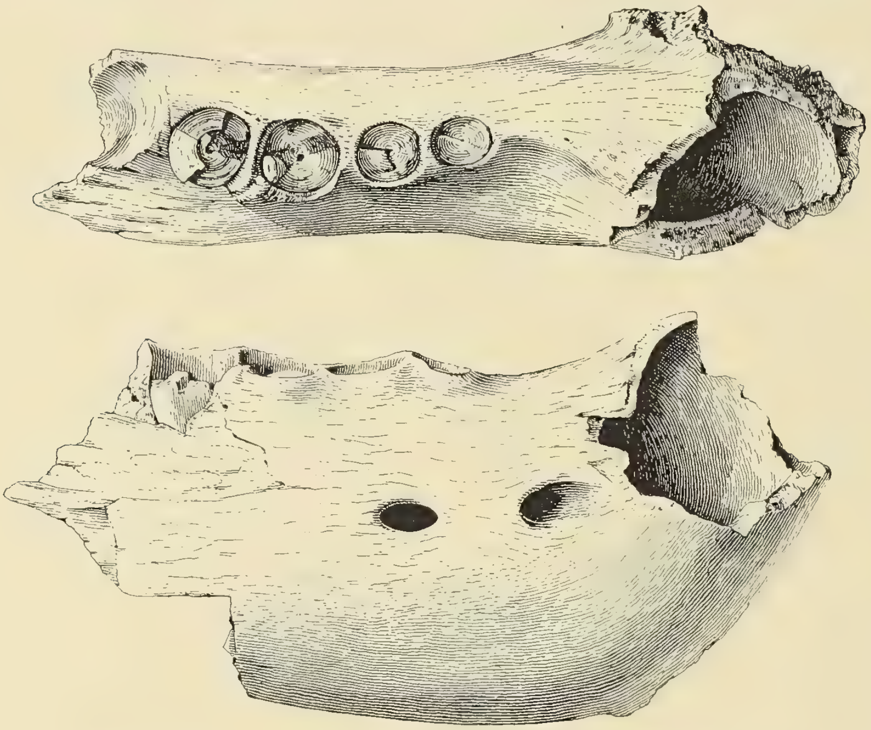

FIG. 152—*Felis* cf. *atrox* Leidy. Fragment of ramus, No. 647, lateral and dorsal views; × 1. Owyhee Pleistocene, Malheur Co., Oregon. California Institute of Technology Collections.

---

[1] Tieje, A. J., *The Pliocene and Pleistocene history of the Baldwin Hills, Los Angeles County, California,* Bull. Amer. Assoc. Petrol. Geol., vol. 10, pp. 502-512, 1 fig. in text, 1926.

La Brea. The specimens doubtless belong to *Smilodon* and may be referred to the species occurring in the asphalt. The vertebræ are not water-worn and could not have been transported for any great distance if they occurred in the boulder bed. The possibility remains that the specimens occurred originally in the fresh-water clays overlying the marine strata of upper San Pedro age and below the boulder bed. In either case the occurrence is particularly noteworthy because it indicates the presence of a sabre-tooth cat in the Los Angeles region in very late geologic time.

GREAT BASIN PROVINCE

Malheur County, Oregon.—In recent years field explorations in the vicinity of Rome on the Owyhee River in southeastern Oregon has furnished a Pleistocene fauna including *Equus* cf. *pacificus*, *Mylodon harlani*, *Camelops*, and a cat of the *Felis atrox* group. The specimen representing the latter form is a fragment of the right ramus, No. 647 Calif. Inst. Coll. Vert. Pale., figure 152. The fragment lacks the teeth although the roots of $P\overline{3}$ and $P\overline{4}$ are in part preserved.

LITERATURE

The literature on the cats, both living and extinct, is voluminous and no attempt is made here to give an exhaustive bibliography. The citations for the most part refer to contributions relating particularly to the study of the Felidæ of Rancho La Brea. The important bibliographies by O. P. Hay (Bull. U. S. Geol. Surv. No. 179, 1902; Carnegie Inst. Wash. Pub. No. 390, 1929.) should be consulted for further references.

ADAMS, G. I.

1896. The extinct Felidæ of North America. Amer. Jour. Sci., ser. 4, vol. 1, pp. 419-444, pls. 10-12.

———, ———,

1897. On the extinct Felidæ. Amer. Jour. Sci., ser. 4, vol. 4, pp. 145-149, figs. 4-8.

AMEGHINO, F.

1889. Contribucion al conocimiento de los mamiferos fosiles de la República Argentina. Act. Acad. Nac. de Ciencias de la Rep. Argentina, vol. 6, pp. 325-342, pl. 3, figs. 3 and 4, 2 figs. in text.

———.

1916. Obras completas y correspondencia cientifica. Vol. 6, Los mamíferos fósiles de la República Argentina. Pt. 1, Planungulados y unguiculados. Buenos Aires. pp. 550-578, 2 figs. in text.

BLAINVILLE, H. M. D. DE.

1839-64. Ostéographie, ou description iconographique comparée du squelette et du systeme dentaire des Mammifères récents et fossiles pour servir de base à la zoologie et à la géologie. Des Felis, vol. 2, 196 pp.; Atlas, vol. 2, pls. 5-20.

BOULE, M.

1901. Revision des espèces Européennes de *Machairodus*. Bull. Soc. Geol. France, ser. 4, vol. 1, pp. 551-573, 17 figs. in text.

———,

1906. Les grands chats des cavernes. Ann. de Paléontologie, vol. 1, pp. 69-95, pls. 4-7, 12 figs. in text.

———, and A. THEVENIN.

1920. Mammifères fossiles de Tarija. Paris, Imprimerie Nationale, pp. 234-241, pl. 26.

BOVARD, J. F.

1907. Notes on Quaternary Felidæ from California. Univ. Calif. Publ. Bull. Dept. Geol., vol. 5, pp. 155-170, pls. 13-14.

BROWN, B.

1908. The Conard fissure, a Pleistocene bone deposit in northern Arkansas: With descriptions of two new genera and twenty new species of mammals. Mem. Amer. Mus. Nat. Hist., vol. 9, pt. 4, pp. 155-208, pls. 14-25.

BURMEISTER, H.

1866. Fauna Argentina, primera parte, mamíferos fosiles. Anales d. Mus. Pub. d. Buenos Aires, vol. 1, pp. 123-141.

———.

1868. Bericht über ein Skelet von Machaerodus, im Staats-Museum zu Buenos Aires. Abh. d. Naturf. Gesellsch. zu Halle, vol. 10, pp. 183-196, 1 pl.

———.

1879. Description physique de la République Argentine d'après des observations personnelles et étrangères. Buenos Aires, vol. 3, animaux vertébrés, pt. 1, mammifères vivants et éteints, pp. 105-136.

———.

1881. Atlas de la description physique de la République Argentine contenant des vues pittoresques et des figures d'histoire naturelle. 2d section, Mammifères, pl. 9.

BURT, W. H.

1931. *Machærodus catocopis* Cope from the Pliocene of Texas. Univ. Calif. Publ. Bull. Dept. Geol. Sci., vol. 20, pp. 261-292, pls. 43-50.

CLERICI, E.

1888. Sopra alcune specie di felini della caverna al Monte delle Gioie presso Roma. Boll. d. R. Comitato Geol. D'Italia, ser. 2, vol. 9, pp. 149-167, pl. 4.

COPE, E. D.

1880. On the extinct cats of America. Amer. Nat., vol. 14, pp. 833-858, 15 figs.

———,

1893. A new Pleistocene sabre-tooth. Amer. Nat., vol. 27, pp. 896-897.

———,

1894. Extinct *Bovidæ*, *Canidæ* and *Felidæ* from the Pleistocene of the Plains. Jour. Acad. Nat. Sci. Phila., ser. 2, vol. 9, pp. 453-459, pls. 21-22.

———,

1895. The fossil vertebrata from the fissure at Port Kennedy, Pa. Proc. Acad. Nat. Sci. Phila., pp. 446-450.

———.

1899. Vertebrate remains from Port Kennedy bone deposit. Jour. Acad. Nat. Sci. Phila., ser. 2, vol. 11, pp. 193-267, pls. 18-21.

DAWKINS, W. B. and W. A. SANFORD.

1866-1871. The British Pleistocene Mammalia. British Pleistocene Felidæ. Mem. Palæontographical Soc., pt. 1, pp. i-L; 1-28, pls. 1-5; pt. 2, pp. 29-124, pls. 6-19; pt. 3, pp. 125-176, pls. 20-23; pt. 4, pp. 177-194, pls. 24-25.

Denton, W.

1875. On an asphalt bed near Los Angeles, Cal., and its contained fossils. Proc. Bost. Soc. Nat. Hist., vol. 18, pp. 185-186.

Doran, A. H. G.

1879. Morphology of the mammalian ossicula auditus. Trans. Linn. Soc. Lond., ser. 2, vol. 1, zool., art. 18, pp. 371-497, pls. 58-64.

Eaton, G. F.

1922. John Day Felidæ in the Marsh collection. Amer. Jour. Sci., ser. 5, vol. 4, pp. 425-452, 12 figs. in text.

Edinger, T.

1929. Die fossilen Gehirne. J. Springer, Berlin, 249 pp., 203 figs. in text. Bibliography of 250 titles.

Fabrini, E.

1890. I Machairodus (Meganthereon) del Valdarno superiore. Boll. d. R. Comitato Geol. D'Italia, ser. 3, vol. 1, pp. 121-144; 161-177, pls. 4-6.

———, 1895. Sopra due Felis di Romagnano. Boll. d. Soc. Geol. Italiana, vol. 14, pp. 164-169, pl. 7.

Filhol, E., and H. Filhol.

1870. Description des ossements de *Felis spelœa,* découverts dans la caverne de l'Herm (Ariége). Ann. d. sci. nat., ser. 5, Zool. et Palé., vol. 14, pp. 1-120, 17 pls.

Freudenberg, W.

1910. Die Säugetierfauna des Pliocäns und Post-Pliocäns von Mexiko. 1: Carnivoren. Geol. und Palæ. Abh., N. F., vol. 9, pp. 195-231, pls. 20-29, 5 figs. in text.

———, 1914. Die Säugetiere des älteren Quartärs von Mitteleuropa. Geol. und Palæ. Abh., N. F., vol. 12, pp. 455-670, pls. 29-48.

Frick, C .

1930. Alaska's frozen fauna. Nat. Hist., vol. 30, pp. 70-80, illus.

Gervais, P.

1855. Recherches sur les mammifères fossiles de l'Amérique meridionale. Ext. de la Zoologie de l'Expedition dans les parties centrales de l'Amérique du Sud, publiée sous la direction de M. le comte Francis de Castelnau. Pages 9-11, pl. 4.

———, 1859. Zoologie et Paléontologie françaises. Nouvelles recherches sur les animaux vertébrés dont on trouve les ossements enfouis dans le sol de la France et sur leur comparaison avec les espèces propres aux autres régions du Globe. Paris, 2nd Ed., pp. 226-231, Atlas, pl. 27.

———, 1878. Sur la dentition des Smilodons. Comptes Rendus, pp. 582-583. (On the dentition of Smilodon, Ann. and Mag. Nat. Hist., ser. 5, vol. 3, pp. 95-96, 1879.).

Gervais, H., and F. Ameghino.

1880. Les mammifères fossiles de l'Amérique du sud. Paris and Buenos Aires, pp. 10-20.

Goldfuss, A.

1821. Osteologische Beiträge zur Kenntniss verschiedener Säugethiere der Vorwelt. IV: Ueber den Schädel des Höhlenlöwen. Verhandl. d. K. Leopold.-Carol. Akad. d. Naturf., vol. 10, pt. 2, pp. 489-494, pl. 45.

Gray, J. E.

1867. Notes on the skulls of the cats (Felidæ). Proc. Zool. Soc. Lond., pp. 258-277, 7 figs. in text.

Hagmann, G.

1899. Die diluviale Wirbeltierfauna von Vöklinshofen (O.E.). I Teil: Raubtiere und Wiederkäuer mit Ausnahme der Rinder. Abh. z. geol. Specialkarte von Elsass-Lothringen, N.F., Hft. 3, pp. 62-73, pl. 3.

Hay, O. P.

1920. Descriptions of some mammalian and fish remains from Florida of probably Pleistocene age. Proc. U. S. Nat. Mus., vol. 56, pp. 103-112, pls. 26-28.

———, 1921. Description of some Pleistocene vertebrates found in the United States. Proc. U. S. Nat. Mus., vol. 58, pp. 83-146, pls. 3-11.

Hilzheimer, M.

1905. Über einige Tigerschädel aus der Strassburger zoologischen Sammlung. Zool. Anz., vol. 28, pp. 594-599; 6 figs. in text.

———, 1922. Die systematische Stellung von *Felis spelæa* Goldf. Zugleich ein Beitrag zur vergleichenden Osteologie von Löwe und Tiger. Sitzber. naturforsch. Freunde, No. 1-2, 24 pp.

Hollister, N.

1917. Some effects of environment and habit on captive lions. Proc. U. S. Nat. Mus., vol. 53, pp. 177-193, pls. 22-25.

———, 1918. East African mammals in the United States National Museum. Pt. 1: Insectivora, chiroptera and carnivora. U. S. Nat. Mus. Bull. 99, 194 pp., 55 pls., 3 figs. in text.

Jaekel, O.

1927. Prähistorische Löwen aus dem Formenkreis der Felis spelæa. Zool. Anz., vol. 70, pp. 225-236, 4 figs. in text.

Jayne, H.

1898. Mammalian anatomy. A preparation for human and comparative anatomy. Pt. 1: The skeleton of the cat. J. B. Lippincott Co., Phila., xix, 816 pp., 611 figs. in text, many tables.

Kampen, P. N. van

1905. Die Tympanalgegend des Säugetierschädels. Gegenbaurs Morph. Jahrb., vol. 34, pp. 501-508, figs. 45-46.

Klaauw, C. J. van der.

1931. The auditory bulla in some fossil mamals with a general introduction to this region of the skull. Bull. Amer. Mus. Nat. Hist., vol. 62, 352 pp., 18 figs. in text.

Klinghardt, F.

1931. Vergleichende Untersuchungen über das Gehirn und Gehirnrelief einiger rezenter und fossiler Raubtiere nebst Bemerkungen über die Schädel. Palæontographica, vol. 74, pp. 135-176, pls. 24-25.

Kretzoi, N.

1929. Materialien zur phylogenetischen Klassifikation der Æluroïdeen. X^e Congrès International de Zoologie tenu à Budapest (Sept. 4-10, 1927), pt. 2, pp. 1293-1355.

Landau, E.

1908. Beitrag zur Kenntnis des Katzenhirns (Hirnfurchen). Morph. Jahrbuch, vol. 38, pp. 1-35, pls. 1-4, appended bibliog. of 26 titles.

Leidy, J.

1853. Description of an extinct species of American lion: *Felis atrox*. Trans. Amer. Philos. Soc., vol. 10, n.s., pp. 319-321, pl. 34.

———, 1868. Notice of some vertebrate remains from Harden Co., Texas. Proc. Acad. Nat. Sci. Phila., pp. 174-176.

———, 1869. The extinct mammalian fauna of Dakota and Nebraska, etc. Jour. Acad. Nat. Sci. Phila., ser. 2, vol. 7, pp. I-VII, 8-472, 30 pls.

———, 1873A. Remarks on extinct mammals from California. Proc. Acad. Nat. Sci. Phila., pp. 259-260.

———, 1873B. Contributions to the extinct vertebrate fauna of the western territories. In Report of United States Geological Survey of the Territories by F. V. Hayden, vol. 1, pt. 1, 358 pp., 37 pls.

———, 1889A. The saber-tooth tiger of Florida. Proc. Acad. Nat. Sci. Phila., pp. 29-31.

———, 1889B. Description of mammalian remains from a rock crevice in Florida. Trans. Wagner Free Inst. Sci., vol. 2, pp. 13-16, pl. 3, fig. 1.

Lull, R. S.

1921. Fauna of the Dallas sand pits. Amer. Jour. Sci., ser. 5, vol. 2, pp. 159-176, 5 figs. in text.

Lund, P. W.

1842. Blik paa Brasiliens dyreverden för sidste jordomvaeltning. Fjerde afhandling: Fortsaettelse af pattedyrene. K. danske videnskabernes selskabs naturvid. og mathem., Afd., vol. 9, pp. 190-193, pls. 36-37.

———, 1846. Meddelelse af det udbytte de I 1844 undersögte knoglehuler have afgivet til kundskaben om Brasiliens dyreverden för sidste jordomvaeltning. K. danske videnskabernes selskabs naturvid. og mathem., Afd., vol. 12, pp, 82-84, pls. 47-48.

Lydekker, R.

1884. Indian tertiary and post-tertiary vertebrata. Siwalik and Narbada carnivora. Mem. Geol. Surv. India., Palae. Indica, ser. 10, vol. 2, pp. 313-348, pls. 40-45.

Matthew, W. D.

1902. List of the Pleistocene fauna from Hay Springs, Nebraska. Bull. Amer. Mus. Nat. Hist., vol. 16, pp. 317-322.

———, 1910. The phylogeny of the Felidæ. Bull. Amer. Mus. Nat. Hist., vol. 28, pp. 289-316, 15 figs. in text.

———, 1918. Contributions to the Snake Creek fauna with notes upon the Pleistocene of western Nebraska, American Museum Expedition of 1916. Bull. Amer. Mus. Nat. Hist., vol. 38, pp. 226-229.

———, 1929. Critical observations upon Siwalik mammals. Bull. Amer. Mus. Nat. Hist., vol. 56, pp. 437-560, 55 figs. in text.

Merriam, J. C.

1905. A new sabre-tooth from California. Univ. Calif. Publ. Bull. Dept. Geol., vol. 4, pp. 171-175, 1 fig. in text.

———, 1906. Recent discoveries of Quaternary mammals in southern California. Science, n.s., vol. 24, pp. 248-250.

———, 1909. The skull and dentition of an extinct cat closely allied to ***Felis atrox*** Leidy. Univ. Calif. Publ. Bull. Dept. Geol., vol. 5, pp. 291-304, pl. 26, 3 figs. in text.

———, 1910. New mammalia from Rancho La Brea. Univ. Calif. Publ. Bull. Dept. Geol., vol. 5, pp. 391-395.

———, 1912. Recent discoveries of carnivora in the Pleistocene of Rancho La Brea. Univ. Calif. Publ. Bull. Dept. Geol., vol. 7, pp. 39-46, 10 figs. in text.

———, 1915. An occurrence of mammalian remains in a Pleistocene lake deposit at Astor Pass, near Pyramid Lake, Nevada. Univ. Calif. Publ. Bull. Dept. Geol., vol. 8, pp. 377-384, pl. 41, 3 figs. in text.

———, 1918A. New mammalia from the Idaho formation. Univ. Calif. Publ. Bull. Dept. Geol., vol. 10, pp. 523-530, 5 figs. in text.

———, 1918B. New puma-like cat from Rancho La Brea. Univ. Calif. Publ. Bull. Dept. Geol., vol. 10, pp. 535-537, 2 figs. in text.

———, 1919. Tertiary mammalian faunas of the Mohave Desert. Univ. Calif. Publ. Bull. Dept. Geol., vol. 11, pp. 543-546, fig. 155.

Meyer, A. B.

1903. The antiquity of the lion in Greece. Smithson. Ann. Rpt., pp. 661-667.

Mivart, St. G.

1881. The cat. An introduction to the study of back-boned animals especially mammals. Charles Scribner's Sons, N. Y., 557 pp., illustrated.

Moodie, R. L.

1922. On the endocranial anatomy of some Oligocene and Pleistocene mammals. Jour. Comp. Neur., vol. 34, pp. 343-379, 25 figs. in text, bibliography.

———, 1927. Studies in Paleopathology, XX. Vertebral lesions in the sabre-tooth, Pleistocene of California, resembling the so-called myositis ossificans progressiva, compared with certain ossifications in the dinosaurs. Ann. Med. Hist., vol. 9, pp. 91-102, 11 figs. in text.

———, 1929. Studies in Paleodontology, XVI. The California sabre-tooth; the mandibular teeth and associated structures. Pacific Dental Gazette, vol. 37, pp. 317-321, 6 figs. in text.

———,
1930A. Studies in Paleopathology, XXV. Hypertrophy in the sacrum of the sabre-tooth, Pleistocene of southern California. Amer. Jour. Surgery, n.s., vol. 8, pp. 1313-1315, 2 figs. in text.

———,
1930B. Studies in Paleopathology, XXVIII. The phenomenon of sacralization in the Pleistocene sabre-tooth. Amer. Jour. Surgery, n.s., vol. 10, pp. 587-589, 2 figs. in text.

Nordmann, A. von.
1858. Palaeontologie Suedrusslands II. Felis, Hyæna, Canis, Thalassictis, Mustela, Lutra, Spermophilus, Arvicola, Spalax, Castor, Lepus and Equus. Helsingfors, text quarto, atlas folio, pp. 111-115, pl. 1, figs. 1-4.

Osborn, H. F.
1915. Review of the Pleistocene of Europe, Asia and northern Africa. Annals N. Y. Acad. Sci., vol. 26, pp. 281-282.

Owen, R.
1846. A history of British fossil mammals, and birds. Carnivora. London. Pp. 161-183, figs. 63-70.

Pavlow, M.
1908. Quelques carnivores fossiles du gouv. de Kherson et de Bessarabia. Mém. Soc. des Naturalistes de la Nouvelle-Russie, Odessa, vol. 32, pp. 27-49, 2 pls.

Ping, C.
1926. On the skeleton of Felis tigris. Contrib. Biol. Lab. of Sci. Soc. of China, vol. 2, no. 1, 6 pp., 5 figs. in text.

———,
1927. On the structures of the hard palate of *Felis tigris*. Proc. Zool. Soc. Lond., pt. 1, pp. 135-139.

Pocock, R. I.
1917. The classification of existing Felidæ. Ann. and Mag. Nat. Hist., ser. 8, vol. 20, pp. 329-350.

———,
1929. Tigers. Jour. Bombay Nat. Hist. Soc., vol. 33, pp. 505-541, 13 pls.

Reichenau, W. von.
1906. Beiträge zur näheren Kenntnis der Carnivoren aus den Sanden von Mauer und Mosbach. Abh. d. grossherzoglich hessischen geol. Landesanstalt z. Darmstadt, vol. 4, pp. 301-312, pls. 9-10, 12-14.

Reighard, J., and H. S. Jennings.
1929. Anatomy of the cat. Henry Holt and Co., N. Y., 2d ed., 498 pp., 173 figs. in text.

Riabinin, A.
1919. Les lions fossiles de la chaîne de l'Oural et de la région du Volga. Mem. Com. Geol., N. S., Publ. 168, Petrograd, 24 pp., 5 pls. (Russian with French résumé).

Roemer, F.
1883. Die Knochenhöhlen von Ojcow in Polen, Palæontographica, vol. 29, pp. 193-233, pls. 22-33.

Schlosser, M.
1903. Die fossilen Säugethiere Chinas nebst einer Odontographie der recenten Antilopen. Abh. K. Bayer. Akad. Wiss., class 2, vol. 22, pt. 1, pp. 37-40, pl. 1.

Stock, C.
1918. The Pleistocene fauna of Hawver Cave. Univ. Calif. Publ. Bull. Dept. Geol., vol. 10, pp. 461-515, 32 figs. in text.

———,
1929A. Significance of abraded and weathered mammalian remains from Rancho La Brea. Bull. South. Calif. Acad. Sci., vol. 28, pt. 1, 5 pp., 2 pls.

———.
1929B. A census of the Pleistocene mammals of Rancho La Brea, based on the collections of the Los Angeles Museum. Jour. Mammalogy, vol. 10, pp. 281-289, 3 figs. in text.

———.
1930. Rancho La Brea. A record of Pleistocene life in California. L. A. Mus. Publ. No. 1, 84 pp., 27 figs. in text.

Straus-Durckheim, H.
1845. Anatomie descriptive et comparative du Chat, type des Mammifères en général et des Carnivores en particulier. Paris. 2 vols. and atlas.

Tscherski, J. D.
1892. Wissenschaftliche Resultate der von der kaiserlichen Akademie der Wissenschaften zur Erforschung des Janalandes und der Neusibirischen Inseln in den Jahren 1885 und 1886 ausgesandten Expedition. Abtheil. 4: Beschreibung der Sammlung posttertiärer Säugethiere. Mem. Imp. Acad. Sci. St. Petersburg, ser. 7, vol. 40, pp. 1-522, pls. 1-6.

True, F. W.
1889. The puma, or American lion: *Felis concolor* of Linnæus. Rpt. U. S. Nat. Mus., pp. 591-608, pl. 94.

Vernay, A. S.
1930. The lion of India. An account of the Vernay-Faunthorpe expedition to India, Dec., 1928, to March, 1929. Nat. Hist., vol. 30, pp. 81-89, illust.

Wilder, B. G., and S. H. Gage.
1886. Anatomical technology as applied to the domestic cat. An introduction to human, veterinary, and comparative anatomy. 2d ed., rev., A. S. Barnes and Co., N. Y. and Chicago, 575 pp. illustrated.

Winge, H.
1895. Jordfundne og nulevende Rovdyr *(Carnivora)* fra Lagoa Santa, Minas Geraes, Brasilien. Med udsigt over Rovdyrenes indbyrdes Slaegtskab. E Museo Lundii, Copenhagen, vol. 2, pt. 4, 103 pp., 8 pls. French résumé, pp. 105-130.

Wurm, A.
1912. Beiträge zur Kenntniss der diluvialen Säugethierfauna von Mauer a. d. Elsenz (bei Heidelberg). I. Felis leo fossilis. Jahres-Berichte u. Mitteil. d. Oberrheinischen geol. Vereines, N.F., vol. 2, Hft. 1, pp. 77-102, pls. 2-4, 2 figs. in text. Bibliography of 100 titles.

PLATES

PLATE 1

PLATE 1

Smilodon californicus Bovard

FIG. 1, skull and mandible, No. 2001–1, lateral view; × 1/3.

FIGS. 2 and 3, skull, No. 2001–1. FIG. 2 dorsal view; FIG. 3, ventral view; × 1/3.

Los Angeles Museum Collection. Rancho La Brea Pleistocene.

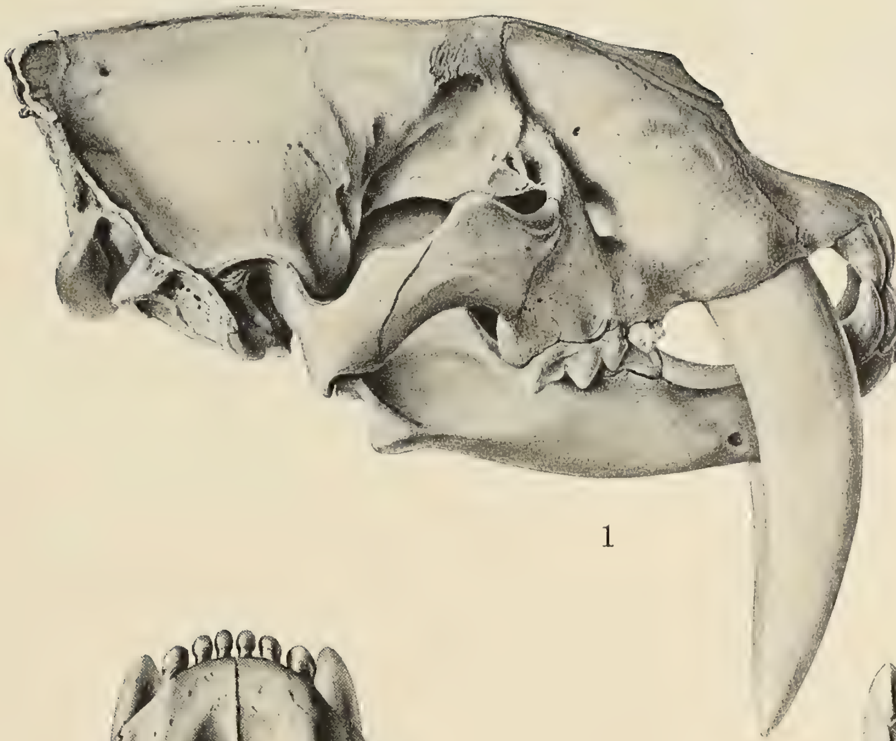

1

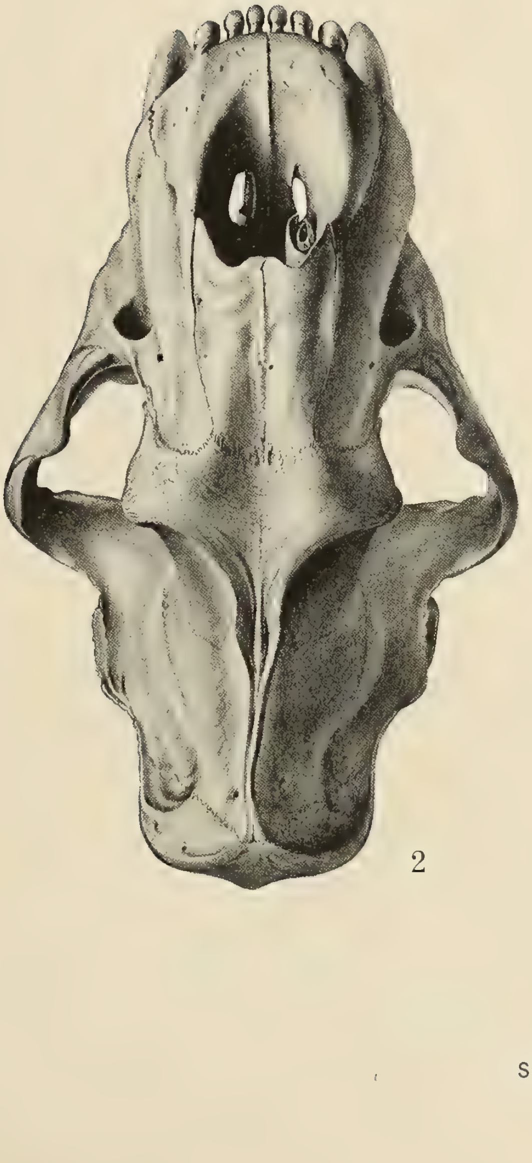

2

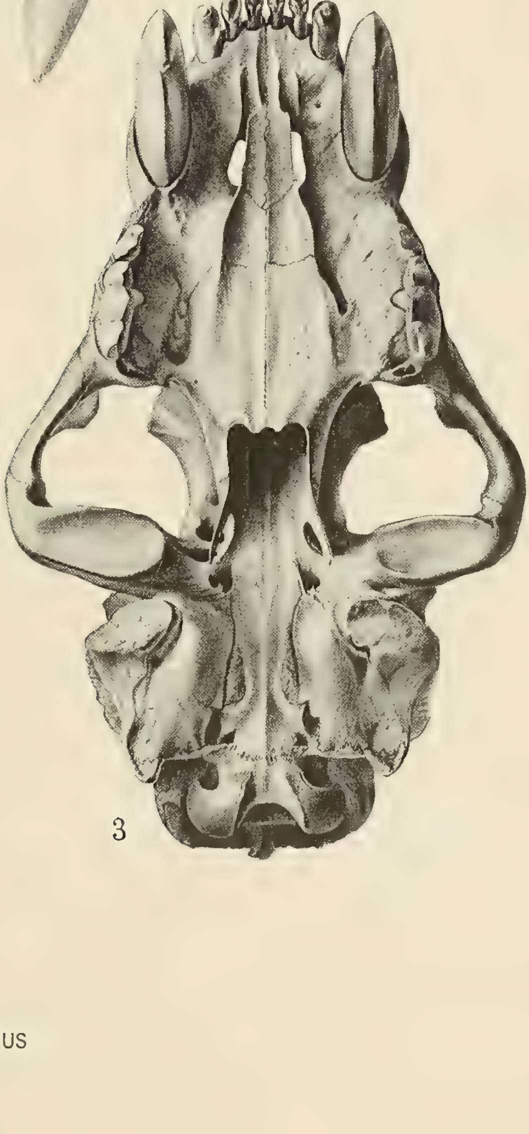

3

SMILODON CALIFORNICUS

PLATE 2

PLATE 2

Smilodon californicus Bovard

FIGS. 1 and 2, skull, No. 2001–1. FIG. 1, lateral view with portion of zygomatic arch removed to show infraorbital region; FIG. 2, posterior view; × 1/3.

FIG. 3, skull and mandible, No. 2001–1, anterior view; × 1/3.

FIGS. 4 and 5, mandible, No. 2002–1. FIG. 4, dorsal view; FIG. 5, lateral view; × 1/3.

FIG. 6, mandible, No. 2002–R–684, inner view; × 1/3.

Los Angeles Museum Collection. Rancho La Brea Pleistocene.

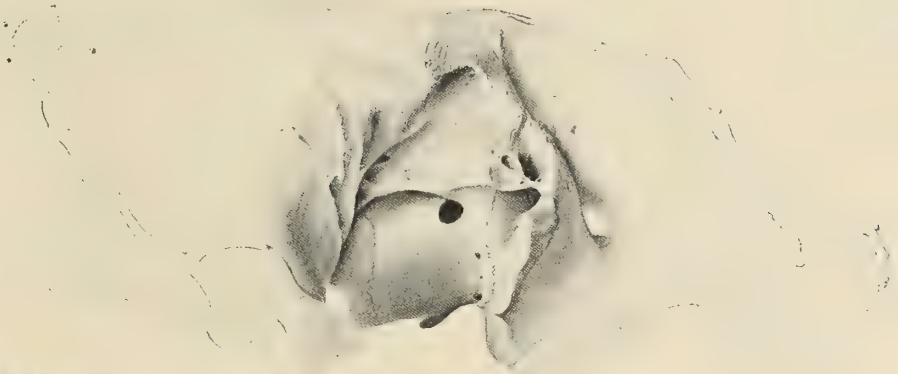

1

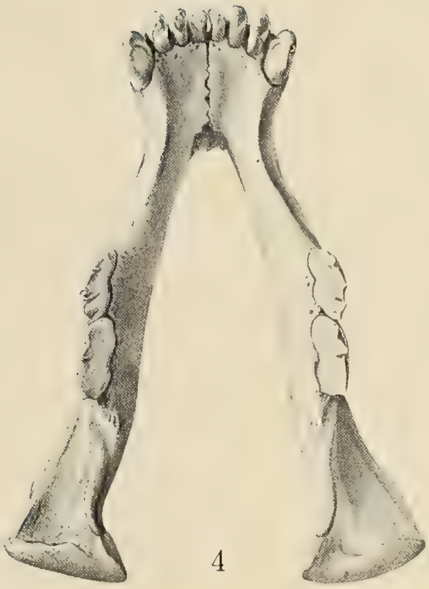

4

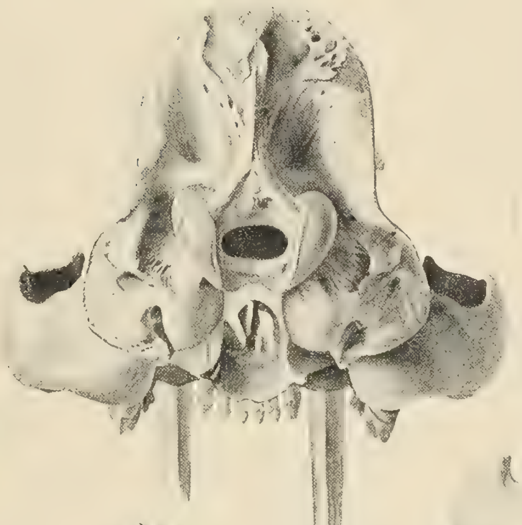

2

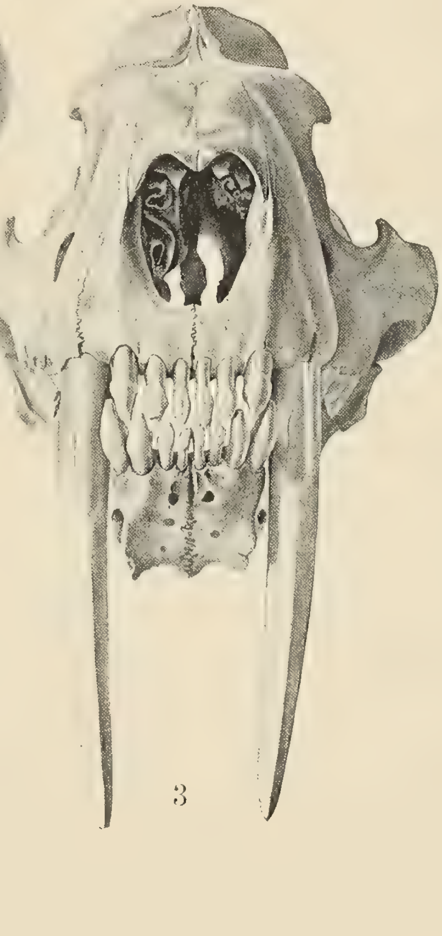

3

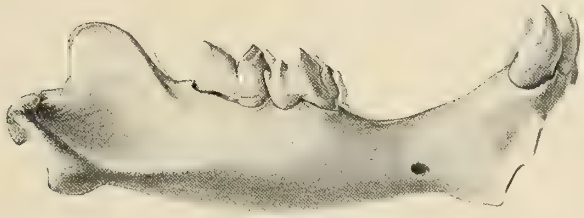

5

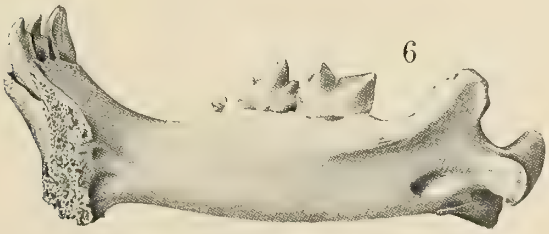

6

SMILODON CALIFORNICUS

PLATE 3

Plate 3

Smilodon californicus Bovard

Smallest and one of the larger skulls of adult individuals, Nos. 2001–148, 2001–225. Figs. 1 and 7, ventral views; Figs. 2 and 5, anterior views; Figs. 3 and 6, dorsal views; Figs. 4 and 8, lateral views; × 2/9. Los Angeles Museum Collection. Rancho La Brea Pleistocene.

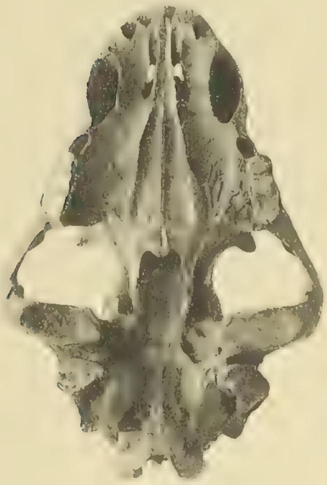
1

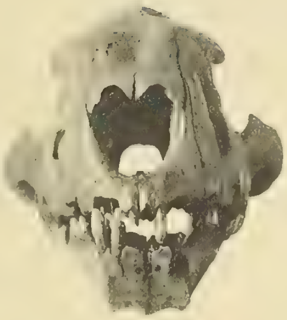
2

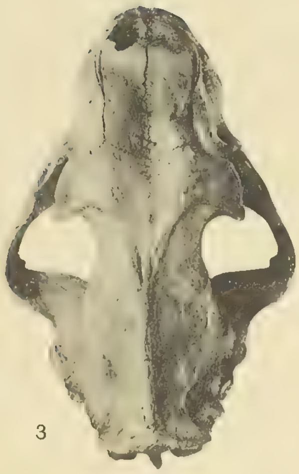
3

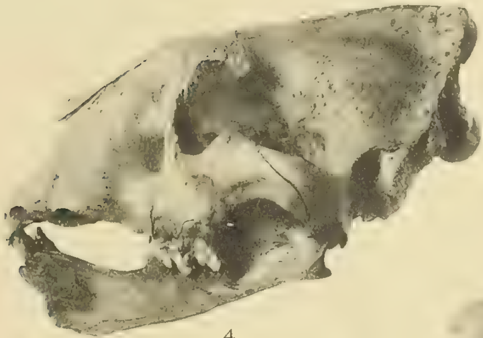
4

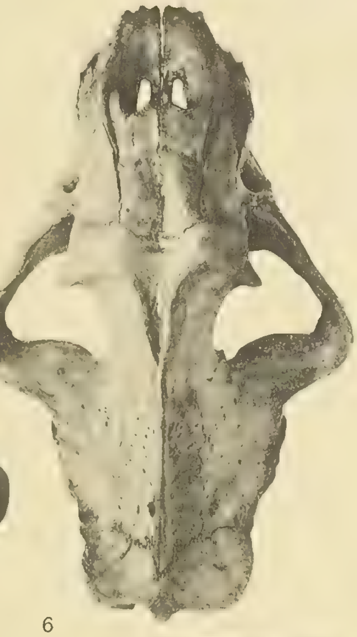
6

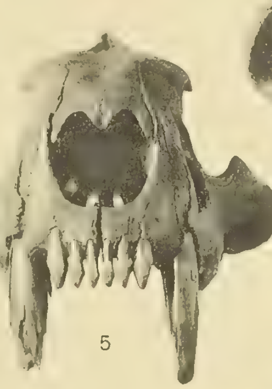
5

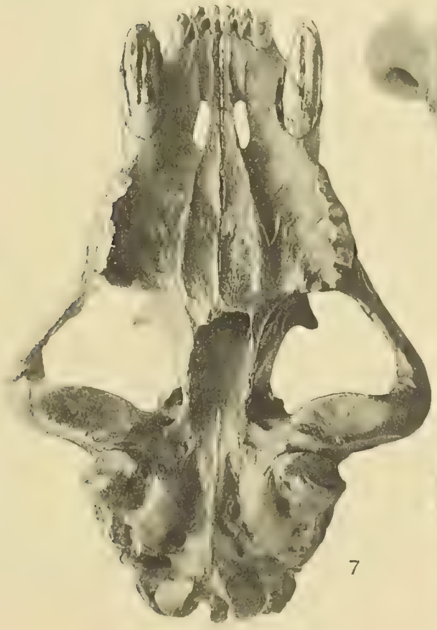
7

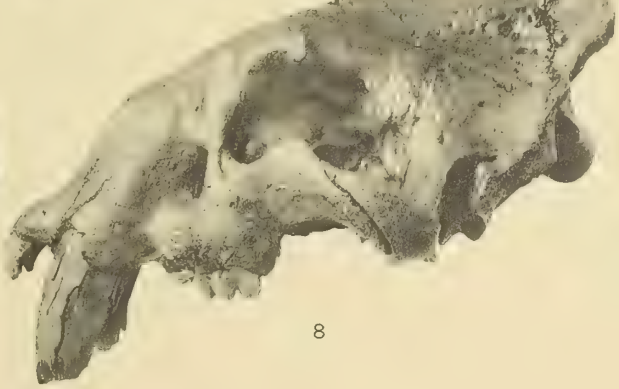
8

HELIOTYPE CO. BOSTON

SMILODON CALIFORNICUS

PLATE 4

Smilodon californicus Bovard

FIGS. 1–10, series of lower jaws including young and adult individuals showing variation in size, Nos. 2002–L–4, R–4, R–68, R–6, R–781, R–10, R–496, R–14, R–16 and R–15, incl. All specimens in lateral view; × 1/2. Specimens shown in FIGS. 1 to 7 possess milk teeth. Permanent dentition shown in FIGS. 8 to 10. Los Angeles Museum Collection. Rancho La Brea Pleistocene.

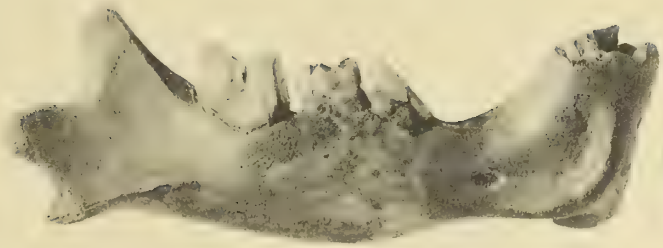
7

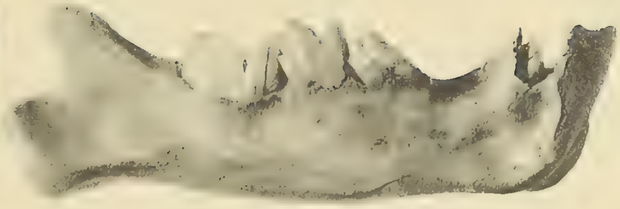
6

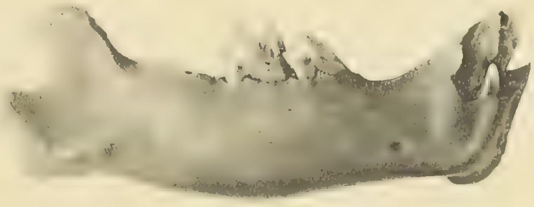
5

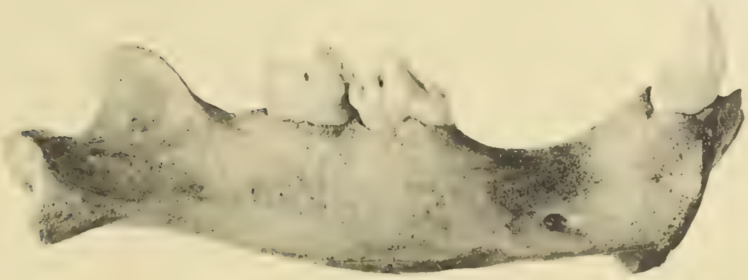
8

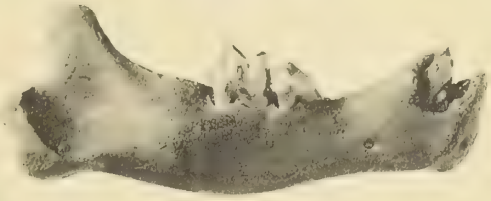
4

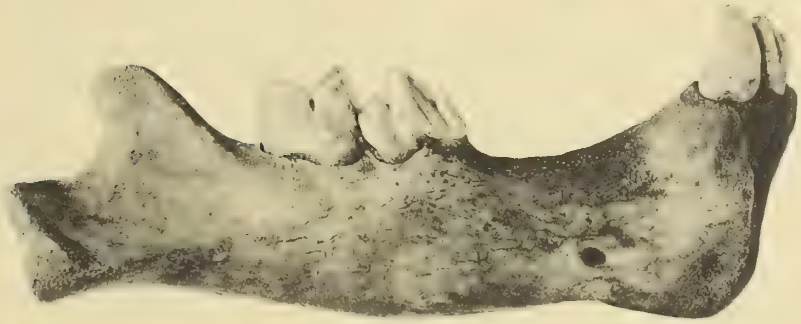
9

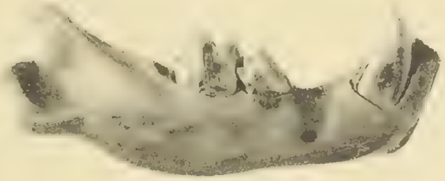
3

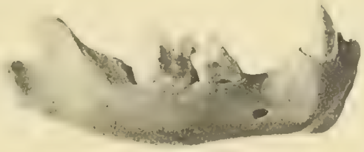
2

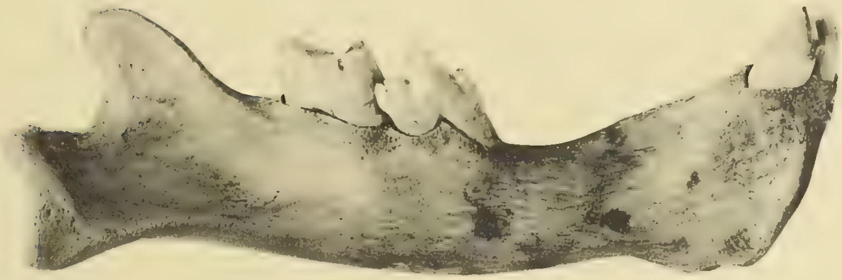
10

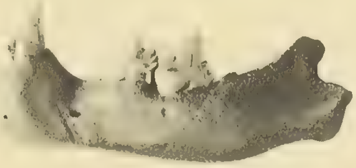
1

HELIOTYPE CO. BOSTON

SMILODON CALIFORNICUS

PLATE 5

PLATE 5

Smilodon californicus Bovard

Skull, No. 2001–10. FIG. 1, lateral view; FIG. 2, anterior view; FIG. 3, dorsal view; FIG. 4, ventral view; × 2/5. The crowns of the permanent canine teeth are appearing along the inner sides of the deciduous canines. Los Angeles Museum Collection. Rancho La Brea Pleistocene.

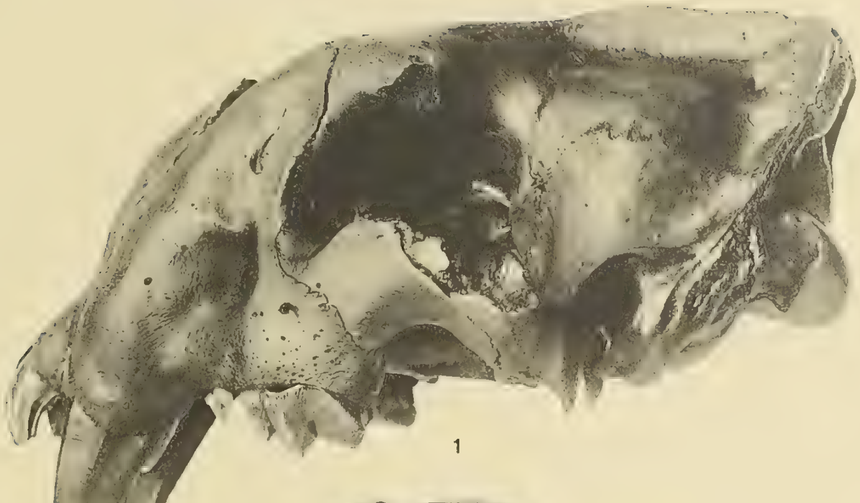

1

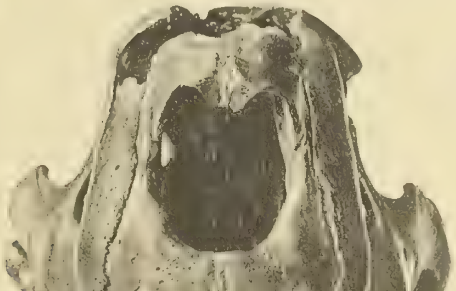

2

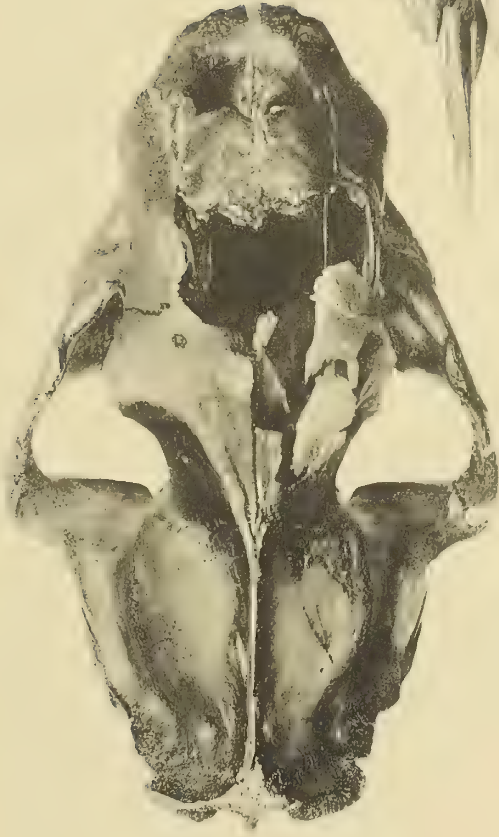

3

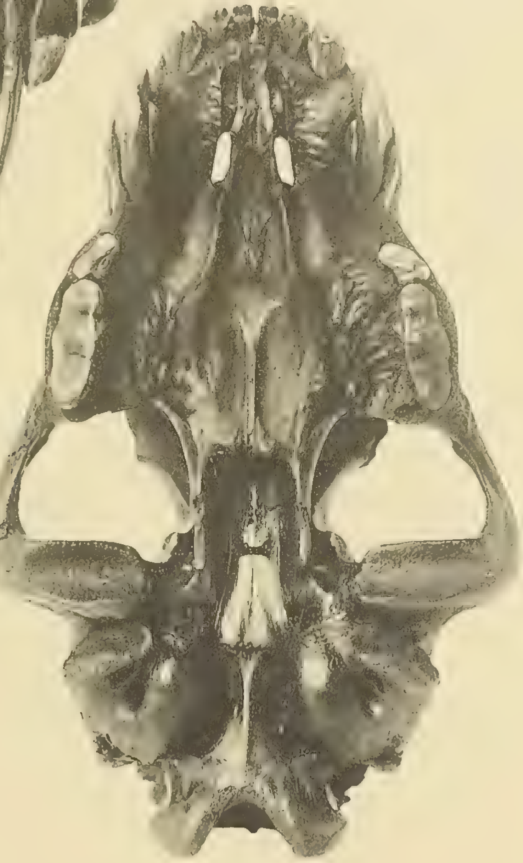

4

HELIOTYPE CO. BOSTON

SMILODON CALIFORNICUS

PLATE 6

PLATE 6

Smilodon californicus Bovard

FIGS. 1, 2, 3 and 4, skull, No. 2001–9. FIG. 1, lateral view; FIG. 2, anterior view; FIG. 3, dorsal view; FIG. 4, ventral view; × 2/5. Los Angeles Museum Collection. Rancho La Brea Pleistocene.

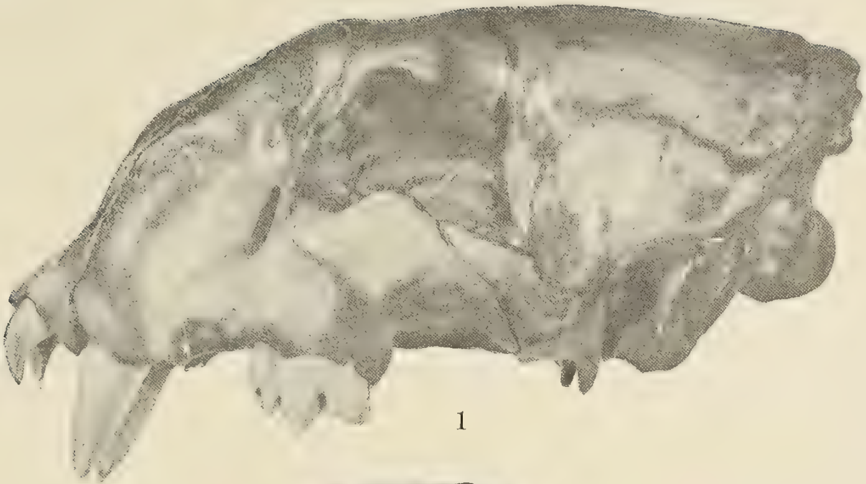

1

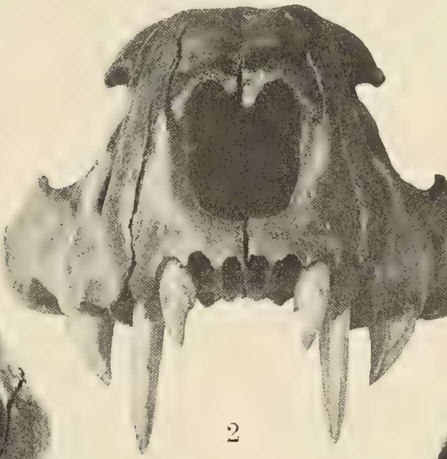

2

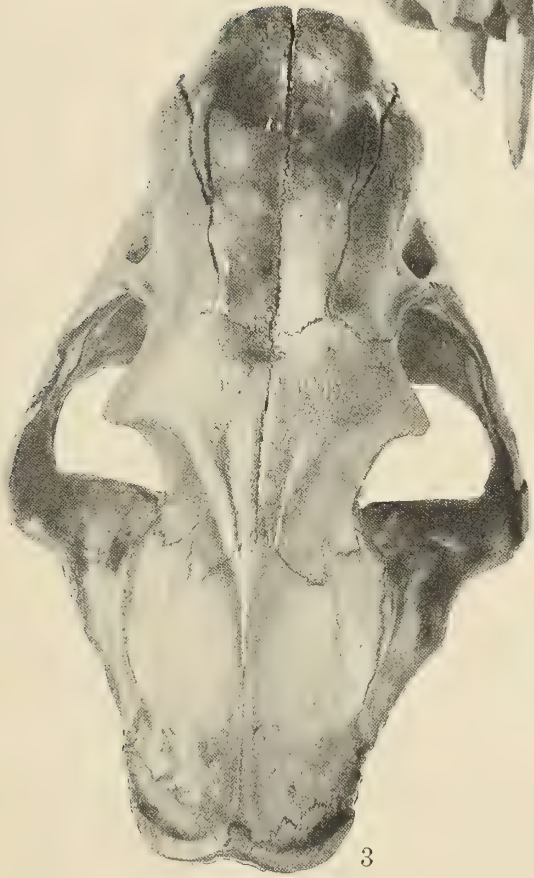

3

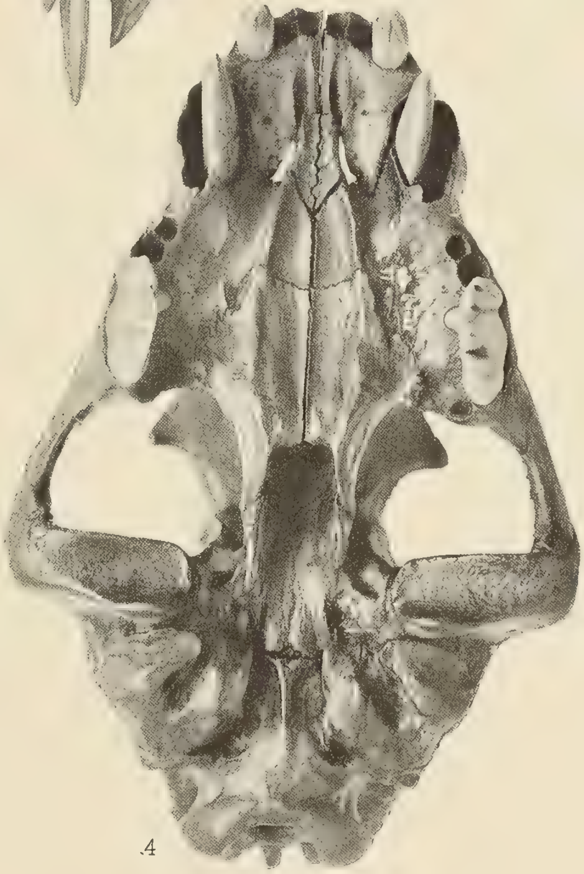

4

SMILODON CALIFORNICUS

PLATE 7

Smilodon californicus Bovard

Skull, No. 2001–7. FIG. 1, lateral view; FIG. 2, anterior view; FIG. 3, dorsal view; FIG. 4, ventral view; × 2/5. Note presence of deciduous and permanent canine teeth on left side. Los Angeles Museum Collection. Rancho La Brea Pleistocene.

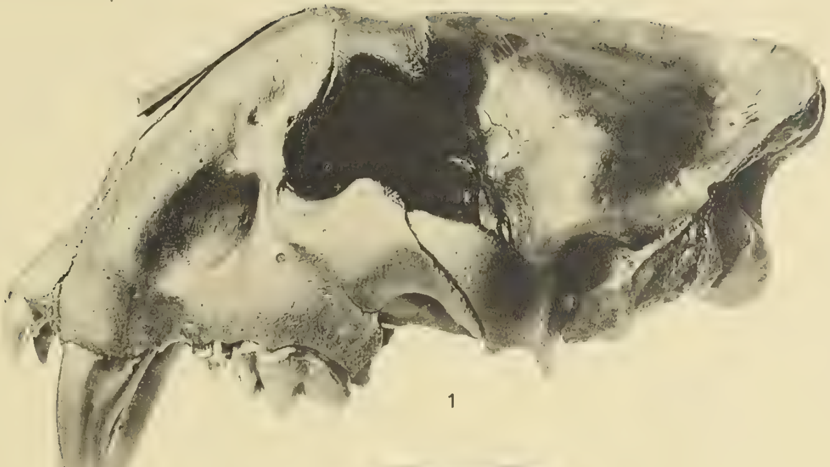

1

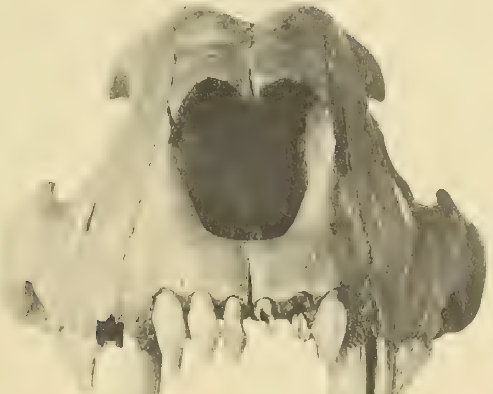

2

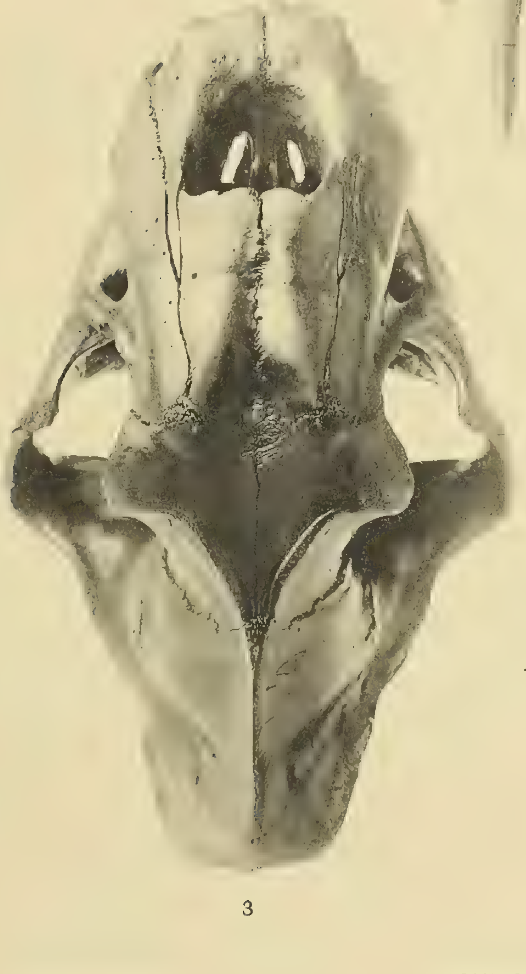

3

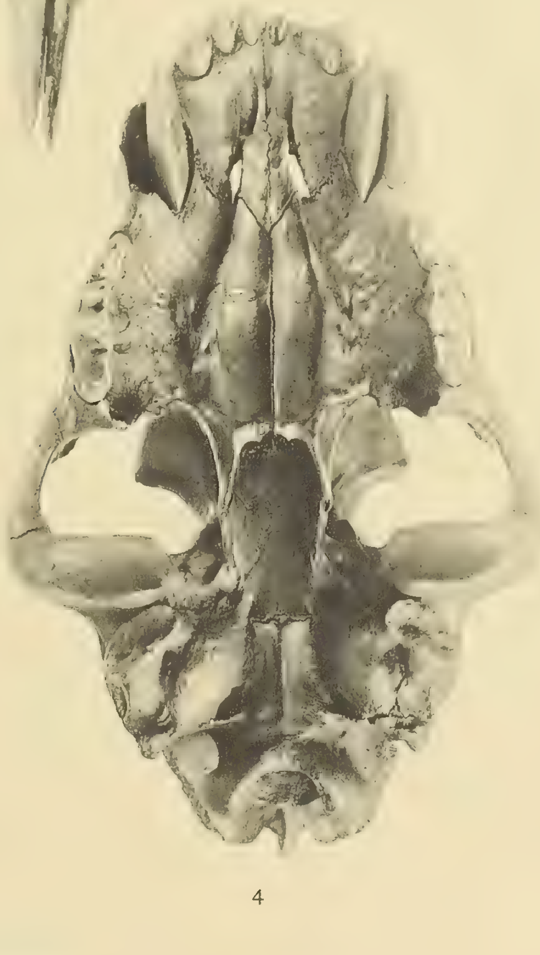

4

HELIOTYPE CO. BOSTON

SMILODON CALIFORNICUS

PLATE 8

Smilodon californicus Bovard

Skull, No. 2001–8. FIG. 1, lateral view; FIG. 2, anterior view; FIG. 3, dorsal view; FIG. 4, ventral view; × 2/5. Note partial emergence of permanent canine teeth. Los Angeles Museum Collection. Rancho La Brea Pleistocene.

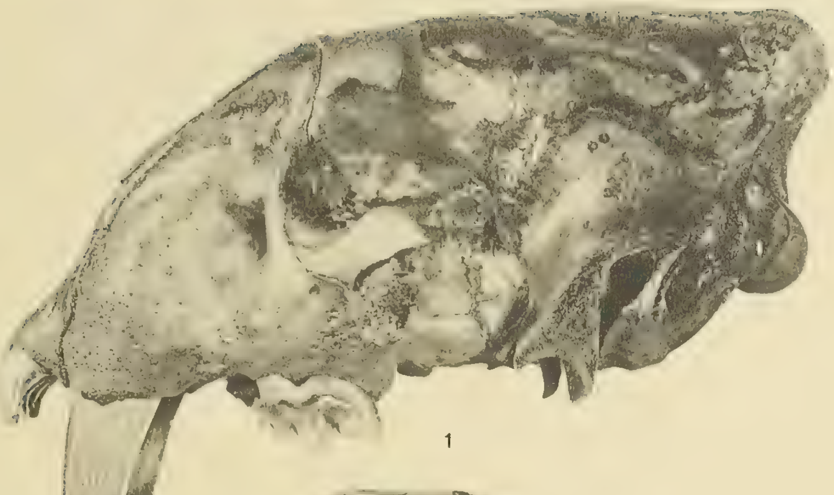

1

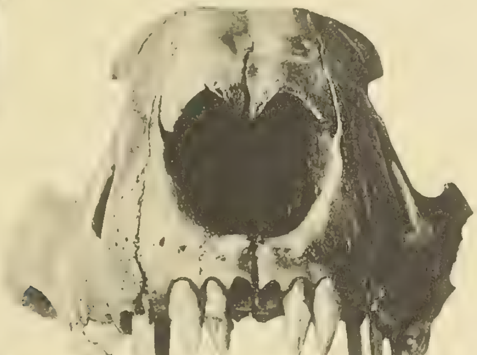

2

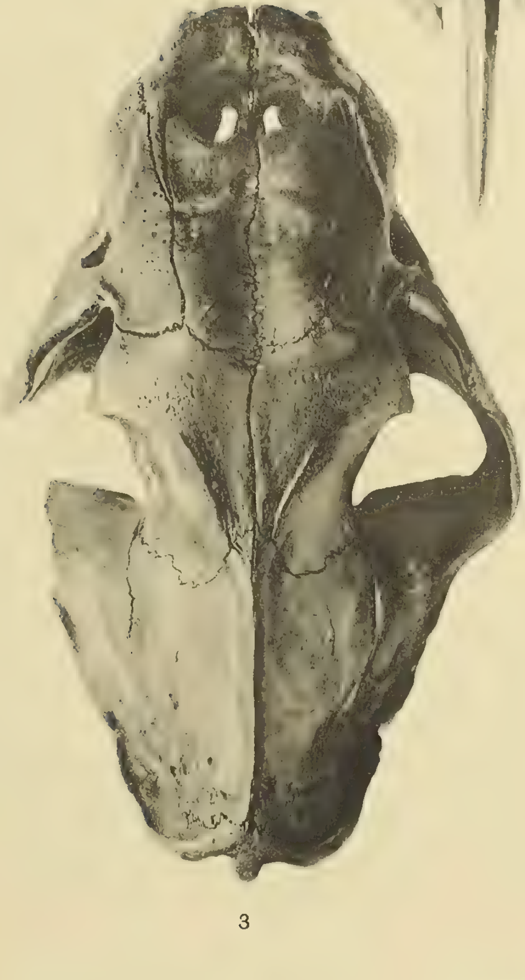

3

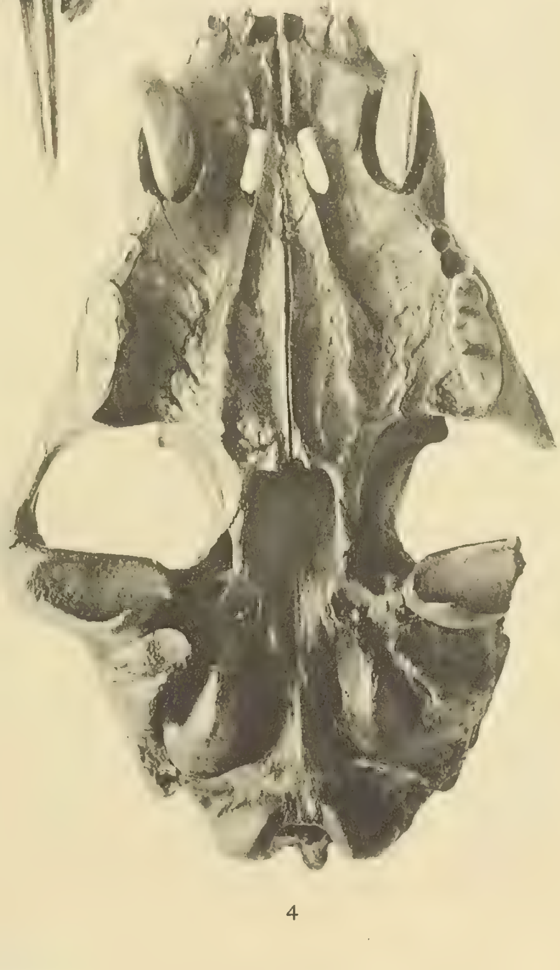

4

HELIOTYPE CO. BOSTON

SMILODON CALIFORNICUS

PLATE 9

PLATE 9

Smilodon californicus Bovard

Skull, No. 2001–6. FIG. 1, lateral view; FIG. 2, anterior view; FIG. 3, dorsal view; FIG. 4, ventral veiw; × 2/5. Permanent canine teeth have not fully emerged in this specimen. Los Angeles Museum Collection. Rancho La Brea Pleistocene.

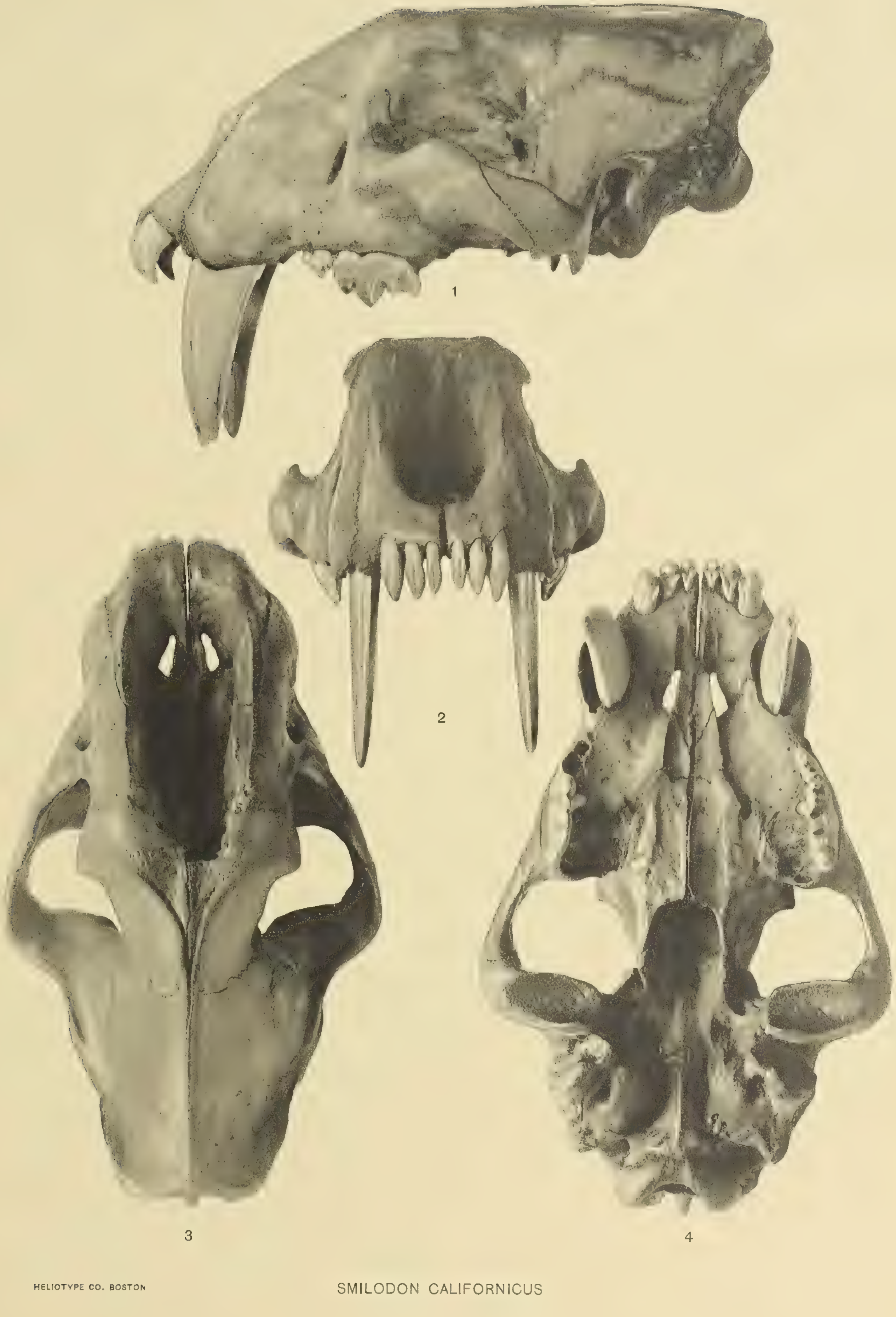

HELIOTYPE CO. BOSTON

SMILODON CALIFORNICUS

PLATE 10

PLATE 10

Smilodon californicus Bovard

Skull, No. 2001–19. FIG. 1, lateral view; FIG. 2, anterior view; FIG. 3, dorsal view; FIG. 4, ventral view; × 1/3. Note broken surfaces of canine teeth which were worn during life of individual. Los Angeles Museum Collection. Rancho La Brea Pleistocene.

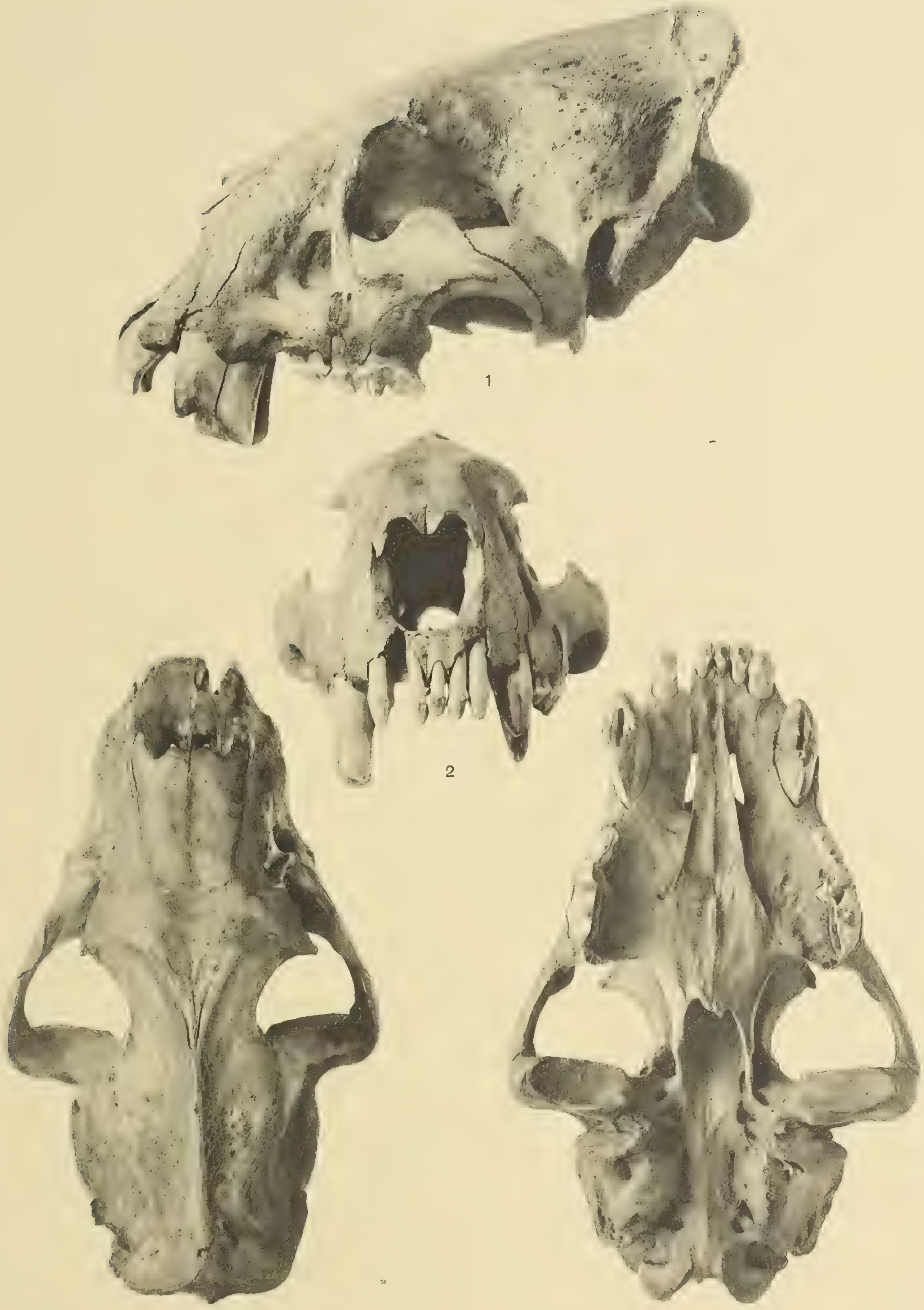

HELIOTYPE CO. BOSTON

SMILODON CALIFORNICUS

PLATE 11

Plate 11

Smilodon floridanus (Leidy)

Type specimen, skull, No. 4072, Wagner Free Institute of Science Collection. Fig. 1, ventral view; Fig. 2, lateral view; × 3/5. Pleistocene, Ocala, Marion Co., Florida.

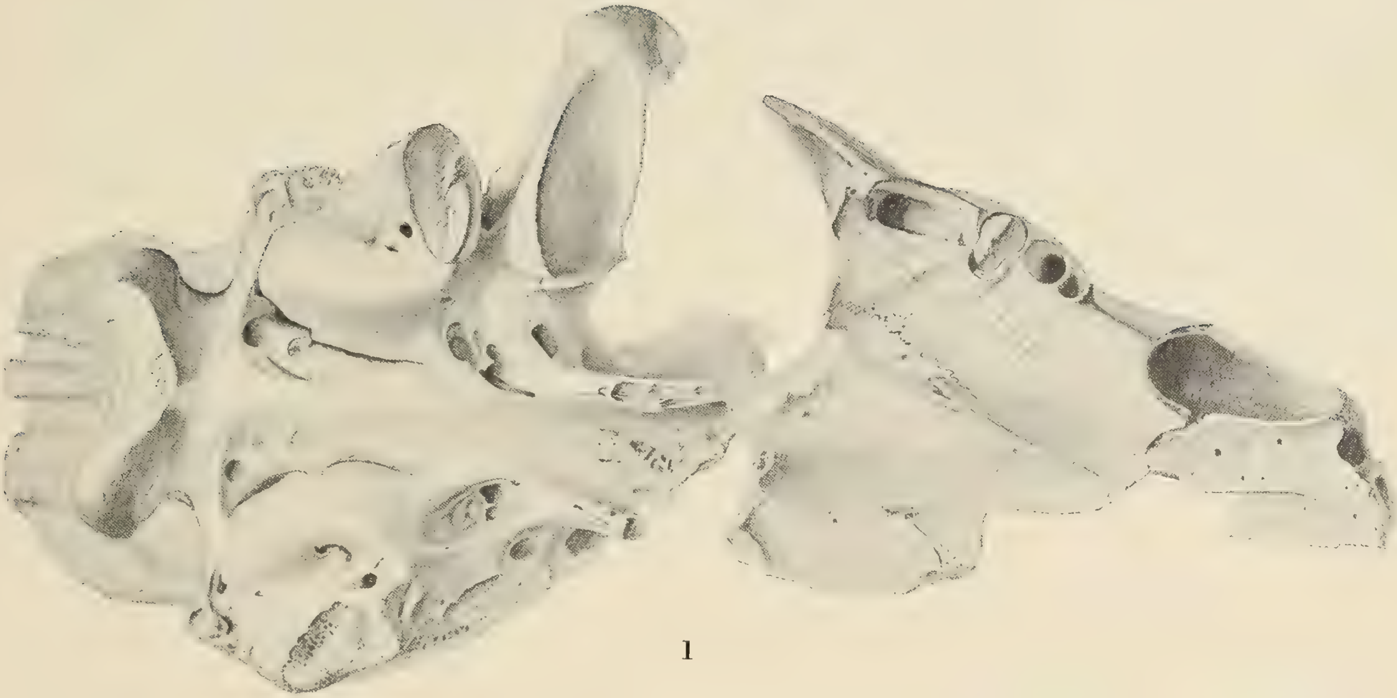

1

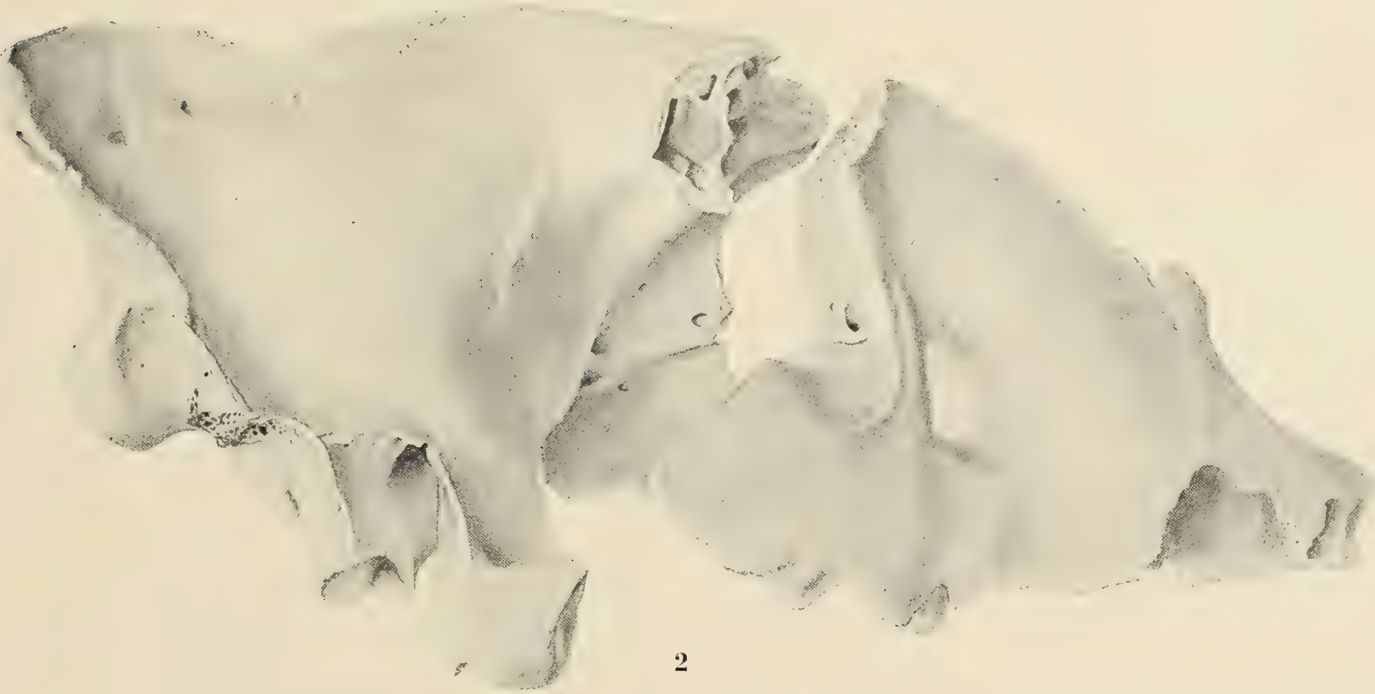

2

SMILODON FLORIDANUS

PLATE 12

Smilodon californicus Bovard

FIGS. 1, 2 and 3, permanent and deciduous canines. FIG. 1, right canine, anterior, inner, outer and posterior views with cross-sections; FIG. 2, portion of crown of canine with anterior and posterior serrations somewhat magnified; FIG. 3, right deciduous canine, same views as in FIG. 1; × 1/2. Los Angeles Museum Collection. Rancho La Brea Pleistocene.

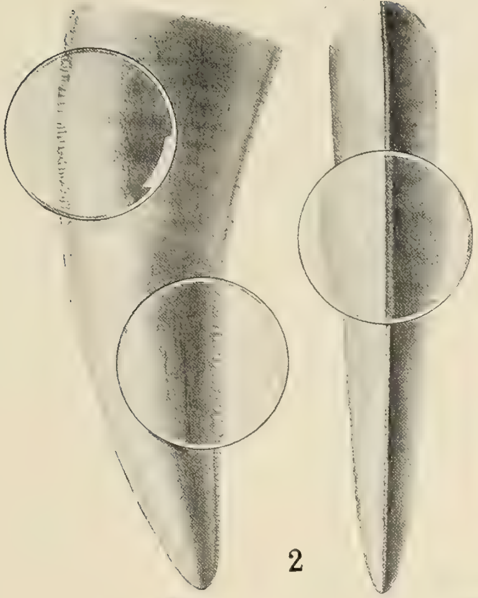

2

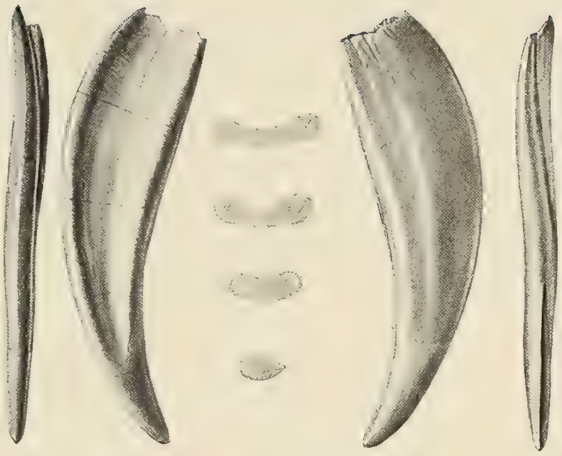

3

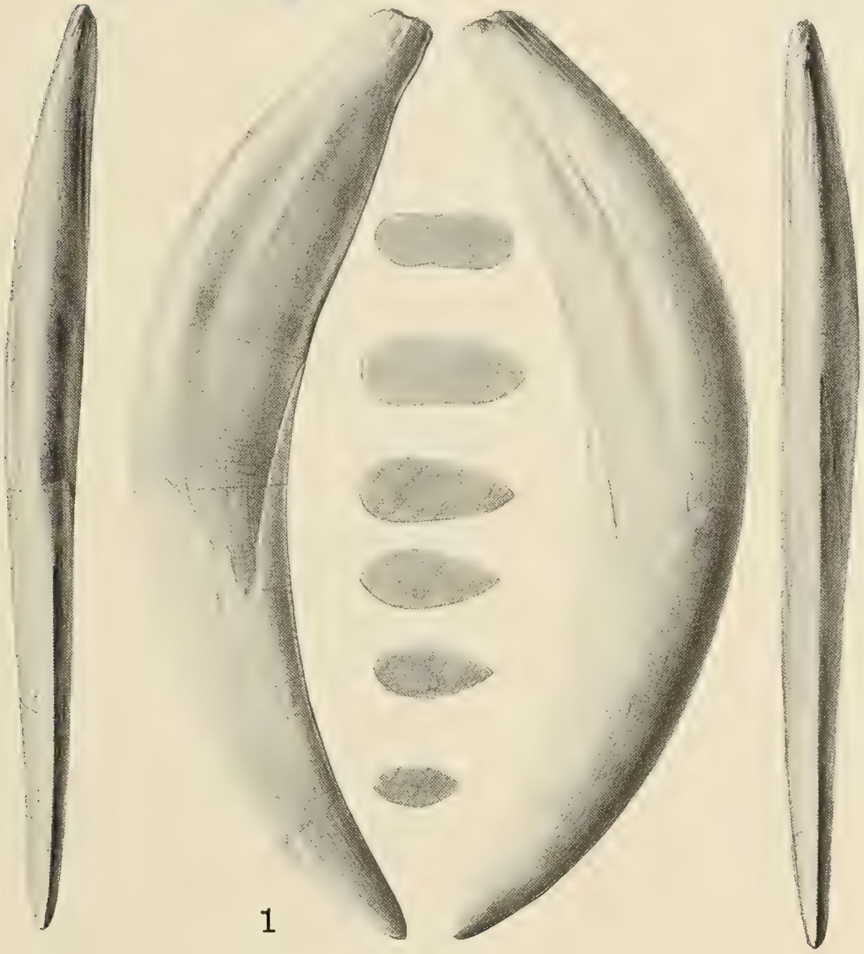

1

SMILODON CALIFORNICUS

Plate 13

Plate 13

Smilodon californicus Bovard

Upper and lower teeth. Figs. 1–1a, $P\underline{4}$, outer and inner views; Figs. 2–2a, $P\underline{3}$, inner and outer views; Figs. 3–3a, Figs. 4–4a, $M\overline{1}$, $P\overline{4}$ respectively, outer and inner views; Figs. 5–5a, Figs. 6–6a, Figs. 7–7a, $I\underline{1}$, $\underline{2}$, $\underline{3}$ respectively, inner and posterior views; Figs. 8–8a, lower canine, inner and posterior views; Figs. 9–9a, Figs. 10–10a, Figs. 11–11a, $I\overline{1}$, $\overline{2}$, $\overline{3}$ respectively, outer and posterior views; × 1. Los Angeles Museum Collection. Rancho La Brea Pleistocene.

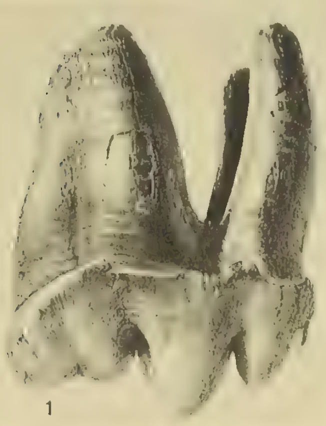
1

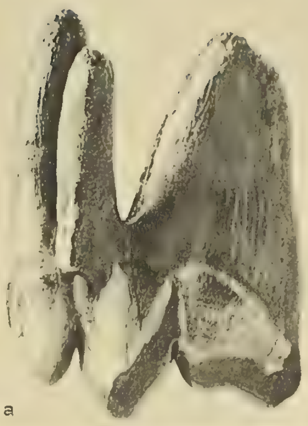
1a

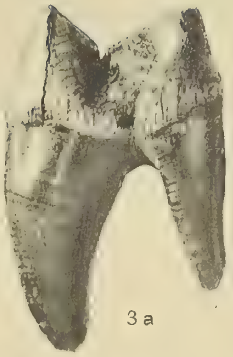
3 a

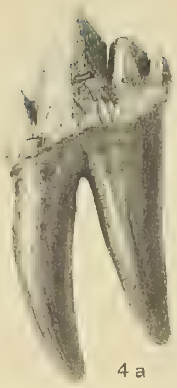
4 a

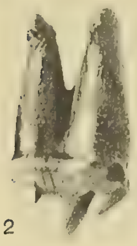
2

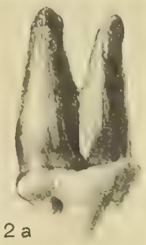
2 a

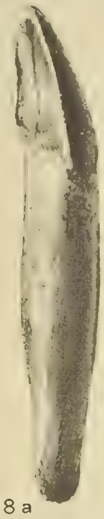
8 a

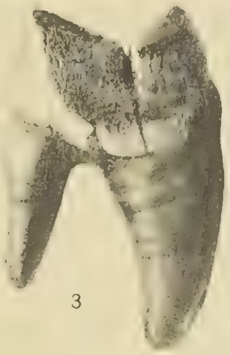
3

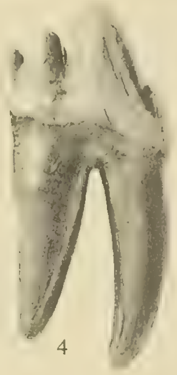
4

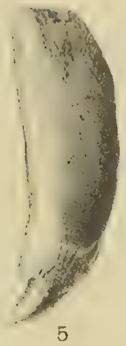
5

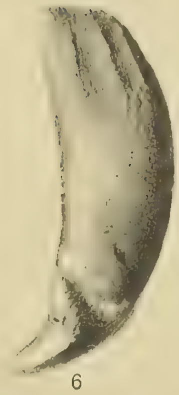
6

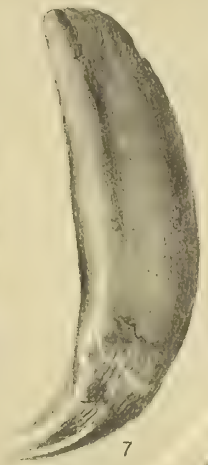
7

9 a

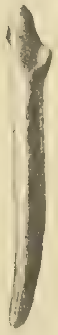
10 a

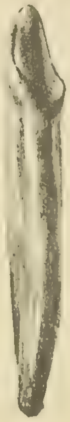
11a

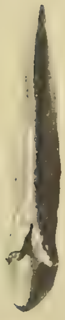
5 a

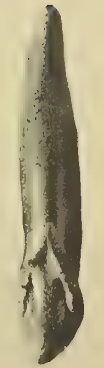
6 a

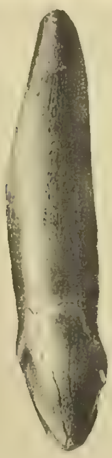
7 a

8

9

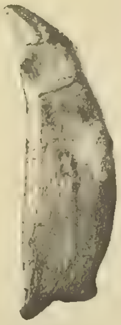
10

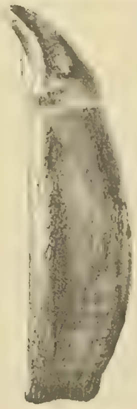
11

HELIOTYPE CO. BOSTON

SMILODON CALIFORNICUS

PLATE 14

Felis atrox Leidy

FIGS. 1, 2 and 3, endocranial cast of skull No. 2900–1. FIG. 1, dorsal view; FIG. 2, lateral view; FIG. 3, ventral view; × 2/3.

Smilodon californicus Bovard

FIGS. 4, 5 and 6, endocranial cast of skull No. 2001–199. FIG. 4, dorsal view; FIG. 5, lateral view; FIG. 6, ventral view; × 2/3.

Los Angeles Museum Collection. Rancho La Brea Pleistocene.

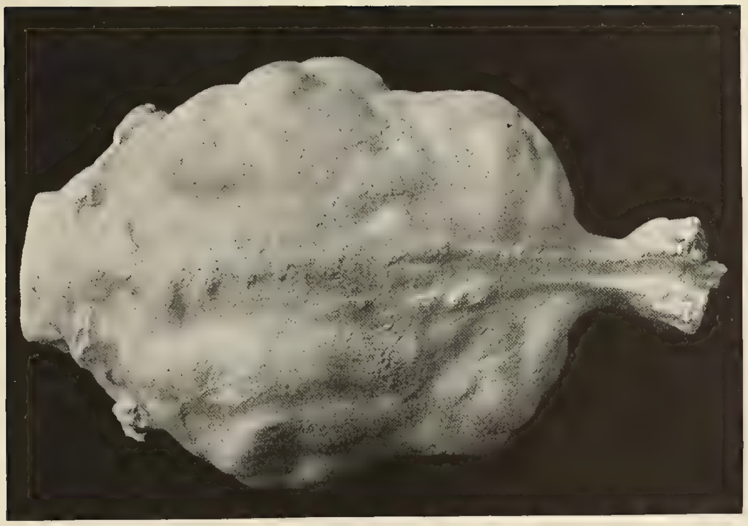

1

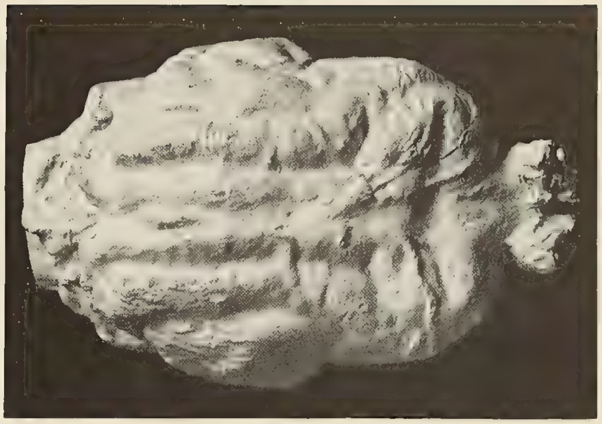

4

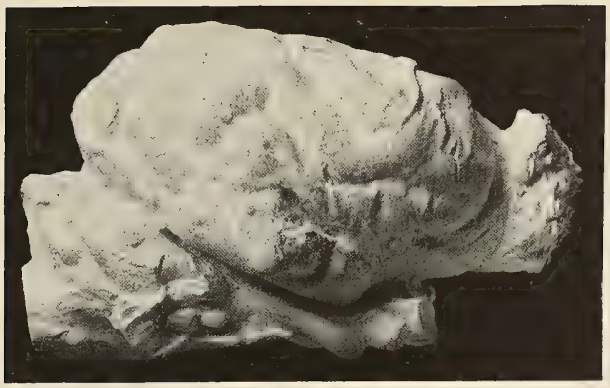

5

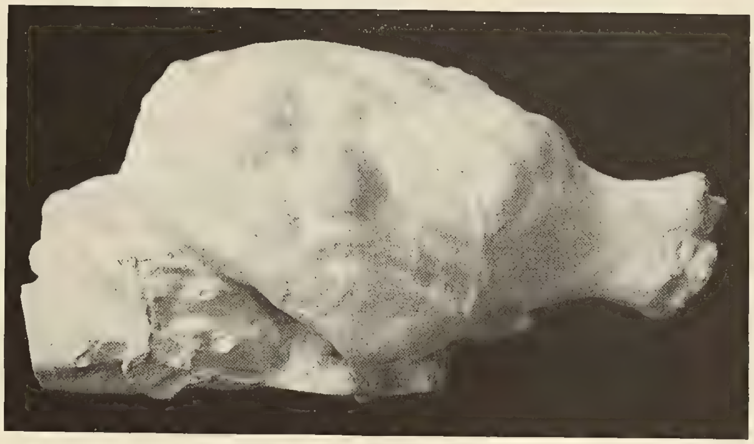

2

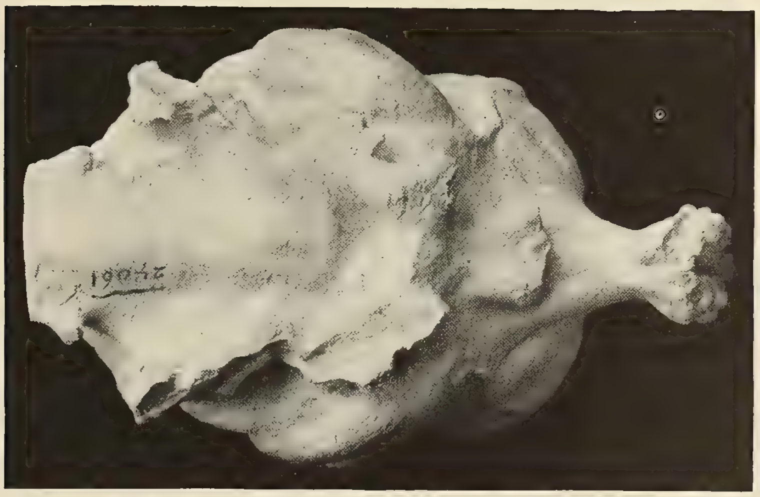

3

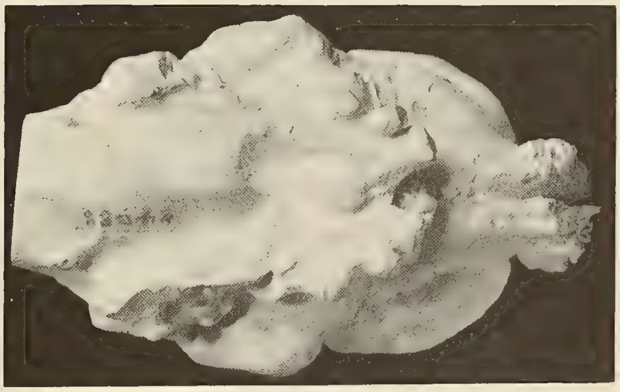

6

FELIS ATROX AND SMILODON CALIFORNICUS

PLATE 15

PLATE 15

Smilodon californicus Bovard

FIG. 1, left ear region of skull cut in transverse sections *a, b, c, d.* Sections *a′, b′, c′* viewed from posterior side; section d′ viewed from anterior side; pg.p., post-glenoid process; m.p., mastoid process; e.c., eustachian canal; f.r., foramen rotundum; f.o., foramen ovale; s.f., stylomastoid foramen; t–hy., tympanohyal pit; c.c., carotid canal; f.l.p., posterior lacerate foramen; c.f., condylar foramen; pa.p., paroccipital process; i.c., inner tympanic chamber; s., septum separating outer tympanic chamber from inner; e.a.m., external auditory meatus; bo., basioccipital; i.a.m., internal auditory meatus; fe.r., fenestra rotunda; pet., petrosal; × 3/4.

FIG. 2, three views of left incus; × 3.

FIG. 3, three views of left malleus; × 3.

Los Angeles Museum Collection. Rancho La Brea Pleistocene.

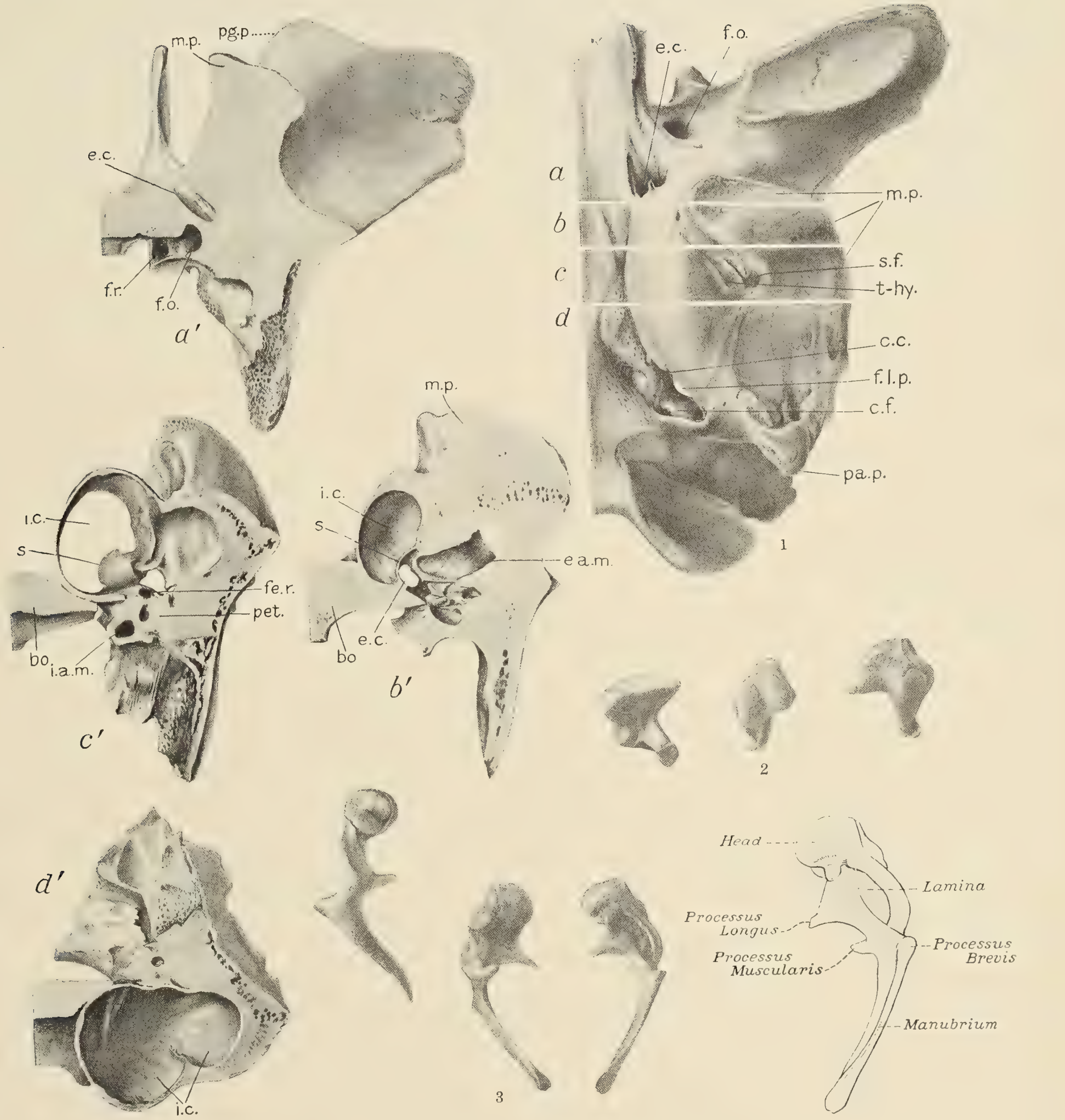

SMILODON CALIFORNICUS

PLATE 16

PLATE 16

Smilodon californicus Bovard

FIGS. 1 and 2, cervical vertebræ, lateral and dorsal views; × 1/3. These vertebræ are not all of the same individual.

Felis atrox Leidy

FIGS. 3 and 4, cervical vertebræ, lateral and dorsal views; × 1/3. Cervicals III-VI are of one individual.

Los Angeles Museum Collection. Rancho La Brea Pleistocene.

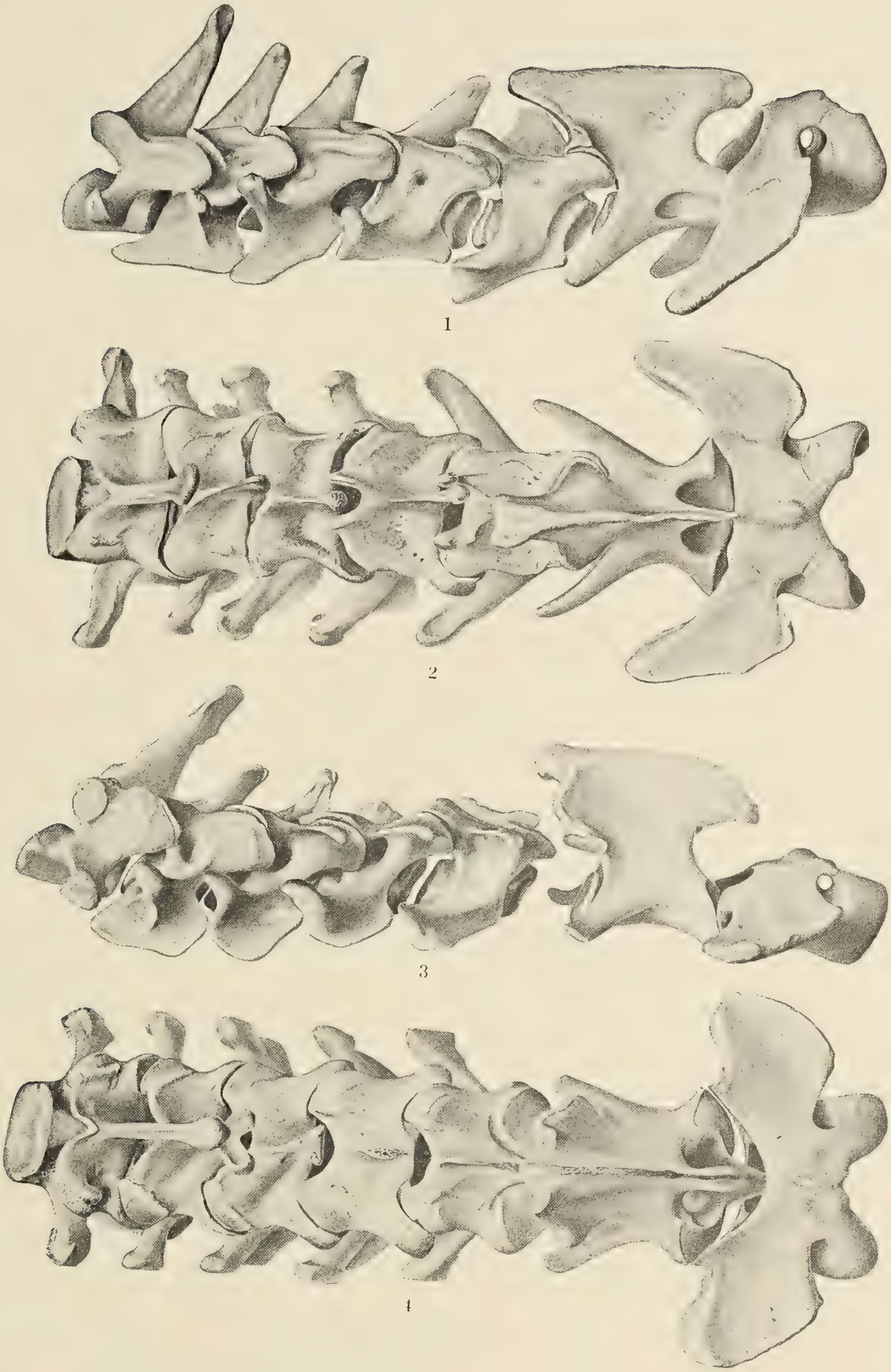

1

2

3

4

SMILODON CALIFORNICUS AND FELIS ATROX

PLATE 17

Smilodon californicus Bovard

FIGS. 1, 2 and 3, axis, No. 2039–1. FIG. 1, dorsal view; FIG. 2, posterior view; FIG. 3, lateral view; × 1/2.

FIGS. 4, 5, 6 and 7, atlas, No. 2038–5. FIG. 4, dorsal view; FIG. 5, anterior view; FIG. 6, posterior view; FIG. 7, ventral view; × 1/2.

Los Angeles Museum Collection. Rancho La Brea Pleistocene.

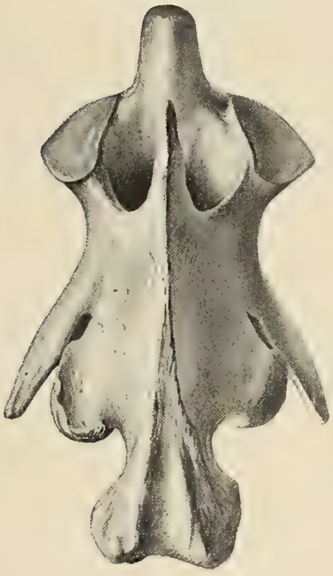

1

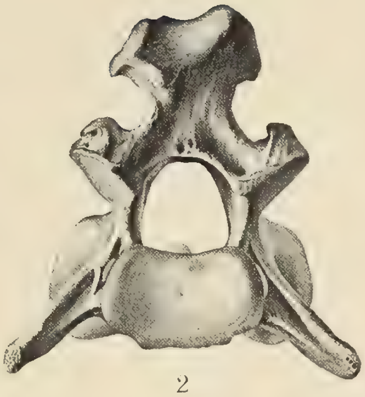

2

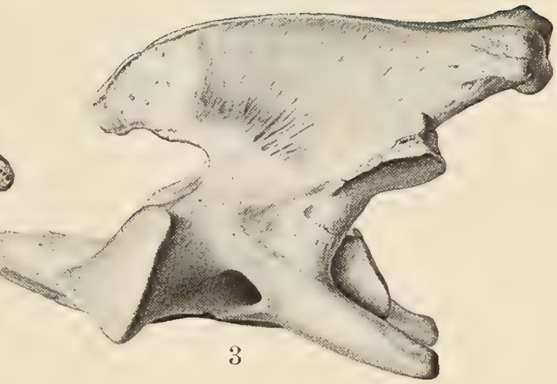

3

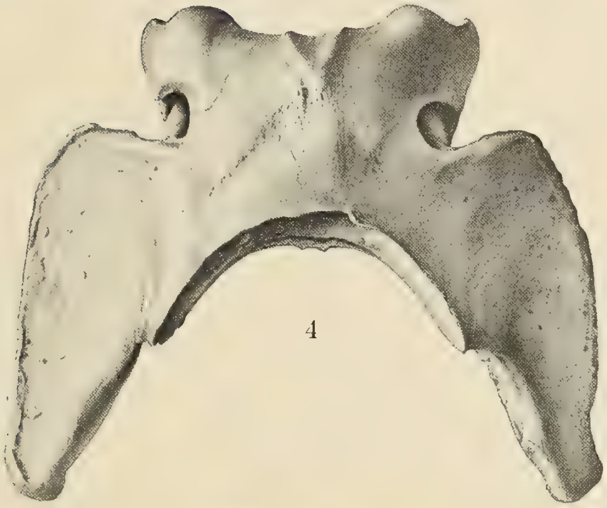

4

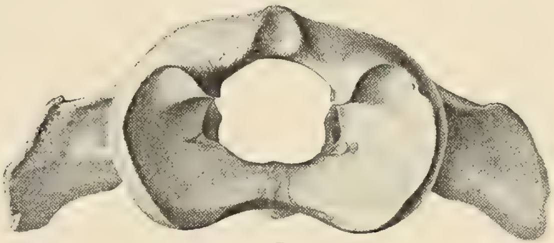

5

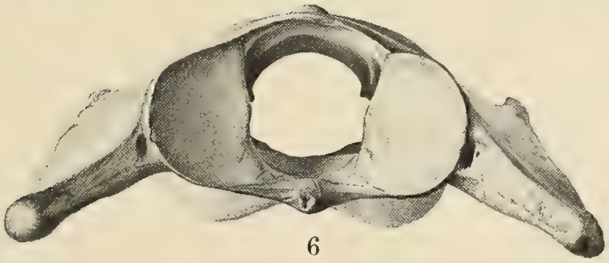

6

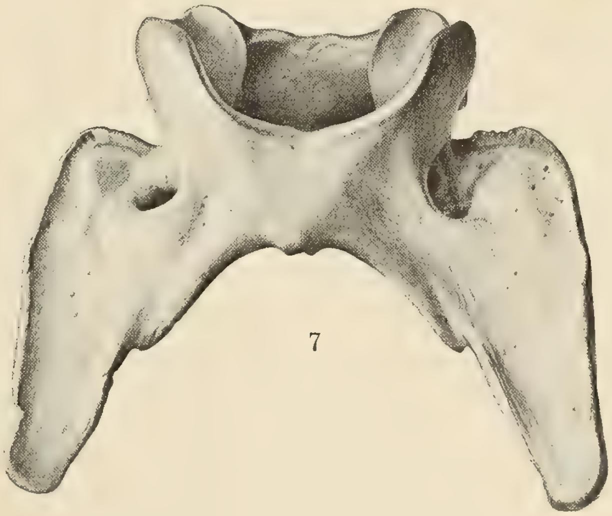

7

SMILODON CALIFORNICUS

Plate 18

Smilodon californicus Bovard

Figs. 1 and 2, thoracic vertebræ, lateral and dorsal views; × 1/3. a′, thirteenth vertebra, No. 2057–12; b′, twelfth vertebra, No. 2056–13; c′, eleventh vertebra, No. 2055–12; d′, seventh vertebra, No. 2051–2; e′, first vertebra, No. 2045–11; anterior views; × 4/9. Los Angeles Museum Collection. Rancho La Brea Pleistocene.

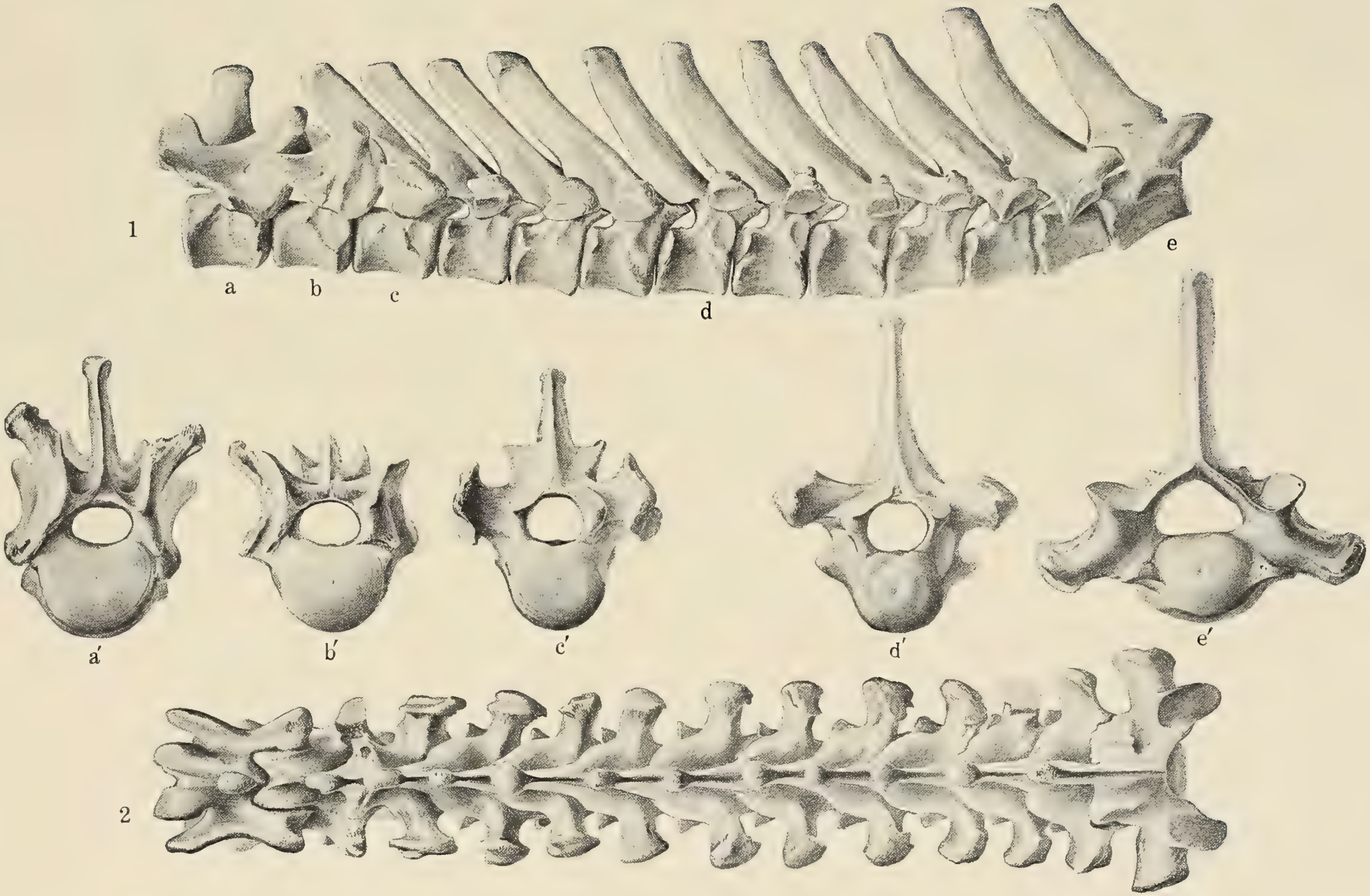

SMILODON CALIFORNICUS

PLATE 19

PLATE 19

Smilodon californicus Bovard

FIGS. 1 and 2, vertebral series from eighth thoracic to last sacral, incl., lateral and dorsal views; × 1/3. a′, seventh lumbar vertebra, No. 2064–12; b′, fourth lumbar vertebra, No. 2061–1; c′, first lumbar vertebra, No. 2058–1; d′, thirteenth thoracic vertebra, No. 2057–11; e′, twelfth thoracic vertebra, No. 2056–12; f′, eleventh thoracic vertebra, No. 2055–11; g′, eighth thoracic vertebra, No. 2052–2; anterior views; × 4/9. Los Angeles Museum Collection. Rancho La Brea Pleistocene.

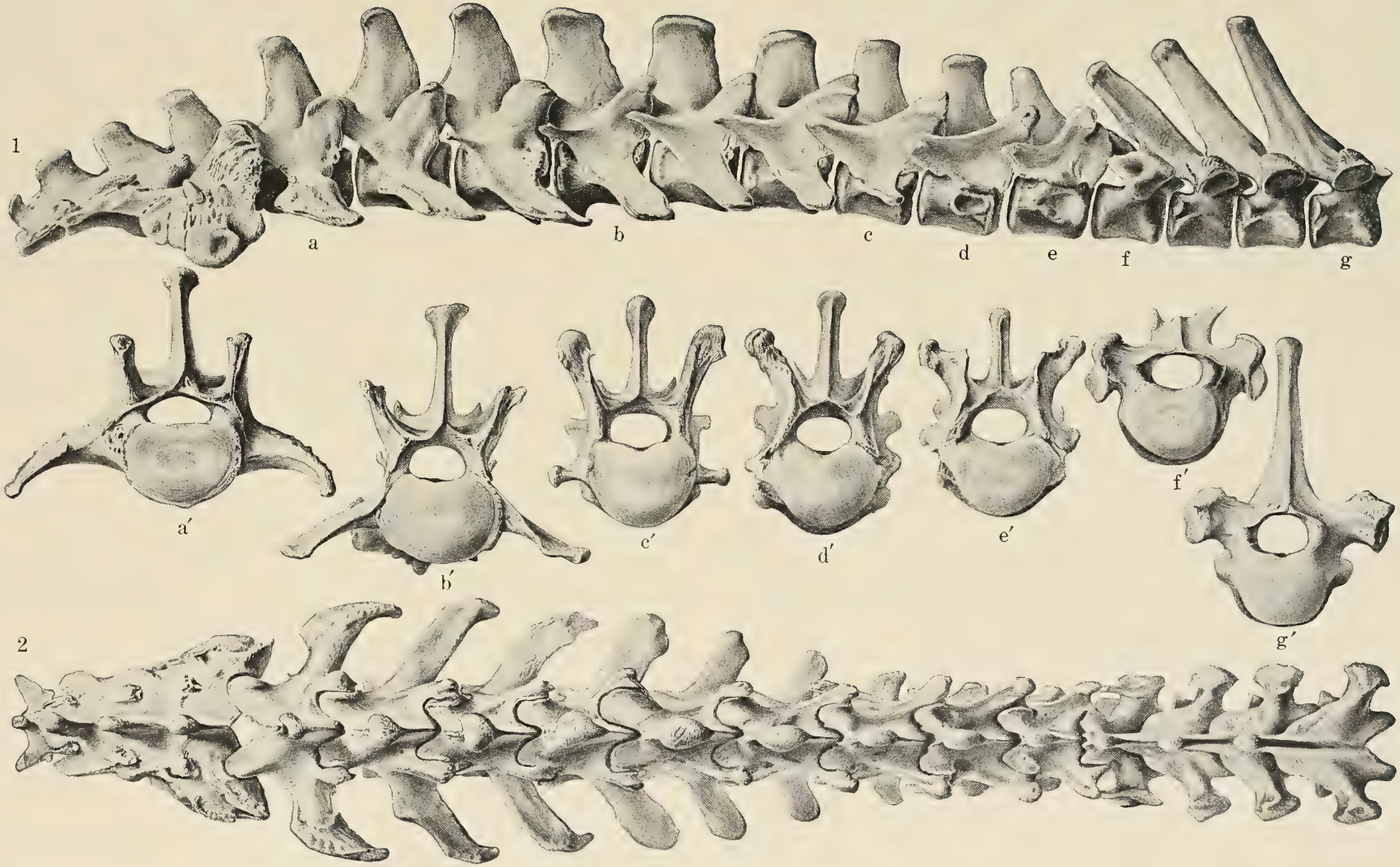

SMILODON CALIFORNICUS

Plate 20

PLATE 20

Smilodon californicus Bovard and *Felis atrox* Leidy

FIGS. 1–7, *Smilodon californicus* Bovard; FIGS. 8–13, *Felis atrox* Leidy; right ribs. FIGS. 1, 1a and FIGS. 8, 8a, first rib; FIGS. 2, 9, second rib; FIGS. 3–7, FIGS. 10–13, ribs posterior to the second; × 4/9. Los Angeles Museum Collection. Rancho La Brea Pleistocene.

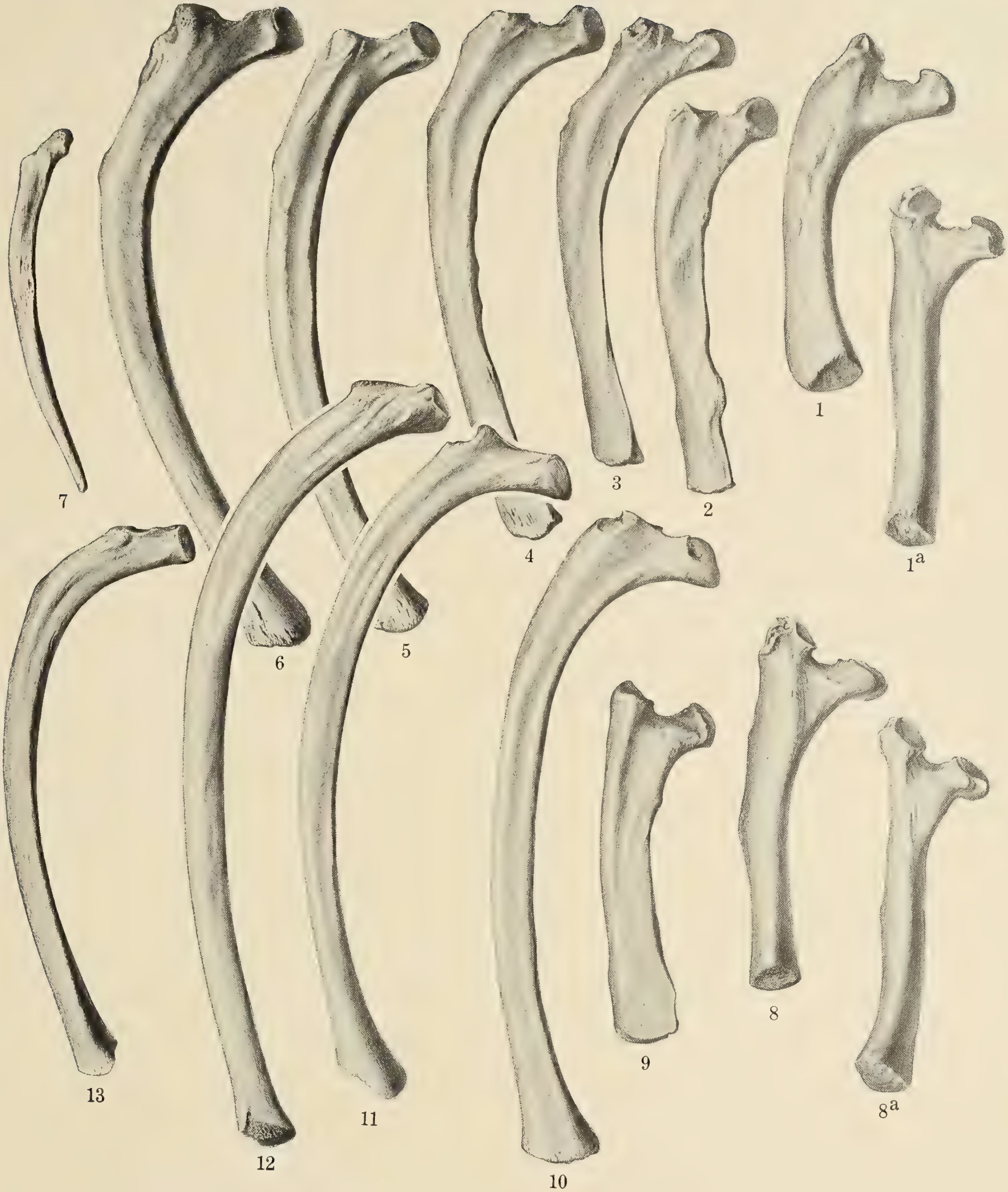

SMILODON CALIFORNICUS AND FELIS ATROX

Plate 21

Smilodon californicus Bovard

Figs. 1, 1a, right scapula, No. 2004–R–10, lateral view and view of articulating end; × 1/3.

Figs. 2, 3, 4 and 5, right humerus, No. 2005–R–6. Fig. 2, inner view; Fig. 3, outer view; Fig. 4, posterior view; Fig. 5, proximal, anterior and distal views; × 1/3. Los Angeles Museum Collection. Rancho La Brea Pleistocene.

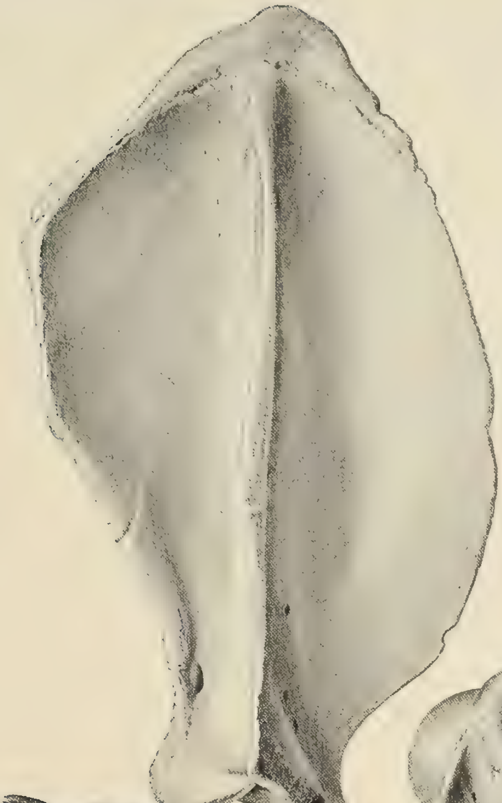

1

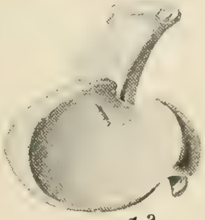

1a

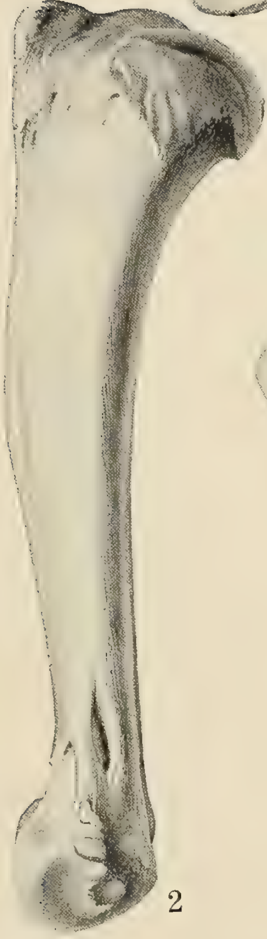

2

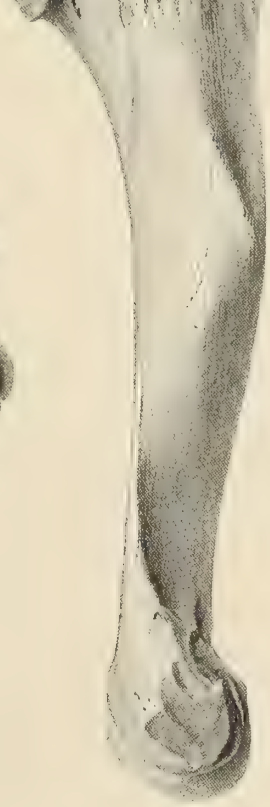

3

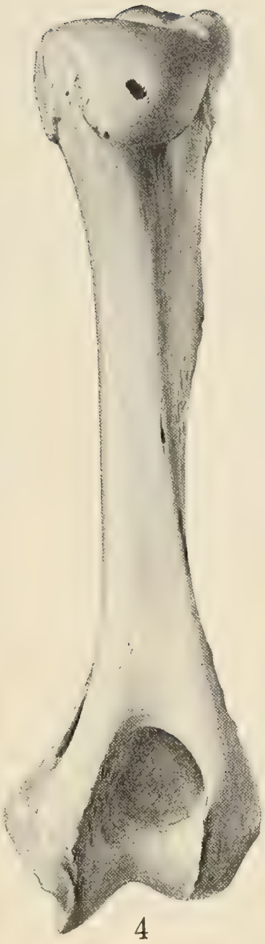

4

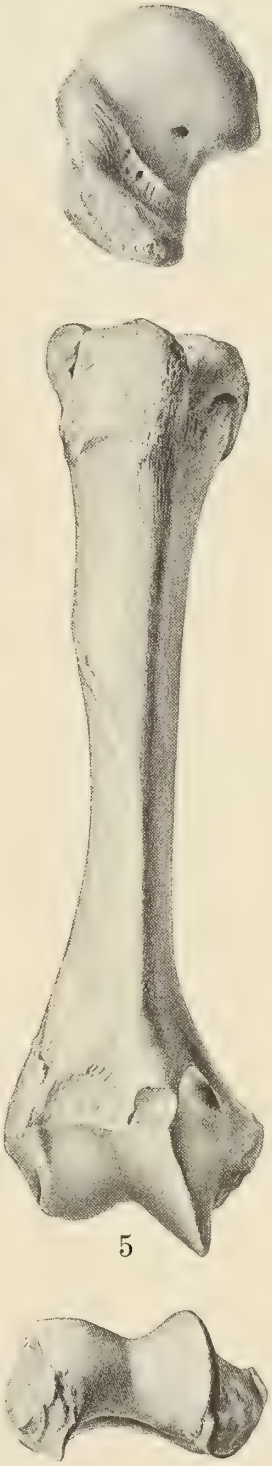

5

SMILODON CALIFORNICUS

Plate 22

PLATE 22

Smilodon californicus Bovard

FIGS. 1, 2 and 3, right ulna, No. 2007–R–6. FIG. 1, radial view; FIG. 2, inner view; FIG. 3, anterior view; × 1/3.

FIGS. 4 and 5, right radius, No. 2006–R–5. FIG. 4, ulnar view; FIG. 5, proximal, outer and distal views; × 1/3.

FIG. 6, right manus, dorsal view; × 1/3.

Los Angeles Museum Collection. Rancho La Brea Pleistocene.

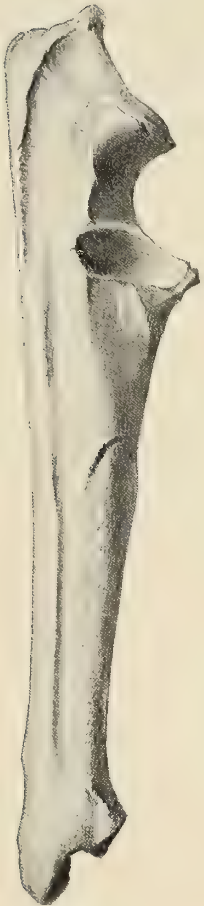

1

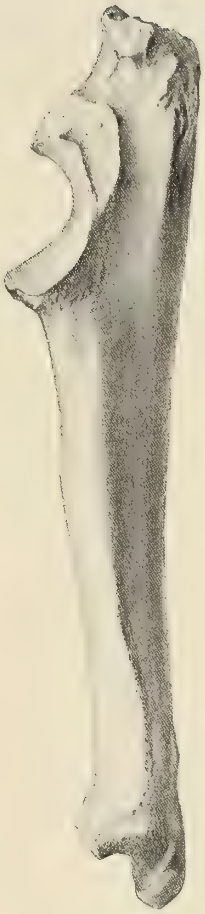

2

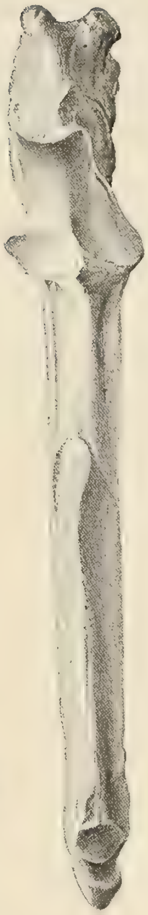

3

4

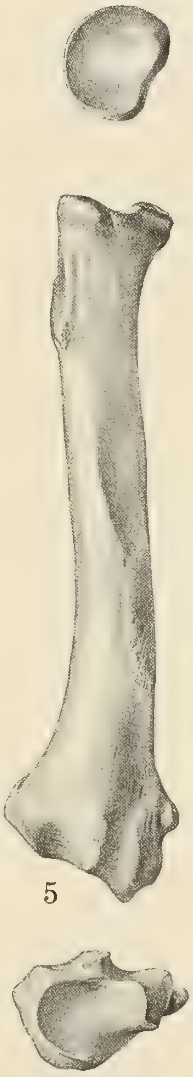

5

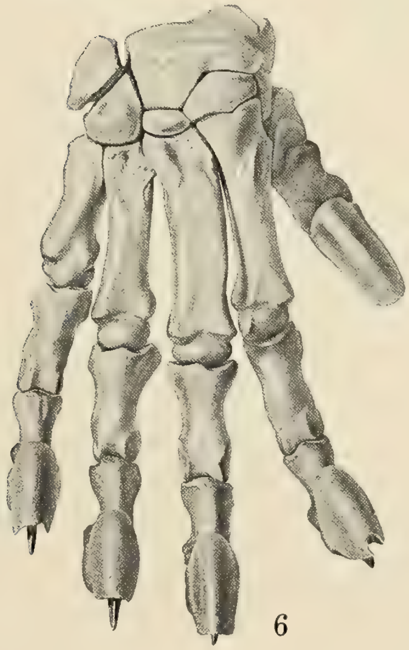

6

SMILODON CALIFORNICUS

Plate 23

PLATE 23

Smilodon californicus Bovard

FIGS. 1 and 2, right femur, No. 2009–R–11. FIG. 1, anterior view; FIG. 2, proximal, posterior and distal views; × 1/3.

FIGS. 3, 4, 5 and 6, right tibia, No. 2010–R–5. FIG. 3, inner view; FIG. 4, outer view; FIG. 5, posterior view; FIG. 6, proximal, anterior and distal views; × 1/3.

FIG. 7, right patella, No. 2012–R–3, anterior and femoral views, and outline of lateral view; × 1/3.

Los Angeles Museum Collection. Rancho La Brea Pleistocene.

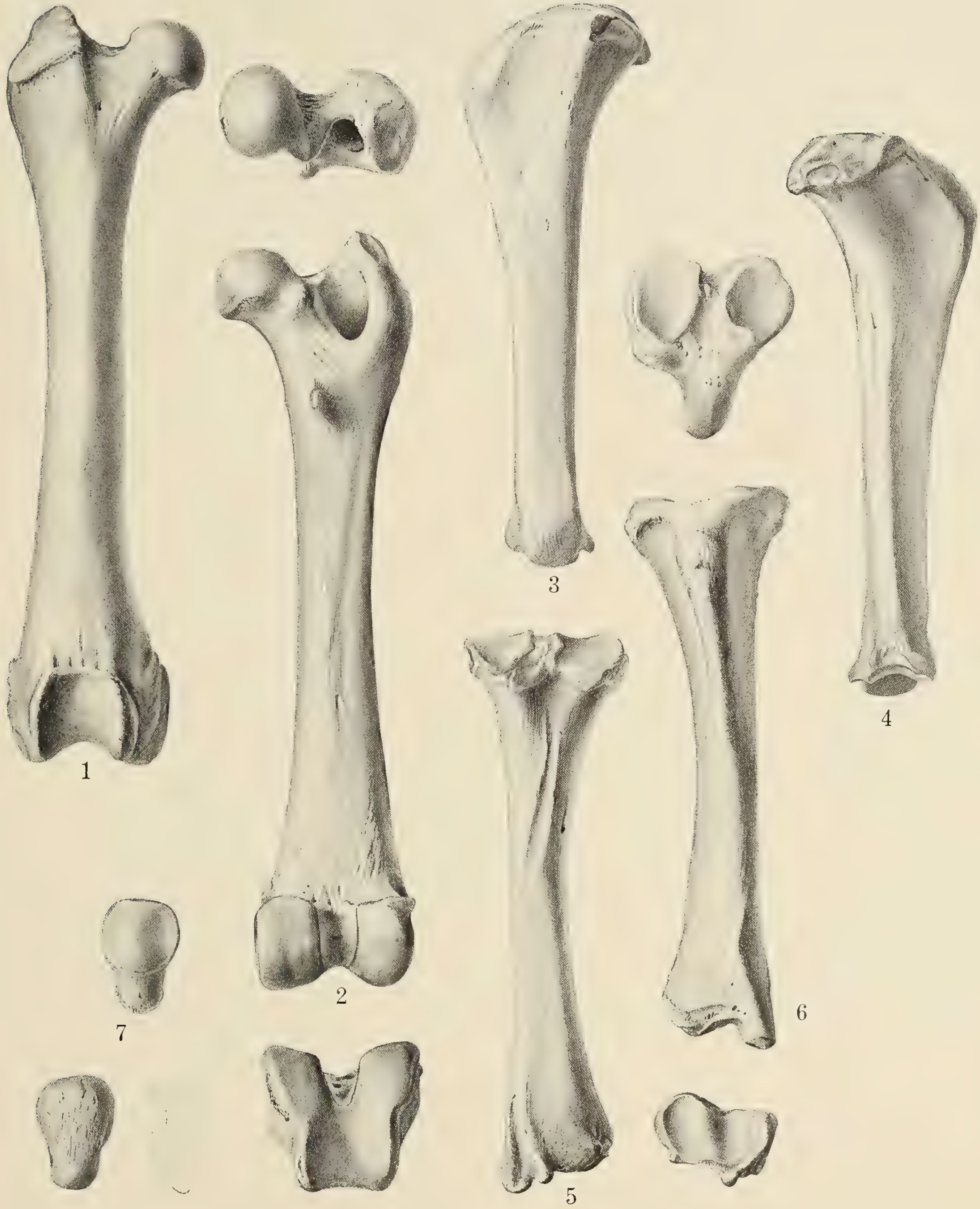

SMILODON CALIFORNICUS

PLATE 24

Smilodon californicus Bovard

FIGS. 1 and 2, pelvis, No. 2008–7. FIG. 1, lateral view; FIG. 2, dorsal view; × 1/3.
FIG. 3, right pes, dorsal view; × 1/3.
FIG. 4, right fibula, No. 2011–R–1, outer, anterior and inner views; × 1/3.

Los Angeles Museum Collection. Rancho La Brea Pleistocene.

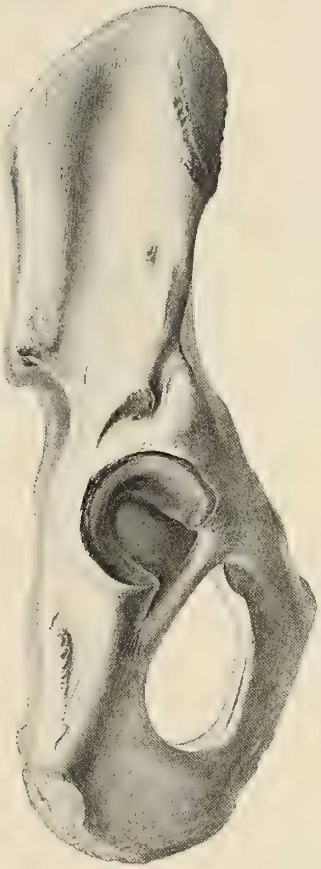

1

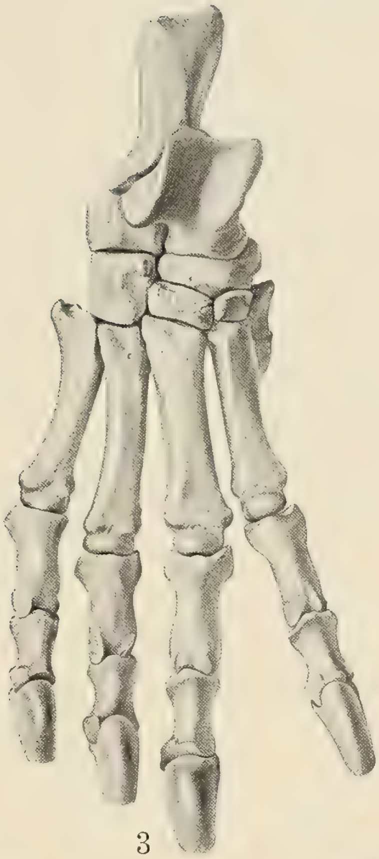

3

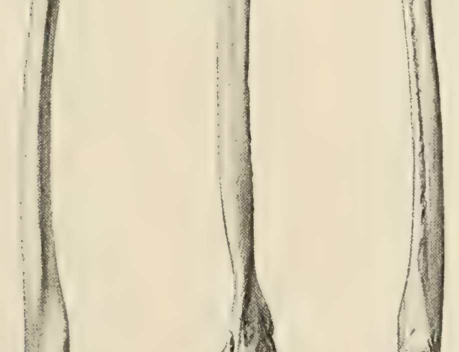

4

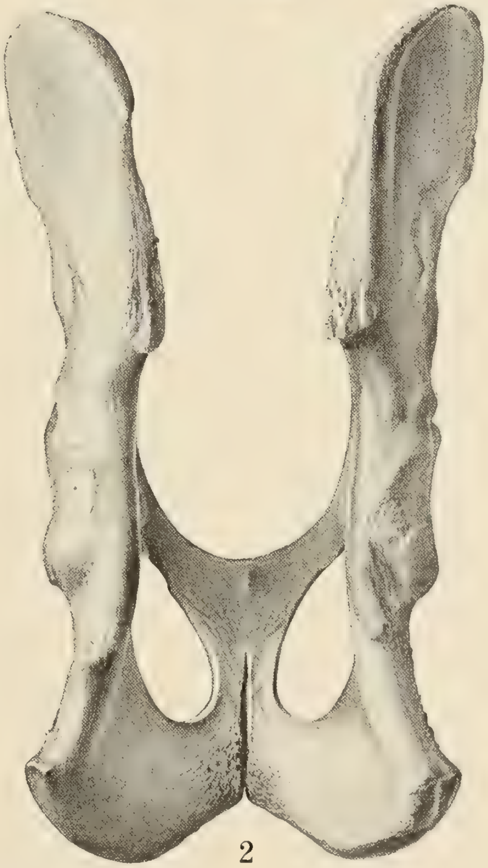

2

SMILODON CALIFORNICUS

PLATE 25

Smilodon californicus Bovard

Mounted skeleton, viewed from right side; approx. × 1/8. Los Angeles Museum Collection. Prepared by J. W. Lytle. Photograph by L. E. Wyman. Courtesy of Los Angeles Museum. Rancho La Brea Pleistocene.

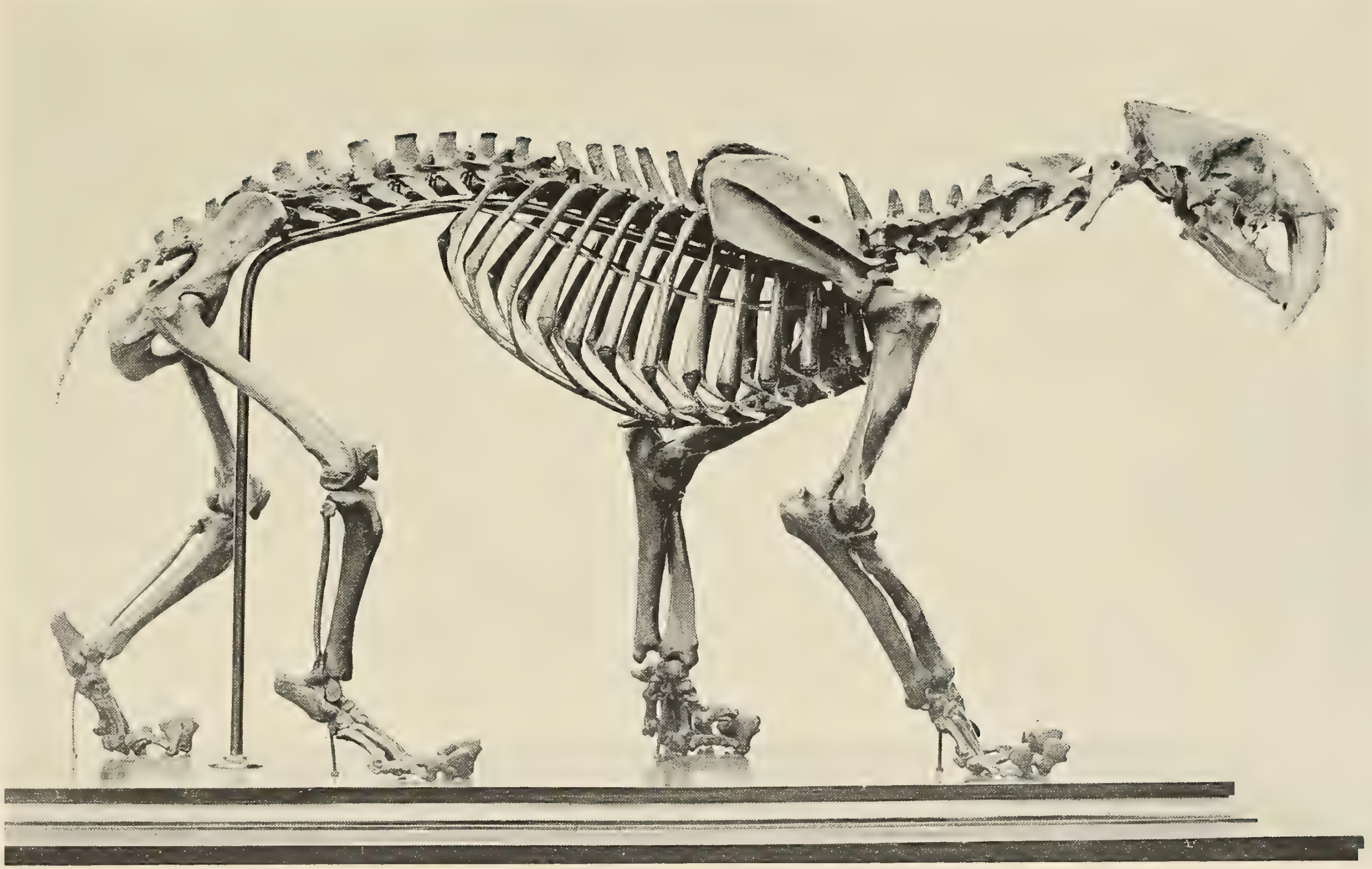

SMILODON CALIFORNICUS

PLATE 26

Felis atrox Leidy

FIG. 1, skull and mandible, No. 20049, lateral view; × 1/3.
FIGS. 2 and 3, skull, No. 20049. FIG. 2, dorsal view; FIG. 3, ventral view; × 1/3.
University of California Collection. Rancho La Brea Pleistocene.

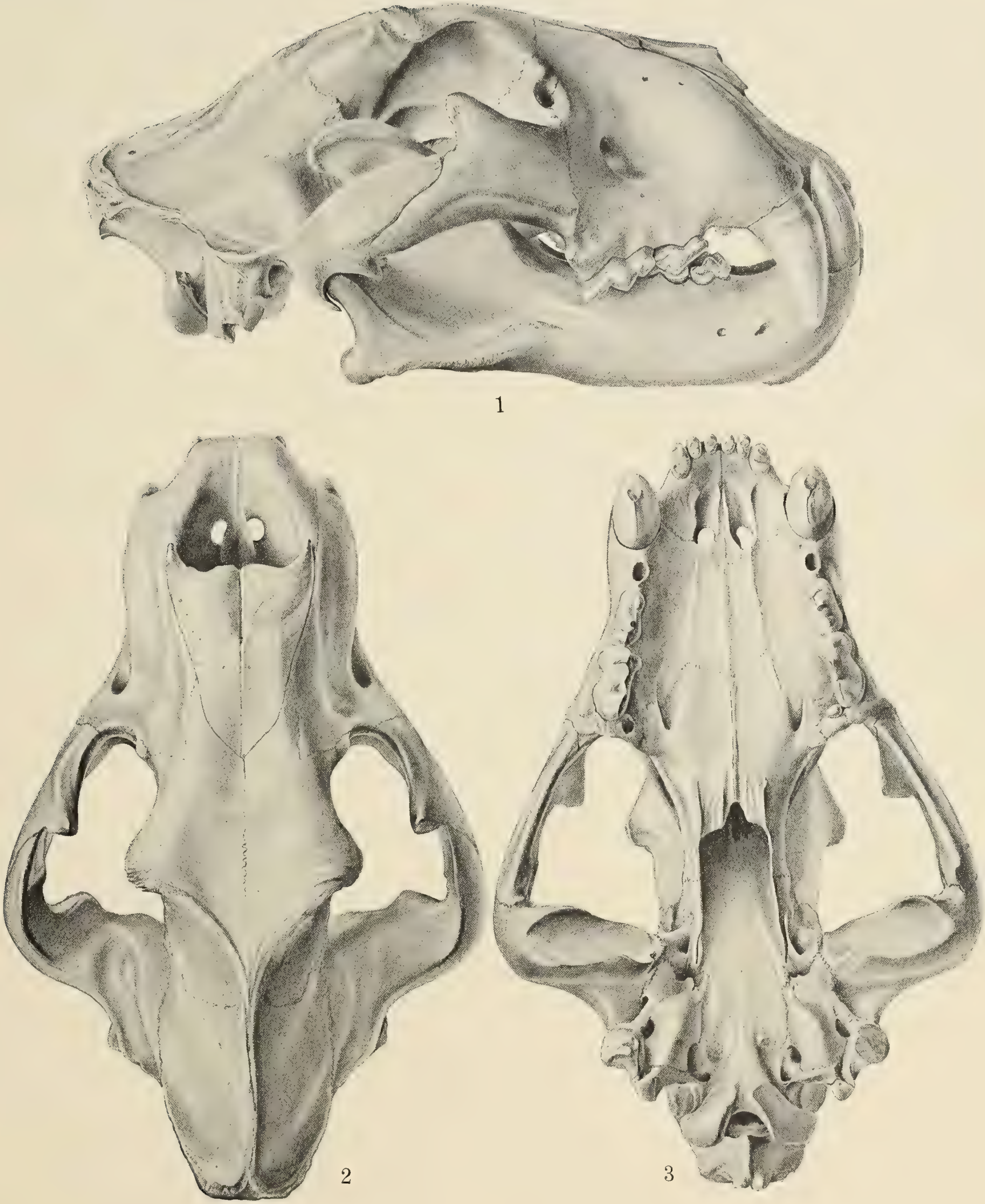

1

2

3

FELIS ATROX

PLATE 27

Felis atrox Leidy

FIGS. 1 and 2, skull, No. 20049. FIG. 1, lateral view with portion of zygomatic arch removed to show infraorbital region; FIG. 2, posterior view; × 1/3.

FIG. 3, skull and mandible, No. 20049, anterior view; × 1/3.

FIGS. 4 and 5, mandible, No. 20049. FIG. 4, dorsal view; FIG. 5, lateral view; × 1/3.

FIG. 6, mandible, No. 2901–4, inner view; × 1/3.

No 20049, University of California Collection; No. 2901–4, Los Angeles Collection. Rancho La Brea Pleistocene.

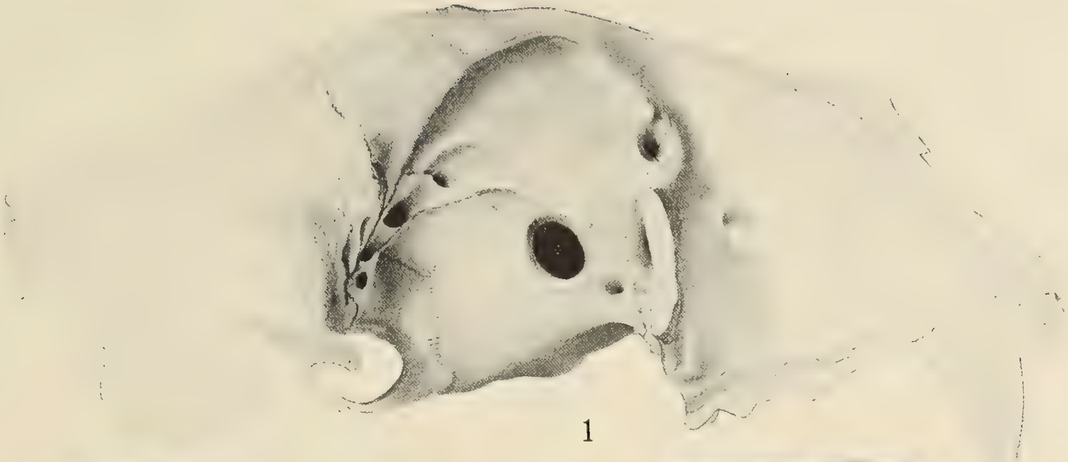

1

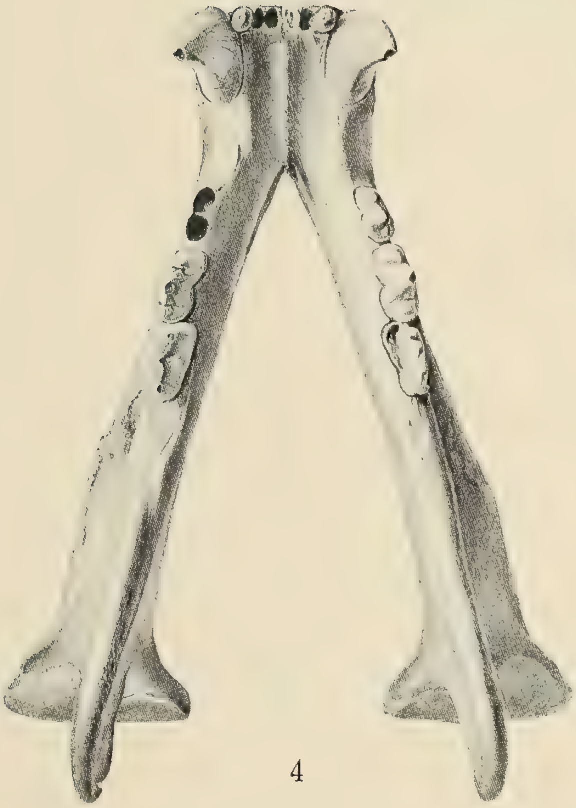

4

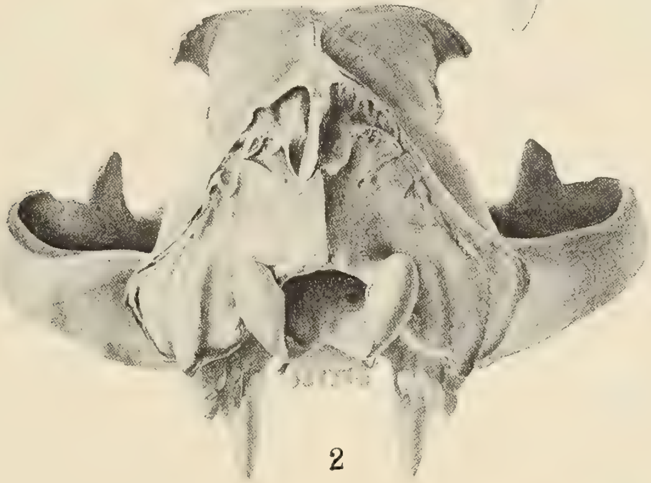

2

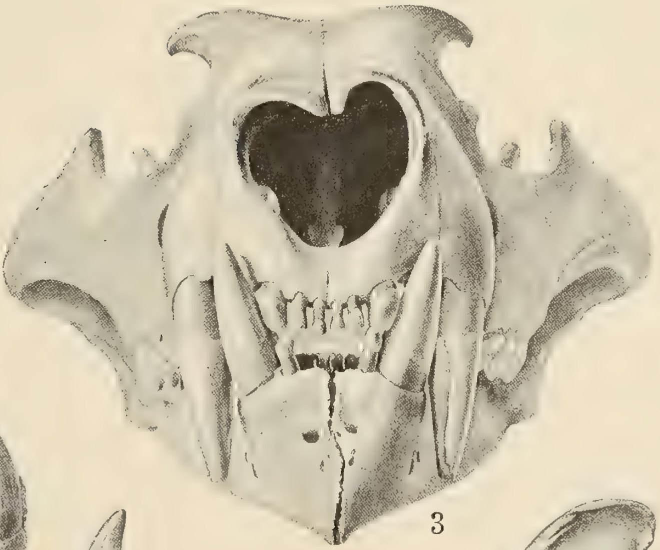

3

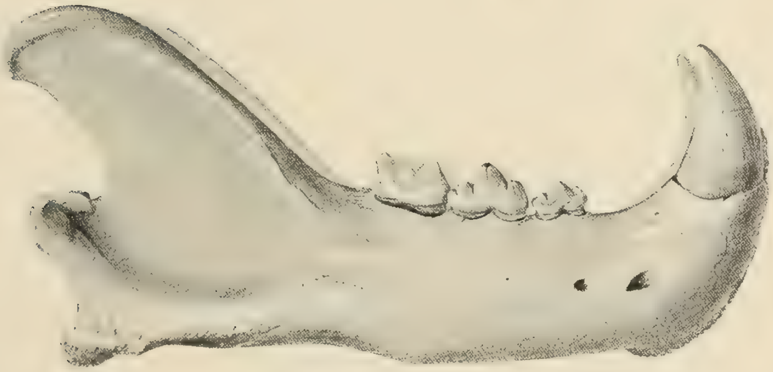

5

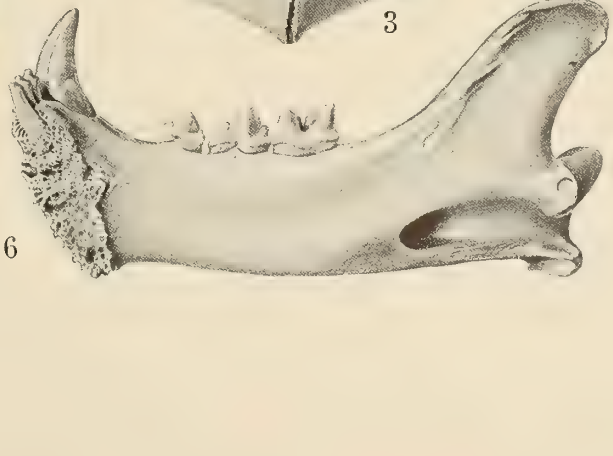

6

FELIS ATROX

PLATE 28

Felis atrox Leidy

Skull, No. 2900–6. FIG. 1, lateral view; FIG. 2, posterior view; FIG. 3, ventral view; FIG. 4, anterior view; FIG. 5, dorsal view; × 1/4. Skulls shown on this and on the three plates that follow represent individuals differing in age and sex. Los Angeles Museum Collection. Rancho La Brea Pleistocene.

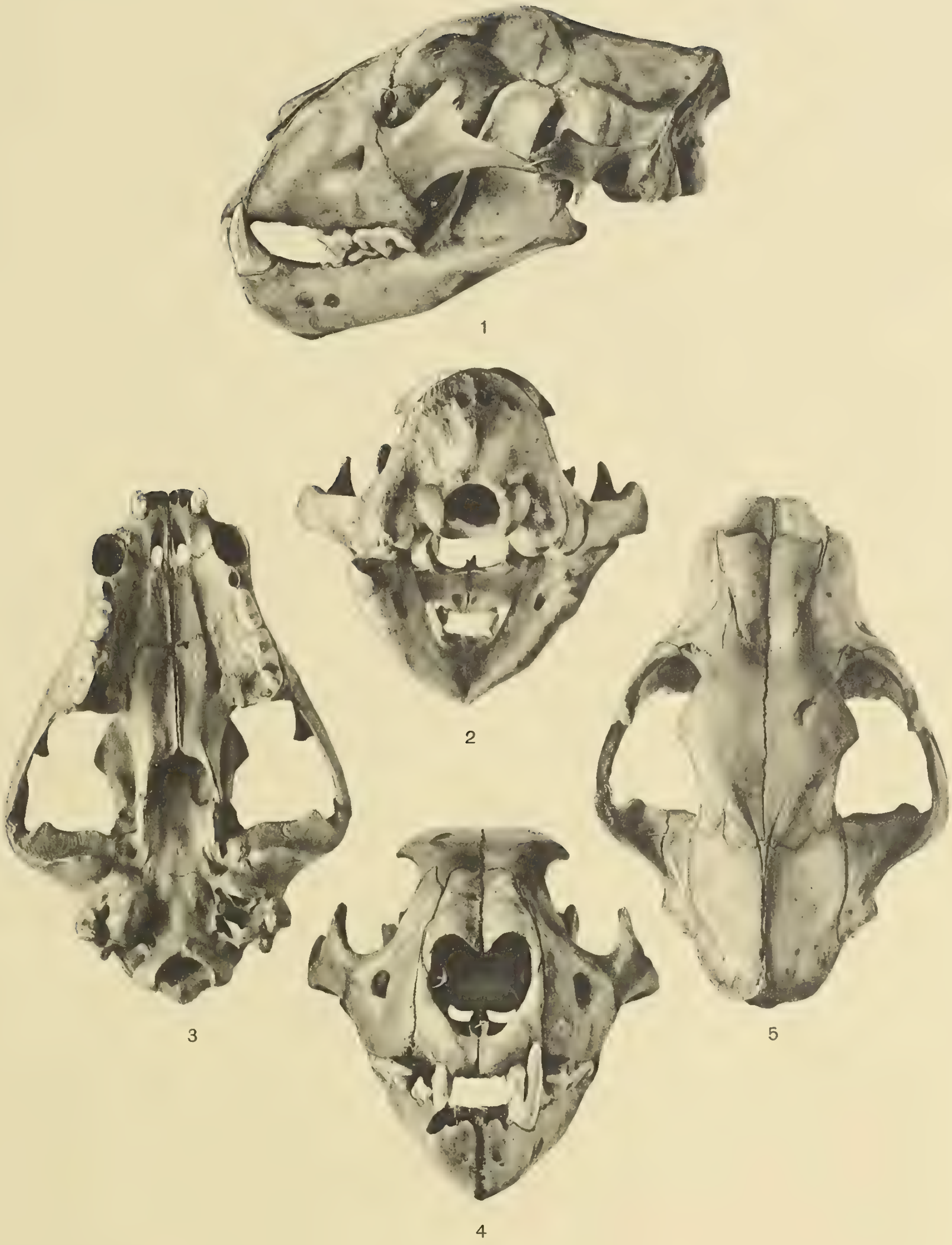

HELIOTYPE CO. BOSTON

FELIS ATROX

PLATE 29

Felis atrox Leidy

Skull, No. 2900–7. FIG. 1, lateral view; FIG. 2, posterior view; FIG. 3, ventral view; FIG. 4, anterior view; FIG. 5, dorsal view; × 1/4. Los Angeles Museum Collection. Rancho La Brea Pleistocene. (See note Plate 28.)

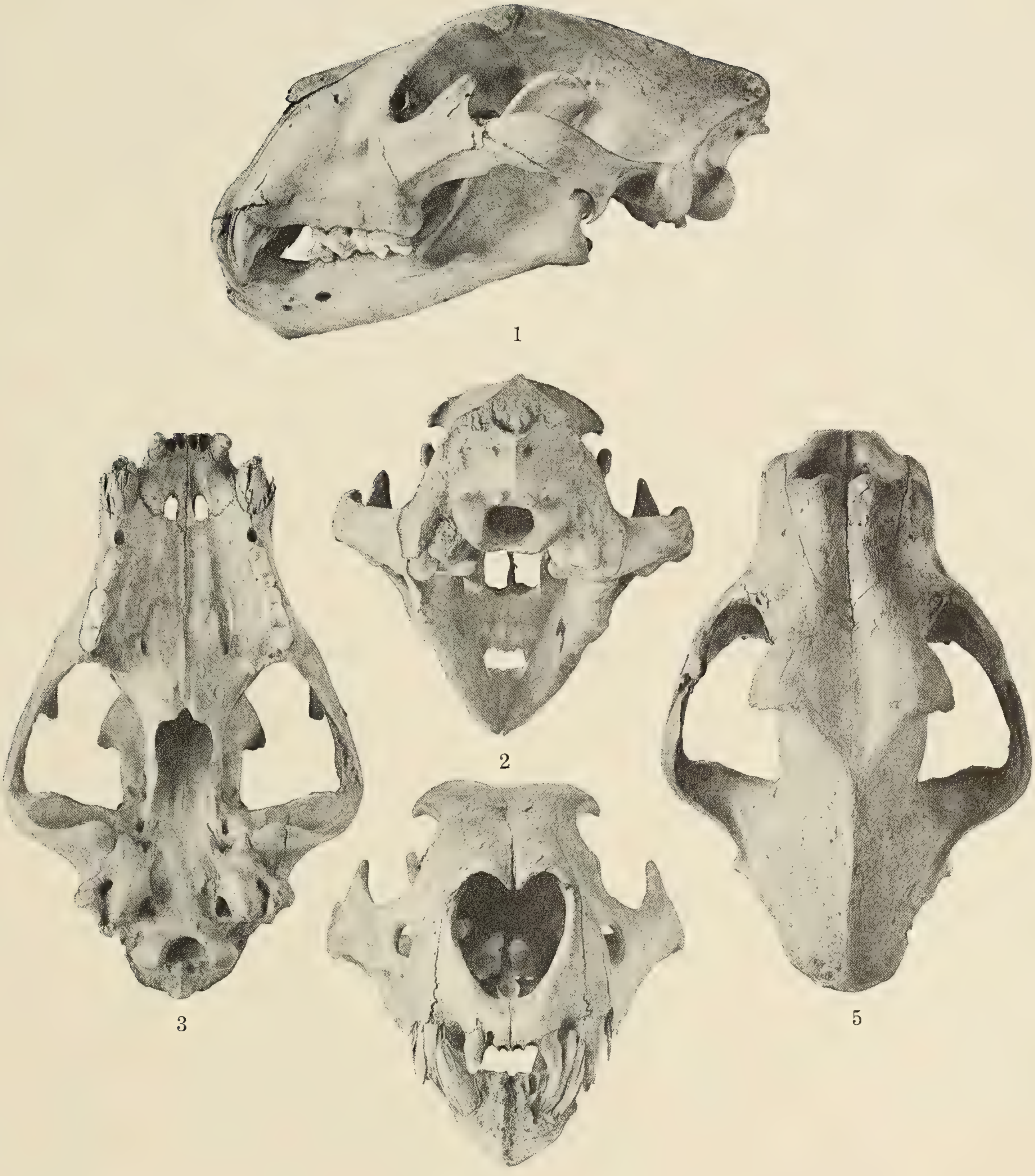

FELIS ATROX

PLATE 30

Felis atrox Leidy

Skull, No. 2900–9. FIG. 1, lateral view; FIG. 2, posterior view; FIG. 3, ventral view; FIG. 4, anterior view; FIG. 5, dorsal view; × 1/4. Los Angeles Museum Collection. Rancho La Brea Pleistocene. (See note Plate 28.)

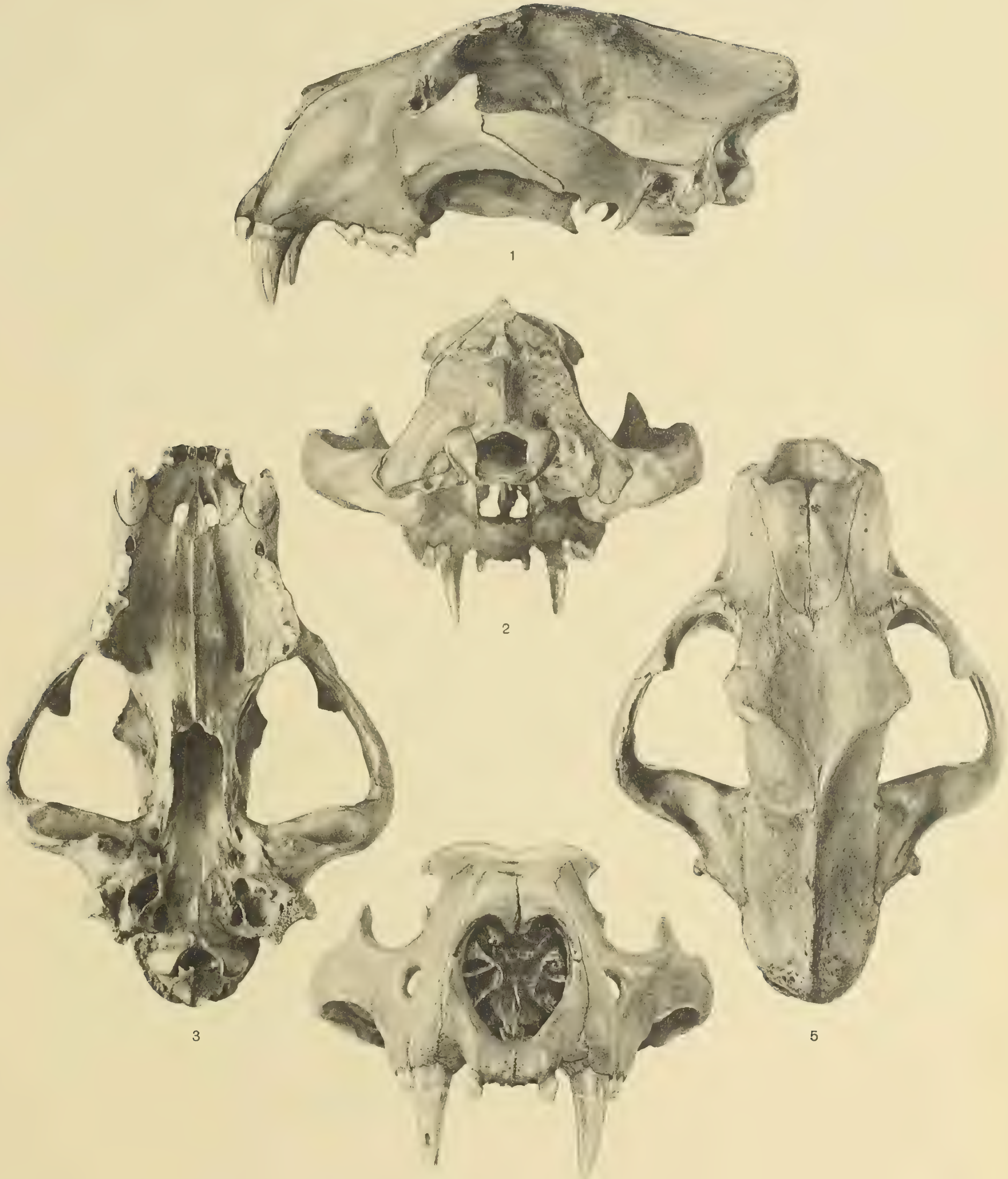

1

2

3

4

5

HELIOTYPE CO. BOSTON

FELIS ATROX

PLATE 31

Felis atrox Leidy

Skull, No. 2900–3. FIG. 1, lateral view; FIG. 2, posterior view; FIG. 3, ventral view; FIG. 4, anterior view; FIG. 5, dorsal view; × 1/4. Los Angeles Museum Collection. Rancho La Brea Pleistocene. (See note Plate 28.)

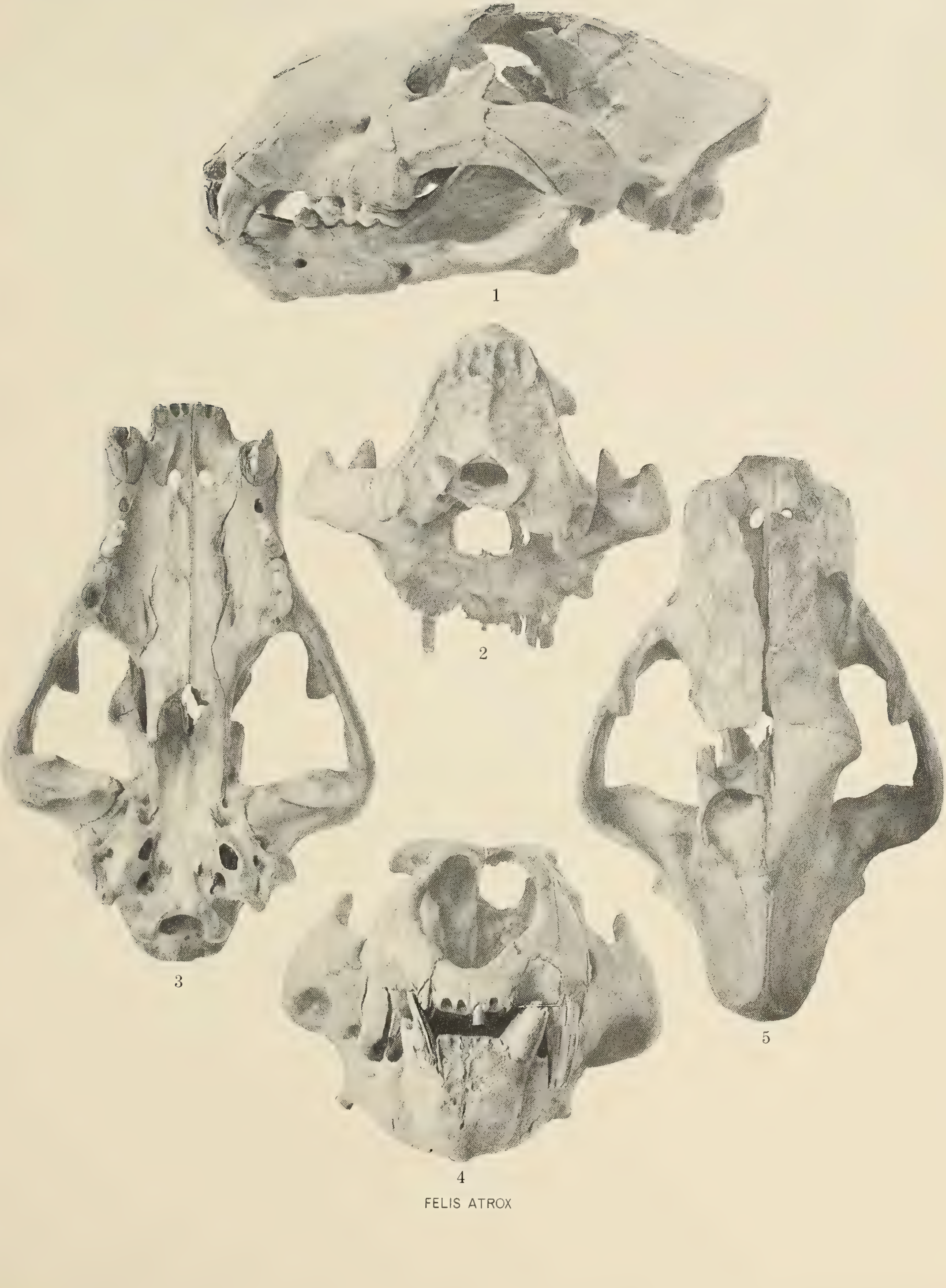

FELIS ATROX

PLATE 32

Felis atrox Leidy

FIGS. 1–5, series of lower jaws including young and adult individuals showing variation in size and shape, Nos. 2901–6, –5, –21, –3, –22, incl.; all specimens × 1/3. Milk teeth present in No. 2901–22.

FIGS. 6–6′, lower canine, inner and posterior views; × 2/3.

FIGS. 7–7′, upper canine, inner and posterior views; × 2/3.

Los Angeles Museum Collection. Rancho La Brea Pleistocene.

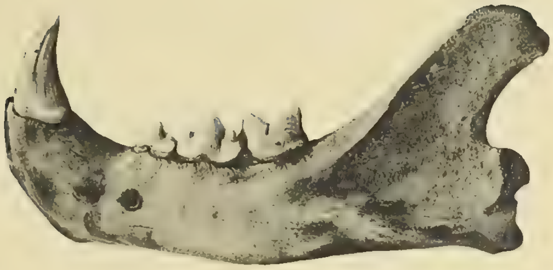
1

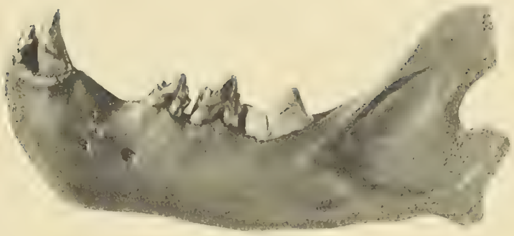
5

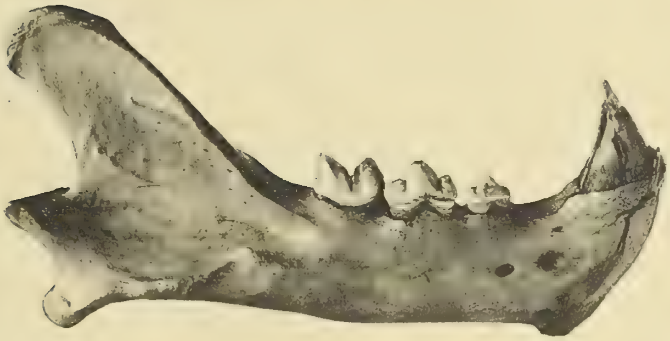
2

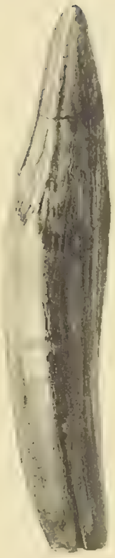
6'

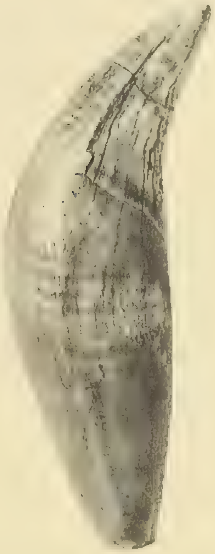
6

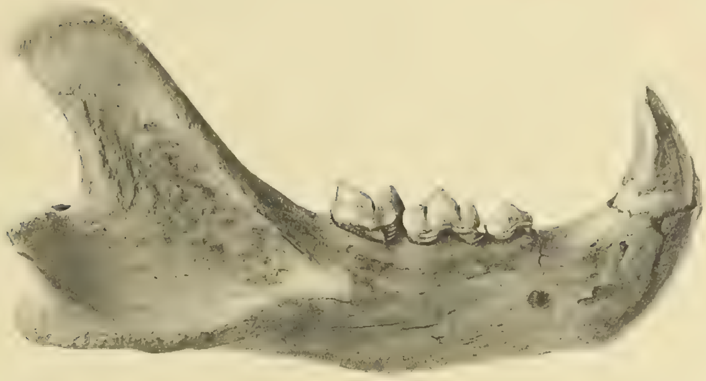
3

7'

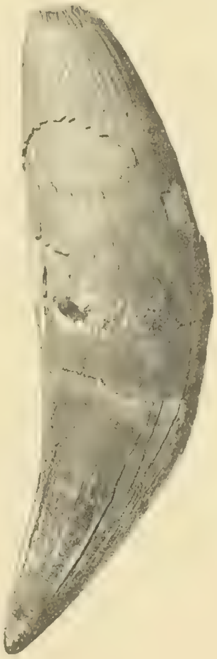
7

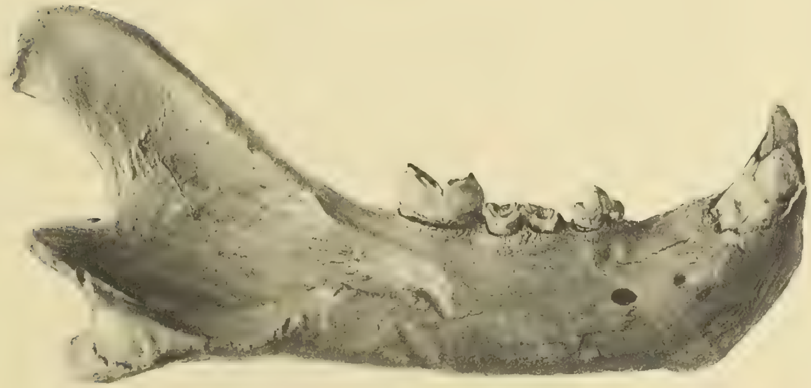
4

HELIOTYPE CO. BOSTON

FELIS ATROX

PLATE 33

Felis atrox Leidy

Upper and lower teeth. FIGS. 1–1a, P$\underline{4}$, outer and inner views; FIGS. 2–2a, P$\underline{3}$, outer and inner views; FIGS. 3–3a, FIGS. 4--4a, FIGS. 5–5a, I$\overline{1}$, $\overline{2}$, $\overline{3}$ respectively, outer and posterior views; FIGS. 6–6a, FIGS. 7–7a, FIGS. 8–8a, M$\overline{1}$, P$\overline{4}$, P$\overline{3}$ respectively, outer and inner views; FIGS. 9–9a, FIGS. 10–10a, FIGS. 11–11a, I$\underline{1}$, $\underline{2}$, $\underline{3}$ respectively, inner and posterior views; × 1. Los Angeles Museum Collection. Rancho La Brea Pleistocene.

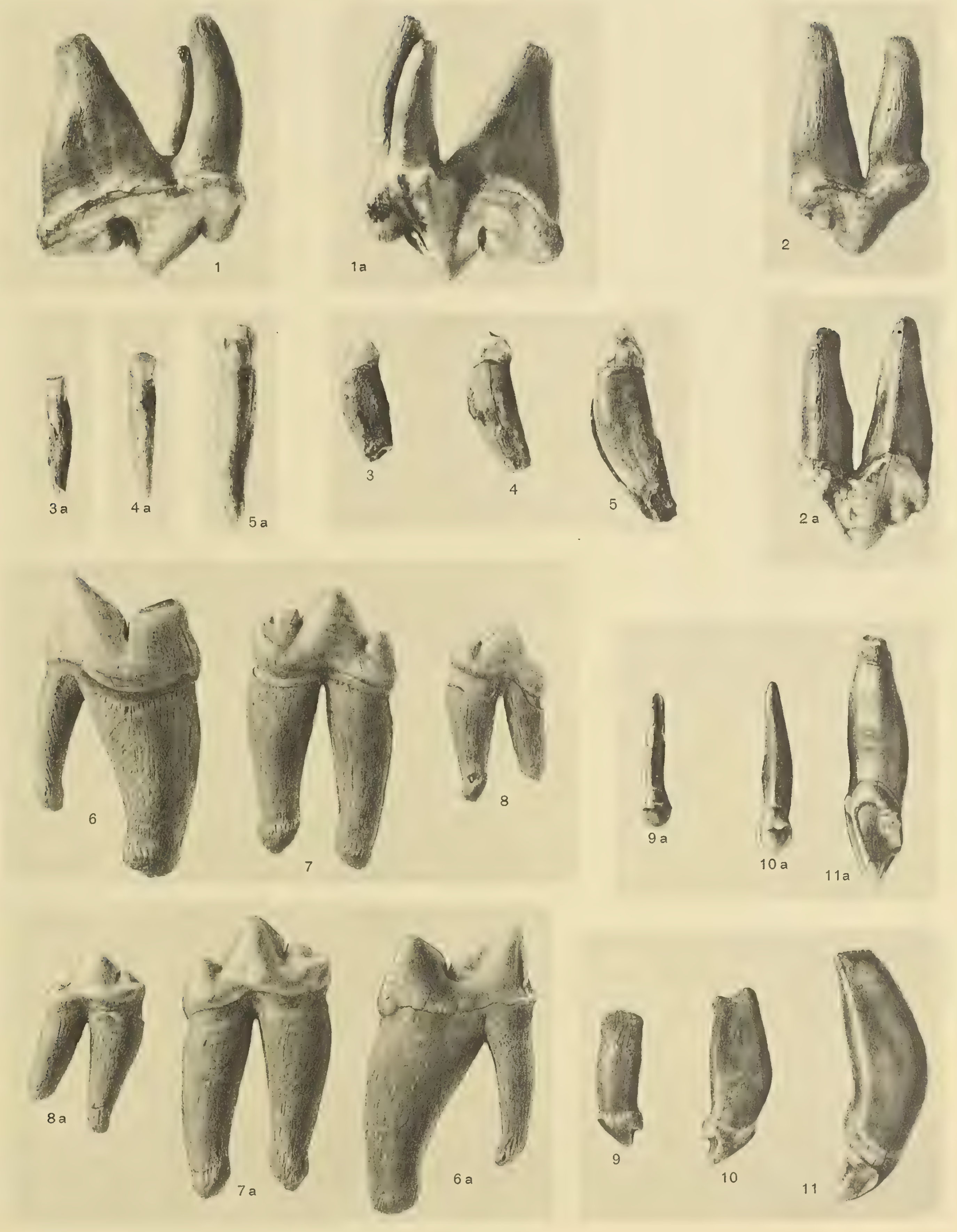

HELIOTYPE CO. BOSTON

FELIS ATROX

PLATE 34

Felis atrox Leidy

FIGS. 1, 2 and 3, axis, No. 2937–7. FIG. 1, dorsal view; FIG. 2, posterior view; FIG. 3, lateral view; × 1/2.

FIGS. 4, 5, 6 and 7, atlas, No. 2936–1. FIG. 4, anterior view; FIG. 5, dorsal view; FIG. 6, ventral view; FIG. 7, posterior view; × 1/2.

Los Angeles Museum Collection. Rancho La Brea Pleistocene.

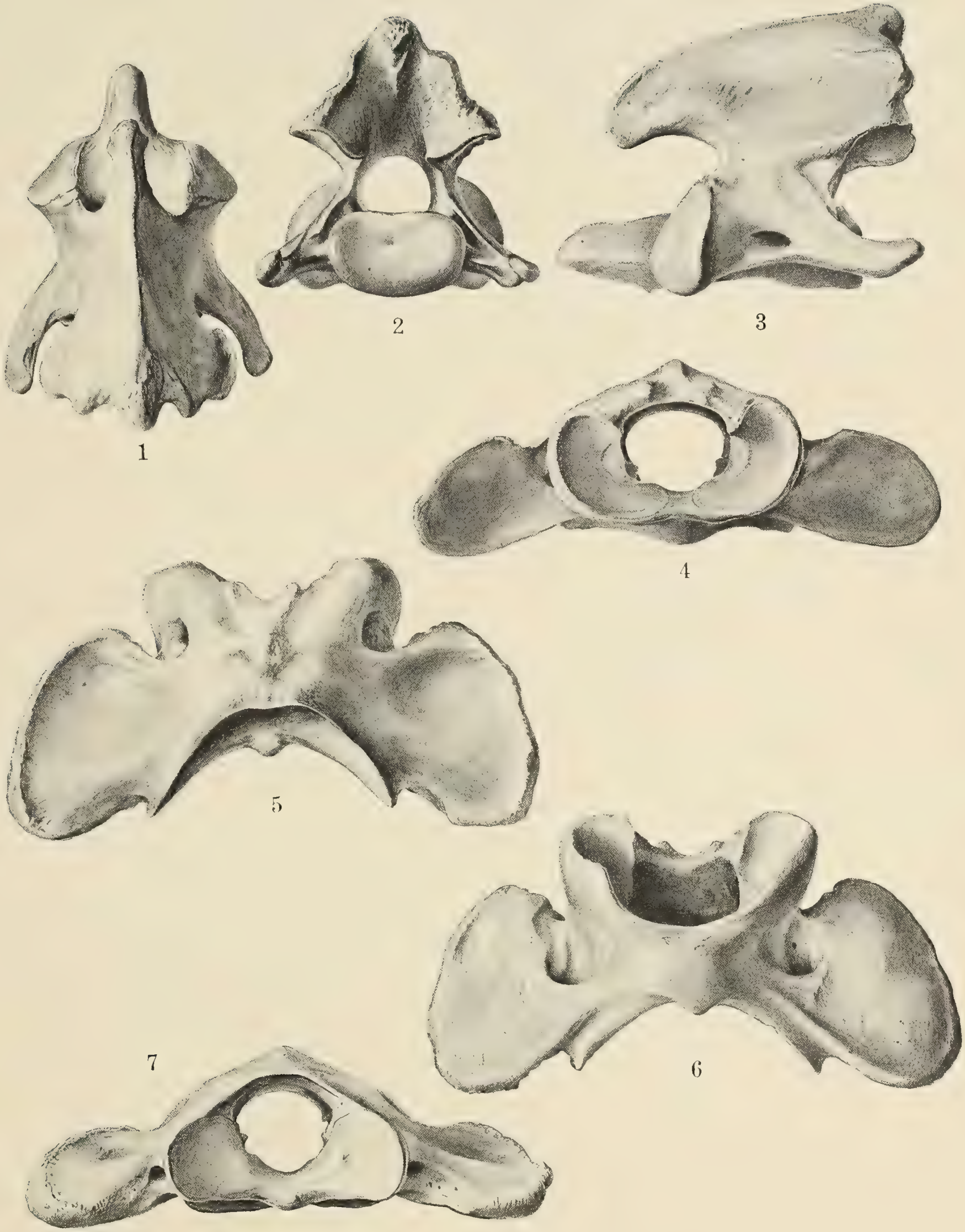

FELIS ATROX

PLATE 35

Felis atrox Leidy

FIG. 1, sacrum, No. 2963–2, lateral view; × 1/3.

FIGS. 2 and 3, lumbar vertebræ, lateral and dorsal views; × 1/3. a′, seventh vertebra, No. 2962–11; b′, fourth vertebra, No. 2959–2; c′, first vertebra, No. 2956–2; anterior views; × 1/3.

FIGS. 4 and 5, thirteenth thoracic vertebra, No. 2955–11, and twelfth thoracic vertebra, No. 2954–12, lateral and dorsal views; × 1/3.

Los Angeles Museum Collection. Rancho La Brea Pleistocene.

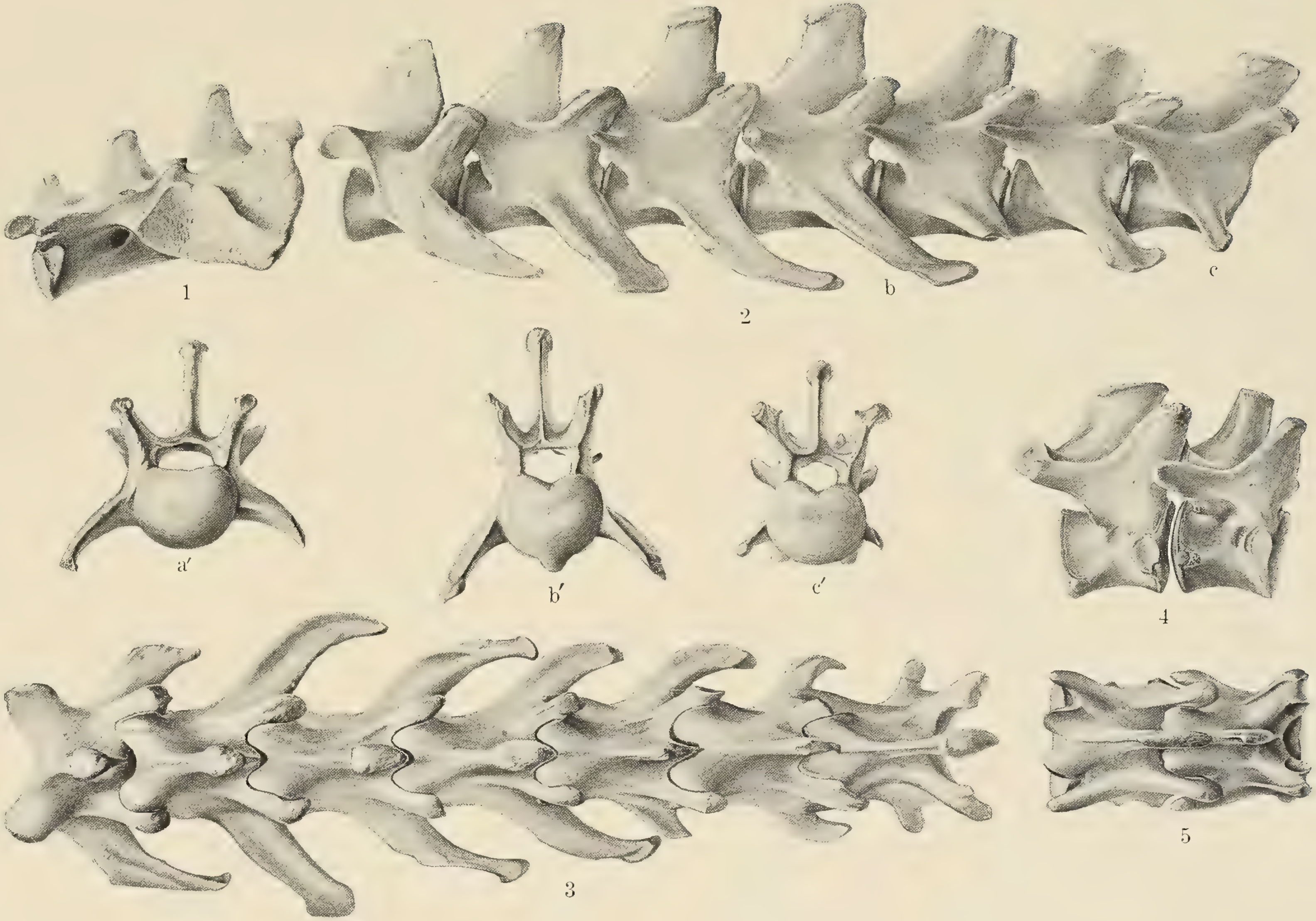

FELIS ATROX

PLATE 36

Felis atrox Leidy

FIG. 1, right scapula, No. 2902–R–1, lateral view and view of articulating end; × 1/3.

FIGS. 2, 3, 4 and 5, right humerus, No. 2903–R–8. FIG. 2, inner view; FIG. 3, outer view; FIG. 4, posterior view; FIG. 5, proximal, anterior and distal views; × 1/3. Los Angeles Museum Collection. Rancho La Brea Pleistocene.

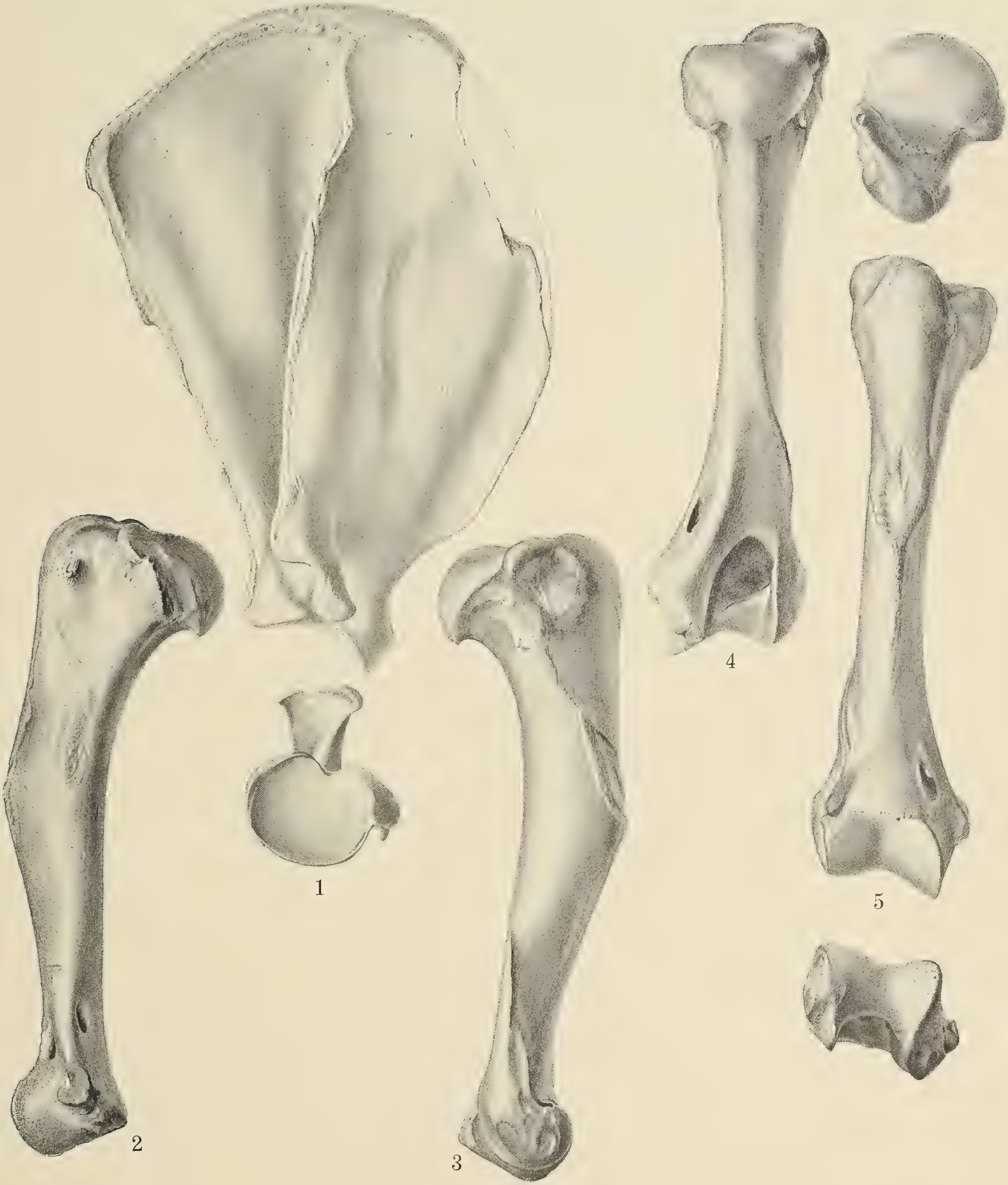

FELIS ATROX

PLATE 37

Felis atrox Leidy

FIGS. 1, 2 and 3, right ulna, No. 2905–R–8. FIG. 1, radial view; FIG. 2, inner view; FIG. 3, anterior view; × 1/3.

FIGS. 4 and 5, right radius, No. 2904–R–7. FIG. 4, ulnar view; FIG. 5, proximal, outer and distal views; × 1/3.

FIG. 6, right manus, dorsal view; × 1/3.

Los Angeles Museum Collection. Rancho La Brea Pleistocene.

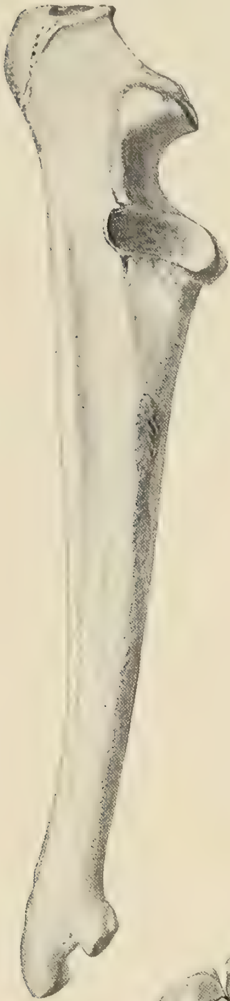
1

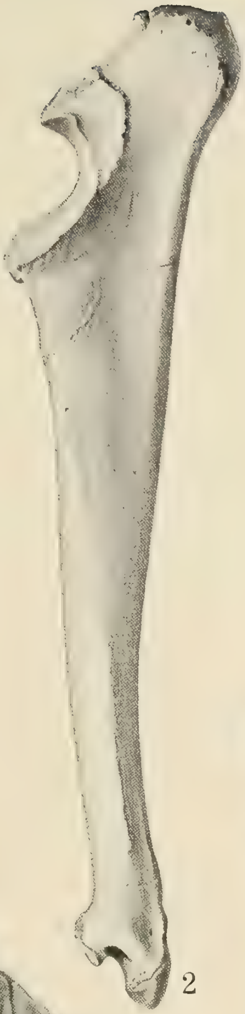
2

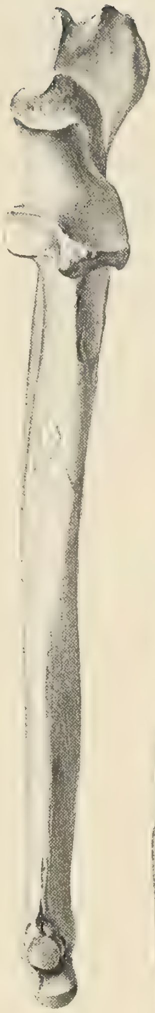
3

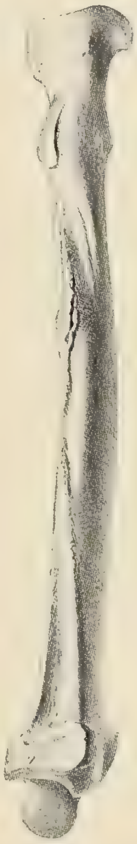
4

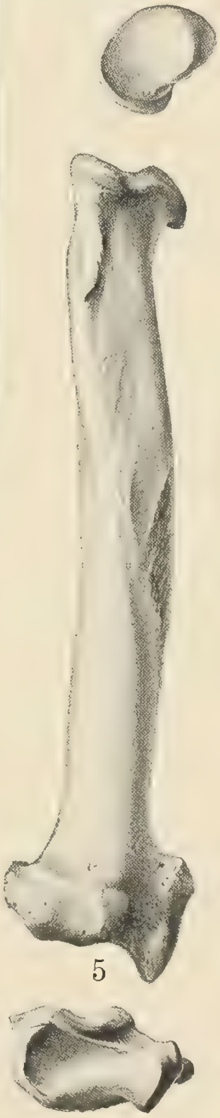
5

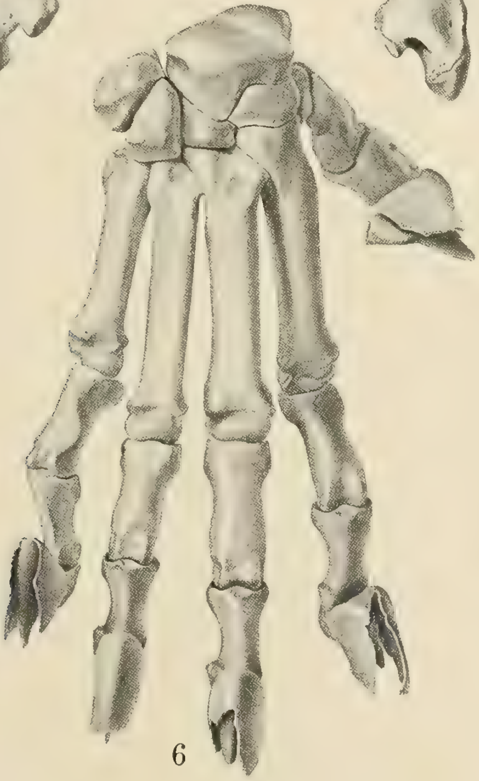
6

FELIS ATROX

PLATE 38

Felis atrox Leidy

FIGS. 1 and 2, right femur, No. 2907–R–11. FIG. 1, anterior view; FIG. 2, proximal, posterior and distal views; × 1/3.

FIGS. 3, 4, 5 and 6, right tibia, No. 2908–R–10. FIG. 3, inner view; FIG. 4, outer view; FIG. 5, posterior view; FIG. 6, proximal, anterior and distal views; × 1/3.

FIG. 7, right patella, No. 2910–R–1, anterior and femoral views, and outline of lateral view; × 1/3.

Los Angeles Museum Collection. Rancho La Brea Pleistocene.

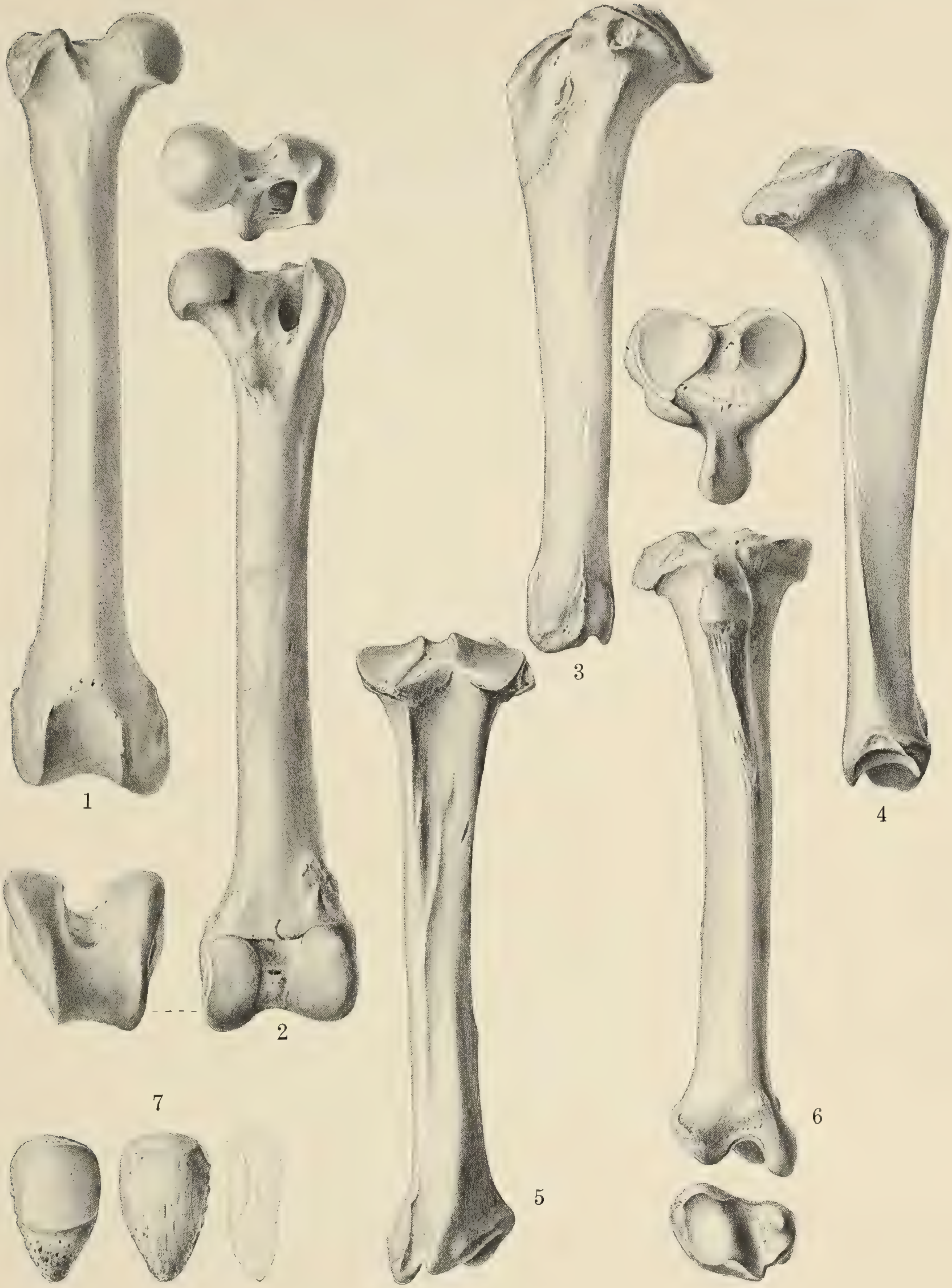

FELIS ATROX

Plate 39

PLATE 39

Felis atrox Leidy

FIGS. 1 and 2, pelvis, No. 2906–1. FIG. 1, lateral view; FIG. 2, dorsal view; × 1/3.
FIG. 3, right pes, dorsal view; × 1/3.
FIGS. 4a, 4b and 4c, right fibula, No. 2909–R–1. FIG. 4a, outer view; FIG. 4b, inner view; FIG. 4c, anterior view; × 1/3.

Los Angeles Museum Collection. Rancho La Brea Pleistocene.

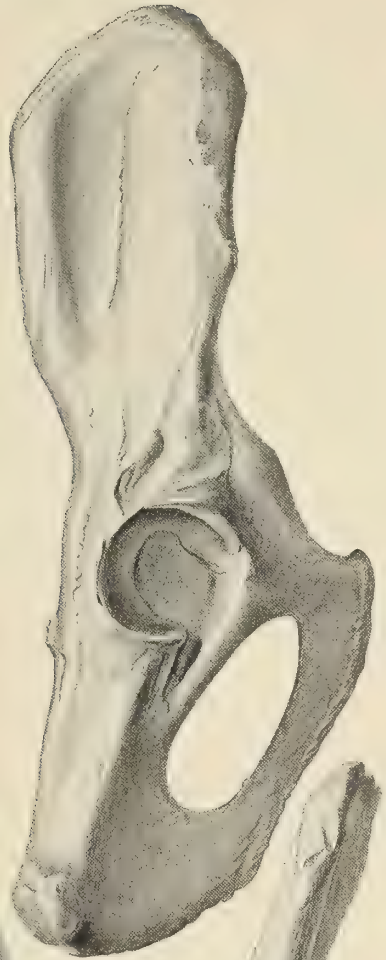

1

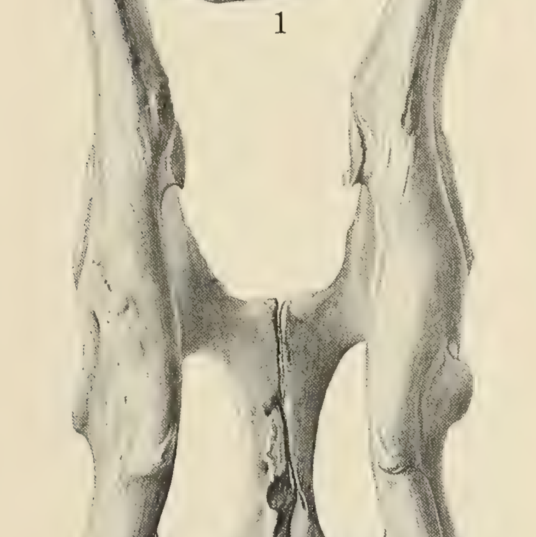

2

4a

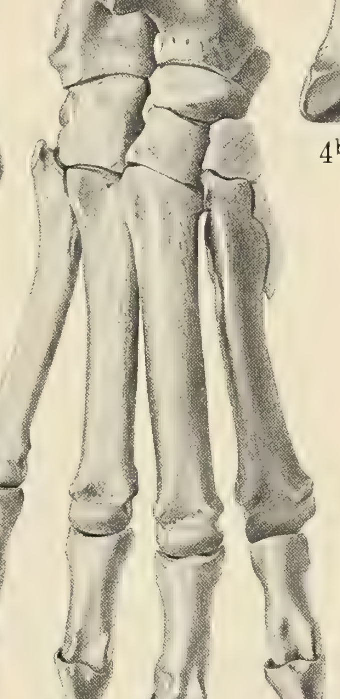

3

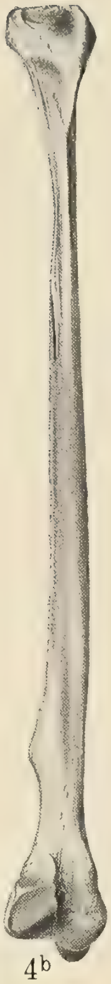

4b

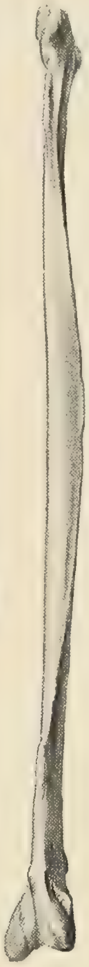

4c

FELIS ATROX

PLATE 40

PLATE 40

Felis atrox Leidy

Mounted skeleton, viewed from right side; approx. × 1/9. Los Angeles Museum Collection. Prepared by J. W. Lytle. Photograph by L. E. Wyman. Courtesy of Los Angeles Museum. Rancho La Brea Pleistocene.

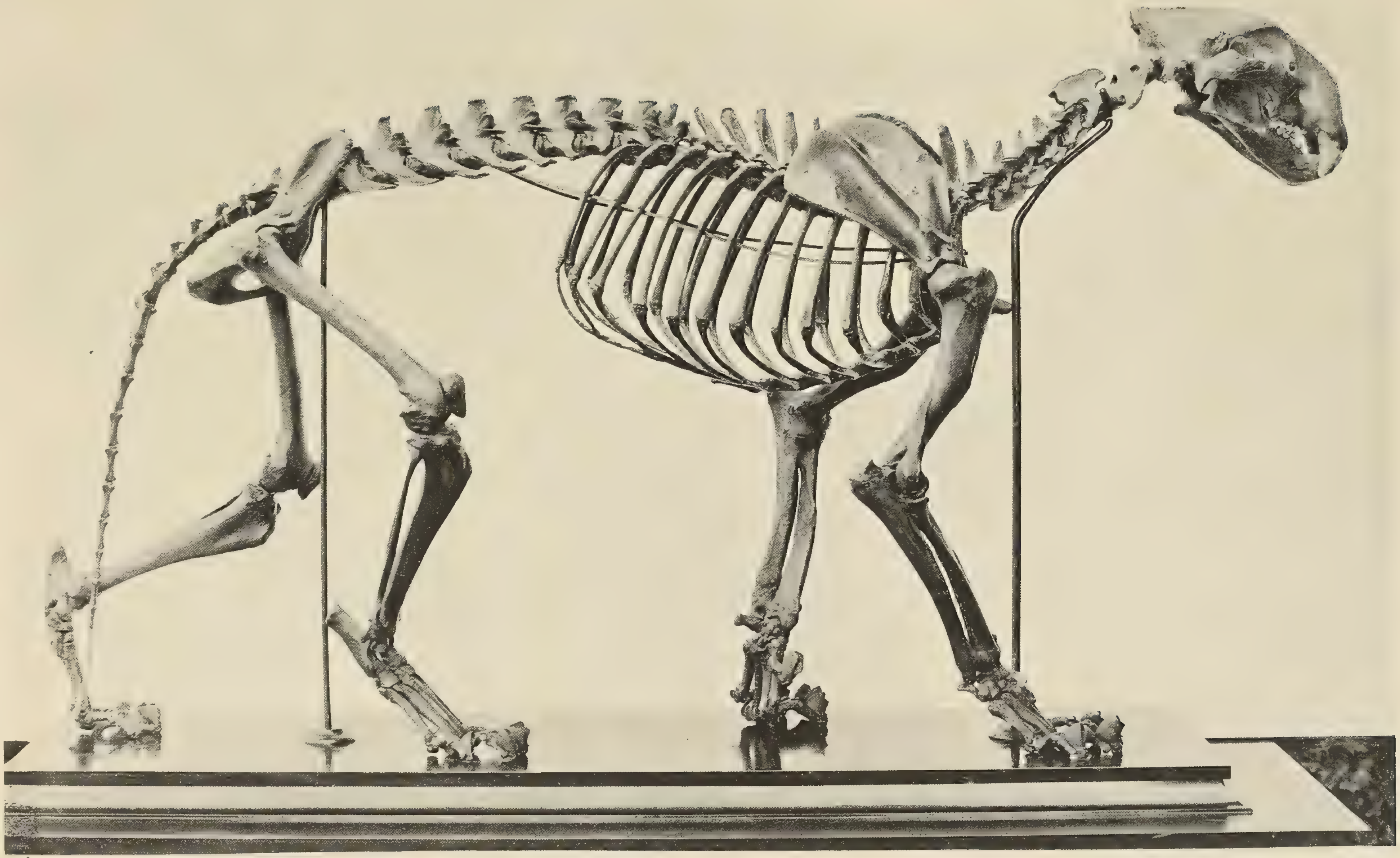

FELIS ATROX

PLATE 41

Felis bituminosa, n. sp.

Holotype, skull, No. X8628. FIG. 1, lateral view of skull and jaw; FIG. 2, dorsal view; FIG. 3, ventral view; × 1/2.

Los Angeles Museum Collection. Rancho La Brea Pleistocene.

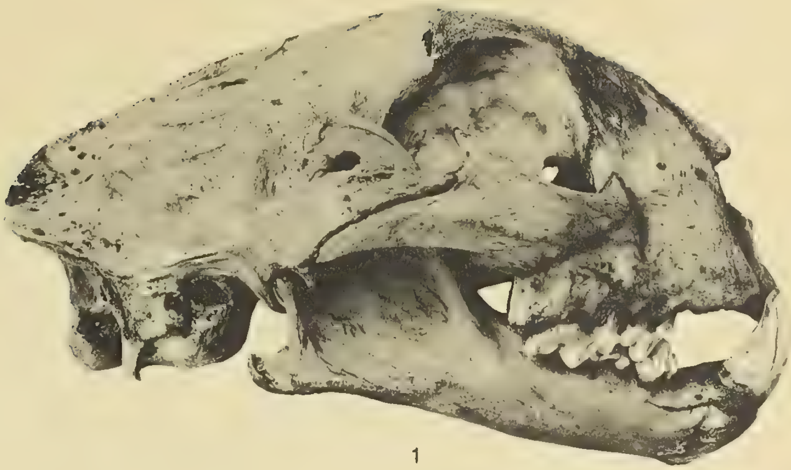

1

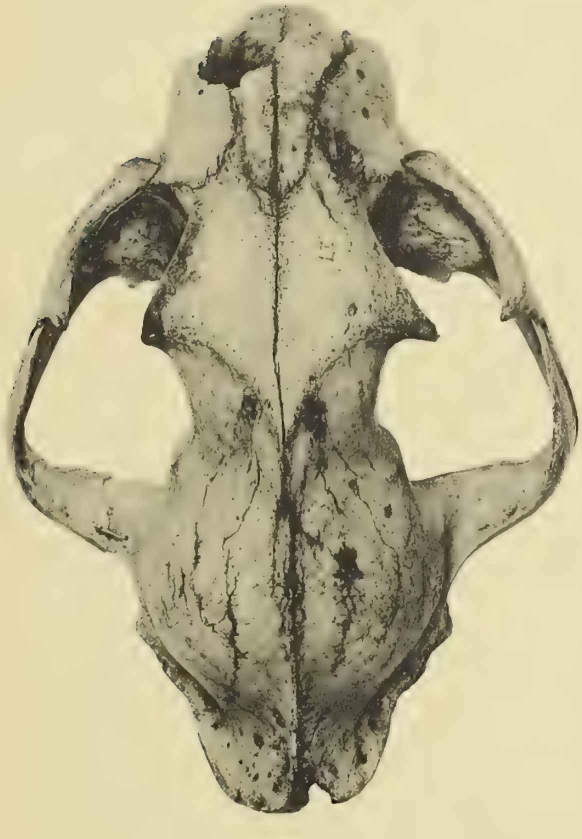

2

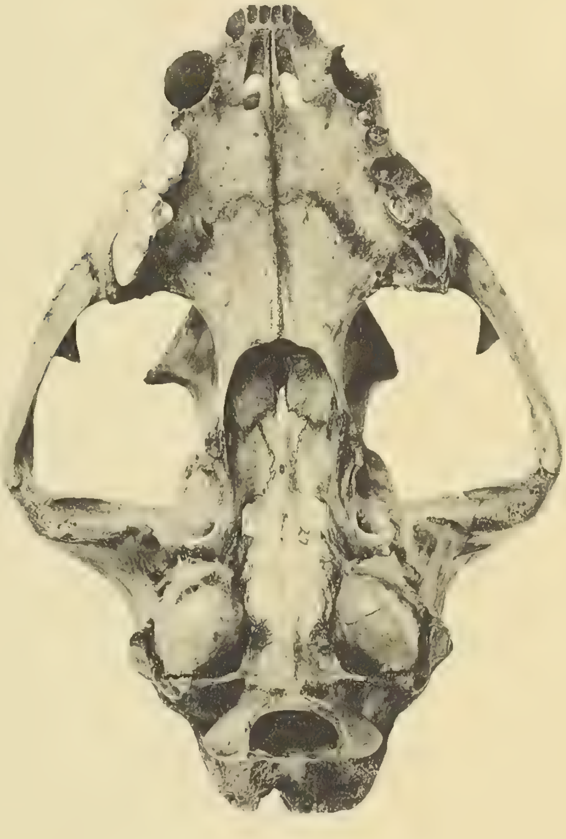

3

HELIOTYPE CO. BOSTON

FELIS BITUMINOSA, N. SP.

PLATE 42

Felis and *Lynx*

FIGS. 1, 2 and 3, *Lynx rufa fischeri* Merriam, skull, No. X9489, dorsal, ventral and lateral views; × 1/2.

FIG. 4, *Lynx rufa fischeri* Merriam, type specimen, ramus of mandible, No. 11283, Univ. Calif. Coll., lateral view; × 1/2.

FIG. 5, *Felis* cf. *bituminosa* n. sp., ramus of mandible, No. X9474, lateral view; × 1/2.

FIG. 6, *Felis daggetti* Merriam, type specimen, No. 21572, Univ. Calif. Coll., lateral view; × 1/2.

FIG. 7, *Lynx rufa fischeri* Merriam, ramus of mandible, No. X9490, lateral view; × 1/2.

FIGS. 8 and 9, *Felis bituminosa* n. sp., skull, No. X8629, dorsal and ventral views; × 1/2.

Los Angeles Museum and University of California Collections.

Rancho La Brea Pleistocene.

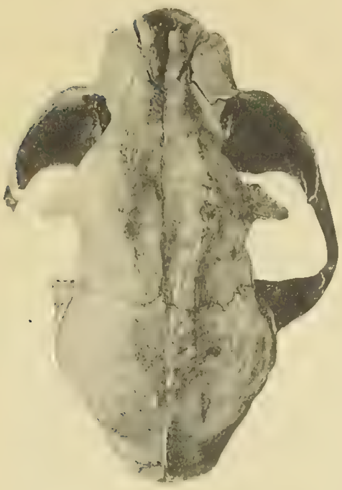
1

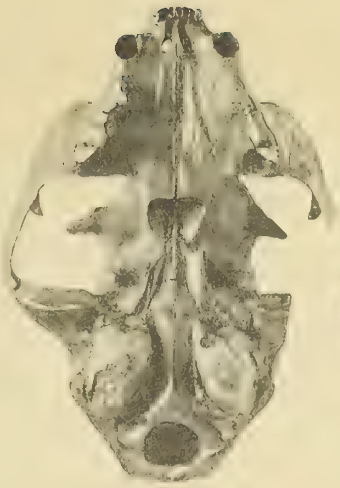
2

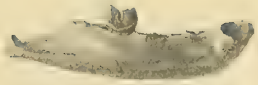
4

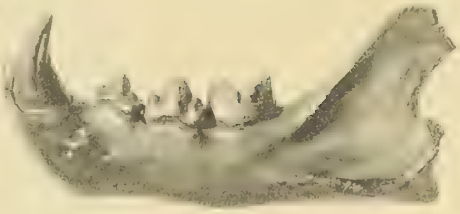
5

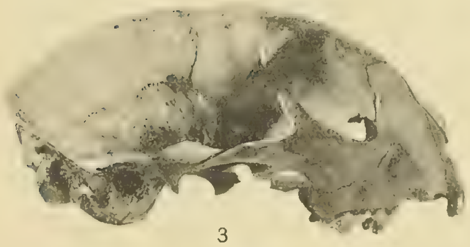
3

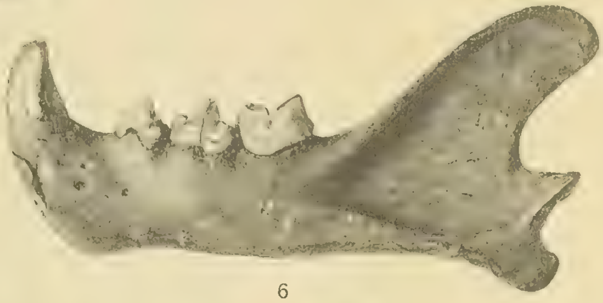
6

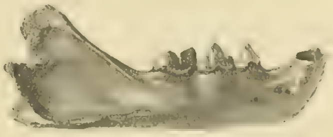
7

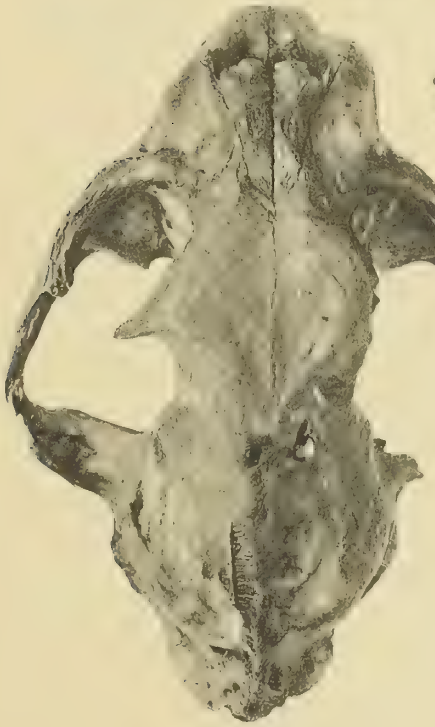
8

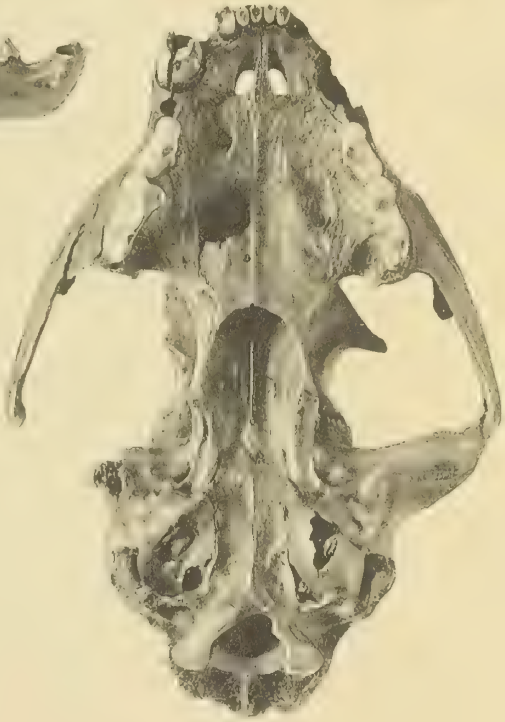
9

HELIOTYPE CO. BOSTON

FELIS AND LYNX

"PALEONTOLOGY AND STRATIGRAPHY BRANCH"

10/7/59

BOUND BY
HNM

SMITHSONIAN INSTITUTION LIBRARIES
3 9088 00733 7710